RESEARCH MODEL INNOVATIONS IN ADVANCING NEONATAL CARE

EDITED BY: Fook-Choe Cheah, Geok Chin Tan and Yuan Shi
PUBLISHED IN: Frontiers in Pediatrics

frontiers Research Topics

frontiers

ISSN 1664-8714
ISBN 978-2-88971-158-1
DOI 10.3389/978-2-88971-158-1

About Frontiers

Frontiers is more than just an open-access publisher of scholarly articles: it is a pioneering approach to the world of academia, radically improving the way scholarly research is managed. The grand vision of Frontiers is a world where all people have an equal opportunity to seek, share and generate knowledge. Frontiers provides immediate and permanent online open access to all its publications, but this alone is not enough to realize our grand goals.

Frontiers Journal Series

The Frontiers Journal Series is a multi-tier and interdisciplinary set of open-access, online journals, promising a paradigm shift from the current review, selection and dissemination processes in academic publishing. All Frontiers journals are driven by researchers for researchers; therefore, they constitute a service to the scholarly community. At the same time, the Frontiers Journal Series operates on a revolutionary invention, the tiered publishing system, initially addressing specific communities of scholars, and gradually climbing up to broader public understanding, thus serving the interests of the lay society, too.

Dedication to Quality

Each Frontiers article is a landmark of the highest quality, thanks to genuinely collaborative interactions between authors and review editors, who include some of the world's best academicians. Research must be certified by peers before entering a stream of knowledge that may eventually reach the public - and shape society; therefore, Frontiers only applies the most rigorous and unbiased reviews.
Frontiers revolutionizes research publishing by freely delivering the most outstanding research, evaluated with no bias from both the academic and social point of view. By applying the most advanced information technologies, Frontiers is catapulting scholarly publishing into a new generation.

What are Frontiers Research Topics?

Frontiers Research Topics are very popular trademarks of the Frontiers Journals Series: they are collections of at least ten articles, all centered on a particular subject. With their unique mix of varied contributions from Original Research to Review Articles, Frontiers Research Topics unify the most influential researchers, the latest key findings and historical advances in a hot research area! Find out more on how to host your own Frontiers Research Topic or contribute to one as an author by contacting the Frontiers Editorial Office: frontiersin.org/about/contact

RESEARCH MODEL INNOVATIONS IN ADVANCING NEONATAL CARE

Topic Editors:
Fook-Choe Cheah, National University of Malaysia, Malaysia
Geok Chin Tan, National University of Malaysia, Malaysia
Yuan Shi, Children's Hospital of Chongqing Medical University, China

Citation: Cheah, F.-C., Tan, G. C., Shi, Y., eds. (2021). Research Model Innovations in Advancing Neonatal Care. Lausanne: Frontiers Media SA. doi: 10.3389/978-2-88971-158-1

Table of Contents

frontiers in Pediatrics

EDITORIAL
published: 16 June 2021
doi: 10.3389/fped.2021.711409

Editorial: Research Model Innovations in Advancing Neonatal Care

Fook-Choe Cheah[1]*, *Geok Chin Tan*[2] and *Yuan Shi*[3]

[1] Department of Paediatrics, Faculty of Medicine, Universiti Kebangsaan Malaysia Medical Centre, Kuala Lumpur, Malaysia,
[2] Department of Pathology, Faculty of Medicine, Universiti Kebangsaan Malaysia Medical Centre, Kuala Lumpur, Malaysia,
[3] Department of Neonatology, Children's Hospital of Chongqing Medical University, Chongqing, China

Keywords: animal models, bronchopulmonary dysplasia, developmental, hypoxic-ischemic encephalopathy, necrotizing enterocolitis, preterm, sex differences, stem cell therapy

Editorial on the Research Topic

Research Model Innovations in Advancing Neonatal Care

INTRODUCTION

Neonatology is a rapidly evolving field. Enormous progress in clinical research and translational studies bring us closer to the understanding and embracing of evidence-based practice in this specialty. While clinical trials bring research ideas of key problems to the test, often to introduce newer therapies, accurate models of diseases provide the fundamental understanding and help to answer or query why we do what we do in practice, thus critical in driving changes to improve neonatal care. In this regard, animal models and innovation prototypes, to be relevant substitutes of patients, are first rigorously studied in pre-clinical trials that simulate real clinical conditions. This special edition aims to highlight original research and innovation in models of pre-clinical studies or prototypes worthy of future clinical testing and application.

BRONCHOPULMONARY DYSPLASIA

Bronchopulmonary dysplasia (BPD) is one of the most common complications of the very premature infant (1). With the rapid development of perinatal care and medical support technology, the survival rate of these infants has significantly improved. This inadvertently leads to also an increase in the rate of a new form of chronic lung disease of prematurity, the "new" BPD. The new BPD is characterized by distal lung tissue disruption that may be initiated by intrauterine inflammation or infection and modified by extrauterine postnatal factors during the critical period of alveolar development, leading to growth arrest and simplification of these alveoli (2). In order to have a better understanding of the etiology and pathophysiology of this new form of BPD, researchers need reliable preterm animal models to study these intrauterine and early perinatal factors that may be preventable or treatable. In the article by Zhang, Chu et al., a premature rat model showed poorer growth with hyperoxia exposure and changes suggestive of alveolar disruption of the new BPD with significantly reduced radial count of the alveoli, which also appeared hyperinflated. The study by Ruan et al. displayed the same growth impairment, dismal overall physical condition, and alveolar simplification from hyperoxia. While many mouse and rat models are studied at term-born, albeit at the saccular stage of lung development, equivalent to that of the human preterm infant, these animal pups could breathe spontaneously and do not require oxygen supplementation (3). The model by Zhang, Chu et al. is interesting and simulates

OPEN ACCESS

Edited and reviewed by:
Arjan Te Pas,
Leiden University, Netherlands

***Correspondence:**
Fook-Choe Cheah
cheahfc@ppukm.ukm.edu.my

Specialty section:
This article was submitted to Neonatology, a section of the journal Frontiers in Pediatrics

Received: *18 May 2021*
Accepted: *24 May 2021*
Published: *16 June 2021*

Citation:
Cheah F-C, Tan GC and Shi Y (2021) Editorial: Research Model Innovations in Advancing Neonatal Care. Front. Pediatr. 9:711409. doi: 10.3389/fped.2021.711409

if additional oxygen could injure the preterm immature lung at an earlier canalicular phase and interfere with growth and their overall physical condition.

Following on the role of intrauterine exposure to infection that could be an antecedent factor in the new BPD development, Cheah et al. studied the effects of low dose intra-amniotic *Gardnerella vaginalis* (GV) injection into a pregnant rabbit model. GV is one of the most common bacteria causing chorioamnionitis in prematurity (4). The major effects were rather similar to that in the model of hyperoxia by Zhang, Chu et al. in terms of growth. The fetal pups were born with significantly lower weight and the number of alveoli was also decreased, although this was not statistically significant but the alveolar septum hypertrophied after intrauterine exposure to GV. It is to be determined if the septal thickening was the result of inflammation, followed by fibromuscular and vascular remodeling that may disrupt oxygenation and gas exchange, as the hallmark changes in the BPD lung. The concept of a "two-hit hypothesis" with antenatal and postnatal factors causing BPD may be explored in the future perhaps with the transgenic mice model reported by Cheah et al. The GM-CSF is a pro-inflammatory cytokine that is induced and elevated by infection. Using this model, the group showed a significant influx of macrophages into the lung interstitium with increased GM-CSF. It will be interesting to study these animals exposed postnatally to hyperoxia and effects on the transition from the inflammatory to the remodeling processes that may result in the development of interstitial or septal fibrosis (5). Of note, despite being different animal models, the hyperoxia and intrauterine infection exposure resulted similarly in growth restriction. Indeed, growth restriction is a potent risk factor for BPD as the associated increase in sFlt-1 (soluble FMS-like tyrosine kinase-1) (6) has a negative impact on growth factors such as VEGF, a mediator that regulates vascular growth closely linked to the alveolarization process (7). As shown by Ruan et al., the effects of oxygen toxicity resulted in increased pulmonary vascular permeability, likely from endothelial damage, and reduced Twist1 that may potentially modify VEGF as well.

It is widely appreciated that BPD is a complex disease of multi-factorial causes and appears inevitable at least in the extremely preterm population but therapy to ameliorate this condition may be in the horizon. Since the first successful cultivation of mice embryonic stem cells in 1981 (8) by Sir Martin J. Evans who eventually won the 2007 Nobel Prize in Physiology or Medicine, stem cells have been widely investigated and regarded as a promising treatment modality of various diseases. In this Research Topic, there are three reviews on the potential use of stem cells in neonatal diseases. Chia et al. described the therapeutic potential of placental stem cells due to its immunomodulating effects on BPD. Based on the current pre-clinical and clinical studies, human amniotic epithelial cells and umbilical cord mesenchymal stem cells are of the greatest potential as therapeutic agents. Liau et al. discussed the current application of mesenchymal stromal cells (MSC) in treating neonatal diseases, discussing the mechanism of action of MSCs through paracrine effects, direct cell contact, and cell fusion. They concluded that MSC therapy while promising, raised concerns in using stem cells with aspects on safety, the risk of transmitting infectious agents, and the heterogeneity in the source of stem cells possessing variable characteristics and differentiating properties. The increasing potential of extracellular vesicles (EVs) such as exosomes is highlighted in these reviews as an emerging and novel therapeutic strategy that may eliminate the worries associated with cellular products.

GASTROINTESTINAL ISSUES

The other "nemesis" that neonatologists face is necrotizing enterocolitis (NEC), occurring more commonly in the very low birth weight preterm infants. Unlike BPD, this gastrointestinal complication occurs earlier, can be acute in onset and progresses unpredictably with a mortality rate that ranges from 20% to above 50% (9, 10). Once NEC sets in, supportive care is the mainstay of treatment and close observation for signs of deterioration and to decide if surgery is required. Holgersen et al. (**Figure 1**) showed in a study of NEC-sensitive piglets that the use of insulin-like growth factor-1 increased intestinal villus length and may be disease modifying, as it was associated with less severe NEC. Furthermore, Villamor-Martinez et al. performed a meta-analysis that concluded, both stem cells and stem cell exosomes reduced all grades of NEC in rodent-exclusive experimental models. These results are promising for future human trials but concerns raised were the lack of robustness in the animal models used, a paucity of clinician involvement and the heterogeneity in the study designs.

The two interventions proven to reduce the risk of NEC are the use of human milk as enteral feeds and probiotics (11). The availability of mother's own milk to infants born preterm are generally insufficient especially during the initial postnatal period and donor human milk (DHM) may be sourced as alternative for enteral feeding. In the article by Cayer et al., the performance of the TEMPO® system to test for human milk bacteriological contamination appears to be reliable with a quick turn-around time for the DHM to be made available for safe consumption by the recipient infants. The use of probiotics, although a standard care of practice to prevent NEC especially among the extremely preterm in some neonatal units, is an area still divided among practitioners as to the optimal timing, dose and strains to be used. Incidentally, the gut microbiome may also affect the health of other organs (12). Zhang, Ran et al. showed that acetate therapy was associated with an abundance of the microbiota that protects the lung from BPD. The mice exposed to hyperoxia but given acetate showed reduction in NLRP3-inflammasome expression and attenuated lung morphological changes of BPD. This mechanism may underlie the observation in a clinical study that showed acetate in parenteral nutrition was associated with a lower rate of BPD (13).

Intriguingly, another preventive measure to be explored that may reduce the incidence of NEC is co-bedding. Brunse et al. showed that co-bedding with skin-to-skin contact of piglet littermates improved gut function and reduced NEC incidence, independent of cortisol effects, which given as hydrocortisone to stabilize blood pressure, predisposed to NEC. Co-bedding of

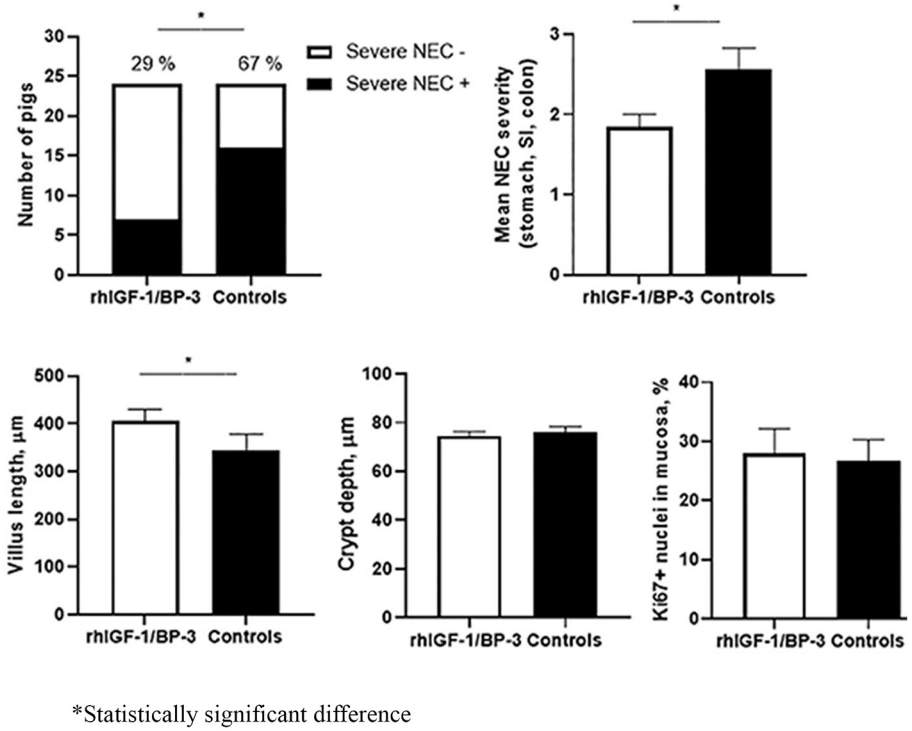

FIGURE 1 | Supplemental insulin-like growth factor-1 and necrotizing enterocolitis in preterm pigs; Holgersen et al.

twins has been practiced in some neonatal intensive care units (NICUs) to simulate the intrauterine couple environment but studies have not shown any positive benefits (14). Conversely, negative implications include potential higher risks of medication errors and cross-infections. Nevertheless, the study by Brunse et al. raised hypothetically whether skin-to-skin contact, an integral feature in kangaroo mother care, gives rise to the various positive effects reported in the preterm infant (15, 16).

The other gastrointestinal-related issues faced by premature infants are gut dysmotility and maturation of the sucking-swallowing processes. These often pose as oral feeding difficulties or challenges when the infant is in the NICU and even after hospital discharge. The article by Kappel et al. provide some insights into how gastrointestinal transit time may vary based on the gestational age, postnatal age, and also the type of feeds. These could help clinicians to approach feeding intolerance occurring in their patients with the appropriate investigation and remedial plans. The review by Lau offers strategies in individualizing care of infants born preterm with different phases of maturational defects in their oral feeding skills.

BRAIN DEVELOPMENTAL DISORDERS AND INJURIES

Brain developmental disorders and injuries to the newborn infant are often devastating and result in significant long-term morbidity such as cerebral palsy. Infants with hypoxic-ischemic encephalopathy (HIE) are currently resuscitated with air and offered therapeutic hypothermia to mitigate the injurious processes in the brain. The review by Liau et al. discussed adjunct therapy with MSC that potentially attenuate the extent of the brain injury. Using the oxygen-glucose deprivation rat model, Shi et al. showed a potential target for further neuroprotection by activating Sirt-1 with the antioxidant such as resveratrol. Another innovative approach that may be explored in the future is the use of hypobaric intervention in stabilization of the asphyxiated infant with early onset and difficult to control seizures. Xie et al. showed in their model that hypobaria, simulating high-altitude environment, increases seizure threshold that may potentially reduce neuronal discharge activity and apoptosis. It may sound counter-intuitive that HIE cases are managed this way, but indeed hypoxic/ischemic pre-conditioning treatment appeared to be protective to the injured neonatal brain (17).

Studying and monitoring the oxygenation status at the cellular level in such critical cases may be complemented by the non-invasive Cellular Oxygen METabolism (COMET) tool that measures *in vivo* mitochondrial oxygen tension. The study by Costerus et al. showed feasibility in its use in neonates and this may be another promising point-of-care test or bedside patient monitoring system to be introduced in the NICU. In hereditary neurological conditions that are largely incurable, Wong et al. reviewed the role of gene-editing models using the Clustered Regularly Interspaced Short Palindromic Repeat (CRISPR) approach, providing a glimmer of hope in therapy in spite of the several drawbacks that need to be overcome such as vulnerability

of neuronal cells and less efficient CRISPR delivery into the brain.

DEVELOPMENTAL ORIGINS AND SEX DIFFERENCES IN HEALTH AND DISEASES

Finally, the developmental origins of health and diseases (DOHaD), a concept that was first proposed by Barker two decades ago, suggests that environmental exposure during the critical period in early life may program the later health in adulthood (18). In the review by Chin and Pang, rodent models of exposure to soy isoflavones during the neonatal period increased bone mineral density in adulthood of especially the female sex. This begs the question if the female or male sex exerts different influences on DOHaD. Sex differences in health outcomes are increasingly being detected with *post-hoc* analyses of clinical studies adjusting for sex as an independent factor (19–21). The gender disparity need to be actively pursued in future research to select sex as an independent and important variable. In the article by Bæk et al. their preterm piglet model receiving a standardized rearing protocol showed increased early mortality among males, which also showed slower growth. The group proposed to use this model for the study of differences in outcomes between the male and female sex with regards to neonatal care and responses to treatment in the future.

AUTHOR CONTRIBUTIONS

All authors listed have made a substantial, direct and intellectual contribution to the work, and approved it for publication.

ACKNOWLEDGMENTS

We wish to convey our appreciation to all the authors who have contributed their scientific papers to this Research Topic and the experts who have participated in the invaluable peer review process of the manuscripts. We would also like to thank Dr. Ooi Kai Shen for his technical assistance.

REFERENCES

1. Jobe AH, Bancalari E. Bronchopulmonary dysplasia. *Am J Respir Critical Care Med.* (2001) 163:1723–9. doi: 10.1164/ajrccm.163.7.2011060
2. Hadchouel A, Franco-Montoya ML, Delacourt C. Altered lung development in bronchopulmonary dysplasia. *Birth Defects Res Part A Clin Mol Teratol.* (2014) 100:158–67. doi: 10.1002/bdra.23237
3. Morty RE. Using experimental models to identify pathogenic pathways and putative disease management targets in bronchopulmonary dysplasia. *Neonatology.* (2020) 117:233–9. doi: 10.1159/000506989
4. Hillier SL, Martius J, Krohn M, Kiviat N, Holmes KK, Eschenbach DA. A case–control study of chorioamnionic infection and histologic chorioamnionitis in prematurity. *N Engl J Med.* (1988) 319:972–8. doi: 10.1056/NEJM198810133191503
5. Hayes D Jr, Feola DJ, Murphy BS, Shook LA, Ballard HO. Pathogenesis of bronchopulmonary dysplasia. *Respiration.* (2010) 79:425–36. doi: 10.1159/000242497
6. Hendrix ML, Bons J, Van Haren A, Van Kuijk S, Van Doorn W, Kimenai D, et al. Role of sFlt-1 and PlGF in the screening of small-for-gestational age neonates during pregnancy: a systematic review. *Ann Clin Biochem.* (2020) 57:44–58. doi: 10.1177/0004563219882042
7. Baker CD, Abman SH. Impaired pulmonary vascular development in bronchopulmonary dysplasia. *Neonatology.* (2015) 107:344–51. doi: 10.1159/000381129
8. Hansen T. The Nobel Prize in physiology or medicine 2007. *Scand J Immunol.* (2007) 66:603. doi: 10.1111/j.1365-3083.2007.02041.x
9. Fitzgibbons SC, Ching Y, Yu D, Carpenter J, Kenny M, Weldon C, et al. Mortality of necrotizing enterocolitis expressed by birth weight categories. *J Pediatric Surg.* (2009) 44:1072–5; discussion: 5–6. doi: 10.1016/j.jpedsurg.2009.02.013
10. Jones IH, Hall NJ. Contemporary outcomes for infants with necrotizing enterocolitis; a systematic review. *J Pediatrics.* (2020) 220:86–92.e3. doi: 10.1016/j.jpeds.2019.11.011
11. Jin YT, Duan Y, Deng XK, Lin J. Prevention of necrotizing enterocolitis in premature infants - an updated review. *World J Clin Pediatrics.* (2019) 8:23–32. doi: 10.5409/wjcp.v8.i2.23
12. Zhuang L, Chen H, Zhang S, Zhuang J, Li Q, Feng Z. Intestinal microbiota in early life and its implications on childhood health. *Genomics Proteomics bioinformatics.* (2019) 17:13–25. doi: 10.1016/j.gpb.2018.10.002
13. Ali A, Ong E-Y, Singh BKS, Cheah F-C. Comparison between sodium acetate and sodium chloride in parenteral nutrition for very preterm infants on the acid-base status and neonatal outcomes. *Pediatric Gastroenterol Hepatol Nutr.* (2020) 23:377. doi: 10.5223/pghn.2020.23.4.377
14. Lai NM, Foong SC, Foong WC, Tan K. Co-bedding in neonatal nursery for promoting growth and neurodevelopment in stable preterm twins. *Cochrane Database Syst Rev.* (2016) 4:CD008313. doi: 10.1002/14651858.CD008313.pub3
15. Pandya D, Kartikeswar GAP, Patwardhan G, Kadam S, Pandit A, Patole S. Effect of early kangaroo mother care on time to full feeds in preterm infants - a prospective cohort study. *Early Human Dev.* (2021) 154:105312. doi: 10.1016/j.earlhumdev.2021.105312
16. Charpak N, Tessier R, Ruiz JG, Hernandez JT, Uriza F, Villegas J, et al. Twenty-year follow-up of Kangaroo mother care versus traditional care. *Pediatrics.* (2017) 139:e20162063. doi: 10.1542/peds.2016-2063
17. Fan X, Wang H, Zhang L, Tang J, Qu Y, Mu D. Neuroprotection of hypoxic/ischemic preconditioning in neonatal brain with hypoxic-ischemic injury. *Rev Neurosci.* (2021) 32:23–34. doi: 10.1515/revneuro-2020-0024
18. Barker DJ. *The Fetal and Infant Origins of Adult Disease*. London: British Medical Journal (1992).
19. Weng Y-H, Yang C-Y, Chiu Y-W. Neonatal outcomes in relation to sex differences: a national cohort survey in Taiwan. *Biol Sex Differ.* (2015) 6:30. doi: 10.1186/s13293-015-0052-8
20. Boghossian NS, Geraci M, Edwards EM, Horbar JD. Sex differences in mortality and morbidity of infants born at less than 30 weeks' gestation. *Pediatrics.* (2018) 142:e20182352. doi: 10.1542/peds.2018-2352
21. Townsel CD, Emmer SF, Campbell WA, Hussain N. Gender differences in respiratory morbidity and mortality of preterm neonates. *Front Pediatr.* (2017) 5:6. doi: 10.3389/fped.2017.00006

Conflict of Interest: The authors declare that the research was conducted in the absence of any commercial or financial relationships that could be construed as a potential conflict of interest.

frontiers in Pediatrics

ORIGINAL RESEARCH
published: 23 April 2020
doi: 10.3389/fped.2020.00190

The Changes of Twist1 Pathway in Pulmonary Microvascular Permeability in a Newborn Rat Model of Hyperoxia-Induced Acute Lung Injury

Ying Ruan, Wenbin Dong, Lan Kang, Xiaoping Lei, Rong Zhang, Fan Wang and Xiaodan Zhu*

Department of Newborn Medicine, The Affiliated Hospital of Southwest Medical University, Luzhou, China

Background: Bronchopulmonary dysplasia (BPD) is a chronic lung disease in preterm infants, which is characterized by alveolar and vascular dysplasia and increased vascular permeability. Hyperoxia is a critical factor in the pathogenesis of BPD, hyperoxia-induced acute lung injury (HALI) model has similar pathological manifestations as human BPD, therefore, may provide insight into the pathogenesis of human BPD. Studies have shown that Twist1 regulates pulmonary vascular permeability of LPS-induced lung injury through the Ang-Tie2 pathway. However, the effect of Twist1 pathway on vascular permeability in HALI has not been reported.

Methods: We randomly exposed newborn rats to the room air or hyperoxia for 14 days. Lung histopathology, immunofluorescence, vascular permeability, mRNA and protein expression was assessed on day 1,7,14.

Results: Our results verified that hyperoxia caused alveolar and vascular developmental disorders and increased pulmonary vascular permeability, which was consistent with previous findings. In hyperoxia-exposed rat lungs, the expressions of Twist1, Ang1, Tie1, Tie2, and pTie2 were significantly reduced, whereas the expression of Ang2 was significantly increased. Next, we observed a significant down-regulation of the Akt/Foxo1 pathway.

Conclusion: In HALI, the pulmonary microvascular permeability was increased, accompanied by changes in Twist1-Tie2 pathway which combined to Angs, and downregulation of Tie1 and Akt/Foxo1 pathway.

Keywords: bronchopulmonary dysplasia, hyperoxia, microvascular permeability, Twist1, Ang, Tie

OPEN ACCESS

Edited by:
Yuan Shi,
The Children's Hospital of Chongqing Medical University, China

Reviewed by:
Yusei Ohshima,
University of Fukui, Japan
Bruce David Uhal,
Michigan State University, United States
Hua Wang,
Sichuan University, China

****Correspondence:***
Wenbin Dong
dongwenbin2000@163.com

Specialty section:
This article was submitted to Neonatology, a section of the journal Frontiers in Pediatrics

Received: *13 February 2020*
Accepted: *31 March 2020*
Published: *23 April 2020*

Citation:
Ruan Y, Dong W, Kang L, Lei X, Zhang R, Wang F and Zhu X (2020) The Changes of Twist1 Pathway in Pulmonary Microvascular Permeability in a Newborn Rat Model of Hyperoxia-Induced Acute Lung Injury. Front. Pediatr. 8:190. doi: 10.3389/fped.2020.00190

INTRODUCTION

In the past few decades, although the survival rate of preterm infants has increased due to the milder oxygen therapy, prenatal steroids and postpartum pulmonary surfactant (PS), the incidence of the "new" BPD which is characterized by the alveolar simplification and disordered angiogenesis has increased year by year (1), which has become an essential factor affecting the survival quality

of premature infants. Lung development includes two stages: alveolar development and pulmonary vascular development. At the same time as alveolar development, the pulmonary microvascular system expands synchronously with the alveolar septum, forming a blood-air barrier (2). There is evidence that the pulmonary microvascular network actively promotes the normal growth of alveoli in the process of lung development, and participates in the maintenance of alveoli structure after birth (3). Angiogenesis regulation plays a necessary role in the formation of the alveolar-capillary network. The deregulation of this process not only impairs the development of the pulmonary microvascular network but also leads to the formation of the immature alveoli, thus leading to lung pathologies such as BPD (4). The pathogenesis of BPD is complicated, the hyperoxia-induced acute lung injury (HALI) is a major contributor to the pathogenesis of BPD (5), which is characterized by increased pulmonary permeability and impairment of alveolar development (6). Therefore, the HALI model may provide insight into the pathogenesis of human BPD. In HALI, the pulmonary microvascular endothelium is damaged, leaving a bare capillary basement membrane area, resulting in increased permeability of the vascular endothelium (7). It has been further found that in the early stage of pulmonary edema of BPD, there is the destruction of the tight connection of the pulmonary vascular endothelium, and the abnormal expression of connexin Cx40 in the lung tissue, which may be related to the increase of the vascular permeability in the stage of pulmonary edema (8). Therefore, maintaining the integrity of the pulmonary microvascular barrier structure and reducing the microvascular permeability is the key to treatment of BPD. However, the specific mechanism of pulmonary vascular permeability changes in BPD is still unclear.

The bHLH transcription factor Twist1 was initially identified in Drosophila by the presence of twisted torsos in embryos that lacked the Twist1 gene (9). It regulates many biological processes such as the epithelial-mesenchymal transition in pulmonary fibrosis (10) and lung cancer (11), in which vascular permeability increases. These different functions of Twist1 are achieved through transcriptional regulation of its targets by recognizing a consensus E-box (CANNTG) motif on the promoter region of target genes to influence their transcription (12) such as tyrosine kinase receptor 2 (Tie2). Twist1 controls angiogenesis and endothelial cell (EC) sprouting through the angiopoietin (Ang)- Tie2 pathway, the disorder of this process mediates the pathological angiogenesis and collagen deposition in bleomycin-induced pulmonary fibrosis model in mice (13). It has also been found that the Twist1-Tie2 pathway is significant to control pulmonary vascular permeability. Twist1 knockdown disrupted cell junction integrity and increased vascular permeability by inhibiting Tie2 expression *in vivo* and *vitro* under physiological conditions (14). Although the Twist1-Tie2 signaling is evident in lung diseases, the role of this signaling in the changes of pulmonary microvascular permeability in HALI has been less explored. Therefore, we hypothesized that the Twist1-Tie2 signaling might participate in the changes of pulmonary vascular permeability in HALI. Given that the Ang-Tie-Akt/Foxo1 pathway plays an important role in the regulation of angiogenesis (15–18), in this research, we further detected whether the Akt-Foxo1 pathway was abnormal in HALI.

In the current study, we showed that the lungs of hyperoxia-exposed rats displayed histological changes consistent with BPD and increased pulmonary vascular permeability. In the lungs, the expressions of Twist1, Ang1, Tie1, Tie2, and pTie2 were significantly reduced, whereas the expression of Ang2 was significantly increased. Next, we observed a significant downregulation of the Akt/Foxo1 pathway. These findings suggest that in HALI, the pulmonary microvascular permeability was increased, accompanied by changes in Twist1-Tie pathway which combined to Angs, and downregulation of Tie1 and Akt/Foxo1 pathway, which may play a vital role in microvascular permeability of HALI.

MATERIALS AND METHODS

Animal Model

A total of 24 time-dated, pregnant SD rats were purchased from the experimental animal center of the Southwest Medical University (Sichuan, China). All animal procedures were reviewed and approved by the Laboratory Animal Ethics Committee of the Southwest Medical University and conducted according to the AAALAC and the IACUC guidelines [License number of the experimental animal: SYXK (Sichuan) 2018-065]. All animals were housed at the experimental animal center of the Southwest Medical University and were permitted access to food and water ad libitum at a temperature range of 20–23°C under a 12:12 h light-dark cycle.

A total of 114 full-term newborn rats were randomly and equally assigned to hyperoxia group and air group within 12 h after birth according to the random number table method. The HALI model was established by high oxygen treatment (8, 19). The hyperoxia group was placed in a closed oxygen tank, and 2L/min of oxygen was continuously introduced to maintain the oxygen concentration at 80∼90%. Sodium lime was used to absorb excessive carbon dioxide. The air group was placed in the same room air (21% oxygen). The nursing mothers were switched every 24 h between the room air and hyperoxia-exposed litters to avoid oxygen toxicity and to eliminate maternal effects. Chamber was opened for 30 min/day for cage cleaning. Nineteen pups were obtained randomly in each group and sacrificed by intraperitoneal sodium pentobarbital injection at the end of 1, 7, 14 days of exposure.

Animal Growth

The survival number, mental state, reaction, feeding status, growth status, and the bodyweight of the newborn rats were recorded every day. At 1, 7, and 14 days of hyperoxia, sixteen newborn rats were randomly taken from each group, and the bodyweight at the time of sampling was recorded. Weight gain

Abbreviations: BPD, bronchopulmonary dysplasia; HALI, hyperoxia-induced acute lung injury; Tie2, tyrosine kinase receptor 2; HE, hematoxylin and eosin staining; MLI, mean linear intercept; IF, immunofluorescence; EBD, Evans blue dye; PDGFB, platelet-derived growth factor B; VEGFR2, vascular endothelial growth factor receptor 2; L-HMVE, lung human microvascular endothelial; ROS, reactive oxygen species; MAOA, monoamine oxidase A; EMT, epithelial-to-mesenchymal transition.

is expressed as a weight gain rate, i.e., body weight growth rate = (body weight at sampling—birth weight)/birth weight.

Sample Collection and Preparation

The lungs were harvested from each group at different time points. The left lung tissues of each group were inflated through the trachea with 4% paraformaldehyde and fixed overnight in the same solution. The fixed tissues were dehydrated and cleared, and five lung tissues were paraffin-embedded for hematoxylin and eosin staining (HE), three lungs were embedded in OCT for immunofluorescence (IF). The lung and body weights of the newborn rats from each group (without formalin fixation) were measured for lung weight /body weight (LW/BW) ratio calculations as an index of lung injury. The remaining lung tissues were immediately frozen at −80°C for reverse transcription-quantitative polymerase chain reaction (RT-qPCR) analysis and immunoblot analysis.

Histopathology and Immunofluorescence Analysis of Lungs

For HE, the paraffin-embedded lung tissues were cut into 4-μm in thickness sections, which were stained with HE for histological analyses of lung injury. From each section, 5–10 random areas were examined at × 20 magnification with an optical microscope. The level of alveolar development was assessed using the mean linear intercept (MLI) methods (20). Ten fields of view were taken at random with the 20 objective on each HE-stained section. Draw a cross line in the center of the collected picture and count the total length of the cross line and the total number of alveolar septa that intersect with the cross line. The MLI calculation method for each field of view: the total length of the cross line divided by the total number of alveolar septa. Finally, the MLI of each section was calculated as the average of the MLI of the 10 fields of view. Large trachea and blood vessels are not included in the calculated field of view.

For IF, the OCT-embedded lung tissues were frozen at −20°C. The frozen tissues were cut into 10-μm sections with a cryostat. The sections were washed with PBST 3 times for 5 min to eliminate OCT, and then incubated in 0.5% TritonX-100 (Amresoo, Washington, USA) for 20 min. The sections were then washed 3 times for 5 min with PBST, blocked with goat serum for 1 h, and incubated with primary antibody. The sections were washed 3 times for 5 min with PBST, and then incubated with fluorescent secondary antibody for 1 h. Finally, the sections were washed 3 times for 5 min with PBST, and then added anti-fluorescence quenching sealing liquid (including DAPI) for sealing. CD31 was detected withing an anti-CD31 primary antibody (1:100, Santa Cruz Biotechnology, CA, USA) and a Rhodamine (TRITC)-conjugated goat anti-rat IgG(H+L) (1:100, Proteintech Group, Inc, USA) secondary antibody. Twist1 was detected withing an anti-Twist1 primary antibody (1:50, Abcam, Cambridge, UK) and a Fluorescein (FITC)-conjugated affinipure goat anti-mouse IgG(H+L) (1:100, Proteintech Group, Inc, USA) secondary antibody. Tie1 was detected withing an anti-Tie1 primary antibody (1:100, Merckmillipore, Germany) and a Coralite488-conjugated affinipure goat anti-rabbit IgG(H+L) (1:250, Proteintech Group, Inc, USA) secondary antibody. Tie2 was detected withing an anti-Tie2 primary antibody (1:100, Merckmillipore, Germany) and a Fluorescein (FITC)-conjugated affinipure goat anti-mouse IgG(H+L) (1:100, Proteintech Group, Inc, USA) secondary antibody. From each section, at least three random areas were examined at × 40 magnification with a fluorescence microscope.

Pulmonary Permeability Assay

Evans blue dye (EBD) can be tightly bound to albumin, and is a sensitive marker of early pulmonary edema and can be used to reflect vascular permeability (21, 22). Lung permeability was measured by LW/BW and by the Evans blue dye (EBD) (Biotopped, Beijing, China) leakage method (23). The lung tissues were homogenated and mixed with formamide (Amresoo, Washington, USA) (1 ml/100 mg tissue), incubated in a 60°C water bath for 24 h, then centrifuged in 5,000 g at room temperature for 30 min, and the absorbance of the supernatant was measured at 620 nm. A standard curve was made according to a series of dilutions of EBD. The concentration of EBD in each group was measured by the standard curve to evaluate the pulmonary vascular endothelial permeability.

Reverse Transcription-Quantitative Polymerase Chain Reaction (RT-qPCR)

The mRNA levels of Twist1, Ang1, Ang2, Tie1, Tei2 were measured by RT-qPCR. The total RNA of each group was extracted from the snap-frozen lung tissues using TRIzol reagent (TIANGEN, Beijing, China) and frozen at −80°C. A total of 1,500 ng RNA from each sample was reverse transcribed to produced cDNA using ReverTra Ace qPCR RT Master Mix (TOYOBO, Japan). The cDNA was then amplified using THUNDERBIRD SYBR qPCR Mix (TOYOBO, Japan). Real-time PCR was conducted using qTOWER 2.0 Real-Time PCR System (Analytik Jena AG, Germany) with Gapdh as an internal control. The amplification reaction was performed as follows: 40 cycles of 95°C for 30 s, 95°C for 5 s, and 60°C for 10 s; and 72°C for 30 s. The relative quantification of mRNA expression for Twist1, Ang1, Ang2, Tie1, Tie2 was conducted using the $2^{\Delta\Delta Ct}$ method following normalization with Gapdh. The specific primers were designed as follows: Twist1, CCGGAGACC TAGATGTCATTGT (forward) and CTGGGAATCTCTGT CCACCG (reverse); Ang1, GGAGTCCAGAAAACGGAGGG (forward) and TTCTCAAGTTTTTGCAGCCAC (reverse); Ang2, CATGATGTCATCGCCCGACT (forward) and TCCA TGTCACAGTAGGCCTTG (reverse); Tie1, AGAGACCAC GCTGGGTAATG (forward) and CTTCACCCGATCCTG ACTGG (reverse); Tie2, AAGAGCGAGTAGACCATGCG (forward) and ACTAGTCCATAAAGGAGCAAGC (reverse); Gapdh, GCAAGTTCAACGGCACAG (forward) and GCCA GTAGACTCCACGACAT (reverse).

Western Bolt

Lung lysate extracts were made, and protein concentration determined by the BCA method. Proteins were separated by SDS-PAGE (10%) and transferred to PVDF membranes followed by

1 h blocking at room temperature (RT) in 7% non-fat milk of PBS with 0.07% Tween-20, and then incubated with anti-Twist1 antibody (1:500, Abcam, Cambridge, UK), anti-Angiopoietin 1 antibody (1:1000, Boster Biological Technology Co., Ltd., China), anti-Angiopoietin 2 (1:1000, Proteintech Group, Inc, USA), Tie1 antibody (1:1000, Thermo Fisher Scientific, Waltham, MA), anti-Tie2 antibody (1:1000, Merckmillipore, Germany), anti-phospho-Tie2 (Ser1119) antibody (1:500, Merckmillipore, Germany), phospho-Akt (Ser473) and Akt antibodies (1:1000, Cell Signaling Technology, Danvers, MA), phospho-FoxO1 (Ser256) and FoxO1 (C29H4) Rabbit mAb Antibodies (1:1000, Cell Signaling Technology, Danvers, MA), Gapdh Mouse Monoclonal Antibody (1:14000, Proteintech Group, Inc, USA) at 4°C, overnight. The following day membranes were washed three times with PBST (Phosphate buffer saline with 0.07% Tween 20), incubated with HRP conjugated secondary antibody [HRP-labeled Goat Anti-Rabbit IgG(H+L) or HRP-labeled Goat Anti-Mouse IgG(H+L); both Beyotime, Shanghai, China] for 1 h at RT, washing and then were measured by ECL chemiluminescence method. The gel analysis imaging system was used for scanning and analysis. The relative protein expression levels of target proteins were normalized to Gapdh.

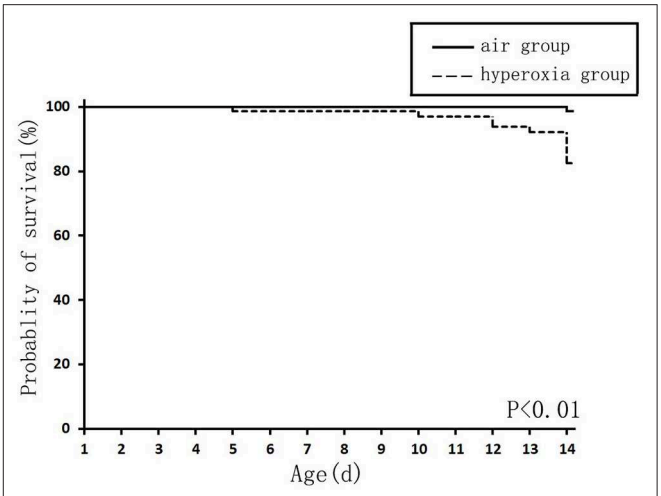

FIGURE 1 | The survival curve of newborn rats in the hyperoxia and air group. The survival rate of the hyperoxia group was significantly lower than that of the air group, $P < 0.01$.

Statistical Analyses

The experimental data were processed by Graphpad prism8.0 software and Image J software and analyzed by SPSS 21.0 statistical software. The values were expressed as mean ± standard deviation. Independent sample *t*-test was used for the comparison between the two groups when normality and homogeneity of variance assumptions were satisfied; otherwise, the non-parametric test Mann-Whitney was used for analysis. In addition, the Kaplan-Meier method was used for survival analysis of each group, and the rank sum test was used for comparison of survival curves between the two groups. $P < 0.05$ was considered statistically significant.

RESULTS

Hyperoxia Exposure Affected the General Health Conditions of the Newborn Rats

The survival rate of newborn rats in the hyperoxia group was significantly lower than that in the air group. The survival rates at 1, 7, and 14 d were 100, 98.56, 82.94%, respectively. With the extension of the hyperoxia time, the newborn rats' mortality gradually increased, and the survival rate gradually decreased. However, no death occurred in the air group at 1 and 7 d, and the survival rate at 14 d was 98.72% (**Figure 1**). We observed the mental state, activity, and hair luster of the newborn rats. With the prolongation of oxygen exposure time, the newborn rats in the hyperoxia group gradually showed weak milk seeking ability, decreased activity, slow response, dull hair, and thin body. Furthermore, from the 7 d after oxygen exposure, the neurological symptoms such as head fibrillation and gait instability began to appear, while the growth and development of the newborn rats in the air group were good, and the above abnormal symptoms did not appear (**Figure 2**). There was no difference in body weight of the newborn rats in both groups at 1 d. The body weight in both groups increased at 7 and 14 d after oxygen exposure compared with 1 d. However, the growth rate of the newborn rats in the hyperoxia group was significantly slower than that in the air group, and the difference between the two groups gradually increased with the extension of the experimental time (**Figure 3A**).

Hyperoxia Could Cause Alveolar Simplification and Lung Injury in Newborn Rats

To determine the role of hyperoxia in lung injury, we analyzed the histological examination of the newborn rats' lungs exposed to air or hyperoxia after birth. It could be seen by the naked eye that the lung tissue of the newborn rats in the air group was pink and elastic, while that of the hyperoxia group was white and less elastic than that of the air group. Under the light microscope, the lung tissue structure of the newborn rats in the air group was gradually completed at 7 d. The alveoli were well-developed and uniform in size. At 14 d, the structure of the alveoli was clear and regular in shape, and the alveolar cavity was small. The alveolar septum was thick, and there was no inflammatory exudation in the alveolar space. In the hyperoxia group, the alveolar space increased, and the alveoli wall became thinner at 7 d. With the extension of oxygen exposure time to 14 d, the lung tissue structure was disordered, and the alveoli structure was simplified and uneven in size. Besides, the alveolar space was significantly enlarged, some of the alveoli fused, the number of alveoli decreased, and inflammatory cells and red blood cells exuded from the alveoli (**Figure 4A**). Upon morphometric analysis, a significant increase in the mean linear intercept (MLI) was noted in newborn rats exposed to hyperoxia (**Figure 4B**). The Lung weight /Bodyweight (LW/BW) ratio is an index of increased cellularity and pulmonary edema; therefore, it can be used to reflect the extent of lung injury. The LW/BW ratios of

FIGURE 2 | The general health conditions of the newborn rats at 1, 7, and 14 d after oxygen exposure. There was no difference between the two groups at 1 d. Newborn rats in the hyperoxia group (H) showed obvious poor development, small body size, inadequate mental response at 7 d, and the difference between the two groups was more evident at 14 d of oxygen exposure. In contrast, the air group (A) has good growth and development.

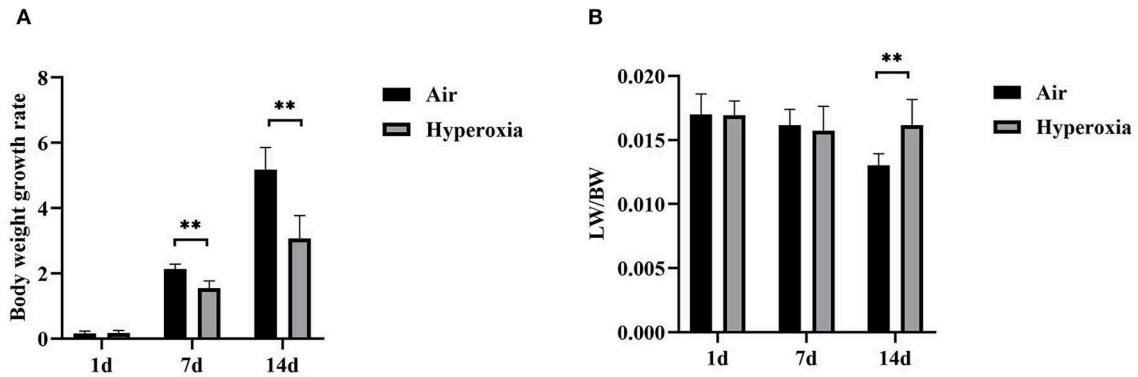

FIGURE 3 | The body weight growth rate and lung/body weight ratios of the air and hyperoxia groups. **(A)** The body weight growth rate of the air and hyperoxia groups at different time points. **(B)** The lung/body weight ratios (LW/BW) of the air and hyperoxia groups at different time points. (**$P < 0.001$).

the newborn rats from the 14 d of the hyperoxia group indicated a significant increase compared with the air group suggesting an increase in lung injury of these animals (**Figure 3B**). The above results indicated that hyperoxia induced lung injury.

Hyperoxia Increased Vascular Permeability in the Newborn Rats' Lung

To further determine whether hyperoxia regulates pulmonary vascular permeability, we measured vascular permeability in newborn rats' lungs by measuring the leakage of Evans blue dye (**Figure 4C**). The leakage of Evans blue dye into lung extravascular space was higher in the lungs of the newborn rats exposed to the hyperoxia compared to that in the air controls at the same time point suggesting that the permeability of pulmonary blood vessels to macromolecules such as Evans blue is gradually increased (**Figure 4D**). In addition, the ratio of LW/BW can also be used to reflect the pulmonary vascular permeability (24). As shown in **Figure 3B**, the LW/BW ratio of the newborn rats on the 14th day is significantly higher than that of the air group. The results above suggest that hyperoxia leads to the increase of pulmonary vascular permeability of the newborn rats.

Hyperoxia Caused Reduced Expression of Twist1, Tie1, and Tie2 in CD31-Positive Cells

We examined the effects of hyperoxia exposure on the levels of Twist1 and Tie receptors in the lung tissues of the newborn rats by IF. IF detection in tissue sections showed that the lungs exposed to high oxygen failed to form septation, resulting in fewer and larger alveoli with less developed vascular structures (CD31-staining vessels), similar to the lungs of premature infants with BPD. The results also showed that the Twist1, Tie1, and Tie2 were specifically expressed in vessel ECs (CD31 positive cells). The Twist1, Tie1, and Tie2 expression were lower in CD31-positive endothelial cells of the hyperoxia group compared to those of the age-matched air controls (**Figures 5A–D**).

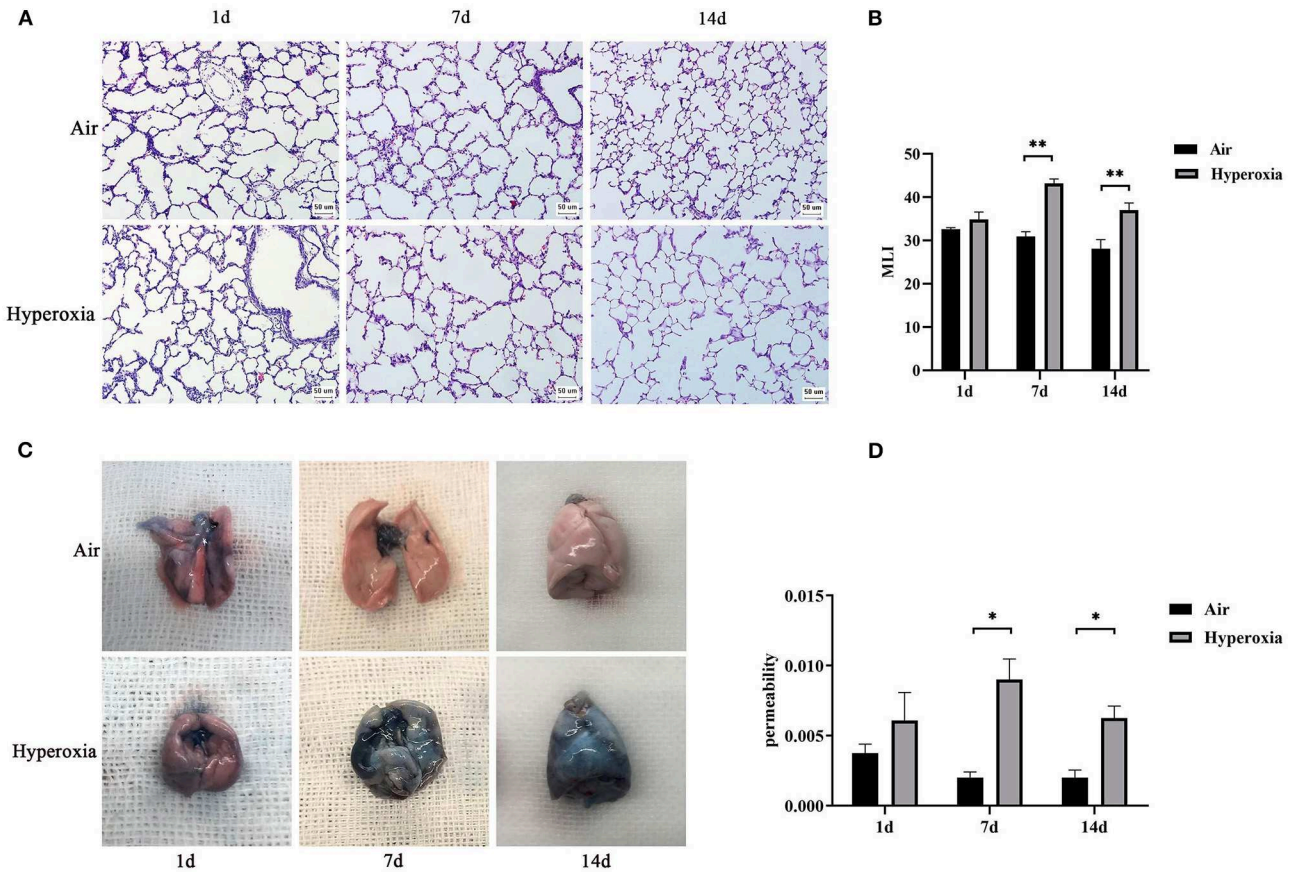

FIGURE 4 | Induction of alveolar simplification and lung injury in newborn rats following hyperoxia. **(A)** The pathological changes of lung tissue were observed by hematoxylin-eosin staining in the air or hyperoxia group. Magnification, × 20. Hyperoxia group at 7 and 14 d showed increased lung injury with disordered lung structure, increased alveolar simplification, and alveolar size. **(B)** The effects of hyperoxia on MLI, which is an index of lung injury, were determined in newborn rats(n = 3–5/group). **(C)** Comparison of Evans blue staining in the lungs of the two groups at different time points. **(D)** Graph showing vascular permeability in the lungs of the two groups at different time points. Vascular permeability was detected by Evans blue dye leakage in the lungs, and extracted dye contents were quantified by measuring at 620 nm. *$P < 0.05$, **$P < 0.001$.

Hyperoxia Down-Regulated Pulmonary Twist1, Tie1, Tie2, and Ang1 mRNAs, While Up-Regulated Ang2 mRNA

Given that hyperoxia could cause pulmonary microvascular endothelial damage, resulting in increased vascular permeability. Therefore, we hypothesized that the Twist1 target gene Tie2 in conjugation with its ligands (Ang1/2) might play a crucial role in hyperoxia-induced pulmonary vascular permeability. To further investigate the mechanism of changes in pulmonary vascular permeability during hyperoxia, we evaluated the pulmonary mRNA levels of Twist1, Tie1, Tie2, Ang1, and Ang2. No significant decrease in the pulmonary Twist1 mRNA level was noted at 1 or 7 d in the hyperoxia group compared with the air controls. However, the Twist1 mRNA level in the hyperoxia group was significantly lower than that in the air group at 14 d. From the 7 d, hyperoxia reduced Tie1, Tie2, Ang1 mRNA significantly compared with the air controls, while induced Ang2 mRNA significantly (**Figures 6A–E**).

Hyperoxia Reduced Pulmonary Twist1, Tie1, Tie2 and Ang1 Protein Levels, While Up-Regulated Ang2 Protein Level, and Inhibited the Expression of Proteins in Akt/Foxo1 Pathway

To further determine the mechanism of Twist1 and its downstream signaling pathways in hyperoxia-induced pulmonary vascular permeability, we evaluated the protein expression in this signaling pathway in the air and hyperoxia groups at different time points by western blot. As shown in **Figure 7**, there was no significant difference in the expression of Twist1 at 1 and 7 d of the hyperoxia group compared with the age-matched air group. With the extension of oxygen exposure time, Twist1 decreased significantly at 14 d of hyperoxia compared with the air group at the same time point (**Figures 7A,D**). Similarly, at 1 d of hyperoxia, the protein levels of Ang1, Ang2, Tie1, pTie2, and Tie2 were not significantly different from those of the air group.

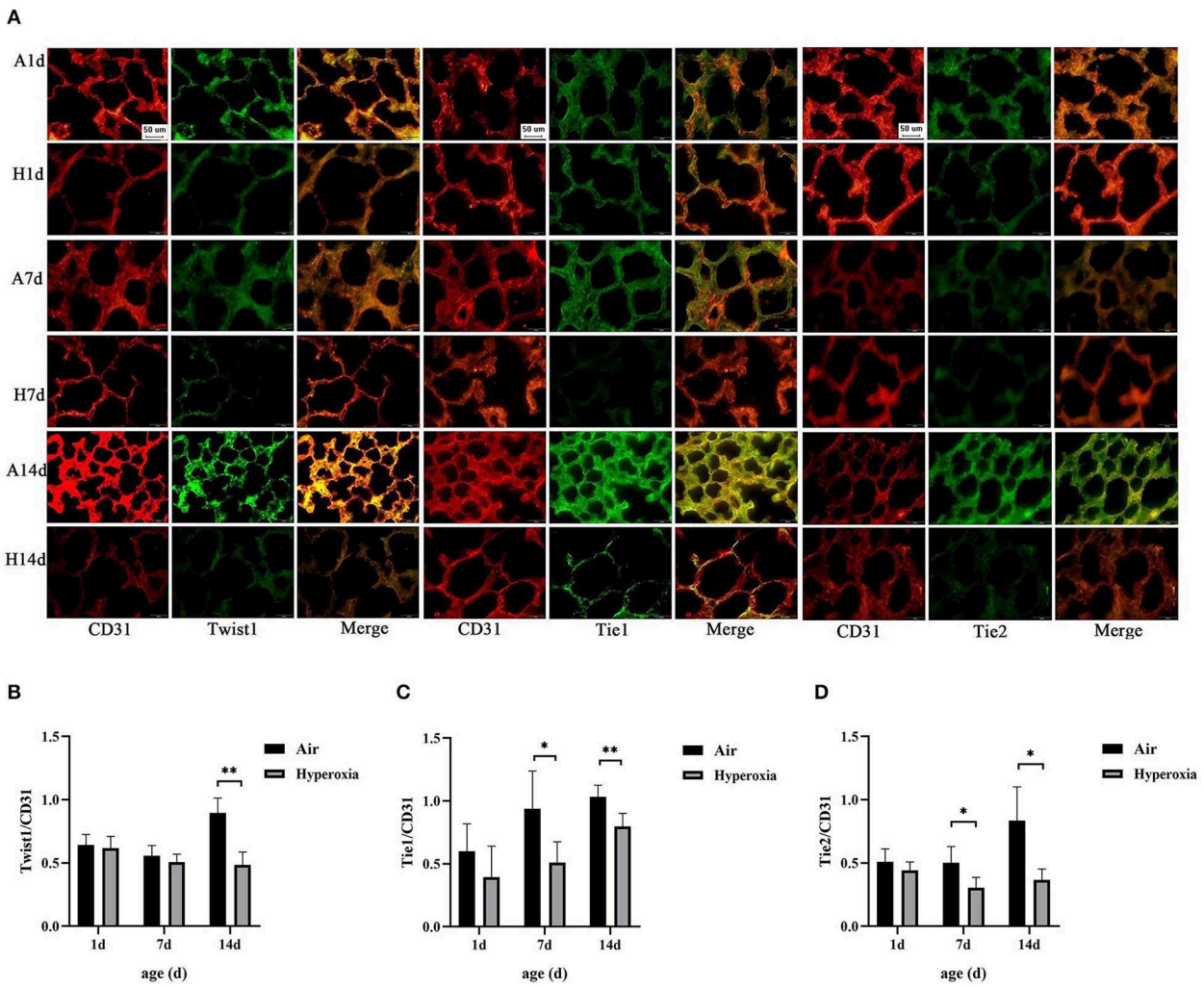

FIGURE 5 | Hyperoxia caused reduced expression of Twist1, Tie1, and Tie2 in CD31-positive cells. **(A)** Immunofluorescence micrographs showed the expression and distribution of Twist1, Tie1, Tie2 in CD31-stained blood vessels of the lungs of the two groups at different time points (Magnification, ×40; bar, 50 μm). **(B)** The expression ratio of Twist1 in CD31 positive endothelial cells of the two groups at different time points ($n = 3$/group). **(C)** The expression ratio of Tie1 in CD31 positive endothelial cells of the two groups at different time points ($n = 3$/group). **(D)** The expression ratio of Tie2 in CD31 positive endothelial cells of the two groups at different time points ($n = 3$/group). $^*P < 0.05$, $^{**}P < 0.001$.

However, with the prolongation of oxygen exposure time, the expression of Ang1, Tie1, ptie2, and Tie2 gradually decreased from the 7 d of hyperoxia, which was significantly different from that of the age-matched air group (**Figures 7A–C,E,F**). Conversely, the expression of Ang2 was significantly higher than that of the air group at 7d of hyperoxia and continued to increase at 14 d of hyperoxia (**Figures 7A,C**). Given that the Tie2 can regulate the activity of Akt and its downstream target protein Foxo1, we also detected the change of Akt/Foxo1 pathway protein in hyperoxia group. Similarly, with the prolongation of oxygen exposure time, the expression of pAkt, Akt, pFoxo1, and Foxo1 proteins decreased significantly from 7 d of hyperoxia, which was significantly different from that of the air group at the same time point (**Figures 8A–C**).

DISCUSSION

BPD is a chronic lung disease in infancy that is associated with significant mortality and long-term morbidity. Previous studies on BPD mainly focused on the mechanism of alveolar dysplasia. However, with the development of new BPD, pulmonary vascular development has gradually received attention, and tight regulation of vascular permeability is the key to maintain lung function. Previous studies have confirmed that the alveolar development process of rats has a similar chronology to humans, the lung development of term newborn rats is in the saccular stage, which is equivalent to that of human at 28 weeks of gestational age (25). Fourteen days after birth is the key period of alveolar formation, the pulmonary blood vessels have also entered a period of significant proliferation (26). It has been

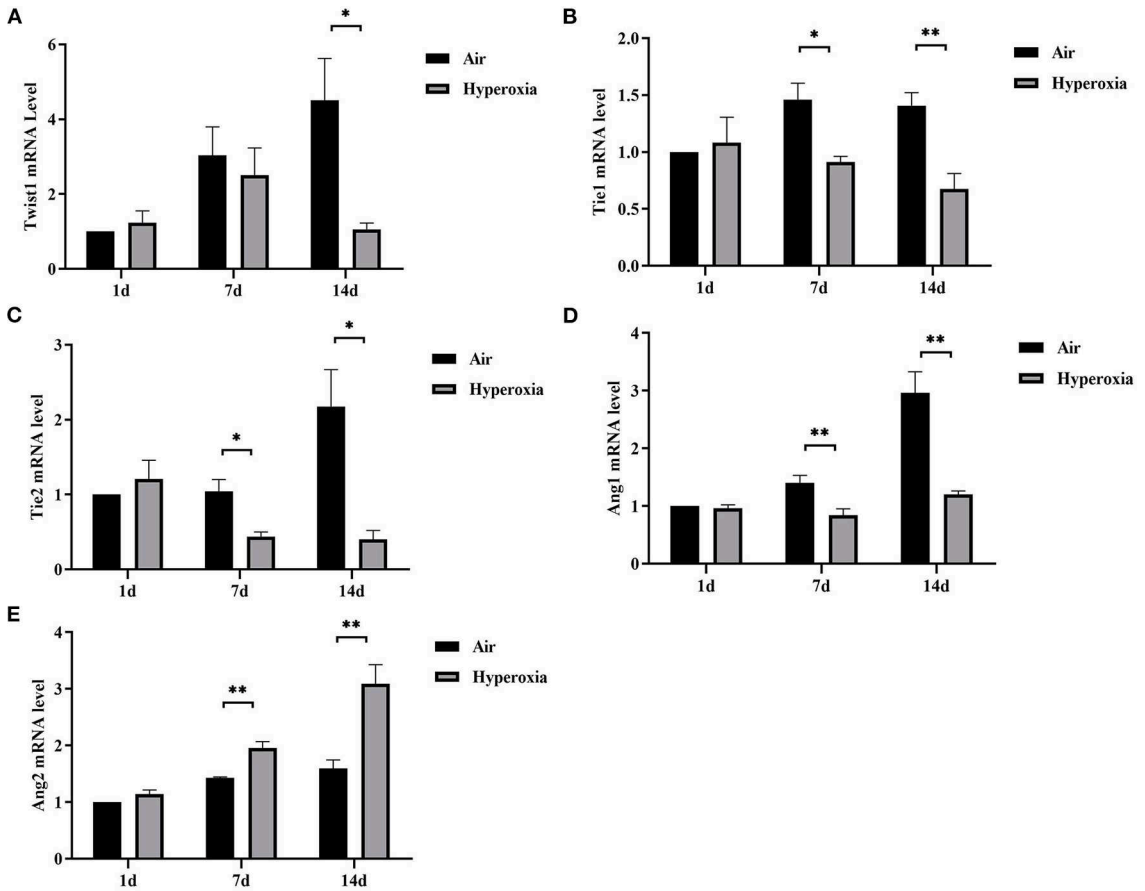

FIGURE 6 | Hyperoxia down-regulated pulmonary Twist1, Tie1, Tie2, and Ang1 mRNAs, while up-regulated Ang2 mRNA. Lungs from all different groups were excised, total RNA was isolated, and Twist1 **(A)**, Tie1 **(B)**, Tie2 **(C)**, Ang1 **(D)**, and Ang2 **(E)** mRNA levels were determined by real time-PCR following cDNA synthesis, as described in the Materials and Methods section ($n = 6$/group). $^{*}P < 0.05$, $^{**}P < 0.01$.

reported that the HALI model in which newborn rats were continuously exposed to 85–90% hyperoxia could simulate the BPD-like lung injury (8, 19, 27). Therefore, in this study, we exposed term newborn rats to 85–90% hyperoxia for 14 days to establish a HALI model. Our data showed a significantly reduced body weight in the hyperoxia group compared with the air group. The newborn rats' mortality gradually increased with the extension of the hyperoxia time. The main pathological changes of BPD are impaired development of alveolar and vascular. Hyperoxia induced decreased number and increased volume of alveolar, disordered lung structure, pulmonary fibrosis and pulmonary vascular dysplasia in newborn rats (27, 28). Our HE staining showed that the obvious structural disorder and simplification of alveolar structure in the lung tissues appeared in the hyperoxia group from the 7th day, and the MLI value was significantly higher than that in the air group, which further indicated that the number of alveoli decreased, reflecting the hypoplasia of lung. The above further proved that the HALI model was successfully established.

In addition, we found that the lung EBD extravasation and LW/BW value of the newborn rats increased after exposure to high oxygen, confirming that pulmonary vascular permeability was increased in HALI (6, 7). Our immunofluorescence results showed that hyperoxia reduced the expression of Twist1, Tie1, and Tie2 in CD31 positive blood vessels. In the lung tissue, CD31 is mainly expressed in pulmonary microvascular endothelial cells and is often used as a marker of vascular endothelial cells (29). With the increase of oxygen exposure time, the CD31 positive blood vessels in the lung tissue of the hyperoxia group were lower than those in the air group, suggesting that there might be pulmonary vascular development obstruction in HALI. Then we examined the changes in mRNA and protein levels of Twist1, Ang1, Ang2, Tie1, and Tie2 in lung tissues. The results showed that the levels of Twist1 mRNA and protein in the hyperoxia group were significantly lower than those in the air group at 14 d. At 7 and 14 d, the mRNA and protein levels of Ang1, Tie1, Tie2, and pTie2 in the hyperoxia group were significantly lower than those in the air group at the same time point. On the contrary, the levels of Ang2 mRNA and protein increased significantly at 7 and 14 d after hyperoxia exposure. In recent years, Twist1 has become a hot spot in the research of vascular-related diseases. It may control the formation of blood vessels

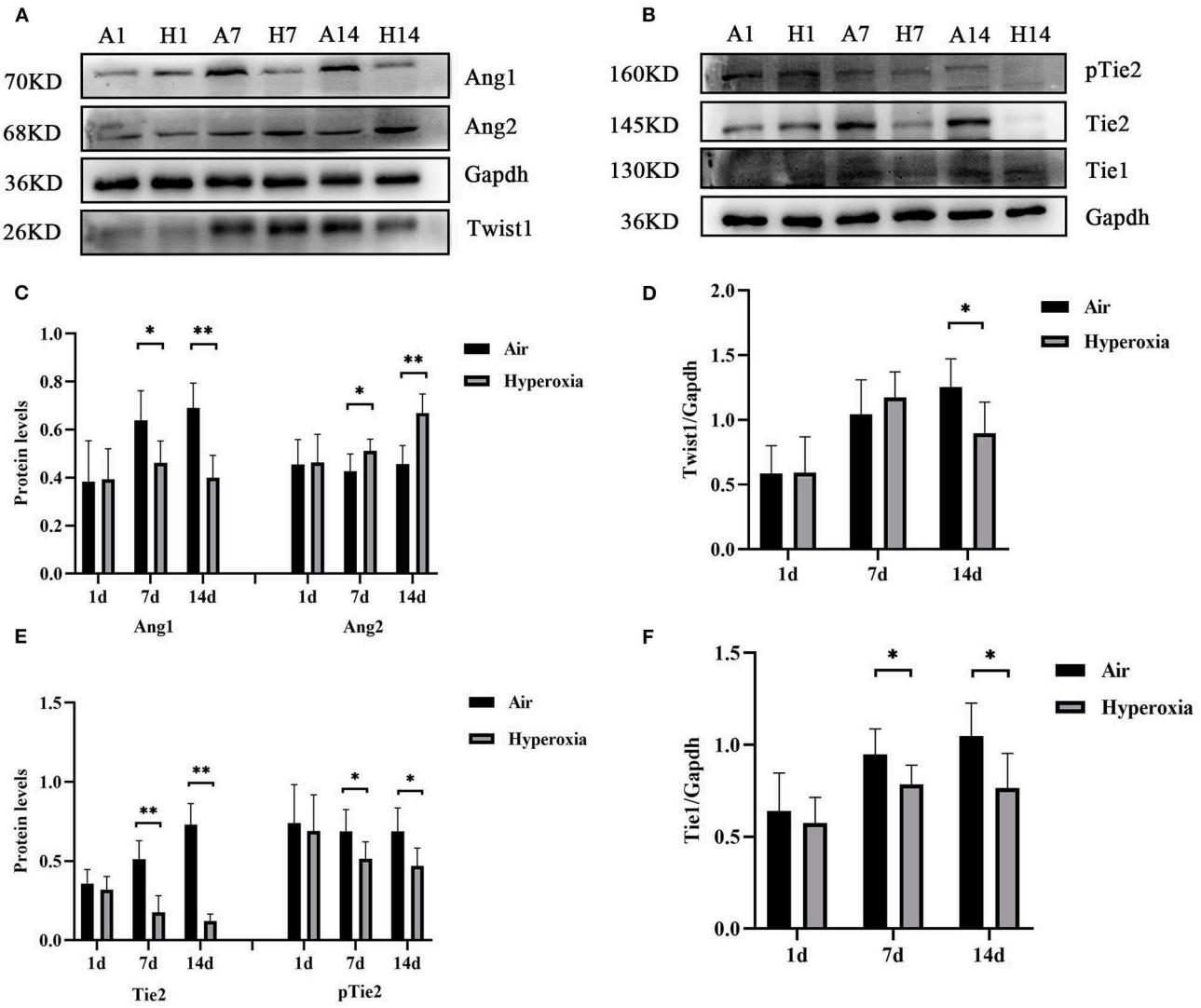

FIGURE 7 | Hyperoxia reduced pulmonary Twist1, Tie1, Tie2, and Ang1 protein levels, while up-regulated Ang2 protein level. The lung homogenates prepared from different groups of newborn rats were subjected to western blots analysis. Western blots showed the expression of Twist1 **(A,D)**, Ang1/2 **(A,C)**, Tie1 **(B,F)**, pTie2/Tie2 **(B,E)** in the lungs. The densitometric intensities of these proteins normalized to Gapdh were quantified and shown separately ($n = 8$–14/group). $^{*}P < 0.05$, $^{**}P < 0.01$.

by regulating the expression of many angiogenic factors and receptors in endothelial cells, such as platelet-derived growth factor B (PDGFB), vascular endothelial growth factor receptor 2 (VEGFR2), Tie2 (14, 30). In cancer and hyperoxia-induced retinopathy models, Twist1 mediated pathological angiogenesis by changing the expression of VEGF and VEGFR2 (30–32). Mammoto et al. (14) found that knockout of Twist1 *in vitro* cultured lung human microvascular endothelial (L-HMVE) cells and *in vivo* adult mouse lung could reduce Tie2 and its phosphorylation status, leading to increased pulmonary vascular permeability in physiological condition where Ang1 is dominant. However, in pathological condition such as endotoxin-induced lung injury, Ang2 was upregulated, knockout of Twist1 failed to increase the pulmonary vascular permeability. These findings demonstrated that the Twist1-Tie2 pathway combined with the Angs controlled the pulmonary vascular permeability in an environment-dependent manner. Angs and Tie receptors are widely expressed in lung tissues, and deregulation of this system contributes to the pathogenesis of various lung diseases such as acute lung injury (ALI) and BPD (33, 34). Ang1 and Ang2 compete with Tie2 receptors to participate in the regulation of endothelial barrier function. Ang1 is secreted by smooth muscle cells and mesenchymal cells around blood vessels (35). As an obligatory Tie2 agonist, Ang1 promotes the germination and branching of blood vessels and vascular stability and maturation, inhibits endothelial cell apoptosis by activating its specific receptor Tie2 (36). In physiological conditions, Ang1 is dominant compared to Ang2 and more likely to combine with Tie2, and induces the transfer of the Tie2 receptor to cell-cell contact or cell-matrix interface, to stabilize the integrity of

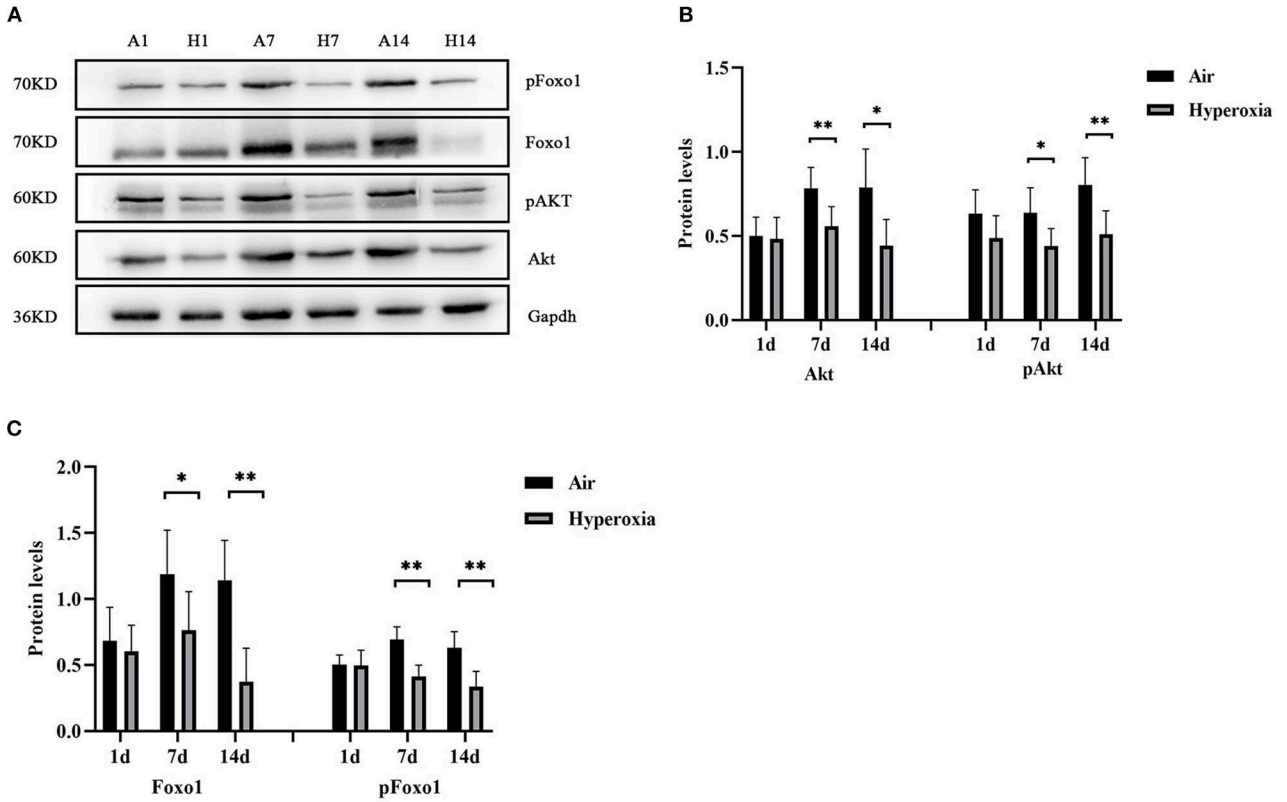

FIGURE 8 | Hyperoxia inhibited the expression of proteins in AKT/Foxo1 pathway. Western blots showed the expression of pAkt/Akt **(A,B)**, pFoxo1/Foxo1 **(A,C)** in the lungs. The densitometric intensities of these proteins normalized to Gapdh were quantified and shown separately (n = 8–14/group). $^{*}P < 0.05$, $^{**}P < 0.01$.

endothelial cell connection (37, 38). Studies have shown that Ang1 could inhibit the permeability of paracellular cells induced by a variety of inflammatory cytokines and growth factors such as thrombin, histamine, and VEGF (39, 40). Therefore, Ang1 plays a vital role in maintaining the continuity and integrity of new blood vessels. In contrast, Ang2 only plays a weak agonist role for Tie2, it almost does not activate Tie2 in physiological condition, it is related to vascular instability and remodeling (41). Ang2 is expressed by ECs and is stored in the endocrine granules in ECs called Weibel Palade body, which can be rapidly secreted when stimulated by inflammatory factors (42). Ang2 promotes vascular leakage by cooperating with inflammatory cytokines. In pathological conditions where Ang2 is dominant, Ang2 combined with Tie2 to play an antagonistic role, making ECs respond quickly to local and systemic stimuli, and destroying the occurrence of connexins between ECs, resulting in increased vascular permeability (43, 44). In our experiment, the Ang1-Tie2 pathway was downregulated in the lungs of newborn rats exposed to hyperoxia, which was consistent with a previous study (34). However, Ang2 was upregulated, Twist1 and Tie2 was downregulated, while the pulmonary vascular permeability was still increased in HALI, this seemed to contradict the conclusion of the research by Mammoto T et al. The possible reasons may be that, in the hyperoxia group, the decrease of Ang1 expression could weaken the Ang1-Tie2 signal, which might lead to vascular development disorder and increase of vascular permeability. Besides, because Ang1 and Ang2 bind to Tie2 in a similar way (45, 46), the binding of Ang2 to Tie2 might lead to the inhibition of the signal transduction of Tie2 induced by Ang1 when the ratio of Ang2/Ang1 increased and make Ang2 play an antagonistic role of Tie2, thus making vascular instability. As a regulator of Tie2 expression, the reduced Twist1 might downregulate the Tie2 expression, which possibly reduce the antagonistic effect of Ang2 on Tie2, and decrease the damage of Ang2 on vascular permeability. Therefore, we speculated that in physiological conditions dominated by Ang1, Twist1 was essential to maintain the stability of pulmonary vessels induced by Ang1-Tie2 signal. In hyperoxia conditions, in which Ang2 was upregulated, the reduction of Twist1might play a compensatory protective role to resist the damage of hyperoxia on pulmonary vascular permeability. Maybe in the natural state without knocking down the Twist1, the decreased extent of Twist1 induced by hyperoxia is not enough to reduce Tie2 to reverse the increase of vascular permeability induced by Ang2-Tie2.

Our experimental data showed that Twist1 had significant difference between the two groups at 14 d, while Ang1, Ang2, Tie2 was significantly different at 7 and 14 d. In the research by Mammoto T et al. knocking down Twist1 did not alter the Ang1 and Ang2 expression, the levels of Ang1 and Ang2 just

determined the effect of the Twist1-Tie2 pathway on vascular permeability. As a regulator of Tie2, the decrease of Twist1 and Tie2 was not synchronous, we analyzed that there were other factors that could regulate Tie2 expression in addition to Twist1, such as micro-RNA (miR)-34a (34). Ang1 and Tie2 were targets of miR-34a, they had conserved miR-34a seed sequence in its 3′UTR. MiR-34a could stimulate cell death and reduce the expression of target protein Ang1 and Tie2. In HALI, micro RNA (miR-34a) was significantly upregulated and Ang1/Tie2 expression was decreased. However, inhibition of miR-34a reduced cell death and enhanced the expression of Ang1/Tie2 in hyperoxia conditions. Therefore, in our experiment, we speculated that both micro RNA (miR-34a) and Twist1 might regulate the Tie2 expression with the prolongation of hyperoxia exposure time. It has not been found that Twist1 can regulate the expression of Tie1. The mechanism of the decline of Tie1 caused by hyperoxia is unclear. Some studies have demonstrated that Tie1 plays an indispensable role in angiopoietin signaling during vascular remodeling and ECs proliferation (47). After treatment with Ad-CAng1 or Ad-Ang2, the tracheal blood vessels of the mice enlarged significantly and endothelial cell proliferation increased, while in Tie1 knockout mice, the above effects were significantly weakened. Tie1 does not bind to angiopoietin directly, but co-precipitates with Tie2 to form a complex at the cell-cell junction (48). The interaction between Tie1 and Tie2 can regulate Ang-induced Tie2 phosphorylation and both Ang1 and Ang2 can increase this interaction through the ectodomain of Tie1 (47). In Tie1-deleted mouse embryos, Ang1-induced Tie2 activation decreased, leading to abnormal blood vessels and leakage (49). In the absence of pathogens, Tie1 was highly activated, and was crucial for the agonist role of Ang1 and Ang2 on Tie2 during vascular remodeling, but inflammation could lead to Tie1 inactivate through ectodomain cleavage, and reduced Ang1-Tie2 signal, and promoted the Tie2 antagonistic effect of Ang2, causing vascular destabilization (47). Although, our current model condition is hyperoxia, some studies have demonstrated that under long-term hyperoxia exposure, lung tissue could produce many inflammatory factors and oxygen radicals such as reactive oxygen species (ROS) which caused inflammatory cells aggregation on the one hand, and on the other hand, inflammatory cells could release a lot of oxygen radicals and inflammatory factors, causing a vicious cycle, leading to lung injury and eventually BPD (50). As a result, oxidative stress and inflammatory responses affected each other. For example, NF-κB is an important transcription factor that regulates inflammatory responses, studies have shown that ROS could cause rapid nuclear translocation of NF-κB, and then promote the expression of downstream pro-inflammatory factors (51). Therefore, we guessed that the changes in Ang-Tie signal were a common result of oxidative stress and inflammation. The down regulation of Ang1-Tie2 might also be related to decreased Tie1 expression.

Ang1-induced Tie2 phosphorylation stimulated the activity of several downstream signaling pathways, which stabilized the VE-cadherin at the EC-EC junction, decreased vascular permeability, and promoted cell survival and anti-apoptosis (52, 53). PI3K/Akt signaling has been demonstrated to be one of the great important downstream signaling pathways of Ang1-Tie2 pathway to play a major role in promoting ECs proliferation and survival at the early stage of angiogenesis (54, 55). The protein expression of PI3K and pAkt decreased after Tie2 inhibitor treatment, indicating that the activation of Tie2 was related to PI3K/Akt pathway transduction (56). Foxo1, can be regulated via the phosphorylation of Akt upon PI3K/Akt signaling activation, its activity is inhibited after phosphorylation (57). Strong evidence showed that Tie2 phosphorylation induced by Ang1 could phosphorylate Foxo1

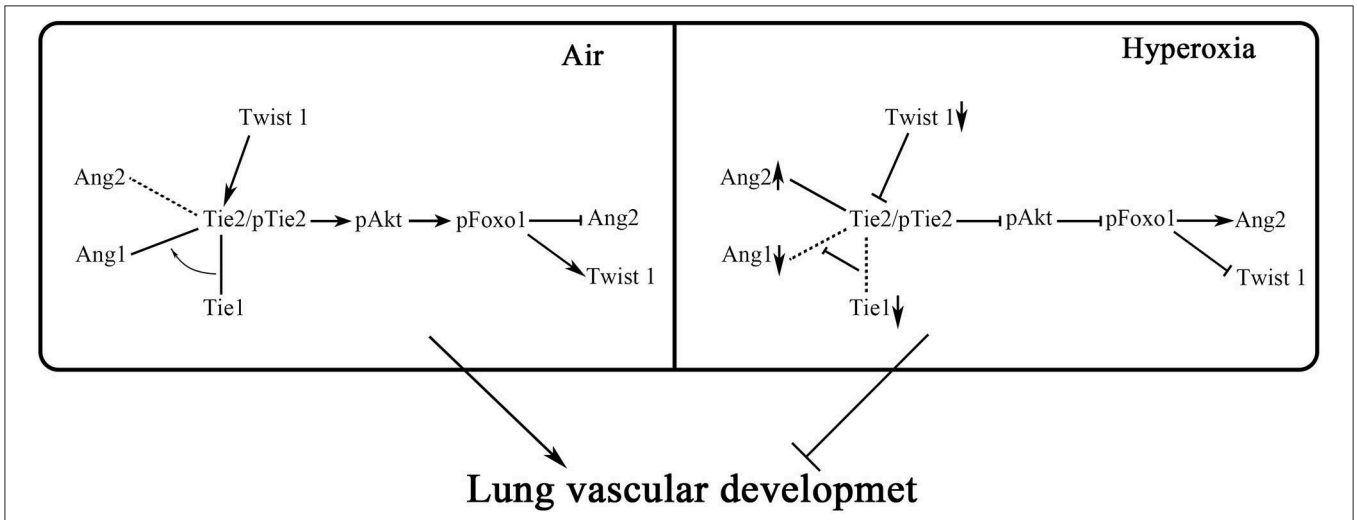

FIGURE 9 | Hypothesis diagram of the regulatory mechanism of Twist1, Tie1, Tie2, Angs, and Akt/Foxo1 in endothelial cells. Twist1-Tie2-Akt/Foxo1 pathway combined to Angs signal may play an important role in hyperoxia-induced increase of pulmonary microvascular permeability. We hypothesize that hyperoxia impaired pulmonary vascular permeability may be associated with disruption of Ang1-Tie2 signaling and decreased Akt/Foxo1 pathways that increase Ang2 production, and the Twist1 and Tie1 may be involved in the regulation of this process.

via Akt, and inhibit Foxo1 transcriptional function by promoting its nuclear rejection and preventing DNA binding (15, 17). Ang1-mediated Foxo1 transcriptional function inhibition induced the expression of target genes related to vascular stability and down-regulated the expression of Ang2 and other genes related to endothelial instability, apoptosis, metabolism, and growth control (15–18), therefore, promoting vascular permeability. It has also been found that in acute inflammatory conditions, in which Ang1 and pAkt levels reduced, decreased Tie2 signaling (including Tie1 deletion) alleviated the inhibition of Foxo1 activity, resulting in increased expression of Ang2 and vascular instability, which is a typical manifestation of vascular leakage (47, 58). In this research, our western blot result showed that at 7 and 14 d, hyperoxia significantly reduced the total protein level and phosphorylation state of Akt and Foxo1 in the lung tissue, suggesting that hyperoxia downregulated the activity of Akt/Foxo1 signaling, probably increasing Ang2 transcription. Wu et al. (59) first proposed the view that Foxo1 could directly regulate Twist1. In the study of prostate tumors (PCa), the increased expression of monoamine oxidase A (MAOA) promoted the production of epithelial-to-mesenchymal transition (EMT), hypoxia, and ROS, which jointly promoted the tumorigenesis, development, and metastasis of PCa. This process was related to MAOA increasing Twist1 expression by promoting Akt-dependent Foxo1 phosphorylation to activate Twist1 transcription. Therefore, we speculated that in this research, downregulation of Twist1 and upregulation of Ang2 in hyperoxia group might probably be related to the decreased Akt-Foxo1 signaling.

In conclusion, our research showed that in HALI, the pulmonary microvascular permeability was increased, accompanied by changes in Twist1-Tie2 pathway which combined to Angs, and downregulation of Akt/Foxo1 pathway. We could speculate that Twist1-Tie2-Akt/Foxo1 pathway combined to Angs signal might play an important role in hyperoxia-induced increase of pulmonary microvascular permeability. In this study, we hypothesized that hyperoxia impaired pulmonary vascular permeability may be associated with disruption of Ang1-Tie2 signaling and decreased Akt/Foxo1 pathways that increased Ang-2 production, and the Twist1 and Tie1 may be involved in the regulation of this process (**Figure 9**). However, this study did not involve direct evidence supporting the direct relationship between pulmonary microvascular permeability and Twist1-Tie2-Akt/Foxo1signal activity in HALI. There needs to be *in vivo* as well as *in vitro* (using pulmonary microvascular endothelial cells) Twist1 knockdown experiments conducted to further explain the mechanistic role of Twist1 pathway in lung microvascular permeability in HALI. Our experimental data just provide further experimental evidence for the important role of the Twist1 signaling pathway on microvascular permeability in hyperoxia-induced lung injury.

DATA AVAILABILITY STATEMENT

The datasets generated for this study are available on request to the corresponding author.

ETHICS STATEMENT

All animal procedures were reviewed and approved by the Laboratory Animal Ethics Committee of the Southwest Medical University and conducted according to the AAALAC and the IACUC guidelines.

AUTHOR CONTRIBUTIONS

All authors fulfill the journal's author requirements. YR conceived, designed, and performed the main experiments. YR, LK, RZ, FW, and XZ had a substantial contribution in acquisition of the main data. YR had a substantial contribution in interpretation and analysis of the data. YR, WD, and XL drafted and revised the article. All authors approved the final version before submission.

FUNDING

This research was supported by the National Natural Science Foundation of China (81571480) and the Science and Technology Department of Sichuan (2014NZ0014).

REFERENCES

1. Fanaroff AA, Hack M, Walsh MC. The NICHD neonatal research network: changes in practice and outcomes during the first 15 years. *Semin Perinatol*. (2003) 27:281–7. doi: 10.1016/S0146-0005(03)00055-7
2. Stenmark KR, Abman SH. Lung vascular development: implications for the pathogenesis of bronchopulmonary dysplasia. *Ann Rev Physiol*. (2005) 67:623–61. doi: 10.1146/annurev.physiol.67.040403.102229
3. Guo Q, Jin J, Yuan JX, Zeifman A, Chen J, Shen B, et al. VEGF, Bcl-2 and Bad regulated by angiopoietin-1 in oleic acid induced acute lung injury. *Biochem Biophys Res Commun*. (2011) 413:630–6. doi: 10.1016/j.bbrc.2011.09.015
4. Jakkula M, Le Cras TD, Gebb S, Hirth KP, Tuder RM, Voelkel NF, et al. Inhibition of angiogenesis decreases alveolarization in the developing rat lung. *Am J Physiol Lung Cell Mol Physiol*. (2000) 279:L600–7. doi: 10.1152/ajplung.2000.279.3.L600
5. Bhandari V. Hyperoxia-derived lung damage in preterm infants. *Semin Fetal Neonatal Med*. (2010) 15:223–9. doi: 10.1016/j.siny.2010.03.009
6. Angara S, Syed M, Das P, Janér C, Pryhuber G, Rahman A, et al. Inhibition of RPTOR Prevents Hyperoxia-induced Lung Injury by Enhancing Autophagy and Reducing Apoptosis in Neonatal Mice. *Am J Respir Cell Mol Biol*. (2016) 55:722–35. doi: 10.1165/rcmb.2015-0349OC
7. Perkett EA, Klekamp JG. Vascular endothelial growth factor expression is decreased in rat lung following exposure to 24 or 48 hours of hyperoxia: implications for endothelial cell survival. *Chest*. (1998) 114:52S−3S. doi: 10.1378/chest.114.1_Supplement.52S
8. Li C, Fu J, Liu H, Yang H, Yao L, You K, et al. Hyperoxia arrests pulmonary development in newborn rats via disruption of endothelial tight junctions and downregulation of Cx40. *Mol Med Rep*. (2014) 10:61–7. doi: 10.3892/mmr.2014.2192
9. Bourgeois P, Stoetzel C, Bolcato-Bellemin AL, Mattei MG, Perrin-Schmitt F. The human H-twist gene is located at 7p21 and encodes a B-HLH protein that is 96% similar to its murine M-twist counterpart, *Mamm Genome*. (1996) 7:915–7. doi: 10.1007/s003359900269

10. Pozharskaya V, Torres-Gonzalez E, Rojas M, Gal A, Amin M, Dollard S, et al. Twist: a regulator of epithelial-mesenchymal transition in lung fibrosis. *PLoS ONE*. (2009) 4:e7559. doi: 10.1371/journal.pone.0007559
11. Wang G, Dong W, Shen H, Mu X, Li Z, Lin X, et al. A comparison of Twist and E-cadherin protein expression in primary non-small-cell lung carcinoma and corresponding metastases. *Eur J Cardiothorac Surg*. (2011) 39:1028–32. doi: 10.1016/j.ejcts.2011.01.023
12. Jan YN, Jan LY. HLH proteins, fly neurogenesis, and vertebrate myogenesis. *Cell*. (1993) 75:827–30. doi: 10.1016/0092-8674(93)90525-U
13. Mammoto T, Jiang A, Jiang E, Mammoto A. Role of Twist1 Phosphorylation in Angiogenesis and Pulmonary Fibrosis. *Am J Respir Cell Mol Biol*. (2016) 55:633–44. doi: 10.1165/rcmb.2016-0012OC
14. Mammoto T, Jiang E, Jiang A, Lu Y, Juan AM, Chen J, et al. Twist1 controls lung vascular permeability and endotoxin-induced pulmonary edema by altering Tie2 expression. *PLoS ONE*. (2013) 8:e73407. doi: 10.1371/journal.pone.0073407
15. Daly C, Wong V, Burova E, Wei Y, Zabski S, Griffiths J, et al. Angiopoietin-1 modulates endothelial cell function and gene expression via the transcription factor FKHR (FOXO1). *Genes Dev*. (2004) 18:1060–71. doi: 10.1101/gad.1189704
16. Potente M, Urbich C, Sasaki, KI, Hofmann WK, Heeschen C, Aicher A, et al. Involvement of Foxo transcription factors in angiogenesis and postnatal neovascularization. *J Clin Invest*. (2005) 115:2382–92. doi: 10.1172/JCI23126
17. Wilhelm K, Happel K, Eelen G, Schoors S, Oellerich MF, Lim R, et al. FOXO1 couples metabolic activity and growth state in the vascular endothelium. *Nature*. (2016) 529:216–20. doi: 10.1038/nature16498
18. Zhang X, Gan L, Pan H, Guo S, He X, Olson ST, et al. Phosphorylation of serine 256 suppresses transactivation by FKHR (FOXO1) by multiple mechanisms. Direct and indirect effects on nuclear/cytoplasmic shuttling and DNA binding. *J Biol Chem*. (2002) 277:45276–84. doi: 10.1074/jbc.M208063200
19. Sun Y, Fu J, Xue X, Yang H, Wu L. BMP7 regulates lung fibroblast proliferation in newborn rats with bronchopulmonary dysplasia. *Mol Med Rep*. (2018) 17:6277–84. doi: 10.3892/mmr.2018.8692
20. Tschanz SA, Makanya AN, Haenni B, Burri PH. Effects of neonatal high-dose short-term glucocorticoid treatment on the lung: a morphologic and morphometric study in the rat. *Pediatr Res*. (2003) 53:72–80. doi: 10.1203/00006450-200301000-00014
21. Udaka K, Takeuchi Y, Movat HZ. Simple method for quantitation of enhanced vascular permeability. *Proc Soc Exp Biol Med*. (1970) 133:1384–7. doi: 10.3181/00379727-133-34695
22. Patterson CE, Rhoades RA, Garcia JG. Evans blue dye as a marker of albumin clearance in cultured endothelial monolayer and isolated lung. *J Appl Physiol*. (1992) 72:865–73. doi: 10.1152/jappl.1992.72.3.865
23. Mammoto T, Parikh SM, Mammoto A, Gallagher D, Chan B, Mostoslavsky G, et al. Angiopoietin-1 requires p190 RhoGAP to protect against vascular leakage *in vivo*. *J Biol Chem*. (2007) 282:23910–8. doi: 10.1074/jbc.M702169200
24. Hu S, Li J, Xu X, Liu A, He H, Xu J, et al. The hepatocyte growth factor-expressing character is required for mesenchymal stem cells to protect the lung injured by lipopolysaccharide *in vivo*. *Stem Cell Res Ther*. (2016) 7:66. doi: 10.1186/s13287-016-0320-5
25. Berger J, Bhandari V. Animal models of bronchopulmonary dysplasia. The term mouse models. *Am J Physiol Lung Cell Mol Physiol*. (2014) 307:L936–47. doi: 10.1152/ajplung.00159.2014
26. Burri PH. Fetal and postnatal development of the lung. *Ann Rev Physiol*. (1984) 46:617–28. doi: 10.1146/annurev.ph.46.030184.003153
27. Nakanishi H, Morikawa S, Kitahara S, Yoshii A, Uchiyama A, Kusuda S, et al. Morphological characterization of pulmonary microvascular disease in bronchopulmonary dysplasia caused by hyperoxia in newborn mice. *Med Mol Morphol*. (2018) 51:166–75. doi: 10.1007/s00795-018-0182-2
28. Jobe AH. Animal models, learning lessons to prevent and treat neonatal chronic lung disease. *Front Med*. (2015) 2:49. doi: 10.3389/fmed.2015.00049
29. Tachezy M, Reichelt U, Melenberg T, Gebauer F, Izbicki JR, Kaifi JT. Angiogenesis index CD105 (endoglin)/CD31 (PECAM-1) as a predictive factor for invasion and proliferation in intraductal papillary mucinous neoplasm (IPMN) of the pancreas. *Histol Histopathol*. (2010) 25:1239–46. doi: 10.14670/HH-25.1239
30. Li J, Liu CH, Sun Y, Gong Y, Fu Z, Evans LP, et al. Endothelial TWIST1 promotes pathological ocular angiogenesis. *Invest Ophthalmol Vis Sci*. (2014) 55:8267–77. doi: 10.1167/iovs.14-15623
31. Mironchik Y, Winnard PT, Vesuna F, Kato Y, Wildes F, Pathak AP, et al. Twist overexpression induces *in vivo* angiogenesis and correlates with chromosomal instability in breast cancer. *Cancer Res*. (2005) 65:10801–9. doi: 10.1158/0008-5472.CAN-05-0712
32. Sossey-Alaoui K, Pluskota E, Davuluri G, Bialkowska K, Das M, Szpak D, et al. Kindlin-3 enhances breast cancer progression and metastasis by activating Twist-mediated angiogenesis. *FASEB J*. (2014) 28:2260–71. doi: 10.1096/fj.13-244004
33. Yan Y, Lou Y, Kong J. MiR-155 expressed in bone marrow-derived lymphocytes promoted lipopolysaccharide-induced acute lung injury through Ang-2-Tie-2 pathway, *Biochem Biophys Res Commun*. (2019) 510:352–7. doi: 10.1016/j.bbrc.2019.01.079
34. Syed M, Das P, Pawar A, Aghai ZH, Kaskinen A, Zhuang ZW, et al. Hyperoxia causes miR-34a-mediated injury via angiopoietin-1 in neonatal lungs. *Nat Commun*. (2017) 8:1173. doi: 10.1038/s41467-017-01349-y
35. Davis S, Aldrich TH, Jones PF, Acheson A, Compton DL, Jain V, et al. Isolation of angiopoietin-1, a ligand for the TIE2 receptor, by secretion-trap expression cloning. *Cell*. (1996) 87:1161–9. doi: 10.1016/S0092-8674(00)81812-7
36. Visconti RP, Richardson CD, Sato TN. Orchestration of angiogenesis and arteriovenous contribution by angiopoietins and vascular endothelial growth factor (VEGF). *Proc Natl Acad Sci USA*. (2002) 99:8219–224. doi: 10.1073/pnas.122109599
37. Saharinen P, Eklund L, Miettinen J, Wirkkala R, Anisimov A, Winderlich M, et al. Angiopoietins assemble distinct Tie2 signalling complexes in endothelial cell-cell and cell-matrix contacts. *Nat Cell Biol*. (2008) 10:527–37. doi: 10.1038/ncb1715
38. Fukuhara S, Sako K, Minami T, Noda K, Kim HZ, Kodama T, et al. Differential function of Tie2 at cell-cell contacts and cell-substratum contacts regulated by angiopoietin-1. *Nat Cell Biol*. (2008) 10:513–26. doi: 10.1038/ncb1714
39. Thurston G, Rudge JS, Ioffe E, Zhou H, Ross L, Croll SD, et al. Angiopoietin-1 protects the adult vasculature against plasma leakage. *Nat Med*. (2000) 6:460–3. doi: 10.1038/74725
40. Baffert F, Le T, Thurston G, McDonald DM. Angiopoietin-1 decreases plasma leakage by reducing number and size of endothelial gaps in venules. *Am J Physiol Heart Circ Physiol*. (2006) 290:H107–18. doi: 10.1152/ajpheart.00542.2005
41. Maisonpierre PC, Suri C, Jones PF, Bartunkova S, Wiegand SJ, Radziejewski C, et al. Angiopoietin-2, a natural antagonist for Tie2 that disrupts *in vivo* angiogenesis. *Science*. (1997) 277:55–60. doi: 10.1126/science.277.5322.55
42. Fiedler U, Scharpfenecker M, Koidl S, Hegen A, Grunow V, Schmidt JM, et al. The Tie-2 ligand angiopoietin-2 is stored in and rapidly released upon stimulation from endothelial cell Weibel-Palade bodies. *Blood*. (2004) 103:4150–6. doi: 10.1182/blood-2003-10-3685
43. Scharpfenecker M, Fiedler U, Reiss Y, Augustin HG. The Tie-2 ligand angiopoietin-2 destabilizes quiescent endothelium through an internal autocrine loop mechanism. *J Cell Sci*. (2005) 118:771–80. doi: 10.1242/jcs.01653
44. Seegar TC, Eller B, Tzvetkova-Robev D, Kolev MV, Henderson SC, Nikolov DB, et al. Tie1-Tie2 interactions mediate functional differences between angiopoietin ligands. *Mol Cell*. (2010) 37:643–55. doi: 10.1016/j.molcel.2010.02.007
45. Yu X, Seegar TCM, Dalton AC, Tzvetkova-Robev D, Goldgur Y, Rajashankar KR, et al. Structural basis for angiopoietin-1-mediated signaling initiation. *Proc Natl Acad Sci USA*. (2013) 110:7205–10. doi: 10.1073/pnas.1216890110
46. Barton WA, Tzvetkova-Robev D, Miranda EP, Kolev MV, Rajashankar KR, Himanen JP, et al. Crystal structures of the Tie2 receptor ectodomain and the angiopoietin-2-Tie2 complex. *Nat Struct Mol Biol*. (2006) 13:524–32. doi: 10.1038/nsmb1101
47. Korhonen EA, Lampinen A, Giri H, Anisimov A, Kim M, Allen B, et al. Tie1 controls angiopoietin function in vascular remodeling and inflammation. *J Clin Invest*. (2016) 126:3495–510. doi: 10.1172/JCI84923
48. Saharinen P, Kerkelä K, Ekman N, Marron M, Brindle N, Lee GM, et al. Multiple angiopoietin recombinant proteins activate the Tie1 receptor

tyrosine kinase and promote its interaction with Tie2. *J Cell Biol*. (2005) 169:239–43. doi: 10.1083/jcb.200411105
49. Puri MC, Rossant J, Alitalo K, Bernstein A, Partanen J. The receptor tyrosine kinase TIE is required for integrity and survival of vascular endothelial cells. *EMBO J*. (1995) 14:5884–91. doi: 10.1002/j.1460-2075.1995.tb00276.x
50. Philip AGS. Bronchopulmonary dysplasia: then and now. *Neonatology*. (2012) 102:1–8. doi: 10.1159/000336030
51. Spilsbury A, Vauzour D, Spencer JPE, Rattray M. Regulation of NF-κB activity in astrocytes: effects of flavonoids at dietary-relevant concentrations. *Biochem Biophys Res Commun*. (2012) 418:578–83. doi: 10.1016/j.bbrc.2012.01.081
52. Frye M, Dierkes M, Küppers V, Vockel M, Tomm J, Zeuschner D, et al. Interfering with VE-PTP stabilizes endothelial junctions *in vivo* via Tie-2 in the absence of VE-cadherin. *J Exp Med*. (2015) 212:2267–87. doi: 10.1084/jem.20150718
53. David S, Ghosh CC, Mukherjee A, Parikh SM. Angiopoietin-1 requires IQ domain GTPase-activating protein 1 to activate Rac1 and promote endothelial barrier defense. *Arterioscler Thromb Vasc Biol*. (2011) 31:2643–52. doi: 10.1161/ATVBAHA.111.233189
54. Cui HJ, Yang AL, Zhou HJ, Wang C, Luo JK, Lin Y, et al. Buyang huanwu decoction promotes angiogenesis via vascular endothelial growth factor receptor-2 activation through the PI3K/Akt pathway in a mouse model of intracerebral hemorrhage. *BMC Complement Altern Med*. (2015) 15:91. doi: 10.1186/s12906-015-0605-8
55. Kim I, Kim HG, So JN, Kim JH, Kwak HJ, Koh GY. Angiopoietin-1 regulates endothelial cell survival through the phosphatidylinositol 3'-Kinase/Akt signal transduction pathway. *Circ Res*. (2000) 86:24–9. doi: 10.1161/01.RES.86.1.24
56. Hu E, Hu W, Yang A, Zhou H, Zhou J, Luo J, et al. Thrombin promotes pericyte coverage by Tie2 activation in a rat model of intracerebral hemorrhage. *Brain Res*. (2019) 1708:58–68. doi: 10.1016/j.brainres.2018.12.003
57. Zhang Y, Gan B, Liu D, Paik JH. FoxO family members in cancer. *Cancer Biol Ther*. (2011) 12:253–9. doi: 10.4161/cbt.12.4.15954
58. Kim M, Allen B, Korhonen EA, Nitschke M, Yang HW, Baluk P, et al. Opposing actions of angiopoietin-2 on Tie2 signaling and FOXO1 activation. *J Clin Invest*. (2016) 126:3511–25. doi: 10.1172/JCI84871
59. Wu JB, Shao C, Li X, Li Q, Hu P, Shi C, et al. Monoamine oxidase A mediates prostate tumorigenesis and cancer metastasis. *J Clin Invest*. (2014) 124:2891–908. doi: 10.1172/JCI70982

Conflict of Interest: The authors declare that the research was conducted in the absence of any commercial or financial relationships that could be construed as a potential conflict of interest.

frontiers in Pediatrics

ORIGINAL RESEARCH
published: 27 May 2020
doi: 10.3389/fped.2020.00271

An Innovative Model of Bronchopulmonary Dysplasia in Premature Infants

*Xiaoyue Zhang, Xiaoyun Chu, Bowen Weng, Xiaohui Gong and Cheng Cai**

Department of Neonatology, Shanghai Children's Hospital, Shanghai Jiao Tong University, Shanghai, China

Bronchopulmonary dysplasia (BPD) is one of the common chronic lung diseases (CLD) of premature infants, which causes unpredictable consequences to the family and society. Therefore, the pathogenesis and prevention methods of BPD are the focus of current research, and the establishment of an effective and appropriate animal model of BPD in premature infants is the key to the research. In this study, premature rats were exposed to hyperoxia environment. Compared with the air group, the body weight and alveolar radiation count of the hyperoxia group decreased significantly, but there was no significant difference in body length. HE staining was used to observe the pathological changes of BPD in the lung tissue. The above results proved that under the hyperoxia condition, the BPD animal model of premature infants was successfully established, which provided a new choice for the future research of BPD.

Keywords: premature, rats, hyperoxia, animal model, bronchopulmonary dysplasia

OPEN ACCESS

Edited by:
Yuan Shi,
Children's Hospital of Chongqing Medical University, China

Reviewed by:
Xiaoguang Zhou,
Nanjing Children's Hospital, China
Ruben Alvaro,
University of Manitoba, Canada

****Correspondence:***
Cheng Cai
caicheng2004@163.com

Specialty section:
This article was submitted to Neonatology, a section of the journal Frontiers in Pediatrics

Received: *06 March 2020*
Accepted: *29 April 2020*
Published: *27 May 2020*

Citation:
Zhang X, Chu X, Weng B, Gong X and Cai C (2020) An Innovative Model of Bronchopulmonary Dysplasia in Premature Infants. Front. Pediatr. 8:271. doi: 10.3389/fped.2020.00271

INTRODUCTION

In recent years, the birth rate of premature infants, especially very low birth weight infants (VLBWI) and extremely low birth weight infants (ELBWI), has increased year by year, which is estimated to account for 11% of all births (1). Bronchopulmonary dysplasia (BPD) is one of the serious diseases that bring long-term adverse prognosis to premature infants. At present, the treatment of BPD is mainly in accordance with the symptoms. Therefore, it is very important to study the pathogenesis, effective prevention, and treatment methods of BPD. The classic pathological features of BPD are severe airway epithelial lesions, extensive metaplasia, and hyperplasia of airway mucous epithelium, extensive alveolar septal fibrosis, and pulmonary vascular remodeling (2), while the *new BPD* emphasizes the simplification of alveolar structure, pulmonary vascular malformation, and interstitial cells and / or fibrous hyperplasia (3). In the study of BPD, the establishment of animal models is essential. The more commonly used animal models are mice, rats, rabbits, sheep, and baboons (4–8). At present, most people think that oxidative stress of lung tissue caused by hyperoxia exposure is an important reason for the occurrence and development of BPD (9), and preterm is an important risk factor for the occurrence of BPD (10). Thanks to BPD brings many harmful effects to family and society, it is the main work to seek effective prevention and treatment strategies, and the establishment of an effective animal model is the basis of the study of BPD. Therefore, this study proposes that the animal model of BPD in premature rats can be established successfully when they are exposed to high concentration of oxygen, in order to provide a new theoretical model for further study on the prevention and treatment of BPD.

MATERIALS AND METHODS

Ethics Approval

The use and care of laboratory rodents was performed according to the Animal Laboratory Center of Pediatrics, Children's Hospital of Fudan University and approved by the Committee of Animal Laboratory Management and Ethics, Shanghai Children's Hospital.

Experimental Animals

250–300 g healthy adult Specific pathogen Free (SPF) grade Sprague-Dawley (SD) rats, 25 females and five males, provided by Shanghai Sipur-Bikai experimental animal Co., Ltd., animal license No. SCXK (Shanghai) 2018-0006.

Cage Closing and Conception of Rats

Male and female SD rats were fed in metabolic cages at 1:5. The mat and excrement of the cage were checked at 6 a.m. every day. Check the vaginal plug of females, and the day that vaginal plug was checked as the day 0 of pregnancy.

Cesarean Section and Milk Substitute of Premature Rats

On the 21st day of gestation, pregnant SD rats were subjected to cesarean sections. The anesthetics (pentobarbital sodium 10 mg diluted in normal saline 20 ml) were intramuscularly injected at the dose of 30–50 mg/kg. The induced anesthetics were given at 30 mg/kg.

The abdomen was sectioned, and the uterus were pulled out gently after anesthesia. The operator pulled out the uterus gently, and took out the fetal rats quickly. Continue to press the chest of premature rats (60–100 times/min) and give 100% oxygen for 30 min by the operator. The premature rats were fed with the breast milk by the mother rats which delivered naturally (**Figures 1A-C**).

FIGURE 1 | (A-C) The premature rats were placed in forage and resuscitated with 100% oxygen by operator.

TABLE 1 | Comparison of weight between two groups at different time (*g*).

Groups	*n*	1d	4d	7d	10d	14d	*F*	*p*
Air group	8	6.85 ± 0.65	12.18 ± 1.80	22.27 ± 1.05	26.09 ± 4.60	37.40 ± 8.25	99.914	<0.001
Hyperoxia	8	7.00 ± 0.79	11.39 ± 0.96	16.00 ± 0.83	19.96 ± 1.03	30.12 ± 3.53	338.388	<0.001
t		−0.422	1.909	15.247	3.894	2.335		
p		0.679	0.063	<0.001	0.004	0.044		

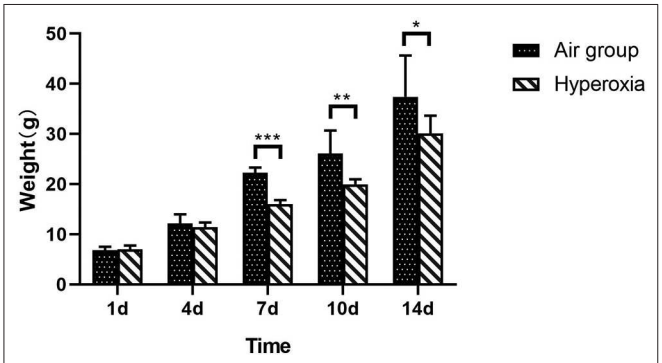

FIGURE 2 | Comparison of weight between two groups at different time. Compare with the air group, weight of premature rats in hyperoxia group at 1d, and the weight of the rats in the hyperoxia group increased slowly at the 7, 10, and 14d, which was statistically significant (*$p < 0.05$, **$p < 0.01$, ***$p < 0.001$).

Premature Rats Exposed to Hyperoxia

Eighty preterm rats were randomly divided into two groups 24 h after birth: the air group and the hyperoxia group. The air group was exposed to room air, and the hyperoxia group was exposed to oxygen concentration with 80 ± 5%. At 1, 4, 7, 10, and 14 days after hyperoxia exposure, the lungs of preterm rats were embedded in paraffin and made into 5 μm sections for HE staining.

General and Pathological Observation of Lung Tissue

All analyses were performed by the same author. The color of the lung surface was observed by naked eyes, and the morphology of the histology slides were analyzed by Hematoxylin-Eosin (HE) staining.

Morphology of Lung Tissue

Morphological changes of lung tissue structure at different time points: the basic morphology of lung tissue, alveolar septal thickness, degree of alveolalization, inflammatory cell infiltration were observed under microscope.

Radial alveolar count (RAC): a vertical line was drawn from the center of respiratory bronchioles to the nearest pleura or fibrous septum. The number of alveoli on this line is called the RAC. One section was randomly selected from each preterm rat and observed under microscope (X 100). Five visual fields were randomly selected from each section to calculate the average number, reflecting the number of alveoli in the end respiratory unit.

Statistical Analysis

The experimental data were analyzed by spss20.0 statistical software. The data were expressed by x ± s. The results of each time point in the two groups were tested by oneway ANOVO, and the results of air group and hyperoxia group were tested by two independent samples *T*-test. $p < 0.05$ was statistically significant.

RESULT

General Condition of Premature SD Rats

Fifteen SD female rats were successfully pregnant, and 116 premature rats were produced during the operation. Twelve premature rats died due to various reasons such as hemorrhage, poor resuscitation, and rescue effect, feeding difficulties in 24 h after the operation, trampled by adult rats, and so on. Finally, 80 premature rats were divided into two groups: the air group and the hyperoxia group. There was no death in the air group, three premature rats died in the hyperoxia group on the 4th day. Each group was divided into five subgroups, the 1, 4, 7, 10, and 14-days. Each subunit contained eight rats.

There was no significant difference in weight between air group and hyperoxia group at 1d ($p = 0.679$). In the air group, the rats had good response, rapid weight growth, and normal growth and development. In the hyperoxia group, the rats began to show poor response, decreased autonomous activity, increased respiratory rate, cyanosis of mouth, nose, and limbs, and other dyspnea symptoms gradually increased in the 4d. At 10d, the rats in the hyperoxia group appeared whole body twitch and head tremor without oxygen, and recovered to normal after oxygen supplied. Compared with the air group, the weight of the rats in the hyperoxia group increased slowly at 7, 10, 14 days, the difference was statistically significant ($p < 0.05$) (**Table 1** and **Figure 2**). At the same time, the color of hair was poor and the time of opening eyes was prolonged. There was no significant difference between the air group and the hyperoxia group in length ($p > 0.05$) (**Table 2** and **Figure 3**).

Histopathology of Lung Tissue in Two Groups of Preterm Rats

Generally speaking, the lung tissue of the two groups was mainly composed of pulmonary interstitium at 1d, the respiratory and circulatory vascular system was immature, the respiratory bronchioles, and their alveoli were less, the lung parenchyma gradually increased and the interstitial decreased at the 4d,

TABLE 2 | Comparison of length between two groups at different time (mm).

Groups	*n*	1d	4d	7d	10d	14d	*F*	*p*
Air group	8	49.40 ± 2.07	60.00 ± 1.41	69.47 ± 5.08	74.67 ± 6.30	86.62 ± 7.53	84.363	<0.001
Hyperoxia	8	50.60 ± 1.35	59.77 ± 1.36	68.47 ± 1.77	74.53 ± 1.06	86.00 ± 2.71	684.800	<0.001
t		−1.538	0.415	0.721	0.081	0.245		
p		0.154	0.682	0.481	0.936	0.809		

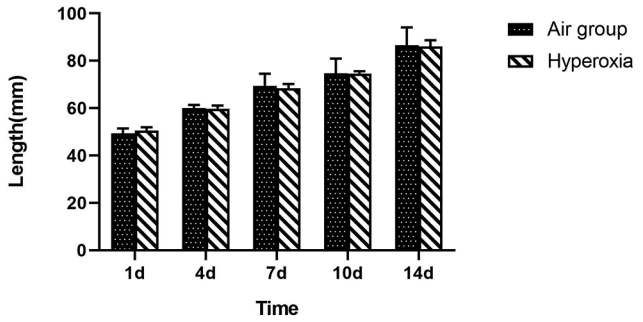

FIGURE 3 | Comparison of length between two groups at different time. Compare with the air group, there was no difference in length of the premature rats in the hyperoxia group, shows that the premature rats exposed to hyperoxia did not affect the development of length.

the number of alveoli gradually increased, and the pulmonary bronchi and vascular system at all levels were refined and increased. In the air group, the structure and morphology of alveoli were clear and regular, the alveoli were well-developed, the size of alveoli was uniform, the walls of alveoli were smooth, the alveoli space was thin, no inflammation or exudate was found in the alveoli. Under the light microscope, the alveoli in the hyperoxia group lost normal regular shape and disordered structure, the alveoli became thinner and enlarged, the number of alveoli decreased, especially at 10 and 14d (**Figure 4**).

RAC of Lung Tissue in Two Groups of Preterm Rats

At each time point, the RAC of hyperoxia group was significantly lower than that of air group ($p < 0.05$), and the RAC of air group gradually increase, while the hyperoxia group gradually decreased (**Table 3** and **Figure 5**).

DISCUSSION

In recent years, with the improvement of treatment for premature infants, the survival rate of premature infants, especially very low birth weight infants (VLBWI) and extremely low birth weight infants (ELBWI) has increased significantly (11), and the incidence rate of bronchopulmonary dysplasia has increased (12). BPD is a kind of chronic lung disease (CLD) that causes the poor long-term prognosis in premature infants. Because the children with BPD need longer hospitalization and long-term oxygen therapy, it has many adverse effects on family and society, it is important to research the etiology, pathophysiology, and the corresponding prevention and treatment measures of BPD. To establish an effective and reliable animal model of BPD is the first problem to be solved by researchers. The main inducing factors of BPD animal model are hyperoxia, mechanical ventilation injury, intrauterine inflammation, postnatal continuous hypoxia, and intrauterine hypoxia (13). At present, it is considered that oxidative stress is one of the main risk factors for BPD, and its pathogenesis is the interruption of lung development through the mechanism of interrupting growth factor signal transduction, cell proliferation, apoptosis, and angiogenesis (14). In 2014, Yang et al. observed that the development of alveoli in lung tissue was weakened, and isolated alveolar epithelial cells (AT2 cells) showed epithelial mesenchymal transition (EMT) in newborn rats by hyperoxia exposed for 21 h after birth (15). Therefore, up to now, the animal model of BPD induced by hyperoxia is still the most commonly used.

The development of lung in human usually goes through five stages, including embryonic stage, pseudoglandular stage, tubule stage, vesicle stage, and alveolar stage (16). The relevant time point of lung development is located in the vesicular phase, usually between the 24 and 38th weeks of pregnancy (corresponding to d0, d4) (17). In the alveolar type II epithelial cells of the full-term rats, the existence of pulmonary surfactant indicates that the lung tissue of the full-term rats is functionally mature (18). The development of lung in premature rats (gestational age 21 days) is in the initial stage of the vesicle, which is closer to the stage of BPD in premature infants. At present, BPD animal models are mainly come from hyperoxia induced animal models, which rodents are the most widely used. As early as 1932, some researchers place newborn rats in an environment having an 83.6% oxygen concentration. A month later, there are thickening and hyalinization of the walls with ultimate thrombosis of many in the lung tissue of rats (19). In the next 100 years, many studies established the animal model of BPD by exposing newborn rats to high concentration of oxygen. In 1978, Yam et al. detected the increase of superoxide dismutase (SOD), glutathione peroxidase (GP), glutathione reductase (GR), and glutathione (GSH) in newborn rats increased by exposing to hyperoxia, which proved that the above substances increased the tolerance of lung tissue to hyperoxia injury, and successfully established a BPD animal model of newborn rats with hyperoxia (20). Recent studies have shown that newborn rats are exposed to different concentrations of oxygen (60, 80, and 100%, respectively), and the probability of BPD is not the same. When FiO_2 is <60%, the probability of BPD is low (21). In this study, the premature SD rats were

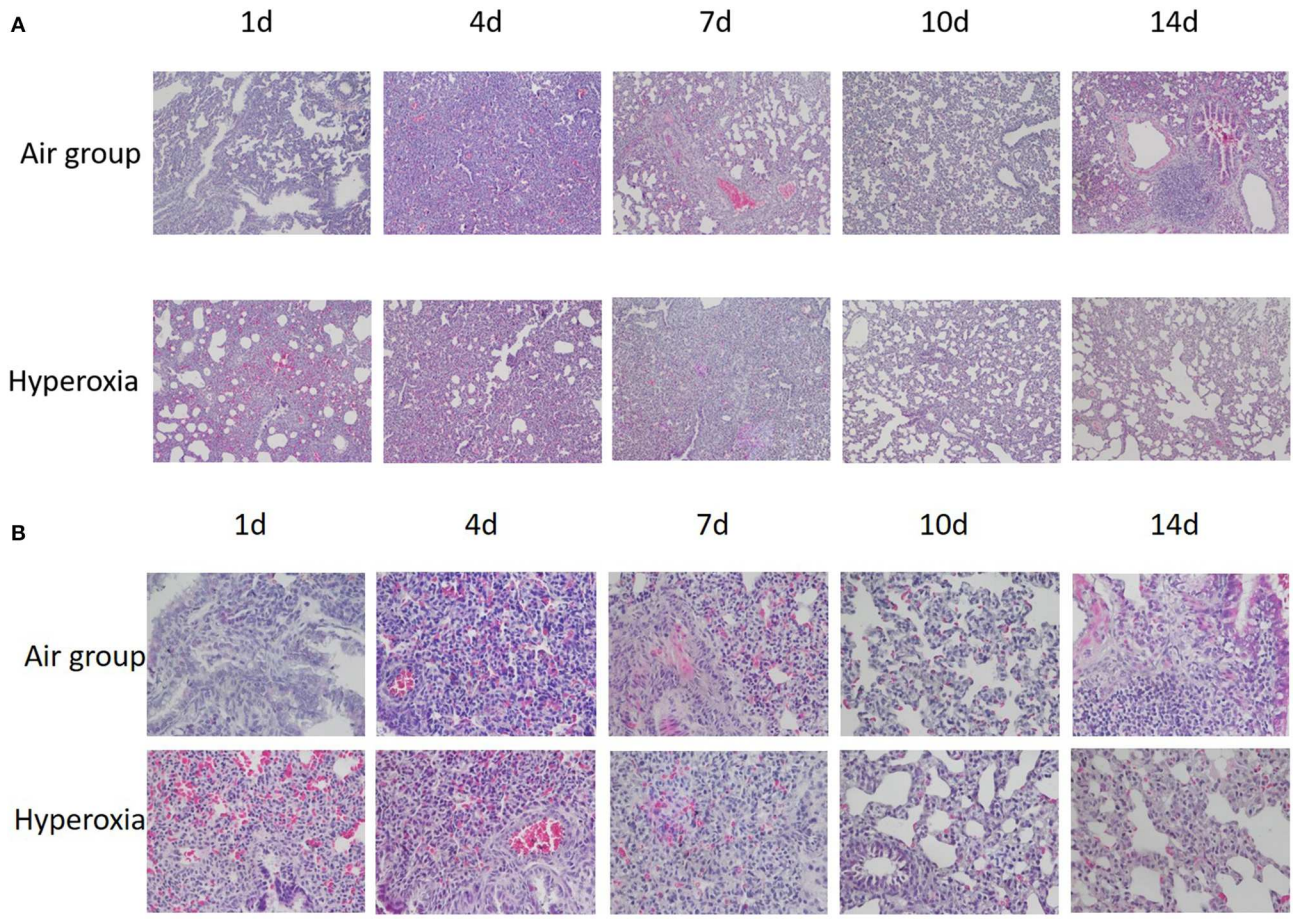

FIGURE 4 | (A) HE staining of lung tissue at different time in two groups (×100). **(B)** HE staining of lung tissue at different time in two groups (×400). When HE stained lung tissue was placed under 100 and 400 times light microscope, it can be seen that compared with the air group, the alveoli in the hyperoxia group lost their normal regular shape and structure disorder, the alveoli space became thinner, the alveoli cavity increased, and the number of alveoli decreased, especially at 10 and 14d.

TABLE 3 | RAC of lung tissue in two groups at different time points.

Groups	*n*	1d	4d	7d	10d	14d	*F*	*p*
Air group	8	2.90 ± 0.30	5.09 ± 0.32	7.18 ± 0.18	8.03 ± 0.31	9.09 ± 0.13	720.663	<0.001
Hyperoxia	8	2.44 ± 0.56	3.14 ± 0.23	5.25 ± 0.38	4.41 ± 0.44	3.41 ± 0.13	63.987	<0.001
t		2.083	11.989	13.069	18.961	87.910		
p		0.056	<0.001	<0.001	<0.001	<0.001		

used as the experimental objects to make the animal model of BPD by exposing to hyperoxia, which has the advantages of easy access to rodents, relatively short pregnancy cycle and convenient management. At present, most of the known experimental animal models of BPD are full-term animal models, and a few are preterm animal models (22). The smaller the gestational age, the higher the severity of BPD, suggesting that premature is another important risk factor for BPD (23). The development of lung in the 21-days pregnant SD rats was in the period of vesicle during delivery, similar to that of the premature infants (24). A number of studies at home and abroad have proved that hyperoxia exposure causes the structural abnormality of pulmonary microvasculature in rats, which is similar to the pathological changes of lung tissue in premature infants with BPD (25). In 1998, the premature rats delivered by cesarean section on the 21st day of pregnancy were exposed to high concentration of oxygen. By comparing the production of pulmonary surfactant, it was confirmed that premature exposure to more than 95% of oxygen for 7–14 days, the clinical morphological characteristics of lung in preterm rats was similar to that of human premature infants (26). Similarly, Zhu et al. proposed that hyperoxia induce lung injury in preterm

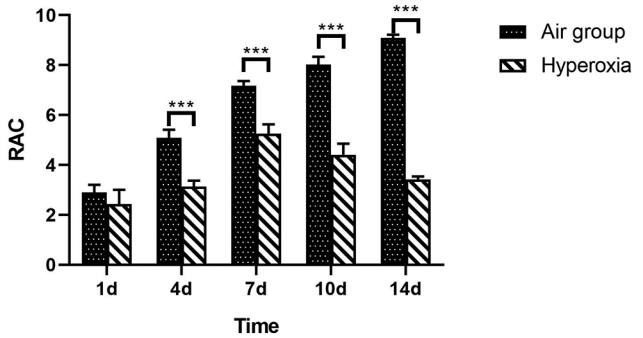

FIGURE 5 | RAC of lung tissue in two groups at different time points. From the center of respiratory bronchioles to the nearest pleura or fibrous septum, a vertical line is drawn. The number of alveoli on this line is the RAC, which reflects the development of alveoli. Compare with the air group, the RAC of hyperoxia group was significantly lower than that of the air group ($p < 0.05$). The RAC of the air group increased while the hyperoxia group decreased gradually after 7 days. ***$p < 0.001$.

rats, in order to explore the dynamic expression and role of SUMO modified C/EBP α in BPD (27). In this experiment, premature SD rats were used as the experimental objects. The rats in hyperoxia group were exposed to high concentration oxygen at 0, 4, 7, 10, 14d, respectively. The experimental results showed that the animal model was established successfully by comparing the weight, length, pathological changes of lung tissue, and RAC count of premature rats, the results have continuity in time as well. Postnatal growth restriction (PTGR) and hyperoxia can reduce the VEGF signal conduction in the lung, and cause abnormal pulmonary vascular and alveolar development in premature and rodent models, resulting in bronchopulmonary dysplasia, and pulmonary hypertension (28). Some studies have confirmed that malnutrition in the early postnatal period will increase the risk of BPD in premature infants (29), so the impact of PTGR on the lungs cannot be ignored.

In this study, compare with the air group, the premature rats in hyperoxia group showed poor response, decreased activity, and dyspnea with the increase of exposure to hyperoxia, and the weight growth was slow from the 7d, the difference was statistically significant ($p < 0.05$), However, there was no significant difference between the two groups in length ($p > 0.05$). Histopathology of lung tissue showed that the alveoli in hyperoxia group lost normal regular shape and structure disorder, the alveoli became thinner and the alveoli cavity enlarged, the number of alveoli decreased, especially on the 10d and 14td, and the RAC was significantly lower than that in air group ($p < 0.05$), these changes are consistent with the pathological changes of BPD in preterm infants (30), indicating that we has successfully established an animal model of hyperoxia exposure to BPD.

The animal model of BPD provides an important basis for the study of the possible mechanism and prevention and control strategy of the disease. However, due to the diversity of the etiology of BPD, there are many ways to establish the animal model of BPD. It is still necessary to further study to find a simpler and more similar with premature infants in BPD. But no matter which animal model is used, it needs to combine the clinical significance to make the experimental data better to reduce the disease.

DATA AVAILABILITY STATEMENT

The data sets used and/or analyzed during the current study are available from the corresponding author on reasonable request.

ETHICS STATEMENT

The animal study was reviewed and approved by Committee of Animal Laboratory Management and Ethics, Shanghai Children's Hospital.

AUTHOR CONTRIBUTIONS

XZ, CC, and XG made substantial contributions to the conception and design, acquisition of data, or analysis, and interpretation of data. XZ and CC were involved in drafting the manuscript or revising it critically for important intellectual content. CC, XG, BW, and XC revised the manuscript and gave final approval of the version to be published. The authors agree to be accountable of the version to be published. The authors agree to be accountable for all aspects of the work in ensuring that questions related to the accuracy or integrity of any part of the work are appropriately investigated and resolved. All authors read and approved the final manuscript.

FUNDING

This work was supported by the National Natural Science Foundation of China (81571467). This study was supported by Key Developing Subject Program from Shanghai Municipal Commission of Health and Family Planning (No. 2016ZB0102).

REFERENCES

1. Harrison MS, Goldenberg RL. Global burden of prematurity. *Semin Fetal Neonatal Med.* (2016) 21:74–9. doi: 10.1016/j.siny.2015.12.007
2. Northway WH Jr, Rosan RC Porter DY. Pulmonary disease following respirator therapy of hyaline-membrane disease. Bronchopulmonary dysplasia. *N Engl J Med.* (1967) 276:357–68. doi: 10.1056/NEJM196702162760701
3. Coalson JJ. Pathology of bronchopulmonary dysplasia. *Semin Perinatol.* (2006) 30:179–84. doi: 10.1053/j.semperi.2006.05.004
4. Shrestha AK, Gopal VYN, Menon RT, Hagan JL, Huang S, Shivanna B. Lung omics signatures in a bronchopulmonary dysplasia and pulmonary hypertension-like murine model. *Am J Physiol Lung Cell Mol Physiol.* (2018) 315:L734–41. doi: 10.1152/ajplung.00183.2018
5. O'Reilly M, Thébaud B. Animal models of bronchopulmonary dysplasia. The term rat models. *Am J Physiol Lung Cell Mol Physiol.* (2014) 307:L948–58. doi: 10.1152/ajplung.00160.2014

6. Salaets T, Gie A, Tack B, Deprest J, Toelen J. Modelling bronchopulmonary dysplasia in animals: arguments for the preterm rabbit model. *Curr Pharm Des.* (2017) 23:5887–901. doi: 10.2174/1381612823666170926123550
7. Albertine KH. Utility of large-animal models of BPD: chronically ventilated preterm lambs. *Am J Physiol Lung Cell Mol Physiol.* (2015) 308:L983–L1001. doi: 10.1152/ajplung.00178.2014
8. Yoder BA, Coalson JJ. Animal models of bronchopulmonary dysplasia. The preterm baboon models. *Am J Physiol Lung Cell Mol Physiol.* (2014) 307:L970–7. doi: 10.1152/ajplung.00171.2014
9. You K, Parikh P, Khandalavala K, Wicher SA, Manlove L, Yang B, et al.. Moderate hyperoxia induces senescence in developing human lung fibroblasts. *Am J Physiol Lung Cell Mol Physiol.* (2019) 317:L525–36. doi: 10.1152/ajplung.00067.2019
10. Tracy MK, Berkelhamer SK. Bronchopulmonary dysplasia and pulmonary outcomes of prematurity. *Pediatr Ann.* (2019) 48:e148–53. doi: 10.3928/19382359-20190325-03
11. Yan J-M, Huang H, Li Q-Q, Deng X-Y. A single-center study on the incidence and mortality of preterm infants from 2006 to 2016. *Clin Res.* (2018) 20:368–72. doi: 10.7499/j.issn.1008-8830.2018.05.006
12. Rutkowska M, Hozejowski R, Helwich E, Borszewska-Kornacka MK, Gadzinowski J. Severe bronchopulmonary dysplasia - incidence and predictive factors in a prospective, multicenter study in very preterm infants with respiratory distress syndrome. *J Matern Fetal Neonatal Med.* (2019) 32:1958–64. doi: 10.1080/14767058.2017.1422711
13. Xiong Z, Zhou X, Yue SJ. Methods for establishing animal model of bronchoplmonary dysplasia and their evaluation. *Zhongguo Dang Dai Er Ke Za Zhi.* (2017) 19:121–5. doi: 10.7499/j.issn.1008-8830.2017.01.020
14. Kalikkot Thekkeveedu R, Guaman MC Shivanna B. Bronchopulmonary dysplasia: a review of pathogenesis and pathophysiology. *Respir Med.* (2017) 132:170–7. doi: 10.1016/j.rmed.2017.10.014
15. Yang H, Fu J, Xue X, Yao L, Qiao L, Hou A, et al. Epithelial-mesenchymal transitions in bronchopulmonary dysplasia of newborn rats. *Pediatr Pulmonol.* (2014) 49:1112–23. doi: 10.1002/ppul.22969
16. Mullassery D, Smith NP. Lung development. *Semin Pediatr Surg.* (2015) 24:152–5. doi: 10.1053/j.sempedsurg.2015.01.011
17. Endesfelder S, Strauß E, Scheuer T, Schmitz T, Bührer C. Antioxidative effects of caffeine in a hyperoxia-based rat model of bronchopulmonary dysplasia. *Respir Res.* (2019) 20:88. doi: 10.1186/s12931-019-1063-5
18. Schmiedl A, Vieten G, Mühlfeld C, Bernhard W. Distribution of intracellular and secreted surfactant during postnatal rat lung development. *Pediatr Pulmonol.* (2007) 42:548–62. doi: 10.1002/ppul.20623
19. Smith FJ, Bennett GA, Heim JW, Thomson RM, Drinker CK. Morphological changes in the lungs of rats living under compressed air conditions. *J Exp Med.* (1932) 56:79–89. doi: 10.1084/jem.56.1.79
20. Yam J, Frank L Roberts RJ. Oxygen toxicity: comparison of lung biochemical responses in neonatal and adult rats. *Pediatr Res.* (1978) 12:115–9. doi: 10.1203/00006450-197802000-00010
21. Greco F, Wiegert S, Baumann P, Wellmann S, Pellegrini G, Cannizzaro V. Hyperoxia-induced lung structure-function relation, vessel rarefaction, and cardiac hypertrophy in an infant rat model. *J Transl Med.* (2019) 17:91. doi: 10.1186/s12967-019-1843-1
22. Hillman NH, Moss TJ, Nitsos I, Jobe AH. Moderate tidal volumes and oxygen exposure during initiation of ventilation in preterm fetal sheep. *Pediatr Res.* (2012) 72:593–9. doi: 10.1038/pr.2012.135
23. Li Y, Wei QF, Pan XN, Meng DH, Wei W, Wu QP. Influencing factors for severity of bronchopulmonary dysplasia in preterm infants. *Zhongguo Dang Dai Er Ke Za Zhi.* (2014) 16:1014-8. doi: 10.7499/j.issn.1008-8830.2014.10.011
24. Chinoy MR. Lung growth and development. *Front Biosci.* (2003) 8:d392–415. doi: 10.2741/974
25. Nakanishi H, Morikawa S, Kitahara S, Yoshii A, Uchiyama A, Kusuda S, et al. Morphological characterization of pulmonary microvascular disease in bronchopulmonary dysplasia caused by hyperoxia in newborn mice. *Med Mol Morphol.* (2018) 51:166–75. doi: 10.1007/s00795-018-0182-2
26. Xu F, Fok TF, Yin J. Hyperoxia-induced lung injury in premature rat: description of a suitable model for the study of lung diseases in newborns. *Chin Med J.* (1998) 111:619–24.
27. Zhu Y, Lu HY, Hao XB, et al. Dynamic Expression and Role of SUMO-modified C/EBPα In Preterm Rats With Bronchopulmonary Dysplasisa Induced by Hyperoxia Exposure. *Zhongguo Dang Dai Er Ke Za Zhi.* (2018). 20:403–9. doi: 10.7499/j.issn.1008-8830.2018.05.013
28. Wedgwood S, Warford C, Agvateesiri SC, Thai P, Berkelhamer SK, Perez M, et al. Postnatal growth restriction augments oxygen-induced pulmonary hypertension in a neonatal rat model of bronchopulmonary dysplasia. *Pediatr Res.* (2016) 80:894–902. doi: 10.1038/pr.2016.164
29. Ehrenkranz RA, Dusick AM, Vohr BR, Wright LL, Wrage LA, Poole WK. Growth in the neonatal intensive care unit influences neurodevelopmental and growth outcomes of extremely low birth weight infants. *Pediatrics.* (2006) 117:1253–61. doi: 10.1542/peds.2005-1368
30. Hwang JS, Rehan VK. Recent advances in bronchopulmonary dysplasia: pathophysiology, prevention, and treatment. *Lung.* (2018) 196:129–38. doi: 10.1007/s00408-018-0084-z

Conflict of Interest: The authors declare that the research was conducted in the absence of any commercial or financial relationships that could be construed as a potential conflict of interest.

frontiers in Pediatrics

HYPOTHESIS AND THEORY
published: 09 June 2020
doi: 10.3389/fped.2020.00296

To Individualize the Management Care of High-Risk Infants With Oral Feeding Challenges: What Do We Know? What Can We Do?

*Chantal Lau**

Department of Pediatrics, Baylor College of Medicine, Houston, TX, United States

The increase in preterm infants' survival over the last 30 years has shed light over their inability to feed by mouth safely and efficiently. With adverse events such as increased risks for oxygen desaturation, bradycardia, penetration/aspiration, infants' hospitalization in neonatal intensive care units (NICUs) are understandably prolonged. Unfortunately, this leads to delayed mother-infant reunion, maternal stress, breastfeeding obstacles, and increased medical costs. Such impediments have stimulated clinicians and researchers to better understand the underlying causes and develop evidence-based solutions to assist these infants. However, it is notable that the research-to-practice translation of this knowledge has been limited as there are still no validated guidelines or protocols as how to best diagnose and care for these infants. This report revisits the immature physiologic functions at the root of these infants' oral feeding difficulties, the current practices, and the recent availability of evidence-based efficacious tools and interventions. Taking advantage of the latter, it presents a renewed perspective of how management strategies can be tailored to the specific needs of individual patients.

Keywords: evidence-based practice, feeding monitors, feeding tools, feeding guidelines, research-to-practice translation, feeding efficiency and safety, prematurity and low birth weight

OPEN ACCESS

Edited by:
Fook-Choe Cheah, National University of Malaysia, Malaysia

Reviewed by:
Marion Aw, National University of Singapore, Singapore
Qianshen Zhang, University of Hong Kong, China
Erin Ross, University of Colorado Boulder, United States

***Correspondence:**
Chantal Lau
clau@bcm.edu

Specialty section:
This article was submitted to Neonatology, a section of the journal Frontiers in Pediatrics

Received: *14 March 2020*
Accepted: *11 May 2020*
Published: *09 June 2020*

Citation:
Lau C (2020) To Individualize the Management Care of High-Risk Infants With Oral Feeding Challenges: What Do We Know? What Can We Do? Front. Pediatr. 8:296. doi: 10.3389/fped.2020.00296

INTRODUCTION

Oral feeding difficulties in children is a *subtle* condition that is not a well-recognized public concern. It has been reported that 20–50% of healthy developing children encounter such complications (1, 2). This incidence can rise to 80% for children with developmental disabilities and complex medical conditions, such as prematurity, cerebral palsy (https://.asha.org/PRPSpecificTopic.aspx?folderid=8589934965&section=Incidence_and_Prevalence). In a recent study of moderate preterm infants [$29^{0/7}$-$33^{6/7}$ weeks gestational age (GA)] from 18 sites within the NICHD Neonatal Research Network, "inadequate oral feeding" was the most prevalent barrier to hospital discharge. Of the 56% (3,376/6,017) of infants who remained hospitalized until 36 weeks postmenstrual age (PMA), 37% (1,262 infants) were clinically stable "feeders and growers" whose only delayed discharge was due to inadequate oral feeding performance (3).

In neonatal intensive care units (NICUs), as the survival of infants born prematurely increased, it has come to light that for many of them, attainment of independent oral feeding is a struggle leading to prolonged hospitalization, while increasing maternal stress and medical cost (3–5). Such condition is often followed by re-hospitalization or visits to feeding disorder clinics as our current knowledge-based practice for the care of these infants has not kept up with their increased survival (5–8). This is reflected by the lack of validated and structured oral feeding guidelines at how to best manage these issues and the large variations in practices between hospitals (3, 9–11). As attainment of independent oral feeding is one of the three criteria infants need to meet prior to home discharge (5), the faster they can wean from tube feeding safely and efficiently, the sooner they can be reunited with their mothers. Such accomplishment is based on their ability to complete all their feedings (breast or bottle) with no adverse events, e.g., oxygen desaturation, bradycardia, within an allotted period of time, e.g., 20–30 min to avoid excessive energy expenditure, while demonstrating appropriate weight gain, e.g., ∼15 g/kg/day.

The purpose of this report is to present a review of the current practices and the efficacious research tools/interventions developed over the last two decades shown to shorten time to safe and efficient attainment of infant independent oral feeding. In combining this research knowledge with current clinical practices, a novel feeding management plan/guidelines catered specifically to the care of *individual* infants in NICUs is presented.

WHAT DO WE KNOW?

Immature Physiologic Functions Are at the Root of Preterm Infants' Oral Feeding Difficulties

Generally, in clinical practice, the evaluation of a particular patient's condition(s) begins by conducting a *differential diagnosis* based on the systematic review of possible causes before his/her management plan is developed. However, it was not until the survival of preterm infants in NICUs increased that healthcare providers' concern over infant oral feeding difficulties came to light. As such there was a limited understanding of the neuro-physiologic and -motor components implicated in their ability to feed by mouth. This led to an increased interest in understanding the maturation of their oral feeding skills and in the development of tools and therapies to assist these young patients more readily wean from tube feeding. It is following the development of the oro-motor kinetic monitoring (OMK) technology that our laboratory began to understand the complex involvement of the different neuro-motor and -physiologic functions required for these infants to feed safely and efficiently (12–16).

At present, for infants with oral feeding challenges, the focus has been primarily on infants' ability to suck, swallow, and breathe. However, amiss in this rationale is the role of the esophageal function (17, 18). Indeed, the transport of a bolus from the mouth to the stomach involves two elements that independently ensure efficiency and safety. Efficiency relates to the proper coordination of the phases of the Swallow Process; namely, the formation of the bolus during the oral phase, its swift transport through the pharynx during the pharyngeal phase, and through the esophagus during the esophageal phase (19). Safety in swallowing, for infants as well as adults, relates to the proper timing of respiratory inhalation/exhalation during the pharyngeal phase of swallowing to prevent O_2 desaturation and/or liquid aspiration/penetration into the lungs during inhalation (20, 21). The difficulty in diagnosing the origin(s) of oral feeding difficulties results from the fact that uncoordinated or improper execution at any phase of the Swallow Process can lead to the same *visual* adverse responses shown in **Figure 1**, e.g., drooling, poor lip seal, oxygen desaturation, pulling away, and feeding aversion. Consequently, based on the commonality of behaviors demonstrated by infants during oral feeding and the lack of appropriate tools to properly monitor the functionality of each phase of the Swallow Process and respiration, it is difficult for caregivers, as observers, to identify the cause(s) responsible for the onset of such events. It is for this reason that the current knowledge-based management plans devised by feeding therapists for bottle- and breast-feeders, i.e., occupational therapists, speech language pathologists, lactation consultants, raise concerns among their multi-disciplinary team members whose viewpoints understandably are influenced by their respective professional training and expertise. Additionally, consensus for best practice is often challenged by the use of qualitative/descriptive over quantitative/objective approaches. This is particularly germane when any resulting benefit may simply be due to infants' normal maturation (22). Other significant factors also impact preterm infants' oral feeding performance. Their abrupt transition from an *in-utero* to *ex-utero* environment forces them to adapt to conditions that they are not developmentally prepared for, e.g., bright lights, loud sounds, varying temperatures, unsupported forced postures (10). As basic physiologic/behavioral/organizational functions, e.g., sleep/awake, calm/agitated, mature at different times, studies have shown that exposure to such variety of NICU stressors has been correlated with changes in infant brain structures and functions (23, 24). In brief, the multitude of maturational and environmental factors that lead preterm infants to exhibit similar adverse events during oral feeding makes it is difficult to identify the culprit(s) at the origin of their oral feeding difficulties.

Current Knowledge-Based Practice Guidelines, Tools, and Interventions

When advancement of infant oral feeding in NICUs is hampered, feeding therapists are commonly consulted (19, 25, 26). Due to the lack of available devices to monitor infants' sucking skills, non-nutritive assessment follows standardized plan based on visual and sensory feedback whether infants are bottle- or breast-feeding. Using a gloved finger, therapists assess the anatomical development of infants' oral structures, e.g., hard/soft palate, gum line, and lingual mobility, e.g., lateralization, cupping, stripping. As the infant is sucking on the therapist's gloved finger, functional development is assessed by visual and tactile feedback, i.e., watching the movement and coordination of cheeks, jaws, and lip seal around the finger, the relative rhythmicity of pressure

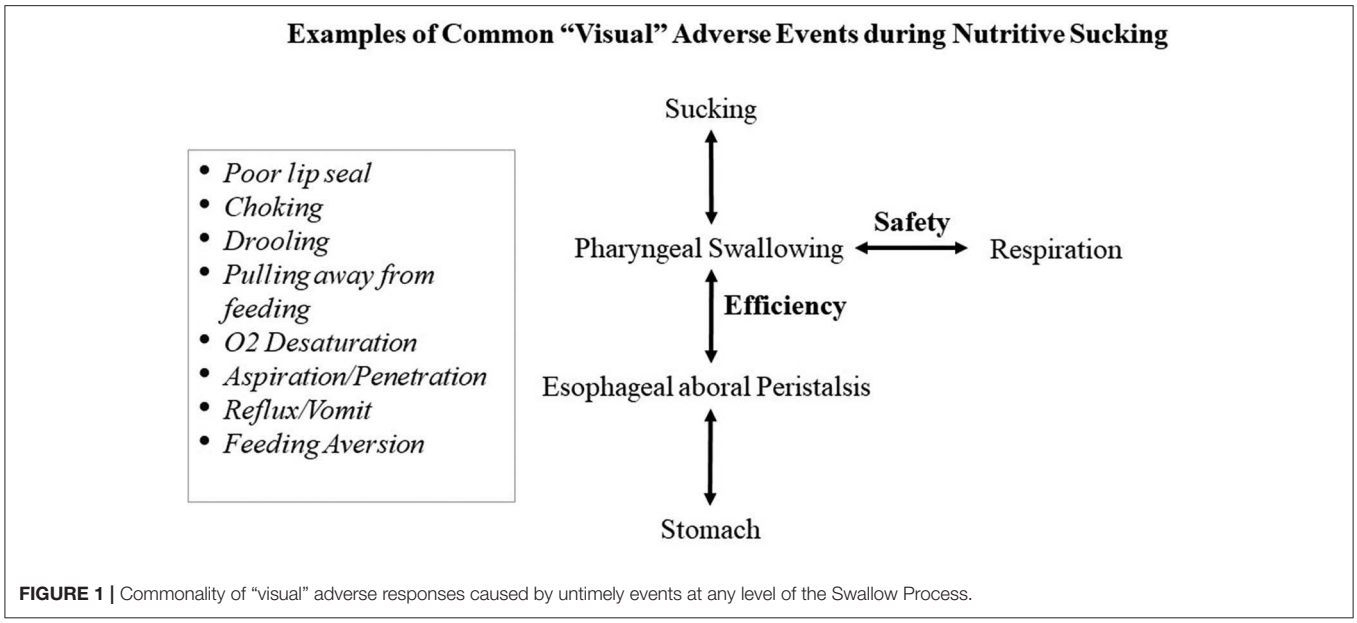

FIGURE 1 | Commonality of "visual" adverse responses caused by untimely events at any level of the Swallow Process.

forces applied on the finger, and respiratory bursts/pauses. Evaluation of nutritive sucking skills conducted during bottle feeding is based on similar visual assessment of cheeks, jaws, lips, and the relative coordination of suck, swallow, and respiration while watching for any adverse events, e.g., choking, O_2 desaturation, pushing back (12). As infant organization/states or external factors such as NICU surroundings, may interfere with performance, a management plan that encompasses the above concerns is proposed that may include varied perioral stimulations, e.g., cheek and chin support, pacing, non-nutritive oral motor stimulation (NNOMT), adjusting feeding positions, e.g., sidelying vs. semi-reclined, dimming overhead lights, etc. (10, 27, 28). In recent years, responsive/cue-based/"infant driven feeding" approaches have grown in popularity. However, in the absence of data providing strong evidence of study design stringencies, a recent Cochrane Intervention Review recommended that "a large RCT [randomized controlled trial] would be needed to confirm "their benefits and determine if such approach may affect other important [preterm infants'] outcomes" (29, 30). When flow rate during bottle feeding is deemed too slow or too fast, it is normally addressed by changing nipples claimed to be slower/faster as per manufacturers (31–34). Insofar as caregivers' decisions are subjective and use trial and error approaches, at times, there lacks a general consensus among the multi-disciplinary members of the NICU team regarding best treatment (27, 28, 35, 36).

The health benefits gained by mothers and infants through breastfeeding are no longer disputed (37–40). In addition to the nutritional advantage mother's milk offers over artificial formulae, breastfeeding is the optimal nurturance infants can receive from their mother through their close physical contact. Indeed, a mother's balanced nutritional and maternal care will benefit her child's not only nutritionally, but also non-nutritionally in the provision of appropriate stimulation of their infants' maturing neuro-physiologic/-motor/-behavioral functions (41–46). Breastfeeding challenges for NICU infants has similarly increased the demand for lactation consultants. Evaluation for breastfeeding difficulties assesses maternal factors e.g., nipple shape, degree of elasticity/protractility as they may interfere with infant's performance and ability to latch-on and remain latched-on during a feeding (6). As breastfeeding requires the involvement of both mother and infant, when infant breastfeeding difficulties arise, any evaluation requires not only assessment of infant oral feeding skills, but just as importantly the lactation performance of their mother. It remains unclear whether a mother's mammary development and function is affected by her shortened gestation. Lactation may be impaired not only by milk supply and milk release during breastfeeding, but also by mother's motivation to breastfeed, her overall well-being, and stress (41, 47). It is well-acknowledged that stress can interfere with the neuro-endocrine regulation of lactation both at the level of milk synthesis and milk release/ejection (6, 41, 46). Although a number of breastfeeding assessment scales have been developed based on a variety of infant behavioral criteria, they are not yet well-recognized (48–53). This situation is similar to that of feeding therapists' evaluation of infant's bottle-feeding difficulties as lactation consultants' feedback lack objective evidence-based studies supporting their proposed treatment(s). Nevertheless, the broad variety of current knowledge-based bottle and breastfeeding approaches proposed by feeding therapists underscores "the importance of strategies for stimulation of [infant] sensory-motor-oral system to decrease the period of transition to full oral feeding system" (35).

Novel Research Tools/Interventions

A small number of devices have been developed to monitor infant non-nutritive and nutritive sucking. As described on their respective website, the NTrainer system (innarahealth.com)

specifically monitors infants' non-nutritive suck and has developed non-nutritive assessments and therapies that "have been proven to reduce time to full oral feeding [. . .] and length of stay [. . .] in the NICU1." The NFANT® Sensor (nfant.com) monitors infant lingual movements during feeding and assist clinicians to "quickly determine optimal feeding parameters through objective metrics" using their Nfant Feeding Solution and Analytics. The Medoff-Cooper Nutritive Sucking Apparatus (M-CNSA) is a research tool that monitors sucking pressure (54).

Due to the commonality of the "visual" adverse symptoms that arise from dysfunctionality(ies) at the various levels of the Swallow Process (**Figure 1**), our approach attempted to examine the proper functionality at these levels. As our intention was first to specifically understand the development of infant nutritive sucking, our studies were conducted during bottle- rather than breast-feeding as the impact of any maternal inputs through their behavior and milk availability would obligatorily add non-controllable external variables that would not be indicative of their infants' *true* competence. As infants comorbidities, e.g., bronchopulmonary dysplasia, post necrotizing enterocolitis, could interfere with infants oral feeding performance, our subjects were recruited from *clinically stable* very low birth weight (VLBW) preterm infants, i.e., "feeders and growers," whose discharge from NICUs were only delayed due to their inability to adequately feed by mouth (3, 13). Following the development of the oro-motor kinetic monitoring (OMK) technology, we gained a substantial understanding of the maturation of VLBW infants' nutritive and non-nutritive sucking and how appropriate synchronization of suck-swallow-breathe was necessary to ensure safe and efficacious oral feeding. With the understanding gained from the OMK technology, the development of additional tools and interventions naturally followed.

The Oro-Motor Kinetic Monitoring Device (OMK) Technology

The OMK Nutritive Assessment Strategy (OMK-NS)

To follow the natural development of infant nutritive sucking, the OMK-NS was developed using miniature sensors appropriately placed on the bottle nipple. As such, it can *directly* monitor the shape/form and strength (mmHg) of the two components of sucking, i.e., Suction and Expression (55). Suction corresponds to the negative intra-oral pressure generated with the closing of the nasal passages by the soft palate and lowering of the jaw that draws milk into the mouth, similar to drinking from a straw. Expression, in turn, corresponds to the compression and stripping of the nipple by the tongue against the hard palate to eject milk into the mouth. With this device, we described five stages of nutritive sucking (NS) maturation based on the presence/absence of suction, expression, their respective rhythmicity, and synchronization with one another (16). We have also shown that this technology can be readily adapted to the breast nipple during breastfeeding.

To simultaneously monitor the sucking-swallowing-breathing events during bottle feeding, two drums placed over the hyoid and diaphragm allowed for the capture the pharyngeal swallow reflex and respiratory effort (56), respectively. This provided evidence for the importance of the proper *temporal* coordination of sucking, swallowing, and respiratory functions (14, 16, 57, 58). If connected to infants' vital signs monitors, **Figure 2** shows how one can monitor at the same time infants' clinical status.

The clinical importance of pediatric esophageal dysphagia is well-recognized by pediatric gastroenterologists (59). As the gastrointestinal (GI) system of the pig is the closest to that of the human (60), we conducted a study on preterm piglets using a 4-port "multi-channel" esophageal catheter provided by our co-author (Omari T) and obtained evidence supporting the importance of the proper maturation of esophageal peristalsis as another essential component for the safe and swift transport of a bolus from the oral cavity to the stomach (17). Preterm piglets demonstrated similar susceptibility to necrotizing enterocolitis and oral feeding issues as their human counterparts, e.g., milk leakage, regurgitation, limited endurance, inability to complete a feeding. When compared to healthy term piglets, the occurrence of the mature pattern of aboral propagating peristaltic waves for bolus transport, i.e., from upper esophageal sphincter to stomach, was significantly less frequent and of slower velocity (17). The development of monitoring devices has been problematic due to infants' fragility and small sizes. However, devices for the assessment of esophageal function, using high resolution manometry with and without impedance (HRIM/HRM) are becoming adaptable to the pediatric population (61–65).

The OMK Non-nutritive Assessment Strategy (OMK-NNS)

The OMK technology can be adapted for non-nutritive sucking assessment on a pacifier or a disposable glove as used by feeding therapists for their consults, providing objective quantitative measures similar to those obtained during nutritive sucking (OMK-NS) e.g., pressure force (mmHg) of suction and expression, NNS frequency, shape/form of these two components, duration of pauses and sucking bursts that cannot be identified otherwise (10, 12, 13). It is advanced that if used for the preliminary clinical evaluation of infant oral feeding skills, therapists' recommendations based on objective outcome measures would be more readily accepted by their NICU team members than currently viewed. Of value, the OMK-glove may be a valuable tool for the objective training of new feeding therapists as they can learn to interpret the variations of their sensory feedback from the recordings obtained. With the OMK technology, we confirmed that nutritive sucking occurs at 1 cps vs. that of non-nutritive sucking at 2 cps (66). This is a useful means to help determine if milk release is occurring when infants are nutritively vs. non-utritively sucking on the breast. When thickeners are added to formula/breastmilk during bottle feeding to decrease reflux, they may occlude the nipple hole preventing milk outflow. This can be readily recognized if infants begin sucking non-nutritively at 2 cps. Of interest, we have observed that infants' non-nutritive sucking is already mature by the time oral feeding is initiated. This implies that the oro-motor competence to generate suction and expression is already attained (12). For this reason, the observation of "rhythmic" sucking on a pacifier/finger is incorrectly used as an index of readiness to feed.

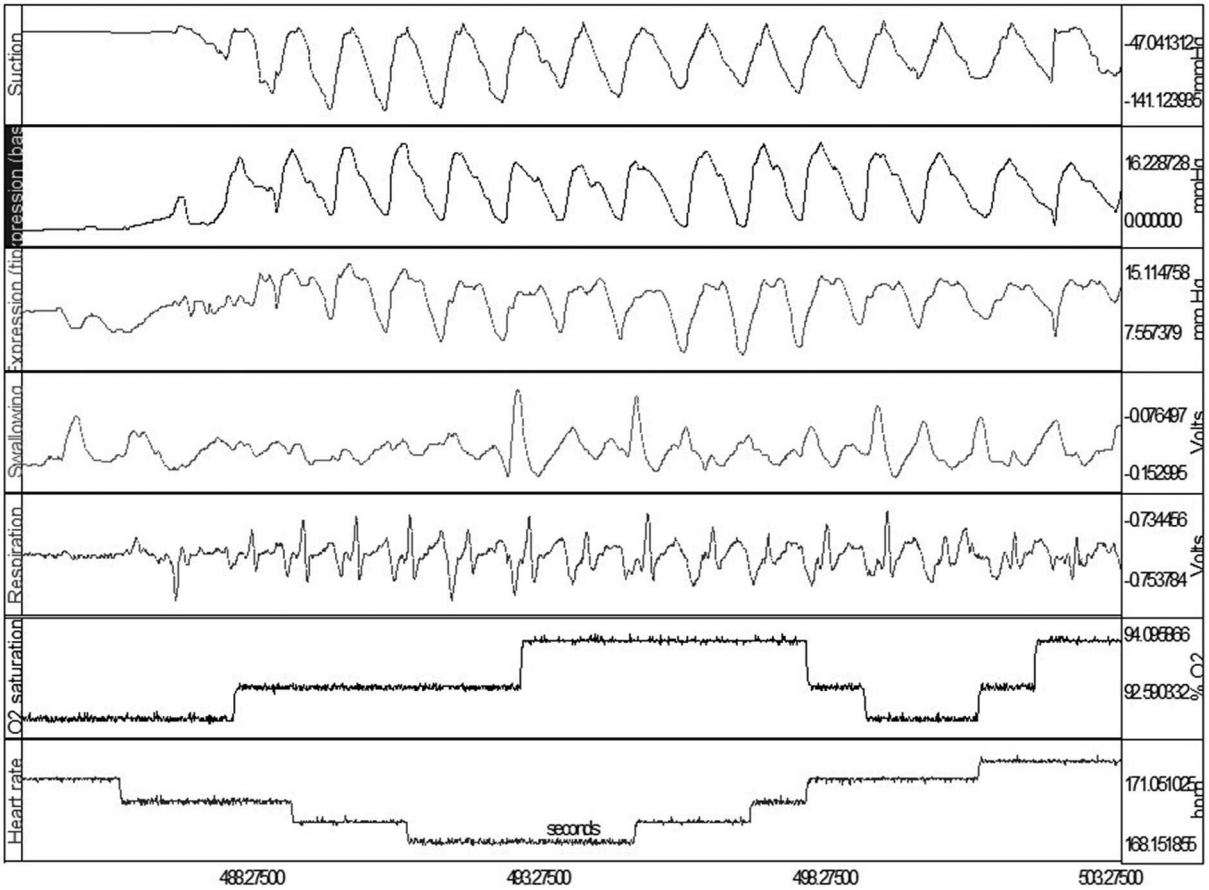

FIGURE 2 | Simultaneous OMK-NS monitoring of nutritive sucking, i.e., suction, expression (base and tip), swallow, respiration, O_2 saturation, heart rate. Note: Expression monitored at base and tip of tongue for assessment of lingual mobility, e.g., compression, stripping.

The Oral Feeding Skills Scale (OFS)

The Oral Feeding Skills scale (OFS) is a 4-level *clinical* scale developed as a simple objective indicator of infants' feeding ability. It has the unique advantage that it does not require any special device, only the recording of the percent volume taken over volume prescribed during the first 5 min of a feeding ("proficiency") and the rate of milk transfer (ml/min) over an entire feeding ("endurance"). The OFS assessment presumes that prior to all oral feedings, infants are left undisturbed 30 min prior in order to ensure minimal fatigue before they are fed. As shown in **Figure 3A**, proficiency on the *X*-axis is used as an estimate of infant's "true" feeding skills *as fatigue is minimal*. Rate of milk transfer on the *Y*-axis is used as an index of endurance or how fatigue impacts an infant's overall feeding performance (67). Four levels of OFS skills are delineated by cut-offs of proficiency set at 30% and "endurance" at 1.5 ml/min for VLBW infants (67), and 40% and 1.5 ml/min for late preterm, respectively (68). These four OFS levels distinguish proficiency (*true* feeding skills) and endurance levels as "high" or "low." **Figure 3B** presents the levels of these two measures at each OFS levels, I–IV, and their correlation with infant overall feeding performance or overall transfer, i.e., percent volume taken/volume prescribed at a feeding. A significant correlation was observed between each OFS levels and % overall transfer (67). It is of interest to note that OFS levels II and III show that proficiency and endurance, on their own, have equal impact on overall transfer [∼80%; **Figure 3B**]. Potential interventions comprising "targeted interventions" and "endurance training" to assist infants when tested at these individual OFS levels are based on their respective proficiency and endurance (**Figure 3B**). **Figure 3C** confirms that preterm infants can demonstrate the whole range of OFS levels I–IV when monitored at their first oral feeding (67). This would explain why, as caregivers, we are familiar with the disparity that infants of same GA and PMA may show broad ranges of oral feeding aptitudes.

The OFS scale offers several advantages: (1) It can be used at any feeding with no special device and without interfering with infant's task because taking a reading of the volume taken at ∼5 min into a feeding coincides with an initial recommended "burping" pause. (2) As it is correlated positively with infants' % overall transfer during a feeding (**Figure 3B**), it becomes an objective index of the correlation between infants' oral feeding skills and performance over time. (3) The observation that infants of similar GA monitored at similar PMA demonstrate all four

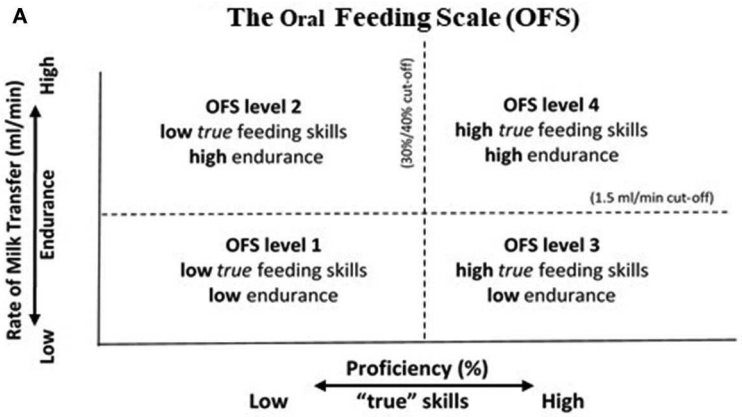

B OFS Scale Interpretations & Clinical Validation

OFS Levels	Feeding skills (Pro)	Endurance (RT)	Overall Transfer (%)	Potential Interventions
I	low	low	~ 30%	Targeted Intervention(s) & endurance training
II	low	high	~ 80%	Targeted Intervention(s)
III	high	low	~ 80%	endurance training
IV	high	high	~ 100%	none

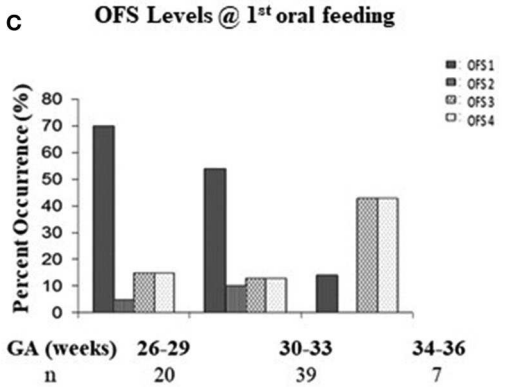

FIGURE 3 | (A) The four OFS levels delineated by: Proficiency on the *X*-axis at 30 and 40% for VLBW and late preterm, respectively; Endurance on the *Y*-axis at 1.5 ml/min. **(B)** Interpretations and Clinical Validation of the OFS Levels, Feeding Skills (Pro: proficiency), Endurance (RT: rate of milk transfer), Overall transfer (% volume taken/volume to be taken), Potential targeted interventions for the respective "low" levels at each OFS levels (see **Figure 5**). **(C)** Percent occurrence of OFS levels (I–IV) in three groups of infants born at 26–29, 30–33, and 34–36 weeks GA at their first oral feeding (~35 weeks PMA); *n*: number of subjects/group. Note: broad variations of OFS levels at each GA.

OFS levels confirms that their oral feeding skills mature at different rates (**Figure 3C**). As such, care should be taken not to interpret that infants falling below "expectation" are delayed. (4) With the ability to monitor the maturational progress of an *individual* infant's proficiency and endurance, the OFS offers the opportunity to differentiate the impact that the maturation of "true" skills (proficiency) and fatigue/endurance can have on infant overall performance (10). Consequently, infants' OFS levels are better indicators of oral feeding competence than the use of PMA or aptitude to suck on a pacifier. (5) The efficacy of an intervention on a particular infant can be verified as it would be reflected by improved OFS level along with corresponding oral feeding performance (10). Providers need to remember that if a particular intervention is not beneficial for one infant, it can be for another as the cause of their respective dysphagia may lie at different levels of the Swallow Process. (6) Finally, when used in patient rounds, the 4-level OFS scale offers team members an objective/quantitative feedback of a patient's performance over time that the current subjective/descriptive approaches cannot, e.g., "baby fed well," "poorly," "better/worse than the day before." Due to its objective feedback, the OFS scale has been adopted into patient's medical records in some hospitals as well as in research.

The Infant Self-Pacing (ISP) Feeding Bottle

The principles of the ISP bottle eliminate two properties of fluid physics that occur within a rigid standard bottle as it empties when an infant is feeding. As a standard bottle empties during a feeding, a natural increase in internal vacuum build-up occurs hindering fluid outflow. This leads infants to suck harder to first overcome the internal vacuum before obtaining milk, likely increasing unnecessary energy expenditure (**Figure 4A**). The positive hydrostatic pressure exerted by milk over the nipple hole when a bottle is tilted naturally leads to a disruptive "milk drip" whether the baby is sucking or not (69) (**Figure 4B**). With

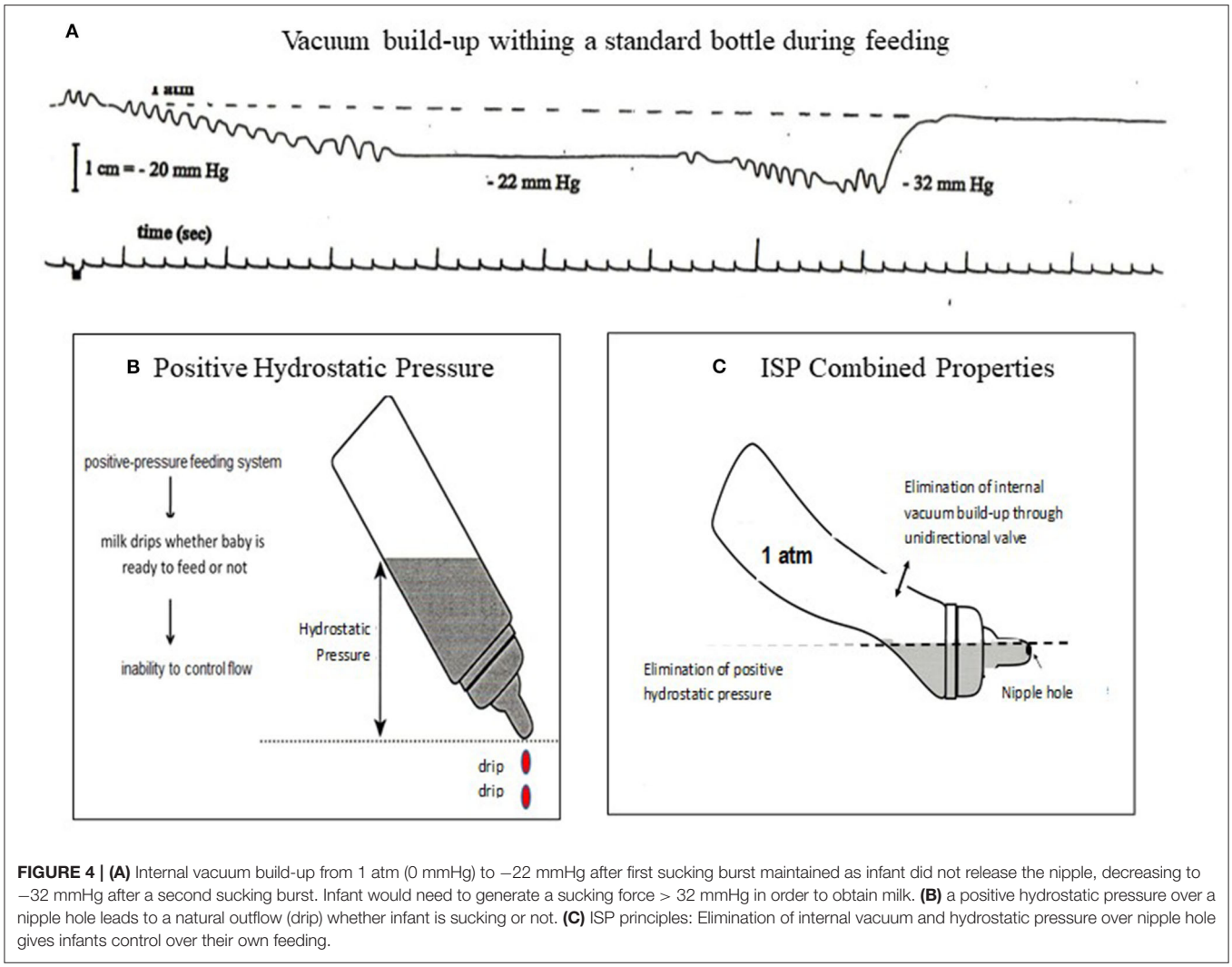

FIGURE 4 | (A) Internal vacuum build-up from 1 atm (0 mmHg) to −22 mmHg after first sucking burst maintained as infant did not release the nipple, decreasing to −32 mmHg after a second sucking burst. Infant would need to generate a sucking force > 32 mmHg in order to obtain milk. **(B)** a positive hydrostatic pressure over a nipple hole leads to a natural outflow (drip) whether infant is sucking or not. **(C)** ISP principles: Elimination of internal vacuum and hydrostatic pressure over nipple hole gives infants control over their own feeding.

the elimination of the natural internal negative pressure build-up after each suck and "milk drip" (**Figure 4C**), the *control of the feeding is given to the infant* and not the caregiver because the infant does not need to suck harder (preserving energy) to overcome the increasing internal negative pressure and can pause to rest/catch-up breathing whenever needed without milk dripping in his/her mouth. Although the volume of a milk "drip" may not appear of significance, it should be noted that the average bolus size of VLBW infants average 0.14 ± 0.06 ml when they transition from tube to independent oral feeding. This is significantly less than the 0.22 ± 0.07 ml monitored in full term infants during their first 2 weeks of life (14).

In general, bottle feeding is controlled by caregivers who, through visual and auditory sensory feedback, determine whether a feeding ought to be maintained or stopped. Unless obvious adverse events occur, e.g., turning blue, pushing away, triggered hospital alarms, the feeding is continued. Caregivers may take different approaches in "assisting" their infant's feeding such as increasing/decreasing milk outflow by using fast or slow flow nipples, offering softer/harder nipples, providing "encouragement" to complete a feeding, or stopping the feeding because infant appears satiated. Under such circumstances, it is unclear the bases upon which such rationales arise because without appropriate devices, we know that immature neuro-motor/-physiologic events cannot be readily detected, e.g., dys-coordination of suck-swallow-respiration-esophageal motility, silent penetration/aspiration, non-overt gastro-esophageal reflux.

To our knowledge, the ISP is the only feeding bottle that gives *control of the feeding* to the babies. Whenever needed, e.g., rest, catch-up breathing, it allows them to stop with the bottle in the mouth without being overwhelmed as milk drip is also eliminated. This assumes no caregivers' inputs during feedings. With the ISP, we observed that a greater percentile of infants completed their feeding with no adverse events. This was achieved at a faster rate while using a more mature OFS level than control counterparts feeding from a standard bottle (69, 70). Therefore, we speculate that infants, *with normally developing central nervous system*, are able to *reflexively* regulate their nutritive sucking *in the absence of external controlling factors*. This assumption is based on anatomical evidence that

the respiratory, sucking, and swallowing centers are anatomically in close proximity from each other in the brainstem, with separate pools of motor neurons implicated in their respective sequential rhythmic movements and regulated by central pattern generators (CPGs) (71, 72). The existence of an intrinsic "tau (τ)" guide acting as a common processor that links timing events of different motor movements has been proposed (73–75). A similar theory of cross-system interactions between suck, swallow, and respiration has been advanced to explain the ability of these functions to rapidly re-adjust to variations occurring at any one of these levels during oral feeding (76). The essential integrity of sensory afferents signaling changes in physiologic and environmental functions has also been proposed for the proper regulatory feedback of these individual functions (77).

From such understanding, the following tools along with evidence-based tested interventions we developed are described below.

Interventions That Enhance Infants' Oral Feeding Aptitude

Infant oral feeding *performance* does not solely relate to the proper maturation of infants' oral feeding skills. Their clinical status, behavioral states, infant's organization, and environmental conditions at feeding time are well-known contributors to a successful feeding (6). Oral feeding is optimized when infants are in drowsy/alert inactive, quiet awake, and/or alert state as defined by the Newborn Individualized Developmental Care and Assessment Program (NIDCAP) (78–80). As mentioned earlier, environmental conditions such as bright light, loud surroundings, fluctuating temperatures, infant unsupported posture are disruptive (10, 81). Consequently, the development of any intervention needs to encompass not only uni-modal approaches targeting physiologic functions, e.g., sucking, swallowing, respiration, esophageal function, but also multi-modal approaches that encompass the above "deterrent" factors. Provision of multi-sensory stimulations to offset these negative factors are varied and have focused on tactile, auditory, and olfactory senses, e.g., skin-to-skin holding/kangaroo care, infant massage/tactile-kinesthetic, music therapy, maternal pheromones. Except for the benefits of the well-acknowledged skin-to-skin holding (82, 83), music and massage therapy along with maternal pheromones will require further confirmation (84–86). We examined the potential benefits of some of these interventions on infant oral feeding difficulties as few of them have been used for this purpose. The OFS scale was used as an index of oral feeding skills, while days from initiation to independent oral feeding was used as index of oral feeding performance. We demonstrated the benefits of a specific *non-nutritive oral motor training* protocol *(NNOMT)* and a *swallow exercis*e directed at sucking and swallowing, respectively (10, 87–89). The use of a protocol consisting of active non-nutritive sucking on a pacifier that followed the same schedule as that of the NNOMT did not replicate the benefit observed with the latter (89). As the general benefits of infant massage for infants and parents are well-recognized (90, 91), we verified its beneficial effect on preterm infants' oral feeding using the *massage protocol* developed by Field for preterm infants (92). This intervention was similarly effective on improving infants' OFS levels and accelerating their attainment of independent oral feeding (87). Over the years, various infant feeding positions have been advocated as "optimal," e.g., the customary semi-reclined (control), upright, and sidelying. As each lacks evidence-based support, we examined VLBW infants' performance when fed under these three conditions. No statistical difference in transition time from tube to independent oral feeding was observed (28). It should be noted that no infants in the above studies demonstrated any adverse events during their feedings.

From a common sense approach, as poor endurance is commonly linked to poor feeding performance, "*endurance training*" is suggested whereby a feeding duration is stopped when the infant shows signs of fatigue, e.g., increased pauses, changes in organization or state, rather than "encouraging" the infant to continue. For instance, if an infant is following a regimen of 2 oral feedings/day (20 min/feeding), but cannot continue after 10 min, a revised schedule of 4 oral feedings/day (10 min/feeding) regimen may be more appropriate and advantageous. Indeed, one may reason that the duration of "practice" time is the same, i.e., 40 min/day, but training during these 40 min in the latter case occurs at a time when the infant has greatest endurance. This principle addresses the common saying that "practice makes perfect" *as long as* the practice duration remains productive. This premise is based on the appreciation that brain plasticity can reorganize sensori-motor areas following beneficial and detrimental practices (93, 94). Consequently, to optimize beneficial sensory inputs, if fatigue were recognized and oral feeding regimen were revised accordingly, detrimental consequences such as oral feeding aversion, regurgitation, aspiration/penetration, may be reduced. Along this line of reasoning, it is proposed that the ISP bottle may be considered an appropriate intervention as it gives control of the feeding to the infants. With control of flow rate and pauses, infants would experience optimal sensory inputs.

WHAT CAN WE DO?

Flexible *Individualized* Management Guidelines

Customarily, the evidence-based efficacy of any intervention on a particular population is confirmed by following appropriately designed studies or randomized clinical trials using appropriate statistical approaches. However, as the functional maturation profiles of preterm infants of same GA and PMA are not uniform, as shown in **Figure 3C**, one ought not presume that if an intervention does not demonstrate statistical efficacy for a group of infants, that it cannot be efficacious for some of them. Insofar as the care of healthcare providers is directed toward *individual* patients, it is advanced that the ease-of-use of the OFS scale can help identify *individual* infants who do or do not benefit from a particular intervention. A fitting example relates to our earlier study on "optimal" feeding positions wherein no statistical difference in transition time from tube to independent oral feeding was observed between positions (28). If the OFS scale had been used to follow *individual* infants' progress as they

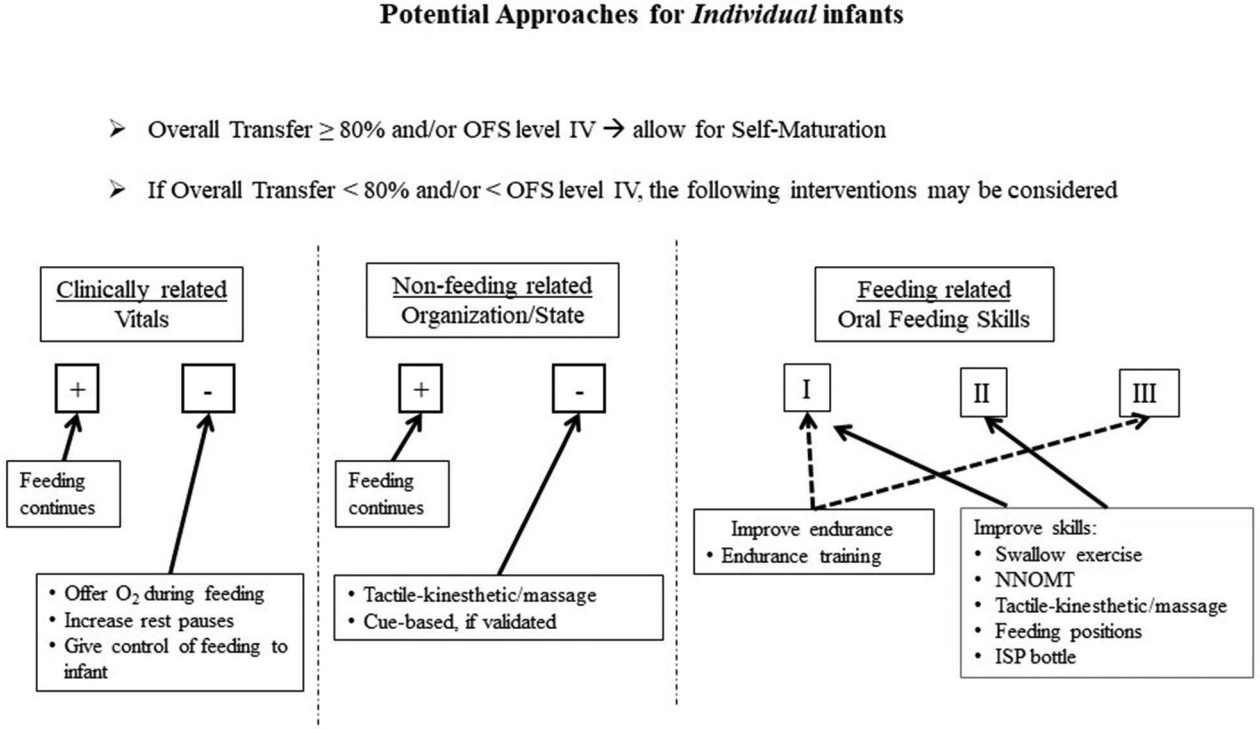

FIGURE 5 | Proposed approaches based on *individual* infant's challenges, i.e., Clinically related, Non-feeding related, Feeding related; (+) Adequate, (–) Inadequate; OFS levels I, II, III.

transition from tube to independent oral feeding, identification of the ones who did and did not benefit from being fed semi-reclined, upright, or sidelying could have been identified. As such, one of the advantages of the OFS scale is to allow close monitoring of the efficacy of any intervention on *individual* infants (10, 89). It is based on the simplicity of use of the OFS scale that the *individualized* management protocol below is presented. This approach is similar to the one used by feeding therapists in the development of their management plans with the advantage that monitoring performance with the OFS scale will provide objective outcome measures that have been shown to correlate with proficiency, endurance, oral feeding skills, and performance (**Figures 3A,B**).

Consequently, it is advanced that the routine use of the OFS scale will allow caregivers to closely monitor the oral feeding skills of their *individual* patients. The guidelines described below make use of a "research-to-practice" translation to complement the current clinical practices. Although we do not know the initial causes of *individual* infants' dysphagia, we do know that they may arise from their clinical status, non-feeding, and feeding related factors, e.g., O_2 desaturation, behavioral organization/state, immature oral feeding skills, respectively. For each of these three categories, there are evidence-based beneficial interventions available as presented earlier (**Figure 5**). Proficiency can be used as an estimate of infants' nutritive sucking ability when fatigue is minimal, while rate of milk transfer can be used as an estimate of infants' endurance *as a function* of their clinical status, behavioral organization/state, and/or stress (95–99). Thus, considering all the factors that may impact preterm infants' ability in attaining independent oral feeding, **Figures 5**, **6** are proposed targeted interventions and general guidelines that may be considered in the management plans of *individual* NICU infants. As the quality of their feeding performance is primarily measured clinically by their % overall transfer, **Figure 5** proposes that with overall transfer ≥ 80% or OFS level IV, no interventions are proposed to allow for infant "self-maturation." With overall transfer < 80% and/or OFS I–III, interventions may be offered to support infants' feeding performance based on their clinically related vitals, non-feeding related organization/state, and/or feeding skills as assessed by their OFS levels. Under each of these categories, targeted interventions are proposed based on clinical practices and objective evidence-based studies presented earlier. In regard to feeding related factors, proposed interventions are based on the interpretation of the OFS levels presented in **Figure 3B**.

Figure 6 is a suggested *flexible* algorithm using the OFS scale as the "monitoring device." The protocol calls for "reassessments" in 2-day block of times to allow for infants "self-maturation." This 2-day block window is based on our clinical observations that some infants, on their own, can show improvement in their oral feeding aptitude within 2 days in the absence of any interventions. Two paths are described. At a feeding therapist's initial bottle feeding consult, if infants demonstrate an OFS level IV and/or overall transfer ≥ 80% (Path I), progression of oral

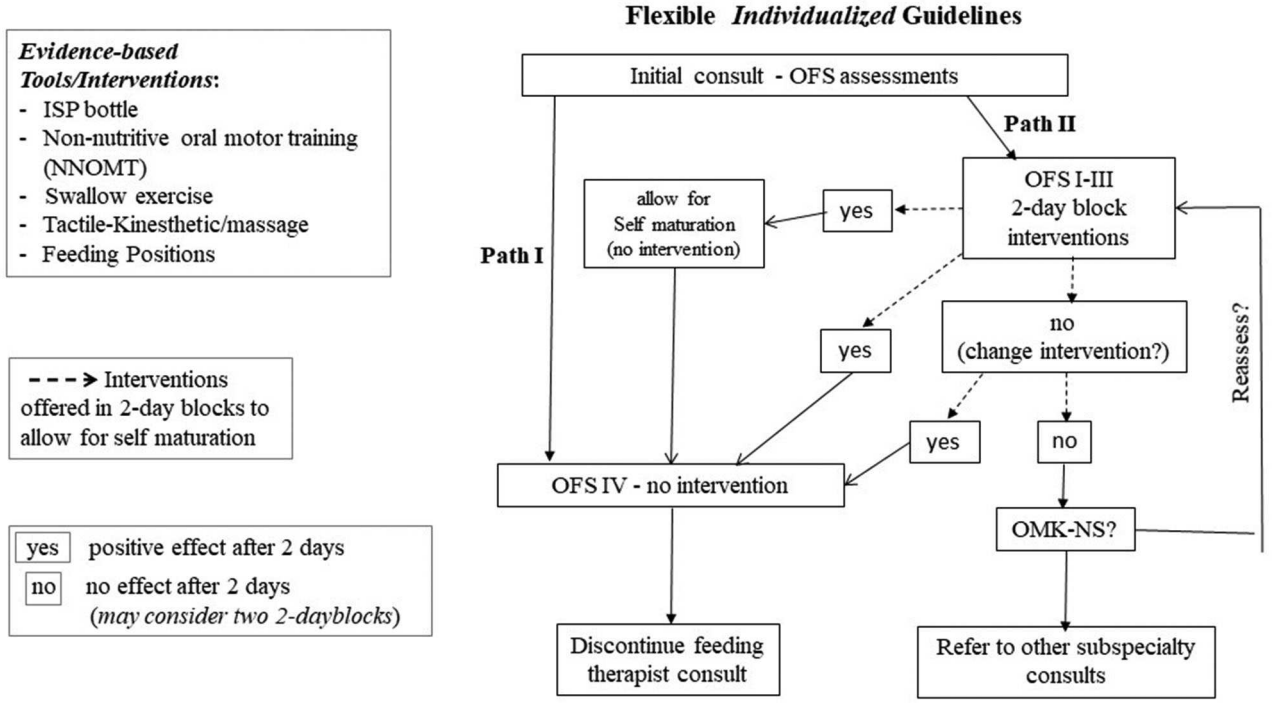

FIGURE 6 | Flexible *individualized* guidelines based on OFS levels; Path I for OFS level IV and Overall Transfer > 80%; Path II for OFS level I to III and Overall Transfer < 80%; interventions provided in 2-day blocks; (yes) positive effect; (no) no effect after 2-day block (see text for details).

feeding would be based on the provider/team's recommendation in oral feeding advancement with no needed intervention. With OFS levels I to III or overall transfer < 80% (Path II), infants will be offered targeted interventions listed in **Figure 5** based upon their clinical stability, organization/state, and/or OFS skill levels. It should be reminded that monitoring infants' OFS levels requires minimal effort as proficiency can be computed at any feeding session by simply measuring the volume taken during the first 5 min at a "burping" pause in addition to the overall transfer and feeding duration that are customarily collected by caregivers. Daily intervention frequency and duration can be offered based on *individual* infants' clinical status, e.g., 15 min/day and reassessed in 2-day blocks. If a positive effect is observed in either OFS levels or % overall transfer, infant can be moved into path I *when* OFS level IV or overall performance ≥ 80% is achieved. If no progress is observed after two 2-day blocks, i.e., 4 days of intervention, a change in intervention may be appropriate as the earlier intervention may not have targeted the appropriate level of the Swallow Process. An assessment using the OMK-NS monitoring system may be recommended in order to directly assess the maturation stage of infants' nutritive skills and suck-swallow-respiratory coordination if necessary. Referral to other pediatric subspecialties, e.g., Pediatric Ear Nose and Throat, Gastroenterology, Pulmonology, Cardiology, may be recommended. Any regression in oral feeding performance would naturally require further medical examination as it may be due to "yet" undetected clinical issues, e.g., sepsis, GI issues, silent gastro-esophageal reflex. The "flexibility" of the proposed guidelines is based on the recognition that due to the broad variations in preterm infants' developmental profiles, caregivers ought to remain flexible in the management plans they devise.

As mentioned above, the focus placed on bottle feeding described in our work does not reflect any partiality for bottle- over breast-feeding, but rather a first step at understanding the development of infants' own skills in the absence of any potential maternal input(s) that may occur during breastfeeding, e.g., poor lactation, maternal own comfort to breastfeeding, infant proper attachment to the nipple-areolar complex. The OFS assessments in the NICU does not threaten infants' breastfeeding opportunities as most infants who are primarily breastfeeding are bottle fed when mother is not present. In fact, their OFS levels may help parents and caregivers identify potential breastfeeding difficulties resulting from infant's proficiency and endurance (**Figure 3A**). One may speculate that improvement of these infants' OFS levels may also lead to improved breastfeeding skills, e.g., latching-on, and earlier breastfeeding success.

Insofar as our tools and intervention programs can be readily used by healthcare providers in hospitals as well as out-patient settings, it is advanced that their adoption in clinics could provide a "Continuum of Care" approach that would allow "feeders and growers" to be discharged earlier from NICU and reduce medical costs, as such care can be readily assumed by out-patient services offering the same oral feeding management protocol.

In brief, the intent of these proposed flexible guidelines is to introduce to clinicians the evidence-based beneficial tools

and interventions developed through research over recent years that could benefit the care of their high-risk patients with oral feeding challenges.

Caveats

It is recognized that the knowledge we gained from our research will require confirmation via additional well-designed studies. However, the above proposed guidelines are based on the following justifications:

1. Preterm infants' difficulties in attaining safe and efficient oral feeding lead to prolonged NICU hospitalization, increased maternal stress, and medical costs. As such, the sooner they attain independent oral feeding safely and efficiently, the better.
2. Due to our limited understanding of the cause(s) leading to oral feeding difficulties, the current practices provided by feeding therapists lack evidence-based backing and consensus from team members as any benefit may be due to the infant's normal maturation.
3. In general, any new treatment/therapy requires additional well-designed studies to confirm and validate their efficacy. Insofar as our proposed guidelines address the care of *individual* infants rather than groups of infants, it is advanced that such approach may not be relevant. As mention earlier, we do not yet have the technology to determine the origination site(s) of an oral feeding problem in the Swallow Process and thus cannot identify the appropriate targeted intervention(s) to best treat them. For instance, if the adverse events observed on a particular patient originated at the "Safety" level, i.e., Respiration-Pharyngeal phase of swallowing (**Figure 1**), providing NNOMT treatment would likely not show any benefit. As such, providers need to remember that if a particular intervention is not efficacious for one infant, it can be for another as the cause(s) of their dysphagia may lie at different levels of the Swallow Process. This is the reason why in the proposed algorithm (**Figure 6**), a "trial and error approach" is used as different targeted interventions would be offered in two 2-day blocks, if no benefits are observed.
4. We speculate that the development of *individualized* management care plans that combine current feeding therapists' practices with the tools and interventions presented would lead to greater success for infants and the team members caring for them.

CONCLUSION

In summary, this report presents a review of the practices currently offered to NICU infants facing oral feeding challenges and the latest research that led to a number of efficacious evidence-based tools and interventions. It is recognized that "the underlying principles of the above model [will need further validation in order] to be clearly disseminated to practitioners of this field" (Research Model Innovations in Advancing Neonatal Care). However, it is hoped that in providing a greater understanding of the potential causes at the root of preterm infants' oral feeding difficulties, our research will improve the current clinical practice and assist "in the development of [additional] diagnostic tools and new therapies." This review presents a new perspective of how combining features of current practices with the use of novel tools/interventions could help practitioners improve their patients' care in developing structured and innovative management plans catered to the *specific* needs of *individual* patient. Additionally, it is proposed that a "Continuum of Care" approach may be envisaged whereby "feeders and growers" could be followed by out-patient clinical or home care services using the same technologies and methodologies. This would allow for earlier discharge, family reunion, and reduced medical cost for all.

DATA AVAILABILITY STATEMENT

The raw data supporting the conclusions of this article will be made available by the authors, without undue reservation, to any qualified researcher.

ETHICS STATEMENT

The studies involving human participants were reviewed and approved by The Baylor College of Medicine Institutional Review Board for Human Research. Parental consent was obtained following approval by attending neonatologists. Written informed consent to participate in this study was provided by the participants' legal guardian/next of kin.

AUTHOR CONTRIBUTIONS

CL is the primary investigator of the above series of studies and was involved in all aspects of the research, i.e., study designs, team members supervision, data collection, statistical analyses, and interpretations, preparation of manuscripts.

FUNDING

General Clinical Research Centers Program (NIH-MO1RR000188): Oral/motor Kinetics in Neonates/Interventions for the enhancement of Oral Feeding in Preterm Infants (2000–2010); NIH Research Project Grant (NIH-R01 HD 44469): Oral Feeding in Infants (2005–2010), PI: CL; Co-I: L.E. Weisman, E.O. Smith, C. Redel; NIH Research Project Grant (NIH-R01 HD 28140): Feeding Strategies for Low Birth Weight Infants (1997–2001), PI: R.J. Schanler; Co-I: CL, K.J. Ellis, E.O. Smith, L.E. Weisman; NIH Research Project Grant (NIH-R01 HD 28140): Feeding Strategies for Low Birth Weight Infants (1992–1997); Co-PI's: R. J. Schanler, R. J. Shulman, CL, M. Heitkemper.

REFERENCES

1. Benjasuwantep B, Chaithirayanon S, Eiamudomkan M. Feeding problems in healthy young children: prevalence, related factors and feeding practices. *Pediatr Rep*. (2013) 5:38–42. doi: 10.4081/pr.2013.e10
2. Han C, Shin J, Jeon GW. Development of swallowing function in infants with oral feeding difficulties. *Int J Pediatr*. (2020) 2020:5437376. doi: 10.1155/2020/5437376
3. Edwards L, Cotten CM, Smith PB, Goldberg R, Saha S, Das A, et al. Inadequate oral feeding as a barrier to discharge in moderately preterm infants. *J Perinatol*. (2019) 39:1219–28. doi: 10.1038/s41372-019-0422-x
4. Bergman NJ, Ludwig R, Westrup B, Welch M. Nurturescience versus neuroscience: a case for rethinking perinatal mother-infant behaviors and relationship. *Birth Defects Res*. (2019) 111:1110–27. doi: 10.1002/bdr2.1529
5. A.A.o. Pediatrics. Hospital discharge of the high-risk neonate. *Pediatrics*. (2008) 122:1119–26. doi: 10.1542/peds.2008-2174
6. Lau C, Hurst N. Oral feeding in infants. *Curr Probl Pediatr*. (1999) 29:105–24. doi: 10.1016/S0045-9380(99)80052-8
7. Manuck TA, Rice MM, Bailit JL, Grobman WA, Reddy UM, Wapner RJ, et al. Preterm neonatal morbidity and mortality by gestational age: a contemporary cohort. *Am J Obstet Gynecol*. (2016) 215:103.e1–e14. doi: 10.1016/j.ajog.2016.01.004
8. Martin JA, Hamilton BE, Osterman MJK, Driscoll AK, Drake P. Births: final data for 2017. National vital statistics reports: from the Centers for Disease Control and Prevention, National Center for Health Statistics. *Natl Vital Stat Syst*. (2018) 67:1–50.
9. Olsen AL, Ammitzbøll J, Olsen EM, Skovgaard AM. Problems of feeding, sleeping and excessive crying in infancy: a general population study. *Arch Dis Child*. (2019) 104:1034–41. doi: 10.1136/archdischild-2019-316851
10. Lau C. Interventions to improve oral feeding performance of preterm infants. *Perspect Swallow Swallow Disord*. (2014) 23:23–45. doi: 10.1044/sasd23.1.23
11. Jadcherla SR, Challenges to eating, swallowing, and aerodigestive functions in infants: a burning platform that needs attention! *J Pediatr*. (2019) 211:7–9. doi: 10.1016/j.jpeds.2019.05.025
12. Lau C, Kusnierczyk I. Quantitative evaluation of infant's nonnutritive and nutritive sucking. *Dysphagia*. (2001) 16:58–67. doi: 10.1007/s004550000043
13. Lau C, Oral feeding in the preterm infant. *NeoReviews*. (2006) 7:e19–e27. doi: 10.1542/neo.7-1-e19
14. Lau C, Smith EO, Schanler RJ. Coordination of suck-swallow and swallow respiration in preterm infants. *Acta Paediatr*. (2003) 92:721–7. doi: 10.1111/j.1651-2227.2003.tb00607.x
15. Amaizu N, Shulman R, Schanler R, Lau C. Maturation of oral feeding skills in preterm infants. *Acta Paediatr*. (2008) 97:61–7. doi: 10.1111/j.1651-2227.2007.00548.x
16. Lau C, Alagugurusamy R, Schanler RJ, Smith EO, Shulman RJ. Characterization of the developmental stages of sucking in preterm infants during bottle feeding. *Acta Paediatr*. (2000) 89:846–52. doi: 10.1111/j.1651-2227.2000.tb00393.x
17. Rasch S, Sangild PT, Gregersen H, Schmidt M, Omari T, Lau C. The preterm piglet - a model in the study of esophageal development in preterm neonates. *Acta Paediatr*. (2010) 99:201–8 doi: 10.1111/j.1651-2227.2009.01564.x
18. Rayyan M, Omari T, Debeer A, Allegaert K, Rommel N. Characterization of esophageal motility and esophagogastric junction in preterm infants with bronchopulmonary dysplasia. *Neurogastroenterol Motil*. (2020). doi: 10.1111/nmo.13849. [Epub ahead of print].
19. Arvedson JC, Lefton-Greif MA. *Pediatric Videofluoroscopic Swallow Studies. A Profession Manual with Caregiver Guidelines*. San Antonio, TX: Communication Skill Builders (1998).
20. Lau C, Development of suck and swallow mechanisms in infants. *Ann Nutr Metab*. 66(Suppl.) (2015) 5:7–14. doi: 10.1159/000381361
21. Martin-Harris B, McFarland D, Hill EG, Strange CB, Focht KL, Wan Z, et al. Respiratory-swallow training in patients with head and neck cancer. *Arch. Phys Med Rehabil*. (2015) 96:885–93. doi: 10.1016/j.apmr.2014.11.022
22. Lau C, Maturation of infant oral feeding skills. In: Ongkasuwan J, Chiou EH, editors, *Pediatric Dysphagia - Challenges and Controversies*. Switzerland: Springer Nature (2018). p. 17–32.
23. Bakewell-Sachs S, Medoff-Cooper B, Escobar GJ, Silber JH, Lorch SA. Infant functional status: the timing of physiologic maturation of premature infants. *Pediatrics*. (2009) 123:e878–e86. doi: 10.1542/peds.2008-2568
24. Smith GC, Gutovich J, Smyser C, Pineda R, Newnham C, Tjoeng TH, et al. Neonatal intensive care unit stress is associated with brain development in preterm infants. *Ann. Neurol*. (2011) 70:541–9. doi: 10.1002/ana.22545
25. Wolf LS, Glass RP. *Feeding and Swallowing Disorders in Infancy: Assessment and Management, Therapy Skills Builders*. Tucson, AZ: Therapy Skill Builders (1992).
26. Howe TH, Oromotor Therapy. In: Ongkasuwan J, Chiou EH, editors, *Pediatric Dysphagia*. Switzerland: Springer Nature (2018). p. 119–134.
27. Mitra S, Reid M, McDougall B, Johnston BC. Are neonatal clinical practice guidelines truly evidence-based? A case for incorporating family values and preferences. *Acta Paediatr*. (2019) 108:1564–6. doi: 10.1111/apa.14879
28. Lau C. Is there an advantage for preterm infants to feed orally in an upright or sidelying position? *J Neonatal Nurs*. (2013) 19:28–32. doi: 10.1016/j.jnn.2012.03.013
29. Lubbe W. Clinicians guide for cue-based transition to oral feeding in preterm infants: an easy-to-use clinical guide. *J Eval Clin Pract*. (2018) 24:80–8. doi: 10.1111/jep.12721
30. Watson J, McGuire W. Responsive versus scheduled feeding for preterm infants. *Cochrane Database Syst Rev*. (2016) CD005255. doi: 10.1002/14651858.CD005255.pub5
31. McGrattan KE, McFarland DH, Dean JC, Hill E, White DR, Martin-Harris B. Effect of single-use, laser-cut, slow-flow nipples on respiration and milk ingestion in preterm infants. *Am J Speech Lang Pathol*. (2017) 26:832–9. doi: 10.1044/2017_AJSLP-16-0052
32. Pados BF, Park J, Dodrill P. Know the flow: milk flow rates from bottle nipples used in the hospital and after discharge. *Adv Neonatal Care*. (2019) 19:32–41. doi: 10.1097/ANC.0000000000000538
33. N. Bell, C. Harding. An investigation of the flow rates of disposable bottle teats used to feed preterm and medically fragile infants in neonatal units across the UK in comparison with flow rates of commercially available bottle teats. *Speech Lang Hear*. (2019) 22:227–35. doi: 10.1080/2050571X.2019.1646463
34. Pados BF, Thoyre SM, Estrem HH, Park J, Knafl GJ, Nix B. Effects of milk flow on the physiological and behavioural responses to feeding in an infant with hypoplastic left heart syndrome. *Cardiol Young*. (2017) 27:139–53. doi: 10.1017/S1047951116000251
35. Lima AH, Cortes MG, Bouzada MC, Friche AA. Preterm newborn readiness for oral feeding: systematic review and meta-analysis. *Codas*. (2015) 27:101–7. doi: 10.1590/2317-1782/20152014104
36. Tian X, Yi LJ, Zhang L, Zhou JG, Ma L, Ou YX, et al. Oral motor intervention improved the oral feeding in preterm infants: evidence based on a meta-analysis with trial sequential analysis. *Medicine*. (2015) 94:e1310. doi: 10.1097/MD.0000000000001310
37. M. Brown Belfort. The science of breastfeeding and brain development. *Breastfeed Med*. (2017) 12:459–61. doi: 10.1089/bfm.2017.0122
38. Victora CG, Bahl R, Barros AJ, Franca GV, Horton S, Krasevec J, et al. Breastfeeding in the 21st century: epidemiology, mechanisms, lifelong effect. *Lancet*. (2016) 387:475–90. doi: 10.1016/S0140-6736(15)01024-7
39. Rollins NC, Bhandari N, Hajeebhoy N, Horton S, Lutter CK, Martines JC, et al. Why invest, and what it will take to improve breastfeeding practices? *Lancet*. (2016) 387:491–504. doi: 10.1016/S0140-6736(15)01044-2
40. Patel S, Patel S. The effectiveness of lactation consultants and lactation counselors on breastfeeding outcomes. *J Hum Lact*. (2016) 32:530–41. doi: 10.1177/0890334415618668
41. Lau C. Breastfeeding challenges and the preterm mother-infant dyad: a conceptual model. *Breastfeed Med*. (2018) 13:8–17. doi: 10.1089/bfm.2016.0206
42. Feldman R. The neurobiology of human attachments. *Trends Cogn Sci*. (2017) 21:80–99. doi: 10.1016/j.tics.2016.11.007
43. Penacoba C, Catala P. Associations between breastfeeding and mother-infant relationships: a systematic review. *Breastfeed Med*. (2019) 14:616–29. doi: 10.1089/bfm.2019.0106
44. Woolridge M. The biomechanics of breastfeeding: bridging the gap between engineering-based studies and clinical practice. *Nestle Nutr Inst Workshop Ser*. (2019) 90:13–32. doi: 10.1159/000490322

45. Mezzacappa ES, Kelsey RM, Katkin ES. Breast feeding, bottle feeding, and maternal autonomic responses to stress. *J Psychosom. Res.* (2005) 58:351–65. doi: 10.1016/j.jpsychores.2004.11.004
46. Lau C. Effects of stress on lactation. *Pediatr Clin North Am.* (2001) 48:221–34. doi: 10.1016/S0031-3955(05)70296-0
47. Lau C, Hurst NM, Smith EO, Schanler RJ. Ethnic/racial diversity, maternal stress, lactation and very low birthweight infants. *J Perinatol.* (2007) 27:399–408. doi: 10.1038/sj.jp.7211770
48. Raskovalova T, Teasley SL, Gelbert-Baudino N, Mauri PA, Schelstraete C, Massoutier M, et al. Breastfeeding assessment score: systematic review and meta-analysis. *Pediatrics.* (2015) 135:e1276–e85. doi: 10.1542/peds.2014-3072
49. Altuntas N, Kocak M, Akkurt S, Razi HC, Kislal MF. LATCH scores and milk intake in preterm and term infants: a prospective comparative study. *Breastfeed Med.* (2015) 10:96–101. doi: 10.1089/bfm.2014.0042
50. Gerçek E, Sarikaya Karabudak S, Ardiç Çelik N, Saruhan A. The relationship between breastfeeding self-efficacy and LATCH scores and affecting factors. *J Clin Nurs.* (2017) 26:994–1004. doi: 10.1111/jocn.13423
51. Tuthill EL, McGrath JM, Graber M, Cusson RM, Young SL. Breastfeeding self-efficacy: a critical review of available instruments. *J Hum Lact.* (2016) 32:35–45. doi: 10.1177/0890334415599533
52. Ho Y-J, McGrath JM. A review of the psychometric properties of breastfeeding assessment tools. *J Obstet Gynecol Neonatal Nurs.* (2010) 39:386–400. doi: 10.1111/j.1552-6909.2010.01153.x
53. Perrella SL, Nancarrow K, Rea A, Murray K, Geddes DT, Simmer KN. Estimates of preterm infants' breastfeeding transfer volumes are not reliably accurate. *Adv Neonatal Care.* (2020). doi: 10.1097/ANC.0000000000000721. [Epub ahead of print].
54. White-Traut R, Rankin K, Lucas R, Shapiro N, Liu L, Medoff-Cooper B. Evaluating sucking maturation using two pressure thresholds. *Early Hum Dev.* (2013) 89:833–7. doi: 10.1016/j.earlhumdev.2013.07.026
55. Sameroff AJ. The components of sucking in the human newborn. *J Exp. Child Psychol.* (1968) 6:607–23. doi: 10.1016/0022-0965(68)90106-9
56. Tarrant SC, Ellis RE, Flack FC, Selley WG. Comparative review of techniques for recording respiratory events at rest and during deglutition. *Dysphagia.* (1997) 12:24–38. doi: 10.1007/PL00009515
57. Lau C, Schanler RJ. Oral motor function in the neonate. *Clin Perinatol.* (1996) 23:161–78. doi: 10.1016/S0095-5108(18)30236-7
58. Mayerl CJ, Gould FDH, Bond LE, Stricklen BM, Buddington RK, German RZ. Preterm birth disrupts the development of feeding and breathing coordination. *J Appl Physiol.* (2019) 126:1681–6. doi: 10.1152/japplphysiol.00101.2019
59. Sanghavi R, Rosen R. Esophageal Dysplagia. In: Ongkasuwan J, Chiou EH, editors, *Pediatric Dysphagia*. Switzerland: Springer Nature, Switzerland (2018). p. 215–38.
60. Sangild PT. Gut responses to enteral nutrition in preterm infants and animals. *Exp. Biol Med (Maywood).* (2006) 231:1695–711. doi: 10.1177/153537020623101106
61. Omari TI, Savilampi J, Kokkinn K, Schar M, Lamvik K, Doeltgen S, et al. The reliability of pharyngeal high resolution manometry with impedance for derivation of measures of swallowing function in healthy volunteers. *Int. J Otolaryngol.* (2016) 2016:2718482. doi: 10.1155/2016/2718482
62. Rommel N, Omari TI, Selleslagh M, Kritas S, Cock C, Rosan R, et al. High-resolution manometry combined with impedance measurements discriminates the cause of dysphagia in children. *Eur. J Pediatr.* (2015) 174:1629–37. doi: 10.1007/s00431-015-2582-9
63. Prabhakar V, Hasenstab KA, Osborn E, Wei L, Jadcherla SR. Pharyngeal contractile and regulatory characteristics are distinct during nutritive oral stimulus in preterm-born infants: Implications for clinical and research applications. *Neurogastroenterol Motil.* (2019) 31:e13650. doi: 10.1111/nmo.13650
64. Li Z-H, Wang D-H, Dong M, Ke M-Y, Wang Z-F. Clinical application of high resolution manometry for examining esophageal function in neonates. *Zhongguo Dang Dai Er Ke Za Zhi.* (2012) 14:607–11.
65. Rayyan M, Omari T, Abu-Assi R, Allegaert K, Rommel N. Effect of esophageal length on high-resolution manometry metrics: extension to the neonatal population. *Neurogastroenterol Motil.* (2020) 32:e13800. doi: 10.1111/nmo.13800
66. Wolff PH. The serial organization of sucking in the young infant. *Pediatrics.* (1968) 42:943–56.
67. Lau C, Smith EO. A novel approach to assess oral feeding skills of preterm infants. *Neonatology.* (2011) 100:64–70. doi: 10.1159/000321987
68. Lau C, Bhat K, Potak DC, Schanler RJ. Oral feeding assessment predicts length of hospital stay in late preterm infants. *J Pediatr Mother Care.* (2015) 1:102. doi: 10.19104/japm.2016.102
69. Lau C, Schanler RJ. Oral feeding in premature infants: advantage of a self-paced milk flow. *Acta Paediatr.* (2000) 89:453–9. doi: 10.1111/j.1651-2227.2000.tb00083.x
70. Lau C, Fucile S, Schanler RJ. A self-paced oral feeding system that enhances preterm infants' oral feeding skills. *J Neonat Nurs.* (2015) 21:121–6. doi: 10.1016/j.jnn.2014.08.004
71. Tanaka S, Kogo M, Chandler SH, Matsuya T. Localization of oral-motor rhythmogenic circuits in the isolated rat brainstem preparation. *Brain Res.* (1999) 821:190–9. doi: 10.1016/S0006-8993(99)01117-8
72. Jean A. Brain stem control of swallowing: neuronal network and cellular mechanisms. *Physiol Rev.* (2001) 81:929–69. doi: 10.1152/physrev.2001.81.2.929
73. Delafield-Butt JT, Freer Y, Perkins J, Skulina D, Schogler B, Lee DN. Prospective organization of neonatal arm movements: a motor foundation of embodied agency, disrupted in premature birth. *Dev Sci.* (2018) 21:e12693. doi: 10.1111/desc.12693
74. Craig CM, Grealy MA, Lee DN. Detecting motor abnormalities in preterm infants. *Exp. Brain Res.* (2000) 131:359–65. doi: 10.1007/s002219900227
75. Craig CM, Lee DN. Neonatal control of nutritive sucking pressure: evidence for an intrinsic tau-guide. *Exp Brain Res.* (1999) 124:371–82. doi: 10.1007/s002210050634
76. McFarland DH, Tremblay P. Clinical implications of cross-system interactions. *Semin. Speech Lang.* (2006) 27:300–9. doi: 10.1055/s-2006-955119
77. Barlow SM, Estep M. Central pattern generation and the motor infrastructure for suck, respiration, and speech. *J Commun. Disord.* (2006) 39:366–80. doi: 10.1016/j.jcomdis.2006.06.011
78. White-Traut RC, Berbaum ML, Lessen B, McFarlin B, Cardenas L. Feeding readiness in preterm infants: the relationship between preterm behavioral state and feeding readiness behaviors and efficiency during transition from gavage to oral feeding. *MCN Am J Matern Child Nurs.* (2005)30:52–9.
79. Gill NE, Behnke M, Conlon M, Anderson GC. Nonnutritive sucking modulates behavioral state for preterm infants before feeding. *Scand J Caring Sci.* (1992) 6:3–7. doi: 10.1111/j.1471-6712.1992.tb00115.x
80. Als H, A synactive model of neonatal behavior organization: framework for the assessment of neurohehavioral development in the preterm infant and for support of infants and parents in the neonatal intensive care environment. *Phys Occup Ther Pediatr.* (1986) 6:3–55. doi: 10.1080/J006v06n03_02
81. DeArmond AC, Yello JR, Bubshait KS, Krueger CA. Revisiting sound in the NICU: implications for the developmental timing, amount and type of sound. *Pediatr Neonatal Nurs.* (2016) 2. doi: 10.16966/2470-0983.116
82. Moore ER, Bergman N, Anderson GC, Medley N. Early skin-to-skin contact for mothers and their healthy newborn infants. *Cochrane Database Syst Rev.* (2016) 11:CD003519. doi: 10.1002/14651858.CD003519.pub4
83. Conde-Agudelo A, Diaz-Rossello JL. Kangaroo mother care to reduce morbidity and mortality in low birthweight infants. *Cochrane Database Syst Rev.* (2016) CD002771. doi: 10.1002/14651858.CD002771.pub4
84. Bieleninik L, Ghetti C, Gold C. Music Therapy for preterm infants and their parents: a meta-analysis. *Pediatrics.* (2016) 138:e20160971. doi: 10.1542/peds.2016-0971
85. Field T. Massage therapy for infants and children. *J Dev Behav Pediatr.* (1995) 16:105–111. doi: 10.1097/00004703-199504000-00008
86. Leleu A, Rekow D, Poncet F, Schaal B, Durand K, Rossion B, et al. Maternal odor shapes rapid face categorization in the infant brain. *Dev Sci.* (2020) 23:e12877. doi: 10.1111/desc.12877
87. Lau C, Fucile S, Gisel EG. Impact of nonnutritive oral motor oral stimulation and infant massage on oral feeding skills in preterm infants. *J Neonatal Perinatol Med.* (2012) 5:311–7. doi: 10.3233/NPM-1262612
88. Fucile S, Gisel E, Lau C. Oral stimulation accelerates the transition from tube to oral feeding in preterm infants. *J. Pediatr.* (2002) 141:230–6. doi: 10.1067/mpd.2002.125731

89. Lau C, Smith E. Interventions to improve the oral feeding performance of preterm infants. *Acta Paediatr.* (2012) 101:e269–e74. doi: 10.1111/j.1651-2227.2012.02662.x
90. Pados BF, McGlothen-Bell K. Benefits of infant massage for infants and parents in the NICU. *Nurs Womens Health.* (2019) 23:265–71. doi: 10.1016/j.nwh.2019.03.004
91. Niemi AK. Review of randomized controlled trials of massage in preterm infants. *Children (Basel, Switzerland).* (2017) 4:21. doi: 10.3390/children4040021
92. Field T, Schanberg SM, Scafidi F, Bauer CR, Vega-Lahr N, Garcia R, et al. Tactile/kinesthetic stimulation effects on preterm neonates. *Pediatrics.* (1986) 77:654–8.
93. Nudo RJ, Wise BM, SiFuentes F, Milliken GW. Neural substrates for the effects of rehabilitative training on motor recovery after ischemic infarct. *Science.* (1996) 272:1791–4. doi: 10.1126/science.272.5269.1791
94. Byl NN, Merzenich MM, Cheung S, Bedenbaugh P, Nagarajan SS, Jenkins WM. A primate model for studying focal dystonia and repetitive strain injury: effects on the primary somatosensory cortex. *Phys Ther.* (1997) 77:269–84. doi: 10.1093/ptj/77.3.269
95. Als H. Toward a synactive theory of development: promise for the assessent and support of infant individuality. *Infant Ment Health J.* (1982) 3:229–43. doi: 10.1002/1097-0355(198224)3:4<229::AID-IMHJ2280030405>3.0.CO;2-H
96. Als H. A manual for naturalistic observation of the newborn (preterm and full term infants). In: Goldson E, editor, *Nurturing the Premature Infant, Developmental Interventions in the Neonatal Intensive Care Nursery.* New York, NY: Oxford University Press (1995). p. 77–85.
97. Vandenberg KA. Individualized developmental care for high risk newborns in the NICU: a practice guideline. *Early Hum Dev.* (2007) 83:433–42. doi: 10.1016/j.earlhumdev.2007.03.008
98. Roué J-M, Kuhn P, Lopez Maestro M, Maastrup RA, Mitanchez D, Westrup B, et al. Eight principles for patient-centred and family-centred care for newborns in the neonatal intensive care unit. *Arch Dis Child Fetal Neonatal Ed.* (2017) 102:F364–F8. doi: 10.1136/archdischild-2016-312180
99. Macho P. Individualized developmental care in the NICU: a concept analysis. *Adv Neonatal Care.* (2017) 17:162–74. doi: 10.1097/ANC.0000000000000374

Conflict of Interest: The author declares that the research was conducted in the absence of any commercial or financial relationships that could be construed as a potential conflict of interest.

frontiers in Pediatrics

ORIGINAL RESEARCH
published: 14 August 2020
doi: 10.3389/fped.2020.00455

Sirt1 Regulates Oxidative Stress in Oxygen-Glucose Deprived Hippocampal Neurons

Lina Shi[1†], *Jing Zhang*[1†], *Yan Wang*[2], *Qingfei Hao*[1], *Haoming Chen*[1] *and Xiuyong Cheng*[1*]

[1] *Department of Neonatology, The First Affiliated Hospital of Zhengzhou University, Zhengzhou, China,* [2] *Department of Pediatrics, Henan Medical College, Xinzheng, China*

Oxidative stress is an important mechanism of neonatal hypoxic-ischemic brain damage. Sirtuin1 (Sirt1) is a deacetylase that depends on NAD^+, which has an important role in antioxidant metabolism. Furthermore, peroxisome proliferator-activated receptor γ-co-activator 1α (PGC-1α) is a key regulator of mitochondrial oxidative stress, which is regulated by Sirt1. Here, we investigated the role of Sirt1 in the pathogenesis of brain injuries after modulating its activity in primary cultured hippocampal neurons. Our study shows that the expression of Sirt1 was downregulated after oxygen-glucose deprivation. Activation of Sirt1 with resveratrol improved cell's resistance to oxidative stress, whereas inhibition of Sirt1 with EX527 significantly reduced cell viability after cellular oxidative stress. Our study also shows that activation of Sirt1 with resveratrol exerts its antioxidant effect by regulating the expression of PGC-1α. In contrast, application of EX527 decreased the expression of PGC-1α. In summary, these results confirmed that Sirt1 is a potent protective factor for neurons subjected to oxidative stress, and the protective effect of Sirt1 is attributed to its regulation of PGC-1α.

Keywords: hypoxic, ischemic, oxidative stress, pgc-1α, sirt1, resveratrol

OPEN ACCESS

Edited by:
Yuan Shi,
Children's Hospital of Chongqing Medical University, China

Reviewed by:
Lai Shuan Wang,
Fudan University, China
Xinlin Hou,
Peking University First Hospital, China

****Correspondence:***
Xiuyong Cheng
fccchengxy@zzu.edu.cn

†These authors have contributed equally to this work

Specialty section:
This article was submitted to Neonatology, a section of the journal Frontiers in Pediatrics

Received: *19 April 2020*
Accepted: *30 June 2020*
Published: *14 August 2020*

Citation:
Shi L, Zhang J, Wang Y, Hao Q, Chen H and Cheng X (2020) Sirt1 Regulates Oxidative Stress in Oxygen-Glucose Deprived Hippocampal Neurons. Front. Pediatr. 8:455. doi: 10.3389/fped.2020.00455

INTRODUCTION

Although therapeutic hypothermia has been widely applied, 40–50% of Hypoxic ischemic encephalopathy (HIE) neonates still have some neurodevelopmental problems (1). Hypoxic ischemia (HI) involves multiple mechanisms, but the detailed pathogenesis is still unclear. Therefore, studies aiming to reducing morbidity and mortality of neonates with brain injuries are still needed.

Oxidative stress is one of the most important mechanisms of perinatal HI. After hypoxia and ischemia, the production of reactive oxygen species (ROS) rapidly accumulates and leads to mitochondrial dysfunction and delayed neuronal death. Oxidative stress-mediated mitochondrial damage has been shown to be involved in apoptosis.

Sirtuins are a class of NAD^+-dependent histone deacetylases widely expressed in living organisms. Sirt1, also named as sirtuin1, is the most widely studied sirtuin has been an important therapeutic target in recent years. The translated protein has a molecular weight of about 60 kD and exhibits NAD^+-dependent deacetylase activity. Previous studies showed that Sirt1 can regulate diabetes-induced cardiac dysfunction and brain ischemic reperfusion injuries by preventing mitochondrial dysfunction and alleviating hepatic steatosis (2–4). A large number *in vitro* and *in vivo* studies have shown that the activation of Sirt1 enhances mitochondrial biogenesis and augments oxidative metabolic capacity through different pathways (5). Studies also show that Sirt1

regulates apoptosis through other pathways, such as the anti-inflammatory pathway of NF-κB acetylation and the regulation of AMPK in autophagy (6, 7). Additionally, evidence has revealed that enhancing Sirt1 activity can reduce ROS production, reduce inflammation of neurons and glial cells, so as to reduce neuronal cell death (8). However, the role of Sirt1 in perinatal brain injuries is not completely understood.

Resveratrol (RSV) is a kind of polyphenol, a plant secondary metabolite extracted from wine, grain, fruit, root, etc., which has a protective effect on cardiovascular and nervous system diseases by regulating anti-inflammatory and anti-oxidation processes. Some studies have also reported that resveratrol is an activator of Sirt1 (9–11). According to a study on diabetic nephropathy by Tao Zhang et al., RSV can improve mitochondrial function, reduce oxidative stress in podocytes, and inhibit apoptosis induction through the Sirt1/PGC-1a axis (12). There is evidence in a brain injury model that RSV has a protective effect (13, 14). In contrast, EX527 is an effective selective Sirt1 inhibitor, which can inhibit Sirt1 deacetylase activity effectively. Maayan Waldman et al. showed that EX527 could increase ROS production by inhibiting Sirt1 activity, which aggravates myocardial injuries caused by diabetes (15). Another study on ischemic strokes also showed that EX527 can aggravate the expression of apoptotic proteins (16).

PGC-1α is a potent stimulator of mitochondrial biogenesis and respiration. It potentially increases neuroprotection while stimulating a broad anti-ROS response via mitochondrial function adaptation in neurological diseases such as Parkinson's disease, Alzheimer's disease, and brain trauma (17, 18). It has been shown that PGC-1α can be activated by deacetylation of Sirt1. Both play an important role in mitochondrial oxidative stress, including anti-oxidative stress, inhibition of inflammatory response, and reduction of apoptosis (19).

HI often causes damage to the hippocampus. In this study, based on a model of oxygen-glucose deprived primary cultured hippocampal neurons, we used RSV and EX527, an agonist and inhibitor of Sirt1, respectively, to investigate the mechanism and potential pathway of Sirt1 in HI.

MATERIALS AND METHODS

Model Construction

Primary Culture of Hippocampal Neurons

All animal studies were approved by the Zhengzhou University committee for animal care and use for animal research. The experimental operation was performed according to the international guidelines for animal studies. Pregnant Sprague-Dawley rats were purchased from the Huaxing experimental animal farm (Zhengzhou, China). We followed an established protocol, obtaining rat embryonic hippocampal neurons from 18-day-old pregnant Sprague-Dawley rats. The hippocampus was detached under a microscope and then digested by trypsin (Hyclone, USA) at 37°C for 10–15 min. Single cells were obtained by blowing and centrifuging. The cell suspension was transferred into planting medium containing DMEM/high glucose (Hyclone, USA), 10% (v/v) fetal bovine serum (Hyclone, USA), 1% (v/v) glutamine (Hyclone, USA), and 1% (v/v) penicillin/streptomycin solution (Hyclone, USA), and subsequently plated on plates pretreated with poly-D-lysine (Sigma, USA). The density was 7×10^5 cells/well in 6-well plates or 2×10^4 cells/well in 96-well plates. After 4 h of incubation, the planting medium was replaced with an equal volume of maintenance medium containing neurobasal medium (Gibco, USA), 2% (v/v) B-27 (Gibco, USA), 1% (v/v) glutamine (Hyclone, USA), and 0.5% penicillin/streptomycin solution (Hyclone, USA). Half of the medium was replaced every 3 days.

Purity Identification

NeuN is a neuronal protein that is localized in the nuclei and the perinuclear cytoplasm of most neurons in the central nervous system of mammals (20). We used immunofluorescent NeuN antibodies that labeled the neurons in order to confirm their purity. The experiment was performed on the 7th *in vitro* day. The coverslips were rinsed in PBS and the cells were fixed in 4% paraformaldehyde in PBS for 30 min. After being incubated in blocking solution (10% donkey serum and 0.06% Triton X-100 in PBS), the coverslips were treated with NeuN antibodies (Millipore, 1:100, USA) and FITC goat anti-mouse antibodies (Abclonal, 1:50, China) in diluting solution (0.01% Triton X-100 and 1% donkey serum in PBS). Then, the coverslips were mounted using DAPI (Vector Lab, Chicago) and the cells were observed under a microscope coupled to a camera. The ratio of the stained cytoplasm and nuclei represented the purity of the neuron.

The Oxygen-Glucose Deprivation Model

The oxygen glucose deprivation (OGD) model is a common cell level model to simulate neonatal hypoxic-ischemic brain damage. Although the time of hypoxia varies (21–23), our previous experiments showed that 30 min of hypoxia can build a successful model for hippocampal neurons (24). To induce OGD, we removed the maintaining medium and switched to DMEM without glucose (Gibco, USA). In this medium, cells were incubated at 37°C for 30 min in a sealed chamber, ventilated with 5% CO_2/95% N_2. At the end, the medium was replaced with normal medium. The cells were incubated for 12 h under normal conditions for subsequent experiments.

RSV and EX527 Treatment and Effect

RSV and EX527 Treatment

Cells were divided into four groups during EX527 treatment (control, OGD, OGD+EX527, OGD+EX527+RSV) and three groups during RSV treatment (control, OGD, OGD+RSV). Cells were pretreated with 25 μM EX527 (MedChemExpress, USA) for 3 hours before OGD, and post-treated with 20 μM RSV (Solarbio, China) immediately after OGD.

MTT for Cell Viability

MTT reduces succinate dehydrogenase in mitochondria of living cells to water-insoluble blue-purple crystalline armor (Formazan) and deposits it in cells. As this process cannot happen in dead cells, it can be used to examine cell viability. Cells were plated into 96-well plates. We analyzed the cells 12 h after OGD induction. We added 10 μl MTT (Amresco, USA) to all groups and

incubated the cells for 4 h. Then, the medium was removed and 100 μl DMSO (Amersco, USA) was added. Finally, we detected absorbance at 562 nm with a microplate reader. Cell viability was calculated as (100%) = (experiment group—blank)/(control group—blank) × 100%.

MDA and SOD Levels

After they were exposed to the different treatments, the neurons were harvested, sonicated, and centrifuged to collect the supernatant. The supernatant was used to examine the levels of SOD and Malondialdehyde (MDA). Cellular MDA content and total SOD activity were examined using commercial assay kits (Jiancheng Institute of Biotechnology, Nanjing, China) according to the manufacturer's instructions. The absorbance was read at 450 nm for SOD activity and at 532 nm for MDA content. The bicinchoninic acid disodium protein assay kit (Solarbio Biotechnology, China) was used to quantify the concentration of total protein.

Flow Cytometry for Cell Apoptosis

Phosphatidylserine, located inside the cell membrane, migrates to the outside of the cell membrane at the early stage of apoptosis. Phosphatidyl binding protein V (Annexin V) is a calcium-dependent phospholipid-binding protein with high affinity to phosphatidylserine. Therefore, the apoptotic cells can be detected by Annexin V and flow cytometry combined with PI rejection. The procedure was performed following the manufacturer's instruction (BD, USA). Cells were analyzed by flow cytometry within 1 h.

Gene Expression With Quantitative RT-PCR

Quantitative RT-PCR assays were performed to measure the mRNA levels of *Sirt1* and *PGC-1α*. Total RNA was extracted using TRIzol Reagent (Invitrogen, USA) according to the manufacturer's protocol. An aliquot of 1 μg of total RNA was reversely transcribed using PrimeScript RT Master Mix (Takara, Japan). Quantitative PCR was performed using TB Green Premix Ex Taq (Takara, Japan). The forward primer for *Sirt1* was ACTGGAGCTGGGGTTTCT and the reverse primer for *Sirt1* was CTTGAGGGTCTGGGGAGGT. The forward primer for *PGC-1α* was TTCCAACAAACACATGCAC and the reverse primer for *PGC-1α* was CGCATTTCTAAAGCACCAG. *GAPDH* was used as an internal reference to normalize the data. The forward primer for *GAPDH* was ACAGCAACAGGGTGGTGG

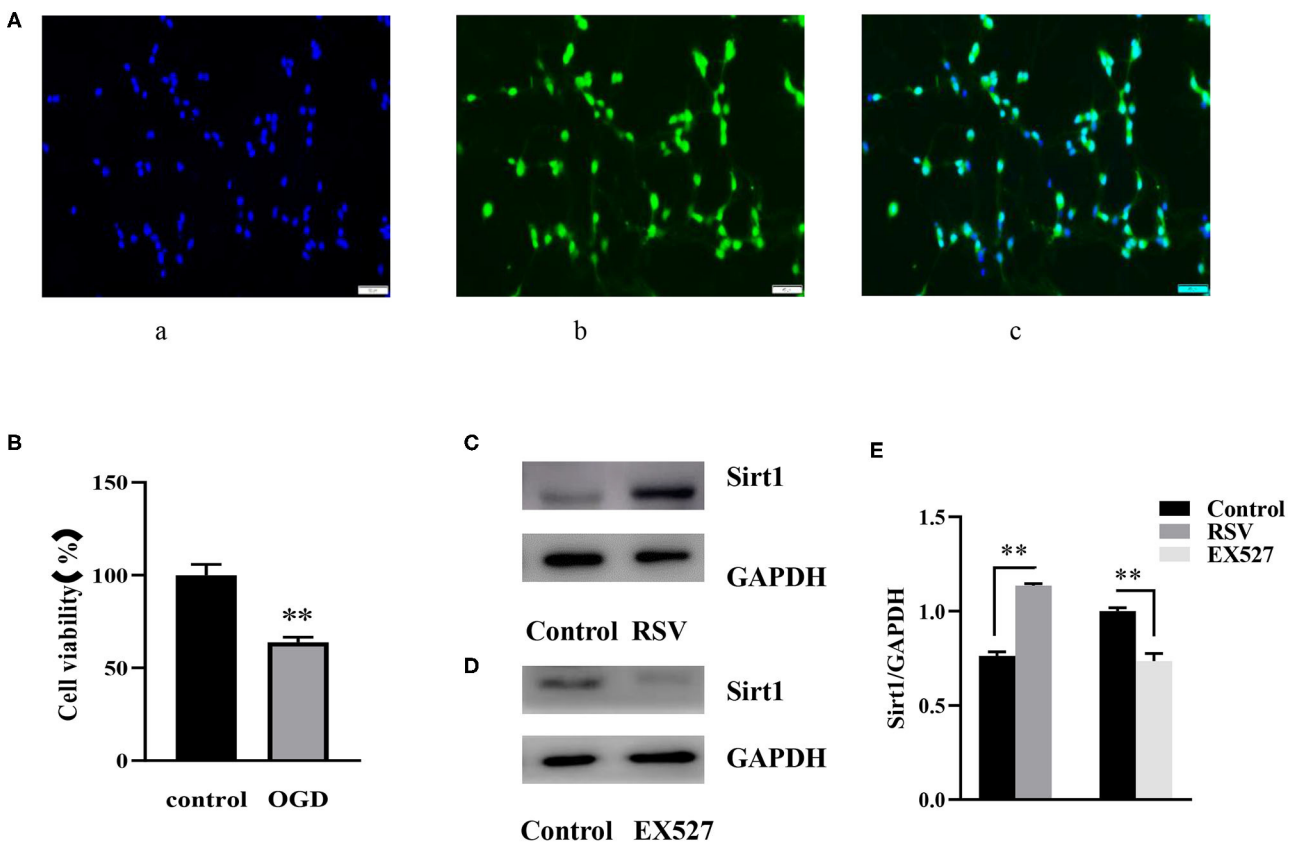

FIGURE 1 | (A) Immunofluorescence of NeuN (400×). **(A)** (a) DAPI-stained nuclei (blue), **(A)** (b) NeuN staining identifies neurons (green), **(A)** (c) Merge image of a and b. A indicates the purity of the cultured cells. **(B)** Effects of OGD on cell viability were determined by an MTT assay ($n = 6$). **(C)** Western blot analysis of Sirt1 in the RSV (20 μM) group compared to the control group ($n = 3$). **(D)** Western blot analysis of Sirt1 in the EX527 (25 μM) group compared to the control group ($n = 3$). **(E)** Bar graph showing the relative *Sirt1* protein levels in each group. Data were obtained from three independent experiments. $^{**}P < 0.01$.

AC and the reverse primer was TTTGAGGGTGCAGCGAACT T. The RT-PCR parameters were as follows: 95°C for 30 s, 40 cycles of 95°C for 30 s, 54°C for 30 s, and 72°C for 45 s. The CT values were recorded as primary data, normalized according to their corresponding internal references, and analyzed using the $2^{-\Delta\Delta CT}$ method. The relative gene expression was noted as the final results and statistically analyzed.

Western Blot

Western blot analysis was performed to measure the protein levels of Sirt1, PGC-1α, and caspase-3 using a standard protocol. Equal amounts of total protein, along with 5 μl of molecular weight marker (Thermo Fisher, USA), were electrophoresed on SDS-PAGE gels. After being incubated with primary antibodies and secondary antibodies, we exploited the Chemiluminescent HRP Substrate (Millipore, USA) to visualize the target proteins (Sirt1, 1:2,000, Bioss, China; PGC-1α, Cell Signaling Technology, 1:1,000; caspase-3, 1:1,000, Cell Signaling Technology, USA; GAPDH and β-actin, 1:10,000, Abclonal, China). The molecular weights of Sirt1 and PGC-1α are 58 and 130 kD, respectively. Finally, we used an Amersham Imager 600 to take pictures and ImageJ to analyze the gray-scale values. Every protein was normalized to its corresponding internal reference. The ratios were noted as the final results and statistically analyzed.

Statistics Analysis

All population data were expressed as means ± SD. Statistical analysis was performed by using GraphPad Prism (GraphPad Software). A $P < 0.05$ was considered significant.

RESULTS

Successful Model Construction

Cell Purity

As shown in **Figure 1A** (c), almost all blue cell nuclei (DAPI) are surrounded by green fluorescence (NeuN), indicating that almost all cultured cells were hippocampal neurons. The result showed that the cultured cells were of high purity and could be used in subsequent experiments.

Cell Viability Decreased After OGD

Twelve hours after OGD, cell viability of the control and OGD group was 100% and 63.785 ± 2.819%, respectively (**Figure 1B**). Compared to the control group, cell viability in the OGD group was significantly decreased, indicating that OGD was successfully induced.

Sirt1 Was Downregulated After OGD

The relative *Sirt1* mRNA levels in the control and the OGD group were 1 and 0.780 ± 0.070, respectively. Compared to the control group, the relative expression in the OGD group was decreased

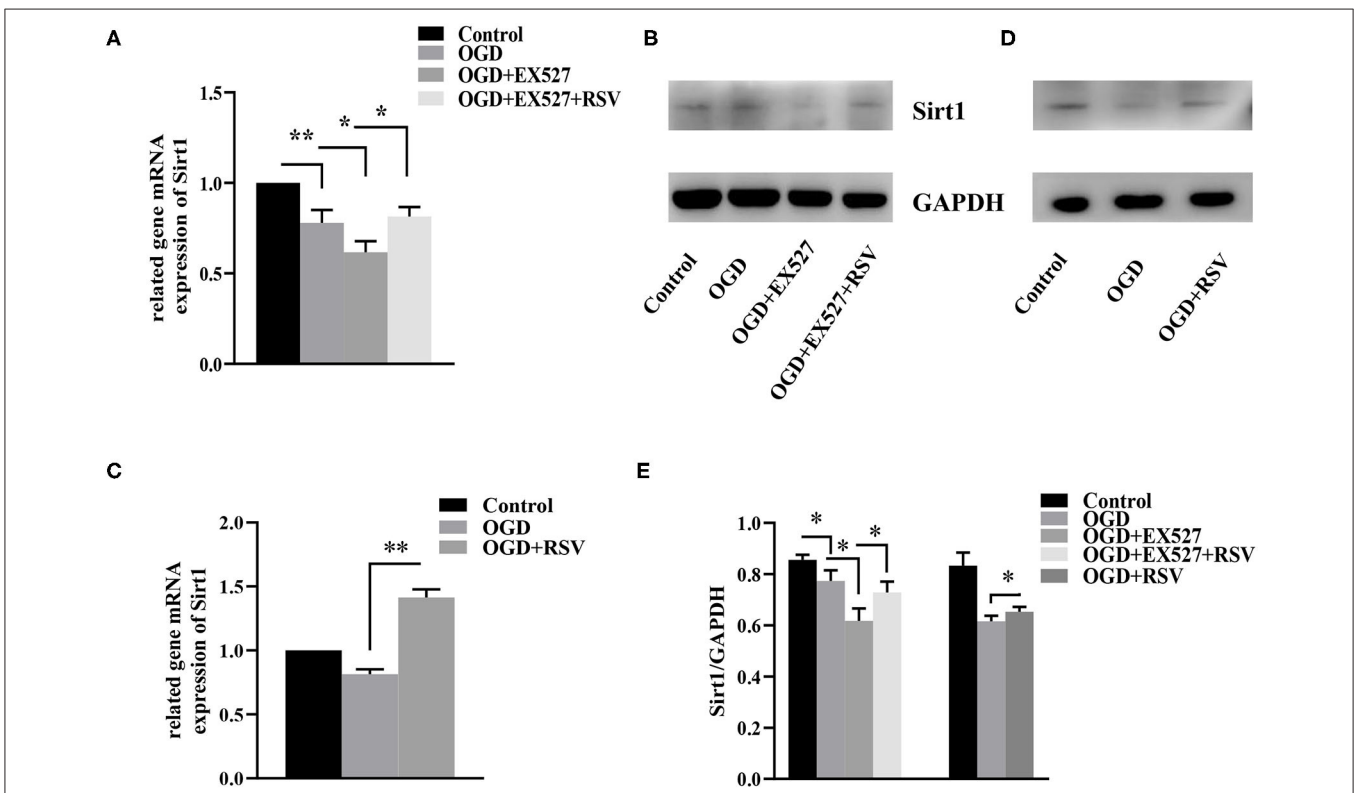

FIGURE 2 | (A) Relative *Sirt1* mRNA levels in different groups after EX527 treatment ($n = 3$). **(B)** Relative Sirt1 protein levels in different groups after EX527 treatment ($n = 3$). **(C)** Relative *Sirt1* mRNA levels in different groups after RSV treatment ($n = 3$). **(D)** Western blot analysis of Sirt1 in different groups after RSV treatment ($n = 3$). **(E)** Bar graph showing the relative *Sirt1* protein levels in each group. Data were obtained from three independent experiments. *$P < 0.05$, **$P < 0.01$.

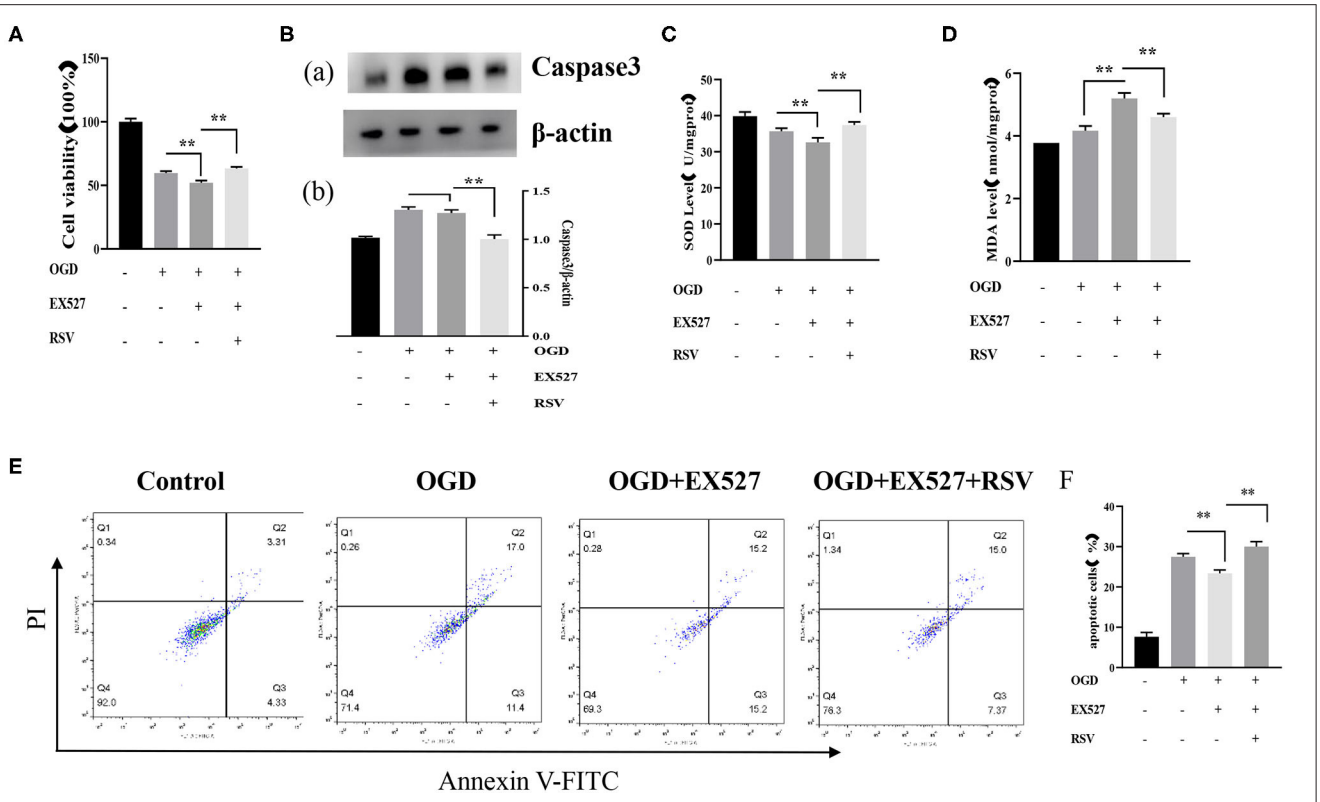

FIGURE 3 | (A) Effects of EX527 treatment on the viability of OGD-treated cells was determined by the MTT assay ($n = 6$). **(B)** (a) Western blot analysis of Caspase-3 in different groups ($n = 3$). (b) Bar graph showing the relative *Caspase-3* protein levels in each group. **(C)** Intracellular SOD levels in different groups ($n = 6$). **(D)** Intracellular MDA levels in different groups ($n = 6$). **(E)** Flow cytometry analysis of apoptotic neurons with different treatments. **(F)** Flow cytometry analysis of apoptotic cells with different treatments ($n = 6$). Data were obtained from three independent experiments $^{**}P < 0.01$.

($P < 0.01$). Sirt1 protein levels were also lower in the OGD group than in the control group (0.856 ± 0.020 vs. 0.773 ± 0.042, $P < 0.05$, **Figures 2A,B**).

Effects of EX527 and RSV at Specific Concentrations on Sirt1 Expression in Normal Cells

After preliminary experiments, we chose to apply 25 μM EX527 3 h before the OGD induction, and 20 μM RSV immediately after OGD. At this concentration, RSV upregulated the expression of Sirt1 protein without affecting cell viability (0.763 ± 0.022 vs. 1.135 ± 0.010, $P < 0.01$, **Figure 1C**). EX527 downregulated the expression of Sirt1 (1.000 ± 0.017 vs. 0.735 ± 0.040, $P < 0.01$, **Figure 1D**). The relative Sirt1 protein levels in each group was showed in Bar graph (**Figure 1E**). Therefore, they can be used to increase or decrease Sirt1 activity, respectively, for subsequent experiments.

EX527 Treatment Effects After OGD

Effect of EX527 on Sirt1 Expression After OGD

The relative levels of *Sirt1* mRNA in the control group, the OGD group, the OGD+EX527 group, and the OGD+EX527+RSV group were 1, 0.780 ± 0.070, 0.620 ± 0.062, and 0.815 ± 0.052, respectively (**Figure 2A**). Sirt1 protein levels were 0.856 ± 0.020, 0.773 ± 0.042, 0.618 ± 0.047, and 0.728 ± 0.042, respectively (**Figure 2B**). The relative Sirt1 protein levels in different groups after EX527 treatment was showed in Bar graph (**Figure 2E**). Compared to the OGD group, the relative levels of both Sirt1 mRNA and protein in the OGD+EX527 group were decreased ($P < 0.05$, $P < 0.05$). The mRNA and protein levels in the OGD+EX527+RSV group were higher than in the OGD+EX527 group ($P < 0.05$, $P < 0.05$). So, EX527 can reduce Sirt1 expression after OGD.

Pretreatment of EX527 Increased Apoptosis and Decreased Cell Viability After OGD

Apoptosis was detected via MTT, caspase-3, and Annexin V-FITC/PI. The cell viability in the OGD+EX527 group was lower than in the OGD group as detected via the MTT method (59.694 ± 1.524% vs. 52.062 ± 1.805%, $P < 0.01$, **Figure 3A**). **Figure 3E** showed the apoptosis in different groups after EX527 treatment. The apoptosis rate of the OGD+EX527 group was higher than in the OGD group as detected by flow cytometry analysis (27.267 ± 0.804% vs. 30.000 ± 1.251%, $P < 0.01$, **Figure 3F**). Oxidative stress results showed that EX527 weakened the protection of ROS. The intracellular SOD level of the OGD+EX527 group was lower than in the OGD group (35.692 ± 0.833 U/mgprot vs. 32.598 ± 1.272 U/mgprot, $P < 0.01$, **Figure 3C**). The intracellular MDA content of the OGD+EX527 group was higher than in the OGD group (4.166

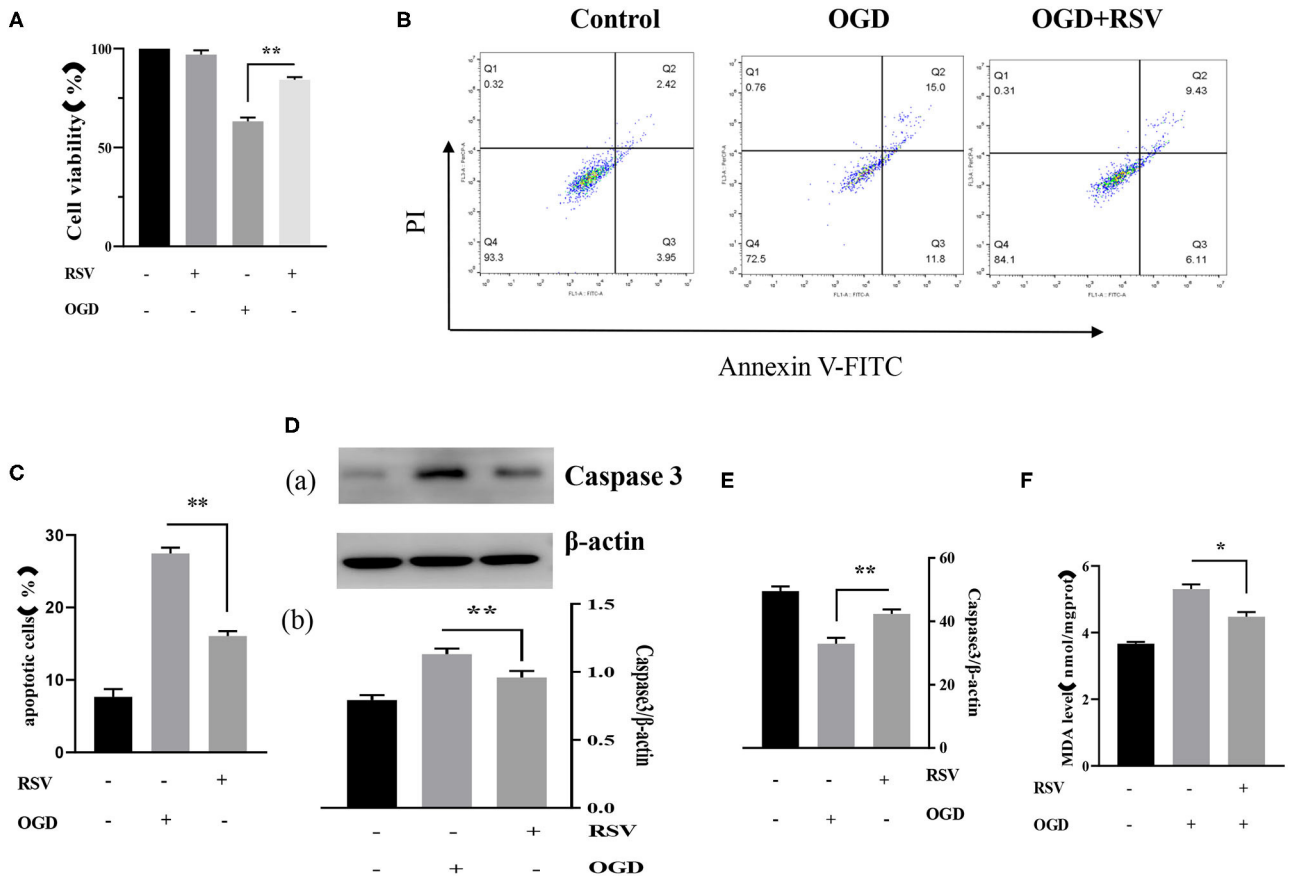

FIGURE 4 | (A) Effects of RSV treatment on the viability of OGD-treated cells was determined by the MTT assay ($n = 6$). **(B)** Flow cytometry analysis of apoptotic neurons with different treatments. **(C)** Flow cytometry analysis of apoptotic cells with different treatments ($n = 6$). **(D)** (a) Western blot analysis of Caspase-3 in different groups ($n = 3$). (b) Bar graph showing the relative *Caspase-3* protein levels in each group. **(E)** Intracellular SOD levels of different groups ($n = 6$). **(F)** Intracellular MDA levels of different groups ($n = 6$). Data were obtained from three independent experiments. $^*P < 0.05$, $^{**}P < 0.01$.

± 0.149 nmol/mgprot vs. 5.196 ± 0.176 nmol/mgprot $P < 0.01$, **Figure 3D**). However, the expression of caspase-3 in the OGD+EX527 group did not increase significantly compared to the OGD group (1.304 ± 0.300 vs. 1.272 ± 0.033, $P > 0.05$, **Figure 3B**). Conversely, RSV increased Sirt1 expression and cell viability. As shown in **Figure 3**, compared to the OGD + EX527 group, the cell viability and oxidative stress indices of the OGD + EX527 + RSV group had corresponding changes.

RSV Treatment Effects After OGD

Effect of RSV on Sirt1 Expression After OGD

The relative levels of *Sirt1* mRNA in the control group, the OGD group, and the OGD+RSV group were 1, 0.814 ± 0.038, and 1.415 ± 0.064, respectively (**Figure 2C**). The protein levels were 0.833 ± 0.051, 0.609 ± 0.011, and 0.653 ± 0.019, respectively (**Figure 2D**). The relative Sirt1 protein levels in different groups after RSV treatment was showed in Bar graph (**Figure 2E**). Compared to the OGD group, Sirt1 mRNA and protein levels were increased in the OGD+RSV group, indicating that RSV can increase Sirt1 expression after OGD ($P < 0.01$, $P < 0.05$).

RSV Treatment Decreased Apoptosis and Increased Cell Viability After OGD

Apoptosis was examined in the same way as described above. Our experiments showed that RSV treatment decreased apoptosis. The cell viability of the OGD+RSV group was higher than in the OGD group, as detected by the MTT method (63.238 ± 1.931% vs. 84.240 ± 1.322%, $P < 0.01$, **Figure 4A**). **Figure 4B** showed the apoptosis in different groups after RSV treatment. The apoptosis rate of the OGD+RSV group was lower than in the OGD group, detected by flow cytometry analysis (27.267 ± 0.804% vs. 16.951 ± 0.679%, $P < 0.01$, **Figure 4C**). The results showed that RSV treatment could reduce caspase-3-mediated apoptosis (1.130 ± 0.041 vs. 0.960 ± 0.470, $P < 0.01$, **Figure 4D**). Intracellular SOD and MDA levels are common indicators of oxidative stress. Our experiments showed that RSV could reduce intracellular oxidative stress. The intracellular SOD level of the OGD+RSV group was higher than in the OGD group (32.904 ± 1.891 U/mgprot vs. 42.339 ± 1.393 U/mgprot, $P < 0.01$, **Figure 4E**). The intracellular MDA levels of the OGD+RSV group were lower than of the OGD group (5.307 ± 0.141 nmol/mgpro vs. 4.477 ± 0.139 nmol/mgprot, $P < 0.01$, **Figure 4F**).

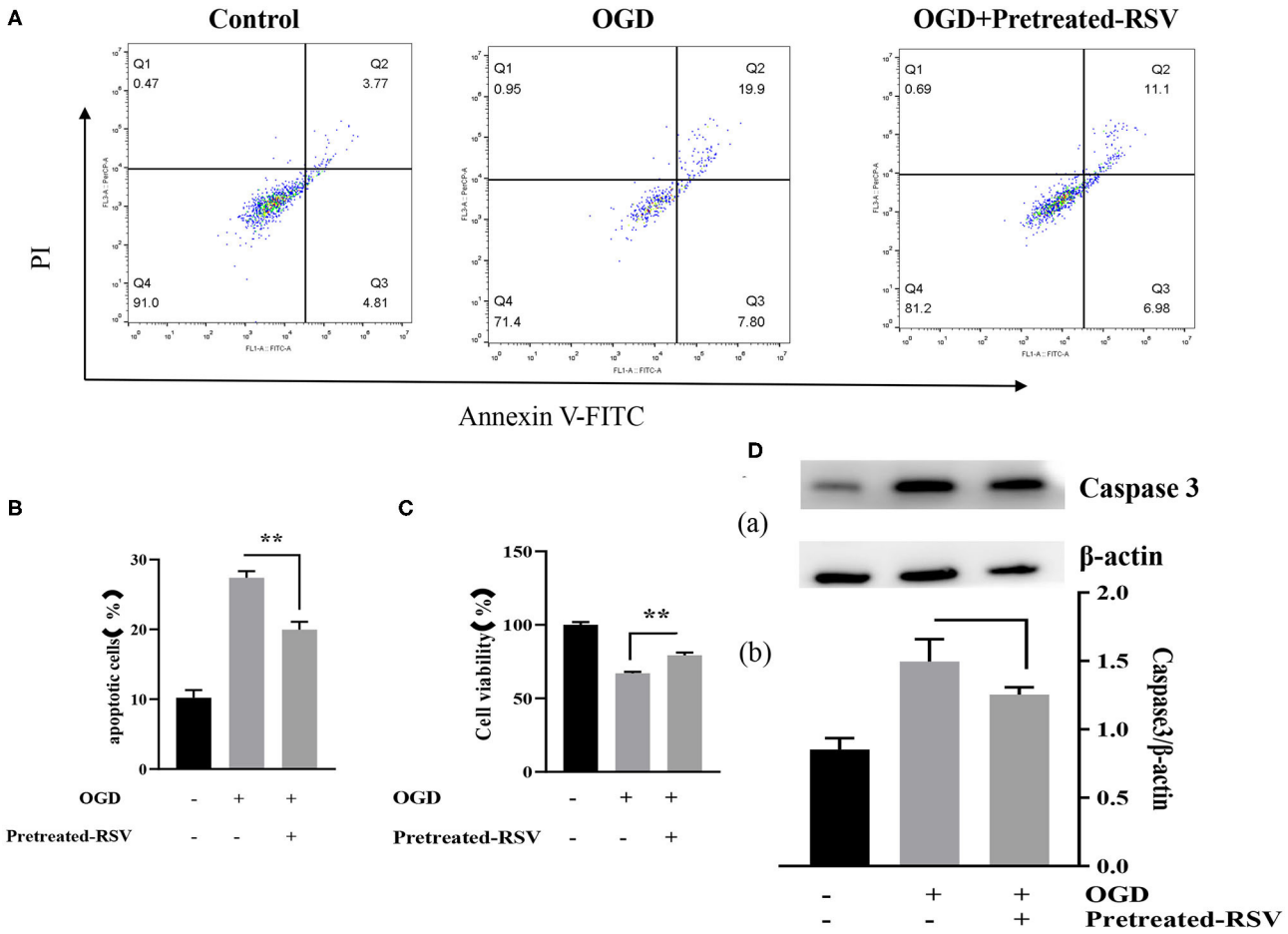

FIGURE 5 | (A) Flow cytometry analysis of apoptotic cells with different treatments. **(B)** Apoptotic cells in different groups are shown as mean ± SD ($n = 6$). **(C)** Cell viability of pretreated-RSV cells compared to the OGD group ($n = 6$). **(D)** (a) Western blot analysis of Caspase-3 in different groups (n = 3). (b) Bar graph showing the relative *Caspase-3* protein levels in each group. Data were obtained from three independent experiments. $^{**}P < 0.01$.

RSV Pretreatment Was Also Protective for OGD

To further investigate the expression of Sirt1, we analyzed protective effects by adding RSV 4 h before OGD. We performed flow cytometry analysis and apoptosis-related protein expression analysis to test the potential benefit of RSV application. **Figure 5A** showed the apoptosis in different groups after RSV pretreatment. The apoptosis rate of the OGD+pretreated RSV group was lower than of the OGD group as assessed by flow cytometry analysis (27.397 ± 0.942% vs. 19.952 ± 1.130%, $P < 0.01$, **Figure 5B**). The cell viability of the OGD+pretreated RSV group was higher than in the OGD group as detected with the MTT method (67.012 ± 1.055% vs. 79.277 ± 1.892%, $P < 0.01$, **Figure 5C**). Therefore, increasing Sirt1 activity before OGD can also reduce apoptosis. However, we did not detect a decrease in caspase-3 expression (1.497 ± 0.163 vs. 1.253 ± 0.054, $P > 0.05$, **Figure 5D**).

Sirt1 Was Involved in Apoptosis by Regulating PGC-1α Levels

PGC-1α is regulated by Sirt1 and is involved in mitochondrial oxidative stress. Therefore, we also tested the change in the expression of PGC-1α after addition of RSV or EX527. As shown in **Figure 6**, compared to the OGD group, the relative levels of Sirt1 and PGC-1α mRNA and protein levels in the OGD+EX527 group were decreased. Compared to the OGD+EX527 group, the relative mRNA levels of *Sirt1* and *PGC-1α* in the OGD+EX527+RSV group were both increased. However, although the relative expression levels of Sirt1 protein was increased, PGC-1α protein levels were not significantly increased, which was mainly because the changes of PGC-1α protein were not synchronized at the time point we selected.

DISCUSSION

Despite the fact that therapeutic hypothermia is an effective treatment in hypoxic ischemia, neonatal brain injury is still one of the main reasons for morbidity and mortality in children (25). Studies in previous decades have shown that reperfusion injury and delayed programmed cell death (apoptosis) of neurons are important pathophysiological mechanisms (26–28). ROS destroy proteins, nucleic acids, and membrane polyunsaturated fatty acids, lead to lipid peroxidation and loss of membrane

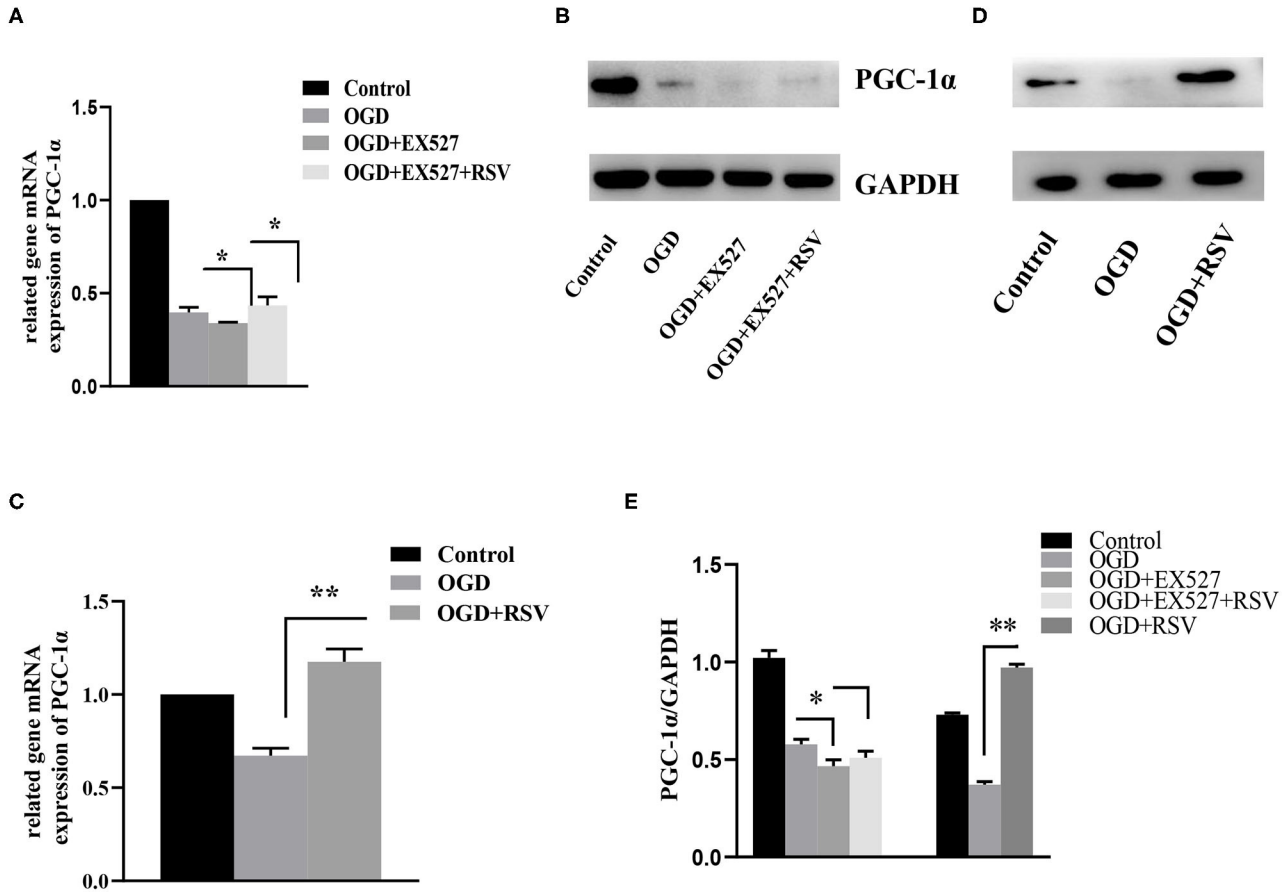

FIGURE 6 | (A) Relative *PGC-1α* mRNA levels in different groups after EX527 treatment ($n = 3$). **(B)** Relative PGC-1α protein levels in different groups after EX527 treatment ($n = 3$). **(C)** Relative *PGC-1α* mRNA levels in different groups after RSV treatment ($n = 3$). **(D)** Relative PGC-1α protein levels in different groups after RSV treatment ($n = 3$). Data were obtained from three independent experiments. **(E)** Bar graph showing the relative expression of PGC-1α in each group. $^*P < 0.05$, $^{**}P < 0.01$.

integrity, reduce mitochondrial membrane potential, increase the membrane permeability to Ca^{2+}, and eventually lead to neuron apoptosis (29–31).

Sirt1 is a member of the sirtuin family, which is a crucial epigenetic regulator involved in many biological and pathological processes including metabolism, genomic stability maintenance, immune responses, and others (32, 33). Earlier studies have shown that Sirt1-related signal pathways mediate oxidative stress in brain injury (34–37). Sirt1 is also an upstream protein of PGC-1α. Therefore, we mainly analyzed the effect of the Sirt1/PGC-1α signal pathway on oxidative stress and neurocytes to investigate its neuroprotective effects in hypoxia/reperfusion.

In our work, we found that Sirt1 expression decreased after OGD, while apoptosis increased and cell viability decreased, indicating that Sirt1 may be related to neuronal apoptosis after OGD. Surprisingly, after adding EX527, a Sirt1 inhibitor, we found that neuronal apoptosis was increased and cell viability was decreased, confirming that Sirt1 was involved in cell apoptosis. Next, when adding RSV, a Sirt1 agonist, we found that neuron apoptosis was decreased and cell viability was increased. Therefore, we hypothesize that Sirt1 may be neuroprotective, which is consistent with results from a previous *in vivo* study (38). Moreover, RSV showed a neuroprotective effect either before or after OGD, indicating its great potential for the treatment of brain injury.

Mitochondria play a key role in regulating cellular calcium levels and activating cell death pathways. The Sirt1/PGC-1α pathway plays an important role in mitochondrial function regulation. Sirt1 can directly regulate PGC-1α activity through phosphorylation and deacetylation. And PGC-1α further induce mitochondrial gene expression in neurons to coordinate energy metabolism, enhance activity, and further regulate mitochondrial biogenesis and function, so as to reduce oxidative stress-mediated neuronal death. The Sirt1/PGC-1 pathway can play a protective role by activating autophagy against oxidative stress-mediated ROS production in systemic endogenous stress syndrome (39). In diabetic peripheral neuropathy, overexpression of Sirt1 can increase axonal growth through Sirt1/ PGC-1α/ TFAM axis and improve mitochondrial oxidative metabolism (40). It has also been shown that Sirt1/PGC-1α signaling pathway can further regulate the role of uncoupling protein 2(UCP2) or Forkhead box protein O1(FOXO1) in reducing oxidative stress and neuronal apoptosis (41, 42). In our study, decreasing Sirt1 reduced the expression of PGC-1α and increased apoptosis, resulting in

intracellular increased MDA and decreased SOD, which are related to cell apoptosis. Therefore, we hypothesize that the neuroprotective effect of Sirt1 in neonatal brain injury is partly exerted by activating PGC-1α.

Although our experiments showed that Sirt1 is involved in the regulation of OGD, the described experiments were only performed *in vitro*. We do not know if the regulatory role described above is the same as *in vivo*. In addition, we selected a single time point after OGD. The trend in Sirt1 changes at different time points is out of scope of this study. Furthermore, the long-term protective effects of Sirt1 after OGD remain unclear, too.

In conclusion, oxidative stress is important for the occurrence of hypoxic brain injury. The antioxidant effect of Sirt1 may be a target of future HI studies. Our study confirms that Sirt1 is involved in apoptosis and is a protective antioxidant, which is regulated by the Sirt1/PGC-1α signaling pathway. Therefore, Sirt1 may serve as an important target in future studies for effective treatments of neonatal brain injury.

DATA AVAILABILITY STATEMENT

The raw data supporting the conclusions of this article will be made available by the authors, without undue reservation.

ETHICS STATEMENT

The animal study was reviewed and approved by Zhengzhou University committee on animal care and use for animal research.

AUTHOR CONTRIBUTIONS

XC designed the project. LS and JZ carried out experiments, analyzed the data, wrote the first draft, and made the final draft. YW and QH participated in the design of the project and revised the manuscript. HC helped perform the experiment. All authors reviewed the manuscript.

FUNDING

This work was support by the National Natural Science Foundation of China (81471491).

ACKNOWLEDGMENTS

This research was completed on the Academy of Medical Sciences of Zhengzhou University Translational Medicine platform.

REFERENCES

1. Herz J, Koster C, Reinboth BS, Dzietko M, Hansen W, Sabir H, et al. Interaction between hypothermia and delayed mesenchymal stem cell therapy in neonatal hypoxic-ischemic brain injury. *Brain Behav Immun.* (2018) 70:118–30. doi: 10.1016/j.bbi.2018.02.006
2. Ding M, Feng N, Tang D, Feng J, Li Z, Jia M, et al. Melatonin prevents Drp1-mediated mitochondrial fission in diabetic hearts through SIRT1-PGC1alpha pathway. *J Pineal Res.* (2018) 65:e12491. doi: 10.1111/jpi.12491
3. Yang Y, Jiang S, Dong Y, Fan C, Zhao L, Yang X, et al. Melatonin prevents cell death and mitochondrial dysfunction via a SIRT1-dependent mechanism during ischemic-stroke in mice. *J Pineal Res.* (2015) 58:61–70. doi: 10.1111/jpi.12193
4. Ren Q, Hu Z, Jiang Y, Tan X, Botchway BOA, Amin N, et al. SIRT1 protects against apoptosis by promoting autophagy in the oxygen glucose deprivation/reperfusion-induced injury. *Front Neurol.* (2019) 10:1289. doi: 10.3389/fneur.2019.01289
5. Supinski GS, Schroder EA, Callahan LA. Mitochondria and critical illness. *Chest.* (2019) 157:310–22. doi: 10.1016/j.chest.2019.08.2182
6. Peng XP, Li XH, Li Y, Huang XT, Luo ZQ. The protective effect of oleanolic acid on NMDA-induced MLE-12 cells apoptosis and lung injury in mice by activating SIRT1 and reducing NF-kappaB acetylation. *Int Immunopharmacol.* (2019) 70:520–9. doi: 10.1016/j.intimp.2019.03.018
7. Zhao H, Chen S, Gao K, Zhou Z, Wang C, Shen Z, et al. Resveratrol protects against spinal cord injury by activating autophagy and inhibiting apoptosis mediated by the SIRT1/AMPK signaling pathway. *Neuroscience.* (2017) 348:241–51. doi: 10.1016/j.neuroscience.2017.02.027
8. Yang X, Si P, Qin H, Yin L, Yan LJ, Zhang C. The neuroprotective effects of SIRT1 on NMDA-induced excitotoxicity. *Oxid Med Cell Longev.* (2017) 2017:2823454. doi: 10.1155/2017/2823454
9. He W, Wang Y, Zhang MZ, You L, Davis LS, Fan H, et al. Sirt1 activation protects the mouse renal medulla from oxidative injury. *J Clin Invest.* (2010) 120:1056–68. doi: 10.1172/JCI41563
10. Zhang Y, Cui G, Wang Y, Gong Y, Wang Y. SIRT1 activation alleviates brain microvascular endothelial dysfunction in peroxisomal disorders. *Int J Mol Med.* (2019) 44:995–1005. doi: 10.3892/ijmm.2019.4250
11. Cai P, Feng N, Zheng W, Zheng H, Zou H, Yuan Y, et al. Treatment with, resveratrol, a SIRT1 activator, prevents zearalenone-induced lactic acid metabolism disorder in rat sertoli cells. *Molecules.* (2019) 24:2474. doi: 10.3390/molecules24132474
12. Zhang T, Chi Y, Ren Y, Du C, Shi Y, Li Y. Resveratrol reduces oxidative stress and apoptosis in podocytes via Sir2-related enzymes, sirtuins1 (SIRT1)/peroxisome proliferator-activated receptor gamma co-activator 1alpha (PGC-1alpha) axis. *Med Sci Monit.* (2019) 25:1220–31. doi: 10.12659/MSM.911714
13. Taherian M, Norenberg MD, Panickar KS, Shamaladevi N, Ahmad A, Rahman P, et al. Additive effect of resveratrol on astrocyte swelling post-exposure to ammonia, ischemia and trauma *in vitro*. *Neurochem Res.* (2020) 45:1156–67. doi: 10.1007/s11064-020-02997-1
14. Xie YK, Zhou X, Yuan HT, Qiu J, Xin DQ, Chu XL, et al. Resveratrol reduces brain injury after subarachnoid hemorrhage by inhibiting oxidative stress and endoplasmic reticulum stress. *Neural Regen Res.* (2019) 14:1734–42. doi: 10.4103/1673-5374.257529
15. Waldman M, Cohen K, Yadin D, Nudelman V, Gorfil D, Laniado-Schwartzman M, et al. Regulation of diabetic cardiomyopathy by caloric restriction is mediated by intracellular signaling pathways involving 'SIRT1 and PGC-1alpha'. *Cardiovasc Diabetol.* (2018) 17:111. doi: 10.1186/s12933-018-0757-1
16. Mei ZG, Tan LJ, Wang JF, Li XL, Huang WF, Zhou HJ. Fermented Chinese formula shuan-tong-ling attenuates ischemic stroke by inhibiting inflammation and apoptosis. *Neural Regen Res.* (2017) 12:425–32. doi: 10.4103/1673-5374.202946
17. Li X, Wang H, Wen G, Li L, Gao Y, Zhuang Z, et al. Neuroprotection by quercetin via mitochondrial function adaptation in traumatic brain injury: PGC-1alpha pathway as a potential mechanism. *J Cell Mol Med.* (2018) 22:883–91. doi: 10.1111/jcmm.13313
18. Tian L, Cao W, Yue R, Yuan Y, Guo X, Qin D, et al. Pretreatment with tilianin improves mitochondrial energy metabolism and oxidative stress in rats with myocardial ischemia/reperfusion injury via AMPK/SIRT1/PGC-1 alpha signaling pathway. *J Pharmacol Sci.* (2019) 139:352–60. doi: 10.1016/j.jphs.2019.02.008

19. Tanno M, Kuno A, Horio Y, Miura T. Emerging beneficial roles of sirtuins in heart failure. *Basic Res Cardiol.* (2012) 107:273. doi: 10.1007/s00395-012-0273-5
20. Gusel'nikova VV, Korzhevskiy DE. NeuN as a neuronal nuclear antigen and neuron differentiation marker. *Acta Nat.* (2015) 7:42–7. doi: 10.32607/20758251-2015-7-2-42-47
21. Sun S, Hu F, Wu J, Zhang S. Cannabidiol attenuates OGD/R-induced damage by enhancing mitochondrial bioenergetics and modulating glucose metabolism via pentose-phosphate pathway in hippocampal neurons. *Redox Biol.* (2017) 11:577–85. doi: 10.1016/j.redox.2016.12.029
22. Ye L, Wang X, Cai C, Zeng S, Bai J, Guo K, et al. FGF21 promotes functional recovery after hypoxic-ischemic brain injury in neonatal rats by activating the PI3K/Akt signaling pathway via FGFR1/beta-klotho. *Exp Neurol.* (2019) 317:34–50. doi: 10.1016/j.expneurol.2019.02.013
23. Chen W, Xu B, Xiao A, Liu L, Fang X, Liu R, et al. TRPM7 inhibitor carvacrol protects brain from neonatal hypoxic-ischemic injury. *Mol Brain.* (2015) 8:11. doi: 10.1186/s13041-015-0102-5
24. Zhang J, Cheng XY, Sheng GY. AP4M1 is abnormally expressed in oxygen-glucose deprived hippocampal neurons. *Neurosci Lett.* (2014) 563:85–9. doi: 10.1016/j.neulet.2014.01.034
25. Jinnou H, Sawada M, Kawase K, Kaneko N, Herranz-Perez V, Miyamoto T, et al. Radial glial fibers promote neuronal migration and functional recovery after neonatal brain injury. *Cell Stem Cell.* (2018) 22:128–37.e9. doi: 10.1016/j.stem.2017.11.005
26. Xu Y, Wang J, Song X, Wei R, He F, Peng G, et al. Protective mechanisms of CA074-me (other than cathepsin-B inhibition) against programmed necrosis induced by global cerebral ischemia/reperfusion injury in rats. *Brain Res Bull.* (2016) 120:97–105. doi: 10.1016/j.brainresbull.2015.11.007
27. Vaibhav K, Shrivastava P, Tabassum R, Khan A, Javed H, Ahmed ME, et al. Delayed administration of zingerone mitigates the behavioral and histological alteration via repression of oxidative stress and intrinsic programmed cell death in focal transient ischemic rats. *Pharmacol Biochem Behav.* (2013) 113:53–62. doi: 10.1016/j.pbb.2013.10.008
28. Qiao L, Fu J, Xue X, Shi Y, Yao L, Huang W, et al. Neuronalinjury and roles of apoptosis and autophagy in a neonatal rat model of hypoxia-ischemia-induced periventricular leukomalacia. *Mol Med Rep.* (2018) 17:5940–9. doi: 10.3892/mmr.2018.8570
29. Sun AY, Wang Q, Simonyi A, Sun GY. Resveratrol as a therapeutic agent for neurodegenerative diseases. *Mol Neurobiol.* (2010) 41:375–83. doi: 10.1007/s12035-010-8111-y
30. Noh KM, Yokota H, Mashiko T, Castillo PE, Zukin RS, Bennett MV. Blockade of calcium-permeable AMPA receptors protects hippocampal neurons against global ischemia-induced death. *Proc Natl Acad Sci USA.* (2005) 102:12230–5. doi: 10.1073/pnas.0505408102
31. Roth TL, Nayak D, Atanasijevic T, Koretsky AP, Latour LL, McGavern DB. Transcranial amelioration of inflammation and cell death after brain injury. *Nature.* (2014) 505:223–8. doi: 10.1038/nature12808
32. Yu Q, Dong L, Li Y, Liu G. SIRT1 and HIF1alpha signaling in metabolism and immune responses. *Cancer Lett.* (2018) 418:20–6. doi: 10.1016/j.canlet.2017.12.035
33. Alves-Fernandes DK, Jasiulionis MG. The role of SIRT1 on DNA damage response and epigenetic alterations in cancer. *Int J Mol Sci.* (2019) 20:3153. doi: 10.3390/ijms20133153
34. Li D, Liu N, Zhao HH, Zhang X, Kawano H, Liu L, et al. Interactions between Sirt1 and MAPKs regulate astrocyte activation induced by brain injury *in vitro* and *in vivo*. *J Neuroinflammation.* (2017) 14:67. doi: 10.1186/s12974-017-0841-6
35. Nikseresht S, Khodagholi F, Ahmadiani A. Protective effects of ex-527 on cerebral ischemia-reperfusion injury through necroptosis signaling pathway attenuation. *J Cell Physiol.* (2019) 234:1816–26. doi: 10.1002/jcp.27055
36. Zhao L, An R, Yang Y, Yang X, Liu H, Yue L, et al. Melatonin alleviates brain injury in mice subjected to cecal ligation and puncture via attenuating inflammation, apoptosis, and oxidative stress: the role of SIRT1 signaling. *J Pineal Res.* (2015) 59:230–9. doi: 10.1111/jpi.12254
37. Jablonska B, Gierdalski M, Chew LJ, Hawley T, Catron M, Lichauco A, et al. Sirt1 regulates glial progenitor proliferation and regeneration in white matter after neonatal brain injury. *Nat Commun.* (2016) 7:13866. doi: 10.1038/ncomms13866
38. Karalis F, Soubasi V, Georgiou T, Nakas CT, Simeonidou C, Guiba-Tziampiri O, et al. Resveratrol ameliorates hypoxia/ischemia-induced behavioral deficits and brain injury in the neonatal rat brain. *Brain Res.* (2011) 1425:98–110. doi: 10.1016/j.brainres.2011.09.044
39. Liang D, Zhuo Y, Guo Z, He L, Wang X, He Y, et al. SIRT1/PGC-1 pathway activation triggers autophagy/mitophagy and attenuates oxidative damage in intestinal epithelial cells. *Biochimie.* (2020) 170:10–20. doi: 10.1016/j.biochi.2019.12.001
40. Chandrasekaran K, Anjaneyulu M, Choi J, Kumar P, Salimian M, Ho CY, et al. Role of mitochondria in diabetic peripheral neuropathy: influencing the NAD^+-dependent SIRT1-PGC-1alpha-TFAM pathway. *Int Rev Neurobiol.* (2019) 145:177–209. doi: 10.1016/bs.irn.2019.04.002
41. Huang J, Liu W, Doycheva DM, Gamdzyk M, Lu W, Tang J, et al. Ghrelin attenuates oxidative stress and neuronal apoptosis via GHSR-1alpha/AMPK/Sirt1/PGC-1alpha/UCP2 pathway in a rat model of neonatal HIE. *Free Radic Biol Med.* (2019) 141:322–37. doi: 10.1016/j.freeradbiomed.2019.07.001
42. Hong YA, Bae SY, Ahn SY, Kim J, Kwon YJ, Jung WY, et al. Resveratrol ameliorates contrast induced nephropathy through the activation of SIRT1-PGC-1alpha-Foxo1 signaling in mice. *Kidney Blood Press Res.* (2017) 42:641–53. doi: 10.1159/000481804

Conflict of Interest: The authors declare that the research was conducted in the absence of any commercial or financial relationships that could be construed as a potential conflict of interest.

frontiers in Pediatrics

BRIEF RESEARCH REPORT
published: 02 September 2020
doi: 10.3389/fped.2020.00532

Mitochondrial Oxygen Monitoring During Surgical Repair of Congenital Diaphragmatic Hernia or Esophageal Atresia: A Feasibility Study

Sophie A. Costerus[1], Mark Wefers Bettink[2], Dick Tibboel[1], Jurgen C. de Graaff[2] and Egbert G. Mik[2]*

[1] Department of Pediatric Surgery, Erasmus University Medical Center-Sophia Children's Hospital, Rotterdam, Netherlands,
[2] Department of Anesthesiology, Erasmus University Medical Center, Rotterdam, Netherlands

Current monitoring techniques in neonates lack sensitivity for hypoxia at cellular level. The recent introduction of the non-invasive Cellular Oxygen METabolism (COMET) monitor enables measuring *in vivo* mitochondrial oxygen tension (mitoPO$_2$), based on oxygen-dependent quenching of delayed fluorescence of 5-aminolevulinic acid (ALA)-enhanced protoporphyrin IX. The aim is to determine the feasibility and safety of non-invasive mitoPO$_2$ monitoring in surgical newborns. MitoPO$_2$ measurements were conducted in a tertiary pediatric center during surgical repair of congenital diaphragmatic hernia or esophageal atresia. Intraoperative mitoPO$_2$ monitoring was performed with a COMET monitor in 11 congenital diaphragmatic hernia and four esophageal atresia neonates with the median age at surgery being 2 days (IQR 1.25–5.75). Measurements were done at the skin and oxygen-dependent delayed fluorescence was measurable after at least 4 h application of an ALA plaster. Pathophysiological disturbances led to perturbations in mitoPO$_2$ and were not observed with standard monitoring modalities. The technique did not cause damage to the skin, and seemed safe in this respect in all patients, and in 12 cases intraoperative monitoring was successfully completed. Some external and potentially preventable factors—the measurement site being exposed to the disinfectant chlorohexidine, purple skin marker, or infrared light—seemed responsible for the inability to detect an adequate delayed fluorescence signal. In conclusion, this is the first study showing it is possible to measure mitoPO$_2$ in neonates and that the cutaneous administration of ALA to neonates in the described situation can be safely applied. Preliminary data suggests that mitoPO$_2$ in neonates responds to perturbations in physiological status.

Keywords: mitochondria, oxygen, neonate, surgery, monitoring

OPEN ACCESS

Edited by:
Fook-Choe Cheah, Medical Centre, National University of Malaysia, Malaysia

Reviewed by:
Brian William Pogue, Dartmouth College, United States
Gorm Greisen, Rigshospitalet, Denmark

****Correspondence:***
Sophie A. Costerus
s.costerus@erasmusmc.nl

Specialty section:
This article was submitted to Neonatology, a section of the journal Frontiers in Pediatrics

Received: *12 May 2020*
Accepted: *27 July 2020*
Published: *02 September 2020*

Citation:
Costerus SA, Bettink MW, Tibboel D, de Graaff JC and Mik EG (2020) Mitochondrial Oxygen Monitoring During Surgical Repair of Congenital Diaphragmatic Hernia or Esophageal Atresia: A Feasibility Study. Front. Pediatr. 8:532. doi: 10.3389/fped.2020.00532

INTRODUCTION

Major (non-cardiac) neonatal surgery is challenging for clinicians. The neonatal homeostasis is a frail equilibrium and is highly affected by general anesthesia and surgical manipulation (1, 2). The anesthesiologist aims to monitor the physiology with the help of the heart rate, invasive blood pressure, saturation, end-tidal carbon dioxide, skin perfusion, urine output, and serum lactate.

These broad range of monitoring modalities are used as surrogate of end-organ perfusion with adequate oxygen transport as a prime goal. To date, the optimal blood pressure in neonates for adequate perfusion of peripheral and cerebral tissue is unknown. Invasive techniques available for effective monitoring of the circulation/cardiovascular system are seldom used due to technical restraints in neonates or are simply not feasible during neonatal surgery (3). Yet, the incidence of brain injury after (non-cardiac) neonatal surgery is increasingly reported (4, 5) as well as altered long–term neurodevelopmental outcomes (6–9). Several factors are thought to contribute to the postoperative brain injury, including alterations in the perioperative neonatal hemodynamics.

Adequate oxygen supply to tissues is of pivotal importance. A non-invasive, bedside monitoring modality for cellular oxygenation could provide direct information about oxygen transport. This allows clinician to adjust their management on actual measurements of tissue perfusion and oxygenation instead of systemic circulatory measures. In this light, monitoring of cellular oxygenation has been suggested to be beneficial during neonatal-cardiac surgery due to the highly affected hemodynamics (10). Yet, major non-cardiac congenital anomalies which requires surgery within the 1st days causes alterations in the neonatal physiology as well (4, 7). The recent introduction of the non-invasive Cellular Oxygen METabolism (COMET) monitor (Photonics Healthcare B.V., Utrecht, The Netherlands) makes it possible to measure *in vivo* mitochondrial oxygen tension (mitoPO$_2$). Although mitochondrial oxygen sensing has been recognized as a promising technique for pediatric ICU and anesthesia (11, 12), until now reported use has been limited to adults (13–16). The present study tests feasibility and safety of intraoperative use of COMET monitoring in infants for the first time.

The COMET monitor measures mitoPO$_2$ by means of oxygen-dependent quenching of delayed fluorescence (17). Green pulsed laser excitation of protoporphyrin IX (PpIX) leads to a relatively long-lived red-light emission, called "delayed fluorescence." The intensity of the delayed fluorescence decays with an oxygen-dependent lifetime, meaning more oxygen results in a shorter lifetime and *vice versa*. PpIX is the final precursor of heme in the heme-biosynthetic pathway, synthesized inside the mitochondria. Under normal (non-sensitized) conditions PpIX concentrations in human skin are very low and non-detectable with COMET. Administration of 5-aminolevulinic acid (ALA) increases mitochondrial PpIX concentrations and ensures the mitochondrial origin of the delayed fluorescence signal (15). Therefore, to enable measurements with the COMET monitor, ALA needs to be applied on skin to induce PpIX, the latter acting as mitochondrially located oxygen-sensitive dye (17, 18).

ALA is registered for use in adults, for example for photodynamic therapy in dermatologic pathology (19, 20) and to visualize brain tumors during fluorescence-guided surgery (21, 22) and was not used in pediatric patients until recently. Research with cutaneous ALA administration up to 354 mg in infants of 5 years and older reported no side effects (23). Oral administration of 20 mg/kg ALA in infants of 1 year and older showed a transient increase of alanine aminotransferase (24–26). Rarely, the administration of 5-aminolevulinic acid led to an allergic reaction, in here contact dermatitis are the only reported allergies (27). Therefore, we assumed the safety on a systemic level of a very low dosage of ALA—8 mg—on the skin of neonates, providing an opportunity to use COMET monitoring in neonates for the first time. Primary outcomes of this study were feasibility and safety, especially local (photo)toxicity, of cutaneous ALA administration in combination with using the COMET monitor in neonates perioperatively. A secondary outcome was preliminary evaluation of anesthesiologic and surgical procedures influencing mitoPO$_2$.

MATERIALS AND METHODS

The institutional research board approved a feasibility study of 15 neonates (MEC 2017-145).

After obtained informed consent from both parents, measurements were performed during surgical treatment of neonates with congenital diaphragmatic hernia (CDH) or esophageal atresia (EA). Surgery took place in the operating theater, unless the neonate was on extracorporeal membrane oxygenation (ECMO), in which case the surgery was performed in the pediatric intensive care unit due to logistics.

In this study the feasibility was defined as the possibility of priming the skin with ALA and to measure mitoPO$_2$ in neonates. The safety was defined as (the lack of) any adverse event of the skin after cutaneous administration of ALA and measurement with COMET until 48 h after the COMET-skin sensor was removed.

An Alacare® plaster has a square format of 2 by 2 cm and contains 2 mg per cm^2 ALA (Alacare, photonamic, Pinneberg, Germany). The plaster is covered by an aluminum layer to protect the primed skin to light exposure (**Figure 1**) (28). The plaster was applied in the pediatric intensive care unit (ambient temperature of ∼22°C) on the skin on the frontal side of the upper leg for at least 4 h before starting the measurement. Research in adults showed that a priming time of 4 h or more was needed to synthesize the suitable concentration of PpIX to enables measurements of mitoPO2 in the skin (15). The same minimal priming time was maintained in this study.

The COMET-skin sensor has a biocompatible housing of 7 × 2 × 2 cm. The skin sensor was placed on the primed skin and was attached to the skin by a double-sided plaster provided by the COMET manufacturer (**Figure 1**). The influence of light on the primed skin during the application of the COMET-skin sensor was minimized by turning off the surgical luminaires/lamps. After the application of the skin sensor, the biocompatible housing was covered with aluminum foil.

Continuous registration of routine vital parameters, regional cerebral oxygenation (rSO$_2$) (INVOS^{TM} 5100C) and mitochondrial saturation (COMET) were obtained and stored for off-line analyses. Sampling rate of the vital parameters was every second, rSO$_2$ every 6 s and mitochondrial oxygen tension (mitoPO$_2$) every 60 s. Intraoperative management was registered in our Patient Data Management System. Patients received general anesthesia with sevoflurane/midazolam, rocuronium

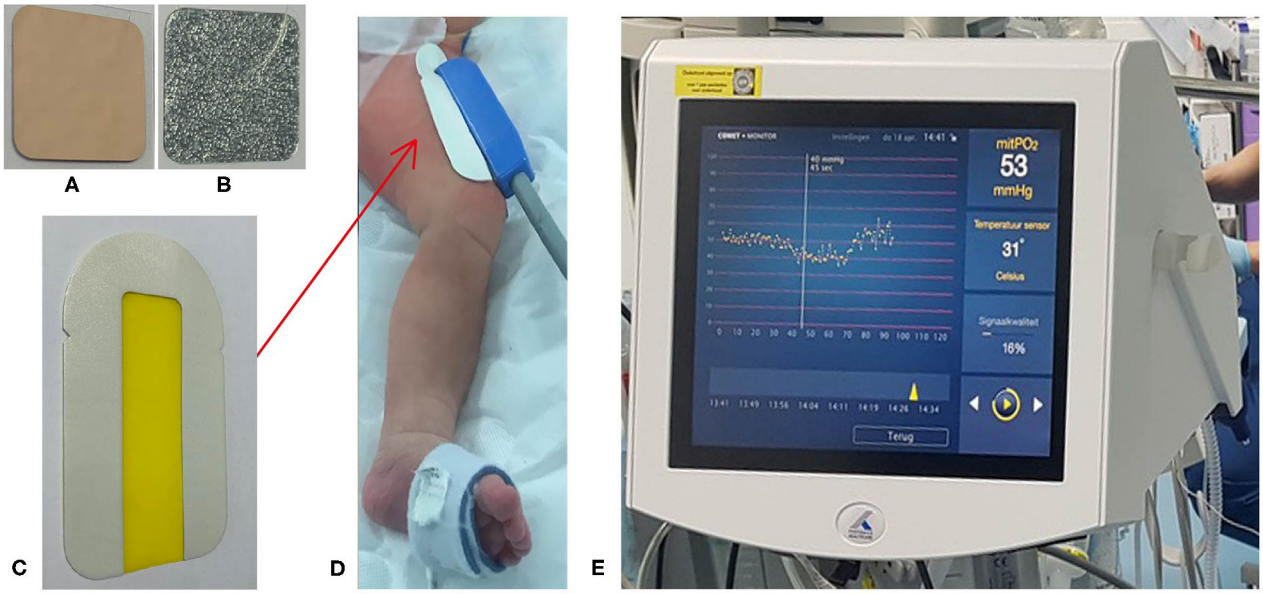

FIGURE 1 | The ALA plaster with the aluminum cover **(A)** and the ALA side **(B)**, double-sided tape **(C)** which is used for the application of the COMET-skin sensor (red arrow) on the frontal side of the upper leg **(D)** and the Cellular Oxygen METabolism (COMET) monitor **(E)**.

TABLE 1 | Patient demographics.

n = 15	Median (IQR)
Male gender, *n* (%)	8 (53%)
Gestational age, wk	38.1 (37.7–40.2)
Birth weight, grams	3,000 (2,400–3,340)
Age at surgery, days	2 (2–5.5)
Duration of surgery, min	106 (95–116)
Priming time skin, min	465 (413–720)
Duration MitoPO$_2$ measurement	116 (98–133)
Surgical approach	
Thoracoscopy, *n* (%)	5 (33%)
Thoracotomy, *n* (%)	2 (13%)
Laparotomy, *n* (%)	8 (53%)
Surgery during ECMO, *n* (%)	2 (13%)

TABLE 2 | Median and IQR values of the 12 successfully obtained measurements.

	HR	MABP	Saturation	rSO$_2$	MitoPO$_2$
Start measurement	133 (113–142)	41 (37–44)	96 (94–97)	87 (66–93)	58 (51–60)
+10 min	130 (112–146)	48 (40–53)	94 (91–97)	83 (69–92)	57 (55–64)
+20 min	133 (118–140)	49 (40–62)	96 (93–97)	88 (69–93)	54 (53–63)
+30 min	133 (122–151)	47 (44–49)	95 (94–97)	81 (74–93)	53 (49–60)
+40 min	146 (135–160)	42 (35–46)	92 (90–97)	79 (70–88)	53 (52–56)
+50 min	144 (137–156)	41 (35–48)	95 (91–99)	82 (72–89)	50 (48–54)
+60 min	149 (137–164)	43 (39–45)	97 (91–99)	88 (77–95)	51 (49–54)
+70 min	154 (136–166)	45 (40–48)	96 (92–97)	87 (65–94)	52 (49–58)
+80 min	150 (137–168)	45 (35–46)	96 (95–99)	86 (71–95)	52 (47–59)
+90 min	151 (133–168)	42 (37–48)	97 (91–99)	83 (67–94)	53 (52–59)
+100 min	157 (124–163)	42 (39–45)	96 (92–99)	78 (65–91)	51 (50–63)
+110 min	133 (121–168)	46 (42–52)	97 (93–99)	84 (68–91)	53 (50–64)
+120 min	137 (127–171)	42 (37–52)	96 (92–99)	77 (74–91)	48 (45–53)

and fentanyl. MitoPO$_2$ measurements started before surgery and continued until after surgery. After completion of the measurement the primed skin was shielded against light with an aluminum plaster for 48 h. This is based on the pharmacological characteristics of ALA. The mean half-life fluorescence clearance of PpIX is 30 ± 10 h.

RESULTS

Informed consent was obtained in 11 CDH and 4 EA patients. Intraoperative measurements were performed in all 15 included neonates. Neonates had a median gestational age of 38 weeks (IQR 37.7–40.2), a median birth weight of 3,000 grams (IQR 2,400–3,340) and a median age at surgery of 2 days (IQR 2–5.5). Median duration of the surgical procedure was 106 min (IQR 95–116) and two patients received surgical repair of CDH on ECMO in the pediatric intensive care unit (**Table 1**). Median skin priming time with ALA was 7 h 45 m (IQR 6 h 50 m−12 h 0 m). Twelve out of 15 measurements were successful with a median duration of the MitoPO$_2$ measurement of 116 min (IQR 98–133) (**Table 1**). The first measurement failed due to the radiant warmer (infra-red light), the second due to pink chlorohexidine-alcohol disinfectants and the third due to purple skin marker on the primed skin.

In the 12 successful measurements (**Table 2**) the mitoPO$_2$ interquartile range at start of the measurement was 51–60 mmHg. In all neonates the skin was examined on regular timepoints; after removing the ALA plaster after priming of the skin, directly after removing the COMET-sensor, at 24 and 48 h after removing the COMET-sensor. No adverse events such as erythema or other signs of an irritated skin were observed.

Two cases illustrate fluctuations in mitoPO$_2$ in relation to surgical and anesthetic actions. Case 1 (**Figure 2A**) is a female neonate, gestational age 37 weeks, birth weight 2,500 grams, with CDH requiring veno-arterial ECMO treatment due to therapy-resistant pulmonary hypertension. Surgical treatment was on day 8 of life, during ECMO. Priming of the skin with ALA was 6 h. During surgery bleeding intercostal arteries caused significant blood loss. Vital parameters and rSO$_2$ remained unchanged, but mitoPO$_2$ decreased from 62 mmHg at start surgery to 36 mmHg (a reduction of 42%) during blood loss and partially recovered after supplementation with erythrocyte transfusion with a mitoPO$_2$ up to 53 mmHg at the end of the surgery.

Case 2 (**Figure 2B**) is a male neonate, gestational age 34 weeks, birth weight 1,950 grams, with EA type C with a trachea-esophageal fistula. Surgical repair took place on day 1 of life. Skin priming time with ALA was 8 h. The patient was positioned on the left side during surgery. Surgical compression of the lung caused hypoxia which required increasing FiO$_2$ from 35 to 75% to maintain peripheral saturation between 90 and 95%. Blood pressure and heart rate remained stable, rSO$_2$ responded on the increased FiO$_2$ firstly, but mitoPO$_2$ decreased soon after the compression started and continues to decrease from 69 mmHg at start surgery to 37 mmHg (a reduction of 47%) and restored within minutes after manipulation of the lung was finished with a mitoPO$_2$ up to 62 mmHg at the end of the surgery.

DISCUSSION

This is the first study showing feasibility of mitoPO$_2$ measurements in neonates, and importantly, in a clinically relevant high-risk perioperative setting. Measurements with the COMET monitor proved feasible and safe in terms of local damage to the skin. Furthermore, pathophysiological disturbances led to perturbations in mitoPO$_2$. In 12 out of 15 patients mitoPO$_2$ measurements were successful. Failures were

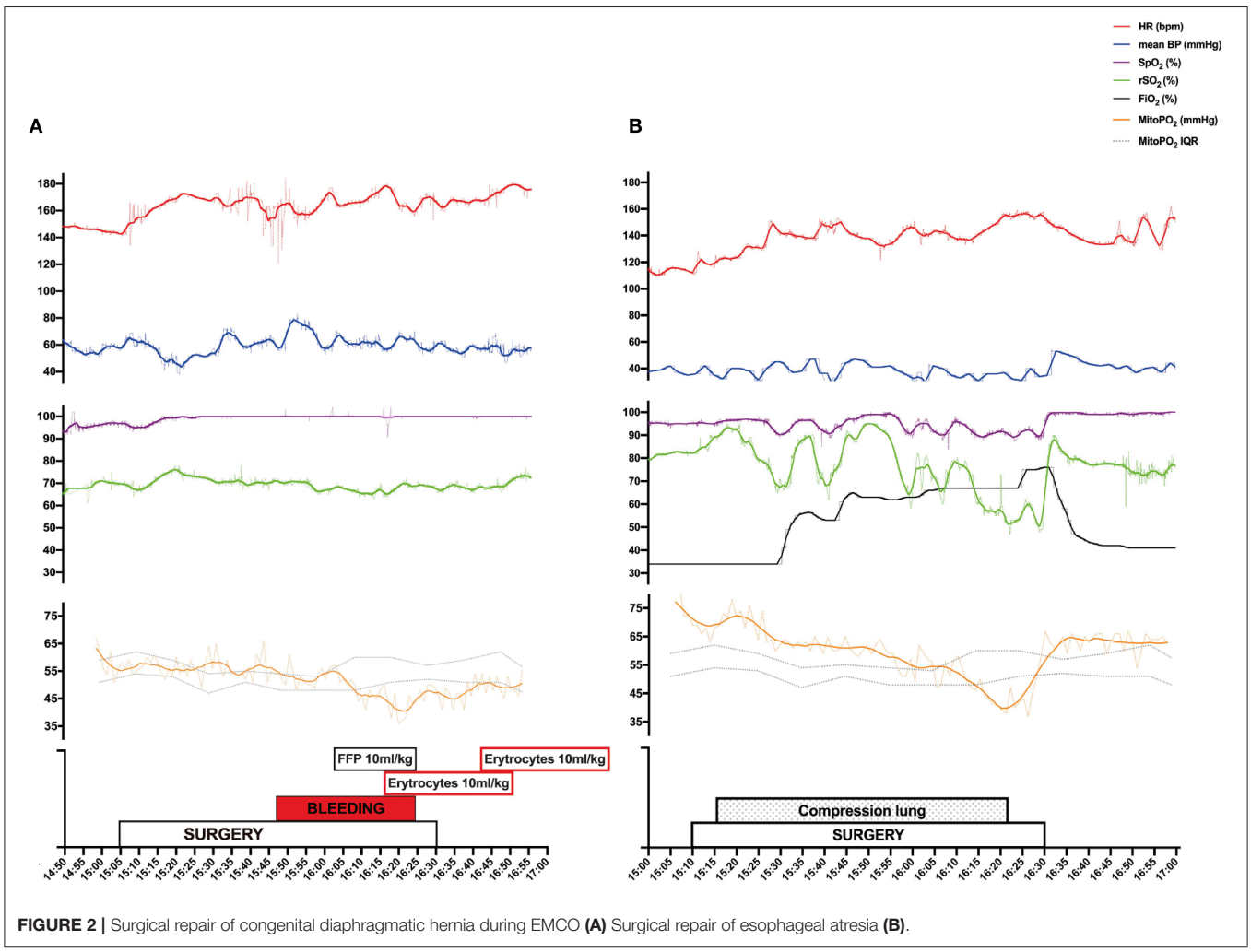

FIGURE 2 | Surgical repair of congenital diaphragmatic hernia during EMCO **(A)** Surgical repair of esophageal atresia **(B)**.

caused by external and potentially preventable factors, disabling detection of an adequate delayed fluorescence signal. In one case infrared warming lamp heat or radiation interfered with the priming of the skin with ALA. Aluminum foil is a strong infrared reflector and was successfully used to shield the ALA plaster against infrared radiation during priming of the skin in the following cases. In the two other failed cases colored substances on the skin interfered with measurements, chlorohexidine with pink pigment and skin marker are both significant sources of delayed fluorescence and thereby potent disturbers of the mitochondrial PpIX light emission.

Safety of ALA administration with Alacare plasters was a major concern for the ethics committee due to the off-label use of ALA for measuring mitoPO$_2$ with the COMET. The reaction of the neonatal skin on ALA administration was unknown and consequently we only obtained approval to perform this feasibility and safety study. ALA makes the skin sensitive for light, consequently it is frequently used for photodynamic therapy in different sorts of dermatologic pathology. In children of 5 years and older, the administration of ALA up to 354 mg, which is over 40 times higher than de 8 mg ALA that was applied on the skin in this study, did not have any side effects (23). Oral administration of 20 mg/kg ALA in infants of 1 year and older showed a transient increase of alanine aminotransferase (24–26). Systemic effects of topical/local administration of ALA on the skin have not been reported and in this study, we focused on potential local side effects in neonatal skin.

There is a risk for erythema and burns when the skin is exposed to (day)light after the administration of ALA. Therefore, precautionary measures were taken to shield the skin for light for 48 h after the measurement with the COMET was ended and the skin sensor was removed. In none of the cases local damage or irritation of the skin was observed, so the combination of ALA-plaster and COMET measurements seems safe.

The pharmacokinetic properties of topical ALA administration with Alacare in neonates are unknown, but in adults the reported skin priming time with ALA takes 4 till 8 h (13). In this study, the same priming times were maintained for neonates. In a following efficacy study, the power calculation/sample size will be focused on validating mitoPO$_2$ measurements in neonates and analyzing the ideal priming time of the neonatal skin. This will create insight in the reaction of the skin to the application of ALA in term and preterm neonates.

For this study two major non-cardiac congenital anomalies were included: congenital diaphragmatic hernia (CDH) and esophageal atresia (EA). These congenital anomalies were chosen to be eligible because major surgery is required within the 1st days of life and postoperative brain injury are reported in children with these congenital anomaly (4, 7). CDH neonates suffer from lung hypoplasia and abnormal morphology of the pulmonary vasculature which results in respiratory insufficiency and severe (therapy-resistant) pulmonary hypertension (29, 30). CDH neonates are a challenge for clinicians to manage due this altered physiology. In EA neonates, the physiology is less affected by the congenital anomaly itself, but requires complex surgery with major intrathoracic manipulation which highly affects the neonatal physiology (31). In these children, our preliminary results suggest that monitoring mitochondrial oxygenation might register changes in neonatal physiology which could not have been observed using standard monitoring devices. Clearly, further research into the clinical usability of COMET is warranted but seems justified based on this pilot. Although this was only a feasibility and safety study, these results confirm that mitochondrial hypoxia may occur without clear signs of central hypoxia and are in line with previous research in animals and humans (32–35). A piglets study demonstrated cutaneous mitoPO$_2$ changed earlier than MABP and lactate during ongoing hemodilution (32). In a sepsis rat model as well as in rats with induced right ventricular failure due to pulmonary arterial hypertension, mitoPO$_2$ proved an additional parameter monitoring physiological changes (33, 34). The clinical prototype of the COMET was tested in healthy volunteers and showed measuring mitochondrial oxygenation and oxygen consumption in humans (13). Previous reports demonstrated the intraoperative use of COMET in adults (15) and also demonstrated that mitoPO$_2$ measurements are not limited to the skin (35). The first study using COMET during upper gastro-intestinal endoscopy showed it is technically feasible and safe (35).

Adequate oxygen supply to tissues is of pivotal importance to sustain mammalian life. Aerobic metabolism is maintained through inhalation of air in the lungs and subsequent transport of the absorbed oxygen to tissues *via* the circulation. The flow of hemoglobin-bound oxygen through the macro- and microcirculation and diffusion of molecular oxygen into the tissue cells brings oxygen to the mitochondria. In the mitochondria, oxygen is used in oxidative phosphorylation in order to efficiently produce adenosine triphosphate (ATP) that acts as the energy source for many cellular processes. Furthermore, mitochondria are essential for homeostasis of the cell, they play a major role in (programmed) cell death (apoptosis). Opening of the mitochondrial permeability transition pore, as a result of a stressful stimulus such as calcium or reactive oxygen species overload, leads to loss of the mitochondrial membrane potential (36). The collapse of the membrane potential results in ATP depletion and necrosis (37), and the release of mitochondrial content such as cytochrome c leads to apoptosis (38). A correlation to outcome after perturbations in cellular oxygenation have not yet been shown, but it could be used as an early warning sign. Importantly, in both a preclinical (32) and clinical setting (15) mitoPO$_2$ provided different information than hemoglobin saturation-based techniques like near- infrared spectroscopy (NIRS). Although visible light spectroscopy and near-infrared spectroscopy failed to show any response on a perturbation, mitoPO$_2$ clearly dropped. This was observed during hemodilution in piglets, where mitoPO$_2$ was measured simultaneously with tissue oxygen saturation on the thoracic wall. The mitoPO$_2$ decreased after the hemoglobin dropped below a threshold, but tissue oxygen saturation, which was measured with NIRS, did not (32).

We previously published a clinical example in which mitoPO$_2$ showed a different response than microvascular hemoglobin-saturation. During peripheral vasoconstriction, which was

induced by the administration of clonidine, microvascular flow, and velocity parameters measured with laser-doppler decreased both. The venous-capillary oxygen saturation did not decrease, however, mitoPO$_2$ in the skin measured by COMET decreased along with the decrease in flow and velocity (15). While mitoPO$_2$ and microvascular flow provided similar information here, we expect additional value of mitoPO$_2$ measurements in clinical situations in which microvascular shunting (39) and loss of hemodynamic coherence occur (40), for example in sepsis and hemodilution. During sepsis microcirculatory dysfunction occurs which causes shunting and loss of the coherence between blood flow and tissue oxygenation. Here microvascular, and ultimately mitochondrial, oxygen measurements can be of additional value (39). The same holds true during a hyperdynamic circulation due to hemodilution, causing erythrocytes to pass too quickly through the microcirculation. This phenomenon is referred to as functional shunting and involves the inability of hemoglobin to off-load oxygen fast enough to the tissues as it passes through the microcirculation, causing cellular hypoxia while hemoglobin saturation is normal or increased (40, 41).

In this study we found baseline mitoPO$_2$ values in the range of 51–60 mmHg. In a previous study in healthy volunteers we reported mean mitoPO$_2$ to be 44 mmHg, and in a very recently published study in critical care patients mean mitoPO$_2$ was reported to be around 60 mmHg (42). Such relatively high values match well with other oxygen measurements in skin (43). The differences between the studies could well be attributed to factors like skin temperature, filling status of the patient, and use of sedation/anesthesia, since such factors are known to influence skin perfusion. Clinical data until now are scarce and normal values for mitoPO$_2$ remain to be determined, as well as the influence of patient factors (such as age) and clinical circumstances. Although we do think mitochondrial oxygen tension is in general higher than anticipated (12), the reader should realize that mitoPO$_2$ in other organs and tissues is likely to differ. Differences in tissue oxygen levels exist between organs, tissues, and tissue compartments (43) and metabolic activity (for example muscle contraction) is also of influence.

To date, clinicians are in the dark about the effect of the altered neonatal (patho)physiology during major high-risk surgery on cellular oxygenation. In the past the focus was to optimize macrohemodynamics although the microcirculation has been increasingly recognized as an import variable in the critically ill neonate (44). To measure tissue oxygenation, a modality based on the principle of near infrared spectroscopy (NIRS) became popular. The optode of the NIRS emits near-infrared light, which easily penetrates biological tissue at a depth of ∼2–3 cm (45, 46). It measures the oxygenation of a combination of 75% venous, 20% arterial, and 5% capillary blood, but does not provide information about the oxygen concentration at cellular level. Unfortunately, the clinical use of additional monitoring with NIRS have not been established yet (47). The COMET allows us to look at oxygen availability at a cellular level. The neonatal skin is an ideal target organ for COMET measurements. It is the biggest organ in neonates and has a relative bigger surface and is more vascularized compared to adults. Skin blood circulation is very sensitive to changes in vascular resistance and blood pressure (48), potentially making the skin a good indicator for the (general) cardiopulmonary status of the neonate.

Compared to interstitial measurements with for example oxygen electrodes COMET has some distinct advantages, such as no need for calibration, non-destructiveness (no need for needle placement), well-defined measurement compartment and very fast response time (no need for signal integration over longer periods of time). A disadvantage of the COMET technique is the necessary priming with ALA. Although previous studies in adults and this study in neonates, show that with some precaution's application of ALA to the skin can be done without harm, it requires planning and currently prevents its use in emergency situations. In elective situations in the operating room and for use in the intensive care this proved not a major issue.

In conclusion, this is the first study showing it is possible to measure mitoPO$_2$ in neonates and that the cutaneous administration of ALA to neonates in the described situation can be safely applied. Preliminary data suggests that mitoPO$_2$ in neonates responds to perturbations in physiological status. The added value of mitochondrial measurements for clinical decision making remains to be determined in future studies.

DATA AVAILABILITY STATEMENT

All datasets presented in this study are included in the article/supplementary material.

ETHICS STATEMENT

The studies involving human participants were reviewed and approved by Erasmus Medical Center. Written informed consent to participate in this study was provided by the participants' legal guardian/next of kin.

AUTHOR CONTRIBUTIONS

All authors had a substantial contribution to conception and design, acquisition of data, analysis, interpretation of data, participated in drafting the article or revising it critically for important intellectual content, and gave final approval of the version to be submitted.

REFERENCES

1. Martin LD, Dissen GA, McPike MJ, Brambrink AM. Effects of anesthesia with isoflurane, ketamine, or propofol on physiologic parameters in neonatal rhesus macaques (*Macaca mulatta*). *J Am Assoc Lab Anim Sci.* (2014) 53:290–300.
2. Smits A, Thewissen L, Dereymaeker A, Dempsey E, Caicedo A, Naulaers G. The use of hemodynamic and cerebral monitoring to study

pharmacodynamics in neonates. *Curr Pharm Des.* (2017) 23:5955–63. doi: 10.2174/1381612823666170918124419
3. Conforti A, Giliberti P, Mondi V, Valfre L, Sgro S, Picardo S, et al. Near infrared spectroscopy: experience on esophageal atresia infants. *J Pediatr Surg.* (2014) 49:1064–8. doi: 10.1016/j.jpedsurg.2014.01.010
4. Stolwijk LJ, Keunen K, de Vries LS, Groenendaal F, van der Zee DC, van Herwaarden MYA, et al. Neonatal surgery for noncardiac congenital anomalies: neonates at risk of brain injury. *J Pediatr.* (2017) 182:335–41.e1. doi: 10.1016/j.jpeds.2016.11.080
5. McCann ME, Schouten ANJ, Dobija N, Munoz C, Stephenson L, Poussaint TY, et al. Infantile postoperative encephalopathy: perioperative factors as a cause for concern. *Pediatrics.* (2014) 133:e751–75. doi: 10.1542/peds.2012-0973
6. Leeuwen L, Schiller RM, Rietman AB, van Rosmalen J, Wildschut ED, Houmes RJM, et al. Risk factors of impaired neuropsychologic outcome in school-aged survivors of neonatal critical illness. *Crit Care Med.* (2018) 46:401–10. doi: 10.1097/CCM.0000000000002869
7. Stolwijk LJ, Lemmers PM, Harmsen M, Groenendaal F, de Vries LS, van der Zee DC, et al. Neurodevelopmental outcomes after neonatal surgery for major noncardiac anomalies. *Pediatrics.* (2016) 137:e20151728. doi: 10.1542/peds.2015-1728
8. Danzer E, Gerdes M, D'Agostino JA, Hoffman C, Bernbaum J, Bebbington MW, et al. Longitudinal neurodevelopmental and neuromotor outcome in congenital diaphragmatic hernia patients in the first 3 years of life. *J Perinatol.* (2013) 33:893–8. doi: 10.1038/jp.2013.47
9. Schiller R, IJsselstijn H, Hoskote A, White T, Verhulst F, van Heijst A, et al. Memory deficits following neonatal critical illness: a common neurodevelopmental pathway. *Lancet Child Adolesc Heal.* (2018) 2:281–9. doi: 10.1016/S2352-4642(17)30180-3
10. Weindling M, Paize F. Peripheral haemodynamics in newborns: best practice guidelines. *Early Hum Dev.* (2010) 86:159–65. doi: 10.1016/j.earlhumdev.2010.01.033
11. Skowno JJ. Hemodynamic monitoring in children with heart disease: overview of newer technologies. *Paediatr Anaesth.* (2019) 29:467–74. doi: 10.1111/pan.13590
12. Mik EG, Balestra GM, Harms FA. Monitoring mitochondrial PO2. *Curr Opin Crit Care.* (2020) 26:289–95. doi: 10.1097/MCC.0000000000000719
13. Harms F, Stolker RJ, Mik E. Cutaneous respirometry as novel technique to monitor mitochondrial function: a feasibility study in healthy volunteers. *PLoS ONE.* (2016) 11:e0163399. doi: 10.1371/journal.pone.0163399
14. Baysan M, Arbous MS, Mik EG, Juffermans NP, Van Der Bom JG. Study protocol and pilot results of an observational cohort study evaluating effect of red blood cell transfusion on oxygenation and mitochondrial oxygen tension in critically ill patients with anaemia: the Insufficient Oxygenation in the Intensive Care Unit (INOX ICU-2) study. *BMJ Open.* (2020) 10:e036351. doi: 10.1136/bmjopen-2019-036351
15. Ubbink R, Bettink MAW, Janse R, Harms FA, Johannes T, Munker FM, et al. A monitor for Cellular Oxygen METabolism (COMET): monitoring tissue oxygenation at the mitochondrial level. *J Clin Monit Comput.* (2017) 31:1143–50. doi: 10.1007/s10877-016-9966-x
16. Baumbach P, Neu C, Derlien S, Bauer M, Nisser M, Buder A, et al. A pilot study of exercise-induced changes in mitochondrial oxygen metabolism measured by a cellular oxygen metabolism monitor (PICOMET). *Biochim Biophys Acta Mol Basis Dis.* (2019) 1865:749–58. doi: 10.1016/j.bbadis.2018.12.003
17. Mik EG. Special article: measuring mitochondrial oxygen tension: from basic principles to application in humans. *Anesth Analg.* (2013) 117:834–46. doi: 10.1213/ANE.0b013e31828f29da
18. Mik EG, Stap J, Sinaasappel M, Beek JF, Aten JA, van Leeuwen TG, et al. Mitochondrial PO2measured by delayed fluorescence of endogenous protoporphyrin IX. *Nat Methods.* (2006) 3:939–45. doi: 10.1038/nmeth940
19. Eber AE, Perper M, Verne SH, Magno R, ALOmair IAO, ALHarbi M, Nouri K. Photodynamic therapy. *Lasers Dermatol Med.* (2018) 261–73. doi: 10.1007/978-3-319-76118-3_16
20. Blume JE, Oseroff AR. Aminolevulinic acid photodynamic therapy for skin cancers. *Dermatol Clin.* (2007) 25:5–14. doi: 10.1016/j.det.2006.09.005
21. Hadjipanayis CG, Stummer W. 5-ALA and FDA approval for glioma surgery. *J Neurooncol.* (2019) 141:479–86. doi: 10.1007/s11060-019-03098-y
22. Ferraro N, Barbarite E, Albert TR, Berchmans E, Shah AH, Bregy A, et al. The role of 5-aminolevulinic acid in brain tumor surgery: a systematic review. *Neurosurg Rev.* (2016) 39:545–55. doi: 10.1007/s10143-015-0695-2
23. Kumar N, Warren CB. Photodynamic therapy for dermatologic conditions in the pediatric population: a literature review. *Photodermatol Photoimmunol Photomed.* (2017) 33:125–34. doi: 10.1111/phpp.12296
24. Burford C, Thamenah Kalyal N, Pandit A, Tailor J, Pedro Lavrador J, Bravo A, et al. The UK's first case series of 5-aminolevulinic acid use in paediatric brain tumours. *EANS Acad.* (2016) 19:i11. doi: 10.1093/neuonc/now293.039
25. Stummer W, Rodrigues F, Schucht P, Preuss M, Wiewrodt D, Nestler U, et al. Predicting the "usefulness" of 5-ALA-derived tumor fluorescence for fluorescence-guided resections in pediatric brain tumors: a European survey. *Acta Neurochir.* (2014) 156:2315–24. doi: 10.1007/s00701-014-2234-2
26. Beez T, Sarikaya-Seiwert S, Steiger HJ, Hänggi D. Fluorescence-guided surgery with 5-aminolevulinic acid for resection of brain tumors in children—a technical report. *Acta Neurochir.* (2014) 156:597–604. doi: 10.1007/s00701-014-1997-9
27. Wulf HC, Philipsen P. Allergic contact dermatitis to 5-aminolaevulinic acid methylester but not to 5-aminolaevulinic acid after photodynamic therapy. *Br J Dermatol.* (2004) 150:143–5. doi: 10.1111/j.1365-2133.2004.05723.x
28. *Samenvatting Van De Productkenmerken.* Available online at: https://db.cbg-meb.nl/smpc/h113539_smpc.pdf (accessed July 17, 2020).
29. Reiss I, Schaible T, Van Den Hout L, Capolupo I, Allegaert K, Van Heijst A, et al. Standardized postnatal management of infants with congenital diaphragmatic hernia in Europe: the CDH EURO consortium consensus. *Neonatology.* (2010) 98:354–64. doi: 10.1159/000320622
30. Snoek KG, Reiss IKM, Greenough A, Capolupo I, Urlesberger B, Wessel L, et al. Standardized postnatal management of infants with congenital diaphragmatic hernia in Europe: the CDH EURO Consortium Consensus-−2015 Update. *Neonatology.* (2016) 110:66–74. doi: 10.1159/000444210
31. van Hoorn CE, Costerus SA, Lau J, Wijnen RMH, Vlot J, Tibboel D, et al. Perioperative management of esophageal atresia/tracheo-esophageal fistula: an analysis of data of 101 consecutive patients. *Paediatr Anaesth.* (2019) 29:1024–32. doi: 10.1111/pan.13711
32. Römers LHL, Bakker C, Dollée N, Hoeks SE, Lima A, Raat NJH, et al. Cutaneous mitochondrial P o 2, but not tissue oxygen saturation, is an early indicator of the physiologic limit of hemodilution in the pig. *Anesthesiology.* (2016) 125:124–32. doi: 10.1097/ALN.0000000000001156
33. Harms FA, Bodmer SIA, Raat NJH, Mik EG. Non-invasive monitoring of mitochondrial oxygenation and respiration in critical illness using a novel technique. *Crit Care.* (2015) 19:343. doi: 10.1186/s13054-015-1056-9
34. Balestra GM, Mik EG, Eerbeek O, Specht PAC, van der Laarse WJ, Zuurbier CJ. Increased *in vivo* mitochondrial oxygenation with right ventricular failure induced by pulmonary arterial hypertension: mitochondrial inhibition as driver of cardiac failure? *Respir Res.* (2015) 16:6. doi: 10.1186/s12931-015-0178-6
35. van Dijk LJD, Ubbink R, Terlouw LG, van Noord D, Mik EG, Bruno MJ. Oxygen-dependent delayed fluorescence of protoporphyrin IX measured in the stomach and duodenum during upper gastrointestinal endoscopy. *J Biophotonics.* (2019) 12:e201900025. doi: 10.1002/jbio.201900025
36. Jones DP, Mason HS. Gradients of O_2 concentration in hepatocytes. *J Biol Chem.* (1978) 253:4874–80.
37. Longmuir IS. Respiration rate of rat-liver cells at low oxygen concentrations. *Biochem J.* (1957) 65:378–82. doi: 10.1042/bj0650378
38. Wilson DF, Rumsey WL, Green TJ, Vanderkooi JM. The oxygen dependence of mitochondrial oxidative phosphorylation measured by a new optical method for measuring oxygen concentration. *J Biol Chem.* (1988) 263:2712–8.
39. Ince C. The microcirculation is the motor of sepsis. *Crit Care.* (2005) 9:S13–9. doi: 10.1186/cc3753
40. Ince C, Mik EG. Microcirculatory and mitochondrial hypoxia in sepsis, shock, and resuscitation. *J Appl Physiol.* (2016) 120:226–35. doi: 10.1152/japplphysiol.00298.2015
41. Ince C. Hemodynamic coherence and the rationale for monitoring the microcirculation. *Crit Care.* (2015) 19:S8. doi: 10.1186/cc14726
42. Neu C, Baumbach P, Plooij AK, Skitek K, Götze J, von Loeffelholz C, et al. Non-invasive assessment of mitochondrial oxygen metabolism in the critically ill patient using the protoporphyrin IX-triplet state

lifetime technique—a feasibility study. *Front Immunol.* (2020) 11:757. doi: 10.3389/fimmu.2020.00757
43. Keeley TP, Mann GE. Defining physiological normoxia for improved translation of cell physiology to animal models and humans. *Physiol Rev.* (2019) 99:161–234. doi: 10.1152/physrev.00041.2017
44. Erdem Ö, Ince C, Tibboel D, Kuiper JW. Assessing the microcirculation with handheld vital microscopy in critically ill neonates and children: evolution of the technique and its potential for critical care. *Front Pediatr.* (2019) 7:273. doi: 10.3389/fped.2019.00273
45. Dix LML, van Bel F, Lemmers PMA. Monitoring cerebral oxygenation in neonates: an update. *Front Pediatr.* (2017) 5:46. doi: 10.3389/fped.2017.00160
46. Brown DW, Picot PA, Naeini JG, Springett R, Delpy DT, Lee TY. Quantitative near infrared spectroscopy measurement of cerebral hemodynamics in newborn piglets. *Pediatr Res.* (2002) 51:564–70. doi: 10.1203/00006450-200205000-00004
47. Costerus S, van Hoorn C, Hendrikx D, Kortenbout J, Hunfeld M, Vlot J, et al. Towards integrative neuromonitoring of the surgical newborn: a systematic review. *Eur J Anaesthesiol.* (2020) 37:701–12. doi: 10.1097/EJA.0000000000001218
48. Wu PYK, Wong WH, Guerra G, Miranda R, Godoy RR, Preston B, et al. Peripheral blood flow in the neonate. 1. Changes in total, skin, and muscle blood flow with gestational and postnatal age. *Pediatr Res.* (1980) 14:1374–8. doi: 10.1203/00006450-198012000-00023

Conflict of Interest: EM is founder and shareholder of Photonics Healthcare B.V., the company that developed and commercializes the COMET monitor. Photonics Healthcare B.V. holds the exclusive licenses to several patents regarding this technology, filed and owned by the Academic Medical Center in Amsterdam and the Erasmus University Medical Center Rotterdam, the Netherlands.

The remaining authors declare that the research was conducted in the absence of any commercial or financial relationships that could be construed as a potential conflict of interest.

frontiers in Pediatrics

ORIGINAL RESEARCH
published: 02 September 2020
doi: 10.3389/fped.2020.00494

Evaluation of the Tempo® System: Improving the Microbiological Quality Monitoring of Human Milk

Marie-Pierre Cayer[1], *Nathalie Dussault*[1], *Marie Joëlle de Grandmont*[1], *Marc Cloutier*[1,2], *Antoine Lewin*[1,3] *and Danny Brouard*[1,4]*

[1] *Affaires Médicales et Innovation, Héma-Québec, Québec, QC, Canada,* [2] *Département de biochimie, Université Laval, Québec, QC, Canada,* [3] *Département d'obstétrique et gynécologie, Université de Sherbrooke, Québec, QC, Canada,* [4] *Département de chimie, Université Laval, Québec, QC, Canada*

Background: Bacteriological testing of donor human milk is mostly done both before and after pasteurization to control contamination in the end-product and meet the microbiological standards. Although the plate count method represents a reliable and sensitive technique and is considered the gold standard for bacteriological testing, it is recognized for being time-consuming and requiring qualified personnel. Recently, faster testing technologies, mostly geared toward the food industry, have been developed. Among these, the bioMérieux TEMPO® system uses the most probable number method to assess microbiological content in a semi-automated fashion.

Objective: The performances of the TEMPO® system in enumerating bacterial quality indicators in human milk were assessed and compared to the reference plate count method.

Methods: Naturally and artificially contaminated human milk samples were used to compare the analytical performances of the TEMPO® system to the plate count technique. More specifically, bacteria belonging to the genera *Bacillus*, *Enterobacteriaceae*, *Staphylococcus aureus,* and total aerobic flora were screened using both methods. Bacteria isolated on agar plates containing selective media were identified by supplemental testing. Bacterial testing results and method parameters were compared using linear regression analyses and Bland-Altman approaches.

Results: Naturally contaminated milk samples ($n = 55$) tested for total aerobic flora showed < 1 log (CFU/ml) discrepancy between the two methods in the output results for 98% of the samples. Comparative linear regression analyses demonstrate good correlations between the two methods ($R^2 > 0.9$). At lower levels of bacterial contamination, the TEMPO® method precision (C.V. < 8%) and accuracy (> 83%) were comparable to plate counts.

Conclusions: The analytical performances of the TEMPO® system for human milk bacteriological testing are equivalent to the reference plate count method. Results from the TEMPO® system are available within a 24-h turnaround time from sample inoculation

OPEN ACCESS

Edited by:
Yuan Shi,
Children's Hospital of Chongqing Medical University, China

Reviewed by:
Sanjeet K. Panda,
Texas Tech University Health Sciences Center El Paso, United States
Joseph M. Bliss,
Women & Infants Hospital of Rhode Island, United States

****Correspondence:***
Danny Brouard
danny.brouard@hema-quebec.qc.ca

Specialty section:
This article was submitted to Neonatology, a section of the journal Frontiers in Pediatrics

Received: *25 March 2020*
Accepted: *14 July 2020*
Published: *02 September 2020*

Citation:
Cayer M-P, Dussault N, de Grandmont MJ, Cloutier M, Lewin A and Brouard D (2020) Evaluation of the Tempo® System: Improving the Microbiological Quality Monitoring of Human Milk. Front. Pediatr. 8:494. doi: 10.3389/fped.2020.00494

without the need for further supplemental testing, suggesting that this semi-automated method could be implemented within milk bank operations as an in-process monitoring technology to optimize end-product quality and safety.

Keywords: donor human milk, human milk bank, bacteriology testing, donor screening, *Bacillus*, quality control, in-process monitoring

INTRODUCTION

A human milk diet has multiple, well-established benefits for all infants and reduces many risks associated with prematurity. Human milk banks provide an essential source to allow human milk diet for infants whose needs exceed what their own mothers can provide. These institutions need to follow standard safety guidelines regarding end-product bacteriological screening to ensure product safety (1–3). Since the inception of its Public Mother's Milk Bank in 2014, Héma-Québec has overseen the milk donation process and is responsible for the processing and distribution of pasteurized donor human milk (PDHM) to premature infants born at 32 weeks or earlier who require medical care and whose mother is unable to breastfeed. Recent studies have shown that breast tissue itself may contain several hundred bacterial species whose diversity may vary according to lactation stages (4–6). Although a normal milk microflora contributes to the establishment of a healthy intestinal flora in neonates, harmful pathogens in human milk can resist thermal processing and have been related to premature babies' infections (7–11).

Bacterial content analysis of pooled mother's milk prior to thermal processing helps identifying potential sources of contamination and allows educational feedback to donors when inadequate collection processes are suspected. The Human Milk Banking Association of North America (HMBANA) guidelines provide recommendations on bacteriological testing of heat-processed milk. Specifically, the guidelines states that any bacterial growth is deemed unacceptable for banked human milk (1). These recommendations on PDHM have been implemented by most milk banks. However, bacteriological screening of milk before pasteurization has not been systematically implemented in all milk banks and there is still no consensus regarding the microbiological criteria to be applied (12–14). Monitoring contaminants in "raw" milk remains relevant, since some pathogens produce toxins or spores that may resist thermal processing (15, 16). Spore-forming bacteria including *Bacillus* and *Bacillus*-derived bacterial genera species, represent the most common contaminants found in PDHM and are responsible for a significant fraction of rejected batches (14, 17). Most milk banks who apply pre-pasteurization milk screening use a total aerobic flora (TAF) threshold of 10^5-10^6 colony-forming units per milliliter (CFU/ml) (18, 19). Threshold values for maximal bacterial counts vary among milk banks and countries. For instance, the National Institute for Health and Care Excellence (NICE) in the UK recommends a maximal bacterial count of 10^4 CFU/ml for *Staphylococcus aureus* (*S. aureus*) and *Enterobacteriaceae*, and maximum of 10^5 for total colony count. In contrast to Australian guidelines, which do not accept any *Enterobacteriaceae*, Enterococci or potential pathogens capable of producing heat-stable enterotoxins (2, 20–22). Héma-Québec's Public Mother's Milk Bank adopted post-pasteurization microbiological criteria based on practices and guidelines; accordingly, unpasteurized milk containing a TAF $> 10^5$ CFU/ml or an *Enterobacteriaceae* content $> 10^4$ CFU/ml or any harmful pathogens including *S. aureus*, *Bacillus,* and *Bacillus*-like species, is discarded.

The plate count method (PCM) is currently the best practice recommended by the HMBANA for bacterial content testing of milk (1). This method can require up to 4 days for the results to be available and its application might lack standardization since procedure variations such as media composition, sample plating volume and raw milk preparations (i.e. dilutions) have been observed among milk banks (23–25). This methodology precludes a rapid intervention upon the human milk processing chain and can result in time, material and product wastage.

New bacteriological testing technologies with higher throughput have been recently introduced, among others, by the food and cosmetic industries as a means of intervening faster on their production chain (26, 27). The TEMPO® system (bioMérieux, Marcy-l'Étoile, France) is the first semi-automated bacteriological testing technology able to identify contaminants typically found in human milk. This system uses testing cards with specific culture media allowing rapid bacterial growth. After distribution of culture media-sample mixtures in the wells of the card, bacteria multiply during incubation and metabolize culture media containing a fluorescent indicator. The TEMPO® system relies upon the detection of the number and volume of positive wells (fluorescent or non-fluorescent) and statistical methods that are based on the most probable number (MPN) approach to perform bacterial enumeration (28, 29). The TEMPO® system is increasingly used in the food industry, which takes advantage of its semi-automated process, built-in sample scanner for traceability purposes and its speed in achieving bacteriological count and identification without additional identification tests (30, 31). Human milk and dairy products have similar matrices in terms of fat and inhibitory substances, which suggest that the TEMPO® system might be an asset for milk banks. This technology could potentially be used as a faster means to perform in-process bacteriological monitoring of raw mother's milk and PDHM (32, 33).

The objective of this study was to conduct a performance evaluation of the TEMPO® system for the enumeration of four typical bacterial quality indicators observed in mother's milk (TAF, *Enterobacteriaceae*, *S. aureus,* and *Bacillus*) and to compare the results with standard PCM. The impacts of the milk matrix on the reliability of the TEMPO® method were assessed along with the precision and accuracy. To the best of our knowledge,

TABLE 1 | Protocol details for human milk bacterial testing.

	Total aerobic flora		*Enterobacteriaceae*		*S. aureus*		*Bacillus cereus*group	
Conditions	**TEMPO®**	**PCM**	**TEMPO®**	**PCM**	**TEMPO®**	**PCM**	**TEMPO®**	**PCM**
Initial sample dilutions	10^0, 10^2	10^0-10^3	10^1	10^0-10^3	10^0	10^0	10^0	10^0-10^3
Sample volume (mL)	1	0.1	1	0.1	1	0.1	1	0.1
Agar media or TEMPO® tests	AC	Blood sheep	EB	MacConkey	STA	Mannitol-salt	BC	Blood sheep
Incubation period (h)	24	48	22	24–48	24	48	22	24–48
Incubation temperature (°C)	35	35	35	35	35	35	30	30
Detection method	Fluorescence+	All colonies	Fluorescence–	Purple colonies	Fluorescence–	Yellow colonies	Fluorescence+	Hemolysis
Supplemental tests	No	No	No	TSI*	No	Coagulase	No	Sporulation

**Triple-sugar iron agar.*

this study represents the first assessment of the TEMPO® system performances for human milk bacterial testing.

MATERIALS AND METHODS

Milk Samples

Before collection, donors were asked to fill a milk donation qualification form providing relevant personal and medical information and to sign an informed donation consent form, in accordance with Héma-Québec's (HQ) Research Ethics Committee guidelines. Qualified donors were subjected to the same serological screening performed for regular blood donations at HQ's blood bank (i.e., hepatitis B and C, syphilis, HIV, CMV, and HTLV-I/II). Expressed milk was self-collected and frozen in a household refrigerator by mothers at their home. Periodically, milk was sent to the Public Mothers' Milk Bank using validated HQ shipping containers. All milk donations were stored at −20°C until analysis. On the day of the analysis, milk samples were rapidly thawed in a water bath at 37°C. Naturally Contaminated Milk Samples (NCMS), and uncontaminated milk samples sterilized by pasteurization were spiked with known concentrations of specific bacterial strains and labeled as Artificially Contaminated Milk Samples (ACMS). *Escherichia coli* (ATCC 25922), *Staphylococcus aureus* (ATCC 27217) and *Bacillus cereus* spores (isolated from a milk donation) were used to prepare ACMS. Mother's milk bacteriological contents were confirmed by PCM and diluted to final target concentrations in order to generate ACMS. For NCMS ($n = 55$) and ACMS ($n = 3$), 10-fold serial dilutions (10^{-1}, 10^{-2}, or 10^{-3}) were prepared in Buffered Peptone Water (BPW; bioMérieux) for bacterial enumeration, as described in **Table 1**.

Enumeration of Bacterial Quality Indicators by the Plate Count Method (PCM)

The PCM, performed by the spread plate technique, was used to enumerate all four bacterial quality indicators in milk samples. The method's performances had been previously validated following controlled quality assurance protocols. Briefly, 100 µl of milk sample were seeded on different media in duplicate. Plates were inverted and incubated at 35°C for 48 h. For the enumeration of TAF and *Bacillus* species, sheep blood agar medium was used (Oxoid; Thermo Fisher Scientific, Waltham, MA, USA). Colonies characterized by a clear zone halo, which can be attributed to hemolytic activity, were ascribed to *Bacillus*. After isolation on blood sheep agar, gram staining and inoculation of sporulation agar medium were performed to confirm the *Bacillus* identification. *Enterobacteriaceae* and *S. aureus* were enumerated on MacConkey and mannitol medium (Laboratoire de santé publique du Québec, Québec), respectively. For NCMS, characterized by a competitive flora, only presumptive pink to purple colonies fermenting lactose were counted as *Enterobacteriaceae*. Triple-Sugar-Iron agar (TSI) medium plates were seeded with bacteria to confirm the presence of *Enterobacteriaceae*. *S. aureus* in NCMS could not be quantified using the previous PCM because coagulase-negative *Staphylococcus* (CONS) and coagulase-positive Staphylococci (CPS; *S. aureus*) could both grow in mannitol medium. CPS identification was confirmed by the observation of presumptive bright yellow colonies on sheep blood agar after a 24-h incubation period at 35°C. CPS was differentiated from CONS using a coagulase test, following the manufacturer's instructions (BD BBL™ Rabbit Coagulase Plasma). For all samples, average counts from duplicates are reported as original concentrations, considering the applied dilution factor.

Enumeration of Bacterial Contaminants by the TEMPO® MPN Method

The bioMérieux TEMPO® system consists of two independent work stations, the semi-automated sample preparation module and the reading/recording module. In this study, the TEMPO® system was used according to the manufacturer's recommendations. Briefly, each individual bacterial analysis was performed using its own specific testing card, which contains a growth-triggered fluorescent transducer scattered in a selective culture medium and a predefined sample dilution pattern for determination of the MPN. Each card contains 48 analysis wells of three different volumes (225, 22.5, and 2.25 µl), from which a fluorescence signal can be recorded and interpreted to deduce the initial bacterial content reported in CFU/ml.

Before each bacterial analysis, a 1 mL milk sample was transferred into a previously rehydrated disposable vial containing 3 mL of sterile water. The seeded medium was subsequently transferred to its attached testing card and sealed

using the TEMPO® Filler. Each testing card was incubated for a specific time and temperature, following the manufacturer's recommendations (see **Table 1**). In this study, the TEMPO® AC testing card was used to characterize TAF and was incubated for 24–28 h at 35°C before reading. *Enterobacteriaceae* were enumerated using the TEMPO® EB testing card and was incubated at 35°C for 22–27 h. The TEMPO® STA testing card was used to determine the *S. aureus* concentration at 35°C for 24–27 h. Finally, a 22–27 h incubation period at 30°C was used with the TEMPO® BC testing card to assay *Bacillus* species belonging to the *Bacillus cereus* group (i.e., *B. cereus*, *B. anthracis*, *B. thuringiensis*, *B. mycoides*, *B. pseudomycoides*, *B. weihenstephanensis,* and *B. cytotoxicus*). After their respective incubation period, all cards were analyzed sequentially in an automated fashion using the TEMPO® reader station. Results are reported in CFU/ml for the original sample after manually entering the initial dilution factor (34).

Comparison of the Methods' Performances TEMPO® vs. PCM

A total of 55 NCMS were tested for TAF and *Enterobacteriaceae* by the TEMPO® MPN and PCM methods, and results were directly compared. Since the TEMPO® BC testing card is specific to the *Bacillus cereus* group, comparison of enumeration results with PCM, which uses blood sheep agar allowing growth of other *Bacillus* species, could not be done. Since CONS and CPS could both grow in mannitol medium, the measured concentration of *S. aureus* could also not be determined by PCM. Hence, the comparison of methods' performances for *S. aureus* and *Bacillus* detection was made from the number of positive samples (% of the population of $n = 55$) analyzed by both methods. Regarding the PCM method for TAF, *Enterobacteriaceae* and *Bacillus*, plate counts were obtained by seeding the undiluted sample along with 10^{-1}, 10^{-2}, and 10^{-3} dilutions. Detection of *S. aureus* was performed by spreading the original undiluted milk sample. Every plate was prepared in duplicate, and results are reported as the average count from both plates.

For TEMPO® measurements, two TEMPO® AC testing cards seeded, respectively, with 10^{0} and 10^{-2} dilutions of the undiluted milk sample were used to cover the TAF enumeration range (1-490 000 CFU/ml, or 0–5.7 log CFU/ml). TEMPO® EB testing cards were seeded with 10^{-1} dilutions giving a detection range of 10–49 000 CFU/ml, or 0–4.7 log CFU/ml. Finally, the TEMPO® STA and BC testing cards were also seeded with the original milk sample (i.e., 10^{0} dilution), and their enumeration range is 1–4,900 CFU/ml, or 0–3.7 log CFU/ml.

Evaluation of the Analytical TEMPO® MPN Method Parameters

The accuracy of the TEMPO® method for each bacterial quality indicator and the milk matrix effect were assessed using the corresponding PCM results as reference. A high concentration of NCMS was used for the determination of the TEMPO® accuracy and precision for the enumeration of TAF (i.e. 5 log CFU/ml). ACMS were prepared by spiking *Escherichia coli* for *Enterobacteriaceae* enumeration, *Bacillus cereus* spores for *Bacillus* testing and *S. aureus* for the detection of CPS. PDHM or BPW was used as diluent to decrease the bacterial concentration. To cover an enumeration ranging from 1 to 5 log CFU/ml, 10^{0}-10^{-2} sample dilutions were seeded on plates or TEMPO® cards.

Selectivity and Linearity

To assess the impacts of the milk matrix on the reliability of the TEMPO® method, milk samples were diluted in PDHM or BPW to obtain standard concentrations ranging between 1 and 5 log CFU/ml for TAF and *Enterobacteriaceae*, and between 1 and 4 log CFU/ml for *S. aureus* and *Bacillus cereus*. From each standard, four 10-fold serial dilutions were prepared for TAF, and five 10-fold serial dilutions were needed for *Enterobacteriaceae*, *S. aureus* and *Bacillus cereus* enumeration tests. Negative control samples previously determined to contain 0 CFU/ml were also prepared and analyzed. The TEMPO® and PCM enumeration results for each bacterial quality indicators diluted in either pasteurized milk or BPW were compared by regression analysis. All experiments were performed in triplicate.

Accuracy and Precision

The precision of each method was assessed from six individual measurements of six test samples prepared from the same mother's milk sample. The accuracy of the analytical method for each bacterial quality indicator was determined using three individual test samples prepared from mother's milk samples, and final target concentrations were 5 log CFU/ml for TAF, 4 log CFU/ml for *Enterobacteriaceae*, 3 log CFU/ml for *S. aureus* and 1 log CFU/ml for *Bacillus cereus*. All test samples were analyzed using both the PCM and TEMPO® method. Seeding on media or TEMPO® cards was performed using sample dilutions of 10^{-2} for TAF, 10^{-1} for *Enterobactericeae* and *S. aureus*, and no dilution (10^{0}) for *Bacillus cereus*. The results of the precision tests are expressed by the coefficient of variation (CV), which is the relative standard error compared to the mean. The method's accuracy (%) for each quality indicator was calculated by reporting the experimentally measured concentrations to the expected values.

Statistical Analysis

Bacterial counts were converted to logarithmic values. The latter were analyzed with standard statistical methods for means and standard deviations (SD). The correlation between the PCM and TEMPO® results was assessed by linear regression analysis and the coefficient of determination (R^2) was used to estimate the model accuracy. The agreement between methods was evaluated by performing a Bland-Altman analysis (OriginPro8.0, OriginLab Corporation, Northampton, MA, USA; SAS 9.4, SAS Institute, Cary, NC, USA).

RESULTS

Comparison of TEMPO® and PCM Performances With NCMS

Samples ($n = 55$) were tested for all four bacterial quality indicators by both methods. Comparing bacterial counts

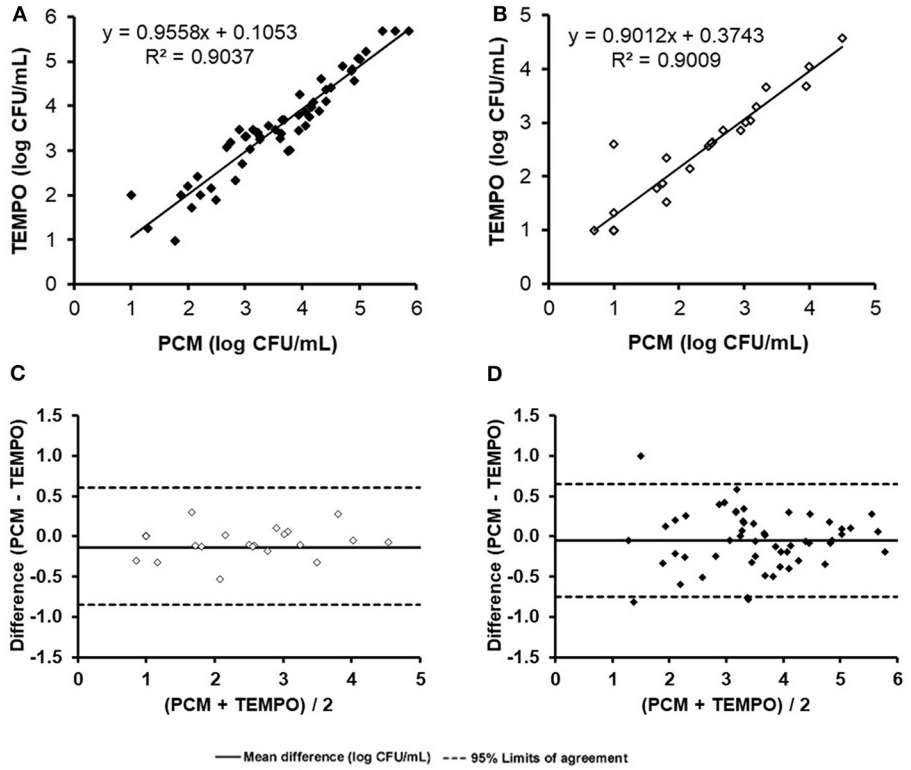

FIGURE 1 | Comparison of total aerobic flora and *Enterobacteriaceae* enumerations (log count per mL) for the 55 naturally contaminated samples by the TEMPO® and plate count methods. Linear regression curve **(A)** and Bland-Altman analysis **(C)** for total aerobic flora. Linear regression curve **(B)** and Bland-Altman analysis **(D)**.

TABLE 2 | Comparative detection of four bacterial quality indicators in 55 NCMS using TEMPO® and PCM methods.

		PCM							
		Total aerobic flora		***Enterobacteriaceae***		***S. aureus***		***Bacillus sp.***	
		Positive	**Negative**	**Positive**	**Negative**	**Positive**	**Negative**	**Positive**	**Negative**
TEMPO method	**Positive**	55	0	24	2	1	0	4	5
	Negative	0	0	1	28	2	52	1	45

obtained for each sample tested by the PCM and TEMPO® methods, there was no more than a 1 log CFU/ml difference in the results, irrespective of the bacterial target.

Total Aerobic Flora

When comparing enumeration results obtained from both methods for TAF using a linear regression analysis, the coefficient of determination obtained was 0.90 (**Figure 1A**). The concentration of one milk sample was out of the quantification range for both methods, and was therefore excluded from the analysis. According to the Bland-Altman analysis (**Figure 1C**), there was a good agreement between both methods, with a mean difference of < 0.5 log CFU/ml across the entire range of values. Only a few samples ($n = 4$) were found to be outside the agreement limits of the Bland-Altman analysis set at $2 \times$ SD. The degree of correlation and agreement between measurements is highlighted by the narrow 95% CI (−0.8 to 0.7 log CFU/ml) and an analytical bias of only 0.1 log CFU/ml for the TEMPO® method over the PCM.

Enterobacteriaceae

Only 44% (24/55) of milk samples were found positive for *Enterobacteriaceae* after analysis by both methods. At low concentrations ($<$ 1.3 log CFU/ml), two samples were positive according to the TEMPO® EB test, but only one showed growth by PCM using MacConkey agar medium (**Table 2**). A statistical analysis was performed on the 24 positive samples, and a linear regression coefficient of 0.90 was obtained (**Figure 1B**). The Bland-Altman plot (**Figure 1D**) shows a good agreement between the two methods, as all results are within the 95% C.I. limits (−0.9 to 0.6 log CFU/ml), with an analytical bias of only 0.1 log CFU/ml

TABLE 3 | Correlation coefficients between plate count and TEMPO® methods for the enumeration of bacterial quality indicators in ACMS and NCMS contaminated samples.

	Total aerobic flora	*Enterobacteriaceae*	*S. aureus*	*Bacillus cereus*
Enumeration range* (log/ml)	0–5	0–5	0–4	0–4
Correlation (R^2)				
NCMS	0.976	n.a.	n.a.	n.a.
ACMS buffered peptone water	n.a.	0.996	0.990	0.994
Artificially contaminated milk	n.a.	0.995	0.948	0.990

**A minimum of four dilutions were teste (n = 3).*
n.a., not available.

TABLE 4 | Evaluation of the accuracy and precision of the plate count and TEMPO® methods at concentrations close to the acceptance criteria for human milk before pasteurization.

	Expected concentration (log CFU/ml)	Measured concentration (log CFU/ml)	CV (%)	Accuracy¥ (%)
Plate count method				
Total aerobic flora	5.3	5.2 ± 0.1	1.7	98.1
Enterobacteriaceae	4.0	4.0 ± 0.1	1.4	100.0
S. aureus	3.0	2.7 ± 0.1	2.0	90.0
Bacillus cereus (spores)	1.0	0.8 ± 0.6	81.6	80.0
TEMPO® method				
Total aerobic flora	5.3	5.3 ± 0.1	2.9	100.0
Enterobacteriaceae	4.0	4.1 ± 0.1	3.0	102.5
S. aureus	3.0	2.5 ± 0.1	5.3	83.3
Bacillus cereus (spores)	1.0	1.2 ± 0.1	9.1	120.0

¥Accuracy = (measured concentration/expected concentration) × 100 (n = 3).
Coefficient of variation = (standard deviation/mean) × 100 (n = 6).

and a calculated ICC of 0.94, suggesting an excellent reliability for the TEMPO® method.

S. aureus

S. aureus was detected by the PCM and the strain identity was confirmed by the coagulase test (**Table 2**) for three of the 55 milk samples (5.4%). The TEMPO® STA test gave a positive result for only one of them associated with an error (code 19). The code 19 is associated to an inconsistent result generated by the TEMPO® reader system. When an incoherent result is obtained, fluorescence is present in the upper wells of the card, confirming the presence of bacteria in the sample, but without a concentration estimate. Despite the fact that it was not possible to obtain a bacterial count for this sample due to a code 19, but considering that the error is associated with growth, they were identified as being contaminated. Consequently, there were two human milk samples unconfirmed positive for the presence of *S. aureus* by the TEMPO® system out of the 55 analyzed.

Bacillus

Bacillus was detected in nine of the 55 samples by TEMPO®, compared to only five by the reference PCM. Only one of the five positive samples identified by PCM was detected exclusively by the gold standard method. On the other hand, five of the nine positive samples by TEMPO were considered negative by PCM. In the end, four samples were tested positive for *bacillus* by both methods (**Table 2**). Interestingly, the single colony of a presumptive *bacillus* that grew on blood agar did not generate beta hemolysis, thereby questioning the identity as a *cereus* species. However, analysis by mass spectrometry (MALDI-TOF) confirmed that the bacterium belongs to the cereus group, and therefore should have been detected by the TEMPO® BC test; however the concentration was only 5 CFU/ml. Overall, both methods demonstrated their capacities to detect low levels of *bacillus* i.e., from 0 to 3.7 log CFU/ml (1–4,900 CFU/ml).

Evaluation of the Analytical TEMPO® MPN Method Parameters

Selectivity and Linearity

The TEMPO® system enables the quantification of bacterial quality indicators over a concentration range of four to five orders of magnitude. To assess the impacts of the complex milk matrix on the TEMPO® method's analytical performances, enumeration results for all bacterial target were compared in ACMS vs. BPW, with the exception of TAF, which was performed in NCMS only (**Table 3**). The statistical analysis shows a good overall agreement between the PCM and TEMPO® methods for all tested bacterial strains and sample matrices. More specifically, the linearity coefficient between the PCM and TEMPO® results for the enumeration of the TAF in milk is $R^2 = 0.976$. Furthermore, bacterial counts obtained for *Enterobacteriaceae* by the PCM using MacConkey medium correlated just as well in a matrix composed of either milk ($R^2 = 0.995$) or BPW ($R^2 = 0.996$). The linear correlation coefficients observed when plotting *S. aureus* counting results by TEMPO® vs. PCM are $R^2 = 0.990$ and $R^2 = 0.948$ for BPW and milk matrices, respectively. Finally, there were no significant differences in the results obtained by the two methods for the enumeration of *B. cereus* using BPW ($R^2 = 0.994$) or milk ($R^2 = 0.990$) samples artificially contaminated with spores. Note that an R^2 value of 1.0 indicates a perfect fit between variables and indicating that the model explains all the relationship, between the two factors.

Precision and Accuracy

Table 4 presents the results obtained for the characterization of the precision and accuracy of both methods. For the precision expressed as the CV, a series of six measurements were taken from samples prepared so that their final concentration was strategically located within the quantification range of each bacterial target. For TAF, the expected sample concentration was 5 log CFU/ml. A CV of 3% was obtained for TEMPO, compared

to 2% for PCM for paired samples. For *Enterobacteriaceae*, the enumeration target was set to 4 log CFU/ml and, similar to the TAF result, a slightly lower CV was obtained for PCM (1%) compared to TEMPO (3%), which was identical to the CV for TAF. A lower target concentration of 3 log CFU/ml was chosen for *S. aureus*, given the more stringent human milk release criteria for gram-positive bacteria. For this target species and concentration, CV of 5 and 2% were obtained for TEMPO® and PCM, respectively. A low 1 log CFU/ml concentration target was chosen for *Bacillus*; given this target, a CV of 9% was obtained with TEMPO®, and a much higher variability was observed in the results for PCM, with a CV of 82%.

The accuracy of each method was calculated from the difference observed between the average experimental value, calculated from three separate measurements, and the expected value for each sample whose final concentration was adjusted so as to be in the quantification range. **Table 4** presents the PCM and TEMPO® accuracy results observed for each target bacterium. In the case of TAF and *Enterobacteriaceae*, values approaching 100% were obtained with both enumeration methods at 4 and 5 log CFU/ml, respectively. For *S. aureus*, the target concentration to assess the accuracy of the PCM and TEMPO® methods was 3 log CFU/ml; at that concentration, the accuracy was 90 and 83% for PCM and TEMPO® method, respectively. Finally, a 1 log CFU/ml target concentration was used with *Bacillus*; at that target, the PCM method underestimated the milk sample contamination (80%), and the TEMPO® method overestimated it (120%).

DISCUSSION

The TEMPO® system is currently used in several countries, mainly as a quality control tool in the food industry. Indeed, all TEMPO® bacterial tests have been approved by international quality and standards organizations, such as AOAC International, AFNOR and ISO for food and environmental samples (35–38). Evaluations of the performances of the TEMPO® MPN method for the characterization of bacterial content in food products, including dairy milk, have been reported (39–45). Most of them have demonstrated a good agreement in the results between the plate count method and TEMPO® for all types of targeted bacteria. The main objective of this performance evaluation was to compare the enumeration capability of the TEMPO® system aimed at the characterization of human milk microflora and the detection of specific bacterial contaminants of interest at concentration levels as low as 1 log CFU/ml in < 24 h. The enumeration results for TAF and *Enterobacteriaceae* obtained from 55 NCMS demonstrated a good agreement between the PCM and TEMPO® methods and, more importantly, no significant analytical bias was observed for the TEMPO® system using plate counts as reference. Differences in the output values were not > 1 log CFU/ml for all samples, which testify to the reliability of the TEMPO® system. Interestingly, occasional discrepancies were observed between enumeration counts obtained from TEMPO® AC cards inoculated with 10^0 and 10^{-2} dilutions of the same mother's milk sample. The upper detection limit threshold of 490 000 CFU/ml was exceeded with the undiluted sample, while the 10^{-2} dilution generated bacterial counts within the 1–4,900 CFU/ml enumeration range. This result could be attributed to an apparent fluorescence quenching caused by diffusion or absorption of the output signal by the complex milk matrix, interpreted by the system as a sample of high bacterial content. A dilution of the sample seems to attenuate the matrix effect on the fluorescence output signal and allows obtaining results within the quantification range of the TEMPO® AC card. This in turn enables to identify milk samples with an aerobic flora content that exceeds the quality criterion of $> 10^5$ CFU/ml with a good level of confidence.

Testing a 10^{-1} sample dilution would be recommended for the enumeration of *S. aureus*; this dilution, corresponding to a limit of detection of < 10 CFU/ml, conforms to the quality criterion threshold for this bacterial species and corresponds to the current plate count method performed on mannitol agar in terms of limit of detection. Finally, 10^0 and 10^{-1} dilutions of the mother's milk sample would be recommended to span appropriate concentration ranges for the enumeration of *Bacillus* and *Enterobacteriaceae* with TEMPO® BC and EB cards, according to the quality criteria applicable to these bacterial species. During the evaluation of the TEMPO® analytical performances, a few samples, independently of the targeted bacteria, generated an error code (code 19), which could be attributed to incoherent results according to the TEMPO® user's manual. The error code is believed to be associated to the opacity of the human milk matrix since all events were observed with undiluted samples. Light absorption by proteins or scattering by the milk fat globules, among others, could interfere with the bacterial growth transducer excitation of its fluorescence emission resulting in a noisy optical signal. According to bioMérieux's technical staff, adherence to the incubation period recommended for each testing card should allow sufficient growth from the lower wells and solve the issue. Repeating the same sample analyses with new testing cards and using the upper recommended limit as the incubation period, the same error code was obtained. One must conclude on the possibility that some human milk constituents may interfere with the TEMPO® detection process. Proper identification of the principal interfering constituents and, extensively, of maternal factors impacting detection performances of the TEMPO® system could be investigated. Nevertheless, to maintain a detection limit of 1 CFU/ml for *S. aureus* and *Bacillus* sp. it requires performing TEMPO® analyses on undiluted samples. Consequently, it would be well-advised to conduct secondary testing in the case of positive samples for *S. aureus* or *Bacillus* sp. in order to determine the bacterial concentration. It is worth noting that some *Bacillus* species outside the *cereus* group would not be detected by the TEMPO® BC test. However, this test remains efficient at quantifying some of the most harmful contaminants with pathogenic potential related to this genus (46). Finally, TEMPO®'s precision and accuracy were comparable to the PCM and, interestingly, the semi-automated detection method performed better than the PCM at low concentration levels, which might prevent the distribution use of human milk contaminated with small numbers of bacteria belonging to the *Bacillus cereus* group.

Within a 24-h period, characterization of the bacterial content in mother's milk donations and pasteurized human milk bottles were performed using the TEMPO® technology from bioMérieux. More specifically, TEMPO® was used for the enumeration of the total aerobic bacterial flora, *Enterobacteriaceae*, *B. cereus* group and *S. aureus* from raw human milk with sample dilutions as the only sample preparation steps prior to the incubation and detection. Rapid and reliable detection of bacterial content would help screening for contaminated milk donations with heat-resistant bacteria prior to pasteurization, thereby reducing rejection rates, and improving overall end-product safety and quality. The bioMérieux TEMPO® system includes a built-in scanning device ensuring sample traceability. It is designed to be integrated within a human milk production line for in-process testing and determining pooling strategies before thermal processing. This study underlines the importance for human milk banks to keep an eye on innovative technologies, especially those dealing with the characterization of bacterial content, as these could lead to enhancements in productivity but most of all, in the safety of a precious product intended for preterm infants.

DATA AVAILABILITY STATEMENT

All data sets are stored on a dedicated external hard drive. They can be made available upon request to the corresponding author.

ETHICS STATEMENT

The studies involving human participants were reviewed and approved by the legal affairs department at Héma-Québec. The patients/participants provided written informed consent to participate in this study.

AUTHOR CONTRIBUTIONS

M-PC, MG, and DB conceived and designed the study and wrote the article. ND collected the data and contributed to the discussion of the results. AL performed the statistical analysis. MC provided suggestions concerning the content of the article and were responsible for critically revising the manuscript. All authors contributed to the article and approved the submitted version.

ACKNOWLEDGMENTS

The authors would like to thank, Manon Landry for her role in supervising the activities of the human milk bank at Héma-Québec (Montreal), Dr. Gilles Delage, France Bernier, and Jean-François Leblanc for critically reading the manuscript, and bioMérieux Canada for their technical support all along the study.

REFERENCES

1. Human Milk Banking of North America (HMBANA). *Guidelines for the Establishment and Operation of a Donor Human Milk Bank*. 10th ed. Raleigh, NC: Human Milk Bank Association of North America (2018).
2. National Institute for Health and Care Excellence (NICE). Donor Breast Milk Banks: The Operation of Donor Milk Bank Services. service operation. NICE Clinical Guidelines, No. 93 (2010).
3. Moro GE, Billeaud C, Rachel B, Calvo J, Cavallarin L, Christen L, et al. Processing of donor human milk: update and recommendations from the European milk bank association (EMBA). *Front Pediatr.* (2019) 7:49. doi: 10.3389/fped.2019.00049
4. Urbaniak C, Gloor GB, Brackstone M, Scott L, Tangney M, Reid G. The microbiota of breast tissue and its association with breast cancer. *Appl Environ Microbiol.* (2016) 82:5039–48. doi: 10.1128/AEM.01235-16
5. Le Doare K, Holder B, Bassett A, Pannaraj PS. Mother's milk: a purposeful contribution to the development of the infant microbiota and immunity. *Front Immunol.* (2018) 9:361. doi: 10.3389/fimmu.2018.00361
6. Cabrera-Rubio R, Collado MC, Laitinen K, Salminen S, Isolauri E, Mira A. The human milk microbiome changes over lactation and is shaped by maternal weight and mode of delivery. *Am J Clin Nutr.* (2012) 96:544–51. doi: 10.3945/ajcn.112.037382
7. Lombard F, Marchandin H, Jacquot A, Cambonie G, Rodiere M, Filleron A. *Streptococcus agalactiae* late-onset neonatal infections: should breast milk be more systematically tested for bacterial contamination? *Acta Paediatr.* (2012) 101:e529–30. doi: 10.1111/apa.12006
8. Hilliard NJ, Schelonka RL, Waites KB. *Bacillus cereus* bacteremia in a preterm neonate. *J Clin Microbiol.* (2003) 41:3441–4. doi: 10.1128/JCM.41.7.3441-3444.2003
9. Decousser JW, Ramarao N, Duport C, Dorval M, Bourgeois-Nicolaos N, Guinebretiere MH, et al. *Bacillus cereus* and severe intestinal infections in preterm neonates: putative role of pooled breast milk. *Am J Infect Control.* (2013) 41:918–21. doi: 10.1016/j.ajic.2013.01.043
10. Nakamura K, Kaneko M, Abe Y, Yamamoto N, Mori H, Yoshida A, et al. Outbreak of extended-spectrum beta-lactamase-producing *Escherichia coli* transmitted through breast milk sharing in a neonatal intensive care unit. *J Hosp Infect.* (2016) 92:42–6. doi: 10.1016/j.jhin.2015.05.002
11. Byrne PA, Miller C, Justus K. Neonatal group B streptococcal infection related to breast milk. *Breastfeed Med.* (2006) 1:263–70. doi: 10.1089/bfm.2006.1.263
12. Picaud JC. VIII. Human milk banks: How to organize the collection of human milk to feed preterm infants. *J Pediatr Gastroenterol Nutr.* (2015) 61(Suppl. 1):S10–2. doi: 10.1097/01.mpg.0000471456.78296.a6
13. Weaver G, Bertino E, Gebauer C, Grovslien A, Mileusnic-Milenovic R, Arslanoglu S, et al. Recommendations for the establishment and operation of human milk banks in Europe: a consensus statement from the European milk bank association (EMBA). *Front Pediatr.* (2019) 7:53. doi: 10.3389/fped.2019.00053
14. Froh EB, Vanderpool J, Spatz DL. Best practices to limit contamination of donor milk in a milk bank. *J Obstet Gynecol Neonatal Nurs.* (2018) 47:547–55. doi: 10.1016/j.jogn.2017.12.002
15. Necidova L, Bogdanovicova K, Harustiakova D, Bartova K. Short communication: pasteurization as a means of inactivating staphylococcal enterotoxins A, B, and C in milk. *J Dairy Sci.* (2016) 99:8638–43. doi: 10.3168/jds.2016-11252
16. Alles AA, Wiedmann M, Martin NH. Rapid detection and characterization of postpasteurization contaminants in pasteurized fluid milk. *J Dairy Sci.* (2018) 101:7746–56. doi: 10.3168/jds.2017-14216
17. Jang HL, Cho JY, Kim MJ, Kim EJ, Park EY, Park SA, et al. The experience of human milk banking for 8 years: Korean perspective. *J Korean Med Sci.* (2016) 31:1775–83. doi: 10.3346/jkms.2016.31.11.1775
18. Arslanoglu S, Bertino E, Tonetto P, De Nisi G, Ambruzzi AM, Biasini A, et al. Guidelines for the establishment and operation of a donor human milk bank. *J Matern Fetal Neonatal Med.* (2010) 23:1–20. doi: 10.3109/14767058.2010.512414
19. Ministère de la Santé, de la Jeunesse et des Sports. *Décrets, Arrêtés, Circulaires. Textes Généraux. Décision du 3 Décembre 2007 Définissant les Règles de Bonnes*

Pratiques Prévues à L'alinéa 3 L'article L. 2323-1 du Code de la Santé Publique. JORF; texte 22 sur 165 (2008).
20. Hartmann BT, Pang WW, Keil AD, Hartmann PE, Simmer K. Best practice guidelines for the operation of a donor human milk bank in an Australian NICU. *Early Hum Dev.* (2007) 83:667–73. doi: 10.1016/j.earlhumdev.2007.07.012
21. Omarsdottir S, Casper C, Akerman A, Polberger S, Vanpee M. Breastmilk handling routines for preterm infants in Sweden: a national cross-sectional study. *Breastfeed Med.* (2008) 3:165–70. doi: 10.1089/bfm.2007.0033
22. Chang FY, Cheng SW, Wu TZ, Fang LJ. Characteristics of the first human milk bank in Taiwan. *Pediatr Neonatol.* (2013) 54:28–33. doi: 10.1016/j.pedneo.2012.11.004
23. Mullie C, Obin O, Outurquin G, Grognet S, Leke A, Adjide C. Breastmilk donations: bacteriological assessment, analysis of causes of non-compliance and suggestions for improvement. *Arch Pediatr.* (2018) 25:263–8. doi: 10.1016/j.arcped.2018.02.006
24. Owen M, Willis C, Lamph D. Evaluation of the TEMPO((R)) most probable number technique for the enumeration of enterobacteriaceae in food and dairy products. *J Appl Microbiol.* (2010) 109:1810–6. doi: 10.1111/j.1365-2672.2010.04810.x
25. Lee DY, Kim HY, Cho YS. Comparison of TEMPO BC and MYP plate methods for the enumeration of bacillus cereus in various foods. *J Food Hyg Saf.* (2017) 32:249–53. doi: 10.13103/JFHS.2017.32.4.249
26. Yossa N, Smiley J, Huang MJ, Yin L, Bell R, Tallent S, et al. Comparison of TEMPO((R)) BC with spiral plating methods for the enumeration of *bacillus cereus* in cosmetic products either naturally preserved or preserved with phenoxyethanol. *J AOAC Int.* (2019) 102:1080–90. doi: 10.5740/jaoacint.18-0375
27. Yörük NG. Most probable number technique in *Escherichia coli* count using ISO 16649-3, ISO 7251, and rapid test enumeration device (TEMPO EC) methods in milk and dairy products. *J Food Saf.* (2018) 38:e12502. doi: 10.1111/jfs.12502
28. Cochran WG. Estimation of bacterial densities by means of the "most probable number". *Biometrics.* (1950) 6:105–16. doi: 10.2307/3001491
29. Woodward RL. How probable is the most probable number? *J Am Water Works Assoc.* (1957) 49:1060–8. doi: 10.1002/j.1551-8833.1957.tb16906.x
30. Tallent SM, Hait JM, Ferguson M. Comparative study of tempo BC automated MPN for the enumeration of bacillus cereus group in food. *J Food Saf.* (2018) 38:e12472. doi: 10.1111/jfs.12472
31. Lobacz A, Kowalik J, Zulewska J. Determination of the survival kinetics of *Salmonella* spp. on the surface of ripened raw milk cheese during storage at different temperatures. *Int J Food Sci Technol.* (2020) 55:610–8. doi: 10.1111/ijfs.14315
32. Crowley ES, Bird PM, Torontali MK, Agin JR, Goins DG, Johnson R. TEMPO TVC for the enumeration of aerobic mesophilic flora in foods: collaborative study. *J AOAC Int.* (2009) 92:165–74. doi: 10.1093/jaoac/92.1.165
33. Lindemann S, Kmet M, Reddy R, Uhlig S. Matrix-specific method validation of an automated most-probable-number system for use in measuring bacteriological quality of grade "A" milk products. *J Food Prot.* (2016) 79:1911–8. doi: 10.4315/0362-028X.JFP-16-141
34. U. S. Food and Drug Administration. *Bacteriological Analytical Manual. Appendix 2*. (2010). Available online at: https://www.fda.gov/food/laboratory-methods-food/bam-appendix-2-most-probable-number-serial-dilutions (accessed February 18, 2020).
35. Association française de normalisation (AFNOR). *Validation Certificate for Alternative Analytical Method According to Standard EN ISO 16140: 2003, Certificate no. BIO 12/13-02/05: TEMPO EC- Method Validated for the Enumeration of Escherichia coli in Food Products*. (2005). Available online at: http://www.afnor-validation.com/afnor-validation-validated-methods/e-coli.html (accessed February 18, 2020).
36. Association française de normalisation (AFNOR). *Validation Certificate for Alternative Analytical Method According to Standard EN ISO 16140: 2003, Certificate no. BIO 12/17-12/05: TEMPO TC- Method Validated for the Enumeration of Total Coliforms in Food Products*. (2005). Available online at: http://www.afnor-validation.com/afnor-validation-validated-methods/coliforms.html (accessed February 18, 2020).
37. Association française de normalisation (AFNOR). *Validation Certificate for Alternative Analytical Method According to Standard NF EN ISO 16140-2: 2016, Certificate no. BIO 12/35-05/13: TEMPO AC- Method Validated for the Enumeration of Aerobic Mesophilic Flora in Human Food, Pet Food and Environmental Samples*. (2016). Available online at: https://nf-validation.afnor.org/wp-content/uploads/2014/03/Synt-BIO-12-35-05-13 (accessed February 18, 2020).
38. Association française de normalisation (AFNOR). *ISO 16140 – Part 2: Validation Study of a TEMPO Method for Bacillus Cereus Enumeration in Food Samples and Environmental Samples*. (2016). Available online at: https://assets.bettyblocks.com/2e826c3765f4401c84671a06de961fc7_e1e4b8ec2b22479080d36038777c5403/17066/2014LR47_-_TEMPO_BC_-_SUMMARY_REPORT___MicroVal_-_Version_1_.pdf (accessed February 18, 2020).
39. Katase M, Tsumura K. Enumeration of micro-organisms in processed soy products with an automated most probable number method compared with standard plate method. *Lett Appl Microbiol.* (2011) 53:539–45. doi: 10.1111/j.1472-765X.2011.03143.x
40. Torlak E, Akan IM. Evaluation of TEMPO STA for the enumeration of coagulase-positive staphylococci in cheese. *Food Sci Technol.* (2012) 18:645–50. doi: 10.3136/fstr.18.645
41. Paulsen P, Schopf E, Smulders FJ. Enumeration of total aerobic bacteria and *Escherichia coli* in minced meat and on carcass surface samples with an automated most-probable-number method compared with colony count protocols. *J Food Prot.* (2006) 69:2500–3. doi: 10.4315/0362-028X-69.10.2500
42. Paulsen P, Borgetti C, Schopf E, Smulders FJ. Enumeration of *Enterobacteriaceae* in various foods with a new automated most-probable-number method compared with petrifilm and international organization for standardization procedures. *J Food Prot.* (2008) 71:376–9. doi: 10.4315/0362-028X-71.2.376
43. Line JE, Stern NJ, Oakley BB, Seal BS. Comparison of an automated most-probable-number technique with traditional plating methods for estimating populations of total aerobes, coliforms, and *Escherichia coli* associated with freshly processed broiler chickens. *J Food Prot.* (2011) 74:1558–63. doi: 10.4315/0362-028X.JFP-11-024
44. Kunicka A. Evaluation of the TEMPO system: an automated method for food microbiological quality control. *J Biotechnol.* (2007) 131:69–72. doi: 10.1016/j.jbiotec.2007.07.119
45. Zitz U, Domig KJ, Hoehl A, Weiss H, Wilrich PT, Kneifel W. Evaluation of three applications of a semi-automated most-probable-number for the assessment of microbiological parameters in dairy products. *Accred Qual Assur.* (2011) 16:299–309. doi: 10.1007/s00769-011-0772-3
46. Ehling-Schulz M, Lereclus D, Koehler TM. The *Bacillus cereus* group: *Bacillus* species with pathogenic potential. *Microbiol Spectr.* (2019) 7:GPP3-0032-2018. doi: 10.1128/microbiolspec.GPP3-0032-2018

Conflict of Interest: The authors declare that the research was conducted in the absence of any commercial or financial relationships that could be construed as a potential conflict of interest.

frontiers in Pediatrics

ORIGINAL RESEARCH
published: 10 September 2020
doi: 10.3389/fped.2020.00561

The Effects of High-Altitude Environment on Brain Function in a Seizure Model of Young-Aged Rats

Yao Xie[1], *Shenglan Qin*[2], *Rui Zhang*[1], *Hong Wu*[2], *Guoyu Sun*[1], *Lili Liu*[1]* *and Xinlin Hou*[1]*

[1] *Pediatric Department, Peking University First Hospital, Beijing, China,* [2] *Pediatric Department, People's Hospital of Tibet Autonomous Region, Tibet, China*

OPEN ACCESS

Edited by:
Yuan Shi,
Children's Hospital of Chongqing Medical University, China

Reviewed by:
Zhihui Rong,
Huazhong University of Science and Technology, China
Lan Zhang,
Anhui Provincial Hospital, China

***Correspondence:**
Lili Liu
liliszm@163.com
Xinlin Hou
07711@pkufh.com

Specialty section:
This article was submitted to Neonatology, a section of the journal Frontiers in Pediatrics

Received: *30 May 2020*
Accepted: *03 August 2020*
Published: *10 September 2020*

Citation:
Xie Y, Qin S, Zhang R, Wu H, Sun G, Liu L and Hou X (2020) The Effects of High-Altitude Environment on Brain Function in a Seizure Model of Young-Aged Rats. Front. Pediatr. 8:561. doi: 10.3389/fped.2020.00561

In this study, we examined the effects of high-altitude environment on the brain function of a young-rat seizure model. Two-hundred healthy, 3-week old, male rats were selected and equally divided into the plateau and plain groups. The plateau group was preconditioned in a simulated 5,000-m altitude (barometric pressure [PB], 405 mmHg; partial pressure of oxygen [PO_2], 84 mmHg) for 6 h/day for 7 days, while the plain group was kept in the ordinary atmospheric environment (PB, 760 mmHg; PO_2, 157 mmHg) for 7 days. After preconditioning, rats were administered pentylenetetrazol (PTZ) to generate level-4 or stronger seizures. Electroencephalogram (EEG) signals were recorded (16 rats/group); the histology and apoptosis of hippocampal tissue were evaluated (6 rats/group); and spatial learning and memory were examined in the Morris water maze (12 rats/group; 6-weeks old). To induce a level 4 or stronger seizure successfully, a significantly higher PTZ dose was used in the plateau (81.32 ± 21.57 mg/kg) than in the plain group (63.41 ± 19.77 mg/kg, $p < 0.01$); however, the plateau group survival rate was significantly lower than that of the plain group (26.2 vs. 42.9%, $p < 0.05$). EEG parameters did not differ between the two groups. Histological analysis revealed that in the plateau group, more neurons were observed ($p < 0.001$), especially in DG and CA1 areas, and less apoptotic cells were found in DG areas ($p = 0.035$), comparing with the plain group. No differences were found between the two groups in any of the parameters examined in the Morris water maze. Our results show that the disease outcome caused by low pressure and low oxygen environment in the plateau group was different to that in the plain group. The high drug dosage to induce seizures in the plateau group, accompanied by increased mortality rates after seizures, indicates that the seizure threshold may be higher in the plateau than in the plain group. Moreover, based on the histological findings, the plateau environment seems to exert a protective effect on brain development after seizures only for survived individuals with mild conditions.

Keywords: high altitude, seizures, brain function, hypoxia, young-aged rats

INTRODUCTION

Tibet is an area with an average altitude of about 4,000 m, with a pressure and partial pressure of oxygen significantly lower than those in plain areas. Tibet's special geographical state not only results in differences between disease spectra but also between the physiological states within the same disease. During one of our author's work as aid for Tibet, she found that for the young children especially the neonates with convulsion in Tibet, the outcome of survival children seemed to be better than in plain areas. It has been established that sustained severe hypoxia can lead to brain hypoxia, ischemia, and edema, eventually leading to neuronal necrosis and irreversible brain damage (1). However, recent studies suggest that moderate hypoxia may have a protective effect on brain injury-related diseases. To train pilots, the concept of "hypoxic training" was proposed as early as the 1930s (2). It is believed that moderate hypoxia training can increase the tolerance of human body, especially that of the cardiovascular system, to subsequent hypoxia. The training method can be a stay at high altitude camps for several weeks, regular high-altitude flights by airplane, training in altitude chambers, and inhalation of a low-oxygen mixture. Follow-up studies found that the low-pressure hypoxic preconditioning can improve other organs' tolerance to hypoxic-ischemic injury; this effect is also encountered in the brain, providing protection to cerebral ischemia and neurodegenerative diseases (3, 4). However, the degree to which hypoxia can induce damage or protection, and against which degree of brain injury hypoxia can provide protection is not clear and is still controversial. Therefore, the impact of plateau environment on diseases needs to be further studied.

Convulsions are common neurological symptoms in childhood and can be caused by a variety of reasons (5). The infantile, especially the neonatal period, is a critical period for nervous system development; thus, the convulsion-induced damage to the nervous system during this period can be considerable. The severity and duration of convulsive seizures are crucial factors influencing the outcomes. A study showed that in 89 patients, 23 (36%) had neurological abnormalities upon examination without an apparent functional impact, neonatal mortality due to convulsive seizures in term infants has been reported at 7%; while 28% of the survivors have poor long-term outcomes. Among the infants with overall poor neurological outcomes (25 patients), 20 (80%) had severe and 5(20%) had moderate neurological impairment (6). Recurrent epileptic seizures cause neuronal loss in the developing brain through apoptosis and necrosis and induce progressive memory deficits (7). In order to reduce those poor outcomes, many studies have been conducted to search for brain protective measures. Research on preconditioning has resulted in various promising strategies for the treatment of patients with acute brain injury (8). Among them, low-pressure hypoxic preconditioning has been widely studied. A study by Zhen et al. (9) suggested that moderate hypoxic preconditioning after epilepsy had a protective effect on brain injury. However, there is paucity of studies examining whether these protective effects are present at different hypoxic levels.

The Tibetan plateau provides a natural low-pressure hypoxic environment. The characteristics of children's convulsion in Tibet are special in outcomes compared with those in plain areas. However, it is still not clear whether the low-pressure hypoxia provided by the plateau environment leads to protection or damage as relevant research is lacking. And if the convulsions are severe, whether the low-pressure hypoxia plays a role is also a problem we want to clarify. To better understand the effect of the plateau environment on the severe convulsion and prognosis, we generated a convulsion rats model with sever levels (level 4–5). First, we preconditioned rats in a low-pressure hypoxia oxygen environment to simulate the plateau environment. Next, we monitored the rats' brain electrical activity, observed the pathological changes of brain tissues, and analyzed the results of the Morris water maze experiment to evaluate the effects of low-pressure hypoxia on brain function.

MATERIALS AND METHODS

Animals

All animal experiments were approved by the local Animal Welfare Committee. We randomly divided 200 3-week-old (the earliest time to withdraw breastfeeding is 21 days after birth), healthy male, Sprague–Dawley rats (weight 60–80 g) into an experimental group (100 rats), and a control group (100 rats). We chose male rats to exclude any effects on epilepsy produced by estrogens or the estrous cycle of female rats (10). The animal experimental protocols were performed in accordance with the Animal Management Rule of the Chinese Ministry of Health and the Animal Care Committee of Peking University First Hospital, Beijing, China. All rats were born and raised at Beijing Vital River Laboratory Animal Technologies Co., Ltd., for the first 21 days, then were transferred to PKUFH Experimental Animal Center. The rats were housed in wire mesh cages in an air-conditioned room (22 ± 2°C) on a 12-h light/dark cycle (06:00–18:00) and *ad libitum* access to food and water. The plateau group was preconditioned to a simulated altitude of 5,000 m (barometric pressure [PB], 405 mmHg; partial pressure of oxygen [PO_2], 84 mm) for 6 h/day, for a total of 7 days. The plateau environment was stimulated by the high pressure/low pressure oxygen tank in The Sixth Medical Center of PLA General Hospital. We placed the rats of plateau group into the tank at same time each day (in light cycle) and provide them the same foods and temperature as outside. The plain group was exposed to ordinary atmospheric conditions (PB, 760 mmHg; PO_2, 157 mmHg) for 7 days.

Young-Rat Seizure Model

After preconditioning, all experimental animals received an intraperitoneal injection (i.p.) of 20 mg/kg (The dosage was a moderate dosage compared with those reported by other institutions) pentylenetetrazol (PTZ, Sigma, USA) to generate the convulsion model freely dissolved in saline (solution: 20 mg PTZ dissolved in 1 ml saline) (11, 12). Extracorporeal electroencephalogram (EEG) electrodes was placed on 16 rats of each group to monitor the seizure (which don't get the additional PTZ). Behavioral seizures were graded according to the Racine scale (13) as follows: stage 1—behavioral arrest with mouth/facial

TABLE 1 | Electroencephalogram parameters in the plateau and plain groups. Values are the mean±SEM.

	Plateau ($n = 16$)	Plain ($n = 16$)	p-value
Frequency of sharp wave (Hz)	5.78 ± 1.90	4.81 ± 1.88	0.051
Duration (s)	54.30 ± 51.29	65.87 ± 84.22	0.490
Amplitude (μV)	783.42 ± 247.40	830.17 ± 281.21	0.409
Interval of crest (s)	0.23 ± 0.99	0.18 ± 0.75	0.067
Duration of post-seizure electrical suppression(s)	8.19 ± 8.76	10.35 ± 7.25	0.316

movements; stage 2—head nodding; stage 3—forelimb clonus; stage 4—rearing or hind limb extension; and stage 5—continuous rearing and falling and loss of balance. Rats were observed for 25 min after drug administration. If the seizures of the rest 84 rats were not severe enough to reach stage 4, an additional dose of 15 mg/kg (solution: 15 mg PTZ dissolved in 1 ml saline) was administered until the occurrence of a convulsive seizure enduring the duration of 5 min. The operation was repeated for up to 3 days; we remeasure the rats' weight daily before giving the drug. If the seizure reached grade 4 or 5 in 2 days, the model was defined as "successful" and the follow-up experiment was performed. If the seizure of any rats lasted for 10 min, 5% chloral hydrate was given to stop the attack (40–60 mg/kg, i.p., Sigma, USA).

Brain Function Evaluation

Evaluation of Brain Electrical Signals

Randomly selected rats from the plateau and plain groups (16 rats per group), for all rat models, 15% chloral hydrate were administered 150 mg/kg intraperitoneally, then fixated on a stereotaxic apparatus. Cranial were exposed and drilled at bilateral frontal and temporal area. Bilateral frontal electrodes were placed 2 mm anterior and 2 mm lateral to the bregma. Bilateral temporal electrodes were placed 4 mm lateral to the bregma and as close to the ear as possible. Four stainless steel screws, 0.5 mm in diameter, were placed epidurally. Wirings were connected and fixed with self-curing denture acrylic. Aseptic techniques were observed during the whole procedure. Then the rats were administered PTZ and then were connected with a signal analysis system (BL-420N Biological, Signal Acquisition, and Analysis System) to monitor the brain electric signals at baseline—before the onset of convulsion—and signals in the middle and after the termination of convulsion, with a duration of 5 min each. The severe stage, duration, amplitude of convulsion, frequency of onset spike, interval of wave peak, and voltage suppression time after convulsion were recorded.

Histopathological Analysis of Acute Brain Injury

Six successful rats models were randomly selected from the plateau and plain groups, and brain tissue was collected at 24 h (3 rats per group) and 72 h (3 rats per group) after the last seizure. After receiving an i.p. injection of 10% chloral hydrate (600 mg/kg), rats were transcardially perfused with 0.9% NaCl followed by 4% phosphate-buffered saline (PBS). The brains were carefully removed and the tissue was fixed in PBS at 4°C for 72 h. The tissue was embedded in paraffin and cut into a series of 4-μm sections. A total of nine sections were examined per brain: three were stained with hematoxylin-eosin (HE) (Servicebio, G1005, Wuhan, China) for the study of cellular morphology; three were stained with cresyl violet (Nissl) to identify neuronal cells (200× fields); and the remaining three were examined with the terminal deoxynucleotidyl transferase dUTP nick end labeling (TUNEL) assay to identify apoptotic cells.

The histological structure was observed under a light microscope (Nikon Eclipse E100, Japan). We chose the hippocampus because it is closely associated with memory and cognition, and is known to be actively involved in epileptogenesis, with CA1, CA3, and DG being the most representative and sensitive regions (14, 15). Three fields of vision were randomly selected from the CA1, CA3, and dentate gyrus (DG) areas of the hippocampus for each. The number of dark Nissl-stained neurons were counted. TUNEL-positive cells were counted with the Pannoramic viewer (3D HISTECH, Hungary), after the sections were scanned (Pannoramic MIDI, 3DHISTECH, Hungary) (16).

Evaluation of Spatial Learning and Memory

The Morris water maze was used to evaluate any spatial learning and memory differences between the plateau and plain groups. Twelve rats from each group were randomly selected at 6-weeks of age. The experiment was performed in a circular pool with a 120-cm diameter, 50-cm wall height, and 25-cm water depth. The water temperature was set at 26°C, and the color of the water was turned white with the use of a milk powder. The escape platform was placed in the second quadrant, 1 cm below the water surface. Three objects of different shapes were placed on the shore of the pool as spatial cues. The camera was placed directly above the pool, and the rat's head was dyed black before entering the water to facilitate the camera recording. Once rats were placed in the pool, they started swimming until they successfully found the hidden platform (success rate, 100%); if after 60 s they did not find the platform, they were removed from the pool (success rate, 0%). During the first 5 days of the experiment, known as the place navigation test, the rats' spatial learning and memory were analyzed. Each entry point was randomly selected from the edge of the pool. Each rat was tested five times per day for a total of 5 days. When a test finished, the rat stayed on the platform to rest for 30 s, and was then moved on to the next training session. The swimming distance traveled (cm), the escape latency to successfully find the hidden platform for the first time after each entry (s), the total distance swum in the platform quadrant (cm), the duration in the platform quadrant (s), and the total distance swum before reaching the platform for the first time (cm) were recorded and analyzed (17, 18). On the sixth day, rats underwent the reversal test at the same time as that during the first 5 days to investigate the rat's ability to retain spatial memory. For this, the platform was removed and placed at the point furthest from the original position. The number of crossings within the area where the original platform had been during a time interval of 120 s, the stay duration (s) and swimming distance (cm) in the

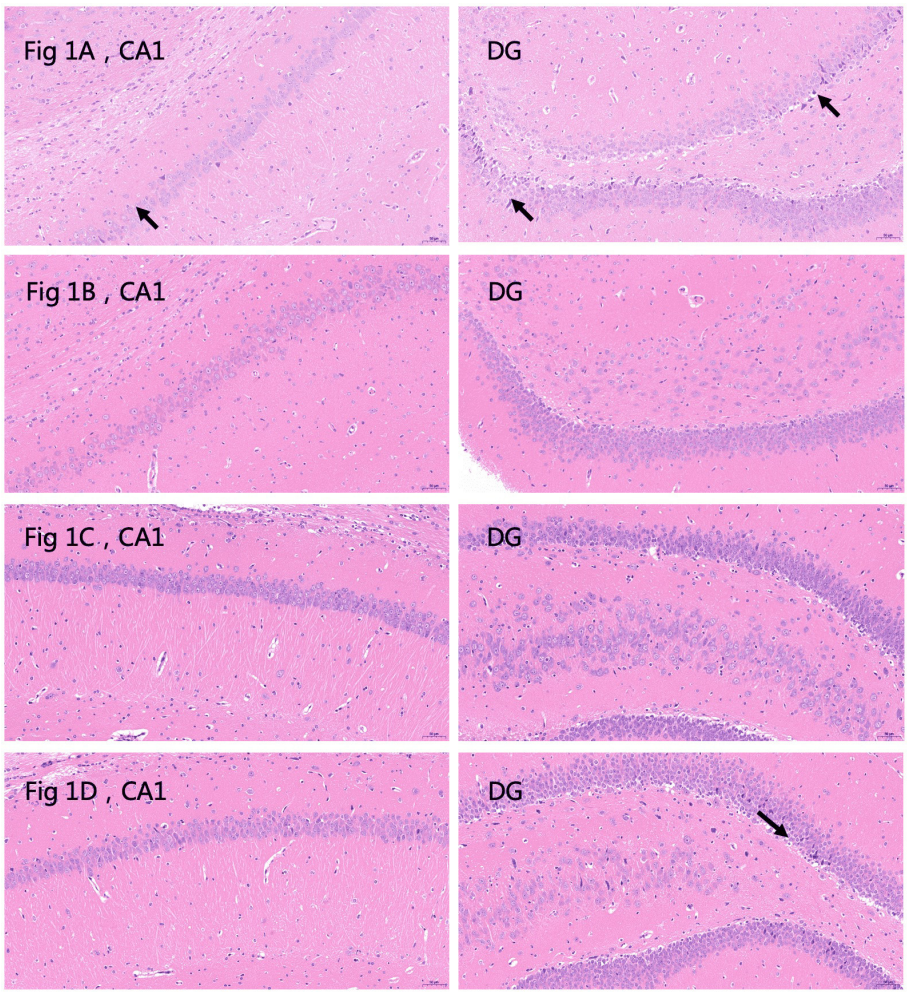

FIGURE 1 | Hematoxylin and eosin (HE) stained sections depicting the CA1 and dentate gyrus (DG) areas of the hippocampus. **(A)** Plain group, 24 h after the last seizure. The arrows indicate deeply stained cells. Neurons are abundant and closely arranged with clear boundaries. A small number of pyramidal cells are deeply stained, and the boundaries between cytoplasm and nucleus are unclear (black arrow). No other obvious abnormalities are observed (20.0×). **(B)** Plain group, 72 h after the last seizure. Neurons are abundant and closely arranged, with clear boundaries and normal morphology. The boundaries between cytoplasm and nucleus are clear, and no obvious abnormalities are observed (20.0×). **(C)** Plateau group, 24 h after the last seizure. Neurons are abundant and regularly arranged, with normal morphology and structure of neurons, clear boundaries of cytoplasm and nucleus, and no obvious inflammation (20.0×). **(D)** Plateau group 72 h after the last seizure. The arrows indicate deeply stained cells. The number of neurons in the hippocampal CA1 region is abundant and regular, the morphology and structure of neurons are normal, and the boundaries of nuclei and cytoplasm are clear. A small number of neurons are wrinkled in the DG region, the cells are deeply stained, and the boundaries of the nuclei and cytoplasm are unclear (black arrow) (20.0×).

original platform quadrant, the numbers of crossing the original platform quadrant, the total distance traveled (cm), and the time point (s) when the original platform was crossed for the first time were recorded.

Statistical Analysis

Quantitative data are expressed as the mean ± standard error of the mean (SEM). The data were statistically analyzed using the SPSS 21.0 software. Independent sample *T*-test was used to compare the statistical difference of electroencephalogram parameters (duration, amplitude of convulsion, frequency of onset spike, interval of wave peak, and voltage suppression time after convulsion) and neuronal counts, analysis of variance for repeated data was used for parameters of Morris water maze (the escape latency, total distance traveled, distance spent in platform quadrant/total distance traveled, and platform quadrant duration/escape latency period). A value of $P < 0.05$ was considered as statistically significant.

RESULTS

Seizure Manifestation and Electroencephalogram Parameters

After preconditioning, all rats were given PTZ to generate seizure models. After the end of seizures, the survival rate in the plateau group was significantly lower than in the plain group (26.2 vs.

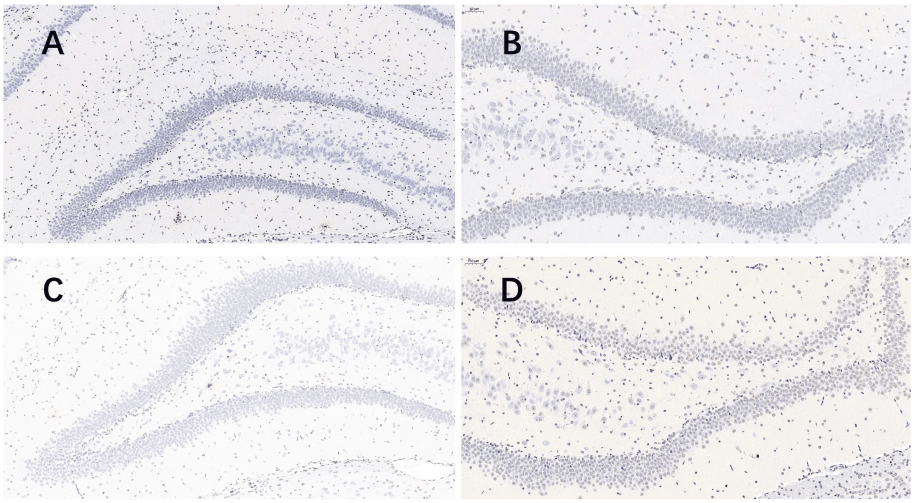

FIGURE 2 | Nissl stained pictures of the hippocampus. When taking screenshots, try to fill the field of whole tissue, make sure that the background light of each photo is consistent. The nuclei of the surviving neurons were large and round, pale blue or blue, with clear nucleoli and abundant cytoplasm. **(A)** plateau group, 24 h after the last seizure; **(B)** plain group, 24 h after the last seizure; **(C)** plateau group, 72 h after the last seizure; **(D)** plain group, 72 h after the last seizure (20.0×).

TABLE 2 | Neuronal counts revealed by Nissl staining in the plateau and plain groups at 24 and 72 h after the last seizure.

		Plateau	Plain	*p*-value
24 h	CA1	252.44 ± 35.15	264.33 ± 27.60	0.224
	CA3	255.00 ± 25.61	267.78 ± 19.97	0.279
	DG	946.33 ± 17.27	803.78 ± 24.49	< 0.001
72 h	CA1	289.11 ± 15.15	206.78 ± 51.75	0.003
	CA3	270.56 ± 27.30	266.33 ± 31.90	0.827
	DG	954.78 ± 23.82	758.00 ± 85.77	< 0.001

Values are the mean ± SEM.
DG, dentate gyrus.

42.9%, respectively; $p < 0.05$). The drug dose for inducing stage 4 or 5 seizures successfully was significantly higher in the plateau group compared to in the plain group (81.32 ± 21.57 vs. 63.41 ± 19.77 mg/kg, respectively; $p < 0.01$).

The baseline characteristic showed slow waves of 3–5 Hz in all rats in intermittent period. No differences in EEG signals during and after the seizures were observed between the plateau and the plain group (frequency of sharp wave: 5.78 ± 1.90 vs. 4.81 ± 1.88 Hz, respectively; $p = 0.051$). Similarly no differences between the two groups were observed in seizure duration and amplitude, interval of crest, and duration of post-seizure electrical suppression (**Table 1**).

Histopathological Findings

Histological examination of HE sections revealed that in the plain group, 24 h after the last seizure, CA1 and DG cell morphology were normal, except for a small amount of cytoplasm that was deeply stained and showed unclear cytoplasmic and nuclear boundaries (**Figure 1A**); 72 h after the last seizure the CA1 and DG hippocampal areas appeared normal (**Figure 1B**). In the plateau group, 24 h after the last seizure, CA1 and DG neuronal morphology appeared normal (**Figure 1C**); however, 72 h after the last seizure, a few neurons in the DG appeared wrinkled, the cell staining was darker, and the cytoplasmatic boundaries were unclear (**Figure 1D**). These results suggest that 72 h after the seizure cell morphology seems to be affected in the plateau but not the plain group.

Nissl staining (**Figure 2**) was used to evaluate neuronal survival in the brains of rats with seizures. Neuronal counts revealed a significant increase in the number of Nissl-positive cells in the DG of the plateau group compared to that in the plain group both at 24 and 72 h after the last seizure and in CA1 of the plateau group compared to that in the plain group at 72 h. No differences between groups were observed in the number of neuronal cells in the CA3 hippocampal areas (**Table 2**).

The TUNEL (**Figure 3**) assay revealed a significant increase in hippocampal apoptotic cell death rate in the plain group of DG areas compared to that in the plateau group at 72 h after the last seizure ($p = 0.009$); however, no differences were observed in the apoptotic rates between the two groups at 24 h after the last seizure (**Table 3**).

Morris Water Maze Performance

In the place navigation test, the escape latency, total distance traveled, distance spent in platform quadrant/total distance traveled, platform quadrant duration/escape latency period (**Table 4**) were analyzed, and there were no statistical differences between the two group.

In the reversal phase of the experiment on day 6, there was no statistical difference between the two groups in the number of crossings around the area of the original platform, total distance traveled, swimming distance in the original platform quadrant/total distance, and the number of times entering the platform quadrant (**Table 5**).

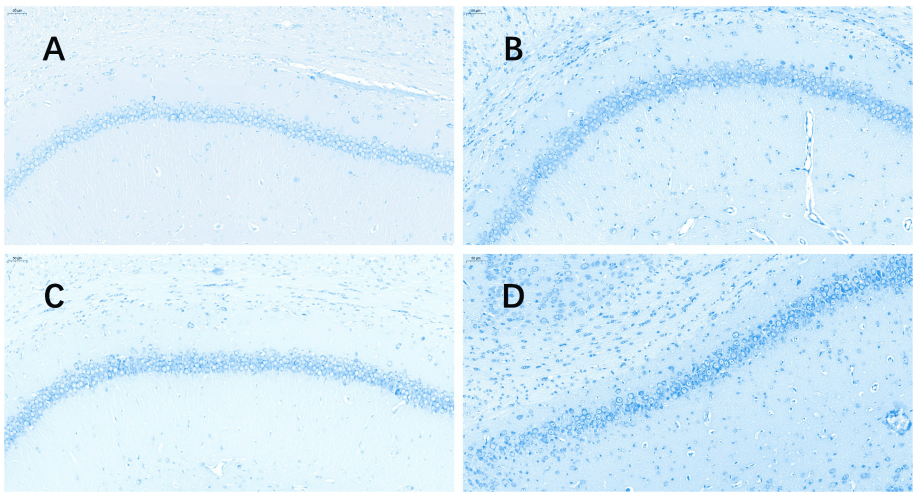

FIGURE 3 | TUNEL stained pictures of the hippocampus. The software nuclei quant automatically identified all the neurons with dark brown, claybank, and light yellow nuclei as positive and blue nuclei as negative. The positive rate was the apoptosis rate (%). **(A)** Plateau group, 24 h after the last seizure; **(B)** plain group, 24 h after the last seizure; **(C)** plateau group, 72 h after the last seizure; **(D)** plain group, 72 h after the last seizure (20.0×).

TABLE 3 | Apoptotic rates revealed by TUNEL staining in the plateau and plain groups at 24 and 72 h after the last seizure.

		Plateau	Plain	*p*-value
24 h apoptotic rate (%)	CA1	51.19 ± 15.20	51.52 ± 8.64	0.485
	CA3	47.55 ± 27.75	57.13 ± 22.97	0.461
	DG	40.97 ± 24.05	50.04 ± 12.48	0.513
72 h apoptotic rate (%)	CA1	38.34 ± 25.14	68.38 ± 15.92	0.312
	CA3	45.24 ± 13.54	63.76 ± 15.39	0.342
	DG	39.88 ± 4.63	71.17 ± 8.45	0.035

Values are the mean ± SEM.

DISCUSSION

Plateau areas are a special survival and living environment. Plateaus' hypoxic and hypobaric conditions can produce complex overall responses from the various physiological functions of the human body. This, in turn, has led to differences in the disease spectra, disease characteristics, and prognosis between populations in Tibet and the plains. Convulsions are abnormal movements, behaviors, and autonomic nervous system functions, caused by the excessive depolarization and abnormal synchronous discharge of neurons. During infancy, the particularity of neurotransmitter development and the susceptibility of immature brain tissue to injury imply that the incidence of convulsions in this period is higher than that in children of other age groups and adults. Convulsions are not only the most common symptom of neurological injury, but can also lead to brain damage, residual epilepsy, developmental delay, other neurological sequelae, and even death in severe cases, affecting the patient's prognosis. However, existing research findings on convulsions and convulsive brain injury are all based on clinical data of pediatric patients from plain areas, whereas the incidence and prognosis of convulsions in children from plateau areas are still unclear. There is a lack of clinical research data on the effects of hypoxia and hypobaria on children's brain functions after convulsions. This is because, on one hand, Tibet covers a wide area and is sparsely populated, which makes it difficult to collect follow-up data. On the other hand, patient prognosis is affected by various factors such as whether medical attention was sought in time and the cause of convulsions. Thus, it is difficult to reflect on the role of hypoxic and hypobaric environments in the prognosis of infantile convulsions based on clinical follow-up alone. For these reasons, this study performed an animal experiment to investigate the onset and prognosis of seizures in young rats under a plateau environment, in order to provide a theoretical basis for the clinical treatment of pediatric patients with convulsions in plateau areas, and to clarify whether hypoxia and hypobaria have possible protective effects on the brain in pediatric patients with convulsions.

With respect to the occurrence of induced convulsions, stage 4–5 seizures were induced in 84 young rats each in the plateau and plain groups. Regarding the drug dose needed for the successful induction of stage 4–5 seizures in young rats, the plateau group required a significantly higher dose than the plain group, that means with the same PTZ dosage, less rats in plateau group would reach stage 4–5 seizures compared with the plain group, in other words, the threshold for convulsion in the plateau group was higher than that in the plain group. This indicates that preconditioning with the hypobaric and hypoxic conditions of the plateau environment may increase an individual's threshold to convulsions and make them less prone to the occurrence of convulsions. Hypobaric and hypoxic preconditioning has now been applied to the prevention and treatment of diseases that may cause organ hypoxia and ischemia, such as respiratory failure, coronary heart disease, and stroke. The underlying mechanism

TABLE 4 | Analysis of place navigation of the Morris water maze.

	Escape Latency (s)		Total distance (cm)		Distance in platform quadrant/total distance		Platform quadrant duration/escape latency	
	Plateau	Plain	Plateau	Plain	Plateau	Plain	Plateau	Plain
Day 1	38.81 ± 21.41	30.77 ± 22.49	8,207.20 ± 4,447.56	8,031.70 ± 5123.23	0.32 ± 0.13	0.31 ± 0.14	0.37 ± 0.17	0.46 ± 0.32
Day 2	24.57 ± 20.42	27.56 ± 20.21	5,387.09 ± 4,463.94	6,547.84 ± 5198.70	0.39 ± 0.19	0.30 ± 0.16	0.49 ± 0.28	0.33 ± 0.18
Day 3	25.05 ± 20.66	22.80 ± 16.07	5,296.64 ± 4,018.47	6,275.21 ± 3974.32	0.31 ± 0.19	0.32 ± 0.13	0.39 ± 0.23	0.50 ± 0.35
Day 4	22.86 ± 17.71	23.27 ± 21.18	4,764.52 ± 3,378.02	5,143.16 ± 4653.78	0.35 ± 0.19	0.32 ± 0.21	0.44 ± 0.27	0.39 ± 0.26
Day 5	22.39 ± 20.17	25.83 ± 18.85	4,740.10 ± 3,867.63	5,866.05 ± 3909.33	0.29 ± 0.14	0.33 ± 0.13	0.36 ± 0.23	0.39 ± 0.20
F	0.053		0.968		0.233		0.019	
P-value	0.818		0.330		0.631		0.890	

Values are the mean ± SEM.

TABLE 5 | Analysis of the reversal phase of the Morris water maze.

	Plateau	Plain	*p*-value
Number of crossings through the original platform	1.57 ± 0.79	1.00 ± 1.22	0.345
Number of entering the platform quadrant	6.28 ± 1.60	5.60 ± 1.82	0.505
Total distance (cm)	12,200.98 ± 976.21	12,290.79 ± 1,395.34	0.898
Swimming distance in the original platform quadrant/total distance	0.33 ± 0.06	0.31 ± 0.11	0.874

Values are the mean ± SEM.

is related to the combined actions of multiple factors and signaling pathways, such as the involvement of glial glutamate transporter-1 (GLT-1) (19), heat-shock protein 70 (HSP70) (20), nitric oxide synthase (NOS) (21), and the Bcl-2 (22) family in the apoptotic pathway. Our study suggests that hypobaric and hypoxic environments may play a role in protecting the damage of convulsions, but the specific mechanisms that underline this will need to be verified by further basic research.

In terms of the short-term prognosis of convulsions in young rats in a plateau environment, we found that although the threshold of the drug dose for inducing convulsions was higher in this group, upon the induction of seizures, the mortality rate of young rats in the acute stage was significantly higher than the plain group. One of the mechanisms by which convulsions cause brain damage and even death is loss of oxygen (23), the results of some previous studies suggest that hypobaric and hypoxic preconditioning can improve the body's tolerance, and increase the tolerance of organs to the re-occurrence of hypoxia (9, 24). However, other studies have differing views, supporting instead that whether hypoxic preconditioning is damaging or protective is mainly determined by the degree of hypoxia (9). Our experimental results indicate that the dosage to induce severe convulsion in plain group is not enough to induce the same stage convulsion in plateau group, young rats that died following severe stage 4–5 seizures were critically ill. In such cases, even prior hypobaric and hypoxic preconditioning could not reverse disease progression, but instead it might cause serious consequences due to the underlying hypobaric and hypoxic state. We supposed maybe the tolerance increase in a certain range, once breakthrough the threshold, the ability to protect and compensate is broken, there is a cliff-like mechanism leading to a high mortality rate. The causes of death from severe epilepsy are very complex, including cerebral edema, respiratory arrest (25), capillary telangiectasias in the hippocampus (26), damage to other organs, and some unclear causes. According to the results of our research, we speculate that the reason lead to the high mortality with the low neuronal apoptosis rate in the plateau group may be that the hypobaria and hypoxia environment actually protects the neurons, but it does not prevent the other causes that directly cause the death. But the mechanism is only a hypothesis, which needs to be verified in future studies. Although the mortality rate of young rats in the plateau preconditioning group was higher than that in the plain group, rats that survived after seizure induction showed lower neuronal apoptosis in the acute stage than the plain group, while the neuronal survival rate in the DG at both time points and in the CA1 at 72 h was higher than that in the plain group. These observations indicate that for young rats with relatively mild conditions, hypobaria and hypoxia may still have a certain protective effect on the brain in the acute stage.

With regards to long-term prognosis, our water maze findings indicate that the performance of the young rats in the plateau and plain groups are comparable. This reflects, to a certain extent, that although the preconditioning environment of the plateau group did not improve the prognosis of the neurological development of young rats with convulsions, it also did not aggravate the impact of brain injury on their learning and memory abilities. The degree of convulsions induced in this study was severe, and the early mortality rate was high. Hence, the protective effect of hypobaric and hypoxic preconditioning in critical cases was not apparent. However, for surviving young rats with relatively mild conditions, hypobaria, and hypoxia might have exerted protective effects on the brain, which were manifested as increased neuronal survival rate in some brain regions and decreased neuronal apoptosis. In future studies, we could attempt to induce relatively mild seizures in young rats and evaluate their long-term prognosis, to investigate the protective

effects of hypobaric and hypoxic preconditioning in young rats with mild seizures.

There are limitations to this study. We investigated the incidence and prognosis of young rats with convulsions by preconditioning them to a simulated altitude of 5,000 m with intermittent hypobaria and hypoxia, however, residents of Tibet live at an average altitude of ∼4,000 m and are in a continuous state of hypobaria and hypoxia, experimental conditions that more closely simulate the real environment should be designed in the future to further explore the incidence and neurological prognosis of infantile convulsions in plateau areas. Secondly, because the drug dose in two groups are different, this may be one of the reason attribute to the high mortality rate, but since the induced convulsions stages were ultimately the same, we think our results are credible, but more studies on the dose-effect relationship would be helpful to eliminate the dosage bias. Last but not least, in this manuscript, we mainly described the phenomena we discovered, which we thought could be attributable to a neuro-protective effect, but confirmation as well as further research into the mechanism is needed.

CONCLUSION

Our results suggest that the effect of the plateau environment on young rats with convulsive brain injury may be related to their disease severity. For individuals in critical condition, hypobaria and hypoxia are factors that will aggravate their poor prognosis, whereas for normal individuals or those with mild conditions, hypobaria and hypoxia may have a protective effect against convulsive brain injury. However, the specific mechanisms involved still require further investigation.

DATA AVAILABILITY STATEMENT

The raw data supporting the conclusions of this article will be made available by the authors, without undue reservation.

ETHICS STATEMENT

The animal study was reviewed and approved by Peking University First Hospital Ethics Committee.

AUTHOR CONTRIBUTIONS

YX wrote the manuscript and conducted the statistical analysis. SQ and RZ conducted the experiments with the help of GS, under the supervision of LL, XH, and HW. All authors contributed to the article and approved the submitted version.

FUNDING

This work was supported by the Tibet Autonomous Region Natural Science Fund (No. XZ2017ZR-ZY017 to XH and No. XZ2018ZRG-110 to HW), Beijing Municipal Science and Technology Commission (No. Z191100006619049 to XH), Clinical Medicine Plus X—Young Scholars Project, Peking University (No. PKU2020LCXQ010 to LL), Scientific Research Seed Fund of Peking University First Hospital (No. 2019SF12 to RZ).

REFERENCES

1. Johnston MV. Hypoxic-ischemic encephalopathy. *Am J Perinatol.* (2000) 17:113–20. doi: 10.1055/s-2000-9293
2. Serebrovskaya TV. Intermittent hypoxia research in the former Soviet Union and the commonwealth of independent States: history and review of the concept and selected applications. *High Alt Med Biol.* (2002) 3:205. doi: 10.1089/15270290260131939
3. Goryacheva AV, Kruglov SV, Pshennikova MG, Smirin BV, Malyshev IY, Barskov IV, et al. Adaptation to intermittent hypoxia restricts nitric oxide overproduction and prevents beta-amyloid toxicity in rat brain. *Nitric Oxide.* (2010) 23:289–99. doi: 10.1016/j.niox.2010.08.005
4. Rybnikova E, Samoilov M. Current insights into the molecular mechanisms of hypoxic pre- and postconditioning using hypobaric hypoxia. *Front Neurosci.* (2015) 9:388. doi: 10.3389/fnins.2015.00388
5. Silverstein FS, Jensen FE. Neonatal seizures. *Ann Neurol.* (2007) 62:112–20. doi: 10.1002/ana.21167
6. Tekgul H, Gauvreau K, Soul J, Murphy L, Robertson R, Stewart J, et al. The current etiologic profile and neurodevelopmental outcome of seizures in term newborn infants. *Pediatrics.* (2006) 117:1270–80. doi: 10.1542/peds.2005-1178
7. Henshall DC, Murphy BM. Modulators of neuronal cell death in epilepsy. *Curr Opin Pharmacol.* (2008) 8:75–81. doi: 10.1016/j.coph.2007.07.005
8. Dirnagl U, Becker K, Meisel A. Preconditioning and tolerance against cerebral ischaemia: from experimental strategies to clinical use. *Lancet Neurol.* (2009) 8:398–412. doi: 10.1016/S1474-4422(09)70054-7
9. Zhen JL, Wang WP, Zhou JJ, Qu ZZ, Fang HB, Zhao RR, et al. Chronic intermittent hypoxic preconditioning suppresses pilocarpine-induced seizures and associated hippocampal neurodegeneration. *Brain Res.* (2014) 1563:122–30. doi: 10.1016/j.brainres.2014.03.032
10. Li Q, Han Y, Du J, Jin H, Zhang J, Niu M, et al. Alterations of apoptosis and autophagy in developing brain of rats with epilepsy: Changes in LC3, P62, Beclin-1 and Bcl-2 levels. *Neurosci Res.* (2018) 130:47–55. doi: 10.1016/j.neures.2017.08.004
11. Lüttjohann A, Fabene PF, van Luijtelaar G. A revised Racine's scale for PTZ-induced seizures in rats. *Physiol Behav.* (2009) 98:579–86. doi: 10.1016/j.physbeh.2009.09.005
12. Hussein AM, Eldosoky M, El-Shafey M, El-Mersery M, Abbas KM, Ali AN, et al. Effects of GLP-1 receptor activation on a pentylenetetrazole-kindling rat model. *Brain Sci.* (2019) 9:108. doi: 10.3390/brainsci 9050108
13. Racine RJ. Modification of seizure activity by electrical stimulation. II. Motor seizure. *Electroencephalogr Clin Neurophysiol.* (1972) 32:281–94. doi: 10.1016/0013-4694(72)90177-0
14. Zhvania MG, Ksovreli M, Japaridze NJ, Lordkipanidze TG. Ultrastructural changes to rat hippocampus in pentylenetetrazol- and kainic acid-induced status epilepticus: a study using electron microscopy. *Micron.* (2015) 74:22–9. doi: 10.1016/j.micron.2015.03.015
15. Bliss TV, Collingridge GL. A synaptic model of memory: long-term potentiation in the hippocampus. *Nature.* (1993) 361:31–9. doi: 10.1038/361031a0
16. Li Q, Han Y, Du J, Jin H, Zhang J, Niu M, et al. Recombinant human erythropoietin protects against hippocampal damage in developing rats with seizures by modulating autophagy via the S6 protein in a time-dependent manner. *Neurochem Res.* (2018) 43:465–76. doi: 10.1007/s11064-017-2443-1
17. Vorhees CV, Williams MT. Morris water maze: procedures for assessing spatial and related forms of learning and memory. *Nat Protoc.* (2006) 1:848–58. doi: 10.1038/nprot.2006.116

18. Schoenfeld R, Schiffelholz T, Beyer C, Leplow B, Foreman N. Variants of the Morris water maze task to comparatively assess human and rodent place navigation. *Neurobiol Learn Mem.* (2017) 139:117–27. doi: 10.1016/j.nlm.2016.12.022
19. Gong SJ, Chen LY, Zhang M, Gong JX, Ma YX, Zhang JM, et al. Intermittent hypobaric hypoxia preconditioning induced brain ischemic tolerance by up-regulating glial glutamate transporter-1 in rats. *Neurochem Res.* (2012) 37:527–37. doi: 10.1007/s11064-011-0639-3
20. Lin HJ, Wang CT, Niu KC, Gao C, Li Z, Lin MT, et al. Hypobaric hypoxia preconditioning attenuates acute lung injury during high-altitude exposure in rats via up-regulating heat-shock protein 70. *Clin Sci.* (2011) 121:223–31. doi: 10.1042/CS20100596
21. Huang YJ, Yuan YJ, Liu YX, Zhang MY, Zhang JG, Wang TC, et al. Nitric oxide participates in the brain ischemic tolerance induced by intermittent hypobaric hypoxia in the hippocampal CA1 subfield in rats. *Neurochem Res.* (2018) 43:1779–90. doi: 10.1007/s11064-018-2593-9
22. Wu Q, Yu KX, Ma QS, Liu YN. Effects of intermittent hypobaric hypoxia preconditioning on the expression of neuroglobin and Bcl-2 in the rat hippocampal CA1 area following ischemia-reperfusion. *Genet Mol Res.* (2015) 14:10799–807. doi: 10.4238/2015.September.9.18
23. Björkman ST, Miller SM, Rose SE, Burke C, Colditz PB. Seizures are associated with brain injury severity in a neonatal model of hypoxia-ischemia. *Neuroscience.* (2010) 166:157–67. doi: 10.1016/j.neuroscience.2009.11.067
24. Cuomo O, Vinciguerra A, Cerullo P, Anzilotti S, Brancaccio P, Bilo L, et al. Ionic homeostasis in brain conditioning. *Front Neurosci.* (2015) 9:277. doi: 10.3389/fnins.2015.00277
25. Kommajosyula SP, Randall ME, Brozoski TJ, Odintsov BM, Faingold CL. Specific subcortical structures are activated during seizure-induced death in a model of sudden unexpected death in epilepsy (SUDEP): a manganese-enhanced magnetic resonance imaging study. *Epilepsy Res.* (2017) 135:87–94. doi: 10.1016/j.eplepsyres.2017.05.011
26. Liu Y, Liang Y, Tong F, Huang W, Tinzing L, Le Grange JM, et al. Sudden death from an epileptic seizure due to capillary telangiectasias in the hippocampus. *Forensic Sci Med Pathol.* (2019) 15:243–8. doi: 10.1007/s12024-018-0075-7

Conflict of Interest: The authors declare that the research was conducted in the absence of any commercial or financial relationships that could be construed as a potential conflict of interest.

frontiers in Pediatrics

MINI REVIEW
published: 11 September 2020
doi: 10.3389/fped.2020.00563

Skeletal Effects of Early-Life Exposure to Soy Isoflavones—A Review of Evidence From Rodent Models

Kok-Yong Chin[1,2]* *and Kok-Lun Pang*[1]

[1] Department of Pharmacology, Faculty of Medicine, Universiti Kebangsaan Malaysia, Kuala Lumpur, Malaysia, [2] State Key Laboratory of Oncogenes and Related Genes, Department of Urology, Renji-Med X Clinical Stem Cell Research Center, School of Medicine, Ren Ji Hospital, Shanghai Jiao Tong University, Shanghai, China

Isoflavones are dietary phytoestrogens commonly found in soy-based products. The widespread presence of isoflavones in soy infant formula and breast milk may have long-lasting effects on the development of sex hormone-sensitive organs like the skeleton. Animal early-life programming models are suitable for testing the skeletal effects of pre- and neonatal exposure of soy isoflavones. This review aims to collate the impacts of early-life exposure of soy isoflavones as evidenced in animal models. The isoflavones previously studied include daidzein, genistein, or a combination of both. They were administered to rodent pups during the first few days postnatal, but prolonged exposure had also been studied. The skeletal effects were observed when the animals reached sexual maturity or after castration to induce bone loss. In general, neonatal exposure to soy isoflavones exerted beneficial effects on the skeletal system of female rodents, but the effects on male rodents seem to depend on the time of exposure and require further examinations. It might also protect the animals against bone loss due to ovariectomy at adulthood but not upon orchidectomy. The potential benefits of isoflavones on the skeletal system should be interpreted together with its non-skeletal effects in the assessment of its safety and impacts.

Keywords: bone, daidzein (CID 5281708), genistein (CID 5280961), neonates, life cycle, imprinting, perinatal, diethylstilbestrol (DES)

OPEN ACCESS

Edited by:
Yuan Shi,
Children's Hospital of Chongqing Medical University, China

Reviewed by:
Branka Šošić-Jurjević,
University of Belgrade, Serbia
Patrick Diel,
German Sport University Cologne, Germany

***Correspondence:**
Kok-Yong Chin
chinkokyong@ppukm.ukm.edu.my

Specialty section:
This article was submitted to Neonatology, a section of the journal Frontiers in Pediatrics

Received: *10 April 2020*
Accepted: *03 August 2020*
Published: *11 September 2020*

Citation:
Chin K-Y and Pang K-L (2020) Skeletal Effects of Early-Life Exposure to Soy Isoflavones—A Review of Evidence From Rodent Models. Front. Pediatr. 8:563. doi: 10.3389/fped.2020.00563

INTRODUCTION

Developmental programming or imprinting refers to the phenomenon whereby changes in the early development of an organism can exert long-lasting impacts that manifest during adulthood (1). Antenatal glucocorticoid use among pregnant women at risk of preterm delivery to assist the maturation of lungs of newborns is an example (2). Recent studies suggest the development of metabolic and cardiovascular abnormalities during adulthood in the offspring of mothers receiving glucocorticoids (3). This phenomenon has been replicated in primate models recently, whereby antenatal glucocorticoid exposure led to obesity in adult male baboons (4). The prevailing theory about the mechanism of developmental programming is epigenetic regulation by DNA methylation and histone modification induced by various factors (5).

The skeletal system is responsive to hormones and hormone-like substances. Prenatal and neonatal exposure of the skeletal system to hormonal stimuli might alter the trajectory of skeletal

development. A single dose of estrogen at the first postnatal day could increase the bone mineral density (BMD) and cortical thickness of male mice at the prepubertal stage, but the inverse happened at the stage of peak bone mass acquisition (6). Prenatal and postnatal exposure of bisphenol A, a synthetic xenoestrogen, lowered the femoral bone stiffness of female rats but not in males (7). These studies highlight that early exposure of xenoestrogens can potentially impact bone development.

Isoflavones are phytoestrogens present abundantly in soy-based products (8) and are also an important source of dietary xenoestrogens to human infants. The average isoflavone content in soy infant formula ranges from 25 to 28 mg/100 g of powder, consisting of daidzein (DAI), genistein (GEN), and glycitein (9). Additionally, these isoflavones are also present in breast milk (10). Setchell et al. reported that circulating isoflavones of infants were 13,000–22,000 times higher than the estradiol level, and the exposure level was 6–11 times higher than the dose in adults with regular soy food intake (11). The American Academy of Pediatrics Committee on Nutrition only recommends soy formula to infants with inherited galactosemia, lactose intolerance, or from vegan families (12). Soy formulation is not recommended to infants with cow milk protein allergy because some of them also experience allergy to soy protein (12). A study in the United States showed that 11.6% of the infants ≤12 months consuming formula were being fed with soy-based products (13). The prevalent use of soy infant formula that may imply the reason to consume these products is based on preference rather than medical reasons. Other committees around the world take a stricter stand against the use of soy infant formula over concerns of the biological activities of phytoestrogens (14).

The skeletal effects of soy isoflavones take decades to develop, and the planning of epidemiological studies or interventional trials on this topic is difficult. Animal models of prenatal and neonatal programming enable us to have a glimpse of the potential effects of soy isoflavones on skeletal developments. Animals like rodents have a relatively short life cycle, so developmental changes can be examined within a shorter time. The purpose of this review is to examine the skeletal effects of early-life exposure to soy isoflavones in animal models of prenatal and neonatal programming.

ANIMAL MODELS

In toxicity testing, the neonatal life stage refers to the period from birth to 3 weeks of age (15), but the definition is debatable because newborn rodents are very immature due to the short gestation period, and some researchers suggest they better resemble human preterm infants (16). A similar definition has been used for rats (17). Thus, this review will focus on rodent models supplemented with soy isoflavones within this period. We noted that most neonatal and prenatal studies are the collective work of one research group, so the reader should take note of potential publication bias.

Most studies examining neonatal exposure of soy isoflavones on the skeletal system used mice as the model organism. The soy isoflavones studied included DAI, GEN, or a combination of both. Since the binding affinity of different types of isoflavones on biological targets, like estrogen receptors (18), are different, this could contribute to the variation of the results among the studies. Notably, a study reported that skeletal effects of a combination of GEN and DAI were less prominent compared to individual isoflavones (19), suggesting that the less active isoflavone could attenuate the effects of the more potent isoflavone.

The soy isoflavones were administered subcutaneously during the first few postnatal days, and the skeletal outcomes were assessed when the mice reached maturity (4 months of age), with diethylstilbestrol (DES) as the positive control. The dose and type of isoflavone used in each study were different [GEN, 4 μg/day sc or 5 mg/kg body weight (bw)/day sc; DAI, 2 mg/kg bw/day sc; GEN + DAI, 7 mg/kg bw/day sc]; thus, the skeletal effects may not be comparable between studies. Other variations of the models exist. Two studies assessed the skeletal effects of prenatal exposure of folic acid (FA) and postnatal exposure of isoflavones on mice (20, 21); thus, the effects of isoflavones were confounded by prenatal FA treatment.

In the prenatal and postnatal rat model (22, 23), soy isoflavones were administered through food, in contrast to subcutaneous for studies in mice. Soy isoflavones like DAI are known to be metabolized by gut microbiomes to equol and O-desmethylangolensin with different biological activities compared to the parent compounds (24). However, in all studies reviewed, the bioavailability of the isoflavones and their metabolites were not measured. Along with the doses that were not readily translatable between the mouse and rat studies, these factors prevent effective comparisons between different research groups.

Another study exposed the mouse pups with isoflavones, castrated them in the fourth month, and assessed their bone health status in the eighth month (25). The castration model is a classic bone loss model due to sex hormone deficiency (26), so the mentioned study examined the antiosteoporosis effects of early exposure to isoflavones.

The composition of the control diet is essential to ensure a fair comparison between the isoflavone-supplemented and control groups. Long-term supplementation of different diet regimens with and without soy isoflavones or protein can modify body composition and metabolic profile of the animals (27). Most studies indicated the use of soy-free diet. Modified AIN93G diet without isoflavones is the most common diet used (19, 23, 28), while other studies indicated the use of diet without DAI (23) or isoflavones (22), or amino acid-based diet without isoflavones (20, 21). The difference in the composition of these diets could cause variation in the results of the studies reviewed.

The design of the studies is shown in **Table 1** for comparison.

NEONATAL EXPOSURE

Effects on Bone Mass

Bone mineral density (BMD) assessment through dual-energy X-ray absorptiometry in animals allows non-invasive longitudinal changes in bone mass (29). Neonatal exposure to GEN increased the femoral BMD of mice at sexual maturity. Additionally, it

TABLE 1 | Skeletal effects of prenatal and/or neonatal exposure of soy isoflavones derived from animal studies.

Study	Study design	Bone mineral density	Bone microstructure	Bone strength	Bone remodeling and biochemical markers
Peikarz and Ward (28)	CD-1 mouse pups were exposed to corn oil, GEN (4 μg/day sc), or DES (2 μg/day sc) for the first 5 days of life. Outcomes measured at 4 months of age. Control diet: AIN93G diet without ISO	Male Femoral BMD: GEN = corn oil < DES Lumbar BMD: GEN > DES = corn oil	NA	Male Femoral peak load: GEN = corn oil < DES Lumbar peak load: GEN > DES = corn oil	Male Serum osteocalcin: GEN = DES < corn oil Serum CTX-1: NS
		Female Femoral BMD: GEN = DES > corn oil Lumbar BMD: GEN = DES > corn oil	NA	Female Femoral Peak load: NS Lumbar peak load: GEN = DES > corn oil	Female Serum osteocalcin & CTX-1 NS
Kaludjerovic and Ward (19)	CD-1 mouse pups were exposed to corn oil, DAI (2 mg/kg bw/day sc), GEN (5 mg/kg bw/day sc), DAI + GEN (ISO, 7 mg/kg bw/day sc), or DES (2 mg/kg bw/day sc) for the first 5 days of life. Outcomes measured at 4 months of age. Control diet: AIN93G diet without estrogenic compounds.	Male Lumbar BMD: DES = all isoflavones group > corn oil Femoral midpoint BMD: DAI > GEN = ISO = DES = corn oil	NA	Male Lumbar peak load: NS Femoral midpoint yield: NS Femoral midpoint peak load: DES < DAI = ISO, DES = corn oil = GEN Femoral midpoint stiffness: NS Femoral neck yield: DAI > DES, ISO > DES, corn oil = DES = GEN Femoral neck peak load: DAI > corn oil = GEN = ISO ≥ DES Femoral neck stiffness: NS	NA
		Female Lumbar BMD: DES > all isoflavones group = corn oil Femoral midpoint BMD: DAI > GEN = ISO = DES = CON	Female ***Lumbar*** BV/TV: DAI = DES > corn oil > GEN, ISO = corn oil = GEN BS/BV: DAI > all groups Tb/Th: GEN = ISO > corn oil = DAI = DES Tb.N: DAI = GEN = DES > corn oil = ISO Tb.Sp: DAI = DES > GEN = ISO > corn oil ***Femoral neck*** BV/TV: DAI = GEN > corn oil = ISO = DES BS/BV: DES > DAI, = other groups, DAI = other groups Tb/TH: DAI > DES = corn oil = GEN = ISO Outer cortical perimeter: DAI > corn oil = DES = GEN = ISO Cortical area: DAI > corn oil = ISO, DAI > DES, DES = corn oil Marrow area: GEN = corn oil > DES, GEN = DAI, DES = DAI, DAI = ISO ***Femoral midpoint*** Tb.Sp: DAI = GEN > DES, DES = ISO = corn oil Cortical area: DAI > corn oil = DES, ISO = GEN = DES = corn oil, ISO = DAI Cortical thickness: DAI > corn oil = DES, DAI = GEN = ISO	Female Lumbar peak load: DAI = DES > ISO = corn oil Femoral midpoint yield: DES > all isoflavones = corn oil Femoral midpoint peak load: corn oil < DES > GEN = ISO, isoflavones > corn oil Femoral midpoint stiffness: corn oil < all isoflavones, DES = DAI > GEN = ISO Femoral neck yield, peak load, stiffness: NS	NA
Kaludjerovic and Ward (25)	CD-1 mouse pulps were exposed to corn oil, DAI + GEN (ISO, 7 mg/bw/day sc), or DES (2 mg/bw/day sc) for the first 5 days of life. Castration was performed at 4th month. Outcomes measured at 8th month of life. Control diet: AIN93G diet	Male Lumbar BMD: NS Whole femur BMD: NS	NA	Male Lumbar peak load: NS Femoral midpoint peak load, yield, stiffness: NS Femoral neck peak load: ISO > DES, DES = corn oil Femoral neck yield, stiffness: NS	NA

(Continued)

TABLE 1 | Continued

Study	Study design	Bone mineral density	Bone microstructure	Bone strength	Bone remodeling and biochemical markers
		Female Lumbar BMD, BMC: ISO > corn oil = DES Whole femur BMD: ISO > corn oil, = DES, corn oil = DES	Female ***Lumbar*** BV/TV: NS Tb/Th: DES = ISO > corn oil Tb.N: DES > corn oil, ISO = DES = corn oil Tb.Sp: NS ***Femoral neck***: All NS	Female Lumbar peak load: DAI + GEN > corn oil = DES Femoral midpoint peak load: ISO > corn oil = DES Femoral midpoint yield, stiffness: NS Femoral neck peak load, yield, stiffness: NS	NA
Hertrampf et al. (22)	Sprague–Dawley female rats Dams fed with diet without isoflavones (IDD), mixed isoflavone diet (IRD: GEN 240 μg/g + DAI 232 μg/g), or GEN (700 μg/g diet). Pups fed with the same diet as dams for 80 days postnatal*	Tibial BMD at Day 21: GEN = IRD > IDD	NA	NA	NA
Kaludjerovic and Ward (20)	CD-1 mouse dams fed with low (0 mg/kg bw/day), adequate (2 mg/kg bw/day) and supplementary (8 mg/kg bw/day) FA. Pups fed with either corn oil or DAI + GEN (ISO, 7 mg/kg bw/day, sc) from day 1–10 after birth. Outcomes measured at 4 months of age. Only male pulps are studied. Control diet: amino acid-based diet without ISO	Male Lumbar BMD: Overall ISO > no ISO Whole femur BMD: ISO + adequate FA group > FA only	NA	Male Lumbar peak load: Overall ISO > no ISO Whole and midpoint femur peak load: ISO + adequate FA group > FA only	Male Serum biomarkers OPG and OPG/RANKL ratio: ISO + supplementary FA group > FA only
Kaludjerovic and Ward (21)	CD-1 mouse dams fed with low (0 mg/kg bw/day), adequate (2 mg/kg bw/day), and supplementary (8 mg/kg bw/day) FA. Pups fed with either corn oil or DAI + GEN (ISO, 7 mg/kg bw/day, sc) from days 1–10 after birth. Outcomes measured at 4 months of age. Only female pulps are studied. Control diet: amino acid based diet free from ISO	Female Femur and lumbar BMD: adequate FA + ISO group > FA only	Female Lumbar BV/TV, Tb.N: Overall ISO > no ISO Lumbar Tb.Sp: Overall ISO < no ISO Femur Tb.Th, Tb.N: Adequate FA + ISO > FA only	Female Lumbar peak load: NS Femur midpoint peak load: ISO + adequate FA group > FA only	Female OPG, OPG/RANKL, IGF-1: Adequate FA + ISO > FA only Dnmt3a mRNA: Adequate FA + ISO < FA only; Supplemental FA + ISO > FA only NPY mRNA: Adequate FA + ISO < FA only
Tousen et al. (23)	Control: Sprague–Dawley dams and offspring fed on DAI-free diet. D1: Sprague–Dawley dams and offspring fed with DAI (0.5 g/kg diet) till postnatal day 13**	Male ***Whole femur BMD*** Day 22: D1 = control Day 35: D1 < control Day 77: D1 < control	NA	NA	Male ***Serum osteocalcin*** Day 22: D1 < control Day 35: D1 = control Day 77: D1 = control
		Female ***Whole femur BMD*** Day 22: D1 = control Day 35: D1 < control Day 77: D1 = control	NA	NA	Female ***Serum osteocalcin*** Day 22: D1 = control Day 35: D1 < control Day 77: D1 = control

BMD, bone mineral density; BV/TV, bone volume; bw, body weight; CTX-1, C-terminal telopeptide of type 1 collagen; DAI, daidzein; DES, diethylstilbestrol; Dmnt3a, DNA methyltransferase 3a; FA, folic acid; GEN, genistein; IDD, dams fed with diet without isoflavones; IGF-1, insulin-like growth factor-1; IRD, dams fed with mixed isoflavones diet (GEN + DAI); ISO, isoflavone mixture (GEN + DAI); NA, not available; NS, not significant among all the groups; NPY, neuropeptide Y; OPG, osteoprotegerin; RANKL, receptor activator of nuclear factor kappa-B ligand; Tb.N, trabecular number; Tb.Th, trabecular thickness; Tb.Sp, trabecular separation; sc, subcutaneous.

**Only data till day 21 is included in this table. **There was another group fed till postnatal day 77.*

also increased the lumbar BMD of female mice (28). The effects of GEN was greater than DES in males but on par with DES in female mice (28). In another study, DAI was more potent than GEN, DAI + GEN, and DES in increasing the femoral midpoint BMD of mice (19). However, DES exerted greater effects on female, while all treatments exerted similar effects on male lumbar BMD (19). In prenatal FA and postnatal isoflavone (DAI + GEN) models, femoral and lumbar BMD increased significantly in male mice exposed to adequate FA (2 mg/kg bw/days) and postnatal isoflavone compared to other treatment

groups (20). Similar treatment resulted in higher lumbar and femoral BMD of the female mice (21). Neonatal isoflavone exposure (DAI + GEN) also prevented deterioration of lumbar and femoral BMD due to castration in female rats but not in male rats (25).

Overall, neonatal exposure to isoflavones increased BMD of the mice at sexual maturation, and the effects were slightly better in male mice. However, it did not protect male mice against bone loss due to sex hormone deficiency. These observations suggest that both androgenic and estrogenic stimulation are essential in the development of the skeleton in males (30, 31). On the other hand, the adverse effects of androgen deprivation on bone are tremendous and cannot be displaced by earlier BMD gain caused by soy isoflavones.

BMD cannot differentiate between the trabecular and cortical compartment, and it has a low resolution (8). Microcomputed tomography assessment, which is discussed below, provides a more complete picture of the microstructure in each bone compartment.

Effects on Bone Microarchitecture

Skeletal microarchitecture is a major determinant of bone strength, which can be studied through microcomputed tomography (32). Neonatal exposure of DAI significantly improved the trabecular microstructure indices of the lumbar spine and femoral neck, and the trabecular separation of the femoral midpoint in female mice (19). The effects of GEN were superior to those of DAI on lumbar trabecular thickness (19). Similarly, neonatal isoflavone exposure independently increased lumbar trabecular microstructure in female offspring from dams supplemented with FA during gestation (21).

On cortical bone indices, DAI increased the cortical area of the femoral neck and midpoint (19). DAI, GEN, and DAI + GEN also improved cortical thickness of the midpoint but not at the femoral neck (19).

Overall, data on neonatal exposure of isoflavones on bone microarchitecture is limited. The available study showed that improvements were site specific. The lumbar spine and femoral neck are trabecular rich; therefore, the improvement in trabecular indices is better. The femoral midshaft is cortical rich; hence, cortical improvement is more apparent. The variations in bone composition could significantly influence the effects of isoflavones on different bone regions, which dictates bone strength.

Effects on Bone Strength

The ultimate measure of bone health is skeletal strength, which predicts fracture risk. The usual indices include ultimate/peak load, which refers to bone strength under certain specific loading conditions, and stiffness, which refers to the resistance of the bone against deformation (33). Neonatal GEN significantly increased the lumbar, but not the femoral, peak load of adult male mice compared to DES, and the normal control (28). The effects of neonatal GEN and DES exposure on lumbar peak load were similar in adult female mice, whereby an improvement over normal control was observed (28). Both compounds did not alter the femoral peak load in adult female mice (28). Since the lumbar spine is rich in trabecular bone, the improvement in strength could be a result of enhanced trabecular bone structure.

On the other hand, neonatal DAI exposure increased the femoral neck and midpoint peak load in adult male mice but not in female mice (19). The effects of DAI were greater than those of DES in male mice, while the effects of GEN or DAI + GEN were intermediary (19). Neonatal isoflavone exposure only retained the peak load of the femoral neck in male mice and the peak load of the femoral midpoint in female mice after castration (25). Adequate prenatal FA and postnatal isoflavone exposure increased the lumbar and femoral peak loads in male mice (20). Contradictory to BMD results, the femoral midpoint, but not the lumbar peak load, was higher in female mice treated with adequate prenatal FA + postnatal isoflavone (21). The beneficial effects on cortical-rich regions in these studies due to DAI or isoflavone mixture with DAI correspond to the results of skeletal microstructure, whereby DAI increased cortical thickness. It also warrants further investigation on whether the skeletal action of DAI is selective on cortical bones.

Overall, neonatal isoflavone exposure generally improves the bone strength of mice, but the skeletal sites vary due to the type of isoflavones present.

Effects on Bone Remodeling

Bone remodeling refers to the tightly regulated process of bone resorption by osteoclasts and formation by osteoblasts (34). The bone remodeling process can be inferred by circulating markers of bone resorption and formation, which are the products of bone cell activities (35). Neonatal GEN exposure did not change the serum C-terminal telopeptide of type I collagen (CTX-1; bone resorption markers) and osteocalcin level (bone formation markers) in mice (28). On the other hand, adequate prenatal FA plus postnatal isoflavone increased osteoprotegerin (OPG) and OPG/receptor activator of nuclear factor kappa-β ligand (RANKL) ratio in male mice (20) and female mice (21). Since OPG prevents the action of RANKL in stimulating osteoclast differentiation, this observation indicates the suppression of bone resorption (36). Additionally, the serum level of insulin-like factor-1, a bone anabolic hormone, was increased in female mice (21).

Overall, neonatal isoflavone exposure might suppress the formation of osteoclasts, but this observation was not reflected in the bone resorption markers. Perhaps this change is transient and has normalized upon adulthood.

MODELS AND PRENATAL AND NEONATAL EXPOSURE

Other studies reported a longer period of isoflavone exposure involving the prenatal and neonatal periods. We limit our discussion to studies with postnatal exposure within the limit of the neonatal period of life. Tousen et al. (23) reported on the skeletal effects of rat dams fed with DAI from gestation till postnatal day 13 and their offspring fed with control diet until weaning. The whole BMD of the male and female offspring was

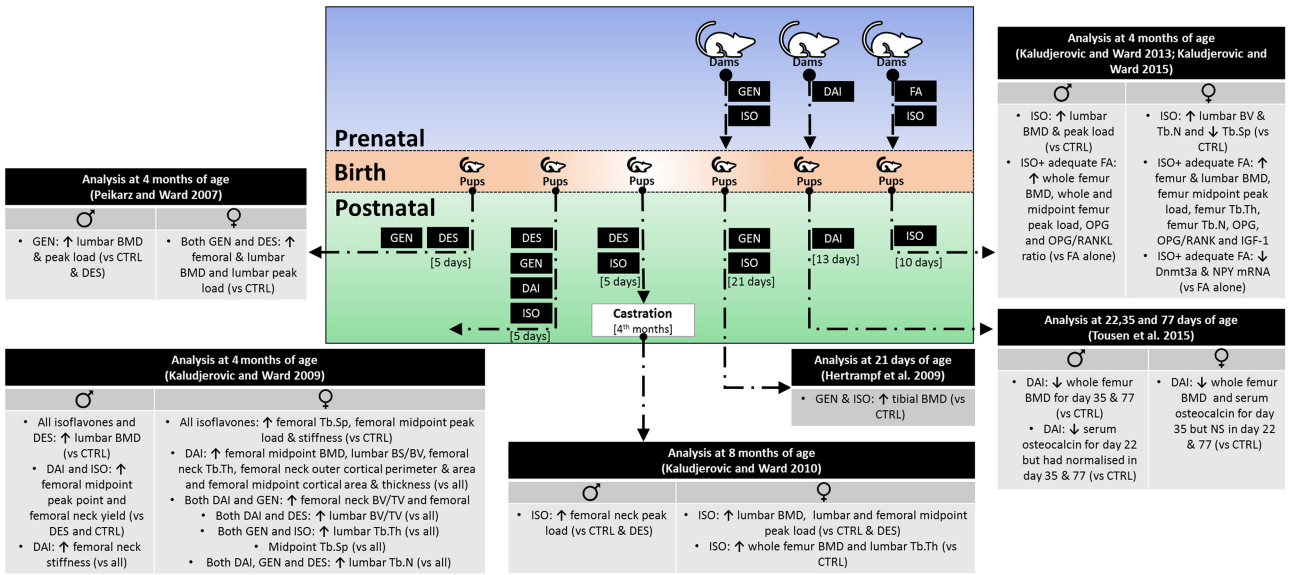

FIGURE 1 | Skeletal effects of early life exposure to soy isoflavones. BMD, bone mineral density; BV/TV, bone volume over total volume; CTRL, control; DAI, daidzein; DES, diethylstilbestrol; Dnmt3a, DNA methyltransferase 3a; FA, folic acid; GEN, genistein; IGF-1, insulin-like growth factor-1; ISO, isoflavone mixture (DAI + GEN); NPY, neuropeptide Y; OPG, osteoprotegerin; RANKL, receptor activator of nuclear factor kappa-B ligand; Tb.N, trabecular number; Tb.Th, trabecular thickness; Tb.Sp, trabecular separation.

significantly lower at the prepubertal stage (day 35) compared to the control rats (23). Upon sexual maturation (day 77), the BMD of the male remained lower compared to that of the normal control, but the BMD of the female returned to control values (23). The serum osteocalcin level of the exposed rats was lower compared to that of the control rats at the prepubertal stage, but the level returned to control values upon sexual maturity (23). Another study reported a lower tibial BMD in female offspring of rat dams exposed to GEN or isoflavones during gestation and lactation period (postnatal 21 days) (22). These effects persisted when the rats reached adulthood, but it should be noted that the offspring were fed with the same diet as the dams' lifelong (22).

Overall, in contrast to neonatal exposure, prenatal plus postnatal exposure of isoflavones exerted negative effects to the bone. This observation might be related to the critical period of intrauterine exposure. It was reported that soy isoflavones could regulate the epigenetic process of embryonic stem cells (37). Whether these changes are beneficial or harmful to the development of the skeletal system remains a question.

Current findings from animal experiments are summarized in **Figure 1**.

Prepubertal exposure of soy isoflavones also influences skeletal health at adulthood. Zhang et al. (38) showed that female rats fed with soy protein isolates for 14 days from postnatal day 20, had higher bone formation markers (alkaline phosphatase, ALP, and osteocalcin), bone resorption markers (RatLap), and sclerostin level (a negative regulator of bone formation) compared to the control. Chen et al. (39) compared the rats fed with casein or soy protein isolate-based diet starting from the postnatal day 24 till postnatal day 55 and subsequently switched to standard diet or continue with soy protein isolates till 6 months old. Some of the rats were castrated at the age of 6 months and sacrificed 1–3 weeks later. They reported that the total BMC and BMD, and trabecular and cortical BMD of the soy protein isolate group were greater than those of the casein group. After castration, rats on short-term or long-term soy protein isolates had better bone health than those on the casein diet. Overall, prepubertal exposure of soy isoflavones exerts skeletal beneficial effects similar to those of neonatal exposure models. In contrast, prenatal and postnatal exposures of soy isoflavones exert negligible or negative effects on rats in adulthood. However, apart from the period of exposure, the dose and type of isoflavones supplemented should be considered in interpreting the results of these studies.

Hotchkiss et al. (40) compared the skeletal effects of GEN in rats supplemented continuously for 2 years or switched to the control diet after postnatal day 140. Lifelong exposure to high-dose GEN resulted in lower lumbar BMC and area, as well as higher pyridinoline (a bone resorption marker) compared to those of rats supplemented with lower doses. In female rats treated till postnatal day 140, pyridonoline was lower and ALP was higher with higher GEN dose, indicating that GEN induced higher bone formation rate in these rats. In rats treated with GEN till weaning and male rats at all life stages, no skeletal effects were observed. The data may indicate that androgenic regulation is essential for skeletal development in males and that phytoestrogenic effects of isoflavones may not be as important as in females.

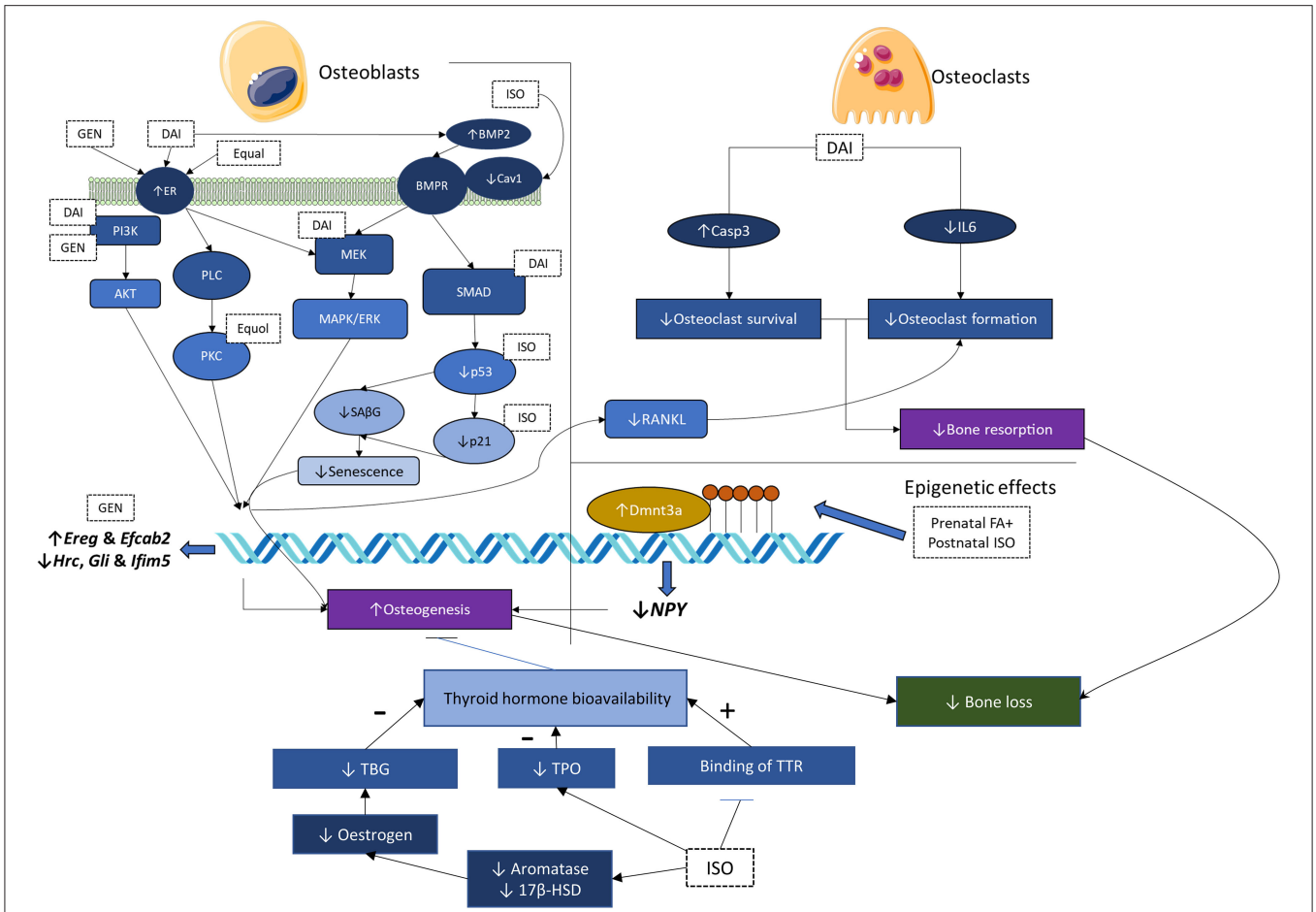

FIGURE 2 | Mechanisms of action of soy isoflavones and soy protein isolates. 17-β-HSD, 17-β-hydroxysteroid dehydrogenase; BMP-2, bone morphogenetic protein-2; Cav1, caveolin-1; DAI, daidzein; Dnmt3a, DNA methyltransferase 3a; ER, estrogen receptor; ER-α/β, estrogen receptor-α/β; FA, folic acid; GEN, genistein; IL-6, interleukine-6; ISO, isoflavone mixture; MAPK, mitogen-activated protein kinase; MEK/ERK, MAPK kinase/extracellular-regulated kinase; NPY, neuropeptide Y; PI3K/Akt, phosphoinositide 3-kinase/protein kinase B; PKC, protein kinase C; PLC, phospholipase C; RANKL, receptor activator of nuclear factor kappa-B ligand; SAβG, senescence-associated beta-galactosidase; T4, thyroxine; TBG, thyroxine-binding globulin; TH, thyroid hormone; TPO, thyroid peroxidase; TTR, transthyretin.

MECHANISM OF ACTION OF ISOFLAVONES ON BONE DEVELOPMENT

Soy isoflavones affect skeletal development through direct and indirect action on bone cells. In this section, the actions of soy isoflavones on bone cells, through DNA methylation and thyroid hormones (TH), are discussed.

GEN exerts a positive effect on bone remodeling by reducing osteoclast and increasing osteoblast number. It lowers the osteoclast number in neonatal bone marrow cell culture through decreasing the survival of osteoclasts or attenuating their formation (41). It also increases the differentiation and migration of primary rat calvarial osteoblasts by estrogen receptor (ER) and nitric oxide synthase pathway (42). Mitogen-activated protein kinase (MAPK) and phosphoinositide 3-kinase (PI3K) transduction systems are shown to involve in the pro-osteogenesis effects of GEN (42). Surprisingly, in a coculture of osteoblasts and monocytes, GEN increased the formation of osteoclast-like cells (42), probably through stimulating factors from osteoblasts. Another study suggested the upregulation of *Ereg* and *Efcab2*, as well as downregulation of *Hrc*, *Gli*, and *Ifim5* in MC3T3-E1 preosteoblastic cells (43).

Similarly, DAI promoted apoptosis of osteoclast-like cells derived from porcine bone marrow cells by caspase-3 cleavage and upregulation of nuclear ER (44). DAI improved osteoblastic differentiation of OCT-1 cells via upregulation of bone morphogenetic protein-2 (BMP-2) and activation of the SMAD pathway (44). DAI also improved proliferation, differentiation of MG-63 osteoblasts primarily through ERα signaling and at least partly through MAPK kinase/extracellular regulated kinase (MEK/ERK) and the PI3K/protein kinase B (Akt) signaling pathway (45). Another study showed an increased expression of ERα, ERβ, and steroid receptor (SR) comprising the classic estrogen-responsive elements in MG-63 osteoblasts induced by DAI (46). It also reduced the expression of stimuli for osteoclastogenesis [RANKL and interleukin-6 (IL-6)] while increasing the expression of OPG in MG-63 osteoblasts (46).

Equol and O-desmethylangolensin, derived from DAI metabolism, could also inhibit the formation of osteoclast-like cells from bone marrow cells from male mice (47). Equol also promoted osteoblast differentiation from primary osteoblast precursors, probably through ER and the protein kinase C-α (PKC-α) pathway (48).

DNA methylation is an epigenetic process mediating gene expression, which plays an important role in skeletal development. It is regulated by DNA methyltransferase (Dnmt) (49). The differentiation of mesenchymal stem cells to osteoblastic or non-osteoblastic progenitors is linked to the methylation rate of critical genes encoding BMP-2 and ALP, which is responsive to the Wnt signaling pathway (50). Methylation of the gene encoding interferon regulatory factor eight facilitates osteoclastogenesis (51). Previous studies have demonstrated that the antiestrogenic effects of isoflavones could be partially attributed to its effects on the methylation of steroidogenic factor 1 (49, 52). Exposure of mouse embryonic tissues to GEN also modified the regulation level of genes (37). Since DNA methylation is the prevailing theory for neonatal imprinting effects, the effects of prenatal FA plus postnatal isoflavones on Dnmt in the bone for female mice have been explored. Postnatal isoflavone exposure decreased Dnmt3a expression in the adequate FA group but increased Dnmt3a expression in the supplemental FA group, indicating a significant interaction between FA and isoflavones (21). Gene expression analysis demonstrated that neuropeptide Y (NPY) level, a potent osteogenesis inhibitor, was suppressed in the adequate FA plus isoflavone group (21). Other epigenetic factors, like histone modifications, could also influence bone health, but the role of soy isoflavones in mediating bone health through this mechanism is less clear.

On the other hand, soy isoflavones exert their effects on the skeletal system indirectly through interference with TH homeostasis (53). Congenital and juvenile hypothyroidism can delay skeletal development, while thyrotoxicosis can accelerate skeletal aging and premature closure of growth plate. These phenomena have been replicated in genetically modified rodent models with altered thyroid hormone signaling (54). On the other hand, the skeletal effects of over hypo/hyperthyroidism and thyroid-stimulating hormone (TSH) are well-known (55, 56). Epidemiological studies showed that soy isoflavone consumption could influence TH levels. Intakes of soy isoflavones or protein are associated with high TSH, especially among women (57), which could be a result of the thyroid suppressive effect of isoflavones. In contrast, urinary isoflavone levels are found to be associated with higher serum thyroxine (T4) in women but not in men (58), in which the authors attribute the higher T4 to the suppressive effects of isoflavones on deiodination of T4 to T3. Mechanistically, soy isoflavones suppress the level of TH by inhibiting thyroid peroxidase (TPO) activity competitively (59) and inhibit the binding of TH to thyroid transport protein [transthyretin (TTR)] in the blood (60, 61). Soy isoflavones, especially GEN, are also deiodinase (Dio) inhibitors, specifically type 1 (Dio1) (62). However, Dio1 is not expressed in the bone (63). *In silico* analysis showed that isoflavones could bind to thyroid receptors, but this effect has not been validated *in vitro* (64). Isoflavones were reported to enhance transcription mediated by triiodothyronine-liganded thyroid receptor (64). Soy isoflavones also inhibit aromatase and 17-β-hydroxysteroid dehydrogenase (17-β-HSD) (65), which prevent the conversion of androgens to estrogens, thereby lowering thyroxine-binding globulin (TBG) and decreasing T4 level (66). However, TTR, instead of TBG, is the main carrier of thyroid hormones in rodent blood (67).

Soy isoflavones may also affect skeletal health through other indirect mechanisms. A multigeneration supplementation study showed that soy protein concentrates and soy isoflavones slowed down the weight gain and reduced the insulin level of the rats (27). The reduction in mechanical loading exerted by body weight and the bone anabolic insulin signaling may be harmful to the bone. Soy protein isolates also decreased the expression of caveolin-1, a membrane protein that anchors other proteins to the membrane, accompanied by activation of BMP-2/SMAD signaling in bone and osteoblasts (38). In another study, long-term soy protein isolate supplementation caused concurrent reductions in caveolin-1, p 53, p 21, and senescence-associated beta-galactosidase in the bone of rats and osteoblasts cultured with the serum of treated rats (39), thus, preventing senescence of osteoblasts. These are translated to a beneficial effect on the bone.

Overall, soy isoflavones modulate a complex network of factors influencing bone health. The net effects seem to be beneficial, considering the phenotypic response of the skeletal system on soy isoflavone supplementation. The mechanisms of action of soy isoflavones and soy protein isolates are summarized in **Figure 2**.

CONCLUSION

Early-life exposure to isoflavones, especially during the neonatal period, enhances BMD, skeletal microstructure, and strength in adulthood. Similarly, prepubertal or life-long supplementation suggested beneficial skeletal effects, which may reduce the skeletal negative effects of castration at adulthood. On the other hand, the prenatal plus postnatal exposure models reveal the negative effects of isoflavones. Further, basic research on the influence of isoflavones on the epigenetic process in embryos would explain the skeletal phenotypes observed. Mechanistically, the skeletal protection may be due to their direct actions on bone cells favoring osteogenesis and DNA methylation. The effects of isoflavones on TH homeostasis could bring more harm than benefits to the skeleton at this life stage. Therefore, soy infant formulation should not be initiated without proper evaluation of the risk and benefits. The evidence presented in this review should also be interpreted together with evidence from other organ systems, especially sex hormone-sensitive organs to assess the impacts of early-life exposure of isoflavones on developmental health holistically.

AUTHOR CONTRIBUTIONS

K-YC and K-LP conceived the review. K-YC performed the literature search and drafted the manuscript. K-LP validated the search results and reviewed the manuscript. All authors contributed to the article and approved the submitted version.

FUNDING

The researchers are funded by the Fundamental Research Grant Scheme (FRGS/1/2018/SKK10/UKM/03/1) provided by the Ministry of Education, Malaysia. K-LP is a postdoctoral research fellow funded by Universiti Kebangsaan Malaysia through Postdoctoral Research Scheme Modal Insan Penyelidikan (RGA1).

REFERENCES

1. Goudochnikov VI. Role of hormones in perinatal and early postnatal development: Possible contribution to programming/imprinting phenomena. *Russ J Dev Biol.* (2015) 46:237–45. doi: 10.1134/S1062360415050045
2. Saccone G, Berghella V. Antenatal corticosteroids for maturity of term or near term fetuses: systematic review and meta-analysis of randomized controlled trials. *BMJ.* (2016) 355:i5044. doi: 10.1136/bmj.i5044
3. Jobe AH, Goldenberg RL. Antenatal corticosteroids: an assessment of anticipated benefits and potential risks. *Am J Obstet Gynecol.* (2018) 219:62–74. doi: 10.1016/j.ajog.2018.04.007
4. Kuo AH, Li J, Li C, Huber HF, Schwab M, Nathanielsz PW, et al. Prenatal steroid administration leads to adult pericardial and hepatic steatosis in male baboons. *Int J Obes (Lond).* (2017) 41:1299–302. doi: 10.1038/ijo.2017.82
5. Zhu Z, Cao F, Li X. Epigenetic programming and fetal metabolic programming. *Front Endocrinol.* (2019) 10:764. doi: 10.3389/fendo.2019.00764
6. Connelly KJ, Larson EA, Marks DL, Klein RF. Neonatal estrogen exposure results in biphasic age-dependent effects on the skeletal development of male mice. *Endocrinology.* (2015) 156:193–202. doi: 10.1210/en.2014-1324
7. Lind T, Lejonklou MH, Dunder L, Kushnir MM, Ohman-Magi C, Larsson S, et al. Developmental low-dose exposure to bisphenol A induces chronic inflammation, bone marrow fibrosis and reduces bone stiffness in female rat offspring only. *Environ Res.* (2019) 177:108584. doi: 10.1016/j.envres.2019.108584
8. Chin KY, Ima-Nirwana S. Can soy prevent male osteoporosis? A review of the current evidence. *Curr Drug Targets.* (2013) 14:1632–41. doi: 10.2174/13894501146661312162226l2
9. Westmark CJ. Soy-based therapeutic baby formulas: testable hypotheses regarding the pros and cons. *Front Nutr.* (2017) 3:59. doi: 10.3389/fnut.2016.00059
10. Franke AA, Halm BM, Custer LJ, Tatsumura Y, Hebshi S. Isoflavones in breastfed infants after mothers consume soy. *Am J Clin Nutr.* (2006) 84:406–13. doi: 10.1093/ajcn/84.2.406
11. Setchell KD, Zimmer-Nechemias L, Cai J, Heubi JE. Exposure of infants to phyto-oestrogens from soy-based infant formula. *Lancet (London, England).* (1997) 350:23–7. doi: 10.1016/S0140-6736(96)09480-9
12. Bhatia J, Greer F. Use of soy protein-based formulas in infant feeding. *Pediatrics.* (2008) 121:1062–8. doi: 10.1542/peds.2008-0564
13. Rossen LM, Simon AE, Herrick KA. Types of infant formulas consumed in the United States. *Clin Pediatr (Phila).* (2016) 55:278–85. doi: 10.1177/0009922815591881
14. Canadian Paediatric Society. Concerns for the use of soy-based formulas in infant nutrition. *Paediatr Child Health.* (2009) 14:109–18. doi: 10.1093/pch/14.2.109
15. Mcclain RM, Keller D, Casciano D, Fu P, Macdonald J, Popp J, et al. Neonatal mouse model: review of methods and results. *Toxicol Pathol.* (2001) 29 (Suppl.):128–137. doi: 10.1080/019262301753178537
16. Puiman P, Stoll B. Animal models to study neonatal nutrition in humans. *Curr Opin Clin Nutr Metab Care.* (2008) 11:601–6. doi: 10.1097/MCO.0b013e32830b5b15
17. Dye JA, Gibbs-Flournoy EA, Richards JH, Norwood J, Kraft K, Hatch GE. Neonatal rat age, sex and strain modify acute antioxidant response to ozone. *Inhal Toxicol.* (2017) 29:291–303. doi: 10.1080/08958378.2017.1369602
18. Nikov GN, Hopkins NE, Boue S, Alworth WL. Interactions of dietary estrogens with human estrogen receptors and the effect on estrogen receptor-estrogen response element complex formation. *Environ Health Perspect.* (2000) 108:867–72. doi: 10.1289/ehp.00108867
19. Kaludjerovic J, Ward WE. Neonatal exposure to daidzein, genistein, or the combination modulates bone development in female CD-1 mice. *J Nutr.* (2009) 139:467–73. doi: 10.3945/jn.108.100115
20. Kaludjerovic J, Ward WE. Adequate but not supplemental folic acid combined with soy isoflavones during early life improves bone health at adulthood in male mice. *J Nutr Biochem.* (2013) 24:1691–6. doi: 10.1016/j.jnutbio.2013.02.008
21. Kaludjerovic J, Ward WE. Bone-specific gene expression patterns and whole bone tissue of female mice are programmed by early life exposure to soy isoflavones and folic acid. *J Nutr Biochem.* (2015) 26:1068–76. doi: 10.1016/j.jnutbio.2015.04.013
22. Hertrampf T, Ledwig C, Kulling S, Molzberger A, Möller FJ, Zierau O, et al. Responses of estrogen sensitive tissues in female Wistar rats to pre- and postnatal isoflavone exposure. *Toxicol Lett.* (2009) 191:181–8. doi: 10.1016/j.toxlet.2009.08.019
23. Tousen Y, Ishiwata H, Takeda K, Ishimi Y. Assessment of safety and efficacy of perinatal or peripubertal exposure to daidzein on bone development in rats. *Toxicol Rep.* (2015) 2:429–36. doi: 10.1016/j.toxrep.2014.12.012
24. Atkinson C, Frankenfeld CL, Lampe JW. Gut bacterial metabolism of the soy isoflavone daidzein: exploring the relevance to human health. *Exp Biol Med (Maywood).* (2005) 230:155–70. doi: 10.1177/153537020523000302
25. Kaludjerovic J, Ward WE. Neonatal administration of isoflavones attenuates deterioration of bone tissue in female but not male mice. *J Nutr.* (2010) 140:766–72. doi: 10.3945/jn.109.116343
26. Chin KY, Ima-Nirwana S. The biological effects of tocotrienol on bone: a review on evidence from rodent models. *Drug Des Devel Ther.* (2015) 9:2049–61. doi: 10.2147/DDDT.S79660
27. Camacho L, Lewis SM, Vanlandingham MM, Juliar BE, Olson GR, Patton RE, et al. Comparison of endpoints relevant to toxicity assessments in three generations of CD-1 mice fed irradiated natural and purified ingredient diets with varying soy protein and isoflavone contents. *Food Chem Toxicol.* (2016) 94:39–56. doi: 10.1016/j.fct.2016.05.014
28. Piekarz AV, Ward WE. Effect of neonatal exposure to genistein on bone metabolism in mice at adulthood. *Pediatr Res.* (2007) 61:48–53. doi: 10.1203/01.pdr.0000250200.94611.03
29. Kim HS, Jeong ES, Yang MH, Yang SO. Bone mineral density assessment for research purpose using dual energy X-ray absorptiometry. *Osteoporos Sarcopenia.* (2018) 4:79–85. doi: 10.1016/j.afos.2018.09.003
30. Chin KY, Ima-Nirwana S. Sex steroids and bone health status in men. *Int J Endocrinol.* (2012) 2012:208719. doi: 10.1155/2012/208719
31. Mohamad NV, Soelaiman IN, Chin KY. A concise review of testosterone and bone health. *Clin Interv Aging.* (2016) 11:1317–24. doi: 10.2147/CIA.S115472
32. Campbell GM, Sophocleous A. Quantitative analysis of bone and soft tissue by micro-computed tomography: applications to *ex vivo* and *in vivo* studies. *Bonekey Rep.* (2014) 3:564. doi: 10.1038/bonekey.2014.59
33. Cole JH, Van Der Meulen MCH. Whole bone mechanics and bone quality. *Clin Orthop Relat Res.* (2011) 469:2139–49. doi: 10.1007/s11999-011-1784-3
34. Siddiqui JA, Partridge NC. Physiological bone remodeling: systemic regulation and growth factor involvement. *Physiology (Bethesda, Md).* (2016) 31:233–45. doi: 10.1152/physiol.00061.2014
35. Shetty S, Kapoor N, Bondu JD, Thomas N, Paul TV. Bone turnover markers: emerging tool in the management of osteoporosis. *Indian J Endocrinol Metab.* (2016) 20:846–52. doi: 10.4103/2230-8210.192914
36. Boyce BF, Xing L. Biology of RANK, RANKL, and osteoprotegerin. *Arthritis Res Ther.* (2007) 9(Suppl. 1):S1. doi: 10.1186/ar2165
37. Sato N, Yamakawa N, Masuda M, Sudo K, Hatada I, Muramatsu M. Genome-wide DNA methylation analysis reveals phytoestrogen modification of promoter methylation patterns during embryonic stem cell differentiation. *PLoS ONE.* (2011) 6:e19278. doi: 10.1371/journal.pone.0019278

38. Zhang J, Lazarenko OP, Wu X, Tong Y, Blackburn ML, Gomez-Acevedo H, et al. Differential effects of short term feeding of a soy protein isolate diet and estrogen treatment on bone in the prepubertal rat. *PLoS ONE.* (2012) 7:e35736. doi: 10.1371/journal.pone.0035736
39. Chen J-R, Lazarenko OP, Blackburn ML, Shankar K. Dietary factors during early life program bone formation in female rats. *FASEB J.* (2017) 31:376–87. doi: 10.1096/fj.201600703r
40. Hotchkiss CE, Weis C, Blaydes B, Newbold R, Delclos KB. Multigenerational exposure to genistein does not increase bone mineral density in rats. *Bone.* (2005) 37:720–7. doi: 10.1016/j.bone.2005.06.005
41. Sliwiński L, Folwarczna J, Janiec W, Grynkiewicz G, Kuzyk K. Differential effects of genistein, estradiol and raloxifene on rat osteoclasts in vitro. *Pharmacol Rep.* (2005) 57:352–9.
42. Cepeda SB, Sandoval MJ, Crescitelli MC, Rauschemberger MB, Massheimer VL. The isoflavone genistein enhances osteoblastogenesis: signaling pathways involved. *J Physiol Biochem.* (2020) 76:99–110. doi: 10.1007/s13105-019-00722-3
43. Kim M, Lim J, Lee JH, Lee KM, Kim S, Park KW, et al. Understanding the functional role of genistein in the bone differentiation in mouse osteoblastic cell line MC3T3-E1 by RNA-seq analysis. *Sci Rep*. (2018) 8:3257. doi: 10.1038/s41598-018-21601-9
44. Yu B, Tang DZ, Li SY, Wu Y, Chen M. Daidzein promotes proliferation and differentiation in osteoblastic OCT1 cells via activation of the BMP-2/Smads pathway. *Pharmazie.* (2017) 72:35–40. doi: 10.1691/ph.2017.6502
45. Jin X, Sun J, Yu B, Wang Y, Sun WJ, Yang J, et al. Daidzein stimulates osteogenesis facilitating proliferation, differentiation, and antiapoptosis in human osteoblast-like MG-63 cells via estrogen receptor-dependent MEK/ERK and PI3K/Akt activation. *Nutr Res.* (2017) 42:20–30. doi: 10.1016/j.nutres.2017.04.009
46. Sun J, Sun WJ, Li ZY, Li L, Wang Y, Zhao Y, et al. Daidzein increases OPG/RANKL ratio and suppresses IL-6 in MG-63 osteoblast cells. *Int Immunopharmacol.* (2016) 40:32–40. doi: 10.1016/j.intimp.2016.08.014
47. Ohtomo T, Uehara M, Peñalvo JL, Adlercreutz H, Katsumata S, Suzuki K, et al. Comparative activities of daidzein metabolites, equol and O-desmethylangolensin, on bone mineral density and lipid metabolism in ovariectomized mice and in osteoclast cell cultures. *Eur J Nutr.* (2008) 47:273–9. doi: 10.1007/s00394-008-0723-x
48. Wang J, Xu J, Wang B, Shu FR, Chen K, Mi MT. Equol promotes rat osteoblast proliferation and differentiation through activating estrogen receptor. *Genet Mol Res.* (2014) 13:5055–63. doi: 10.4238/2014.July.4.21
49. Ghayor C, Weber FE. Epigenetic regulation of bone remodeling and its impacts in osteoporosis. *Int J Mol Sci.* (2016) 17:1446. doi: 10.3390/ijms17091446
50. Cho YD, Yoon WJ, Kim WJ, Woo KM, Baek JH, Lee G, et al. Epigenetic modifications and canonical wingless/int-1 class (WNT) signaling enable trans-differentiation of nonosteogenic cells into osteoblasts. *J Biol Chem.* (2014) 289:20120–8. doi: 10.1074/jbc.M114.558064
51. Ivashkiv LB. Metabolic-epigenetic coupling in osteoclast differentiation. *Nat Med.* (2015) 21:212–3. doi: 10.1038/nm.3815
52. Wang W, Sun Y, Guo Y, Cai P, Li Y, Liu J, et al. Continuous soy isoflavones exposure from weaning to maturity induces downregulation of ovarian steroidogenic factor 1 gene expression and corresponding changes in DNA methylation pattern. *Toxicol Lett.* (2017) 281:175–83. doi: 10.1016/j.toxlet.2017.09.021
53. Pistollato F, Masias M, Agudo P, Giampieri F, Battino M. Effects of phytochemicals on thyroid function and their possible role in thyroid disease. *Ann N Y Acad Sci.* (2019) 1443:3–19. doi: 10.1111/nyas.13980
54. Bassett JHD, Williams GR. Role of thyroid hormones in skeletal development and bone maintenance. *Endocr Rev.* (2016) 37:135–87. doi: 10.1210/er.2015-1106
55. Chin K-Y, Ima-Nirwana S, Mohamed IN, Aminuddin A, Johari MH, Ngah WZW. Thyroid-stimulating hormone is significantly associated with bone health status in men. *Int J Med Sci.* (2013) 10:857–63. doi: 10.7150/ijms.5870
56. Tuchendler D, Bolanowski M. The influence of thyroid dysfunction on bone metabolism. *Thyroid Res.* (2014) 7:12–12. doi: 10.1186/s13044-014-0012-0
57. Tonstad S, Jaceldo-Siegl K, Messina M, Haddad E, Fraser GE. The association between soya consumption and serum thyroid-stimulating hormone concentrations in the Adventist Health Study-2. *Public Health Nutr.* (2016) 19:1464–70. doi: 10.1017/S1368980015002943
58. Janulewicz PA, Carlson JM, Wesselink AK, Wise LA, Hatch EE, Edwards LM, et al. Urinary isoflavones levels in relation to serum thyroid hormone concentrations in female male adults in the U.S. general population. *Int J Environ Health Res.* (2019) 6:1–12. doi: 10.1080/09603123.2019.1663497
59. Doerge DR, Sheehan DM. Goitrogenic and estrogenic activity of soy isoflavones. *Environ Health Perspect.* (2002) 110(Suppl. 3):349–53. doi: 10.1289/ehp.02110s3349
60. Radović B, Mentrup B, Köhrle J. Genistein other soya isoflavones are potent ligands for transthyretin in serum cerebrospinal fluid. *Br J Nutr.* (2006) 95:1171–6. doi: 10.1079/BJN20061779
61. Šošić-Jurjević B, Ajdžanović V, Filipović B, Severs W, Milošević V. Thyroid mediation of the isoflavone effects on osteoporotic bone: the endocrine interference with a beneficial outcome. *Front. Endocrinol.* (2019) 10:688. doi: 10.3389/fendo.2019.00688
62. Renko K, Schäche S, Hoefig CS, Welsink T, Schwiebert C, Braun D, et al. An improved nonradioactive screening method identifies genistein and xanthohumol as potent inhibitors of iodothyronine deiodinases. *Thyroid.* (2015) 25:962–8. doi: 10.1089/thy.2015.0058
63. Williams AJ, Robson H, Kester MHA, Van Leeuwen JPTM, Shalet SM, Visser TJ, et al. Iodothyronine deiodinase enzyme activities in bone. *Bone.* (2008) 43:126–34. doi: 10.1016/j.bone.2008.03.019
64. Ariyani W, Iwasaki T, Miyazaki W, Yu L, Takeda S, Koibuchi N. A possible novel mechanism of action of genistein and daidzein for activating thyroid hormone receptor-mediated transcription. *Toxicol Sci.* (2018) 164:417–27. doi: 10.1093/toxsci/kfy097
65. Swart AC, Johannes ID, Sathyapalan T, Atkin SL. The effect of soy isoflavones on steroid metabolism. *Front Endocrinol.* (2019) 10:229. doi: 10.3389/fendo.2019.00229
66. Refetoff S. Thyroid hormone serum transport proteins. In: Feingold KR, Anawalt B, Boyce A, Chrousos G, Dungan K, Grossman A, editors. *Endotext*. South Dartmouth, MA: MDText.com, Inc. (2000).
67. Palha JA, Episkopou V, Maeda S, Shimada K, Gottesman ME, Saraiva MJ. Thyroid hormone metabolism in a transthyretin-null mouse strain. *J Biol Chem.* (1994) 269:33135–9.

Conflict of Interest: The authors declare that the research was conducted in the absence of any commercial or financial relationships that could be construed as a potential conflict of interest.

frontiers in Pediatrics

REVIEW
published: 04 November 2020
doi: 10.3389/fped.2020.591693

The Potential of Mesenchymal Stromal Cell as Therapy in Neonatal Diseases

*Ling Ling Liau[1], Maimonah Eissa Al-Masawa[2], Benson Koh[2], Qi Hao Looi[3], Jhi Biau Foo[4], Sau Har Lee[5], Fook Choe Cheah[6] and Jia Xian Law[2]**

[1] Department of Physiology, Faculty of Medicine, Universiti Kebangsaan Malaysia Medical Centre, Kuala Lumpur, Malaysia, [2] Centre for Tissue Engineering and Regenerative Medicine, Faculty of Medicine, Universiti Kebangsaan Malaysia Medical Centre, Kuala Lumpur, Malaysia, [3] Future Cytohealth Sdn Bhd, Bandar Seri Petaling, Kuala Lumpur, Malaysia, [4] School of Pharmacy, Faculty of Health and Medical Sciences, Taylor's University, Subang Jaya, Malaysia, [5] School of Biosciences, Faculty of Health and Medical Sciences, Taylor's University, Subang Jaya, Malaysia, [6] Department of Paediatrics, Faculty of Medicine, Universiti Kebangsaan Malaysia Medical Centre, Kuala Lumpur, Malaysia

Mesenchymal stromal cells (MSCs) can be derived from various tissue sources, such as the bone marrow (BMSCs), adipose tissue (ADSCs), umbilical cord (UC-MSCs) and umbilical cord blood (UCB-MSCs). Clinical trials have been conducted to investigate the potential of MSCs in ameliorating neonatal diseases, including bronchopulmonary dysplasia (BPD), intraventricular hemorrhage (IVH) and necrotizing enterocolitis (NEC). In preclinical studies, MSC therapy has been tested for the treatment of various neonatal diseases affecting the heart, eye, gut, and brain as well as sepsis. Up to date, the number of clinical trials using MSCs to treat neonatal diseases is still limited. The data reported thus far positioned MSC therapy as safe with positive outcomes. However, most of these trials are still preliminary and generally smaller in scale. Larger trials with more appropriate controls and a longer follow-up period need to be conducted to prove the safety and efficacy of the therapy more conclusively. This review discusses the current application of MSCs in treating neonatal diseases, its mechanism of action and future direction of this novel therapy, including the potential of using MSC-derived extracellular vesicles instead of the cells to treat various clinical conditions in the newborn.

Keywords: cell therapy, clinical trial, neonatal diseases, extracellular vesicles, mesenchymal stromal cells

OPEN ACCESS

Edited by:
Eugene Dempsey,
University College Cork, Ireland

Reviewed by:
Kazumichi Fujioka,
Kobe University, Japan
Gangaram Akangire,
Children's Mercy Hospital,
United States

****Correspondence:***
Jia Xian Law
danieljx08@gmail.com;
lawjx@ppukm.ukm.edu.my

Specialty section:
This article was submitted to Neonatology, a section of the journal Frontiers in Pediatrics

Received: *05 August 2020*
Accepted: *05 October 2020*
Published: *04 November 2020*

Citation:
Liau LL, Al-Masawa ME, Koh B, Looi QH, Foo JB, Lee SH, Cheah FC and Law JX (2020) The Potential of Mesenchymal Stromal Cell as Therapy in Neonatal Diseases. Front. Pediatr. 8:591693. doi: 10.3389/fped.2020.591693

INTRODUCTION

Mesenchymal stromal cells (MSCs) possess several unique properties which render them an ideal candidate for cell-based therapy in various neonatal diseases. MSCs are multipotent and can migrate to the damaged tissues or organs in response to the inflammatory mediators. At the injured sites, the cells can replicate and differentiate to regenerate the loss or damaged tissues. Besides, MSCs also secrete paracrine factors such as growth factors, cytokines and chemokines which diffuse to local tissue environment and interact with the surrounding cells. These paracrine factors can remedy tissue injury and inflammation as well as mediate tissue repair and regeneration by exerting its anti-inflammatory, anti-apoptotic and pro-mitotic effects (1–3).

MSCs are classified into various groups according to the cell source, such as bone marrow-derived MSCs (BMSCs), adipose-derived MSCs (ADSCs), umbilical cord-derived MSCs (UC-MSCs), and umbilical cord blood-derived MSCs (UCB-MSCs) (4). BMSCs were favored by some researchers since the cells are proven to be safe, easily accessible and can be extracted from the patient's bone marrow (autologous) thus minimizing the risk of immune rejection (5, 6). On the other hand, UC-MSCs and UCB-MSCs appear as attractive sources of allogeneic MSCs due to their availability and immune evasive nature (7–9). Generally, the procedure of BMSC preparation is more time consuming and costlier compared to UC-MSCs and UCB-MSCs, thus the use of UC-MSCs and UCB-MSCs may be preferred.

Regardless of the tissue sources, MSCs have low immunogenicity and can suppress the activation of immune cells (10). Therefore, both autologous and allogeneic MSCs can be used clinically as the cells have a very low risk of being rejected by the host immune system. A significant advantage of allogeneic MSCs is that the cells can be developed into an off-the-shelf product that is convenient to be used clinically. **Table 1** highlights the advantages and disadvantages of different MSCs.

MSC therapy can be instituted during the first month of life and is reportedly quite safe. MSC therapy has been introduced to treat neonatal diseases such as severe intraventricular hemorrhage (IVH), bronchopulmonary dysplasia (BPD), and necrotizing enterocolitis (NEC) (11–13) (**Figure 1**). MSCs are more widely used clinically to treat neonatal diseases as the cells do not have ethical concerns and have a very low risk of tumor formation compared to the embryonic stem cells (ESCs) and induced pluripotent stem cells (iPSCs). In preclinical studies, MSCs have been experimented to treat congenital heart, eye, gut and brain diseases as well as sepsis.

In this review, literature search was conducted using the keywords (1) neonate and (2) clinical and (3) mesenchymal stem cells on Pubmed and Medline databases and all the relevant articles were included in the review.

TABLE 1 | Comparison between BMSCs, ADSCs, UC-MSCs and UCB-MSCs for stem cell therapy.

Characteristic	BMSCs	ADSCs	UC-MSCs UCB-MSCs
Ethical conundrum	No	No	No
Tissue collection	Invasive	Invasive	None invasive (unwanted tissue after delivery)
Tissue processing and cell culture	Easy	Easy	Easy
Effect of donor age on cells	Quantity and quality decline with age	Quantity and quality decline with age	Unaffected
Cell proliferative potential	Lower	Lower	Higher
Expression of embryonic markers	Lower	Lower	Higher
Anti-inflammatory property	Good	Good	Good
Allogeneic cell rejection	No	No	No
Risk of tumor formation	Very low	Very low	Very low

BMSCs, Bone marrow-derived mesenchymal stromal cells; ADSCs, adipose tissue-derived mesenchymal stromal cells; UC-MSCs, umbilical cord-derived mesenchymal stromal cells; UCB-MSCs, Umbilical cord blood-derived mesenchymal stromal cells.

MSCs FOR THE TREATMENT OF NEONATAL LUNG DISEASES

Bronchopulmonary Dysplasia (BPD)

BPD is a chronic lung disease affecting mostly preterm neonates and is characterized by disrupted alveolar growth and pulmonary vascularization. Recent years have witnessed an increased incidence of BPD due to the spike in the population of preterm survivors as a result of the improvement in neonatal care. Pulmonary hypertension is common in severe cases of BPD. Affected infants may require oxygen support and commonly develop respiratory problems that need hospitalization (14, 15).

Currently, clinical trials evaluating MSC therapeutic and preventive effects on BPD are still limited (**Table 2**). The majority of the studies are small in scale, non-randomized and lack proper comparison groups. To the best of our knowledge, the first clinical study was reported by Chang et al. in 2014 which followed-up the patients up to 2 years (11, 16). The study examined the safety and feasibility of single intratracheal transplantation of 1×10^7 and 2×10^7 allogeneic UCB-MSCs/kg in 9 preterm infants with a high risk of developing BPD at the age of 7–14 days. Results showed that UCB-MSC therapy helped to reduce BPD severity and inflammatory markers as well as to minimize the risk of neurodevelopmental morbidities. Powell et al. treated 12 preterm infants with BPD using the same protocol as Chang et al. and found that disease severity improved after the stem cell treatment (19). Alvarez-Fuente et al. reported suppression of pro-inflammatory as well as improvement in pulmonary hypertension and diminished levels of surfactant protein D (SP-D) expression, a biomarker for lung injury, in 2 preterm infants given multiple dosages of allogeneic BMSCs intravenously (17). Nonetheless, both patients received stem cell therapy at the very advanced stages of BPD and passed away 6 weeks after the initiation of MSC therapy. Lin et al. reported improvement in respiratory functions after intratracheal administration of maternal BMSC (6.25×10^6 cells/kg) in a 10-month old preterm infant with BPD that developed acute respiratory distress syndrome (ARDS) (18). Results from these clinical studies suggested that the beneficial effects of MSCs might be attributed to paracrine effects that stimulate alveolarization and vascularization rather than cell engraftment and proliferation as traces of donor cells in the recipients were absent.

The optimal dosage regimen, including the optimal MSC per dose, number of doses, timing of transplantation, time between doses, and route of administration, is essential in determining

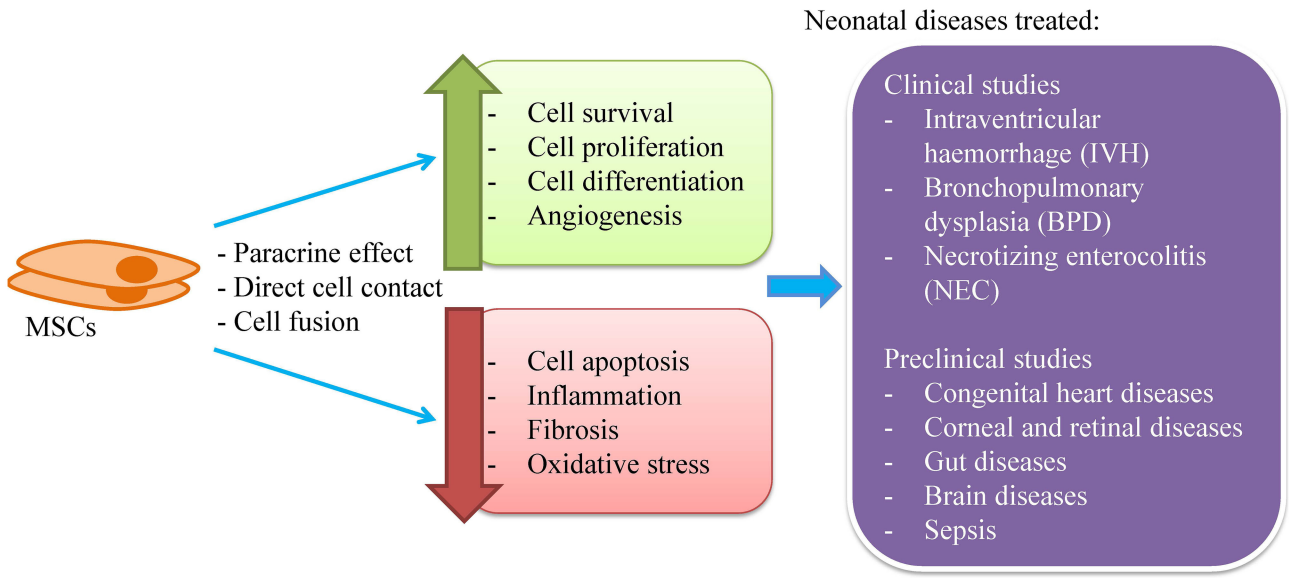

FIGURE 1 | MSCs for the treatment of neonatal diseases. MSCs are known to exert its therapeutic effect through paracrine secretion, direct cell contact and cell fusion to enhance cell survival, proliferation and differentiation, and angiogenesis as well as to reduce cell apoptosis, inflammation, fibrosis, and oxidative stress. Clinically, MSCs have been used to treat intraventricular hemorrhage, bronchopulmonary dysplasia, and necrotizing enterocolitis. Besides, MSCs have been tested for the treatment of congenital heart diseases, eye, gut, and brain diseases as well as sepsis.

MSC efficacy. However, this regimen has not been established yet. The identified clinical studies used MSC dose of 1–20 $\times$ 10^6 cells/kg body weight. Studies that compared high and low doses (1 $\times$ 10^7 vs. 2 $\times$ 10^7 cells/kg) found no difference in outcome (11, 19). Majority of the studies gave a single dose except for Alvarez-Fuente et al. that applied multiple infusions (17). Chang et al. noticed that respiratory function improvement started to decline after 7 days of transplantation (11). This finding supports the notion of the inadequacy of a single-dose approach and the authors suggested that day 7 could be the time for the second dosage of MSCs. Another issue is determining the optimal timing of MSC transplantation. Generally, researchers agreed that early intervention is more beneficial for BPD patients. Most studies administered the cells using the intratracheal route to ensure high cell homing at the targeted tissue while evading systemic side effects (11, 18, 19). Besides, the airway is easily accessible through the endotracheal tube in preterm neonates assisted with mechanical ventilation. Although there are concerns over the risk of delivering a large number of MSCs to the premature lungs, nonetheless, intratracheal administration has been shown to be safe and feasible. Intravenous administration also has been reported to be safe and this route might be preferred in infants that do not require invasive ventilation (17). Preclinical studies showed that intravenously administered MSCs reach the lungs within 24 h and dissipate in 7 days after infusion with no traces in other organs (20).

In spite of the inconsistencies on the degree of effectiveness of MSCs, all reported studies support the apparent safety profile of MSCs regardless of the dose and route of administration. There was no anaphylactic shock, no immune rejection, no mass formation and no dose-limiting toxicities reported. This has led to much excitement about the potential of using MSCs in the prevention and treatment of BPD. There are many more studies that are currently underway (**Table 3**).

MSCs FOR THE TREATMENT OF NEONATAL BRAIN DISEASES

Neonatal brain diseases, including intraventricular hemorrhage (IVH), neonatal stroke (NS), hypoxic-ischemic encephalopathy (HIE) and periventricular leukomalacia (PVL), are the major contributor to the high mortality and morbidity rates among the neonate (21). Experimental investigations have identified multiple causes for these diseases, including perinatal-induced neuronal cell death due to depleted tissue energy reserve, placental disruption, prolapsed umbilical cord, dysfunctional mitochondria, accumulated free oxygen radical species, persistent inflammatory reactions, defective maturation, and myelination of neuronal cells, as well as the loss of endogenous stem cell pool that is responsible for cell differentiation and tissue repair (22, 23). In the developing brain, pre-oligodendrocytes normally present in high number to form mature oligodendrocytes for the production of myelin sheath. Unfortunately, these pre-oligodendrocytes are more vulnerable than its mature counterpart, hence are more easily lost in the presence of the injurious assaults leading to the development of neonatal brain diseases (22). Despite the advances and progress in neonatal therapeutic medicine, there is still a lack of therapy that is effective to prevent or cure developmental brain

TABLE 2 | Clinical trials used MSCs to treat neonatal diseases.

References/ year/study location	ClinicalTrials.gov identifier	Study design	Disease/ pathology	Age group	No. of patient		Cell source	Route of administration	Dose	Frequency of cell administration	Follow up period	Safety outcome	Key efficacy outcome
					C	T							
Chang et al. (11), 2014, South Korea	NCT01297205	Phase 1 dose-escalation clinical trial	BPD	5 to 14-day old (23–29 gestational weeks)	0	9	Allogeneic UCB-MSCs (Pneumostem®)	Intratracheal	Group A: 3 patients received 1 × 10^7 cells/kg Group B: 6 patients received 2 × 10^7 cells/kg	Single dose	84 days	- No MSC related AE - No dose-limiting toxicities - No tumor formation	- BPD severity reduced - Retinopathy of prematurity demanding surgery occurred less in the MSC-treated group compared to the historical corresponding control group - Significant declined in IL-6, IL-8, MMP-9, TNF-a, and TGF-b1 levels in tracheal aspirates at day 7
Ahn al. (16), 2014, South Korea	NCT01632475	Phase I trial	BPD	5 to 14-day old (23–29 gestational weeks)	0	9	Allogeneic UCB-MSCs (Pneumostem®)	Intratracheal	Group A: 3 patients received 1 × 10^7 cells/kg Group B: 6 patients received 2 × 10^7 cells/kg	Single dose	24 months	- No MSC-related AE	- Infants treated with MSCs did not require supplemental oxygen upon discharge compared to 22% in the historical corresponding control group - Infants treated with MSCs did not develop asthma and did not need persistent steroid/bronchodilator therapy as long as 24 months of CA - MSC treatment minimized risk of neurodevelopmental morbidities.
Álvarez-Fuente et al. (17), 2018, Spain	–	Phase 1 trial	BPD	Patient1: 5-month old Patient 2: 85-day old	0	2	Allogeneic BMSCs	Intravenous	Patient1: Increasing weekly dose: 1.1 × 10^6 cells/kg up to 13.9 × 10^6 cells/kg Patient 2: 5 × 10^6 cells/kg per week for 3 consecutive weeks	Patient 2 received 3 doses	–	- No MSC-related AE	- Inflammatory and lung injury biomarkers decreased - MSCs failed to reverse late stage of lung fibrosis, thus patients did not survive
Lin et al. (18), 2018, Taiwan	–	Case study	BPD with ARDS	10-month old	0	1	Allogeneic BMSCs	Intratracheal	6.25 × 10^6 cells/kg	Single dose	-	- No MSC-related AE	- Improvement in respiratory functions - ECMO support was detached at 25 days after transfusion - Improvement in lung fibrosis
Powell and Silvestri (19), 2019, USA	NCT02381366	Phase 1, open-label, dose-escalation trial	BPD	6 to 14-day old	0	12	Allogeneic UCB-MSCs (Pneumostem®)	Intratracheal	Group A: 6 patients received 1 × 10^7 cells/kg Group B: 6 patients received 2 × 10^7 cells/kg	Single dose	Up to 20 months CA	- No severe AEs related to MSCs - No dose-limiting toxicities.	- All patients developed BPD - 10/12 patients developed severe BPD showed improvement at day 84 after transfusion - Potential effectiveness could not be established.

(Continued)

TABLE 2 | Continued

References/ year/study location	ClinicalTrials.gov identifier	Study design	Disease/ pathology	Age group	No. of patient		Cell source	Route of administration	Dose	Frequency of cell administration	Follow up period	Safety outcome	Key efficacy outcome
					C	T							
Ahn et al. (12), 2018, South Korea	NCT02274428	Phase I dose-escalation clinical trial	IVH (Grade 4)	11.6 ± 0.9-day old	0	9	Allogeneic UCB-MSCs	Intraventricular	Group A: 3 patients received 5×10^6 cells/kg Group B: 6 patients received 1×10^7 cells/kg	Single dose	NA	- No fatality - No anaphylactic reaction - Severe AEs observed were not related to MSC transplantation	–
Akduman et al. (13), 2019, Turkey	–	Case study	NEC (SVT related)	22-day old	0	1	Allogeneic UC-MSCs	Intravenous	1×10^7 cells/transfusion	Single dose	12 months	- No AE	- Intestinal blood supply improved - Saved the remaining of the necrotic intestine after laparotomy - Helped maintain the baby growth and neurodevelopment on par with babies of his age.

AE, adverse event; ARDS, acute respiratory distress syndrome; BMSCs, bone marrow derived mesenchymal stromal cells; BPD, bronchopulmonary dysplasia; CA, corrected age; C- control; T, treatment; UC-MSCs, umbilical cord derived mesenchymal stromal cells; UCB-MSCs, umbilical cord blood derived mesenchymal stromal cells; IVH, intraventricular hemorrhage; NEC, necrotizing enterocolitis; SVT, supraventricular tachycardia.

injuries in neonates. Therefore, research for a newer, safer and more effective therapeutic approach is necessary to improve the outcome of these conditions. Thus, far, the use of stem cell-based therapy has been well-researched as an intervention to ameliorate complications associated with brain diseases. MSCs have been used clinically to treat IVH, whilst pre-clinical studies have been conducted to unveil the potential of MSCs to attenuate or to repair the brain injury present in various disease models, including NS, HIE, and PVL.

Intraventricular Hemorrhage (IVH)

IVH is a perinatal brain morbidity that results from the rupture and bleeding of the germinal matrix that is restricted to the ventricular area of the brain. Premature neonates are at a higher risk of developing IVH (24). IVH continues to be one of the leading causes of mortality and lifetime disability in infants. A recent systematic review concluded that prematurity and IVH are major contributing factors to the increased risk for cerebral palsy (CP) in neonates (25).

Clinical research examines MSC therapeutic and preventive effect on IVH is still in its infancy. To the best of our knowledge, the first clinical trial for the evaluation of MSC therapy in IVH patients was revealed by Ahn et al. in South Korea in 2018 (12). It was an uncontrolled phase I dose-escalation study intended to investigate the safety and feasibility of the intraventricular transplantation of allogeneic UCB-MSCs. Nine premature newborns of gestational age 23–34 weeks with severe IVH of grade 3 and 4 were recruited and received a single dose of UCB-MSCs. The average age at transplantation was 11.6 days, around 7 days after IVH diagnosis. UCB-MSCs were injected directly to the lateral ventricle through the anterior fontanelle. Two different UCB-MSC concentrations were tested. The lowest dose used was 5×10^6 cells/kg and the highest dose was 1×10^7 cells/kg given to 3 and 6 patients, respectively. Preliminary findings showed that transplantation was well-tolerated with no immune rejection, anaphylactic shock, dose-related toxicity, death, or any MSC infusion-related severe adverse events. Eight infants developed prematurity related disorders including BPD, sepsis, retinopathy of prematurity, and NEC. Additionally, 5/9 MSC recipients needed shunt placement. The 2-year follow-up study to evaluate the safety of MSC transplantation on these infants is still ongoing (NCT02673788). The same research group is currently conducting a phase II trial to assess the therapeutic efficacy of MSC therapy in preterm infants with IVH (NCT02890953). Of note, the narrow therapeutic window and utilization of brain injury biomarkers should be considered when designing MSC therapeutic protocols for IVH. More well-designed clinical studies to confirm the safety and efficacy of MSC transplantation in IVH patients are necessary.

Neonatal Stroke (NS)

NS involves injury to the cerebral tissue, usually caused by a disruption in arterial blood flow or major cerebral vein due to the presence of thrombus or embolism. It is a neonatal brain disease with high mortality and morbidity. The use of MSCs has been attempted by Kim et al. for the attenuation of brain injuries in a middle cerebral artery occlusion-induced

TABLE 3 | Clinical trials using MSCs to treat neonatal diseases recorded in ClinicalTrials.gov.

ClinicalTrials.gov identifier	Cell source	Route of administration	Age eligibility	Disease	Phase	No. of patient	Country
NCT03356821	BMSCs	Intranasal	newborns with gestational age ≥36 weeks	PAIS	I/II	10	Netherlands
NCT04255147	UC-MSCs	Intravenous	up to 21-day old	BPD	I	9	Canada
NCT03683953	MSCs	Intrathecal	newborns with gestational age between 28 and 37 weeks	BPD	I	200	China
NCT03601416	UC-MSCs	Intravenous	up to 1-year old	BPD	II	57	China
NCT03645525	UC-MSCs	Intratracheal	up to 3-week old	BPD	I/II	180	China
NCT03774537	UC-MSCs	Intravenous	up to 14-day old	BPD	I/II	20	China
NCT01207869	UC-MSCs	Intrathecal	up to 6-month old	BPD	I	10	China
NCT03631420	UC-MSCs	–	36 to 48-week old	BPD	I	9	Taiwan
NCT03857841	BMSCs-EVs (UNEX-42)	Intravenous	up to 14-day old	BPD	I	18	United States
NCT02443961	MSCs	–	1-month to 28-week old	BPD	I	10	Spain
NCT04062136	UC-MSCs	Intravenous	1 to 6-month old	BPD	I	10	Vietnam
NCT03873506	UC-MSCs	Intravenous	1-month to 5-year old	BPD	I	30	China
NCT03558334	UC-MSCs	Intravenous	all ages	BPD	I	12	China
NCT03392467	UCB-MSCs (Pneumostem®)	–	up to 13-day old	BPD	II	60	Korea
NCT04003857	UCB-MSCs (Pneumostem®)	Intratracheal	6 to 60-month old	BPD	follow-up of NCT03392467	60	South Korea
NCT01828957	UCB-MSCs (Pneumostem®)	Intratracheal	up to 14-day old	BPD	II	69	South Korea
NCT01897987	UCB-MSCs (Pneumostem®)	Intratracheal	7-month old	BPD	follow-up of NCT01828957	70	South Korea
NCT02023788	UCB-MSCs (Pneumostem®)	Intratracheal	45 to 63-month old	BPD	follow-up of NCT01632475	8	South Korea
NCT03378063	UCB-MSCs	–	1 to 3-month old	BPD	I	100	China
NCT03635450	UC-MSCs	Intravenous	up to 48-hour old	HIE	I	6	United States
NCT02854579	a. hFF-NPCs b. MSCs-derived paracrine factors c. hFF-NPCs + MSCs-derived paracrine factors	Intrathecal	up to 14-day old	HIE	–	120	China
NCT01962233	UC-MSCs	Intravenous	all ages	HIE	I	10	China
NCT03525418	BMSCs	Intramyocardial	up to 1-year old	HLHS	I/II	30	United States
NCT03079401	MPCs	Intramyocardial	up to 5-year old	HLHS	I/II	24	United States
NCT03525418	BMSCs	Intramyocardial	up to 1-year old	HLHS	I/II	30	United States
NCT02855112	ADSCs	Intrathecal	5 to 12-month old	ISMA	I/II	10	Iran
NCT02274428	UCB-MSCs (Pneumostem®)	Intraventricular	23 to 34-week gestational age	IVH	I/II	9	South Korea
NCT02673788	UCB-MSCs (Pneumostem®)	–	6-month to 2-year old	IVH	follow-up of NCT02274428	9	South Korea
NCT02890953	UCB-MSCs (Pneumostem®)	Intraventricular	within 28 postnatal days	IVH	IIa	22	South Korea

ADSCs, adipose tissue-derived mesenchymal stromal cells; BPD, bronchopulmonary dysplasia; BMSCs, bone marrow-derived mesenchymal stromal cells; CP, cerebral palsy; CM, conditioned medium; EVs, extracellular vesicles; hFF-NPCs, aborted human fetal forebrain-derived neural progenitor cells; HIE, hypoxic-ischemic encephalopathy; HLHS, hypoplastic left heart syndrome; UCB-MSCs, umbilical cord blood-derived mesenchymal stromal cells; UC-MSCs, umbilical cord-derived mesenchymal stromal cells; ISMA, infantile spinal muscular atrophy; IVH, intraventricular hemorrhage; MPC, mesenchymal precursor cells; PAIS, perinatal arterial ischemic stroke; UC-HSCs umbilical cord-derived hematopoietic stem cells; uAVC, unbalanced atrioventricular canal.

newborn rat model (26). They observed a reduction in brain infarct volume, improvement of functional tests and enhanced astrogliosis post-MSC transplantation. Similarly, van Velthoven et al. delivered MSCs intranasally to the stroke-affected newborn rats and discovered that the extent of brain injury was reduced, as shown by the decreased size of the infarct, reduced loss of brain matter as well as improved motor functions (27). In another study, exosomes isolated from MSCs were used to treat lipopolysaccharide-induced neuroinflamed 3-day old rat pups intranasally (28). As a result, the expression of inflammatory genes and pro-inflammatory cytokines were suppressed by the exosomes, therefore decreasing the microglia-mediated brain injuries. These exosomes primarily worked by interfering with the Toll-like receptor 4 signaling of microglial cells, hence preventing degradation of NFκB inhibitor (IκBα), as well as phosphorylation of MAP kinase family of proteins.

Hypoxic-ischemic Encephalopathy (HIE)

HIE refers to a type of brain injury whereby insufficient blood flow is delivered to the brain tissue, resulting in death or severe disabilities such as epilepsy, intellectual disability and CP (29). The current widely used treatment option for HIE is hypothermia, although it only provides a neuroprotective effect rather than a neurorestorative function. Therefore, researchers are working hard to establish a therapy that could improve the prognosis of this neonatal disease.

The combined therapy of hypothermia and UCB-MSCs significantly reduced the cerebral infarcted area and improved the sensorimotor function of rats with HIE (30). This improved diseased condition is thought to be contributed by the paracrine factors released by MSCs, including IGF-1, bFGF, neural cell adhesion molecules, nerve growth factors, and anti-inflammatory cytokines, which stimulated neurogenesis. Moreover, MSCs enhanced expression of genes that triggered cell proliferation while suppressing genes involved in inflammatory responses. Through the inhibition of apoptosis, induction of nerve fibers to remyelinate and axons to regenerate, the administered MSCs were also able to reduce the loss of brain matter while improving sensorimotor functions (31, 32). The potential neurorestorative function of MSCs is further demonstrated in the study by van Velthoven et al. (27). In the control group, inflammatory and cell death activities in the affected rodent brain tissue stopped after 4 days, indicating the therapeutic window to be up to 4 days after the initial attack. However, intranasal transplantation of 1×10^7 MSCs/kg at day 10 post-hypoxia-ischemia attack in the experimental group was still able to limit the brain tissue damage. This implies that tissue reparative activity is ongoing and responsive to MSCs that migrated to the ischemic zone to induce a microenvironmental change which favors neurogenesis (27, 33). Functionality wise, newborn rodents treated with MSCs also showed long-lasting improvement in cognitive and motor functions, up to 14 weeks post-injury (34). In a pre-clinical study, Ophelders et al. reported that intravenous administration of BMSC-derived extracellular vesicles (EVs) to the fetus improved the brain function using a preterm sheep model of hypoxic-ischemic brain injury (35).

Periventricular Leukomalacia (PVL)

PVL is characterized by a loss of oligodendrocyte and its progenitor cell. This disease is one of the clinical complications of HIE that lead to CP. Other than HIE, the predisposing factors include birth trauma, and immature brain development. In neonates affected by PVL, their periventricular tissue undergoes necrosis while the surrounding white matter experiences diffused gliosis. These changes in brain tissue will disrupt the cognitive, adaptive, motor, and social functions in the infant. Unlike other brain diseases with some limited therapeutic option, there is no specific treatment for PVL except for expectant and supportive management (36). Thus, researchers have begun exploring the use of MSCs for the treatment of PVL.

In the cystic PVL rat model used by Chen et al., excitotoxic ibotenic acid was injected into the white matter of rat brain leading to loss of myelin with transient formation of cysts, activation of microglia and development of CP-like behavioral defects (37). With this animal model, the research group injected the animals intracerebrally with BMSCs 1 day after PVL induction. Results showed that MSCs migrated to the lesion areas in the brain to increase the proliferation of glial cells, hence resulting in improvement of the myelination process with better motor function outcome. Using a different PVL study model that is established through ligation of the left common carotid artery inducing 4 h of hypoxia, the rats were treated with intraperitoneal UC-MSC injection for 3 consecutive days (38). Similarly, functional outcomes improved with decreased microglia and astrocyte activities. Another study by Morioka et al. also demonstrated the suppression of pro-inflammatory cytokines in the affected brain treated with UC-MSCs to reverse the lipopolysaccharide-induced PVL-like injury in newborn rats (39).

MSCs FOR THE TREATMENT OF NEONATAL GUT DISEASES

There are several types of neonatal gut diseases that affect the neonate, with higher prevalence in the preterm infant. Currently, MSC therapy has been used to treat NEC in one clinical study involving a neonatal patient. Conversely, several preclinical studies have examined the safety and efficacy of MSC therapy to ameliorate NEC and gastroschisis.

Necrotizing Enterocolitis (NEC)

NEC is the most common devastating gastrointestinal disease affecting the neonate, with a mortality rate between 15 and 30 % (40). It may affect both full-term and preterm neonates with the latter group having an increased risk. Predisposing factors include prematurity, low birth weight, formula feeding, intrauterine growth retardation, postnatal asphyxia, sepsis, and congenital heart diseases (41, 42). In NEC, bowel inflammation causes necrosis and perforation which may lead to intestinal surgical removal, death or a lifetime severe neurodevelopmental impairment (43, 44)

MSCs have emerged as a promising therapeutic choice for intestinal anomalies such as ulcerative colitis and Crohn's disease

(45, 46). However, the therapeutic benefit of MSCs for NEC has yet to be fully explored in clinical setting. A case report of a full-term, 22-day old male neonate weighed 3.350 kg who experienced NEC as a consequence to repeated supraventricular tachycardia (SVT) leading to the resection of 60 cm of the intestine because of gangrene revealed a noticeable improvement after intravenous infusion of MSCs (13). A single dose of 1×10^7 allogeneic UC-MSCs was transfused 4 days after colectomy with no complications. Improved intestinal blood supply was confirmed 3 days post-transplantation, enteral nutrition was resumed at day 8, and the jejunal stoma was closed 46 days post-transplantation. The authors speculated that MSC therapy helped to salvage the remaining of the resected intestine thus prevent short bowel syndrome. Overall, MSC transplantation may offer substantial practical advantages to NEC patients. Nonetheless, findings of this single case report should be interpreted with caution.

In an animal study conducted by Taymen et al. BMSCs were administered to a rat model of NEC (47). The rat showed significant weight gain and improvement in clinical sickness scores after BMSC transplantation. The number of BMSCs homing to the bowel was significantly higher in the treated group. In fact, the severity of bowel damage was significantly reduced in histopathological evaluation. A similar study was conducted by McCulloh et al. using 4 different sources of stem cells, i.e., BMCSs, amniotic fluid-derived MSCs (AF-MSCs), amniotic fluid-derived neural stem cells and neonatal enteric neural stem cells (48). The results indicated that all sources of stem cells reduced the incidence and severity of experimental NEC equally.

Gastroschisis

Gastroschisis is a full-thickness paraumbilical defect in the abdominal wall that results in herniation of the fetal midgut with a significant mortality rate of 5–10% (49). Feng et al. evaluated the efficacy of intraamniotic delivery of concentrated AF-MSCs to treat gastroschisis (50). The cells were injected into rat fetuses with surgically-created gastroschisis. A significantly thicker muscular layer was observed in the AF-MSC group compared to the control group. It was concluded that AF-MSCs mitigated bowel damage in experimental gastroschisis after intraamniotic injection. A further study was conducted by the same research group but in a larger animal model, i.e., the rabbit (51), which reported similar results.

Since heterotopic cell fusion has been demonstrated between MSCs and various cells, as such, the similar mechanism of protection was also proposed in congenital gut diseases. Nevertheless, preclinical data do not support this hypothesis (52, 53). It seems that MSC homing and paracrine effects are better accepted as the protective mechanism in congenital gut diseases. MSCs may be attracted to the injured site, differentiate to replace damaged cells or interact with native intestinal stem cells to upregulate the Wnt/β-catenin pathway, which promotes auto-regeneration of the intestinal epithelium (54). MSCs secrete a myriad of paracrine factors that promote gut healing and reconstruction. MSC secretome has been shown to improve the severity in a rat NEC model (47).

MSCs FOR THE TREATMENT OF NEONATAL EYE DISEASES

Corneal disease is a challenging condition to manage particularly in the neonatal age group. However, successful preclinical studies in the past 10 years have shed some light on the usage of MSCs to treat neonatal corneal diseases. Liu et al. evaluated the efficacy of MSC transplantation in treating congenital corneal disease *in vivo* (55). The corneal disease was simulated using a Lumican null mice model where the cornea is manifested as thin and cloudy due to the disorganization of stromal extracellular collagen matrix and down-regulated expression of keratocan. Results showed that stromal thickness increased significantly and transparency improved in MSC-treated corneas as early as 8 weeks after treatment compared to the control group. This exciting finding has spurred the interest of other research groups to use the similar strategy to treat neonatal patients with corneal diseases.

Mucopolysaccharidosis (MPS) VII is a disease caused by the mutation of β-glucuronidase. Patients with this disease often suffer from developmental defects including short stature, corneal clouding and delayed development. In 2013, Coulson-Thomas et al. transplanted UC-MSCs into the cornea of MPS VII mice (56). MSC-transplanted corneas demonstrated reduced corneal haze 1–3 months post-transplantation. Corneas treated during the first and second month presented significantly improved corneal integrity in comparison to those treated at the third month, suggesting that prophylactic treatment upon diagnosis could prevent the development of corneal clouding. An overall decrease in glycosaminoglycan content was detected in corneas treated at all time points in comparison to the untreated corneas.

Collagen V is a critical protein in the regulation of corneal collagen fibrillogenesis and function development. It has been reported that collagen V knockout stroma demonstrated severe dysfunctional regulation of fibrillogenesis (57). Call et al. treated this congenital and acquired corneal opacity associated with the loss of collagen V in $Col5a1^{\Delta st/\Delta st}$ mice (58). The mice were subjected to keratectomy in which the corneal epithelium and the anterior stroma were removed before received UC-MSC transplantation via intrastromal injection. MSC therapy reduced corneal opacity by re-establishing the collagen fibril arrangement via the production of collagen V.

Retinal neovascularization is an unhealthy development which leads to visual diminution and even blindness. Xu et al. studied the therapeutic effect of BMSCs against retinal neovascularization and found that BMSCs migrated and integrated into the host retina, significantly inhibited retinal neovascular tufts and remodeled the capillary network after injection (59). In addition, BMSCs increased the retinal vascular density, decreased the number of acellular capillaries and inhibited retinal cell death.

The therapeutic effect of MSCs in congenital cornea diseases is believed to be attributed to supplementation or replacement

of corneal cells. In lumican null cornea model by Liu et al., the injected UC-MSCs acquired the characteristics of keratocytes in which lumican and keratocan were laid down in the stroma cornea (55). The treated animal regained normal corneal thickness and transparency due to reorganization of the collagen fibrils in the cornea. Likewise, MSC transplanted into MPS VII mice cornea also acquired the characteristics of keratocytes. The transplanted cells supplied functional β-glucuronidase to degrade accumulated glycosaminoglycans thereby assisting in lysosome recycling (60). On the other hand, MSCs also secrete paracrine factors that exert anti-inflammation and anti-fibrosis functions, thus suppressing inflammatory neovascularization (61, 62). Through these mechanisms, MSCs can mitigate the inflammation, fibrosis and neovascularisation of the cornea.

MSCs FOR THE TREATMENT OF NEONATAL HEART DISEASES

Research has been conducted to investigate the application of MSCs in 28-day old mice/rats for the treatment of heart diseases. In an *in vitro* experiment, it was found that neonatal thymus-derived MSCs (ntMSCs) secreted higher level of sonic hedgehog (Shh) in comparison to neonatal bone marrow-derived MSCs (nbMSCs) (63). Shh is involved in cell growth, cell specialization and morphogenesis of the corpus during embryonic development. Animal studies have revealed that ntMSC transplantation improved the left ventricular function, increased revascularization, decreased scar size and decreased cardiomyocyte death, 4 weeks after infarction. The protective mechanism in this study could be attributed to heterotopic cell fusion. This mechanism occurs when two cells from different lineages merge into one cell, transmitting information and mediators in the process (64). Fusion has been demonstrated between BMSCs with cardiomyocytes, Purkinje neurons and hepatocytes (65). These results warrant further consideration as therapy for heart diseases resulting in early-onset heart failure, such as the cardiomyopathies.

Kang et al. compared the pro-angiogenic, anti-apoptotic and inflammation-modulatory potential of MSCs derived from patients of cyanotic congenital heart disease (C-CHD) and acyanotic congenital heart disease (A-CHD) (66). The purpose of the study is to locate the best source of MSCs for engineered heart tissue treatment (EHT). *In vitro* results showed that MSCs from C-CHD patients expressed higher levels of VEGF-A and VEGFR2, and secreted more pro-angiogenic and anti-inflammatory cytokines under hypoxic condition in comparison to the cells from A-CHD patients. Interestingly, 4 weeks after right ventricular outflow tract reconstruction, cytokine-immobilized patches seeded with C-CHD MSCs exhibited preserved morphology, prolonged cell survival and enhanced angiogenesis compared to A-CHD MSCs. Considering the "naturally hypoxic preconditioning," MSCs from C-CHD donors might be more adaptable to the hypoxic environment upon transplantation.

MSCs FOR THE TREATMENT OF NEONATAL SEPSIS

In sepsis, the host immune system responsible for the clearing of infection may be dysregulated and becomes no longer protective to the host when it is too exuberant. Such an injurious hyperinflammatory response frequently involves excessive release of cytokines and over-activation of the complement system. Unnecessary stimulation of the coagulation system and pro-thrombogenesis is another characteristic of sepsis, which eventually leads to poorer tissue perfusion, cell death and organ dysfunction (67).

A variety of animal sepsis models have been established depending on the use of different bacterial pathogens such as *P. aeruginosa* and *E.coli*, induction with a toxic agent such as lipopolysaccharide (LPS) as well as disruption to the tissue barrier integrity such as cecal ligation and puncture (CLP) (67–70). Using these animal models, the effects of a variety of MSC variables have been tested, including dosage, timing, and route of MSC administration. Reports have shown that MSC dosage as low as 2.5×10^5 cells was effective in reducing the mortality rate of the septic animals though the effect was better when increasing the cell number to 10^6 cells per animal. Furthermore, the treatment efficacy may be affected by the timing of MSC administration as some researchers failed to identify any positive effects of MSC when administered 6 h post-CLP induction while other identified positive correlation when used at 24 h pre-CLP induction and up to 24 h post-induction. Similar contradictory findings were seen in the route of administration used whereby intraperitoneal injections of MSCs were able to decrease demise of LPS-induced septic mice in one study while the same method resulted in slightly more deaths among CLP-induced septic rats in another investigation (68, 70).

Notably, most of the studies reported that the higher survival rate of septic animals post-MSC treatment is attributable to improved organ function presumably from the MSC anti-apoptotic and anti-oxidant properties as well as reduction of the inflammation-associated tissue injury (68, 71). This is because the administration of MSCs is capable in limiting immune cell infiltration to target organs such as the liver, intestine, lung, and kidney. MSC administration also balances the enhanced expression of pro-inflammatory cytokines seen during the sepsis with higher production of anti-inflammatory cytokines (72).

In addition, MSC may reduce the bacterial burden causing sepsis and increase the survival rate of septic animals. In the study by Zhu et al., treatment with UC-MSCs enhanced the clearance of *E. coli* in 3-day old septic rats with a decreased influx of neutrophils coupled with the increased phagocytic activity of macrophages (73). The antimicrobial activity of MSCs is also due in part to its ability to synthesize anti-microbial peptides. Krasnodembskaya et al. discovered the secretion of LL-37 anti-microbial peptide by MSCs after exposure to *E. coli*, *P. aeruginosa*, and *S. aureus* (74). Likewise, Lee et al. reported the increased clearance of *E. coli* through the effects of KGF secreted by MSCs (75). A more recent study demonstrated the potential of pre-treating MSCs with polyinosinic:polycytidylic acid (an agonist for Toll-like receptor 3) to further improve its anti-microbial activity (76).

LIST OF REGISTERED CLINICAL TRIALS

Apart from the various completed clinical studies discussed earlier, there are various clinical trials currently registered in the ClinicalTrials.gov database that have yet to publish results (**Table 3**). These clinical trials use MSCs to treat BPD, perinatal arterial ischemic stroke (PAIS), infantile spinal muscular atrophy (ISMA), hypoplastic left heart syndrome (HLHS), HIE, and IVH. The treatment of neonatal diseases with MSCs is still at the early stage whereby the majority of these trials are either phase I, II or I/II. Of note, MSC-derived EVs, and paracrine factors are also being evaluated clinically for the treatment of BPD (NCT03857841) and HIE (NCT02854579).

FUTURE PERSPECTIVES

Large-Scale Production of MSCs

A sustainable strategy of MSC expansion is essential to fulfilling the large cell number needed for clinical applications. To achieve a scalable MSC expansion, multi-layered flask, spinner flask, and bioreactor were introduced and gained more attention as a potential for mass production. The multi-layered flask is a static culture system while the spinner flasks and bioreactors are dynamic expansion system. Each of the aforementioned systems has its unique features, whereby the selection should base on preferences or requirements in different situations.

Multi-layered flask offers a simple and straight forward up-scale process. However, due to its larger size compared to conventional flasks, cell monitoring throughout the culture period is almost impossible. Also, the uniform distribution of cells will be relatively harder to achieve and possibly will lead to culture heterogeneity and suboptimal yield of cells (77).

Three-dimensional culture in bioreactor simulates the environment of cells *in vivo*, therefore providing an optimal condition that possibly enhances cellular activities that are not observed in standard monolayer culture (78). Unlike traditional MSC culture protocol, microcarriers are usually added into the culture to provide sufficient growth areas for cells (79). Compared to the multi-layered flask, bioreactor offers better monitoring of cells throughout the culture period and precise control of the culture environment can be done with the aid of computerized sensors in the bioreactor. For more information about the large-scale expansion of MSCs, the readers may refer to the systematic review by Hassan et al. (80).

Cell-Free Approaches

Recently, EVs, including microvesicles and exosomes, have been identified as one of the vital components of stem cell paracrine potency (**Figure 2**). Many researchers suggested that, if purified and concentrated, the therapeutic potential of EVs can be greater compared to the parent cell (81, 82). In addition, it is still unclear in the long-term regarding the safety of MSC transplantation, e.g., the possibility of malignant transformation. Hence, the use of EVs may be a safer approach and a better alternative to MSC therapy.

EVs are nano-sized particles secreted by cells and are delimited by a phospholipid bilayer. However, EVs do not possess a functional nucleus, hence do not replicate (83). EVs carry various proteins, lipids, and nucleic acids, particularly in the form of RNA, which function in intercellular signaling (84).

EV therapy has been demonstrated to exhibit promising results in ameliorating neonatal diseases in animal model studies (28, 35). A clinical trial (NCT03857841) has recently been developed to evaluate EV therapeutic potential. Nonetheless, there are several challenges to overcome in the bench to bedside translation of EV therapy. One of the major challenges is to identify and quantify the content of EVs, especially the nature of their therapeutically active components. Much effort is made to understand the bioactive elements of these EV-cargoes. EVs are reported to contain proteins, lipids, and nucleic acids, yet there is still a lack of understanding regarding the role of some of these components, particularly the non-coding RNA species. Similarly, the function and mechanism of action of the DNA found in EVs remain unclear.

Besides these cargoes, another vital aspect to consider in EV therapy is the potency. Currently, there are several methods to quantify EV doses based on cell equivalent calculation, protein concentration, EV number and particle size using specialized quantitative analytical measurements, such as nanoparticle tracking analysis (85). EVs are known for having short half-life, as such the therapeutic effect could be short-lived (86). Therefore, a repeat or multiple dosage model is preferred compared to single administration for sustained therapeutic effects over time (87). Sjöqvist et al. observed that repeated administration of EVs was more important than the dose in promoting wound healing in a pig model of esophageal wound repair (88). Furthermore, repeat administration of a lower dose reduces the risk of toxicity and immunogenicity (89, 90).

Another major challenge is to isolate highly purified EVs (91). Currently, purity of EVs is normally expressed as the ratio between protein content and the number of EVs. It has been reported that the purity of EVs is directly related to the isolation technique (91). The isolation technique may impact on EV yield, size distribution and potential biological effects. Currently, many techniques, including ultracentrifugation, size-based filtration, immunoaffinity capture, precipitation and microfluidics-based isolation are used to isolate EVs (92). Different isolation methods yielded a different amount of EVs and Antounians et al. recently reported that significant biological variations were also observed when EVs isolated with different methods were used to treat an *in vitro* lung epithelial injury model (93). The dose-dependent effects have been reported by in several studies (94–96). To date, it is uncertain which isolation technique can provide an optimal yield and the best outcome.

Apart from purity considerations, quality control of EV preparation is also vital. It is proposed that the doses for EVs should be specifically quantified, e.g., by the copies of their microRNAs, so as to reduce the inherent biological variation.

CONCLUSION

MSC therapy is a promising treatment for neonatal diseases. The safety and efficacy of MSC therapy have been reported

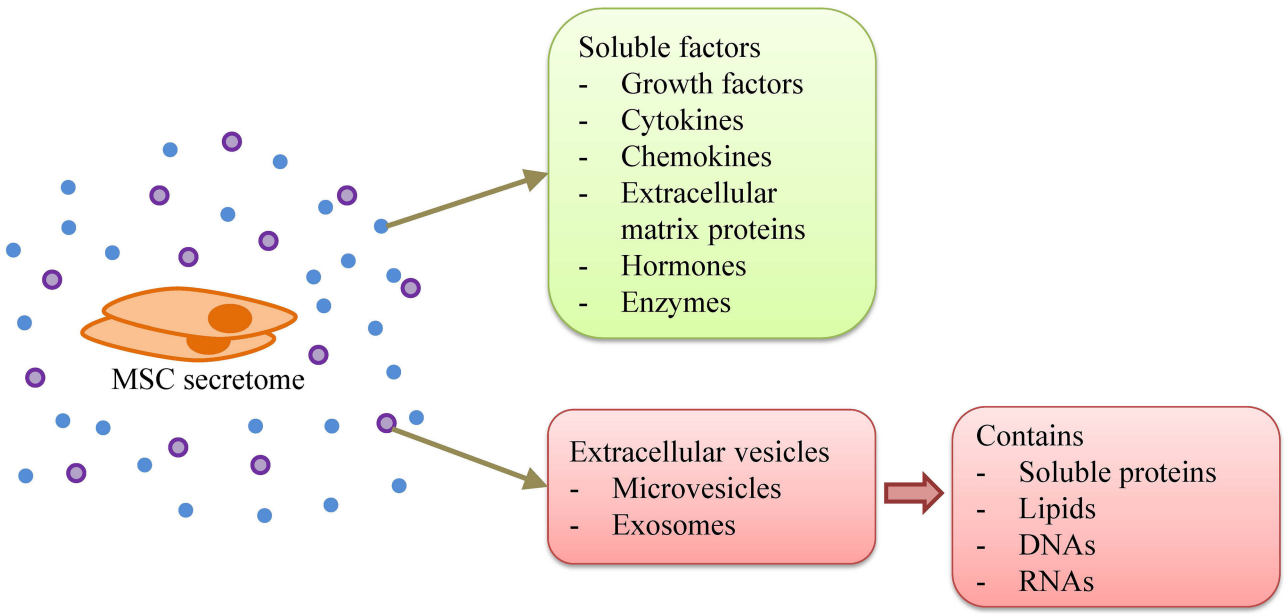

FIGURE 2 | MSC secretome. MSC secretome consists of soluble factors, i.e., growth factors, cytokines, chemokines, extracellular matrix proteins, hormones, and enzymes, as well as extracellular vesicles that contain soluble proteins, lipids, DNAs, and RNAs.

in numerous preclinical and several clinical studies. MSC transplantation can be conducted safely as early as the first month of life. Future studies should be well-designed, i.e., controlled, randomized, involving a larger group of patients, and with a longer follow-up period, to further assure the safety and efficacy of this novel therapy. Besides, more focus is needed to improve on the dosage regimen, to investigate the influence of adjunct therapies on MSC effectiveness and to identify molecular biomarkers to indicate MSC efficacy. In addition, MSC-EV has emerged as a highly potential therapy for neonatal diseases as MSC exerts its therapeutic potential via the paracrine mechanism.

AUTHOR CONTRIBUTIONS

FC and JL revised it critically for important intellectual content. All authors substantially contributed to the conception and design of the article and interpreting the relevant literature, drafted the article, and approved the final draft.

FUNDING

This work was supported by research grants from the Universiti Kebangsaan Malaysia Medical Center (FF-2019-450/1 and FF-2020-038).

REFERENCES

1. Liau LL, Ruszymah BHI, Ng MH, Law JX. Characteristics and clinical applications of Wharton's jelly-derived mesenchymal stromal cells. *Curr Res Transl Med.* (2020) 68:5–16. doi: 10.1016/j.retram.2019.09.001
2. Hofer HR, Tuan RS. Secreted trophic factors of mesenchymal stem cells support neurovascular and musculoskeletal therapies. *Stem Cell Res Ther.* (2016) 7:131. doi: 10.1186/s13287-016-0394-0
3. Looi QH, Eng SP, Liau LL, Tor YS, Bajuri MY, Ng MH, et al. Mesenchymal stem cell therapy for sports injuries-From research to clinical practice. *Sains Malaysiana.* (2020) 49:825–38. doi: 10.17576/jsm-2020-4904-12
4. Lim WL, Liau LL, Ng MH, Shiplu RC, Law JX. Current progress in tendon and ligament tissue engineering. *Tissue Eng Regen Med.* (2019) 16:549–71. doi: 10.1007/s13770-019-00196-w
5. Hafez P, Chowdhury SR, Jose S, Law JX, Ruszymah BHI, Ramzisham ARM, et al. Development of an *in vitro* cardiac ischemic model using primary human cardiomyocytes. *Cardiovasc Eng Technol.* (2018) 9:529–38. doi: 10.1007/s13239-018-0368-8
6. Hafez P, Jose S, Chowdhury SR, Ng MH, Ruszymah BHI, Abdul Rahman Mohd R. Cardiomyogenic differentiation of human sternal bone marrow mesenchymal stem cells using a combination of basic fibroblast growth factor and hydrocortisone. *Cell Biol Int.* (2016) 40:55–64. doi: 10.1002/cbin.10536
7. Lim J, Razi ZRM, Law JX, Nawi AM, Idrus RBH, Chin TG, et al. Mesenchymal stromal cells from the maternal segment of human umbilical cord is ideal for bone regeneration in allogenic setting. *Tissue Eng Regen Med.* (2018) 15:75–87. doi: 10.1007/s13770-017-0086-6
8. Lim J, Razi ZRM, Law J, Nawi AM, Idrus RBH, Ng MH. MSCs can be differentially isolated from maternal, middle and fetal segments of the human umbilical cord. *Cytotherapy.* (2016) 18:1493–502. doi: 10.1016/j.jcyt.2016.08.003
9. Lee M, Jeong SY, Ha J, Kim M, Jin HJ, Kwon SJ, et al. Low immunogenicity of allogeneic human umbilical cord blood-derived mesenchymal stem cells *in vitro* and *in vivo*. *Biochem Biophys Res Commun.* (2014) 446:983–9. doi: 10.1016/j.bbrc.2014.03.051
10. Liau LL, Looi QH, Eng SP, Yazid MD, Sulaiman N, Busra MFM, et al. Mesenchymal stem cells for the treatment of immune-mediated diseases. In: Haider KH, editor. *Stem Cells*. Singapore: World Scientific (2020). p. 178–210.
11. Chang YS, Ahn SY, Yoo HS, Sung SI, Choi SJ, Oh W Il, et al. Mesenchymal stem cells for bronchopulmonary dysplasia: phase 1 dose-escalation clinical trial. *J Pediatr.* (2014) 164:966–72. doi: 10.1016/j.jpeds.2013.12.011

12. Ahn SY, Chang YS, Sung SI, Park WS. Mesenchymal stem cells for severe intraventricular hemorrhage in preterm infants: phase I dose-escalation clinical trial. *Stem Cells Transl Med.* (2018) 7:847–56. doi: 10.1002/sctm.17-0219
13. Akduman H, Dilli D, Ergün E, Çakmakçi E, Çelebi SK, Çitli R, et al. Successful mesenchymal stem cell application in supraventricular tachycardia-related necrotizing enterocolitis: a case report. *Fetal Pediatr Pathol.* (2019) 1–6. doi: 10.1080/15513815.2019.1693672. [Epub ahead of print].
14. Higgins RD, Jobe AH, Koso-Thomas M, Bancalari E, Viscardi RM, Hartert T V, et al. Bronchopulmonary dysplasia: executive summary of a workshop. *J Pediatr.* (2018) 197:300–8. doi: 10.1016/j.jpeds.2018.01.043
15. Kwon HW, Kim HS, An HS, Kwon BS, Kim GB, Shin SH, et al. Long-term outcomes of pulmonary hypertension in preterm infants with bronchopulmonary dysplasia. *Neonatology.* (2016) 110:181–9. doi: 10.1159/000445476
16. Ahn SY, Chang YS, Kim JH, Sung SI, Park WS. Two-year follow-up outcomes of premature infants enrolled in the phase I trial of mesenchymal stem cells transplantation for bronchopulmonary dysplasia. *J Pediatr.* (2017) 185:49–54.e2. doi: 10.1016/j.jpeds.2017.02.061
17. Álvarez-Fuente M, Arruza L, Lopez-Ortego P, Moreno L, Ramírez-Orellana M, Labrandero C, et al. Off-label mesenchymal stromal cell treatment in two infants with severe bronchopulmonary dysplasia: clinical course and biomarkers profile. *Cytotherapy.* (2018) 20:1337–44. doi: 10.1016/j.jcyt.2018.09.003
18. Lin HC, Wang CC, Chou HW, Wu ET, Lu FL, Ko BS, et al. Airway delivery of bone marrow-derived mesenchymal stem cells reverses bronchopulmonary dysplasia superimposed with acute respiratory distress syndrome in an infant. *Cell Med.* (2018) 10:2155179018759434. doi: 10.1177/2155179018759434
19. Powell SB, Silvestri JM. Safety of intratracheal administration of human umbilical cord blood derived mesenchymal stromal cells in extremely low birth weight preterm infants. *J Pediatr.* (2019) 210:209–13.e2. doi: 10.1016/j.jpeds.2019.02.029
20. Guess AJ, Daneault B, Wang R, Bradbury H, La Perle KMD, Fitch J, et al. Safety profile of good manufacturing practice manufactured interferon γ-primed mesenchymal stem/stromal cells for clinical trials. *Stem Cells Transl Med.* (2017) 6:1868–79. doi: 10.1002/sctm.16-0485
21. Ahn SY, Chang YS, Park WS. Stem cells for neonatal brain disorders. *Neonatology.* (2016) 109:377–83. doi: 10.1159/000444905
22. Mitsialis SA, Kourembanas S. Stem cell-based therapies for the newborn lung and brain: possibilities and challenges. *Semin Perinatol.* (2016) 40:138–51. doi: 10.1053/j.semperi.2015.12.002
23. Mueller M, Wolfs TG, Schoeberlein A, Gavilanes AW, Surbek D, Kramer BW. Mesenchymal stem/stromal cells-a key mediator for regeneration after perinatal morbidity? *Mol Cell Pediatr.* (2016) 3:6. doi: 10.1186/s40348-016-0034-x
24. Szpecht D, Szymankiewicz M, Nowak I, Gadzinowski J. Intraventricular hemorrhage in neonates born before 32 weeks of gestation-retrospective analysis of risk factors. *Childs Nerv Syst.* 2016) 32:1399–404. doi: 10.1007/s00381-016-3127-x
25. Gotardo JW, de Freitas Valle Volkmer N, Stangler GP, Dornelles AD, de Athayde Bohrer BB, Carvalho CG. Impact of peri-intraventricular haemorrhage and periventricular leukomalacia in the neurodevelopment of preterms: a systematic review and meta-analysis. *PLoS ONE.* (2019) 14:e0223427. doi: 10.1371/journal.pone.0223427
26. Kim ES, Ahn SY, Im GH, Sung DK, Park YR, Choi SH, et al. Human umbilical cord blood-derived mesenchymal stem cell transplantation attenuates severe brain injury by permanent middle cerebral artery occlusion in newborn rats. *Pediatr Res.* (2012) 72:277–84. doi: 10.1038/pr.2012.71
27. van Velthoven CT, Kavelaars A, van Bel F, Heijnen CJ. Mesenchymal stem cell transplantation changes the gene expression profile of the neonatal ischemic brain. *Brain Behav Immun.* (2011) 25:1342–8. doi: 10.1016/j.bbi.2011.03.021
28. Thomi G, Surbek D, Haesler V, Joerger-Messerli M, Schoeberlein A. Exosomes derived from umbilical cord mesenchymal stem cells reduce microglia-mediated neuroinflammation in perinatal brain injury. *Stem Cell Res Ther.* (2019) 10:105. doi: 10.1186/s13287-019-1207-z
29. Allen KA, Brandon DH. Hypoxic ischemic encephalopathy: pathophysiology and experimental treatments. *Newborn Infant Nurs Rev.* (2011) 11:125–33. doi: 10.1053/j.nainr.2011.07.004
30. Park WS, Sung SI, Ahn SY, Yoo HS, Sung DK, Im GH, et al. Hypothermia augments neuroprotective activity of mesenchymal stem cells for neonatal hypoxic-ischemic encephalopathy. *PLoS ONE.* (2015) 10:e0120893. doi: 10.1371/journal.pone.0120893
31. Bruschettini M, Romantsik O, Moreira A, Ley D, Thébaud B. Stem cell-based interventions for the prevention of morbidity and mortality following hypoxic-ischaemic encephalopathy in newborn infants. *Cochrane Database Syst Rev.* (2018) 2018:CD013202. doi: 10.1002/14651858.CD013202
32. Cánovas-Ahedo M, Alonso-Alconada D. Combined therapy in neonatal hypoxic-ischaemic encephalopathy. *An Pediatría.* (2019) 91:59–9.e6. doi: 10.1016/j.anpede.2019.04.007
33. McDonald CA, Djuliannisaa Z, Petraki M, Paton MCB, Penny TR, Sutherland AE, et al. Intranasal delivery of mesenchymal stromal cells protects against neonatal hypoxic-ischemic brain injury. *Int J Mol Sci.* (2019) 20:2449. doi: 10.3390/ijms20102449
34. Wagenaar N, Nijboer CH, van Bel F. Repair of neonatal brain injury: bringing stem cell-based therapy into clinical practice. *Dev Med Child Neurol.* (2017) 59:997–1003. doi: 10.1111/dmcn.13528
35. Ophelders DRMG, Wolfs TGAM, Jellema RK, Zwanenburg A, Andriessen P, Delhaas T, et al. Mesenchymal stromal cell-derived extracellular vesicles protect the fetal brain after hypoxia-ischemia. *Stem Cells Transl Med.* (2016) 5:754–63. doi: 10.5966/sctm.2015-0197
36. Wang Y, Long W, Cao Y, Li J, You L, Fan Y. Mesenchymal stem cell-derived secretomes for therapeutic potential of premature infant diseases. *Biosci Rep.* (2020) 40:BSR20200241. doi: 10.1042/BSR20200241
37. Chen A, Siow B, Blamire AM, Lako M, Clowry GJ. Transplantation of magnetically labeled mesenchymal stem cells in a model of perinatal brain injury. *Stem Cell Res.* (2010) 5:255–66. doi: 10.1016/j.scr.2010.08.004
38. Zhu LH, Bai X, Zhang N, Wang SY, Li W, Jiang L. Improvement of human umbilical cord mesenchymal stem cell transplantation on glial cell and behavioral function in a neonatal model of periventricular white matter damage. *Brain Res.* (2014) 1563:13–21. doi: 10.1016/j.brainres.2014.03.030
39. Morioka C, Komaki M, Taki A, Honda I, Yokoyama N, Iwasaki K, et al. Neuroprotective effects of human umbilical cord-derived mesenchymal stem cells on periventricular leukomalacia-like brain injury in neonatal rats. *Inflamm Regen.* (2017) 37:1. doi: 10.1186/s41232-016-0032-3
40. Niemarkt HJ, de Meij TG, van Ganzewinkel CJ, de Boer NKH, Andriessen P, Hütten MC, et al. Necrotizing enterocolitis, gut microbiota, and brain development: role of the brain-gut axis. *Neonatology.* (2019) 115:423–31. doi: 10.1159/000497420
41. Lin H, Mao S, Shi L, Tou J, Du L. Clinical characteristic comparison of low birth weight and very low birth weight preterm infants with neonatal necrotizing enterocolitis: a single tertiary center experience from eastern China. *Pediatr Surg Int.* (2018) 34:1201–7. doi: 10.1007/s00383-018-4339-9
42. Lu Q, Cheng S, Zhou M, Yu J. Risk factors for necrotizing enterocolitis in neonates: a retrospective case-control study. *Pediatr Neonatol.* (2017) 58:165–70. doi: 10.1016/j.pedneo.2016.04.002
43. Zozaya C, Shah J, Pierro A, Zani A, Synnes A, Lee S, et al. Neurodevelopmental and growth outcomes of extremely preterm infants with necrotizing enterocolitis or spontaneous intestinal perforation. *J Pediatr Surg.* (2020). doi: 10.1016/j.jpedsurg.2020.05.013. [Epub ahead of print].
44. Eaton S, Zani A, Pierro A, De Coppi P. Stem cells as a potential therapy for necrotizing enterocolitis. *Expert Opin Biol Ther.* (2013) 13:1683–9. doi: 10.1517/14712598.2013.849690
45. Shi X, Chen Q, Wang F. Mesenchymal stem cells for the treatment of ulcerative colitis: a systematic review and meta-analysis of experimental and clinical studies. *Stem Cell Res Ther.* (2019) 10:266. doi: 10.1186/s13287-019-1336-4
46. Lightner AL, Wang Z, Zubair AC, Dozois EJ. A systematic review and meta-analysis of mesenchymal stem cell injections for the treatment of perianal Crohn's disease: progress made and future directions. *Dis Colon Rectum.* (2018) 61:629–40. doi: 10.1097/DCR.0000000000001093
47. Tayman C, Uckan D, Kilic E, Ulus AT, Tonbul A, Hirfanoglu IM, et al. Mesenchymal stem cell therapy in necrotizing enterocolitis: a rat study. *Pediatr Res.* (2011) 70:489–94. doi: 10.1203/PDR.0b013e31822d7ef2
48. McCulloh CJ, Olson JK, Zhou Y, Wang Y, Besner GE. Stem cells and necrotizing enterocolitis: a direct comparison of the

efficacy of multiple types of stem cells. *J Pediatr Surg.* (2017) 52:999–1005. doi: 10.1016/j.jpedsurg.2017.03.028
49. Overcash RT, DeUgarte DA, Stephenson ML, Gutkin RM, Norton ME, Parmar S, et al. Factors associated with gastroschisis outcomes. *Obstet Gynecol.* (2014) 124:551–7. doi: 10.1097/AOG.0000000000000425
50. Feng C, Graham CD, Connors JP, Brazzo J, Pan AHS, Hamilton JR, et al. Transamniotic stem cell therapy (TRASCET) mitigates bowel damage in a model of gastroschisis. *J Pediatr Surg.* (2016) 51:56–61. doi: 10.1016/j.jpedsurg.2015.10.011
51. Feng C, Graham CD, Shieh HF, Brazzo JA, Connors JP, Rohrer L, et al. Transamniotic stem cell therapy (TRASCET) in a leporine model of gastroschisis. *J Pediatr Surg.* (2017) 52:30–4. doi: 10.1016/j.jpedsurg.2016.10.016
52. Davies PS, Powell AE, Swain JR, Wong MH. Inflammation and proliferation act together to mediate intestinal cell fusion. *PLoS ONE.* (2009) 4:e6530. doi: 10.1371/journal.pone.0006530
53. de Jong JH, Rodermond HM, Zimberlin CD, Lascano V, De Sousa E Melo F, Richel DJ, et al. Fusion of intestinal epithelial cells with bone marrow derived cells is dispensable for tissue homeostasis. *Sci Rep.* (2012) 2:271. doi: 10.1038/srep00271
54. Zani A, Cananzi M, Fascetti-Leon F, Lauriti G, Smith VV, Bollini S, et al. Amniotic fluid stem cells improve survival and enhance repair of damaged intestine in necrotising enterocolitis via a COX-2 dependent mechanism. *Gut.* (2014) 63:300–9. doi: 10.1136/gutjnl-2012-303735
55. Liu H, Zhang J, Liu CY, Wang IJ, Sieber M, Chang J, et al. Cell therapy of congenital corneal diseases with umbilical mesenchymal stem cells: Lumican null mice. *PLoS ONE.* (2010) 5:e10707. doi: 10.1371/journal.pone.0010707
56. Coulson-Thomas VJ, Caterson B, Kao WWY. Transplantation of human umbilical mesenchymal stem cells cures the corneal defects of mucopolysaccharidosis vii mice. *Stem Cells.* (2013) 31:2116–26. doi: 10.1002/stem.1481
57. Sun M, Chen S, Adams SM, Florer JB, Liu H, Kao WWY, et al. Collagen V is a dominant regulator of collagen fibrillogenesis: dysfunctional regulation of structure and function in a corneal-stroma-specific Col5a1-null mouse model. *J Cell Sci.* (2011) 124:4096–105. doi: 10.1242/jcs.091363
58. Call M, Elzarka M, Kunesh M, Hura N, Birk DE, Kao WW. Therapeutic efficacy of mesenchymal stem cells for the treatment of congenital and acquired corneal opacity. *Mol Vis.* (2019) 25:415–26.
59. Xu W, Cheng W, Cui X, Xu G. Therapeutic effect against retinal neovascularization in a mouse model of oxygen-induced retinopathy: bone marrow-derived mesenchymal stem cells versus conbercept. *BMC Ophthalmol.* (2020) 20:7. doi: 10.1186/s12886-019-1292-x
60. Zhang L, Coulson-Thomas VJ, Ferreira TG, Kao WWY. Mesenchymal stem cells for treating ocular surface diseases. *BMC Ophthalmol.* (2015) 15:54–65. doi: 10.1186/s12886-015-0138-4
61. Navas A, Magaña-Guerrero FS, Domínguez-López A, Chávez-García C, Partido G, Graue-Hernández EO, et al. Anti-inflammatory and anti-fibrotic effects of human amniotic membrane mesenchymal stem cells and their potential in corneal repair. *Stem Cells Transl Med.* (2018) 7:906–17. doi: 10.1002/sctm.18-0042
62. Song HB, Park SY, Ko JH, Park JW, Yoon CH, Kim DH, et al. Mesenchymal stromal cells inhibit inflammatory lymphangiogenesis in the cornea by suppressing macrophage in a TSG-6-dependent manner. *Mol Ther.* (2018) 26:162–72. doi: 10.1016/j.ymthe.2017.09.026
63. Wang S, Huang S, Gong L, Yuan Z, Wong J, Lee J, et al. Human neonatal thymus mesenchymal stem cells promote neovascularization and cardiac regeneration. *Stem Cells Int.* (2018) 2018:8503468. doi: 10.1155/2018/8503468
64. Doster DL, Jensen AR, Khaneki S, Markel TA. Mesenchymal stromal cell therapy for the treatment of intestinal ischemia: defining the optimal cell isolate for maximum therapeutic benefit. *Cytotherapy.* (2016) 18:1457–70. doi: 10.1016/j.jcyt.2016.08.001
65. Alvarez-Dolado M, Pardal R, Garcia-Verdugo JM, Fike JR, Lee HO, Pfeffer K, et al. Fusion of bone-marrow-derived cells with Purkinje neurons, cardiomyocytes and hepatocytes. *Nature.* (2003) 425:968–73. doi: 10.1038/nature02069
66. Kang K, Chuai JB, Xie B dong, Li J zhong, Qu H, Wu H, et al. Mesenchymal stromal cells from patients with cyanotic congenital heart disease are optimal candidate for cardiac tissue engineering. *Biomaterials.* (2020) 230:119574. doi: 10.1016/j.biomaterials.2019.119574
67. Elman JS, Li M, Wang F, Gimble JM, Parekkadan B. A comparison of adipose and bone marrow-derived mesenchymal stromal cell secreted factors in the treatment of systemic inflammation. *J Inflamm.* (2014) 11:1. doi: 10.1186/1476-9255-11-1
68. Lombardo E, van der Poll T, DelaRosa O, Dalemans W. Mesenchymal stem cells as a therapeutic tool to treat sepsis. *World J Stem Cells.* (2015) 7:368–79. doi: 10.4252/wjsc.v7.i2.368
69. Zhao X, Liu D, Gong W, Zhao G, Liu L, Yang L, et al. The toll-like receptor 3 ligand, poly(I:C), improves immunosuppressive function and therapeutic effect of mesenchymal stem cells on sepsis via inhibiting MiR-143. *Stem Cells.* (2014) 32:521–33. doi: 10.1002/stem.1543
70. Korneev K V. [Mouse models of sepsis and septic shock]. *Mol Biol.* (2019) 53:799–814. doi: 10.1134/S0026893319050108
71. Horák J, Nalos L, Martínková V, Beneš J, Štengl M, Matějovič M. Mesenchymal stem cells in sepsis and associated organ dysfunction: a promising future or blind alley? *Stem Cells Int.* (2017) 2017:7304121. doi: 10.1155/2017/7304121
72. Spees JL, Lee RH, Gregory CA. Mechanisms of mesenchymal stem/stromal cell function. *Stem Cell Res Ther.* (2016) 7:125. doi: 10.1186/s13287-016-0363-7
73. Zhu Y, Xu L, Collins JJP, Vadivel A, Cyr-Depauw C, Zhong S, et al. Human umbilical cord mesenchymal stromal cells improve survival and bacterial clearance in neonatal sepsis in rats. *Stem Cells Dev.* (2017) 26:1054–64. doi: 10.1089/scd.2016.0329
74. Krasnodembskaya A, Song Y, Fang X, Gupta N, Serikov V, Lee JW, et al. Antibacterial effect of human mesenchymal stem cells is mediated in part from secretion of the antimicrobial peptide LL-37. *Stem Cells.* (2010) 28:2229–38. doi: 10.1002/stem.544
75. Lee JW, Krasnodembskaya A, McKenna DH, Song Y, Abbott J, Matthay MA. Therapeutic effects of human mesenchymal stem cells in ex vivo human lungs injured with live bacteria. *Am J Respir Crit Care Med.* (2013) 187:751–60. doi: 10.1164/rccm.201206-0990OC
76. Park J, Kim S, Lim H, Liu A, Hu S, Lee J, et al. Therapeutic effects of human mesenchymal stem cell microvesicles in an ex vivo perfused human lung injured with severe E. *coli pneumonia. Thorax.* (2019) 74:43–50. doi: 10.1136/thoraxjnl-2018-211576
77. Hanley PJ, Mei Z, da Graca Cabreira-Hansen M, Klis M, Li W, Zhao Y, et al. Manufacturing mesenchymal stromal cells for phase I clinical trials. *Cytotherapy.* (2013) 15:416–22. doi: 10.1016/j.jcyt.2012.09.007
78. Levenberg S, Huang NF, Lavik E, Rogers AB, Itskovitz-Eldor J, Langer R. Differentiation of human embryonic stem cells on three-dimensional polymer scaffolds. *Proc Natl Acad Sci USA.* (2003) 100:12741–6. doi: 10.1073/pnas.1735463100
79. Koh B, Sulaiman N, Fauzi MB, Law JX, Ng MH, Idrus RBH, et al. Three dimensional microcarrier system in mesenchymal stem cell culture: a systematic review. *Cell Biosci.* (2020) 10:75. doi: 10.1186/s13578-020-00438-8
80. Hassan MNF Bin, Yazid MD, Yunus MHM, Chowdhury SR, Lokanathan Y, Idrus RBH, et al. Large-scale expansion of human mesenchymal stem cells. *Stem Cells Int.* (2020) 2020:9529465. doi: 10.1155/2020/9529465
81. Adamiak M, Cheng G, Bobis-Wozowicz S, Zhao L, Kedracka-Krok S, Samanta A, et al. Induced pluripotent stem cell (iPSC)-derived extracellular vesicles are safer and more effective for cardiac repair than iPSCs. *Circ Res.* (2018) 122:296–309. doi: 10.1161/CIRCRESAHA.117.311769
82. Porzionato A, Zaramella P, Dedja A, Guidolin D, Van Wemmel K, Macchi V, et al. Intratracheal administration of clinical-grade mesenchymal stem cell-derived extracellular vesicles reduces lung injury in a rat model of bronchopulmonary dysplasia. *Am J Physiol Lung Cell Mol Physiol.* (2019) 316:L6–19. doi: 10.1152/ajplung.00109.2018
83. Théry C, Witwer KW, Aikawa E, Alcaraz MJ, Anderson JD, Andriantsitohaina R, et al. Minimal information for studies of extracellular vesicles 2018 (MISEV2018): a position statement of the International Society for Extracellular Vesicles and update of the MISEV2014 guidelines. *J Extracell vesicles.* (2018) 7:1535750. doi: 10.1080/20013078.2018.1461450
84. Lokanathan Y, Law JX, Yazid MD, Chowdhury SR, Busra MFM, Sulaiman N, et al. Mesenchymal stem cells and their role in hypoxia-induced injury. In: Haider KH, editor. *Stem Cells: From Myth to Reality and Evolving. Boston:* De Gruyter (2019). p. 166–86.

85. Willis GR, Kourembanas S, Mitsialis SA. Toward exosome-based therapeutics: isolation, heterogeneity, and fit-for-purpose potency. *Front Cardiovasc Med.* (2017) 4:63. doi: 10.3389/fcvm.2017.00063
86. Bachurski D, Schuldner M, Nguyen P-H, Malz A, Reiners KS, Grenzi PC, et al. Extracellular vesicle measurements with nanoparticle tracking analysis - an accuracy and repeatability comparison between nanoSight NS300 and ZetaView. *J Extracell vesicles.* (2019) 8:1596016. doi: 10.1080/20013078.2019.1596016
87. Aliotta JM, Pereira M, Wen S, Dooner MS, Del Tatto M, Papa E, et al. Exosomes induce and reverse monocrotaline-induced pulmonary hypertension in mice. *Cardiovasc Res.* (2016) 110:319–30. doi: 10.1093/cvr/cvw054
88. Sjöqvist S, Ishikawa T, Shimura D, Kasai Y, Imafuku A, Bou-Ghannam S, et al. Exosomes derived from clinical-grade oral mucosal epithelial cell sheets promote wound healing. *J Extracell vesicles.* (2019) 8:1565264. doi: 10.1080/20013078.2019.1565264
89. Zhu X, Badawi M, Pomeroy S, Sutaria DS, Xie Z, Baek A, et al. Comprehensive toxicity and immunogenicity studies reveal minimal effects in mice following sustained dosing of extracellular vesicles derived from HEK293T cells. *J Extracell vesicles.* (2017) 6:1324730. doi: 10.1080/20013078.2017.1324730
90. Mendt M, Kamerkar S, Sugimoto H, McAndrews KM, Wu CC, Gagea M, et al. Generation and testing of clinical-grade exosomes for pancreatic cancer. *JCI insight.* (2018) 3:e99263. doi: 10.1172/jci.insight.99263
91. Duijvesz D, Luider T, Bangma CH, Jenster G. Exosomes as biomarker treasure chests for prostate cancer. *Eur Urol.* (2011) 59:823–31. doi: 10.1016/j.eururo.2010.12.031
92. Li P, Kaslan M, Lee SH, Yao J, Gao Z. Progress in exosome isolation techniques. *Theranostics.* (2017) 7:789–804. doi: 10.7150/thno.18133
93. Antounians L, Tzanetakis A, Pellerito O, Catania VD, Sulistyo A, Montalva L, et al. The regenerative potential of amniotic fluid stem cell extracellular vesicles: lessons learned by comparing different isolation techniques. *Sci Rep.* (2019) 9:1837. doi: 10.1038/s41598-018-38320-w
94. Tassew NG, Charish J, Shabanzadeh AP, Luga V, Harada H, Farhani N, et al. Exosomes mediate mobilization of autocrine Wnt10b to promote axonal regeneration in the injured CNS. *Cell Rep.* (2017) 20:99–111. doi: 10.1016/j.celrep.2017.06.009
95. Tabak S, Schreiber-Avissar S, Beit-Yannai E. Extracellular vesicles have variable dose-dependent effects on cultured draining cells in the eye. *J Cell Mol Med.* (2018) 22:1992–2000. doi: 10.1111/jcmm.13505
96. Willis GR, Fernandez-Gonzalez A, Anastas J, Vitali SH, Liu X, Ericsson M, et al. Mesenchymal stromal cell exosomes ameliorate experimental bronchopulmonary dysplasia and restore lung function through macrophage immunomodulation. *Am J Respir Crit Care Med.* (2018) 197:104–16. doi: 10.1164/rccm.201705-0925OC

Conflict of Interest: The authors declare that the research was conducted in the absence of any commercial or financial relationships that could be construed as a potential conflict of interest.

frontiers in Pediatrics

SYSTEMATIC REVIEW
published: 09 December 2020
doi: 10.3389/fped.2020.578984

Stem Cells as Therapy for Necrotizing Enterocolitis: A Systematic Review and Meta-Analysis of Preclinical Studies

Eduardo Villamor-Martinez[1], *Tamara Hundscheid*[1], *Boris W. Kramer*[1], *Carlijn R Hooijmans*[2] *and Eduardo Villamor*[1]*

[1] Department of Pediatrics, Maastricht University Medical Center (MUMC+), School for Oncology and Developmental Biology (GROW), Maastricht, Netherlands, [2] Department for Health Evidence Unit SYRCLE, Radboud University Medical Center, Nijmegen, Netherlands

Background: Necrotizing enterocolitis (NEC) is the most common life-threatening gastrointestinal condition among very and extremely preterm infants. Stem cell therapy has shown some promising protective effects in animal models of intestinal injury, including NEC, but no systematic review has yet evaluated the preclinical evidence of stem cell therapy for NEC prevention or treatment.

Methods: PubMed and EMBASE databases were searched for studies using an animal model of NEC with stem cells or their products. The SYRCLE tool was used for the assessment of risk of bias. A random-effects model was used to pool odds ratios (ORs) and 95% confidence interval (CI).

Results: We screened 953 studies, of which nine (eight rat and one mouse models) met the inclusion criteria. All animal models induced NEC by a combination of hypothermia, hypoxia, and formula feeding. Risk of bias was evaluated as unclear on most items for all studies included. Meta-analysis found that both mesenchymal and neural stem cells and stem cell-derived exosomes reduced the incidence of all NEC (OR 0.22, 95% CI 0.16–0.32, $k = 16$), grade 2 NEC (OR 0.41, 95% CI 0.24–0.70, $k = 16$), and grade 3–4 NEC (OR 0.28, 95% CI 0.19–0.42, $k = 16$). k represents the number of independent effect sizes included in each meta-analysis. The effect of the exosomes was similar to that of the stem cells. Stem cells and exosomes also improved 4-day survival (OR 2.89 95% CI 2.07–4.04, $k = 9$) and 7-day survival (OR 3.96 95% CI 2.39–6.55, $k = 5$) after experimental NEC. Meta-analysis also found that stem cells reduced other indicators of intestinal injury.

Conclusion: The data from this meta-analysis suggest that both stem cells and stem cell-derived exosomes prevented NEC in rodent experimental models. However, unclear risk of bias and incomplete reporting underline that poor reporting standards are common and hamper the reliable interpretation of preclinical evidence for stem cell therapy for NEC.

Keywords: stem cells, necrotizing enterocolitis (NEC), preclinical (*in-vivo*) studies, meta-analysis, risk of bias assessment

OPEN ACCESS

Edited by:
Geok Chin Tan, National University of Malaysia, Malaysia

Reviewed by:
Chin Seng Gan, University of Malaya, Malaysia
MaryAnn Volpe, Tufts University School of Medicine, United States

***Correspondence:**
Eduardo Villamor
e.villamor@mumc.nl

Specialty section:
This article was submitted to Neonatology, a section of the journal Frontiers in Pediatrics

Received: *01 July 2020*
Accepted: *13 October 2020*
Published: *09 December 2020*

Citation:
Villamor-Martinez E, Hundscheid T, Kramer BW, Hooijmans CR and Villamor E (2020) Stem Cells as Therapy for Necrotizing Enterocolitis: A Systematic Review and Meta-Analysis of Preclinical Studies. Front. Pediatr. 8:578984. doi: 10.3389/fped.2020.578984

INTRODUCTION

Necrotizing enterocolitis (NEC) is the most common life-threatening gastrointestinal condition among very and extremely preterm infants (1–4). Severe NEC is characterized by full-thickness destruction of the intestine leading to intestinal perforation, peritonitis, bacterial invasion of blood stream, and generalized infection (1–4). NEC has a multifactorial etiology that is largely related to prematurity and the consequent immaturity of the gastrointestinal tract (1–10). However, besides low gestational age (GA), several risk factors such as formula feeds, gut dysbiosis, infection, or intestinal hypoperfusion have been implicated in the etiopathogenesis of NEC (1–10). Furthermore, a clear definition of NEC remains elusive because NEC likely represents different conditions with intestinal injury or necrosis as final outcome (4, 11).

A number of animal models have been developed to investigate the pathophysiology of NEC and to test different preventive and therapeutic strategies (12–18). The most widely used experimental animals are rats, mice, and piglets (12–18). The experimental models try to reproduce the pathogenesis of NEC using one or a combination of potential contributory factors such as intestinal immaturity, formula feeding, bacteria and/or their byproduct, and hypoxic–ischemic stress (12–18). However, after more than five decades of preclinical and clinical research on NEC, the promise of a "magic bullet" for the prevention and/or treatment of NEC has yet to become a reality (11).

Stem cell therapy is increasingly proposed as a novel therapeutic approach for a number of complications of prematurity such as bronchopulmonary dysplasia (19–22), brain injury (22, 23), or retinopathy of prematurity (24) with encouraging preclinical results auspicious for clinical translation (19, 21, 22). A growing number of preclinical studies have investigated the potential therapeutic role of stem cells in experimental NEC (13–21). However, to use stem cell therapy, we need to answer five questions: which cells to give, at what time, via which route, in which dose, and to which babies (25).

Systematic reviews and meta-analyses are common practice in human clinical research, particularly for randomized controlled trials. Although most animal experiments are performed to enrich our clinical understanding of human diseases, systematic reviews of preclinical studies are still scarce (26, 27). Meta-analyses of preclinical studies can be used to inform clinical trial design, to understand the possible discrepancies between findings from preclinical and clinical studies and to improve the quality and translational utility of animal experimentation (28–30). To date, there has been no systematic review and/or meta-analysis on the therapeutic potential of stem cells in experimental NEC. We aimed to provide a comprehensive overview of all studies using stem cells in animal models of NEC and to quantify the effects of stem cells in mortality and development of intestinal injury.

METHODS

Protocol

A protocol was registered on PROSPERO (CRD42018110084) before starting the review (31). We used the Preferred Reporting Items for Systematic Reviews and Meta-Analyses (PRISMA) checklist for the manuscript (32).

Sources and Search Strategy

We searched PubMed and EMBASE databases for original, preclinical studies concerning the effects of stem cells or stem cell products on NEC published until June 2019. The search strategy involved the following four search components: stem cells (and all synonyms) AND (necrotizing enterocolitis OR [neonate AND (intestinal injury OR necrosis)] AND animals (33, 34) (for our complete search strategy, see S 1). No language or date restrictions were applied. Electronic search alerts were set up using Google Scholar to be able to include any studies published after the last search.

Inclusion Criteria and Study Selection

Studies were included in this systematic review when they met all of the following criteria, defined *a priori* in our published protocol: (1) original *in vivo* animal studies using a neonatal experimental NEC model; (2) intervention was randomized, quasi-randomized, or non-randomized; (3) tested as intervention stem cells or stem cell-derived products; and (4) reported on any of the following outcome measures: survival, NEC incidence and/or severity, intestinal injury, weight gain, and clinical sickness scores. Non-interventional studies, studies without controls, and non-neonatal models of intestinal injury were excluded.

The primary outcome was NEC incidence. Secondary outcomes were survival and severity of NEC. Therefore, studies that reported on survival, NEC incidence (determined histologically), and/or severity of NEC (determined histologically and with predetermined scales) were included.

Two independent reviewers (TH and EV-M) screened all studies for inclusion. The first screening was based on title and abstract using Rayyan RCI software (35). In case of doubt, the full text of the article was evaluated. The full text of all preselected publications was subsequently assessed by two independent reviewers (TH and EV-M). Studies were included when they met all the inclusion criteria. Disagreements about inclusion were resolved through discussion and consensus among three reviewers (TH, EV-M, and CH).

One reviewer (TH) extracted the data using a predetermined data extraction sheet. A second reviewer (EV-M) checked data for accuracy. Data were extracted for study characteristics (authors, year of publication, and study location), study design (sample size for intervention, control, and sham groups), intervention characteristics (timing, dose, and mode of stem cell administration), and outcome measures (primary and secondary outcomes as described above). Dichotomous and continuous data provided in numbers were extracted directly. Data on survival and NEC incidence/severity were converted

to odds ratios (ORs), and data on intestinal injury (intestinal permeability and motility), weight, and sickness/severity scores were converted to standardized differences in means. If only graphs were available, Web Plot Digitizer was used to extract numerical values (36).

Risk of Bias

We used the SYRCLE tool (37) to assess the risk of bias in the included studies. Two reviewers (TH and EV-M) independently evaluated the studies, and discrepancies in scoring were resolved through discussion. A "yes" score indicates low risk of bias; a "no" score indicates high risk of bias; and a "?" score indicates unknown risk of bias.

In order to avoid the problem of too many items being evaluated as "unclear risk of bias" due to lack of reporting of experimental details on animals, methods, and materials (38), we added three items on reporting and evaluated whether studies reported (1) any measure of randomization, (2) any measure of blinding, and (3) a sample size calculation. For these three items, a "yes" score indicates "reported," and a "no" score indicates "unreported."

Meta-Analysis, Subgroup Analyses, and Publication Bias

Studies were combined and analyzed using Comprehensive Meta-Analysis V3.0 software (Biostat Inc., Englewood, NJ, USA). The unit of analysis for the meta-analysis (represented as k) was the individual experiments (i.e., one reference could contain multiple independent experiments). All outcome measures that were reported in more than one study were included in meta-analyses. For dichotomous outcomes, the OR with 95% confidence interval (CI) was calculated from the data provided in the studies. For continuous outcomes, we extracted the mean, SD, and n to calculate the standardized mean difference (SMD). If studies used a single control group and multiple experimental groups, we corrected for this by dividing the sample size of the control group by the number of experimental groups. When one of the cells contained a zero value or the risk in either the control or experimental group was 100%, we added 0.5 to each cell to calculate the OR.

Due to anticipated heterogeneity, summary statistics were calculated with a random-effects model. This model accounts for variability between studies as well as within studies. Statistical heterogeneity was assessed by Cochran's Q statistic and by the I^2 statistic, which is derived from Q and describes the proportion of total variation that is due to heterogeneity beyond chance (39).

Subgroup analyses were predefined in the protocol and only carried out if there were at least three independent comparisons per subgroup ($k \geq 3$). The criteria we planned on using for subgroup analyses included cell-type, animal/species, stem cells vs. cell-derived products, control group (placebo/sham vs. no intervention), and definition of neonatal (term vs. preterm model). Subgroup analyses were conducted according to the mixed-effects model (40). In this model, a random-effects model is used to combine studies within each subgroup, and a fixed-effects model is used to combine subgroups and yield the overall effect. We expected the variance to be comparable within the subgroups; therefore, we assumed a common among-study variance across subgroups. For subgroup analyses, we adjusted our significance level according to the conservative Bonferroni method to account for multiple analyses (p/number of comparisons).

Publication bias analysis was carried out for the outcomes with $k > 10$. We used visual inspection of the funnel plot, Duval and Tweedie's trim and fill, and Egger's regression test to assess publication bias (40).

RESULTS

Study Characteristics and Experimental Models

After duplicates were removed, 953 references needed to be screened for eligibility. **Figure 1** shows the PRISMA diagram of the comprehensive search and the reasons for excluding studies. Finally, nine studies could be included in this systematic review (13–21), which encompassed 23 comparisons in total. We did not find additional studies after the search through electronic alerts (until December 2019). Six of the included studies (41–46) were carried out in the same research facility in Columbus, Ohio (USA). One study (47) was carried out in Turkey, and two studies were carried out in the United Kingdom (48, 49). The characteristics of included studies are summarized in **Table 1**. Eight studies used rats, and the study of Wei et al. used mice. All included studies used the method of Barlow et al. (50) for inducing experimental NEC through formula feeding, hypoxia, and hypothermia.

Intervention: Stem Cells and Stem Cell-Derived Products

As shown in **Table 1**, seven studies examined stem cells as the intervention (42, 44–49), one study examined both stem cells and exosomes (43), and one study examined only exosomes as intervention (41). Regarding the type of stem cells, one study (one experiment) (42) examined amniotic fluid (AF) mesenchymal stem cells (MSCs), and two studies (three experiments) (48, 49) examined AF stem cells (AFSCs). AFSCs stained positively for a number of surface markers that are characteristic of MSCs and/or neural stem cells (NSCs) (51, 52) and therefore were analyzed separately from AFMSCs. Five studies (seven experiments) (42, 43, 45, 47, 48) examined bone marrow MSCs (BMMSCs), three studies (three experiments) (42, 44, 46) examined enteric NSCs (ENSCs), and one study (one experiment) (42) examined AFNSCs. Two studies studied exosomes of stem cells as the intervention, with McCulloh et al. (41) studying exosomes of AFMSCs, BMMSCs, ENSCs, and AFNSCs in two experiments, and Rager et al. (43) studying BMMSC exosomes in one experiment. The dosages and timing for each intervention are detailed in **Table 1**.

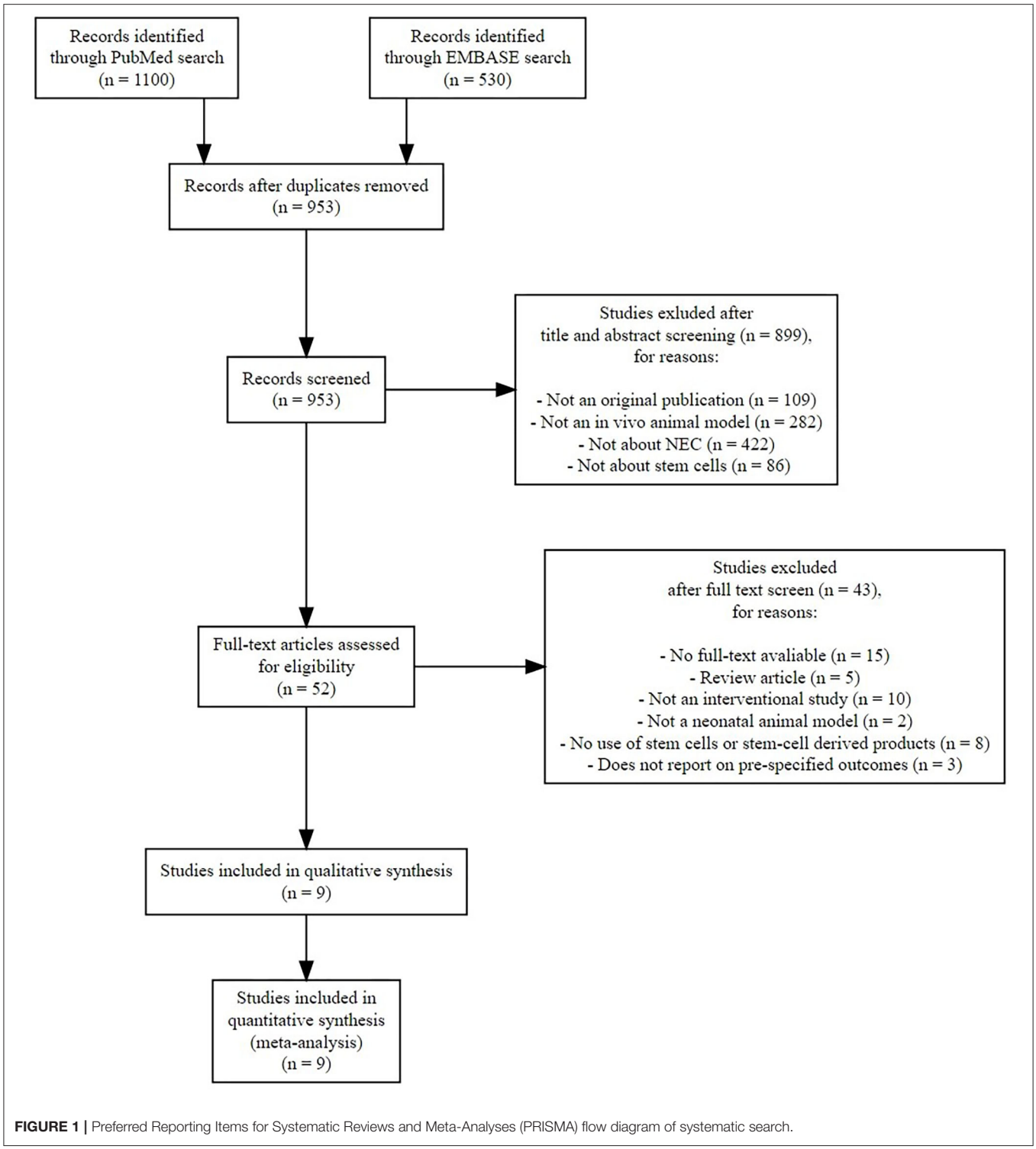

FIGURE 1 | Preferred Reporting Items for Systematic Reviews and Meta-Analyses (PRISMA) flow diagram of systematic search.

Reported Outcomes

Primary Outcomes

Four studies (16 experiments) (41–43, 45) reported on incidence of any grade NEC, incidence of grade 2 NEC, and incidence of severe NEC (grades 3 and 4). Five studies (nine experiments) reported on survival at day 4 of life (45–49), and two studies (five experiments) reported on survival at day 7 of life (46, 48).

Secondary Outcomes

Several studies reported on indicators of intestinal injury. Four studies (10 experiments) (42, 43, 45, 48) reported

TABLE 1 | Summary of the characteristics of studies in each article.

Author	Species	INT	CON	No. INT	No. CON	Dose and time of intervention	Admin mode	NEC induced at age	Outcome measures
McCulloh et al. (42)	Rat	AFMSC BMMSC ENSC AFNSC	PBS	42 48 36 37	62	2 * 10^6 cells in 0.1 ml of PBS after delivery	IP	Preterm (−0.5 day)	NEC incidence, NEC severity
McCulloh et al. (41) Series A	Rat	AFMSC Exo BMMSC Exo ENSC Exo AFNSC Exo	PBS	18 15 9 14	14	8 * 10^7 exosomes < 1 h after birth	IP	Preterm (−1 day), immediately after intervention	NEC incidence, NEC severity
McCulloh et al. (41) Series B	Rat	AFMSC Exo BMMSC Exo ENSC Exo	PBS	20 13 11	14	4 * 10^8 exosomes < 1 h after birth	IP	Preterm (−1 day), immediately after intervention	NEC incidence, NEC severity
Rager et al. (43)	Rat	BMMSC BMMSC Exo	PBS	35 40	46	Cells in 50 ml of PBS, 5 h after delivery	IP	Preterm (−1 day)	NEC incidence, NEC severity, intestinal injury
Tayman et al. (47)	Rat	BMMSC	None	12	12	6 * 10^5 cells in 50 μl of PBS, 3rd day of study	IP	Term (0 days)	Survival, sickness score
Wei et al. (44)	Mouse	ENSC	HBSS	39	48	30 μl of HBSS, 2 h after birth	IP	Term (0 days)	NEC incidence, NEC severity, intestinal injury
Yang et al. (45)	Rat	BMMSC IP BMMSC IV	Vehicle only	25 27	38	300 * 10^3 in 40 μl of vehicle, at birth	IP IV	Preterm (−0.5 day)	Survival, NEC incidence, NEC severity, intestinal injury
Zani et al. (49) (*EJPS*)	Rat	AFS	PBS	92	93	24 h after birth	IP	Unknown	Survival
Zani et al. (48) (*Gut*) Series A	Rat	BMMSC	PBS	26	30	2 * 10^6 cells in 50 μl of PBS, 24 h after birth	IP	Unknown	Survival, NEC severity, intestinal injury, sickness score
Zani et al. (48) (*Gut*) Series B	Rat	BMMSC AFS	PBS	17 40	43	2 * 10^6 cells in 50 μl of PBS, 24 h after birth	IP	Unknown	Survival, NEC severity, intestinal injury, sickness score
Zani et al. (48) (*Gut*) Series C	Rat	AFS	PBS	121	120	2 * 10^6 cells in 50 μl of PBS, 24 h after birth	IP	Unknown	Survival, NEC severity, intestinal injury, sickness score
Zhou et al. (46)	Rat	ENSC	DMEM/F12	9	9	50,000 cells in 50 μl of DMEM, day 3 after birth	IP	Preterm (−1 day)	Survival, intestinal injury

INT, interventional group; CON, control group; Admin, administration; NEC, necrotizing enterocolitis; AF, amniotic fluid; MSC, mesenchymal stem cell; IP, intraperitoneal; exo, exosomes (stem cell product); IV, intravenous; PBS, phosphate-buffered saline; DMEM, Dulbecco's modified Eagle's medium; AFS, amniotic fluid-derived stem cells (stained positively for a number of surface markers characteristic of mesenchymal and/or neural stem cells); AFMSC, amniotic fluid mesenchymal stem cell; AFNSC, amniotic fluid neural stem cell; BMMSC, bone marrow mesenchymal stem cell; ENSC, enteric neural stem cell; HBSS, Hank's Balanced Salt Solution.

on intestinal permeability. Two studies (two experiments) reported on intestinal motility (46, 49). Two studies (two experiments) reported on clinical sickness (47, 48). One study (one experiment) reported on NEC severity score (48).

Risk of Bias Assessment

Selection Bias and Performance Bias

The details for the risk of bias analysis are shown in **Table 2**. None of nine included studies provided sufficient information to assess the risk of bias as either low or high risk of bias for selection bias (*sequence generation*, *baseline characteristics*, and *allocation concealment*) and performance bias (*random housing* and *investigator/caregiver blinding*). We evaluated all six of these items as "unclear" risk of bias due to poor reporting of essential experimental details.

Detection Bias

We evaluated risk of bias for *blinding of outcome assessors* (detection bias) separately for each outcome reported, and the details of this evaluation are provided in **Table 3**. Five studies (41, 42, 44, 45, 47) had low risk of bias for *blinding of outcome assessors*, for the outcome NEC incidence and severity. One study (48) blinded outcome assessors for intestinal motility and scored "low" risk of bias for this outcome, whereas another (46) did not clarify if outcome assessors were blinded and scored "unclear" risk of bias. For all other outcomes (survival, intestinal permeability, and clinical sickness score), studies did not clarify if outcome assessors were blinded, and they were evaluated as "unclear" risk of bias. No study provided information on *random outcome assessment* (detection bias), and we evaluated this for all studies as "unclear" risk of bias.

Attrition Bias

Attrition bias (incomplete outcome data) was evaluated as "low" in one study (44), "high" in another study (41), and "unclear" in seven studies (42, 43, 45–49).

TABLE 2 | Risk of bias assessment.

Study	Adequate sequence generation	Baseline characteristics comparable	Allocation concealment	Random housing	Investigators/ caregivers blinding	Random outcome assessment	Blinding outcome assessment	Incomplete outcome data adequate addressed	Free of reporting bias	Other biases absent	Randomization mentioned?	Blinding mentioned?	Sample size and calculation mentioned?
McCulloh et al. (42)	?	?	?	?	?	?	Yes	?	?	?	Yes	Yes	No
McCulloh et al. (42)	?	?	?	?	?	?	Yes	No	?	?	Yes	Yes	No
Rager et al. (43)	?	?	?	?	?	?	?	?	?	Yes	Yes	No	No
Tayman et al. (47)	?	?	?	?	?	?	Yes	Yes	?	Yes	No	Yes	Yes
Wei et al. (44)	?	?	?	?	?	?	Yes	?	?	Yes	Yes	Yes	No
Yang et al. (45)	?	?	?	?	?	?	Yes	?	?	Yes	Yes	Yes	No
Zani et al. (49) (*EJPS*)	?	?	?	?	?	?	?	?	?	Yes	Yes	Yes	No
Zani et al. (48) (*Gut*)	?	?	?	?	?	?	Yes	?	No	Yes	Yes	Yes	No
Zhou et al. (46)	?	?	?	?	?	?	?	?	?	Yes	No	No	No

TABLE 3 | Risk of bias for blinding of outcome assessment, per outcome.

	Was outcome assessment blinded?		
Study	**Yes**	**Unclear**	**No**
McCulloh et al. (42)	NEC incidence	-	–
McCulloh et al. (42)	NEC incidence	–	–
Rager et al. (43)	–	NEC incidence, intestinal permeability	–
Tayman et al. (47)	NEC incidence, sickness score	Survival, clinical sickness score	–
Wei et al. (44)	NEC incidence	Intestinal permeability	–
Yang et al. (45)	NEC incidence	Survival, intestinal permeability	–
Zani et al. (49) (*EJPS*)		Survival	–
Zani et al. (48) (*Gut*)	Intestinal motility, intestinal permeability	Survival, clinical sickness score	–
Zhou et al. (46)	–	Survival, intestinal motility	–

NEC, necrotizing enterocolitis.

Reporting Bias and Other Bias

Reporting bias (selective outcome reporting) was evaluated as "high" in one study (48) and unclear in eight studies (41–47, 49).

We evaluated seven out of nine studies as low risk of "other biases": there were no indications of unit of analysis errors, and they reported information on funding and conflicts of interest. Two studies did not provide funding and conflict of interest information and were evaluated as "unclear" risk of bias in this category.

Meta-Analyses of Primary Outcomes

Necrotizing Enterocolitis Incidence

As shown in **Figure 2**, meta-analysis showed that stem cells and stem cell-derived products significantly reduced the incidence of any grade of NEC ($k = 16$, OR 0.22, 95% CI 0.16–0.32). Meta-analysis also found that stem cells and stem cell-derived products significantly reduced incidence of grade 2 NEC ($k = 16$, OR 0.41, 95% CI 0.24–0.70, **Figure 3**), as well as incidence of grade 3–4 NEC ($k = 16$, OR 0.28, 95% CI 0.19–0.42, **Figure 4**). As shown in **Figures 2–4**, the protective effects of stem cells were similarly observed in the subgroups of mesenchymal SC, neural SC, and SC-derived exosomes. Sensitivity analyses showed that the removal of the study that used mice instead of rats did not affect the significance of the results, nor did removal of experiments that used SC-derived exosomes (instead of SC) as the intervention (**Supplementary Table 1**).

Survival

Meta-analysis showed that stem cells significantly improved survival at day 4 of life ($k = 9$, OR 2.89, 95% CI 2.07–4.04, **Figure 5**). Moreover, meta-analysis showed that stem cells significantly improved chance of survival at day 7 of life ($k = 5$, OR 3.96, 95% CI 2.39–6.55, **Figure 6**). Subgroup analysis based

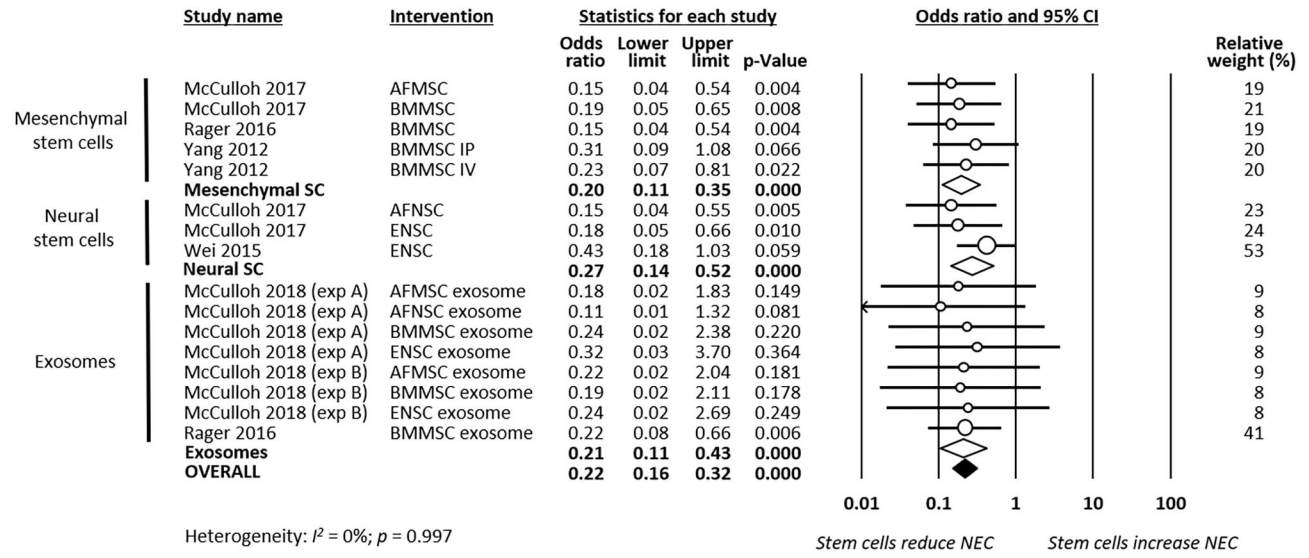

FIGURE 2 | Meta-analysis on stem cells/stem cell-derived products and incidence of any grade necrotizing enterocolitis (NEC). AF, amniotic fluid; BM, bone marrow; ENSC, enteric neural stem cell; IP, intraperitoneal; IV, intravenous; MSC, mesenchymal stem cell; NSC, neural stem cell; SC, stem cell.

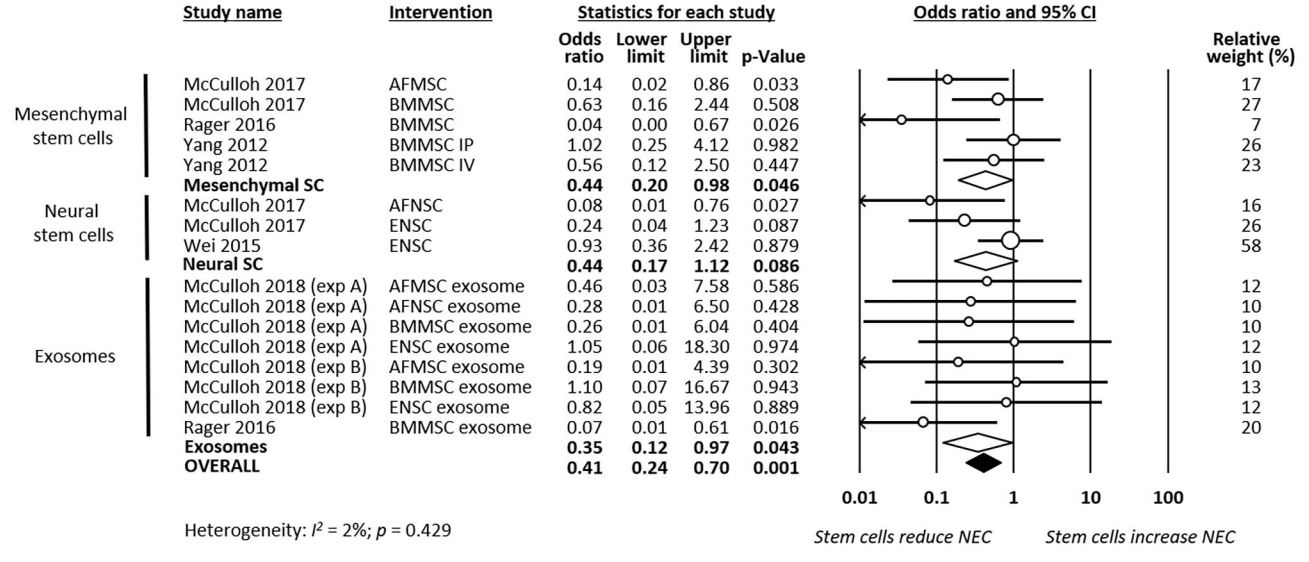

FIGURE 3 | Meta-analysis on stem cells/stem cell-derived products and incidence of grade 2 necrotizing enterocolitis (NEC). AF, amniotic fluid; BM, bone marrow; ENSC, enteric neural stem cell; IP, intraperitoneal; IV, intravenous; MSC, mesenchymal stem cell; NSC, neural stem cell; SC, stem cell.

on the type of stem cells was not performed for this outcome due to the small number of studies in each subgroup.

Meta-Analyses of Secondary Outcomes

Meta-analysis showed that stem cells and stem cell exosomes significantly reduced intestinal permeability (k = 10, SMD −3.48, 95% CI −3.90 to −3.05, **Figure 7**). Sensitivity analyses showed that the reduction remained significant after removing the sole experiment that used exosomes as the intervention and after removing the sole experiment that used mice as the experimental animal (**Supplementary Table 1**). Meta-analysis also found that stem cells improved intestinal motility (k = 2, SMD 3.73, 95% CI 3.09–4.38, **Supplementary Figure 1**) and reduced clinical sickness score (SMD −3.49, 95% CI −6.58 to −0.40, **Supplementary Figure 2**).

Publication Bias

There were sufficient independent effect sizes (k > 10) to test two outcomes (any grade NEC and grade 3–4 NEC incidence) for publication bias. For any grade NEC (k = 16), the visual inspection and trim-and-fill analysis suggested funnel plot asymmetry (**Supplementary Figure 3**), but Egger's regression

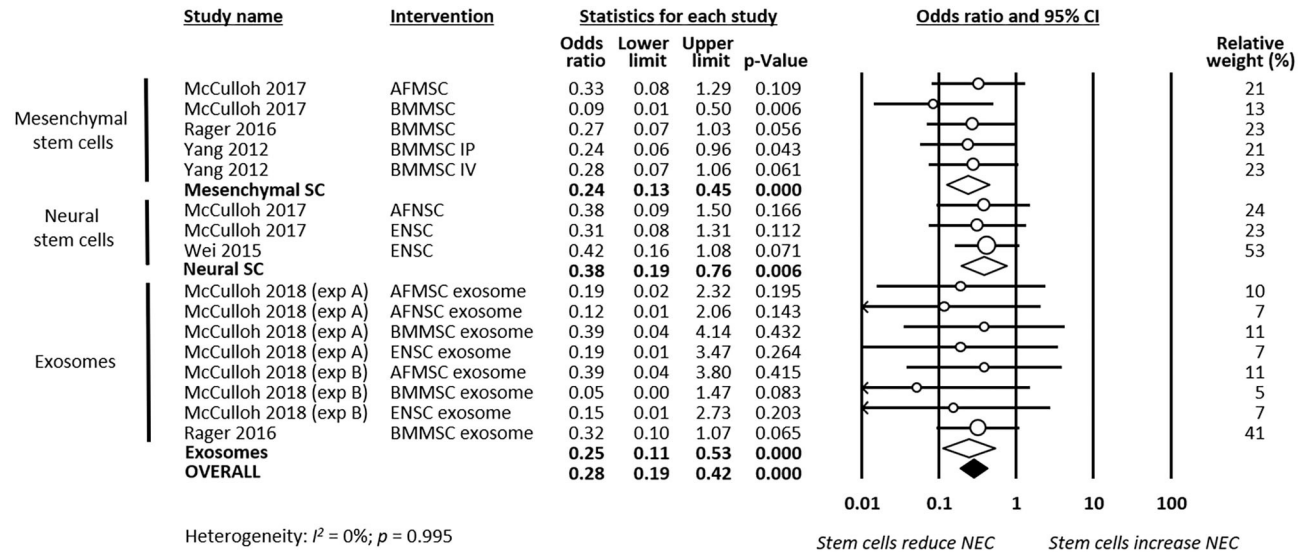

FIGURE 4 | Meta-analysis on stem cells/stem cell-derived products and incidence of grade 3–4 necrotizing enterocolitis (NEC). AF, amniotic fluid; BM, bone marrow; ENSC, enteric neural stem cell; IP, intraperitoneal; IV, intravenous; MSC, mesenchymal stem cell; NSC, neural stem cell; SC, stem cell.

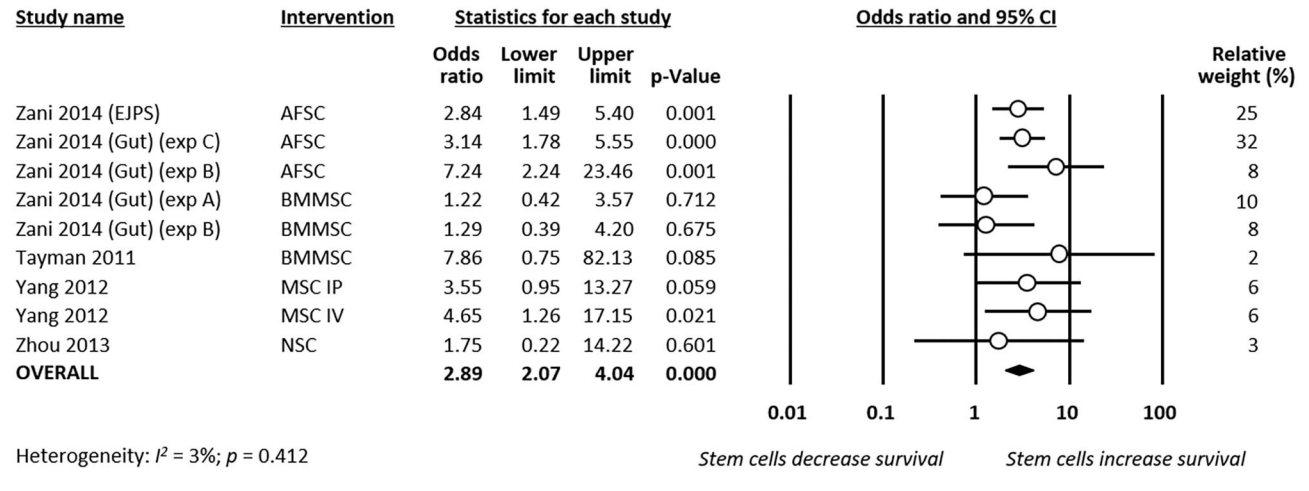

FIGURE 5 | Meta-analysis on stem cells and survival at day 4 of life following necrotizing enterocolitis (NEC). AFSC, amniotic fluid stem cell; BMMSC, bone marrow mesenchymal stem cell; IP, intraperitoneal; IV, intravenous; MSC, mesenchymal stem cell; NSC, neural stem cell.

test was non-significant ($p = 0.090$). For the outcome NEC grade 3–4 ($k = 16$), the visual inspection and trim-and-fill analysis suggested funnel plot asymmetry (**Supplementary Figure 4**), and Egger's regression test supported the presence of significant publication bias ($p < 0.001$).

DISCUSSION

To the best of our knowledge, this is the first systematic review and meta-analysis of preclinical studies investigating the effects of stem cells in experimental NEC. Meta-analysis showed that stem cells and stem cell-derived exosomes increased survival and decreased both incidence and severity of histologically proven NEC in rodent models of the condition. The beneficial effects of stem cells were consistent despite the heterogeneity in the sort of cells or exosomes across the different studies.

The studies included in our review used bone marrow- and AF-derived MSCs, and AF- and fetal intestine-derived NSCs. Among non-embryonic stem cells, MSCs are considered to have a high therapeutic potential due to their ability of proliferation and multilineage differentiation (22, 53–55). MSCs are found in multiple tissues, including bone marrow, adipose tissue, placenta, chorion, amnion, umbilical cord, umbilical blood, and breast milk (22, 55). The data of the meta-analysis suggest that MSCs and NSCs have similar effects on experimental NEC. However, NSCs, compared with MSCs, are challenging to isolate and

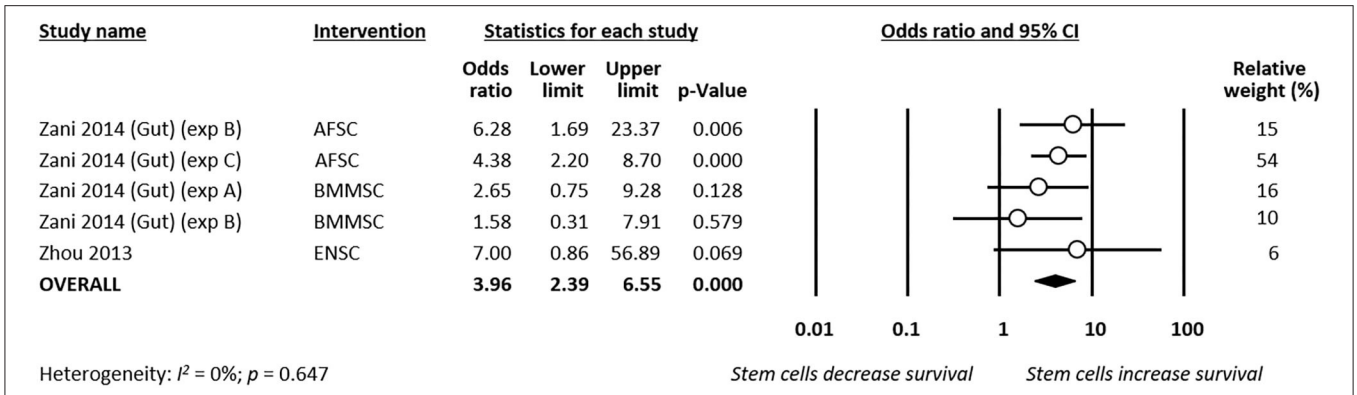

FIGURE 6 | Meta-analysis on stem cells and survival at day 7 of life following necrotizing enterocolitis (NEC). AFSC, amniotic fluid stem cell; BMMSC, bone marrow mesenchymal stem cell; ENSC, enteric neural stem cell.

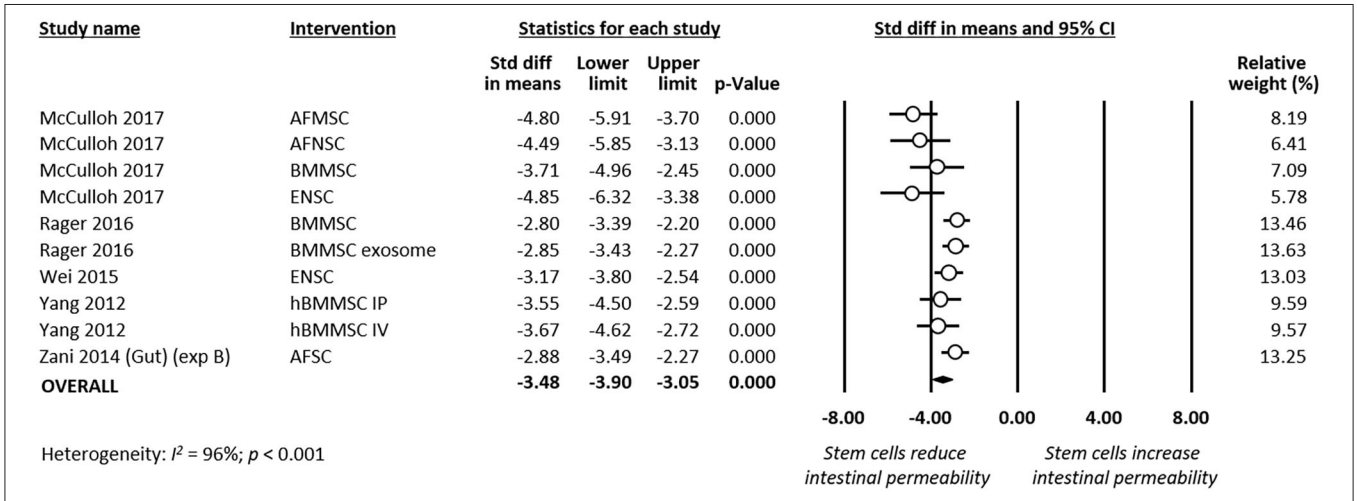

FIGURE 7 | Meta-analysis on stem cells/stem cell-derived products and intestinal permeability following experimental necrotizing enterocolitis (NEC). AF, amniotic fluid; BM, bone marrow; ENSC, enteric neural stem cell; h, human; IP, intraperitoneal; IV, intravenous; MSC, mesenchymal stem cell; SC, stem cell.

culture, potentially limiting their clinical utility (22). Two studies investigated the effects of AFSC (48, 49). AFSC are considered as an intermediate type between embryonic and adult stem cells, and they stained positively for a number of surface markers characteristic of MSCs and NSCs (51, 52). Interestingly, it has been shown that NSCs can be purified and derived from AFSC. As reviewed by McCulloch et al., these amniotic-fluid derived NSCs may have the ability to provide the same therapeutic effects than other NSCs but with the advantage of a greater easiness in obtaining them (52).

The results from this meta-analysis also suggest that exosomes are just as effective in reducing the incidence and severity of experimental NEC as the stem cells from which they derive. Accordingly, a previous meta-analysis showed that cell-free MSC-derived conditioned media had significant therapeutic effects in hyperoxic rodent models of bronchopulmonary dysplasia (21). Paracrine mediators such as stem cell-derived exosomes are emerging as a novel therapeutic strategy to overcome some of the limitations of stem cell therapy (56). Exosomes are small membrane vesicles of endocytic origin that exert their therapeutic actions by involving cell–cell interactions and transferring proteins, RNAs, and microRNAs (56). Interestingly, breast milk-derived exosomes, which are produced by a variety of cells, stimulate intestinal cell proliferation and differentiation (57, 58) and may be protective in experimental NEC (59).

The strengths of our systematic review included the breadth of the search strategy, the clear definition of inclusion and exclusion criteria, and the rigorous data evaluation and reporting by the use of international guidance and standards. However, the review has also a number of limitations that should be discussed. First, the included studies generally had small sample sizes that were not justified by power calculations. Second, evidence of publication bias was detected in some of the analyses (see **supplementary Figure 4**). Publication and other forms of reporting bias appear to occur in a greater proportion in preclinical than in clinical studies (60, 61). Therefore, studies with less positive results might not have been published. Third, a high

number of the included studies came from the same research group (41–46). Fourth, although no statistical heterogeneity was detected, there was evident heterogeneity in the design of the studies, particularly in the type of stem cells (or exosomes) that were used. We conducted subgroup analyses to determine whether some of the stem cell types were more effective than others. However, these subgroups included a limited number of studies. Therefore, the results of the subgroup analysis should be interpreted with caution, and their main value is the generation of hypotheses for future research.

The fifth limitation to discuss was that the risk of bias assessment for the primary studies was hampered by low quality and/or completeness of reporting on relevant domains. This fact has already been highlighted in other systematic reviews of preclinical studies on neonatal pathological conditions (21, 62, 63). In general, studies blinded outcome assessment and had low risk of bias for selective outcome reporting. However, for all other elements of risk of bias, including sequence generation, randomization of intervention, comparability of baseline characteristics, allocation concealment, random housing, investigator blinding, random outcome assessment, and reporting bias, the information contained in the articles was insufficient to draw conclusions about risk of bias. It should be considered that the information may be incomplete because the authors considered some aspects of study design not sufficiently relevant to be mentioned (64). Despite the publication of extensive guidelines such as the ARRIVE guidelines (65), or the Gold Standard Publication Checklist (66), underreporting is a point of concern that harms the internal validity and the generalizability of the results (64). Therefore, it is imperative that studies report all characteristics of their animal, experimental, and intervention models (62, 64). This information, along with information regarding the experimental conditions, is especially important for future study comparisons and meta-analyses and, consequently, to optimize interventions for future translational and clinical studies (62, 64).

One final limitation that is inherent to all preclinical studies is the so-termed indirectness, which is defined as "how well the results translate from animals to the clinical situation" (28). Rodent models of NEC are frequently used by investigators because of their relative low costs and ease of breeding (14, 15). However, the inability to provide intensive care and parenteral nutrition to the pups limits the model to only a few days after NEC induction (14, 15). Moreover, it has been argued that the combination of insults (hypoxia, hypothermia, formula feeds, and bacterial products) that is used in rodent models is not what commonly leads to classical late-onset NEC in very and extremely preterm infants (63). In addition, the effects of an intervention may be species specific, making the extrapolation of experimental NEC to human preterm infants difficult (63). In this sense, it should be noted that some studies were carried out in term pups (see **Table 1**). Finally, the translational applicability of the studies included in this review is limited by the clinical difficulty of identifying those preterm infants who are starting to develop NEC and are therefore susceptible to early treatment with stem cells. Also related to translational applicability, the majority of the included studies administered the stem cells by intraperitoneal (IP) injection. IP administration of drugs in adults seems to be safe (67), but it is not known if this can be extrapolated to very preterm infants. Nevertheless, the IP route appears to be the most adequate for stem cell administration for the treatment of gastrointestinal disorders (68).

In conclusion, the data form this meta-analysis suggest that both stem cells and stem cell-derived exosomes prevented NEC in rodent experimental models. However, there is a need to explore this effect in other species and NEC models. Preclinical studies using animal models are invaluable tools for enriching our understanding of the etiopathogenesis and treatment of human diseases. Nevertheless, there is a need for greater homogeneity and clarity in both the experimental designs and in the way the design and results are reported in the publications. The participation of clinicians in the design of the experimental models would contribute to increase their translational applicability.

DATA AVAILABILITY STATEMENT

All datasets generated for this study are included in the article/**Supplementary Material**.

AUTHOR CONTRIBUTIONS

EV-M conceptualized the study, wrote the review protocol, carried out the systematic search, selected studies for inclusion, supervised data collection, carried out statistical analysis, and reviewed and revised the manuscript. TH carried out the systematic search, selected studies for inclusion, extracted study data, and drafted the first version of the manuscript. BK contributed to interpretation of results and reviewed and revised the manuscript. CH co-wrote the review protocol, supervised study inclusion and data collection, contributed to statistical analyses and interpretation of results, and reviewed and revised the manuscript. EV conceptualized and supervised the study, contributed to statistical analyses and interpretation of results, and reviewed and revised the manuscript. All authors contributed to the article and approved the submitted version.

FUNDING

This study was funded by a ZonMw grant Synthesis of Evidence in practice, within the program More Knowledge with Fewer Animals, project number 114024123 (in Dutch: Meer Kennis met Minder Dieren—Module Kennisinfrastructuur 'De praktijk van een Synthesis of Evidence' voor dierexperimenteel onderzoek).

SUPPLEMENTARY MATERIAL

The Supplementary Material for this article can be found online at: https://www.frontiersin.org/articles/10.3389/fped.2020.578984/full#supplementary-material

REFERENCES

1. Neu J, Walker WA. Necrotizing enterocolitis. *N Engl J Med.* (2011) 364:255–64. doi: 10.1056/NEJMra1005408
2. Neu J. Necrotizing enterocolitis: the mystery goes on. *Neonatology.* (2014) 106:289–95. doi: 10.1159/000365130
3. Hunter CJ, Upperman JS, Ford HR, Camerini V. Understanding the susceptibility of the premature infant to necrotizing enterocolitis (NEC). *Pediatr Res.* (2008) 63:117. doi: 10.1203/PDR.0b013e31815ed64c
4. Neu J, Pammi M. Necrotizing enterocolitis: the intestinal microbiome, metabolome and inflammatory mediators. *Semin Fetal Neonatal Med.* (2018) 23:400–5. doi: 10.1016/j.siny.2018.08.001
5. Cuna A, George L, Sampath V. Genetic predisposition to necrotizing enterocolitis in premature infants: current knowledge, challenges, and future directions. *Semin Fetal Neonatal Med.* (2018) 23:387–93. doi: 10.1016/j.siny.2018.08.006
6. Mai V, Young CM, Ukhanova M, Wang X, Sun Y, Casella G, et al. Fecal microbiota in premature infants prior to necrotizing enterocolitis. *PLoS ONE.* (2011) 6:e20647. doi: 10.1371/journal.pone.0020647
7. Wu SF, Caplan M, Lin HC. Necrotizing enterocolitis: old problem with new hope. *Pediatr Neonatol.* (2012) 53:158–63. doi: 10.1016/j.pedneo.2012.04.001
8. Lim JC, Golden JM, Ford HR. Pathogenesis of neonatal necrotizing enterocolitis. *Pediatr Surg Int.* (2015) 31:509–18. doi: 10.1007/s00383-015-3697-9
9. Rose AT, Patel RM. A critical analysis of risk factors for necrotizing enterocolitis. *Semin Fetal Neonatal Med.* (2018) 23:374–9. doi: 10.1016/j.siny.2018.07.005
10. Bowker RM, Yan X, De Plaen IG. Intestinal microcirculation and necrotizing enterocolitis: the vascular endothelial growth factor system. *Semin Fetal Neonatal Med.* (2018) 23:411–5. doi: 10.1016/j.siny.2018.08.008
11. Gordon PV, Swanson JR, MacQueen BC, Christensen RD. A critical question for NEC researchers: can we create a consensus definition of NEC that facilitates research progress? *Semin Perinatol.* (2017) 41:7–14. doi: 10.1053/j.semperi.2016.09.013
12. Xing T, Camacho Salazar R, Chen YH. Animal models for studying epithelial barriers in neonatal necrotizing enterocolitis, inflammatory bowel disease and colorectal cancer. *Tissue Barriers.* (2017) 5:e1356901. doi: 10.1080/21688370.2017.1356901
13. Topalian SL, Ziegler MM. Necrotizing enterocolitis: a review of animal models. *J Surg Res.* (1984) 37:320–36. doi: 10.1016/0022-4804(84)90196-3
14. Sulistyo A, Rahman A, Biouss G, Antounians L, Zani A. Animal models of necrotizing enterocolitis: review of the literature and state of the art. *Innov Surg Sci.* (2018) 3:87–92. doi: 10.1515/iss-2017-0050
15. Sodhi C, Richardson W, Gribar S, Hackam DJ. The development of animal models for the study of necrotizing enterocolitis. *Dis Model Mech.* (2008) 1:94–8. doi: 10.1242/dmm.000315
16. Lu P, Sodhi CP, Jia H, Shaffiey S, Good M, Branca MF, et al. Animal models of gastrointestinal and liver diseases. animal models of necrotizing enterocolitis: pathophysiology, translational relevance, and challenges. *Am J Physiol Gastrointest Liver Physiol.* (2014) 306:G917–28. doi: 10.1152/ajpgi.00422.2013
17. Crissinger KD. Animal models of necrotizing enterocolitis. *J Pediatr Gastroenterol Nutr.* (1995) 20:17–22. doi: 10.1097/00005176-199501000-00004
18. Ares GJ, McElroy SJ, Hunter CJ. The science and necessity of using animal models in the study of necrotizing enterocolitis. *Semin Pediatr Surg.* (2018) 27:29–33. doi: 10.1053/j.sempedsurg.2017.11.006
19. Thebaud B. Stem cells for extreme prematurity. *Am J Perinatol.* (2019) 36(S 02):S68–73. doi: 10.1055/s-0039-1691774
20. Pierro M, Thebaud B, Soll R. Mesenchymal stem cells for the prevention and treatment of bronchopulmonary dysplasia in preterm infants. *Cochrane Database Syst Rev.* (2017) 11:CD011932. doi: 10.1002/14651858.CD011932.pub2
21. Augustine S, Avey MT, Harrison B, Locke T, Ghannad M, Moher D, et al. Mesenchymal stromal cell therapy in bronchopulmonary dysplasia: systematic review and meta-analysis of preclinical studies. *Stem Cells Transl Med.* (2017) 6:2079–93. doi: 10.1002/sctm.17-0126
22. Nitkin CR, Rajasingh J, Pisano C, Besner GE, Thébaud B, Sampath V. Stem cell therapy for preventing neonatal diseases in the 21st century: Current understanding and challenges. *Pediatr Res.* (2019) 2019:1–12. doi: 10.1038/s41390-019-0425-5
23. Finch-Edmondson M, Morgan C, Hunt RW, Novak I. Emergent prophylactic, reparative and restorative brain interventions for infants born preterm with cerebral palsy. *Front Physiol.* (2019) 10:15. doi: 10.3389/fphys.2019.00015
24. Ma QQ, Liu FY, Shi M, Sun CH, Tan Z, Chang XD, et al. Bone marrow mesenchymal stem cells modified by angiogenin-1 promotes tissue repair in mice with oxygen-induced retinopathy of prematurity by promoting retinal stem cell proliferation and differentiation. *J Cell Physiol.* (2019) 234:21027–38. doi: 10.1002/jcp.28706
25. Mueller M, Kramer BW. Stem cells and bronchopulmonary dysplasia-the five questions: which cells, when, in which dose, to which patients via which route? *Paediatr Respir Rev.* (2017) 24:54–9. doi: 10.1016/j.prrv.2016.12.003
26. Sena ES, Currie GL, McCann SK, Macleod MR, Howells DW. Systematic reviews and meta-analysis of preclinical studies: why perform them and how to appraise them critically. *J Cereb Blood Flow Metabol.* (2014) 34:737–42. doi: 10.1038/jcbfm.2014.28
27. Vesterinen H, Sena E, Egan K, Hirst T, Churolov L, Currie G, et al. Meta-analysis of data from animal studies: a practical guide. *J Neurosci Methods.* (2014) 221:92–102. doi: 10.1016/j.jneumeth.2013.09.010
28. Hooijmans CR, de Vries RB, Ritskes-Hoitinga M, Rovers MM, Leeflang MM, IntHout J, et al. Facilitating healthcare decisions by assessing the certainty in the evidence from preclinical animal studies. *PLoS ONE.* (2018) 13:e0187271. doi: 10.1371/journal.pone.0187271
29. Hooijmans CR, IntHout J, Ritskes-Hoitinga M, Rovers MM. Meta-analyses of animal studies: an introduction of a valuable instrument to further improve healthcare. *ILAR J.* (2014) 55:418–26. doi: 10.1093/ilar/ilu042
30. Hooijmans C, Ritskes-Hoitinga M. Progress in using systematic reviews of animal studies to improve translational research. *PLoS Med.* (2013) 10:e1001482. doi: 10.1371/journal.pmed.1001482
31. Villamor-Martinez E, Hunscheid T, Kramer B, Hooijmans C, Villamor E. *Stem Cells for the Prevention of Experimental Necrotizing Enterocolitis: a Systematic Review and Meta-Analysis of Preclinical Studies: PROSPERO;*. (2018). Available online at: https://www.crd.york.ac.uk/prospero/display_record.php?ID=CRD42018110084 (accessed March 12, 2020).
32. Moher D, Liberati A, Tetzlaff J, Altman DG, The PG. Preferred reporting items for systematic reviews and meta-analyses: The PRISMA statement. *PLOS Med.* (2009) 6:e1000097. doi: 10.1371/journal.pmed.1000097
33. de Vries RB, Hooijmans CR, Tillema A, Leenaars M, Ritskes-Hoitinga M. Updated version of the embase search filter for animal studies. *Lab Anim.* (2014) 48:88. doi: 10.1177/0023677213494374
34. Hooijmans CR, Tillema A, Leenaars M, Ritskes-Hoitinga M. Enhancing search efficiency by means of a search filter for finding all studies on animal experimentation in PubMed. *Lab Anim.* (2010) 44:170–5. doi: 10.1258/la.2010.009117
35. Ouzzani M, Hammady H, Fedorowicz Z, Elmagarmid A. Rayyan—a web and mobile app for systematic reviews. *Syst Rev.* (2016) 5:210. doi: 10.1186/s13643-016-0384-4
36. Rohatgi A. *Web Plot Digitizer San Francisco, California, USA2019.* (2019). Available online at: https://automeris.io/WebPlotDigitizer (accessed March 12, 2020).
37. Hooijmans CR, Rovers MM, de Vries RB, Leenaars M, Ritskes-Hoitinga M, Langendam MW. SYRCLE's risk of bias tool for animal studies. *BMC Med Res Methodol.* (2014) 14:43. doi: 10.1186/1471-2288-14-43
38. Kilkenny C, Parsons N, Kadyszewski E, Festing MF, Cuthill IC, Fry D, et al. Survey of the quality of experimental design, statistical analysis and reporting of research using animals. *PLoS ONE.* (2009) 4:e7824. doi: 10.1371/journal.pone.0007824
39. Borenstein M, Hedges LV, Higgins J, Rothstein HR. Identifying and quantifying heterogeneity. In: *Introduction to Meta-Analysis.* Chichester: John Wiley & Sons, Ltd (2009). p. 107–26. doi: 10.1002/9780470743386.ch16
40. Borenstein M, Hedges LV, Higgins JP, Rothstein HR. Publication bias. In: *Introduction to Meta-Analysis.* Chichester: John Wiley & Sons, Ltd (2009). p. 277:292. doi: 10.1002/9780470743386.ch30
41. McCulloh CJ, Olson JK, Wang Y, Zhou Y, Tengberg NH, D, et al. Treatment of experimental necrotizing enterocolitis with stem cell-derived exosomes. *J Pediatr Surg.* (2018) 53:1215–20. doi: 10.1016/j.jpedsurg.2018.02.086

42. McCulloh CJ, Olson JK, Zhou Y, Wang Y, Besner GE. Stem cells and necrotizing enterocolitis: a direct comparison of the efficacy of multiple types of stem cells. *J Pediatr Surg.* (2017) 52:999–1005. doi: 10.1016/j.jpedsurg.2017.03.028
43. Rager TM, Olson JK, Zhou Y, Wang Y, Besner GE. Exosomes secreted from bone marrow-derived mesenchymal stem cells protect the intestines from experimental necrotizing enterocolitis. *J Pediatr Surg.* (2016) 51:942–7. doi: 10.1016/j.jpedsurg.2016.02.061
44. Wei J, Zhou Y, Besner GE. Heparin-binding EGF-like growth factor and enteric neural stem cell transplantation in the prevention of experimental necrotizing enterocolitis in mice. *Pediatr Res.* (2015) 78:29–37. doi: 10.1038/pr.2015.63
45. Yang J, Watkins D, Chen CL, Bhushan B, Zhou Y, Besner GE. Heparin-binding epidermal growth factor-like growth factor and mesenchymal stem cells act synergistically to prevent experimental necrotizing enterocolitis. *J Am Coll Surg.* (2012) 215:534–45. doi: 10.1016/j.jamcollsurg.2012.05.037
46. Zhou Y, Yang J, Watkins DJ, Boomer LA, Matthews MA, Su Y, et al. Enteric nervous system abnormalities are present in human necrotizing enterocolitis: potential neurotransplantation therapy. *Stem Cell Res Ther.* (2013) 4:157. doi: 10.1186/scrt387
47. Tayman C, Uckan D, Kilic E, Ulus AT, Tonbul A, Murat Hirfanoglu I, et al. Mesenchymal stem cell therapy in necrotizing enterocolitis: a rat study. *Pediatr Res.* (2011) 70:489–94. doi: 10.1203/PDR.0b013e31822d7ef2
48. Zani A, Cananzi M, Fascetti-Leon F, Lauriti G, Smith VV, Bollini S, et al. Amniotic fluid stem cells improve survival and enhance repair of damaged intestine in necrotising enterocolitis via a COX-2 dependent mechanism. *Gut.* (2014) 63:300–9. doi: 10.1136/gutjnl-2012-303735
49. Zani A, Cananzi M, Lauriti G, Fascetti-Leon F, Wells J, Siow B, et al. Amniotic fluid stem cells prevent development of ascites in a neonatal rat model of necrotizing enterocolitis. *Eur J Pediatr Surg.* (2014) 24:57–60. doi: 10.1055/s-0033-1350059
50. Barlow B, Santulli TV. Importance of multiple episodes of hypoxia or cold stress on the development of enterocolitis in an animal model. *Surgery.* (1975) 77:687–90.
51. Perin L, Sedrakyan S, Da Sacco S, De Filippo R. Characterization of human amniotic fluid stem cells and their pluripotential capability. *Methods Cell Biol.* (2008) 86:85–99. doi: 10.1016/S0091-679X(08)00005-8
52. McCulloh C, Zhou Y, Besner GE. Transplantation of amniotic fluid–derived neural stem cells. *Perinatal Stem Cells.* (2018) 2018:39–51. doi: 10.1016/B978-0-12-812015-6.00003-0
53. Slack JM. What is a stem cell? *Wiley Interdiscipl Rev Dev Biol.* (2018) 7:e323. doi: 10.1002/wdev.323
54. McCulloch EA, Till JE. Perspectives on the properties of stem cells. *Nat Med.* (2005) 11:1026. doi: 10.1038/nm1005-1026
55. Cananzi M, Atala A, De Coppi P. Stem cells derived from amniotic fluid: new potentials in regenerative medicine. *Reprod Biomed Online.* (2009) 18:17–27. doi: 10.1016/S1472-6483(10)60111-3
56. Prathipati P, Nandi SS, Mishra PK. Stem cell-derived exosomes, autophagy, extracellular matrix turnover, and miRNAs in cardiac regeneration during stem cell therapy. *Stem Cell Rev Rep.* (2017) 13:79–91. doi: 10.1007/s12015-016-9696-y
57. Chen T, Xie M-Y, Sun J-J, Ye R-S, Cheng X, Sun R-P, et al. Porcine milk-derived exosomes promote proliferation of intestinal epithelial cells. *Sci Rep.* (2016) 6:33862. doi: 10.1038/srep33862
58. Hock A, Miyake H, Li B, Lee C, Ermini L, Koike Y, et al. Breast milk-derived exosomes promote intestinal epithelial cell growth. *J Pediatr Surg.* (2017) 52:755–9. doi: 10.1016/j.jpedsurg.2017.01.032
59. Li B, Hock A, Wu RY, Minich A, Botts SR, Lee C, et al. Bovine milk-derived exosomes enhance goblet cell activity and prevent the development of experimental necrotizing enterocolitis. *PLoS ONE.* (2019) 14:e0211431. doi: 10.1371/journal.pone.0211431
60. Van der Worp HB, Howells DW, Sena ES, Porritt MJ, Rewell S, O'Collins V, et al. Can animal models of disease reliably inform human studies? *PLoS Med.* (2010) 7:e1000245. doi: 10.1371/journal.pmed.1000245
61. Tsilidis KK, Panagiotou OA, Sena ES, Aretouli E, Evangelou E, Howells DW, et al. Evaluation of excess significance bias in animal studies of neurological diseases. *PLoS Biol.* (2013) 11:e1001609. doi: 10.1371/journal.pbio.1001609
62. Archambault J, Moreira A, McDaniel D, Winter L, Sun L, Hornsby P. Therapeutic potential of mesenchymal stromal cells for hypoxic ischemic encephalopathy: a systematic review and meta-analysis of preclinical studies. *PLoS ONE.* (2017) 12:e0189895. doi: 10.1371/journal.pone.0189895
63. Athalye-Jape G, Rao S, Patole S. Effects of probiotics on experimental necrotizing enterocolitis: a systematic review and meta-analysis. *Pediatr Res.* (2018) 83:16–22. doi: 10.1038/pr.2017.218
64. Leenaars CH, Kouwenaar C, Stafleu FR, Bleich A, Ritskes-Hoitinga M, De Vries RB, et al. Animal to human translation: a systematic scoping review of reported concordance rates. *J Transl Med.* (2019) 17:223. doi: 10.1186/s12967-019-1976-2
65. Kilkenny C, Browne WJ, Cuthill IC, Emerson M, Altman DG. Improving bioscience research reporting: the ARRIVE guidelines for reporting animal research. *PLoS Biol.* (2010) 8:e1000412. doi: 10.1371/journal.pbio.1000412
66. Hooijmans CR, Leenaars M, Ritskes-Hoitinga M. A gold standard publication checklist to improve the quality of animal studies, to fully integrate the Three Rs, and to make systematic reviews more feasible. *Altern Lab Anim.* (2010) 38:167–82. doi: 10.1177/026119291003800208
67. Fonnes S, Holzknecht BJ, Arpi M, Rosenberg J. Characterisation and safety of intraperitoneal perioperative administration of antibacterial agents: a systematic review. *Drug Res.* (2017) 67:688–97. doi: 10.1055/s-0043-109565
68. Wang M, Liang C, Hu H, Zhou L, Xu B, Wang X, et al. Intraperitoneal injection (IP), Intravenous injection (IV) or anal injection (AI)? Best way for mesenchymal stem cells transplantation for colitis. *Sci Rep.* (2016) 6:30696. doi: 10.1038/srep30696

Conflict of Interest: The authors declare that the research was conducted in the absence of any commercial or financial relationships that could be construed as a potential conflict of interest.

frontiers in Pediatrics

ORIGINAL RESEARCH
published: 15 January 2021
doi: 10.3389/fped.2020.624915

Radiographic Imaging to Evaluate Food Passage Rate in Preterm Piglets as a Model for Preterm Infants

Susanne Soendergaard Kappel[1,2], *Per Torp Sangild*[1,2,3], *Thomas Scheike*[4], *Christel Renée Friborg*[2], *Magdalena Gormsen*[5] *and Lise Aunsholt*[1,2]*

[1] Comparative Pediatrics and Nutrition, University of Copenhagen, Copenhagen, Denmark, [2] Department of Neonatology, Copenhagen University Hospital Rigshospitalet, Copenhagen, Denmark, [3] Department of Pediatrics, Odense University Hospital, Odense, Denmark, [4] Section of Biostatistics, Department of Public Health, University of Copenhagen, Copenhagen, Denmark, [5] Department of Radiology, Copenhagen University Hospital Rigshospitalet, Copenhagen, Denmark

OPEN ACCESS

Edited by:
Fook-Choe Cheah, National University of Malaysia, Malaysia

Reviewed by:
Shalini Ojha, University of Nottingham, United Kingdom
Roberto Murgas Torrazza, Tecnología e Innovación, Panama

***Correspondence:**
Lise Aunsholt
lise.aunsholt@regionh.dk

Specialty section:
This article was submitted to Neonatology, a section of the journal Frontiers in Pediatrics

Received: *01 November 2020*
Accepted: *18 December 2020*
Published: *15 January 2021*

Citation:
Kappel SS, Sangild PT, Scheike T, Friborg CR, Gormsen M and Aunsholt L (2021) Radiographic Imaging to Evaluate Food Passage Rate in Preterm Piglets as a Model for Preterm Infants. Front. Pediatr. 8:624915. doi: 10.3389/fped.2020.624915

Objectives and study: Gut motility in infants mature with increasing post-menstrual age and is affected by numerous hormonal, immunological and nutritional factors. However, it remains unclear how age and diet influence gut motility and its relation to feeding intolerance and gastric residuals in preterm neonates. Using preterm piglets as a model for infants, we investigated if contrast passage rate, as determined by X-ray contrast imaging, is affected by gestational age at birth, advancing postnatal age and different milk diets.

Methods: Contrast passage rate was evaluated using serial abdominal X-ray imaging on postnatal day 4 and 18 in preterm and near-term piglets fed infant formula, colostrum or intact bovine milk, with or without added fortifier (total $n = 140$).

Results: Preterm piglets had a faster small intestinal passage rate of contrast solution at day 4 of life than near-term piglets (SIEmpty, hazard ratio (HR): 0.52, 95%CI [0.15, 0.88], $p < 0.01$). Formula fed piglets at day 4 had a faster passage rate of contrast to caecum (ToCecum, HR: 0.61, 95%CI [0.25,0.96], $p = 0.03$), and through the colon region (CaecumToRectum, $p < 0.05$, day 4) than colostrum fed preterm piglets. The time for contrast to leave the stomach, and passage through the colon in day 4 preterm piglets were slower than in older piglets at day 18 (both, $p < 0.05$). Adding a nutrient fortifier increased body growth, gastric residuals, intestinal length and weight, but did not affect any of the observed passage rates of the contrast solution.

Conclusion: Serial X-ray contrast imaging is a feasible method to assess food passage rate in preterm piglets. Contrast passage rate through different gut segments is affected by gestational age at birth, postnatal age, and milk diet. The preterm piglet could be a good model to investigate clinical and dietary factors that support maturation of gut motility and thereby feeding tolerance and gut health in preterm infants.

Keywords: enteral nutrition, feeding intolerance, gut motility, bovine colostrum, x-ray

INTRODUCTION

Gut motility secures the continuous movement of nutrients through the gastrointestinal tract (GIT) via coordinated contractions of the smooth muscle layers, regulated by both dietary, neural, and hormonal factors (1). In newborn infants, the maturation stage of gut motility depends on post-menstrual age at birth. At 34–36 weeks gestation, the motility pattern reaches a relatively mature level, although some maturation of motility may continue throughout infancy and childhood in both term and preterm infants (1–3). Adequate physiological maturation of intestinal motility is important for preterm infants to tolerate enteral feeding and to avoid serious gastrointestinal (GI) complications, such as necrotizing enterocolitis (NEC). Early enteral feeding stimulates GI motor activity as shown by manometry studies of the immature intestine in preterm infants (4). This may occur via both physical food stimulation and luminal nutrients affecting the release of motility-promoting hormones, such as neurotensin from enteroendocrine cells in the small intestine (5).

Following preterm birth, mother's own milk or donor human milk is not always available and alternative enteral diets may be required. Diet type and nutrient density (e.g., breast milk, formula, human donor milk, nutrient-fortified human milk) vary widely for preterm infants and all these factors may influence food passage rate and maturation of gut motility patterns. In preterm piglets, bovine colostrum improves GI function compared with formula and human donor milk, as shown by reduced NEC incidence and improved digestive function and immunity (6–8). In ongoing clinical studies, the effects of bovine colostrum on growth, feeding intolerance, and defecation patterns (Amsterdam Stool Scale) are being investigated (9, 10) (Clinical trials: NCT03085277, NCT03537365).

To assess intestinal motility in preterm infants, previous studies have used food colors, abdominal ultrasound, manometry, or scintigraphy (11–14). Most of these studies can only assess motility of the upper or lower part of the GIT, without integrated information about the motility along the entire GIT. All these methods are technically difficult to perform because of the size and fragile condition of preterm infants, and some of them are relatively invasive and may interfere with the infant physiology (1). In clinical practice, standardized abdominal X-ray imaging is performed to evaluate functions in pathological conditions (e.g., obstruction, ileus, NEC), with or without the use of contrast solutions (15). Contrast solution provides detailed information about the gut transit time across different gut regions. This method, has not yet been used to provide information about the age- and diet-related maturation of gut motility in infants, partly because of the potential health risks associated with serial X-ray examinations.

Preterm piglets delivered at 90% gestation have become a well-established animal model of preterm infants to investigate gut development, nutrition, NEC and clinical complications of prematurity (16). Proof-of-concept studies in preterm pigs may pave the way for focused investigations in preterm infants and provide initial information about the factors that affect development of intestinal motility and food passage rate in infants. Using this model, we hypothesized that gestational age at birth, type of nutrition and age after birth are factors that influence contrast passage rate as assessed by X-ray imaging. To assess the possible utility of this method to monitor intestinal motility in immature newborns, we compared recordings from preterm and near-term cesarean-delivered piglets, from preterm piglets fed bovine colostrum or formula, and from piglets at different ages (4 and 18 days), with and without bovine colostrum used as a nutrient fortifier to cow's milk.

MATERIALS AND METHODS

Animals

Preterm and near-term piglets were delivered from sows by cesarean section at 90% gestation (day 105–106 of gestation, 11 litters) and 96% gestation (113 days of gestation, 2 litters), which were used in 5- and 19-day experiments to investigate the effects of different enteral diets on gut structure and function (10, 17, 18). Piglets were placed individually in preheated incubators (37–38°Celcius) and received supplementary oxygen during the first 24 h (1–2 L/min). Two hours after delivery, a feeding tube was placed for enteral nutrition (EN) and a vascular catheter inserted via the umbilical cord for parenteral nutrition (PN). Piglets were orally fed every 2–3 h with gradually increasing volumes of either infant formula ($n = 60$) or dilute bovine milk ($n = 50$). The bovine milk fed was fed with or without fortification, using bovine colostrum powder, to increase protein and energy contents (e.g., protein 27–55 g/L, energy 2426-3602 kJ/L) (10). To ensure adequate fluid and nutrient intake, enteral nutrition was supplemented with PN to reach a total fluid intake of 120–180 ml/kg/d (Kabiven, Fresenius Kabi, Bad Homburg, Germany). In the 19-day study piglets were at day 7 transitioned to voluntary drinking from troughs. To secure that all piglets were healthy, they were continuously monitored by caretakers for clinical symptoms of feeding intolerance, hemorrhagic diarrhea, pain, and/or respiratory distress throughout the study periods. Pigs were euthanized, if they developed severe clinical symptoms. All animal studies were approved by the National Committee on Animal Experimentation, Denmark (license nr: 2014-15-0201-55 00418), and in line with the ARRIVE guidelines (19).

At time of organ harvest, one last bolus meal of 15 mL/kg was administered 60–90 min before tissue collection, when piglets were anesthetized and euthanised with an overdose of sodium pentobarbital. The gastrointestinal organs were removed and separated into stomach, small intestine and caecum-colon. The mass of the gastric residual was determined by weighing the stomach before and after emptying its contents. The small intestine was dissected by cutting along the mesenteric border and the intestine and colon wet weights were determined.

For Study 1, piglets were born preterm ($n = 30$) or close to term ($n = 27$) and fed increasing amounts of formula for 5 days (**Table 1**). For Study 2, preterm piglets were fed increasing amounts of bovine colostrum ($n = 17$) or formula ($n = 33$, **Table 1**), as described previously (17, 18). In study 1 and 2, radiographic recording was performed on day 4. Finally, for Study 3, preterm piglets ($n = 33$) had radiographic recordings done taken both on day 4 and 18 (**Table 1**). Some of these piglets

TABLE 1 | Clinical outcomes.

	Experiment 1			Experiment 2			Experiment 3		
	Preterm	**Near-term**	***P***	**Colostrum**	**Formula**	***P***	**Fortified**	**Non-fortified**	***P***
Total *n*	30	27		17	33		16	17	
Birth weight (g)	1,028 ± 219	1,078 ± 262	NS	1,084 ± 198	1,007 ± 229	NS	1,024 ± 161	1,009 ± 214	NS
End weight (g)	1,114 ± 195	1,179 ± 309	NS	1,224 ± 249	1,095 ± 209	NS	1,954 ± 331	1,502 ± 279	<0.01
Passage of meconium (h)	31 ± 18	37 ± 27	NS	30 ± 19	31 ± 17	NS	25 ± 11	27 ± 16	NS
Gastric residual (g/kg)	16 ±9	19 ± 12	NS	19 ± 6	17 ± 9	NS	12 ± 2	8 ± 3	<0.01
Intestinal length (cm)	483 ± 153	471 ± 91	NS	327 ± 47	466 ± 150	<0.01	473 ± 51	405 ± 41	<0.01
Intestinal weight (g)	35 ± 6	37 ± 10	NS	37 ± 8	37 ± 15	NS	75 ± 12	54 ± 14	<0.01
Relative intestinal weight (g/kg)	32 ± 4	31 ± 4	NS	31 ± 5	34 ± 16	NS	39 ± 4	37 ± 11	NS
Colon weight (g)	11 ± 3	15 ± 3	<0.05	14 ± 5	11 ± 3	NS	33 ± 15	25 ± 7	NS
Relative colon weight (g/kg)	10 ± 1	11 ± 1	NS	11 ± 4	11 ± 3	NS	17 ± 7	18 ± 7	NS

were fed fresh dilute cow's milk (control, $n = 17$) while others were fed the same milk fortified with bovine colostrum powder ($n = 16$), as described previously (10). As the present study aimed to investigate effects of gestational age, maturity at birth and milk diets on intestinal passage rate under normo-physiological, healthy conditions, all piglets with signs of NEC or other severe complications were excluded prior to X-ray examination. We have previously reported the effects of NEC development on gastric residuals and contrast passage rates, as assessed by X-ray imaging (20).

Contrast X-Ray Imaging

Luminal passage of contrast through the GI tract was assessed by transit time recordings for the contrast solution on day 4 or day 18. Briefly, piglets were fasted for 2–3 h and then administered 4 mL/kg contrast (Iodixanol, Visipaque, GE Healthcare, Brøndby Denmark) by a feeding tube. Piglets receiving contrast on day 18, ate the contrast solution from a trough, to minimize the risk of lung aspiration and the potential effect on gastric motility by insertion of the feeding tube. Abdominal X-ray images were captured (80 kV/1,00 mAs) using Mobilett XP Hybrid (Siemens, Germany) at 10, 25, 60, 120, 180, 240 min after contrast was given and every 120 min until the contrast had left the gut completely. The piglets were fed with their normal enteral diet (colostrum, formula or cow's milk) 25 min after intake of the contrast solution and fed every 3 h during X-ray examination. X-rays were performed with piglets restricted and placed in supine position, see **Figure 1**. The procedure lasted ½-1 min and X-ray images were stored digitally. Contrast passage rate was evaluated by a neonatologist and an expert radiologist blinded to age and diets of the piglets. The time periods taken for the contrast to leave the stomach (StEmpty), reaching the cecum (ToCecum), emptied from small intestine (SiEmpty), and reaching the rectum (ToRectum) were recorded. Time taken for the contrast solution to pass through the colon (CecumToRectum) was calculated as the difference in time between ToCecum and ToRectum times.

Statistics

Survival analyses for interval-censored data was used to analyse time-to-event outcomes. When analyzing time-to-event data, the time of interest lies in an interval. In this study we only know whether the time of interest occurred or did not occur at the time of X-ray imaging. If the time of interest did not occur at the latest X-ray imaging, then this is a right censored observation (21).

Comparing preterm with near-term piglets (Study 1), different diets (Study 2) and unfortified with fortified cow's milk (Study 3), interval-censored data was analyzed by the Cox regression model using the R-package icenReg (Statistical software R version 2.0.14). In addition, we validated the results by extensive simulations and other methods for discrete interval-censored data, considering that the intervals were based on observing the piglets at particular time points, as previously described (22). Results are presented as hazard ratio (HR) with 95% confidence interval. To compare StEmpty, ToCecum, CecumToRectum, SiEmpty, and ToRectum at day 4 and 18 (Study 3), we used the paired McNemar test. This was feasible because we had equivalent evaluation times for each piglet. Demographic/clinical data and time for first passage of meconium were analyzed using *t*-test and a non-parametric Wilcoxon test. We did not perform treatment-related power calculations for this initial method validation study because variation of the key outcome variables was unknown. Sample size was based on those sufficient to show age and diet effects in our previous studies (16). A $p < 0.05$ was considered statistically significant different and a $p < 0.1$ was considered as a tendency toward an effect (23).

RESULTS

Comparisons between groups in Experiments 1–3 were based on a total of 140 recordings (**Table 1**) from a total of 110 piglets. All piglets tolerated the X-ray examination well, with no obvious pain or distress during or after the 1 min handling for X-ray (**Figure 1**). The fecal score before intake of contrast was lower than after intake of contrast, indicating some laxative effect of contrast and/or handling ($p < 0.01$).

Study 1: Preterm vs. Near-Term Piglets

Preterm and near-term piglets showed similar organ weights and length, time for first meconium passage and gastric residuals

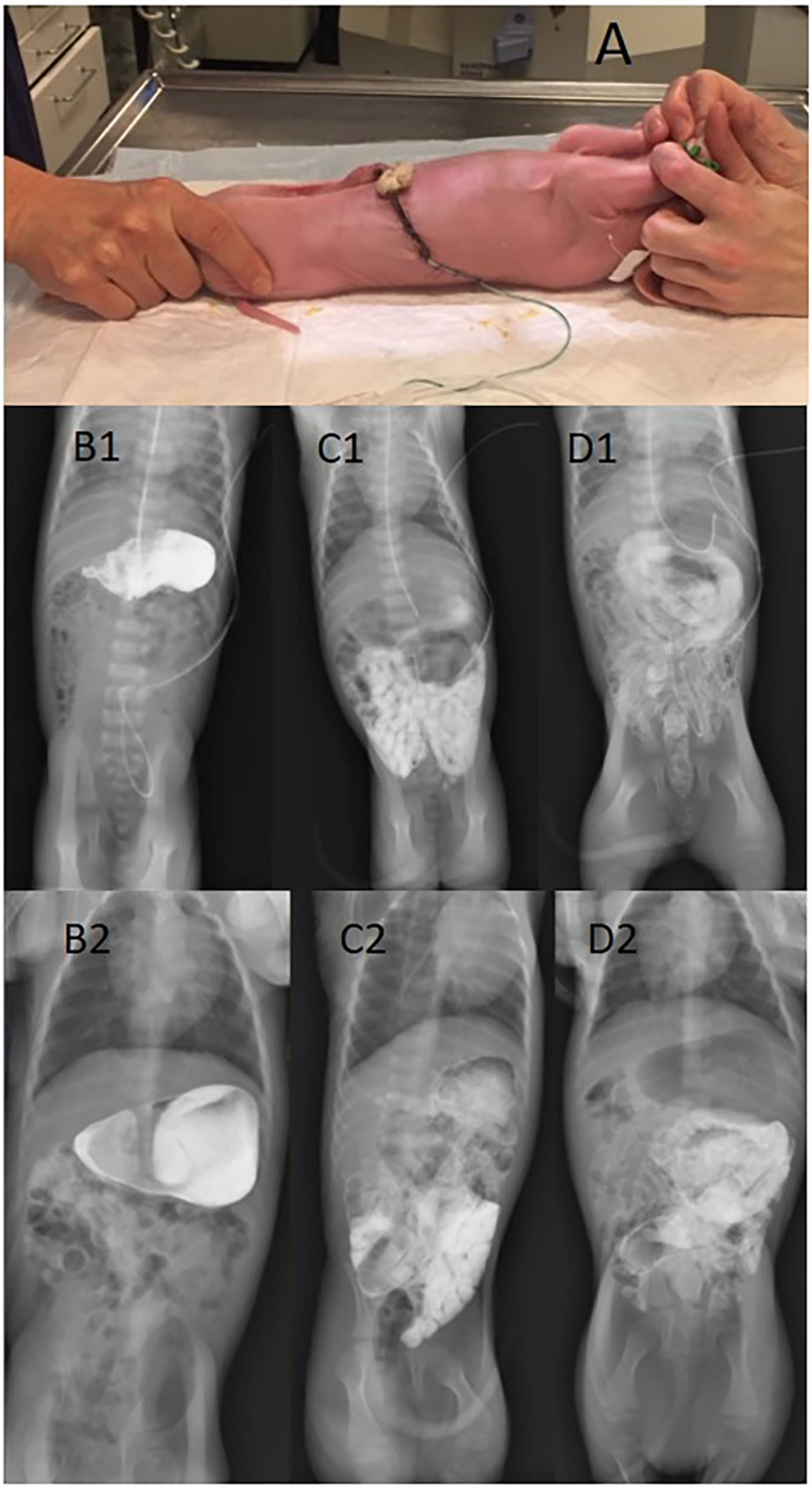

FIGURE 1 | Contrast X-ray imaging of preterm piglets placed in lateral recumbence for taking the X-ray picture **(A)**. The figure also shows a stomach filled with contrast solution **(B1, B2)**, contrast reaching the caecum **(C1, C2)**, and contrast in colon and rectum with a near-empty small intestine **(D1, D2)**. Upper panel: 4 days of age; lower panel: 18 days of age.

(**Table 1**), while colon weight tended to be higher in near-term piglets. For preterm piglets there was a tendency for contrast to leave the stomach at a slower rate compared with near-term piglets (StEmpty, HR: 0.67, 95%CI [0.24, 1.09], $p = 0.1$, **Figure 2A**). Time for contrast to leave the small intestine was faster in preterm piglets than in near-term piglets (SIEmpty, HR:0.52, 95%CI [0.15,0.88], $p < 0.01$, **Figure 2B**), while there were no differences in the time to reach caecum (ToCaecum, HR: 1.32, 95%CI [0.52, 2.11], $p = 0.4$) or rectum (ToRectum, HR:1.34, 95%CI [0.34,2.41], $p = 0.5$). The contrast passage rate through the colon (CaecumToRectum) was slower in preterm vs. near-term piglets ($p < 0.05$).

Study 2: Bovine Colostrum vs. Formula for Preterm Piglets

There were limited differences between the two diets with regards meconium passage, residuals and intestinal weights on day 5 (**Table 1**). The intestinal length was greater in formula-fed piglets. On day 4, similar values across the diets were found for stomach emptying time (StEmpty, HR:0.97, 95%CI [0.41, 1.52]), $p = 0.9$), emptied small intestine (SiEmpty, HR:0.64, 95%CI [0.08, 1.20], $p = 0.2$) and time to reach to rectum (ToRectum, HR:0.85, 95%CI [0.135, 1.56], $p = 0.7$). Contrast passage rate was faster in the formula-fed piglets compared with colostrum-fed piglets (ToCecum, HR:0.61, 95%CI [0.25, 0.96], $p = 0.03$, **Figure 2C**). Likewise, the contrast passage rate through the colon region (CaecumToRectum) was faster in formula-fed vs. colostrum-fed piglets ($p < 0.05$, paired McNemar test).

Study 3: Preterm Piglets Tested on Day 4 and 18, With and Without Milk Fortification

Nutrient fortification increased the growth of preterm piglets, also inducing higher relative weights and lengths of the small intestine, together with larger gastric residuals on day 19 (**Table 1**). On day 4, time for contrast to leave the stomach was slower compared with day 18 ($p < 0.05$). There were no differences in time for the contrast to reach cecum or rectum between day 4 and 18 (ToCeacum, $p = 0.3$ and ToRectum, $p = 0.2$). However, the calculated colon transit time was slower in day 4 piglets compared with day 18 ($p < 0.05$, CaecumToRectum) when assessing the time to events. For comparison between the dilute and the fortified cow's milk, the stomach emptying time (StEmpty, day 4: HR:0.83, 95%CI [0.13, 1.78], $p = 0.7$; day 18: HR: 0.49, 95%CI [0, 1.60], $p = 0.4$), intestinal transit time (Tocecum, day 4: HR:0.67, 95%CI [0.07, 1.42], $p = 0.4$; day 18: HR:3.58, 95%CI [0–25.5], $p = 0.8$), and time to reach to rectum (ToRectum, day4: HR:2.16, 95%CI [0.05, 4.37], $p = 0.3$; day 18: HR: 1.79, 95%CI [0.7,4.3], $p = 0.5$) were similar between the two groups on day 4 and day 18.

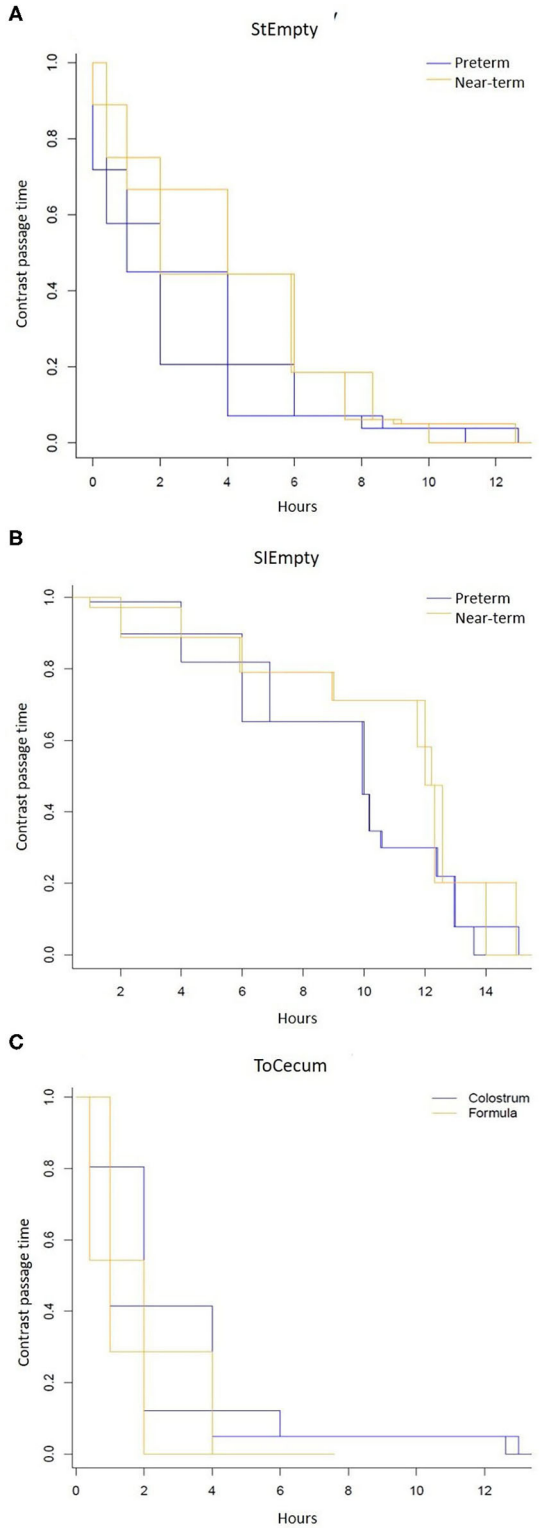

FIGURE 2 | Contrast passage rate measured by serial of x-ray images after intake of contrast solution in 4 d-old immature piglets. **(A)** Stomach emptying time (StEmpty) in preterm and near-term piglets. **(B)** Small intestinal emptying time (SIEmpty) in preterm and near-term piglets. **(C)** Time for the contrast to reach the caecum (ToCaecum) in piglets fed formula or bovine colostrum.

DISCUSSION

Feeding intolerance (FI) and poor gastrointestinal motility is a challenge in the clinical care of preterm infants. Adverse clinical conditions, such as sepsis or gut inflammatory reactions, potentially leading to NEC, affect intestinal motility patterns, as

indicated in our previous study (20). On the other hand, poor gut motility, and impaired food passage may be an inherent sign of physiological immaturity at birth, independent of clinical conditions and diseases, predisposing to large gastric residuals, NEC and sepsis. These interacting factors are difficult to study in infants. Using preterm piglets as a model, we now demonstrate that contrast passage rate is influenced by gestational age at birth, type of milk diet and postnatal age. We conclude that contrast X-ray imaging is a feasible method to investigate food transit rate in piglets, demonstrating region-dependent effects of gestational age at birth, postnatal age and milk diets. This adds information to the few studies in preterm infants on this topic, using a range of other methods (11–14).

Preterm piglets tended to empty their stomach at a slower rate than piglets born close to term. This result concurs with some previous infant perfusion manometry studies (4), indicating maturational changes in proximal gut motility with increasing gestational age at birth (2), and the common clinical observation of feeding intolerance, with large pre-feeding gastric residuals, in the early life of very preterm infants. Likewise, the slower contrast passage rate through the colon in preterm vs. near-term pigs may reflect the frequently reported risk of constipation in preterm infants, reflecting poor hind gut motility (24). Conversely, the faster passage rate through the small intestine in preterm vs. near-term individuals may reflect an inability of the immature intestine to promote an adequately controlled intestinal motility pattern, allowing maximal nutrient absorption, thereby predisposing to nutrient maldigestion (25).

Stomach and colon transit times were longer in piglets shortly after birth, relative to later (day 4 vs. 18), indicating maturational changes, and possibly feeding effects, also in preterm pigs. The results are in accordance with a study in preterm infants, showing that volume, and content of enteral intake increase the frequency of stool passage, independent of the digestibility of the enteral diet (26). Using ultra-sonographic imaging, one preterm infant study showed that bovine-milk-based fortified mother's milk reduced stomach emptying time (27). We observed more gastric residuals in fortified piglets (bovine milk fortified with bovine colostrum) but no difference in stomach emptying time assessed by x-ray contrast imaging. This may reflect that both diet type and density, together with maturation of intestinal motility pattern, affect food passage rates. We cannot exclude that motility effects of bovine colostrum differ from those of standard fortifiers, and the nature of the base diet may also be important (e.g., bovine milk vs. human milk). An ongoing infant study using bovine-colostrum-based fortifier to human milk may help to answer some questions for preterm infants (28).

In the first days after preterm birth, previous studies show that bovine colostrum improves gut functions in pigs, relative to formula, as assessed by less gastric residuals, improved digestive enzyme activities, immunological functions and NEC resistance (7). In this study, we observed no diet-related differences in intestinal wet weight but a longer intestine in formula-fed pigs. This may reflect a longer and thinner intestine in piglets fed formula, consistent with previous observations of structural changes in the gut of formula- vs. colostrum-fed piglets (29). Further, we found no effect of colostrum on contrast passage rate through the gut across piglets without NEC lesions. Since we assessed only healthy preterm piglets, this might indicate that previous observations of altered motility in formula-fed animals that developed mild NEC symptoms, could be a direct result of NEC development and the associated pro-inflammatory effects, rather than a specific effect of diet composition (20, 30). An ongoing clinical trial in preterm infants will help to show if bovine colostrum or formula, used in the first feeds after preterm birth, when mother's own milk is not available, influence gastric residuals, bowel habits, constipation and time to full enteral feeding (ClinicalTrials.gov Identifier: NCT03085277).

In infants, carmine red has been used in several studies to investigate the total transit time through the GIT (12). However, this approach does not accurately reflect food transit, but rather transit of the marker compound used. Furthermore, the osmolarity of the compound and the composition of the nutrient intake (orally or via a feeding tube) may impact the results obtained. In our study, we investigated the total transit time, i.e., from the first intake of our non-absorbable contrast solution (Iodixanol) to its entry into the rectum. We found that intake of contrast affected the fecal score and increased the transit time, indicating that the contrast solution itself may affect the total transit time. The osmolarity of the solution used in this study was 290 mOsm/L (unpublished observations) and therefore comparable to mother's milk (277-303 mOsm/l (31). Its chemical carrier constituents include mainly calcium and sodium which should not have notable direct gut osmotic effects or increase the fecal score, although such effects cannot be excluded (32). Digestive effects of a contrast or color solution are avoided when using Tc^{99m}-DTPA scintigraphy that have also been used for preterm infants (13), despite the ethical limitations in using radioactive constituents. Most scientific methodologies related to gut motility and food passage studies in preterm infants, from color markers to use of serial X-rays or radiolabeled components, have ethical constraints that limits their use in clinical practice.

We used preterm piglets as a model for preterm infants because they show many similarities to infants in their complications after preterm birth, including maldigestion, poor respiration, brain defects, high NEC sensitivity and a degree of feeding intolerance with large gastric residuals (16, 20, 33, 34). The model has translational limitations, not only because preterm piglet anatomy and physiology may differ from infants (e.g., a relatively long small intestine and high NEC sensitivity) but also because serial X-rays are required to accurately assess the passage of contrast through the entire gut. Regardless, preterm piglets may be used effectively to study in detail the influence of medical, nutritional and disease-related factors that affect enteral feeding tolerance and the important transition from parenteral to full enteral feeding in immature newborn infants. We conclude that gestational age at birth, postnatal age, and milk diet influence intestinal motility in piglets, as evaluated by contrast passage rate and X-ray images. The method used was feasible and provided novel information about regional intestinal motility but may not be applicable to human preterm infants. Regardless, there is a great need to investigate different aspects of intestinal motility and food passage rate in human preterm infants, considering the important clinical problem of both primary (immaturity) or

secondary (response to complications) intestinal dysmotility in preterm infants.

DATA AVAILABILITY STATEMENT

The raw data supporting the conclusions of this article will be made available by the authors, without undue reservation.

ETHICS STATEMENT

The animal study was reviewed and approved by National Committee on Animal Experimentation, Denmark.

AUTHOR CONTRIBUTIONS

SK, PS, and LA: conception and design and data interpretation. SK, CF, MG, and LA: data acquisition. TS: data analysis. SK: writing original draft. TS, PS, and LA: critical review and editing. All authors are approval of the final manuscript.

FUNDING

The NEOCOL project granted by Innovation Fund Denmark (NEOCOL Project No. 6150-00004B) and a Ph.D. scholarship from University of Copenhagen (SK).

ACKNOWLEDGMENTS

We would like to thank Thomas Thymann, Elin Skytte, Jane C. Povlsen, Line Møller Willumsen, Wenchao Chen, Marit Navis, Ole Bæk, Agnethe Ahnfeldt, Yanqi Li, Xiaoyu Pan, and Kristina Møller from Comparative Pediatrics and Nutrition for technical support with animal and x-ray procedures.

REFERENCES

1. Berseth CL. Gastrointestinal motility in the neonate. *Clin Perinatol*. (1996) 23:179–90. doi: 10.1016/S0095-5108(18)30237-9
2. Berseth CL. Gestational evolution of small intestine motility in preterm and term infants. *J Pediatr*. (1989) 115:646–51. doi: 10.1016/S0022-3476(89)80302-6
3. Jadcherla SR, Berseth C. Chapter 3 - Development of gastrointestinal motility reflexes. In: Neu J, editor. *Gastroenterology and Nutrition: Neonatology Questions and Controversies*, Second Ed. Philadelphia: W.B. Saunders (2012), p. 27–37. doi: 10.1016/B978-1-4377-2603-9.00003-X
4. Berseth CL. Effect of early feeding on maturation of the preterm infant's small intestine. *J Pediatr*. (1992) 120:947–53. doi: 10.1016/S0022-3476(05)81969-9
5. Berseth CL, Nordyke CK, Valdes MG, Furlow BL, Go VL. Responses of gastrointestinal peptides and motor activity to milk and water feedings in preterm and term infants. *Pediatr Res*. (1992) 31:587–90. doi: 10.1203/00006450-199206000-00010
6. Jensen ML, Sangild PT, Lykke M, Schmidt M, Boye M, Jensen BB, et al. Similar efficacy of human banked milk and bovine colostrum to decrease incidence of necrotizing enterocolitis in preterm piglets. *Am J Physiol Regulat Integrat Comparat Physiol*. (2013) 305:R4–12. doi: 10.1152/ajpregu.00094.2013
7. Shen RL, Thymann T, Ostergaard MV, Stoy AC, Krych L, Nielsen DS, et al. Early gradual feeding with bovine colostrum improves gut function and NEC resistance relative to infant formula in preterm pigs. *Am J Physiol Gastrointest Liver Physiol*. (2015) 309:G310–323. doi: 10.1152/ajpgi.00163.2015
8. Rasmussen SO, Martin L, Østergaard MV, Rudloff S, Li Y, Roggenbuck M, et al. Bovine colostrum improves neonatal growth, digestive function, and gut immunity relative to donor human milk and infant formula in preterm pigs. *Am J Physiol Gastrointestinal Liver Physiol*. (2016) 311:G480–91. doi: 10.1152/ajpgi.00139.2016
9. Bekkali N, Hamers SL, Reitsma JB, Van Toledo L, Benninga MA. Infant stool form scale: development and results. *J Pediatr. (*2009) 154:521–6.e521. doi: 10.1016/j.jpeds.2008.10.010
10. Ahnfeldt AM, Bæk O, Hui Y, Nielsen CH, Obelitz-Ryom K, Busk-Anderson T, et al. Nutrient restriction has limited short-term effects on gut, immunity, and brain development in preterm pigs. *J Nutrit*. (2020) 150:1196–207. doi: 10.1093/jn/nxaa030
11. Berseth CL. Assessment in intestinal motility as a guide in the feeding management of the newborn. *Clin Perinatol*. (1999) 26:1007–15. doi: 10.1016/S0095-5108(18)30032-0
12. Mcclure RJ, Newell SJ. Randomised controlled trial of trophic feeding and gut motility. *Arch Dis Child Fetal Neonatal Ed*. (1999) 80:F54–58. doi: 10.1136/fn.80.1.F54
13. Bodé S, Dreyer M, Greisen G. Gastric emptying and small intestinal transit time in preterm infants: a scintigraphic method. *J Pediatr Gastroenterol Nutr*. (2004) 39:378–82. doi: 10.1097/00005176-200410000-00014
14. Gathwala G, Shaw C, Shaw P, Yadav S, Sen J. Human milk fortification and gastric emptying in the preterm neonate. *Int J Clin Pract*. (2008) 62:1039–43. doi: 10.1111/j.1742-1241.2006.01201.x
15. Hiorns M. Gastrointestinal tract imaging in children: current techniques. *Pediatr Radiol*. (2011) 41:42–54. doi: 10.1007/s00247-010-1743-2
16. Sangild PT, Thymann T, Schmidt M, Stoll B, Burrin DG, Buddington RK. Invited Review: The preterm pig as a model in pediatric gastroenterology. *J Animal Sci*. (2013) 91:4713–29. doi: 10.2527/jas.2013-6359
17. Li Y, Pan X, Nguyen DN, Ren S, Moodley A, Sangild PT. Bovine colostrum before or after formula feeding improves systemic immune protection and gut function in newborn preterm pigs. *Front Immunol*. (2019) 10:3062–2. doi: 10.3389/fimmu.2019.03062
18. Bæk O, Ren S, Brunse A, Sangild PT, Nguyen DN. Impaired neonatal immunity and infection resistance following fetal growth restriction in preterm pigs. *Front Immunol*. (2020) 11:1808. doi: 10.3389/fimmu.2020.01808
19. Kilkenny C, Browne WJ, Cuthill IC, Emerson M, Altman DG. Improving bioscience research reporting: the ARRIVE guidelines for reporting animal research. *PLoS Biol*. (2010) 8:e1000412. doi: 10.1371/journal.pbio.1000412
20. Chen W, Sun J, Kappel SS, Gormsen M, Sangild PT, Aunsholt L. Gut transit time, using radiological contrast imaging, to predict early signs of necrotizing enterocolitis. *Pediatr Res*. (2020). doi: 10.1038/s41390-020-0871-0
21. Jiangsu S. *The Statistical Analysis of Interval-censored Failure Time Data*. USA: Springer (2006).
22. Clifford A-B. icenReg: regression models for interval censored data in R. *J. Stat. softw*. (2017) 81:1–23. doi: 10.18637/jss.v081.i12
23. Greenland S, Senn SJ, Rothman KJ, Carlin JB, Poole C, Goodman SN, et al. Statistical tests, P values, confidence intervals, and power: a guide to misinterpretations. *Eur J Epidemiol*. (2016) 31:337–50. doi: 10.1007/s10654-016-0149-3
24. Bekkali N, Moesker FM, Van Toledo L, Reitsma JB, Hamers SL, Valerio PG, et al. Bowel habits in the first 24 months of life: preterm- versus term-born infants. *J Pediatr Gastroenterol Nutr*. (2010) 51:753–8. doi: 10.1097/MPG.0b013e3181d7c809
25. Demers-Mathieu V, Qu Y, Underwood MA, Borghese R, Dallas DC. Premature infants have lower gastric digestion capacity for human milk proteins than term infants. *J Pediatr Gastroenterol Nutr*. (2018) 66:816–21. doi: 10.1097/MPG.0000000000001835
26. Weaver LT, Lucas A. Development of bowel habit in preterm infants. *Arch Dis Child*. (1993) 68:317–20. doi: 10.1136/adc.68.3_Spec_No.317

27. Perrella SL, Hepworth AR, Simmer KN, Geddes DT. Influences of breast milk composition on gastric emptying in preterm infants. *J Pediatr Gastroenterol Nutr*. (2015) 60:264–71. doi: 10.1097/MPG.0000000000000596
28. Ahnfeldt AM, Hyldig N, Li Y, Kappel SS, Aunsholdt L, Sangild PT, et al. FortiColos - a multicentre study using bovine colostrum as a fortifier to human milk in very preterm infants: study protocol for a randomised controlled pilot trial. *Trials*. (2019) 20:279. doi: 10.1186/s13063-019-3367-7
29. Sangild PT, Siggers RH, Schmidt M, Elnif J, Bjornvad CR, Thymann T, et al. Diet- and colonization-dependent intestinal dysfunction predisposes to necrotizing enterocolitis in preterm pigs. *Gastroenterology*. (2006) 130:1776–92. doi: 10.1053/j.gastro.2006.02.026
30. Cao M, Andersen AD, Li Y, Thymann T, Jing J, Sangild PT. Physical activity and gastric residuals as biomarkers for region-specific NEC lesions in preterm neonates. *Neonatology*. (2016) 110:241–7. doi: 10.1159/000445707
31. Almeida MBDM, Gomes Júnior SC, Silva JBD, Silva DD, Moreira MEL. Osmolality analysis of human milk and an infant formula with modified viscosity for use in infants with dysphagia. *Revista CEFAC*. (2018) 20:770–7. doi: 10.1590/1982-021620182064218
32. Ozturk U, Sungur MA, Karakas T, Mulayim K, Ozturk P. Acute generalized exanthematous pustulosis induced by iodixanol. (Visipaque): a serious reaction to a commonly used drug. *Cutaneous Ocular Toxicol*. (2015) 34:344–6. doi: 10.3109/15569527.2014.961071
33. Markova V, Holm C, Pinborg AB, Thomsen LL, Moos T. Impairment of the developing human brain in iron deficiency: correlations to findings in experimental animals and prospects for early intervention therapy. *Pharmaceuticals (Basel)*. (2019) 12.
34. Kappel SS, Sangild PT, Hilsted L, Hartmann B, Thymann T, Aunsholt L. Gastric residual to predict necrotizing enterocolitis in preterm piglets as models for infants. *JPEN J Parenter Enteral Nutr*. (2020). doi: 10.1002/jpen.1814

Conflict of Interest: The authors declare that the research was conducted in the absence of any commercial or financial relationships that could be construed as a potential conflict of interest.

frontiers in Pediatrics

ORIGINAL RESEARCH
published: 22 January 2021
doi: 10.3389/fped.2020.593802

Intrauterine *Gardnerella vaginalis* Infection Results in Fetal Growth Restriction and Alveolar Septal Hypertrophy in a Rabbit Model

Fook-Choe Cheah[1], Chee Hoe Lai[1], Geok Chin Tan[2], Anushia Swaminathan[1], Kon Ken Wong[3], Yin Ping Wong[2] and Tian-Lee Tan[1]*

[1] Department of Pediatrics, Universiti Kebangsaan Malaysia Medical Center, Kuala Lumpur, Malaysia, [2] Department of Pathology, Universiti Kebangsaan Malaysia Medical Center, Kuala Lumpur, Malaysia, [3] Department of Microbiology, Universiti Kebangsaan Malaysia Medical Center, Kuala Lumpur, Malaysia

Background: *Gardnerella vaginalis* (GV) is most frequently associated with bacterial vaginosis and is the second most common etiology causing intrauterine infection after *Ureaplasma urealyticum*. Intrauterine GV infection adversely affects pregnancy outcomes, resulting in preterm birth, fetal growth restriction, and neonatal pneumonia. The knowledge of how GV exerts its effects is limited. We developed an *in vivo* animal model to study its effects on fetal development.

Materials and Methods: A survival mini-laparotomy was conducted on New Zealand rabbits on gestational day 21 (28 weeks of human pregnancy). In each dam, fetuses in the right uterine horn received intra-amniotic 0.5×10^2 colony-forming units of GV injections each, while their littermate controls in the left horn received sterile saline injections. A second laparotomy was performed seven days later. Assessment of the fetal pups, histopathology of the placenta and histomorphometric examination of the fetal lung tissues was done.

Results: Three dams with a combined total of 12 fetuses were exposed to intra-amniotic GV, and 9 fetuses were unexposed. The weights of fetuses, placenta, and fetal lung were significantly lower in the GV group than the saline-inoculated control group [mean gross weight, GV (19.8 ± 3.8 g) vs. control (27.9 ± 1.7 g), $p < 0.001$; mean placenta weight, GV (5.5 ± 1.0 g) vs. control (6.5 ± 0.7 g), $p = 0.027$; mean fetal lung weight, GV (0.59 ± 0.11 g) vs. control (0.91 ± 0.08 g), $p = 0.002$. There was a two-fold increase in the multinucleated syncytiotrophoblasts in the placenta of the GV group than their littermate controls (82.9 ± 14.9 vs. 41.6 ± 13.4, $p < 0.001$). The mean alveolar septae of GV fetuses was significantly thicker than the control (14.8 ± 2.8 μm vs. 12.4 ± 3.8 μm, $p = 0.007$). Correspondingly, the proliferative index in the interalveolar septum was 1.8-fold higher in the GV group than controls (24.9 ± 6.6% vs. 14.2 ± 2.9%, $p = 0.011$). The number of alveoli and alveolar surface area did not vary between groups.

Discussion: Low-dose intra-amniotic GV injection induces fetal growth restriction, increased placental multinucleated syncytiotrophoblasts and fetal lung re-modeling characterized by alveolar septal hypertrophy with cellular proliferative changes.

OPEN ACCESS

Edited by:
Heber C. Nielsen, Tufts Medical Center, United States

Reviewed by:
Kazumichi Fujioka, Kobe University, Japan
Cherry Wongtrakool, Emory University, United States

****Correspondence:***
Fook-Choe Cheah
cheahfc@ppukm.ukm.edu.my

Specialty section:
This article was submitted to Neonatology, a section of the journal Frontiers in Pediatrics

Received: *11 August 2020*
Accepted: *16 December 2020*
Published: *22 January 2021*

Citation:
Cheah F-C, Lai CH, Tan GC, Swaminathan A, Wong KK, Wong YP and Tan T-L (2021) Intrauterine Gardnerella vaginalis Infection Results in Fetal Growth Restriction and Alveolar Septal Hypertrophy in a Rabbit Model. Front. Pediatr. 8:593802. doi: 10.3389/fped.2020.593802

Conclusion: This intra-amniotic model could be utilized in future studies to elucidate the acute and chronic effects of GV intrauterine infections.

Keywords: bacterial vaginosis, intrauterine growth restriction, bronchopulmonary dysplasia, intra-amniotic, rabbit model, multinucleated syncytiotrophoblasts, fetal lung development, intrauterine infection

INTRODUCTION

Gardnerella vaginalis (GV) is the first bacterium found to play a significant role in bacterial vaginosis (BV), which is a dysbiosis of the vaginal microflora that affects 4.7–58.3% of the female population worldwide, particularly in females of reproductive age (1, 2). The majority of women who harbor GV frequently remain untreated unless they developed severe symptoms (3, 4). Therefore, a significant proportion of women may carry this organism while they are pregnant. The high recurrence rate further complicates the course of GV infection (5).

GV infection during the perinatal period is becoming increasingly important as it is associated with unfavorable outcomes for both the mother and growing fetus (2). It is the second most common etiology of intrauterine infection (6–8) and is associated with an increased risk of preterm birth, spontaneous abortion, and maternal infection (9, 10). Postnatally, several neonatal cases of invasive GV infection causing pneumonia, meningitis, osteomyelitis, septicemia, and death had been reported (11–16).

Besides, GV-associated BV served as an independent risk factor for low in birthweight infants and was responsible for as much as 56% of pregnancies complicated with intrauterine growth restriction (IUGR) (17). Some potential mechanisms which could limit the intrauterine fetal growth include placenta dysfunction, thrombosis of the placenta vessels, and tissue necrosis (18). In humans, a prominent histopathological feature in the placenta of IUGR infant is the increase in syncytial knots (19, 20). The syncytial knot (SK) is characterized by a clustering of five or more syncytiotrophoblast nuclei that bulge on top of the normal villous surface. It is presently uncertain whether intrauterine GV infection may be associated with a similar histological change that may explain the underlying cause of IUGR in such cases.

Intrauterine infection also has an impact on the developing fetal lung (21–23). In animal models, the intra-amniotic injection of *Ureaplasma urealyticum*, *Escherichia coli,* and bacterial lipopolysaccharide were associated with histomorphometric lung changes that resemble bronchopulmonary dysplasia (BPD) (24–26). BPD is a chronic lung disease which primarily affects preterm infants and results in significant morbidity and mortality (27). A recent systematic review concluded that exposure to intrauterine inflammation is associated with a higher risk of developing BPD (28). Nevertheless, the impact of intrauterine GV infection on the development of the fetal lung remains unclear.

Various animal models of intrauterine infection/inflammation have been created to study the effects of pathogens/toxins on the developing fetus (10, 24). In this study, we developed a rabbit model by directly inoculating GV into the amniotic cavity to study its effects on the developing fetus. As opposed to intravaginal inoculation, the direct intra-amniotic route overcomes the issue of vaginal flora variation across species (29–31). Besides, studies have shown that the direct intra-amniotic inoculation of bacteria produces more apparent effects as compared to the deposition of bacteria into the placenta-decidual interface (32–34). Titration of the doses and approach used are crucial to study a specific pathology and reduce attrition from overwhelming infection causing animal deaths (10). As such, we introduced the lowest dose of GV to ensure survival and studied the pathological effects to the fetus after the insult and clearance of the infection.

The female rabbit has a bicornuate duplex uterus, characterized by two completely separated uterine horns with a cervix each. This unique anatomy allows fetuses in one horn to be used as the control littermates for the other horn's as intervention. The littermate-controlled experimental design ensures the standardization of genetic profile, environmental background, and intrauterine condition.

MATERIALS AND METHODS

Animal

Three timed-pregnant New Zealand white rabbits (*Oryctolagus cuniculus*) were obtained from the animal farm of Broga Hill (Selangor, Malaysia), where they were born and bred. They were housed in the experimental facility of the Laboratory Animal Resource Unit (LARU), Universiti Kebangsaan Malaysia under standard care conditions, and fed rabbit chow *ad libitum*. The sample size obtained was 21 (12 in GV-inoculated group; nine in the saline-inoculated group), and based on the "resource equation" calculation formula [degree of freedom, E = total number of animal – total number of groups], the $E = 19$ was in the optimal range of 10–20 and this number was considered adequate (35).

The study protocol and sample size were approved by the Universiti Kebangsaan Malaysia Animal Ethics Committee (UKMAEC) (approval code: FP/PAED/2012/CHEAH/26-SEPTEMBER/460-NOVEMBER-2012-NOVEMBER-2014), and all procedures were conducted in compliance with the Malaysian Code of Practice for the Care and Use of Animals for Scientific Purposes. This novel animal model design is registered under the copyright reference number: UKM.IKB.800-4/1/1084.

Surgical Procedure and Intra-amniotic Inoculation of GV

The pregnant dams were subjected to a surviving mini-laparotomy surgery on day 21 of gestation (equivalent to 28 weeks human gestation). They were anesthetized with intravenous xylazine 5 mg/kg and ketamine 35 mg/kg via the marginal ear vein, placed supine and prepared in a sterile field. The fur at the surgical area was shaved, and the skin was scrubbed with povidone–iodine. A lower midline mini-laparotomy (incision

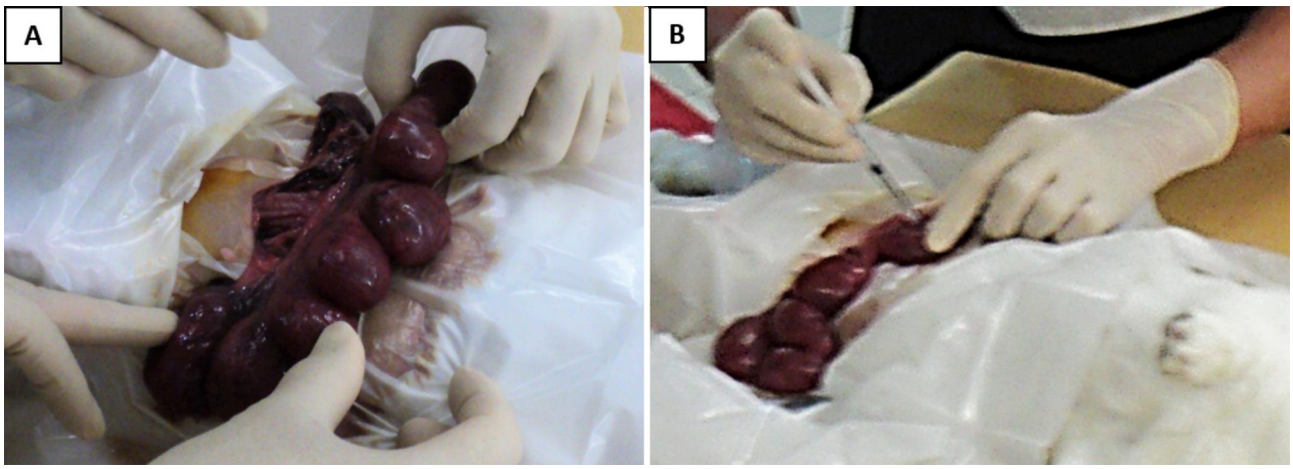

FIGURE 1 | Intra-amniotic injection of GV. **(A)** Following the laparotomy procedure, the gravid uterine horns were externalized and examined. **(B)** Injection was performed directly into the amniotic sac surrounding each of the fetus, with either 0.5×10^2 CFU of GV or sterile saline. The injection was done at a site to avoid hitting the placenta and fetal parts.

size: 1–1.5 in.) was then performed, exposing the two uterine horns. The uterine horns were carefully externalized from the abdominal cavity, and the number of viable fetuses in each horn was identified (**Figure 1A**). The fetuses were assigned to two experimental groups based on the position of the uterine horn. With prefilled standard insulin syringes, the amniotic cavity of fetuses on the right uterine horn was injected with 0.5 mL volume containing GV (10^2 colony-forming units per mL; ATCC 14018) suspended in Hank's Balanced Salt Solution (HBSS) (Gibco, Massachusetts, United States). As controls, the amniotic cavity of fetuses on the left horn was each injected with 0.5 mL sterile HBSS (**Figure 1B**). The site of injection was observed for any leakage and sealed with an adhesion spray if necessary. Routine layered abdominal wall closure was performed. Meanwhile, the remaining aliquot of GV suspension was sent to the laboratory to confirm bacterial viability and back-culture quantification.

Upon recovery from the surgery, the dams were housed in individual cages with 12/12 light cycles and *ad libitum* access to a commercially-available pellet diet and sterile water for the next seven days. The animals were examined daily for wound healing and signs of preterm labor.

The dams were subjected to the second laparotomy on day 28 of gestation (equivalent to 37–38 weeks human gestation). Once sedated, the abdominal and uterine walls were sectioned, the fetuses and placenta were removed. The amniotic fluid surrounding each of the fetuses was gently dabbed onto a sterile cotton swab and sent for culture. At the end of the surgery, the dams and fetuses were humanely euthanized with a lethal dose of xylazine-ketamine mixture (2 mL/kg). Each fetus and placenta were weighed individually. The lungs and placenta were harvested and prepared for the various tissue analyses.

Preparation of GV Suspension

Gardnerella vaginalis (ATCC 14018) was used as stock in this model of intrauterine infection. The Gardnerella selective Columbia Blood Agar with sheep blood (Thermo Scientific, Massachusetts, United States) was streaked with GV from the bacteria stock and incubated for 48 h in a 5% CO_2 atmosphere at 37°C. A 50 mL centrifuge tube was filled with 20 mL of Mueller Hinton Broth (MHB), and a sterile cotton swab was used to roll on the GV colonies on the agar plate and transferred into the MHB to make the inoculum. The concentration of bacteria per mL of the inoculum was determined using a spectrophotometer. The inoculum was then centrifuged, and the bacteria were pelleted down. The supernatant was discarded, and the remaining pellet in the 50 mL centrifuge tube was mixed with 2 mL HBSS (Gibco, Massachusetts, United States). A concentration of 10^2 CFU/mL of GV suspended in HBSS was used for intrauterine inoculation.

In optimizing the dose of inoculum, the lower dose of 10^2 CFU/mL of GV was used based upon our preliminary results that showed intrauterine inoculation with a higher concentration of GV (10^3 and 10^4 CFU/mL) brought about unacceptably high mortality for both the dams and fetuses.

The volume for intraamniotic injection was 0.5 mL, as a volume of more than 0.5 mL resulted in a higher incidence of leakage, resulting in sepsis and mortality to the dams.

Tissue Processing for Histomorphometry and Histopathology

The placenta was fixed in 4% paraformaldehyde (PFA4%) solution, dehydrated, and embedded in paraffin wax. The placenta tissues were sectioned (3–5 μm thickness) and stained using a standard hematoxylin and eosin (H&E) protocol. The slides were evaluated for the inflammatory infiltrates, edema, and necrosis. Aggregation of syncytial nuclei forming multinucleated cells was observed and quantified by counting the number of cells in five different high power fields (HPF; 400x) for each specimen. The average number per HPF was then calculated. An additional macrophage marker antibody MAC387 (Abcam, Cambridge, United Kingdom) staining was performed.

For fetal lung fixation, a 50 cm^3 syringe was filled with 30 mL of chilled PFA4%, and the lungs were placed carefully into a syringe after first removing the plunger. The plunger was then reinserted, excess air expelled and the syringe tip occluded with a stopper. The syringe plunger was drawn with about 15 pulls to create a vacuum to inflate the alveoli for better lung fixation. The tissue was rinsed, dehydrated and embedded in paraffin wax. The lung tissue was then sectioned and stained by routine H&E staining protocol.

The lung morphometry assessment was carried out to assess the number of alveoli, alveolar surface area, and the thickness of alveolar septae. Five random non-overlapping HPF were viewed and measurements taken for each tissue section. Firstly, the number of alveoli was recorded. The alveolar area and the alveolar septal thickness were assessed using the DP2-BSW software (Olympus Corporation, Tokyo, Japan). The average alveolar surface area was determined by the sum of all closed areas, divided by the number of alveoli. The mean alveolar septal thickness was calculated from the average of three thickest septae.

Immunohistochemical Staining of the Lung Tissue

Lung tissues were sectioned at 4 μm thickness and stained with mouse monoclonal Ki-67 antibody (Dako, Glostrup, Denmark) diluted 1:200. The DAKO ARK™ (Animal Research Kit) (Dako, California, United States) detection was used according to the manufacturer's instructions. Briefly, the sections were deparaffinized and dehydrated with xylene and graded alcohols. Antigen retrieval was carried out by heating for 30 min at 110°C in Tris-EDTA solution pH 9, followed by peroxidase blocking to quench endogenous peroxidase. Sections were then incubated for 15 min with the prepared biotinylated primary antibody, followed by streptavidin-peroxidase incubation for 15 min. Finally, 3,3′Diaminobenzidine (DAB) substrate chromogen was applied onto the sections for 5 min and counterstained with Mayer's Hematoxylin solution.

Three random fields of each lung tissue section were image-captured using high magnification (400×) with a B×40 microscope (Olympus Corporation, Tokyo, Japan). Two hundred nuclei in each field were counted manually, and a total of 600 nuclei per tissue section were analyzed. An average percentage of positively stained cells for every 100 nuclei were calculated as the proliferation index.

Statistical Analysis

The Shapiro–Wilk test was applied to assess the normality of data. The mean differences between groups were compared with an unpaired two-tailed Student's *t*-test. The results were expressed as mean ± SD. All statistical analyses were performed with SPSS 22.0 (PASW Statistics, Chicago, USA). The *p*-values of <0.05 were considered to be statistically significant.

RESULTS

Animal Survival and Clearance of GV in Amniotic Fluid After 7 Days of Inoculation

In the experiment, all dams and their fetuses were alive at day 28 of gestation. There was neither preterm labor nor complications of the surgical procedure observed. Of note, no GV was cultured from the amniotic fluid of any of these fetuses after 7 days of inoculation. In contrast, all the bacterial cultures used to inoculate in the preceding 7 days when back-cultured were confirmed positive and yielded 10^2 CFU/mL of GV in each sample.

GV Infection Associated With Decreased Gross Body, Lung, and Placenta Weights

The weight of fetuses in the GV was significantly lower as compared to their littermate controls (mean gross weight, 19.8 ± 3.8 g vs. 27.9 ± 1.7 g, respectively, $p < 0.001$). The fetal lung weight was also significantly lower in the GV as compared with their littermate controls (mean fetal lung weight, 0.59 ± 0.11 g vs. 0.91 ± 0.08 g, respectively; $p = 0.002$). The placenta weight in GV infection was significantly lower as compared to the controls (mean placenta weight, 5.5 ± 1.0 g vs. 6.5 ± 0.7 g, respectively, $p = 0.027$) (**Table 1**).

GV Infection Increases Multinucleated Syncytiotrophoblasts in the Placenta

Microscopically, the histological characteristics of inflammation were not evident in the placenta tissues. However, the number of multinucleated syncytiotrophoblasts per HPF was two-fold higher in the placenta of fetuses exposed to GV than those unexposed (mean cell count per HPF, 83 ± 15 vs. 42 ± 13, respectively, $p < 0.001$). These cells display condensed nuclei without prominent nucleoli, and the surface macrophage marker, MAC387, were negative, together these are characteristics of the multinucleated syncytiotrophoblasts, also present and usually recognized as syncytial knots in the human equivalent (**Figure 2**).

GV Infection Increases the Alveolar Septal Thickness and Proliferative Index in the Lung Interstitium

The alveolar septa measured in the fetuses of the GV infected was approximately 1.2-fold thicker than the control group (**Table 2**). Ki-67 immunohistochemical study revealed that the proliferative index (PI) in the interalveolar septum was 1.8-fold higher in the GV than the control group (**Table 2**). The lung histology and immunohistochemical staining of Ki-67 antibody were illustrated in **Figure 3**.

The histology of lung tissue revealed no alveolar or interstitial inflammation in the GV and control group. The total number of alveoli and their total surface area did not vary between groups (**Table 2**).

DISCUSSION

In this study, we demonstrated that intrauterine GV infection was associated with features indicative of fetal growth restriction, lower gross body, lung, and placenta weights. This is consistent with previous studies on GV infection during pregnancy (36, 37). We found the fetal growth restriction was associated with increased multinucleated cells in the placenta of the GV-inoculated group, which has not been previously reported. These multinucleated cells also exhibited condensed nuclei

TABLE 1 | Comparison of the gross body, lung weights of fetuses, and the placental weights in gram (g) between saline-inoculated and GV-inoculated pregnant rabbits.

Weights, g		Saline (n =9)	GV (n = 12)	p-value
Fetuses Gross body	Dam 1	30.0 28.0 28.0 27.0	14.0 22.0 21.0 22.0	
	Dam 2	25.0 28.0 26.0	15.0 16.0 23.0 21.0	
	Dam 3	30.0 29.0	22.0 15.0 26.0 21.0	
Mean gross body (SD)		27.9 (1.7)	19.8 (3.8)	<0.001
Fetuses Lung	Dam 1	1.00 0.82 1.00 0.92	0.60 0.70 0.60 0.61	
	Dam 2	0.81 0.90 1.00	0.45 0.63 0.72 0.60	
	Dam 3	0.90 0.85	0.55 0.42 0.81 0.50	
Mean fetal lung (SD)		0.91 (0.08)	0.59 (0.11)	0.002
Placenta,	Dam 1	8.0 6.0 6.5 6.0	4.5 5.5 7.0 7.5	
	Dam 2	6.8 6.0 6.5	5.0 4.5 5.5 5.0	
	Dam 3	6.5 7.0	5.5 4.3 6.5 5.5	
Mean placenta (SD)		6.5 (0.7)	5.5 (1.0)	0.027

GV, Gardnerella vaginalis.

and absent nucleoli which appear similar to syncytial knots (SK) in the human placenta. They are pathognomonic of syncytiotrophoblast apoptosis (38, 39), and are present in cases of infants born as IUGR (19, 20, 38). How SKs are formed are still not clearly understood (40). Histologically, they display condensed nuclei, no nucleoli, and devoid of transcriptional activity (41–43). SKs are generally an indicator of placenta aging, and an excessive number of SKs is suggestive of uteroplacental malperfusion (40, 44). The presence of multinucleated cells resembling SK had also been previously reported in the rabbit model of toxemia (45).

We speculate with infection, the direct insult to the trophoblasts could be mediated by the Toll-like Receptor-2 (TLR-2), which is expressed on the trophoblastic membrane (46, 47). TLR-2 recognizes the bacterial peptidoglycan and lipoteichoic acid, which are present on the bacterial wall of GV (47, 48). The ligation of TLR-2 activates MyD88/FADD-dependent caspases and/or NF-kappaB signaling pathways, which lead to cell death (49, 50) and the inflammation cascade. Moreover, *in vitro* peptidoglycan treatment on human trophoblastic cells resulted in a dose-dependent increase in cell apoptosis (50). The next phase of our study will include determination of the inter-related mechanisms underlying these observations.

In addition, intrauterine infection may affect placenta vasculogenesis (51–53). Altered placental vascular re-modeling, causing reduced perfusion and oxygen transport across the feto-maternal interface were observed in animal studies (54, 55). The dysregulation of several angiogenic mediators accompanied by uteroplacental malperfusion leads to hypoxia and adverse pregnancy outcomes (52, 56–58). The hypoxia-inducible factor 1α (HIF-1α) mediates cell apoptosis (59, 60), transcribes upregulation of anti-angiogenic mediators, e.g., sFlt-1 (61), that were increased in the placenta of IUGR infants (62, 63).

The increased SKs observed with GV infection implicates trophoblastic dysfunction and apoptosis, reducing the functional mass of the placenta, thus limiting nutrient transport and restricting intrauterine fetal growth (64). Even so, Burton et al. (40) reported that multinucleated syncytiotrophoblasts, important in placental development, may consist of sprouts. The increased numbers of these cells on the other hand may thus signify trophoblastic proliferative response to an increased need from the insult inflicted by GV.

We noted that there was no viable GV recovered from the amniotic fluid after 7 days of inoculation. The possible explanation could be clearance of the organism by the host immune response. In McDuffie et al. (37) study on chronic chorioamnionitis, a decreasing trend in the amniotic fluid positive cultures of GV from day four through six after inoculation, may support the role of host immune response in eradicating the organisms from the amniotic cavity with time. Additionally, our preliminary experiments with a higher dose of GV led to an increased demise of the dams and rates of abortion. Two earlier studies had used the intrauterine infection model to investigate the impact of higher doses of GV during pregnancy. Field et al. (36) endoscopically inoculated a relatively high concentration of GV into the uterine horns of pregnant rabbits and reported a significantly lower live birth rate (80 vs. 90%), lower live birthweight (12.82 g vs. 16.82 g) and more neuronal necrosis (60 vs. 0%) in GV-inoculated rabbits as compared to the saline-inoculated control. Nearly a decade later, McDuffie et al. (37) used a similar animal model and found a positive association between the duration of infection with the amniotic fluid proinflammatory cytokine (TNF-α) levels and fetal brain histological index scores. In both studies, high dose GV resulted in 20% abortion and 10% preterm labor (31, 36, 65).

In using a relatively lower concentration of inoculum but injected direct intra-amniotically, our study produced a 100% survival rate without any preterm birth or spontaneous abortion.

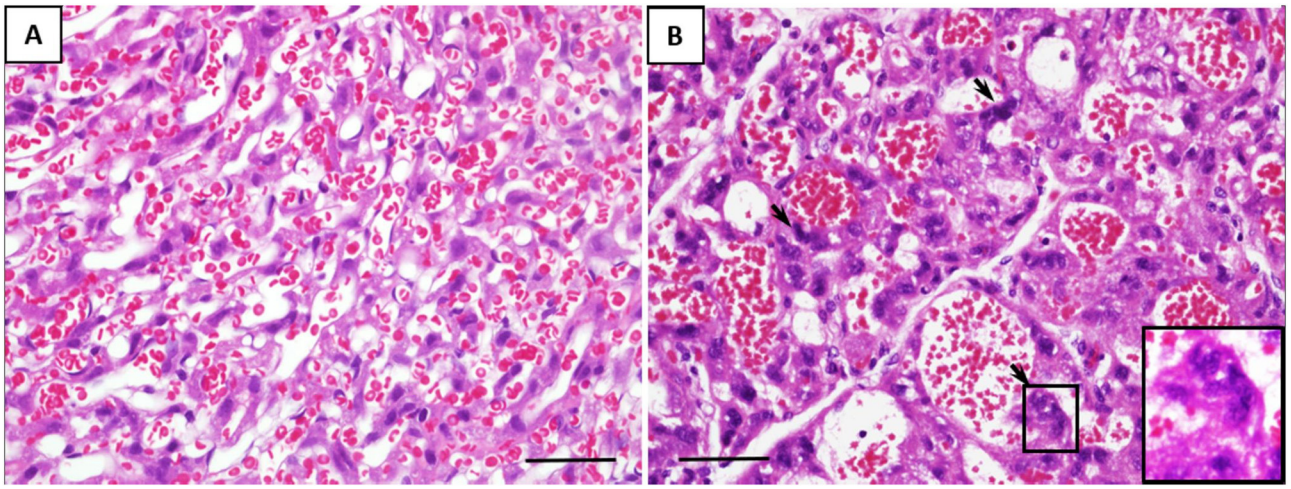

FIGURE 2 | Representative histological changes of the placenta from **(A)** saline-inoculated and **(B)** GV-inoculated groups. GV exposed cases showed dilated vascular spaces and a significant increase in multinucleated syncytiotrophoblasts (arrows). These cells stained negative for the macrophage marker MAC387 (scale bar = 100 μm).

TABLE 2 | Comparison of the fetal lung histomorphometry indices between saline-inoculated and GV-inoculated pregnant rabbits.

Lung indices	Saline	GV	*p*-value
Alveoli number, *n**	15 (3)	14 (3)	0.260
Alveolar surface area, μm^2	1,792.1 (1,006.2)	1,806.0 (1,060.7)	0.800
Alveolar septa thickness, μm	12.4 (3.8)	14.8 (2.8)	0.007
Interstitium—Proliferative index, %	14.2 (2.9)	24.9 (6.6)	0.011

**This number was the average of the total number of alveoli counted in five random non-overlapping high power field (400×).*
Values are expressed as mean (SD).
GV, Gardnerella vaginalis.

A lower dose of GV at 0.5×10^2 CFU, although eventually cleared by the host immune system, could have exerted injury to the fetal organs in the process (66). Changes to the placenta have been discussed above, but we also observed effects on the developing fetal lung. The lungs of low dose GV-infected fetuses demonstrated a significant degree of septal thickening as a result of increased cellular proliferation in the lung interstitium. Several preclinical models of intrauterine infection with low dose pathogens also yielded similar lung histopathology, which resembled the features of BPD in humans (24–26). Intrauterine infection has been shown to induce cellular proliferation via the effects of proinflammatory cytokine. Interleukin 1 beta (IL-1beta) is one of the central cytokines which has been implicated in the pathogenesis of BPD (67–70). The lung of IL-1beta-expressing gene-targeted mice revealed increased alveolar septal thickness accompanied with abnormal deposition of elastin in the interstitium (70) disrupting the lung morphogenesis. Moreover, prophylactic subcutaneous injection of IL-1 receptor antagonists (IL-1Ra) has been shown to prevent the BPD-like lung changes in the mice exposed to intrauterine LPS and postnatal hyperoxia (71). Our results showed unremarkable alteration in the number of alveoli and the total alveolar surface area with GV infection that are features of alveolar simplification reported in the "new BPD" (72). Future studies sufficiently powered with the appropriate sample size are necessary to confirm if these findings are induced with GV infection.

Antigen Ki-67 is a nuclear protein that is associated with cellular proliferation, and as such any cellular mitosis will display a high number of Ki-67. In this study, we demonstrated an increase in the proliferative cell index in the lung interstitium. Lung interstitial cells are derived from the mesenchyme and play a crucial role in alveolarization, along with the epithelium (73). Myofibroblast is the major interstitial cell that is critically involved in secondary septation and alveolarization. The dysregulation of myofibroblast has been implicated in the development of BPD (73, 74). Myofibroblasts markedly decreased after the alveolarization phase, and their persistent high numbers is associated with fibrotic lung diseases (75, 76). The regulatory pathways of myofibroblast during the different phases of lung development are still unclear. We are pursuing further studies to determine if lower dose of GV infection induced an increased interstitial lung myofibroblast activity resulting in alveolar septal hypertrophy. This may potentially impede alveolar gaseous exchange and predispose to pulmonary hypertension, features commonly associated with BPD.

Future studies with this model are in the planning to determine the signaling pathways involved leading to the multinucleated syncytiotrophoblasts formation and alveolar septal hypertrophy. Specific cell staining for alveolar type I, II pneumocytes, interstitial myofibroblasts, vascular bundles,

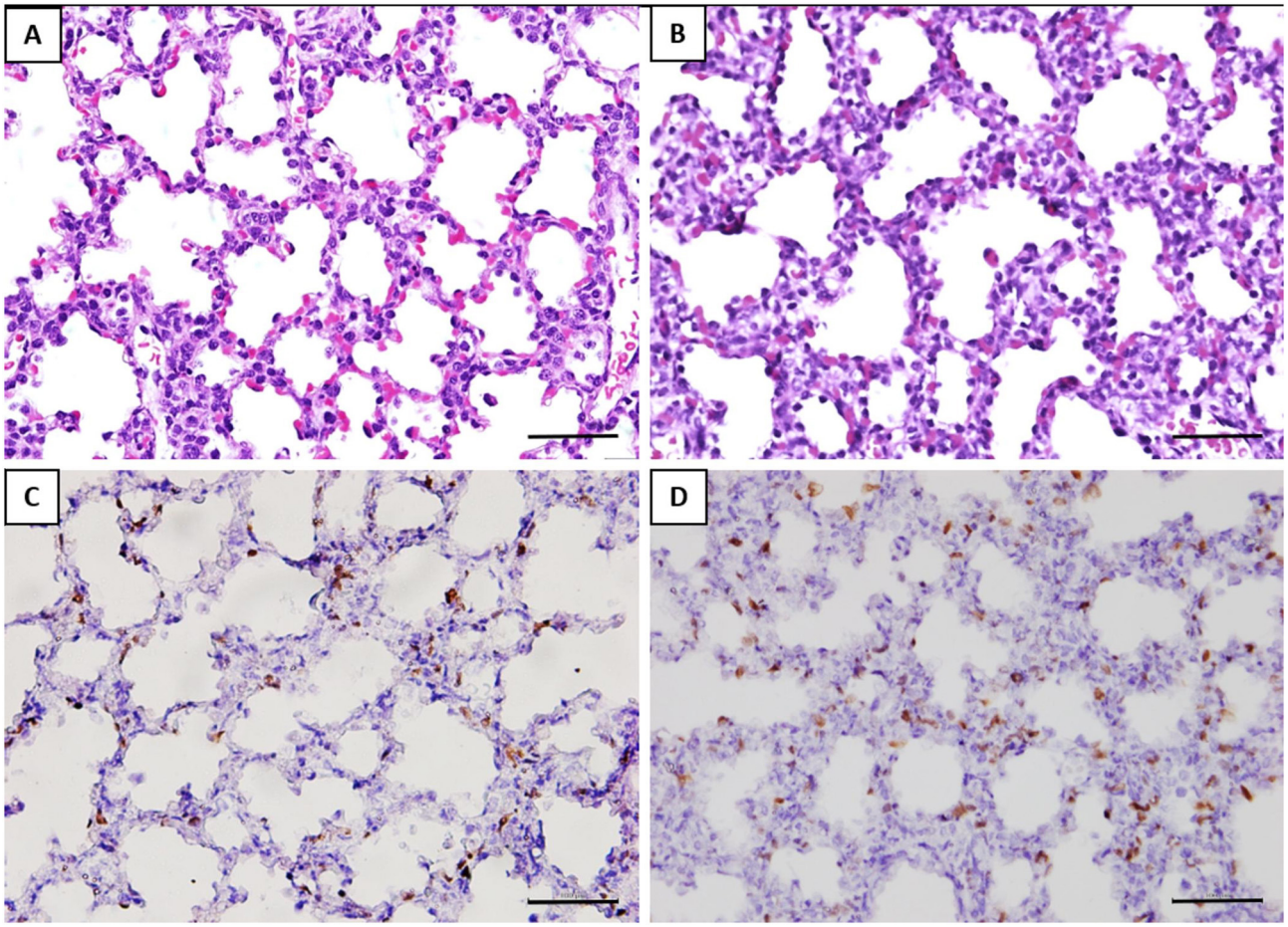

FIGURE 3 | Histomorphometry and immunostaining of the fetal lung with or without exposure to GV. H&E staining of **(A)** saline-inoculated group **(B)** GV-inoculated group. The alveolar septae in the GV-inoculated group were thicker as compared to the saline-inoculated group (scale bar = 100 μm). There was no inflammatory cell infiltration observed in the alveoli or lung interstitium in both groups. Immunohistochemical staining showed significantly more Ki-67 positive cells in the interalveolar septae of fetal lungs in the **(D)** GV-inoculated group than **(C)** saline-inoculated group (scale bar = 100 μm).

and extracellular matrix composition could provide additional insights to the current understanding on the pathogenicity of intrauterine GV infection in modifying fetal lung growth. It would also be valuable to study the postnatal functional outcomes of these fetuses with abnormal growth and lung development.

CONCLUSION

In conclusion, low dose intrauterine GV infection leads to fetal growth restriction, increased placenta multinucleated syncytiotrophoblasts, and disrupted lung morphogenesis with alveolar septal hypertrophy. These findings may lead to studies in human pregnancies to determine if antenatal GV infection with and without treatment similarly results in fetal growth restriction and alveolar septal re-modeling that predisposes to BPD development.

DATA AVAILABILITY STATEMENT

The original contributions presented in the study are included in the article/supplementary materials, further inquiries can be directed to the corresponding author/s.

ETHICS STATEMENT

The animal study was reviewed and approved by Universiti Kebangsaan Malaysia Animal Ethics Committee (UKMAEC).

AUTHOR CONTRIBUTIONS

F-CC designed and created the animal model and was the principal investigator of the study. CL coordinated the breeding, rearing of the rabbits, fine-tuning of the model, and executed majority of the animal experiments. All authors have made a substantial contribution to the research work and manuscript

preparation and reviewed and approved the final version of the manuscript.

FUNDING

This study was funded by the Universiti Kebangsaan Malaysia Research University Grant (DIP-2012-025). The funder had no role in the study design, data collection and analysis, decision to publish, or preparation of the manuscript.

ACKNOWLEDGMENTS

We wish to convey our gratitude to the staff members of the anatomy, pathology and microbiology departments of the Universiti Kebangsaan Malaysia Medical Center for their diligent assistance rendered in this research project. Our gratitude in particular to Mrs. Nur Aqilah Kamaruddin, Mr. Muaatamarulain Mustangin and Mr. Mike Low Kiat Cheong for their technical assistance and advice.

REFERENCES

1. Kenyon C, Colebunders R, Crucitti T. The global epidemiology of bacterial vaginosis: a systematic review. *Am J Obstet Gynecol*. (2013) 209:505–23. doi: 10.1016/j.ajog.2013.05.006
2. Wong YP, Tan GC, Wong KK, Anushia S, Cheah FC. *Gardnerella vaginalis* in perinatology: an overview of the clinicopathological correlation. *Malays J Pathol*. (2018) 40:267–86.
3. Hartmann AA, Elsner P. [*Gardnerella vaginalis* infection—another sexually transmitted disease]. Der Hautarzt; Zeitschrift fur Dermatologie, Venerologie, und verwandte Gebiete. *Hautarzt*. (1984) 35:512–6.
4. Janulaitiene M, Paliulyte V, Grinceviciene S, Zakareviciene J, Vladisauskiene A, Marcinkute A, et al. Prevalence and distribution of *Gardnerella vaginalis* subgroups in women with and without bacterial vaginosis. *BMC Infect Dis*. (2017) 17:394. doi: 10.1186/s12879-017-2501-y
5. Bradshaw CS, Morton AN, Hocking J, Garland SM, Morris MB, Moss LM, et al. High recurrence rates of bacterial vaginosis over the course of 12 months after oral metronidazole therapy and factors associated with recurrence. *J Infect Dis*. (2006) 193:1478–86. doi: 10.1086/503780
6. Hillier SL, Witkin SS, Krohn MA, Watts DH, Kiviat NB, Eschenbach DA. The relationship of amniotic fluid cytokines and preterm delivery, amniotic fluid infection, histologic chorioamnionitis, and chorioamnion infection. *Obstet Gynecol*. (1993) 81:941–8.
7. Goldenberg RL, Hauth JC, Andrews WW. Intrauterine infection and preterm delivery. N *Engl J Med*. (2000) 342:1500–7. doi: 10.1056/NEJM200005183422007
8. Romero R, Mazor M. Infection and preterm labor. *Clin Obstet Gynecol*. (1988) 31:553–84. doi: 10.1097/00003081-198809000-00006
9. Leitich H, Bodner-Adler B, Brunbauer M, Kaider A, Egarter C, Husslein P. Bacterial vaginosis as a risk factor for preterm delivery: a meta-analysis. *Am J Obstet Gynecol*. (2003) 189:139–47. doi: 10.1067/mob.2003.339
10. Galinsky R, Polglase GR, Hooper SB, Black MJ, Moss TJ. The consequences of chorioamnionitis: preterm birth and effects on development. *J Pregnancy*. (2013) 2013:412831. doi: 10.1155/2013/412831
11. Platt MS. Neonatal *Hemophilus vaginalis* (Corynebacterium vaginalis) infection. *Clin Pediatr (Phila)*. (1971) 10:513–6. doi: 10.1177/000992287101000907
12. Venkataramani TK, Rathbun HK. Corynebacterium vaginale (*Hemophilus vaginalis*) bacteremia: clinical study of 29 cases. *Johns Hopkins Med J*. (1976) 139:93–7.
13. Nightingale LM, Eaton CB, Fruehan AE, Waldman JB, Clark WB, Lepow ML. Cephalhematoma complicated by osteomyelitis presumed due to *Gardnerella vaginalis*. *Jama*. (1986) 256:1936–7. doi: 10.1001/jama.1986.03380140106032
14. Furman LM. Neonatal *Gardnerella vaginalis* infection. *Pediatr Infect Dis J*. (1988) 7:890. doi: 10.1097/00006454-198807120-00019
15. Berardi-Grassias L, Roy O, Berardi JC, Furioli J. Neonatal meningitis due to *Gardnerella vaginalis*. *Eur J Clin Microbiol Infect Dis*. (1988) 7:406–7. doi: 10.1007/BF01962348
16. Amaya RA, Al-Dossary F, Demmler GJ. *Gardnerella vaginalis* bacteremia in a premature neonate. *J Perinatol*. (2002) 22:585–7. doi: 10.1038/sj.jp.7210757
17. Svare JA, Schmidt H, Hansen BB, Lose G. Bacterial vaginosis in a cohort of Danish pregnant women: prevalence and relationship with preterm delivery, low birthweight and perinatal infections. *BJOG*. (2006) 113:1419–25. doi: 10.1111/j.1471-0528.2006.01087.x
18. Vedmedovska N, Rezeberga D, Donder GGG. Is abnormal vaginal microflora a risk factor for intrauterine fetal growth restriction? *Asian Pac J Reprod*. (2015) 4:313–6. doi: 10.1016/j.apjr.2015.07.010
19. Hansen AR, Collins MH, Genest D, Heller D, Shen-Schwarz S, Banagon P, et al. Very low birthweight placenta: clustering of morphologic characteristics. *Pediatr Dev Pathol*. (2000) 3:431–8. doi: 10.1007/s100249910044
20. Hecht JL, Allred EN, Kliman HJ, Zambrano E, Doss BJ, Husain A, et al. Histological characteristics of singleton placentas delivered before the 28th week of gestation. *Pathology*. (2008) 40:372–6. doi: 10.1080/00313020802035865
21. Mir IN, Chalak LF, Brown LS, Johnson-Welch S, Heyne R, Rosenfeld CR, et al. Impact of multiple placental pathologies on neonatal death, bronchopulmonary dysplasia, and neurodevelopmental impairment in preterm infants. *Pediatr Res*. (2020) 87:885–91. doi: 10.1038/s41390-019-0715-y
22. Watterberg KL, Demers LM, Scott SM, Murphy S. Chorioamnionitis and early lung inflammation in infants in whom bronchopulmonary dysplasia develops. *Pediatrics*. (1996) 97:210–5.
23. Hallman M, Lappalainen U, Bry K. Clearance of intra-amniotic lung surfactant: uptake and utilization by the fetal rabbit lung. *Am J Physiol*. (1997) 273(1 Pt 1):L55–63. doi: 10.1152/ajplung.1997.273.1.L55
24. Kramer BW, Kallapur S, Newnham J, Jobe AH. Prenatal inflammation and lung development. *Semin Fetal Neonatal Med*. (2009) 14:2–7. doi: 10.1016/j.siny.2008.08.011
25. Pan J, Zhan C, Yuan T, Wang W, Shen Y, Sun Y, et al. Effects and molecular mechanisms of intrauterine infection/inflammation on lung development. *Respir Res*. (2018) 19:93. doi: 10.1186/s12931-018-0787-y
26. Viscardi RM, Atamas SP, Luzina IG, Hasday JD, He JR, Sime PJ, et al. Antenatal *Ureaplasma urealyticum* respiratory tract infection stimulates proinflammatory, profibrotic responses in the preterm baboon lung. *Pediatr Res*. (2006) 60:141–6. doi: 10.1203/01.pdr.0000228322.73777.05
27. Jensen EA, Schmidt B. Epidemiology of bronchopulmonary dysplasia. *Birth Defects Res A Clin Mol Teratol*. (2014) 100:145–57. doi: 10.1002/bdra.23235
28. Villamor-Martinez E, Alvarez-Fuente M, Ghazi AMT, Degraeuwe P, Zimmermann LJI, Kramer BW, et al. Association of chorioamnionitis with bronchopulmonary dysplasia among preterm infants: a systematic review, meta-analysis, and metaregression. *JAMA Netw Open*. (2019) 2:e1914611. doi: 10.1001/jamanetworkopen.2019.14611
29. Spear GT, Gilbert D, Sikaroodi M, Doyle L, Green L, Gillevet PM, et al. Identification of rhesus macaque genital microbiota by 16S pyrosequencing shows similarities to human bacterial vaginosis: implications for use as an animal model for HIV vaginal infection. *AIDS Res Hum Retroviruses*. (2010) 26:193–200. doi: 10.1089/aid.2009.0166
30. Uchihashi M, Bergin IL, Bassis CM, Hashway SA, Chai D, Bell JD. Influence of age, reproductive cycling status, and menstruation on the vaginal microbiome in baboons (*Papio anubis*). *Am J Primatol*. (2015) 77:563–78. doi: 10.1002/ajp.22378
31. Gibbs RS, McDuffie RS Jr, Kunze M, Barr JM, Wolf DM, Sze CI, et al. Experimental intrauterine infection with *Prevotella bivia* in New Zealand White rabbits. *Am J Obstet Gynecol*. (2004) 190:1082–6. doi: 10.1016/j.ajog.2003.10.700
32. Kim CJ, Romero R, Chaemsaithong P, Chaiyasit N, Yoon BH, Kim YM. Acute chorioamnionitis and funisitis: definition, pathologic features,

and clinical significance. *Am J Obstet Gynecol.* (2015) 213(4 Suppl.):S29–52. doi: 10.1016/j.ajog.2015.08.040
33. Steel JH, Malatos S, Kennea N, Edwards AD, Miles L, Duggan P, et al. Bacteria and inflammatory cells in fetal membranes do not always cause preterm labor. *Pediatr Res*. (2005) 57:404–11. doi: 10.1203/01.PDR.0000153869.96337.90
34. Grigsby PL, Novy MJ, Adams Waldorf KM, Sadowsky DW, Gravett MG. Choriodecidual inflammation: a harbinger of the preterm labor syndrome. *Reprod Sci*. (2010) 17:85–94. doi: 10.1177/1933719109348025
35. Charan J, Kantharia ND. How to calculate sample size in animal studies? *J Pharmacol Pharmacother*. (2013) 4:303–6. doi: 10.4103/0976-500X.119726
36. Field NT, Newton ER, Kagan-Hallet K, Peairs WA. Perinatal effects of *Gardnerella vaginalis* deciduitis in the rabbit. *Am J Obstet Gynecol.* (1993) 168(3 Pt 1):988–94. doi: 10.1016/S0002-9378(12)90858-3
37. McDuffie RS Jr., Kunze M, Barr J, Wolf D, Sze CI, Shikes R, et al. Chronic intrauterine and fetal infection with *Gardnerella vaginalis*. *Am J Obstet Gynecol*. (2002) 187:1263–6. doi: 10.1067/mob.2002.127129
38. Levy R, Smith SD, Yusuf K, Huettner PC, Kraus FT, Sadovsky Y, et al. Trophoblast apoptosis from pregnancies complicated by fetal growth restriction is associated with enhanced p53 expression. *Am J Obstet Gynecol*. (2002) 186:1056–61. doi: 10.1067/mob.2002.122250
39. Furukawa S, Kuroda Y, Sugiyama A. A comparison of the histological structure of the placenta in experimental animals. *J Toxicol Pathol.* (2014) 27:11–8. doi: 10.1293/tox.2013-0060
40. Burton GJ, Jones CJ. Syncytial knots, sprouts, apoptosis, and trophoblast deportation from the human placenta. *Taiwanese J Obstetr Gynecol*. (2009) 48:28–37. doi: 10.1016/S1028-4559(09)60032-2
41. Fogarty NM, Ferguson-Smith AC, Burton GJ. Syncytial knots (Tenney-Parker changes) in the human placenta: evidence of loss of transcriptional activity and oxidative damage. *Am J Pathol.* (2013) 183:144–52. doi: 10.1016/j.ajpath.2013.03.016
42. Stanek J. Hypoxic patterns of placental injury: a review. *Arch Pathol Lab Med*. (2013) 137:706–20. doi: 10.5858/arpa.2011-0645-RA
43. Parks WT. Increased syncytial knot formation. In: Khong TY, Mooney EE, Nikkels PGJ, Morgan TK, Gordijn SJ, editors. *Pathology of the Placenta: A Practical Guide*. Cham: Springer International Publishing (2019). p. 131–7.
44. Loukeris K, Sela R, Baergen R. Syncytial knots as a reflection of placental maturity: reference values for 20 to 40 weeks' gestational age. *Pediatr Dev Pathol.* (2009) 13:305–9. doi: 10.2350/09-08-0692-OA.1
45. Abitbol MM, Driscoll SG, Ober WB. Placental lesions in experimental toxemia in the rabbit. *Am J Obstet Gynecol*. (1976) 125:942–8. doi: 10.1016/0002-9378(76)90493-2
46. Holmlund U, Cebers G, Dahlfors AR, Sandstedt B, Bremme K, Ekstrom ES, et al. Expression and regulation of the pattern recognition receptors Toll-like receptor-2 and Toll-like receptor-4 in the human placenta. *Immunology*. (2002) 107:145–51. doi: 10.1046/j.1365-2567.2002.01491.x
47. Koga K, Mor G. Toll-like receptors at the maternal-fetal interface in normal pregnancy and pregnancy disorders. *Am J Reprod Immunol*. (2010) 63:587–600. doi: 10.1111/j.1600-0897.2010.00848.x
48. Sadhu K, Domingue PA, Chow AW, Nelligan J, Cheng N, Costerton JW. *Gardnerella vaginalis* has a gram-positive cell-wall ultrastructure and lacks classical cell-wall lipopolysaccharide. *J Med Microbiol*. (1989) 29:229–35. doi: 10.1099/00222615-29-3-229
49. Aliprantis AO, Yang RB, Weiss DS, Godowski P, Zychlinsky A. The apoptotic signaling pathway activated by Toll-like receptor-2. *EMBO J*. (2000) 19:3325–36. doi: 10.1093/emboj/19.13.3325
50. Abrahams VM, Bole-Aldo P, Kim YM, Straszewski-Chavez SL, Chaiworapongsa T, Romero R, et al. Divergent trophoblast responses to bacterial products mediated by TLRs. *J Immunol*. (2004) 173:4286–96. doi: 10.4049/jimmunol.173.7.4286
51. Girardi G, Yarilin D, Thurman JM, Holers VM, Salmon JE. Complement activation induces dysregulation of angiogenic factors and causes fetal rejection and growth restriction. *J Exp Med.* (2006) 203:2165–75. doi: 10.1084/jem.20061022
52. McDonald CR, Cahill LS, Gamble JL, Elphinstone R, Gazdzinski LM, Zhong KJY, et al. Malaria in pregnancy alters L-arginine bioavailability and placental vascular development. *Sci Transl Med*. (2018) 10:eaan6007. doi: 10.1126/scitranslmed.aan6007
53. Weckman AM, Ngai M, Wright J, McDonald CR, Kain KC. The impact of infection in pregnancy on placental vascular development and adverse birth outcomes. *Front Microbiol*. (2019) 10:1924. doi: 10.3389/fmicb.2019.01924
54. Conroy AL, Silver KL, Zhong K, Rennie M, Ward P, Sarma JV, et al. Complement activation and the resulting placental vascular insufficiency drives fetal growth restriction associated with placental malaria. *Cell Host Microbe*. (2013) 13:215–26. doi: 10.1016/j.chom.2013.01.010
55. Phillips P, Brown MB, Progulske-Fox A, Wu XJ, Reyes L. Porphyromonas gingivalis strain-dependent inhibition of uterine spiral artery remodeling in the pregnant rat. *Biol Reprod.* (2018) 99:1045–56. doi: 10.1093/biolre/ioy119
56. Darling AM, McDonald CR, Conroy AL, Hayford KT, Liles WC, Wang M, et al. Angiogenic and inflammatory biomarkers in midpregnancy and small-for-gestational-age outcomes in Tanzania. *Am J Obstet Gynecol*. (2014) 211: 509.e1–e8. doi: 10.1016/j.ajog.2014.05.032
57. Conroy AL, McDonald CR, Gamble JL, Olwoch P, Natureeba P, Cohan D, et al. Altered angiogenesis as a common mechanism underlying preterm birth, small for gestational age, and stillbirth in women living with HIV. *Am J Obstet Gynecol*. (2017) 217:684.e1–e17. doi: 10.1016/j.ajog.2017.10.003
58. Straughen JK, Misra DP, Helmkamp L, Misra VK. Preterm delivery as a unique pathophysiologic state characterized by maternal soluble FMS-like tyrosine kinase 1 and uterine artery resistance during pregnancy: a longitudinal cohort study. *Reprod Sci*. (2017) 24:1583–9. doi: 10.1177/1933719117698574
59. Bakker WJ, Harris IS, Mak TW. FOXO3a is activated in response to hypoxic stress and inhibits HIF1-induced apoptosis via regulation of CITED2. *Mol Cell*. (2007) 28:941–53. doi: 10.1016/j.molcel.2007.10.035
60. Zhang Z, Huang C, Wang P, Gao J, Liu X, Li Y, et al. HIF1alpha affects trophoblastic apoptosis involved in the onset of preeclampsia by regulating FOXO3a under hypoxic conditions. *Mol Med Rep*. (2020) 21:2484–92. doi: 10.3892/mmr.2020.11050
61. Tal R, Shaish A, Barshack I, Polak-Charcon S, Afek A, Volkov A, et al. Effects of hypoxia-inducible factor-1alpha overexpression in pregnant mice: possible implications for preeclampsia and intrauterine growth restriction. *Am J Pathol*. (2010) 177:2950–62. doi: 10.2353/ajpath.2010.090800
62. Yinon Y, Nevo O, Xu J, Many A, Rolfo A, Todros T, et al. Severe intrauterine growth restriction pregnancies have increased placental endoglin levels: hypoxic regulation via transforming growth factor-beta 3. *Am J Pathol*. (2008) 172:77–85. doi: 10.2353/ajpath.2008.070640
63. Nevo O, Many A, Xu J, Kingdom J, Piccoli E, Zamudio S, et al. Placental expression of soluble fms-like tyrosine kinase 1 is increased in singletons and twin pregnancies with intrauterine growth restriction. *J Clin Endocrinol Metab*. (2008) 93:285–92. doi: 10.1210/jc.2007-1042
64. Scifres CM, Nelson DM. Intrauterine growth restriction, human placental development and trophoblast cell death. *J Physiol.* (2009) 587(Pt 14):3453–8. doi: 10.1113/jphysiol.2009.173252
65. Yoon BH, Kim CJ, Romero R, Jun JK, Park KH, Choi ST, et al. Experimentally induced intrauterine infection causes fetal brain white matter lesions in rabbits. *Am J Obstetr Gynecol*. (1997) 177:797–802. doi: 10.1016/S0002-9378(97)70271-0
66. Knox CL, Dando SJ, Nitsos I, Kallapur SG, Jobe AH, Payton D, et al. The severity of chorioamnionitis in pregnant sheep is associated with *in vivo* variation of the surface-exposed multiple-banded antigen/gene of *Ureaplasma parvum*. *Biol Reprod*. (2010) 83:415–26. doi: 10.1095/biolreprod.109.083121
67. Rindfleisch MS, Hasday JD, Taciak V, Broderick K, Viscardi RM. Potential role of interleukin-1 in the development of bronchopulmonary dysplasia. *J Interferon Cytokine Res*. (1996) 16:365–73. doi: 10.1089/jir.1996.16.365
68. Cayabyab RG, Jones CA, Kwong KY, Hendershott C, Lecart C, Minoo P, et al. Interleukin-1beta in the bronchoalveolar lavage fluid of premature neonates: a marker for maternal chorioamnionitis and predictor of adverse neonatal outcome. *J Matern Fetal Neonatal Med*. (2003) 14:205–11. doi: 10.1080/jmf.14.3.205.211
69. Bose CL, Dammann CE, Laughon MM. Bronchopulmonary dysplasia and inflammatory biomarkers in the premature neonate. *Arch Dis Child Fetal Neonatal Ed*. (2008) 93:F455–61. doi: 10.1136/adc.2007.121327
70. Ambalavanan N, Carlo WA, D'Angio CT, McDonald SA, Das A, Schendel D, et al. Cytokines associated with bronchopulmonary dysplasia or death in extremely low birth weight infants. *Pediatrics*. (2009) 123:1132–41. doi: 10.1542/peds.2008-0526

71. Nold MF, Mangan NE, Rudloff I, Cho SX, Shariatian N, Samarasinghe TD, et al. Interleukin-1 receptor antagonist prevents murine bronchopulmonary dysplasia induced by perinatal inflammation and hyperoxia. *Proc Natl Acad Sci USA*. (2013) 110:14384–9. doi: 10.1073/pnas.1306859110
72. Jobe AH. The new bronchopulmonary dysplasia. *Curr Opin Pediatr*. (2011) 23:167–72. doi: 10.1097/MOP.0b013e3283423e6b
73. Choi CW. Lung interstitial cells during alveolarization. *Korean J Pediatr*. (2010) 53:979–84. doi: 10.3345/kjp.2010.53.12.979
74. Kauffman SL, Burri PH, Weibel ER. The postnatal growth of the rat lung. II. Autoradiography. *Anat Rec*. (1974) 180:63–76. doi: 10.1002/ar.1091800108
75. Bland RD. Neonatal chronic lung disease in the post-surfactant era. *Biol Neonate*. (2005) 88:181–91. doi: 10.1159/000087581
76. Yamada M, Kurihara H, Kinoshita K, Sakai T. Temporal expression of alpha-smooth muscle actin and drebrin in septal interstitial cells during alveolar maturation. *J Histochem Cytochem*. (2005) 53:735–44. doi: 10.1369/jhc.4A6483.2005

Conflict of Interest: The authors declare that the research was conducted in the absence of any commercial or financial relationships that could be construed as a potential conflict of interest.

frontiers in Pediatrics

ORIGINAL RESEARCH
published: 04 February 2021
doi: 10.3389/fped.2020.595157

Acetate Downregulates the Activation of NLRP3 Inflammasomes and Attenuates Lung Injury in Neonatal Mice With Bronchopulmonary Dysplasia

Qian Zhang[1,2,3], *Xiao Ran*[1,2,3], *Yu He*[1,2,3], *Qing Ai*[1,2,3] *and Yuan Shi*[1,2,3]*

[1] Department of Neonatology, Children's Hospital of Chongqing Medical University, Chongqing, China, [2] Chongqing Key Laboratory of Pediatrics, Chongqing, China, [3] Ministry of Education Key Laboratory of Child Development and Disorders, National Clinical Research Center for Child Health and Disorders, China International Science and Technology Cooperation Base of Child Development and Critical Disorders, Chongqing, China

Background: Bronchopulmonary dysplasia (BPD) is a common pulmonary complication in preterm infants. Acetate is a metabolite produced by the gut microbiota, and its anti-inflammatory function is well known. The role of acetate in BPD has not been studied. Here, we investigate the effects of acetate on lung inflammation and damage in mice model of BPD.

Objective: To investigate the role of acetate in the development of BPD.

Methods: C57BL/6 mice were randomly divided into three groups on the 3rd day after birth: room air group, hyperoxia group, and hyperoxia + acetate (250 mM, 0.02 ml/g) group. The expression of inflammatory factors was determined by ELISA and RT-PCR, and NLRP3 and caspase-1 were detected by Western blot. High-throughput sequencing was used to detect bacterial communities in the mice intestines.

Results: After acetate treatment, the expression levels of TNF-α, IL-1β, IL-18, NLRP3, and caspase-1 were significantly reduced, while the expression of GPR43 was increased. In the BPD mice treated with acetate, the proportion of Escherichia-Shigella was lower than in placebo-treated BPD mice, while the abundance of Ruminococcus was increased.

Conclusions: These results indicate that acetate may regulate intestinal flora and reduce inflammatory reactions and lung injury in BPD. Therefore, acetate may be an effective drug to protect against neonatal BPD.

Keywords: GPR43, microbial communities, inflammasome, acetate, bronchopulmonary dysplasia

OPEN ACCESS

Edited by:
Henry J. Rozycki, Virginia Commonwealth University, United States

Reviewed by:
Rashmin C. Savani, University of Texas Southwestern Medical Center, United States
Peter Vitiello, University of Oklahoma Health Sciences Center, United States

***Correspondence:**
Yuan Shi
shiyuan@hospital.cqmu.edu.cn

Specialty section:
This article was submitted to Neonatology, a section of the journal Frontiers in Pediatrics

Received: *15 August 2020*
Accepted: *29 December 2020*
Published: *04 February 2021*

Citation:
Zhang Q, Ran X, He Y, Ai Q and Shi Y (2021) Acetate Downregulates the Activation of NLRP3 Inflammasomes and Attenuates Lung Injury in Neonatal Mice With Bronchopulmonary Dysplasia. Front. Pediatr. 8:595157. doi: 10.3389/fped.2020.595157

INTRODUCTION

Bronchopulmonary dysplasia (BPD) is the most common pulmonary complication of very premature birth (1), and its prevalence is increasing, most likely due to the prolonged survival of preterm infants (2). BPD is characterized by stunted development involving impaired alveolar and vascular growth (3, 4). In addition to preterm birth, inflammation and infection are all related to the

pathogenesis of BPD (4, 5). Pro-inflammatory factors such as tumor necrosis factor (TNF)-α and interleukin (IL)-1β have been associated with the development of BPD (3, 6, 7). Inflammasomes are a series of multiprotein complexes that modulate the innate immune responses (8). NLRP3 is the most commonly studied protein in the inflammasomes and activated by infection, tissue lesion and oxidative stress. Meanwhile, activation of NLRP3 could promote IL-1β and IL-18 secretion (9, 10). Many studies have shown that inflammasome activation is associated with various inflammatory disorders. Previous studies have shown that NLRP3 inflammasome plays an important role in the pathogenesis of BPD (11). Therefore, the regulation of NLRP3 activation may be a therapeutic target of BPD.

Acetate is produced by the intestinal flora, and well known for its anti-inflammatory function (12, 13). In most cases, acetate acts by binding to its receptor. G protein-coupled receptor 43 (GPR43) is the natural receptor for acetate (14). Antunes et al. (12) demonstrated that acetate activated and regulated type 1 responses in lung epithelial cells by GPR43 to prevent RSV infection. Another study showed that acetate binds to GPR43 to reduce the inflammasome in lipopolysaccharide (LPS)-induced endotoxemia through sAC-PKA (15). Despite the acetate have shown anti-inflammatory effects by regulating NLRP3 in several peritonitis models, its role in BPD remains unknown.

In this study, we investigated the effects of acetate on inflammation and lung damage in mice model of BPD and found that acetate intervention could alter the abundance of gut microbiota.

MATERIALS AND METHODS

Animal Model and Experimental Protocol

This study was approved by the Ethics Committee for Animal Protection and Use of Chongqing Children's Hospital. All C57BL/6 mice were purchased from Chongqing Medical University. Mice were housed under environmentally controlled conditions, and pregnant mice were kept in separate cages. All studies used newborn mice, and the number of pups in each litter was adjusted to 5–7 mice in each group to minimize the impact of nutritional differences on lung development. All mice were weighed on the day of birth and during modeling. According to the experimental conditions, newborn mice on postnatal day 3 (P3) were randomly divided into 3 groups (n = 5–7/group): room air (21% O_2) + placebo (phosphate-buffered saline, PBS) group, hyperoxia (85% O_2) + placebo (PBS) group, and hyperoxia (85% O_2) + acetate group. During continuous exposure to hyperoxia, acetate (250 mM, 0.02 ml/g) (15) was given daily for 14 consecutive days. The continuous exposure to 85%O_2 was achieved in a sealed oxygen chamber, and the oxygen concentration inside was continuously monitored with an oxygen meter. To avoid oxygen poisoning of nursing mothers, these mice were exchanged between the hyperoxia and room air conditions every 24 h.

Mouse Lung Tissue Harvesting

The mice were anesthetized by intraperitoneal injection of pentobarbital sodium on P17. The left lung was completely fixed in 4% paraformaldehyde and then embedded in paraffin. The right lung was immediately stored in −80°C for the measurement of gene expression, proteins, and cytokine.

Lung Histopathology

Standard inflation was used in generating the lung histopathology as previously described (6). 4%Paraformaldehyde-fixed lung tissue was embedded in paraffin and cut into 4 μm sections. Lung tissues sections were stained with hematoxylin and eosin (H&E) for morphological analysis by optical microscopy at a magnification of 200x (Nikon, Japan). Six fields of view were randomly selected on each tissue section. Alveolar development was estimated using the mean linear intercept (MLI) and radial alveolar count (RAC) (11, 16). The MLI is used as a method to estimate volume-to-surface ratio of acinar airspaces complex. The RAC is used to quantify alveolarization and estimate lung maturation. All images were evaluated by two blinded investigators. Data analyses were performed using Image-ProPlus software.

RNA Isolation and Quantitative Real-Time PCR

Total RNA was separated and purified using the TRIZOL reagent (Invitrogen). The A260/A280 ratio was measured to determine the RNA concentration. Takara Primescript RT (China) kits were used for reverse transcription according to the instructions.

The primers were as follows: IL-1β (Forward: TGGTGTGTGA CGTTCCCATT Reverse: CAGCACGAGGCTTTTTTGTTG), TNF-α (Forward: GACGTGGAACTGGCAGAAGAG Reverse: CAGGAATGAGAAGAGGCTGAGAC), NLRP3 (Forward: ATTACCCGCCCGAGAAAGG Reverse: CATGAGTGTG GCTAGATCCAAG), GPR43 (Forward: CTTGATCCTCAC GGCCTACAT Reverse: CCAGGGTCAGATTAAGCAGGAG), GAPDH (Forward: AGGTCGGTGTGAACGGATTTG Reverse: GGGGTCGTTGATGGCAACA). Reactions were performed in the Bio-Rad CFX Real-Time PCR system. The software of this instrument was used to compute the threshold cycle (Ct) values of all genes. The expression of each gene was normalized to that of GAPDH.

Cytokine Measurements

The inflammatory cytokine levels in lung homogenates of mice were evaluated. According to the manufacturer's instructions, the pulmonary concentrations of IL-18 (Xinbosheng China), IL-1β (Sizhengbai China), and TNF-α (Sizhengbai China) were measured by mouse cytokine enzyme-linked immunosorbent assay (ELISA) kits.

Western Blotting Analysis

We extracted proteins from whole lung tissues. Western blot was performed according to a protocol described by Chen et al. (6). Antibodies recognizing NLRP3 (Abcam, UK) and caspase-1-p20 (GeneTex, USA) were used.

Microbiome Analysis

After the mice were anesthetized by intraperitoneal injection of pentobarbital sodium on P17, feces were collected under sterile conditions and stored in −80°C. According to the manufacturer's instructions, QIAamp FAST DNA Stool Mini Kit (Qiagen, Hilden, Germany) was used to extract bacterial DNA. PCR was used to amplify the 16S ribosomal DNA variable V3-V4 region, and the primer sequences were 338F (5′-ACTCCTACGG GAGGCAGCAG-3′) and 806R (5′-GGACTACHVGGGTWT CTAAT-3′). The original data obtained by Miseq sequencing were processed and optimized. Operational taxonomic units (OTUs) were clustered at 97% similarity. At the phylum and genus levels, we analyzed the relative abundance of each OTU. Data analyses were run on the free online platform of Majorbio Cloud Platform (www.majorbio.com).

Statistical Analysis

SPSS version 22.0 (SPSS Inc., USA) was used for statistical analysis. Data between multiple groups were analyzed by one-way analysis of variance (ANOVA). P value < 0.05 was considered statistically significant.

RESULTS

Body Weight of Neonatal Mice

Compared with the room air group, the body weight of hyperoxia + placebo group was obviously decreased at P9. However, the body weight of hyperoxia + acetate group increased at P9 compared to that of the hyperoxia + placebo group (**Figure 1A**). Similar weight differences were observed at P17 (**Figure 1B**), but the difference in weight could not be completely reversed.

Acetate Attenuates Morphological Changes of the Lung

H&E staining was used to examine lung morphology (**Figure 2**). In the room air group, the lung exhibited complete lung structures with a normal alveolar epithelium and alveolar septum (**Figure 2A**). However, after 14 days of hyperoxia exposure, the alveoli of the mice were enlarged (**Figure 2B**), the RAC of per unit area significantly reduced, while the MLI significantly increased (**Figures 2D,E**). These data showed that exposure to hyperoxia increased alveolar damage and led to alveolar simplification. Alveolar simplification and alveolar septal improvement were observed in the hyperoxia + acetate group compared to the hyperoxia group (**Figure 2C**). These results demonstrated that acetate therapy could resist high O_2-induced lung injury and partly restore high O_2-induced alveolar simplification.

Acetate Decreases Inflammatory Factors in the Mouse Lung

RT-PCR and ELISA were used to detect the expressions of inflammatory cytokines in lung tissues. Compared with the room air group, the expression of TNF-α was significantly increased after 14 days of exposure to the high O_2 level. However, in the hyperoxia + acetate group, the expression of TNF-α was significantly lower than the hyperoxia group (**Figures 3A,B**). These results indicated that acetate treatment decreases the expressions of TNF-α in the lung caused by hyperoxia.

Acetate Reduces the Expression of NLRP3 Inflammasome-Related Proteins and GPR43

To assess the effect of acetate on the lung NLRP3 inflammasome-related cytokines IL-1β and IL-18, lung tissues were examined by RT-PCR and ELISA. Compared with the room air group, the expression of IL-18 in hyperoxia group was significantly increased (**Figures 4C,D**). However, the expression of IL-18 in the hyperoxia + acetate group was significantly lower than the hyperoxia group. Similar results were also observed for IL-1β (**Figures 4A,B**). Then, RT-PCR and Western blot were used to detect the expressions of NLRP3 inflammasome and caspase-1 in lung tissue.

Compared with the room air group, the expressions of NLRP3 inflammasome and caspase-1 were significantly increased in the hyperoxia group, and these effects could be partially reversed by the acetate treatment (**Figures 4E,G,H**).

Next, we investigated whether acetate could alter the expression level of GPR43 in newborn mice exposed to high oxygen. Compared with the control group, high oxygen exposure reduced the expression of GPR43 in lung tissue (**Figure 4F**). Acetate treatment could partially increase the expression of GPR43. These data showed that acetate affects the expression of NLRP3 and GPR43 in lung tissue after hyperoxia exposure.

Acetate Treatment Affects the Composition of the Gut Microbiota in Mice Exposed to Hyperoxia

To investigate whether acetate could change the composition of intestinal flora, we used the 16S rRNA method to analyze the intestinal contents to determine the changes in intestinal flora. The bacterial compositions of the three groups of mice were significantly different at the phylum and genus levels. Compared with the room air group, the abundance of Proteobacteria in the gut was significantly higher in the hyperoxia group ($P < 0.05$) (**Figure 5A**), while no significant difference was observed in the proportion of Bacteroidetes and Firmicutes in the gut. In the hyperoxia+acetate group, the abundance of Proteobacteria was decreased. In addition, at the genus level (**Figure 5B**), we found an increase in the relative abundance of Escherichia/Shigella in the hyperoxia group compared with the room air group ($P < 0.001$), while the relative abundance of Ruminococcus was significantly decreased ($P < 0.05$). In the hyperoxia+acetate group, the relative abundance of Escherichia/Shigella was decreased, while the relative abundance of Ruminococcus was significantly increased.

DISCUSSION

BPD is a chronic lung disease of prematurity and it is usually accompanied by delayed pulmonary hypertension, persistent pulmonary dysfunction, developmental delay,

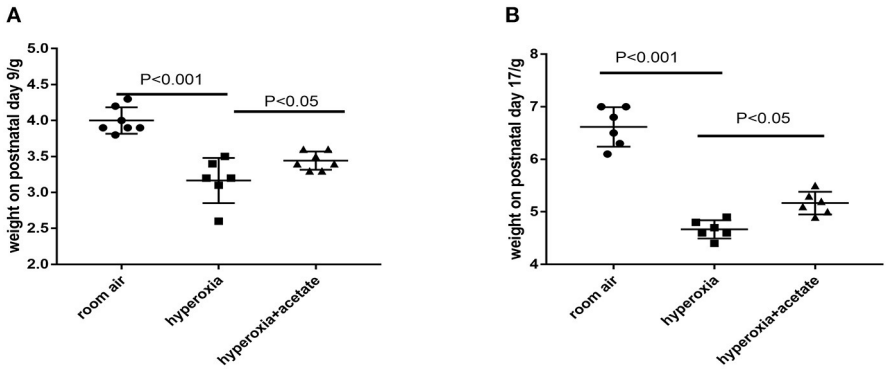

FIGURE 1 | Body weight of neonatal mice. **(A)** Acetate-treated mice in the hyperoxia group had a significantly higher body weight on postnatal day 9 than non-acetate treated mice ($P < 0.001$). **(B)** The body weight on postnatal day 17 ($P < 0.001$). $n = 8$ mice/group. Data are expressed relative to the control group at each time point as the mean ± SEM.

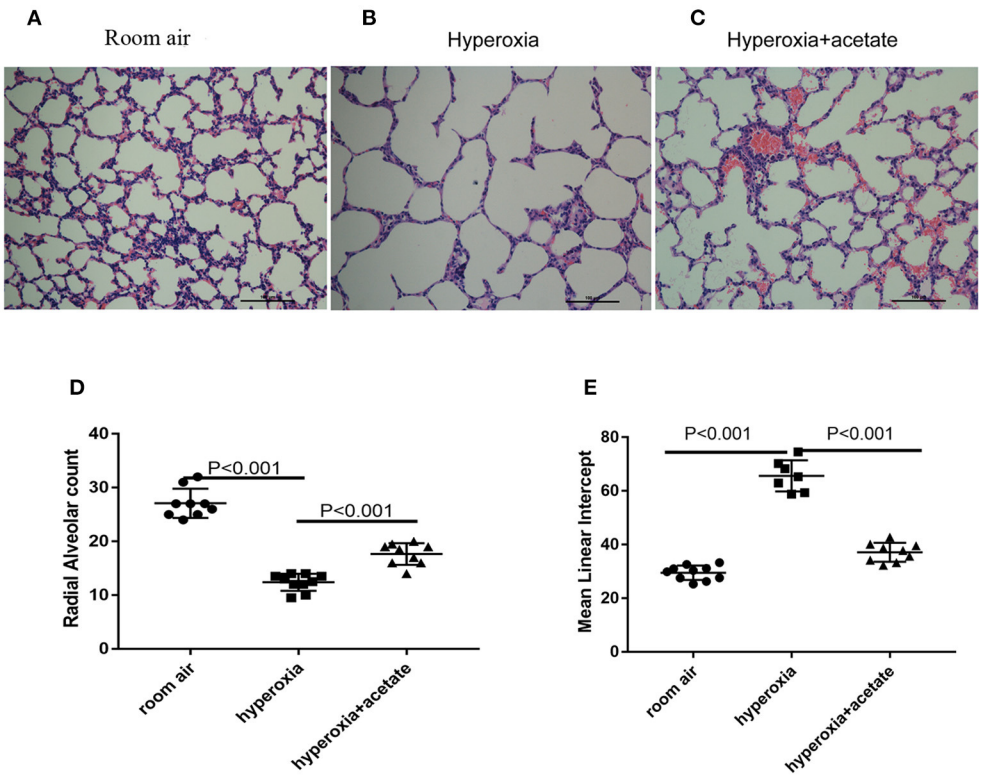

FIGURE 2 | Acetate attenuates morphological changes. Hyperoxia exposure led to marked alveolar simplification as shown by H&E staining and by RAC and MLI assessment. Acetate treatment improved the hyperoxia-induced impairment of alveolar growth. **(A–C)** Representative H&E staining (light microscopy, ×200) of lung tissue slides from each group. Scale bars = 100 μm. **(D)** Semiquantitative pathological determination of RAC in lung tissues. **(E)** Semiquantitative pathological determination of MLI in lung tissues. The values represent the mean ± SD; $n = 6$ mice/group.

and neurocognitive problems in later life (17, 18). In this study, hyperoxia activated the NLRP3-IL-1β axis and induced the pathological features of BPD in newborn mice. We found that acetate downregulated the expression levels of NLRP3-related proteins, alleviated lung inflammation, and improved simplification of alveoli. Acetate intervention could also alter the abundance of gut microbiota.

Lung injury induced by hyperoxia exposure is the most common model of BPD in neonatal mice. Impaired alveolarization and angiogenesis disorders are the main pathological features of BPD (1, 19). Studies have confirmed

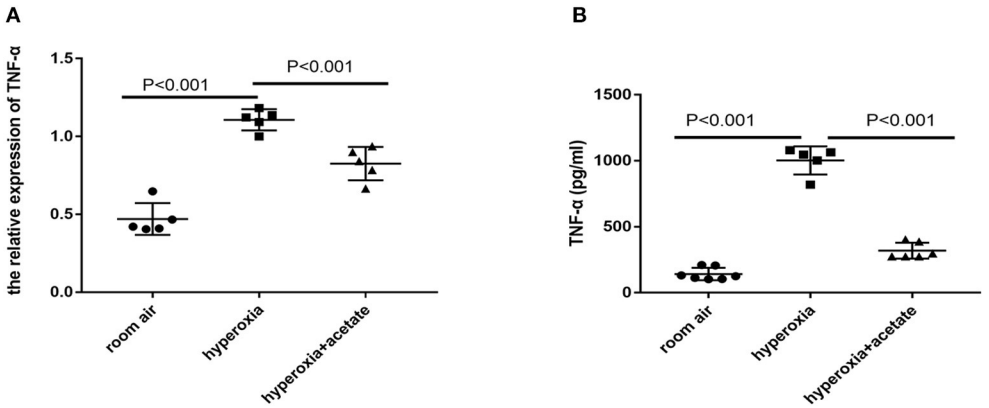

FIGURE 3 | Acetate decreases pro-inflammatory factors in the mouse lung. The pulmonary mRNA levels of TNF-α **(A)**. The pulmonary protein levels of TNF-α **(B)**. $n =$ 5–7/group from 3 independent experiments; data are presented as the means ± SD.

that lung development of mice undergoes five stages: embryonic, pseudoglandular, canalicular, saccular, and alveolar stages, suggesting that the process of alveolarization has a similar time sequence as that in humans (20). However, unlike the development of the human embryonic lung, neonatal mice lung tissue only completes gross morphogenesis, and alveolarization begins 3 days after birth (21, 22). In the present study, a mouse model of BPD was successfully established by selecting 3-day-old newborn mice and continuously exposing them to 85% O_2 for 14 days. H&E staining of the lung tissue demonstrated simplification of alveoli after high O_2 exposure, which is consistent with the pathological features of BPD. NLRP3 activation results in excessive inflammation, which is associated with a variety of inflammatory disorders, including type 1 diabetes, hyperinflammation following influenza infection, asthma and gout (23–26). NLRP3, ASC and pro-caspase-1 are the main components of the NLRP3 inflammasome (10). Infection, tissue lesions and oxidative stress can activate the NLRP3 inflammasome. Activation of this complex processes pro-caspase-1 into an active 20 kDa fragment, which can enzymatically cleave pro-IL-1β into mature IL1β, and process pro-IL-18 into mature IL-18 (27). This process plays an important role in the initiation of inflammation (8). Liao's research showed that NLRP3 activation is one of the primary causes of BPD (11). In the present study, after 14 days of hyperoxia exposure, the levels of NLRP3, caspase-1, IL-1β, IL-18, and TNF-α were significantly increased compared to the room air group. After acetate treatment, the expression levels of NLRP3, caspase-1, IL-1β, IL-18, and TNF-α were significantly decreased. In BPD mice, the increased accumulation of macrophages can be observed (11). After RSV infection, acetate intervention reduces the recruitment of inflammatory cells including macrophages and lymphocytes into the lungs of mice, thus reducing lung inflammation (12, 28). In addition, acetate reduces the activation of NLRP3 through ubiquitination and autophagy and plays an anti-inflammatory role in peritonitis and endotoxemia models (15). Our results are consistent with these studies and suggested that acetate intervention may reduce lung inflammation. However, the effect of acetate intervention on inflammatory cells in BPD needs to be further explored *in vitro*. Subsequently, we explored the mechanism by which acetate reduces NLRP3 expression. Short-chain fatty acids (SCFAs) are metabolites derived from the gut flora, which are produced by the fermentation of indigestible dietary fiber (12) and mainly consist of acetate, propionate, and butyrate. These fatty acids are absorbed into the circulatory system and act through binding G protein-coupled receptors (GPR43 and GPR41) or inhibiting histone deacetylases (HDACs) (29, 30). It is well known that acetate can activate GPR43, and this receptor was originally recognized in colitis (29). Activation of GPR43 can reduce inflammation, and in this manner, SCFAs protect the colon from injury. Our results also indicated that after 14 days of hyperoxia, the expression of GPR43 in the newborn mice decreased and this decrease would be improved by acetate treatment. However, because GPR43 is widely expressed on the membranes of different cells, such as macrophages and epithelial cells (31), it is unclear which cell type plays a key role; further research is needed. In addition, the causal relationship between GPR43 and NLRP3 requires further investigation. Thorburn et al. demonstrated that acetate specifically activates GPR43 and subsequently decreases $Ca2^+$ to activate downstream signals (32). However, an increase in $Ca2^+$ can further promote the activation of NLRP3 (33). It can be concluded that after activation of GPR43 by acetate, NLRP3 activation is inhibited by decreasing $Ca2^+$.

The colonization pattern of microbiota in very low birth weight (VLBW) infants is significantly different from that in healthy full-term infants (34, 35). Because acetate, a main component of SCFAs, significantly ameliorates inflammation in BPD, we speculate that the intestinal microbiota may affect the susceptibility and/or severity of BPD. Previous studies have demonstrated that gut microbiota may affect the immune response of the lungs (36–39), which indicates that gut microbiota may affect the severity of BPD by regulating systemic and lung inflammation. As previous reports, Escherichia/Shigella from the Enterobacteriaceae were significantly increased in

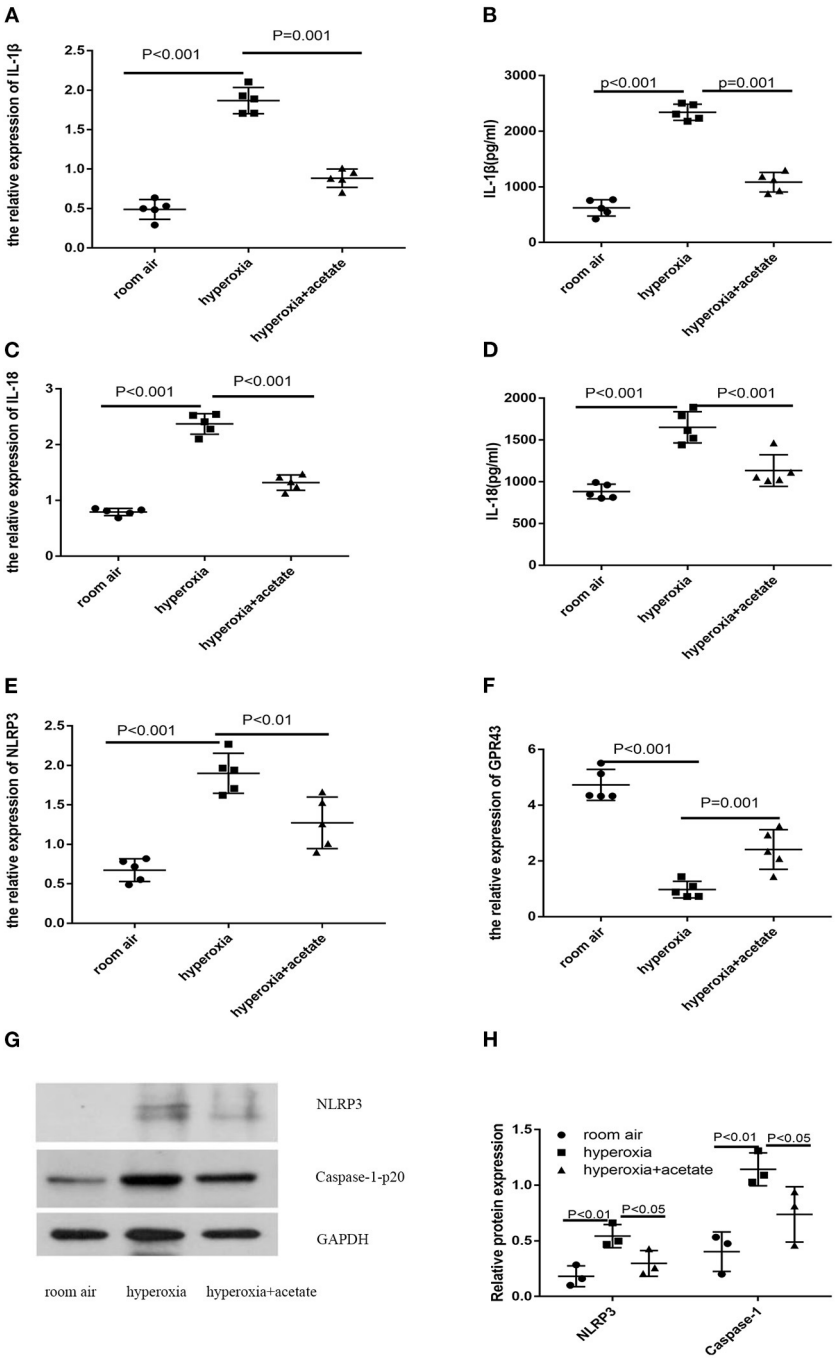

FIGURE 4 | Acetate decreases NLRP3 inflammasome-related protein and GPR43 expression. The pulmonary mRNA levels of IL-1β **(A),** IL-18 **(C)**, NLRP3 **(E)** and GPR43 **(F)**. The pulmonary protein levels of IL-1β **(B)**, IL-18 **(D)**, NLRP3 **(G,H)** and caspase-1 **(G,H)**. $n \geq 3$/group from 3 independent experiments; data are presented as the means ± SD.

infants with BPD (40). Escherichia-Shigella belongs to the Proteobacteria phylum and produces LPS (41). Since the LPS of Escherichia/Shigella may activate the immune system and cause inflammation (41), the increase in the relative abundance of Escherichia/Shigella in the hyperoxia group compared to the acetate group shown in our study suggests that higher levels of inflammation may have occurred in the hyperoxia group. Ruminococcaceae, which is an important source of SCFA production (42), also decreased after hyperoxia exposure but increased after administration of acetate in our study, these results are consistent with previous studies showing that Ruminococcaceae have anti-inflammatory effects (43–45) and

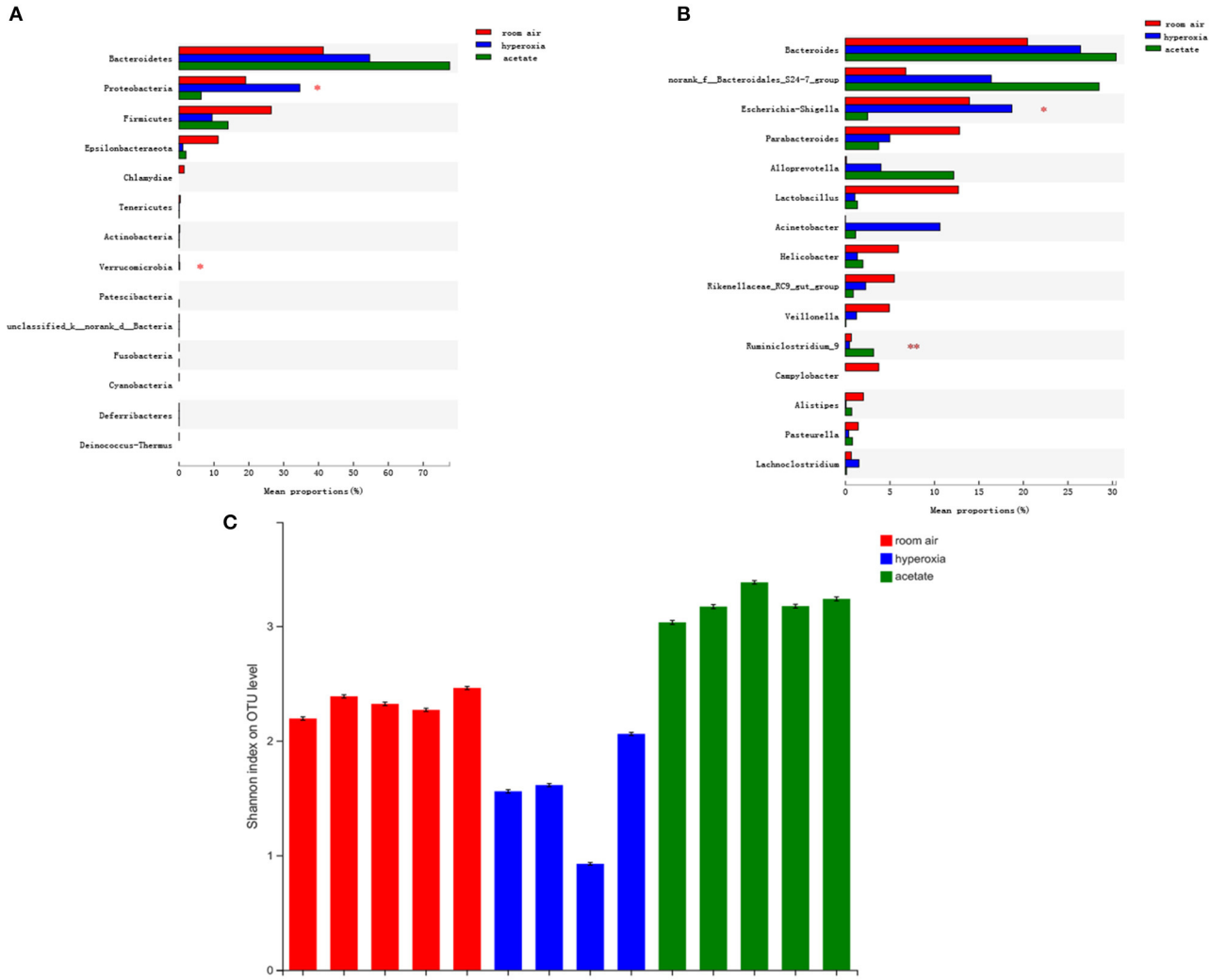

FIGURE 5 | Acetate treatment affects the composition of the gut microbiota in mice exposed to hyperoxia. The relative abundance of microbial communities in the gut of the 3 groups at the phylum **(A)** and genus **(B)** levels. For **(A,B)**, relative abundance >1%, $^{*}P < 0.05$ and $^{**}P < 0.01$. Assessment of the diversity of microbial communities in the intestinal contents **(C)** of the 3 groups by the Shannon Diversity Index (room air: red, hyperoxia: blue, acetate: green).

can ameliorate lung injury (45, 46). All of these findings suggested that intestinal flora may be involved in the protective effect of acetate against lung injury.

In our study, some limitations are to be mentioned. (i) Although we found that acetate could change the composition of intestinal flora in the model of hyperoxia-induced lung injury, the combined effects of hyperoxia + acetate were considered and the independent effect of acetate on the perinatal intestinal was not considered. At present, no studies have investigated the effects of acetate treatment during the perinatal period on gut microbiota. However, a study on hypertension showed that acetate changed the gut microbiota composition, increasing the levels of bacteria from the Bacteroides genus (47). Thus, acetate-independent effects on the perinatal microbiome should be added into the future investigations. (ii) Studies have proven that male neonatal are more susceptible to hyperoxic lung injury (48). In our experimental design, sex was not taken into account as a variable, which may only reflect part of the role of acetate.

In summary, our research showed that acetate treatment can alleviate lung injury after hyperoxia exposure by inhibiting the expression of NLRP3-related proteins, which indicates that acetate treatment may be helpful for the treatment or prevention of BPD. The mechanism remains to be elucidated.

DATA AVAILABILITY STATEMENT

The raw data supporting the conclusions of this article will be made available by the authors, without undue reservation.

ETHICS STATEMENT

The animal study was reviewed and approved by Ethics Committee for Animal Protection and Use of Chongqing Children's Hospital.

AUTHOR CONTRIBUTIONS

QZ, YH, and YS contributed to the concept and design of the study. QZ performed the main experiments. XR performed a portion of the statistical analysis. QZ wrote the first draft of the manuscript. YS, YH, and QA have revised this manuscript. All authors have approved the final version before submission.

FUNDING

This work was supported by the National Key R&D Program of China and West China Cohort Study for Child Health and Development (2019YFC0840703).

REFERENCES

1. Jobe AH. The new bronchopulmonary dysplasia. *Curr Opin Pediatr.* (2011) 23:167. doi: 10.1097/MOP.0b013e3283423e6b
2. Thebaud B, Goss KN, Laughon M, Whitsett JA, Abman SH, Steinhorn RH, et al. Bronchopulmonary dysplasia. *Nat Rev Dis Primers.* (2019) 5:78. doi: 10.1038/s41572-019-0127-7
3. Rudloff I, Cho SX, Bui CB, McLean C, Veldman A, Berger PJ, et al. Refining anti-inflammatory therapy strategies for bronchopulmonary dysplasia. *J Cell Mol Med.* (2017) 21:1128–38. doi: 10.1111/jcmm.13044
4. Gien J, Kinsella JP. Pathogenesis and treatment of bronchopulmonary dysplasia. *Curr Opin Pediatr.* (2011) 23:305–13. doi: 10.1097/MOP.0b013e328346577f
5. Ali Z, Schmidt P, Dodd J, Jeppesen DL. Bronchopulmonary dysplasia: a review. *Arch Gynecol Obstet.* (2013) 288:325–33. doi: 10.1007/s00404-013-2753-8
6. Chen S, Wu Q, Zhong D, Du L. Caffeine prevents hyperoxia-induced lung injury in neonatal mice through NLRP3 inflammasome and NF-kappaB pathway. *Respir Res.* (2020) 21:140. doi: 10.1186/s12931-020-01403-2
7. Hummler JK, Dapaah-Siakwan F, Vaidya R, Zambrano R, Luo S, Chen S, et al. Inhibition of Rac1 signaling downregulates inflammasome activation and attenuates lung injury in neonatal rats exposed to hyperoxia. *Neonatology.* (2017) 111:280–8. doi: 10.1159/000450918
8. Son S, Hwang I, Han SH, Shin JS, Shin OS, Yu JW. Advanced glycation end products impair NLRP3 inflammasome-mediated innate immune responses in macrophages. *J Biol Chem.* (2017) 292:20437–48. doi: 10.1074/jbc.M117.806307
9. Mangan MSJ, Olhava EJ, Roush WR, Seidel HM, Glick GD, Latz E. Targeting the NLRP3 inflammasome in inflammatory diseases. *Nat Rev Drug Discov.* (2018) 17:588–606. doi: 10.1038/nrd.2018.97
10. Yang Y, Wang H, Kouadir M, Song H, Shi F. Recent advances in the mechanisms of NLRP3 inflammasome activation and its inhibitors. *Cell Death Dis.* (2019) 10:128. doi: 10.1038/s41419-019-1413-8
11. Liao J, Kapadia VS, Brown LS, Cheong N, Longoria C, Mija D, et al. The NLRP3 inflammasome is critically involved in the development of bronchopulmonary dysplasia. *Nat Commun.* (2015) 6:8977. doi: 10.1038/ncomms9977
12. Antunes KH, Fachi JL, de Paula R, da Silva EF, Pral LP, Dos Santos AÁ, et al. Microbiota-derived acetate protects against respiratory syncytial virus infection through a GPR43-type 1 interferon response. *Nat Commun.* (2019) 10:3273.
13. Tan J, McKenzie C, Potamitis M, Thorburn AN, Mackay CR, Macia L. The role of short-chain fatty acids in health and disease. *Adv Immunol.* (2014) 121:91–119. doi: 10.1016/B978-0-12-800100-4.00003-9
14. Macia L, Tan J, Vieira AT, Leach K, Stanley D, Luong S, et al. Metabolite-sensing receptors GPR43 and GPR109A facilitate dietary fibre-induced gut homeostasis through regulation of the inflammasome. *Nat Commun.* (2015) 6:6734. doi: 10.1038/ncomms7734
15. Xu M, Jiang Z, Wang C, Li N, Bo L, Zha Y, et al. Acetate attenuates inflammasome activation through GPR43-mediated Ca (2+)-dependent NLRP3 ubiquitination. *Exp Mol Med.* (2019) 51:83. doi: 10.1038/s12276-019-0276-5
16. Hsia CC, Hyde DM, Ochs M, Weibel ER, AEJTFoQAo Structure L. An official research policy statement of the American Thoracic Society/European Respiratory Society: standards for quantitative assessment of lung structure. *Am J Respir Crit Care Med.* (2010) 181:394–418. doi: 10.1164/rccm.200809-1522ST
17. Abman SH, Collaco JM, Shepherd EG, Keszler M, Cuevas-Guaman M, Welty SE, et al. Interdisciplinary care of children with severe bronchopulmonary dysplasia. *J Pediat.* (2017) 181:12–28. e1. doi: 10.1016/j.jpeds.2016.10.082
18. Davidson LM, Berkelhamer SK. Bronchopulmonary dysplasia: chronic lung disease of infancy and long-term pulmonary outcomes. *J Clin Med.* (2017) 6:4 doi: 10.3390/jcm6010004
19. Jobe AH, Bancalari E. Bronchopulmonary dysplasia. *Am J Respir Crit Care Med.* (2001) 163:1723–9. doi: 10.1164/ajrccm.163.7.2011060
20. Mund SI, Stampanoni M, Schittny JC. Developmental alveolarization of the mouse lung. *Dev Dyn.* (2008) 237:2108–16. doi: 10.1002/dvdy.21633
21. Nardiello C, Mizikova I, Morty RE. Looking ahead: where to next for animal models of bronchopulmonary dysplasia? *Cell Tissue Res.* (2017) 367:457–68. doi: 10.1007/s00441-016-2534-3
22. Berger J, Bhandari V. Animal models of bronchopulmonary dysplasia. The term mouse models. *Am J Physiol Lung Cell Mol Physiol.* (2014) 307:L936–47. doi: 10.1152/ajplung.00159.2014
23. Coates BM, Staricha KL, Ravindran N, Koch CM, Cheng Y, Davis JM, et al. Inhibition of the NOD-Like receptor protein 3 inflammasome is protective in juvenile influenza a virus infection. *Front Immunol.* (2017) 8:782. doi: 10.3389/fimmu.2017.00782
24. Hu C, Ding H, Li Y, Pearson JA, Zhang X, Flavell RA, et al. NLRP3 deficiency protects from type 1 diabetes through the regulation of chemotaxis into the pancreatic islets. *Proc Natl Acad Sci USA.* (2015) 112:11318–23. doi: 10.1073/pnas.1513509112
25. Kim RY, Pinkerton JW, Essilfie AT, Robertson AAB, Baines KJ, Brown AC, et al. Role for NLRP3 inflammasome-mediated, IL-1β-dependent responses in severe, steroid-resistant asthma. *Am J Respir Crit Care Med.* (2017) 196:283–97. doi: 10.1164/rccm.201609-1830OC
26. Martinon F, Pétrilli V, Mayor A, Tardivel A, Tschopp J. Gout-associated uric acid crystals activate the NALP3 inflammasome. *Nature.* (2006) 440:237–41. doi: 10.1038/nature04516
27. Sutterwala FS, Haasken S, Cassel SL. Mechanism of NLRP3 inflammasome activation. *Ann N Y Acad Sci.* (2014) 1319:82–95. doi: 10.1111/nyas.12458
28. Vieira AT, Galvao I, Macia LM, Sernaglia EM, Vinolo MA, Garcia CC, et al. Dietary fiber and the short-chain fatty acid acetate promote resolution of neutrophilic inflammation in a model of gout in mice. *J Leukoc Biol.* (2017) 101:275–84. doi: 10.1189/jlb.3A1015-453RRR
29. Maslowski KM, Vieira AT, Ng A, Kranich J, Sierro F, Yu D, et al. Regulation of inflammatory responses by gut microbiota and chemoattractant receptor GPR43. *Nature.* (2009) 461:1282–6. doi: 10.1038/nature08530
30. Theiler A, Barnthaler T, Platzer W, Richtig G, Peinhaupt M, Rittchen S, et al. Butyrate ameliorates allergic airway inflammation by limiting eosinophil trafficking and survival. *J Allergy Clin Immunol.* (2019) 144:764–76. doi: 10.1016/j.jaci.2019.05.002
31. Imoto Y, Kato A, Takabayashi T, Sakashita M, Norton JE, Suh LA, et al. Short-chain fatty acids induce tissue plasminogen activator in airway epithelial cells via GPR41&43. Clinical and experimental allergy: *J Br Soc Allerg Clin Immunol.* (2018) 48:544–54. doi: 10.1111/cea.13119

32. Thorburn AN, Macia L, Mackay CR. Diet, metabolites, and "western-lifestyle" inflammatory diseases. *Immunity.* (2014) 40:833–42. doi: 10.1016/j.immuni.2014.05.014
33. Lee GS, Subramanian N, Kim AI, Aksentijevich I, Goldbach-Mansky R, Sacks DB, et al. The calcium-sensing receptor regulates the NLRP3 inflammasome through Ca2+ and cAMP. *Nature.* (2012) 492:123–7. doi: 10.1038/nature11588
34. La Rosa PS, Warner BB, Zhou Y, Weinstock GM, Sodergren E, Hall-Moore CM, et al. Patterned progression of bacterial populations in the premature infant gut. *Proc Natl Acad Sci USA.* (2014) 111:12522–7. doi: 10.1073/pnas.1409497111
35. Patel AL, Mutlu EA, Sun Y, Koenig L, Green S, Jakubowicz A, et al. Longitudinal survey of microbiota in hospitalized preterm very-low-birth-weight infants. *J Pediatr Gastroenterol Nutr.* (2016) 62:292–303. doi: 10.1097/MPG.0000000000000913
36. Lal CV, Travers C, Aghai ZH, Eipers P, Jilling T, Halloran B, et al. The airway microbiome at birth. *Sci Rep.* (2016) 6:31023. doi: 10.1038/srep31023
37. Berkhout DJC, Niemarkt HJ, Benninga MA, Budding AE, van Kaam AH, Kramer BW, et al. Development of severe bronchopulmonary dysplasia is associated with alterations in fecal volatile organic compounds. *Pediatr Res.* (2018) 83:412–9. doi: 10.1038/pr.2017.268
38. Gray J OK, Worthen G, Alenghat T, Whitsett J, Deshmukh H. Intestinal commensal bacteria mediate lung mucosal immunity and promote resistance of newborn mice to infection. *Sci Transl Med.* (2017) 9:eaaf9412. doi: 10.1126/scitranslmed.aaf9412
39. McAleer JP, Kolls JK. Contributions of the intestinal microbiome in lung immunity. *Eur J Immunol.* (2018) 48:39–49. doi: 10.1002/eji.201646721
40. Ryan FJ, Drew DP, Douglas C, Leong LEX, Moldovan M, Lynn M, et al. Changes in the composition of the gut microbiota and the blood transcriptome in preterm infants at less than 29 weeks gestation diagnosed with bronchopulmonary dysplasia. *mSystems.* (2019) 4:19. doi: 10.1128/mSystems.00484-19
41. Wang W, Chen Q, Yang X, Wu J, Huang F. Sini decoction ameliorates interrelated lung injury in septic mice by modulating the composition of gut microbiota. *Microb Pathog.* (2020) 140:103956. doi: 10.1016/j.micpath.2019.103956
42. Li W, Wu X, Hu X, Wang T, Liang S, Duan Y, et al. Structural changes of gut microbiota in Parkinson's disease and its correlation with clinical features. *Sci China Life Sci.* (2017) 60:1223–33. doi: 10.1007/s11427-016-9001-4
43. Chua HH, Chou HC, Tung YL, Chiang BL, Liao CC, Liu HH, et al. Intestinal dysbiosis featuring abundance of ruminococcus gnavus associates with allergic diseases in infants. *Gastroenterology.* (2018) 154:154–67. doi: 10.1053/j.gastro.2017.09.006
44. Yu W, Su X, Chen W, Tian X, Zhang K, Guo G, et al. Three types of gut bacteria collaborating to improve Kui Jie'an enema treat DSS-induced colitis in mice. *Biomed Pharm.* (2019) 113:108751. doi: 10.1016/j.biopha.2019.108751
45. Abell GC, Cooke CM, Bennett CN, Conlon MA, McOrist AL. Phylotypes related to Ruminococcus bromii are abundant in the large bowel of humans and increase in response to a diet high in resistant starch. *FEMS Microbiol Ecol.* (2008) 66:505–15. doi: 10.1111/j.1574-6941.2008.00527.x
46. Surendran Nair M, Eucker T, Martinson B, Neubauer A, Victoria J, Nicholson B, et al. Influence of pig gut microbiota on Mycoplasma hyopneumoniae susceptibility. *Vet Res.* (2019) 50:86. doi: 10.1186/s13567-019-0701-8
47. Marques FZ. High fibre diet and acetate supplementation change the gut microbiota and prevent the development of hypertension and heart failure in DOCA-salt hypertensive mice. *Circulation.* (2017) 135:964. doi: 10.1161/CIRCULATIONAHA.116.024545
48. Lingappan K, Jiang W, Wang L, Moorthy B. Sex-specific differences in neonatal hyperoxic lung injury. *Am J Physiol Lung Cell Mol Physiol.* (2016) 311:L481–93. doi: 10.1152/ajplung.00047.2016

Conflict of Interest: The authors declare that the research was conducted in the absence of any commercial or financial relationships that could be construed as a potential conflict of interest.

frontiers in Pediatrics

ORIGINAL RESEARCH
published: 04 February 2021
doi: 10.3389/fped.2020.602047

Supplemental Insulin-Like Growth Factor-1 and Necrotizing Enterocolitis in Preterm Pigs

*Kristine Holgersen[1], Xiaoyan Gao[1,2], Rangaraj Narayanan[3], Tripti Gaur[3], Galen Carey[3], Norman Barton[3], Xiaoyu Pan[1], Tik Muk[1], Thomas Thymann[1] and Per Torp Sangild[1,4,5]**

[1] Comparative Pediatrics and Nutrition, Department of Veterinary and Animal Sciences, Faculty of Health and Medical Sciences, University of Copenhagen, Frederiksberg, Denmark, [2] Department of Neonatology, Southern Medical University Affiliated Maternal & Child Health Hospital of Foshan, Foshan, China, [3] Takeda, Cambridge, MA, United States, [4] Department of Neonatology, Rigshospitalet, Copenhagen, Denmark, [5] Department of Pediatrics, Odense University Hospital, Odense, Denmark

Background: Recombinant human IGF-1/binding protein-3 (rhIGF-1/BP-3) is currently tested as a therapy in preterm infants but possible effects on the gut, including necrotizing enterocolitis (NEC), have not been tested. The aim of this study was to evaluate if rhIGF-1/BP-3 supplementation in the first days after birth negatively affects clinical variables like growth, physical activity, blood chemistry and hematology and gut maturation (e.g., intestinal permeability, morphology, enzyme activities, cytokine levels, enterocyte proliferation, NEC lesions), using NEC-sensitive preterm pigs as a model for preterm infants.

Methods: Preterm pigs were given twice daily subcutaneous injections of rhIGF-1/BP-3 or vehicle. Blood was collected for IGF-1 measurements and gut tissue for NEC evaluation and biochemical analyses on day 5.

Results: Baseline circulating IGF-1 levels were low in preterm pigs compared with near-term pigs reared by their mother (<20 vs. 70 ng/ml). Injection with rhIGF-1/BP-3 resulted in increased plasma IGF-1 levels for up to 6 h after injection (>40 ng/mL). rhIGF-1/BP-3 treatment reduced the incidence of severe NEC lesions (7/24 vs.16/24, $p = 0.01$) and overall NEC severity (1.8 ± 0.2 vs. 2.6 ± 0.3, $p < 0.05$, with most lesions occurring in colon). In the small intestine, villi length (405 ± 25 vs. $345 \pm 33\,\mu m$) and activities of the brush border peptidases aminopeptidase N and dipeptidylpeptidase IV were increased in rhIGF-1/BP-3 treated pigs, relative to control pigs (+31–44%, both $p < 0.05$). The treatment had no effects on body weight, blood chemistry or hematology, except for an increase in blood leucocyte and neutrophil counts ($p < 0.05$, i.e., reduced neonatal neutropenia). Likewise, rhIGF-1/BP-3 treatment did not affect intestinal tissue cytokine levels (IL-1β, IL-6, IL-8, TNFα,), enterocyte proliferation, goblet cell density, permeability or bacterial translocation to the bone marrow.

Conclusion: Supplemental rhIGF-1/BP-3 did not negatively affect any of the measured variables of clinical status or gut maturation in preterm pigs. Longer-term safety and efficacy of exogenous rhIGF-1/BP-3 to support maturation of the gut and other critical organs in preterm newborns remain to be investigated in both pigs and infants.

Keywords: IGF-1, infant, intestine, preterm birth, gut, newborn, growth restriction, fetus

OPEN ACCESS

Edited by:
Fook-Choe Cheah, National University of Malaysia, Malaysia

Reviewed by:
Simon Eaton, University College London, United Kingdom
Kok Yong Chin, National University of Malaysia, Malaysia
Adrian Cummins, University of Adelaide, Australia

***Correspondence:**
Per Torp Sangild
pts@sund.ku.dk

Specialty section:
This article was submitted to Neonatology, a section of the journal Frontiers in Pediatrics

Received: *02 September 2020*
Accepted: *18 December 2020*
Published: *04 February 2021*

Citation:
Holgersen K, Gao X, Narayanan R, Gaur T, Carey G, Barton N, Pan X, Muk T, Thymann T and Sangild PT (2021) Supplemental Insulin-Like Growth Factor-1 and Necrotizing Enterocolitis in Preterm Pigs. Front. Pediatr. 8:602047. doi: 10.3389/fped.2020.602047

INTRODUCTION

Preterm birth (<37 weeks gestation) accounts for 5–15% of all live births worldwide or about 15 million infants per year (1). Premature infants are a highly vulnerable population due to immaturity of their organs and the accelerated transition to extrauterine life. Postnatally, infants with gestational age (GA) <32 weeks at birth show clearly reduced serum levels of insulin-like growth factor 1 (IGF-1) relative to term infants and gestational age-matched fetuses *in utero*, probably due to the sudden loss of placental and amniotic fluid supplies (2–4). Recently, a large multi-center international clinical trial was initiated to test the clinical effects of supplemental recombinant human (rh) IGF-1/rhIGFBP-3 (rhIGF-1/BP-3) during the first weeks after extremely preterm birth (<28 weeks GA), with respiratory function as the primary outcome (ClinicalTrials.gov registry NCT03253263).

IGF-1 is a 70-amino acid polypeptide playing an important role in intrauterine and postnatal growth and organ development. In the fetus and newborn, the majority of circulating IGF-1 is generated by the liver in an insulin- and nutrient-dependent manner (4). About 80% of circulating IGF-1 is bound to IGF-binding protein (IGFBP)-3 and an acid labile subunit, regulating the action and biological availability of IGF-1 in peripheral tissues (5). Free IGF-1 binds to the type 1 IGF-receptor, a transmembrane tyrosine kinase receptor highly homologous to the insulin receptor, that activates intracellular signaling cascades like the mitogen-activated protein (MAP)-kinase and phosphatidylinositol 3(PI3-K)-kinase/Akt pathways (6, 7). In addition to its endocrine effects *via* the blood stream, IGF-1 is also produced locally in a variety of tissues exerting cellular paracrine and autocrine effects. In the gastrointestinal tract, IGF-1 may promote enterocyte proliferation and differentiation and inhibits apoptosis, thus supporting cell survival and mucosal growth (8–10). In young rodents, parenteral IGF-1 administration attenuates intestinal injury by decreasing apoptosis and increasing proliferation of epithelial cells after hypoxia/reoxygenation (11), sepsis (9) or thermally-induced damage (10). In weaned rats, an anabolic effect on the small intestine was observed only after subcutaneous, but not enteral IGF-1 administration (12). Inconsistent effects on intestinal growth have also been observed in neonatal pigs after enteral IGF-1 administration (13–15) and effects beyond the gut are poorly investigated. Considering the multifunctional actions of IGF-1, it is critical to understand how circulating IGF-1 levels relate to development of both the gut and other organs in the short and longer term.

Hellström et al. (16) demonstrated an association between persistently low serum concentrations of IGF-1 and several morbidities in preterm infants. In support, a recent phase II clinical trial indicated that exogenous rhIGF-1/BP-3 reduced the occurrence of severe bronchopulmonary dysplasia (BPD) and intraventricular hemorrhage (IVH) in extremely premature infants (17). The same study showed no effect on the overall incidence of necrotizing enterocolitis (NEC) (6/61 vs. 5/60), but the number of fatal NEC cases was highest in the rhIGF-1/BP-3 group (3 vs. 0). Generally, NEC is associated with high mortality (20–30%) and occurs in 5–10% of extremely preterm infants within the first weeks of life (18–22). Despite comprehensive research, in part using animal models, the pathogenesis of NEC remains ambiguous and worldwide the NEC incidence is constant or increasing (19, 21).

Preterm pigs reflect many clinical aspects of preterm infants, thus enabling pathophysiological investigation and drug development. Comparison between preterm pigs and preterm infants is organ-dependent but judged by their immature gut and immune systems, and high sensitivity to NEC and sepsis, 90% gestation in pigs may reflect gut and immunity development in extremely preterm infants (23–25). Within a few days of advancing enteral feeding with infant formula, 40–70% of preterm pigs spontaneously develop NEC-like lesions, including pneumatosis intestinalis, mucosal necrosis, villus atrophy and digestive dysfunction (26–29). We have previously shown that circulating IGF-1 levels remain low until at least 26 days after birth in preterm pigs vs. term pigs (30). However, data concerning the relationship between IGF-1 levels and comorbidities in preterm pigs are lacking.

We hypothesized that parenteral rhIGF-1/BP-3 supplementation in preterm pigs, to reach physiological levels in corresponding term individuals, would not negatively affect clinical variables, gut maturation and NEC incidence. To test this hypothesis, we first compared circulating IGF-1 levels in preterm pigs with values in near-term pigs reared artificially or reared naturally by their sow. Next, we tested the pharmacokinetics (PK) of rhIGF-1/BP-3 to establish an appropriate dosing regimen in preterm pigs. Finally, we investigated how restoration of circulating IGF-1 levels in preterm pigs affected clinical variables, parameters of gut function and NEC in 5-day-old formula-fed preterm pigs, known to be highly sensitive to spontaneous development of NEC-like lesions throughout the gut.

MATERIALS AND METHODS

Animal studies were conducted in accordance with the European Communities Council Directive 2010/63/EU for the protection of animals used for experimental purposes and approved by the Danish Animal Experiments Inspectorate, Ministry of Environment and Food of Denmark.

Experiment 1: Basal Circulating IGF-1 Levels in Piglets

Groups of pigs (Landrace x Yorkshire x Duroc) were born at different gestational ages in relation to normal full term [117 ± 2 days] and reared artificially or naturally, as previously described (31). In brief, these pigs were born vaginally on day 112 and housed with their mother under natural rearing conditions ($n = 12$), by cesarean section at day 115 and housed in incubators ($n = 14$), or groups of pigs delivered by cesarean section on day 106 and housed in incubators (total $n = 145$). Blood samples were obtained at day 1 (cord blood), day 5 or day 19 (**Figure 1**).

Experiment 2: Pharmacokinetics of IGF-1

A 1:1 molar ratio of the non-covalent complex rhIGF-1/rhIGFBP-3 (rhIGF-1/BP-3, mecasermin rinfabate) and

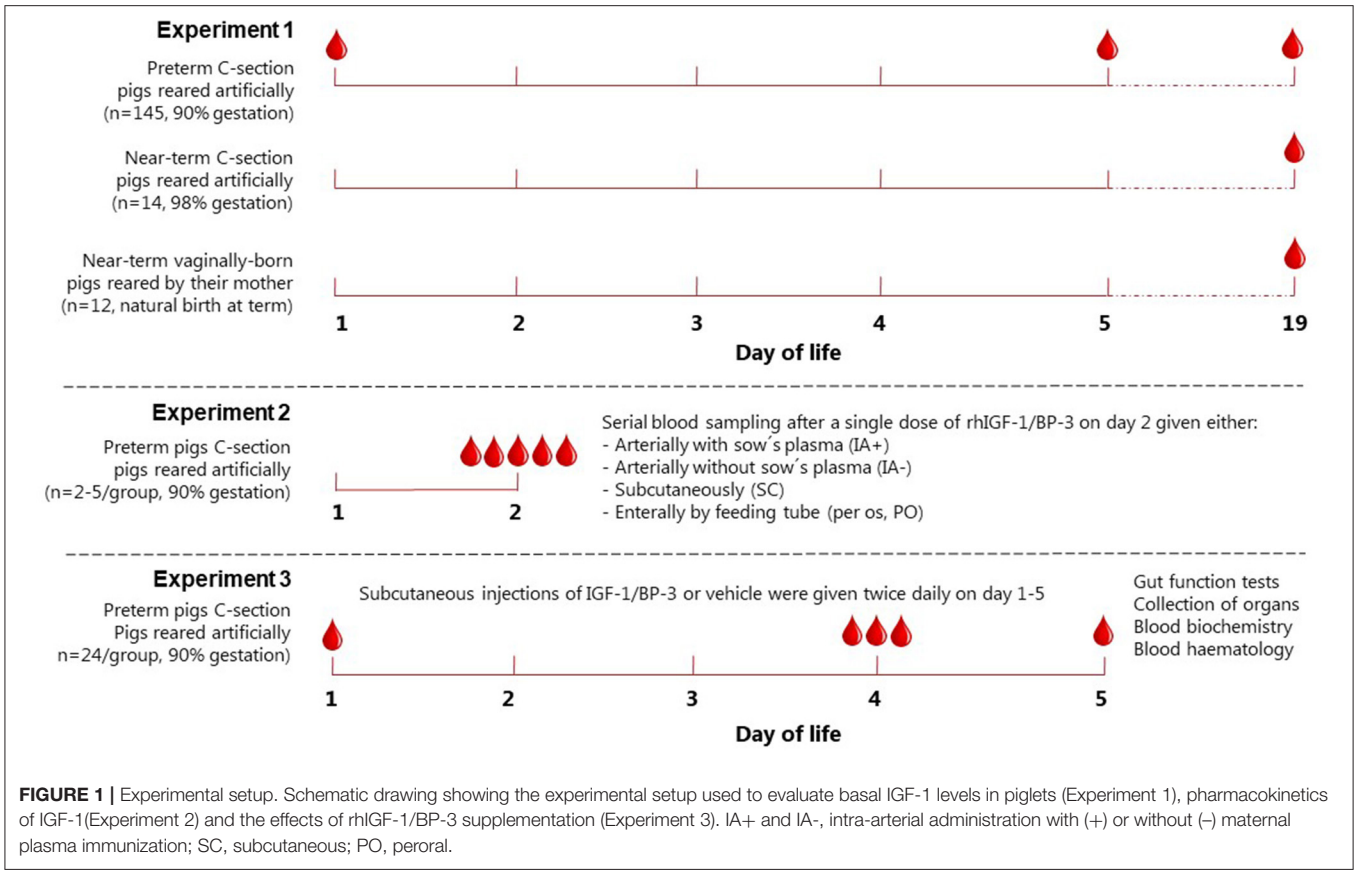

FIGURE 1 | Experimental setup. Schematic drawing showing the experimental setup used to evaluate basal IGF-1 levels in piglets (Experiment 1), pharmacokinetics of IGF-1(Experiment 2) and the effects of rhIGF-1/BP-3 supplementation (Experiment 3). IA+ and IA-, intra-arterial administration with (+) or without (–) maternal plasma immunization; SC, subcutaneous; PO, peroral.

formulation vehicle were provided by Takeda, Cambridge, MA, USA. Based on our literature studies from both infants and pigs (3, 4, 30), we aimed for a target physiological IGF-1 range of 30–110 ng/ml in the circulation. Preterm pigs for the pharmacokinetic study were delivered from one sow by cesarean section at day 106 and reared in incubators. All pigs received 4 ml/kg/h total parenteral nutrition (TPN) for 3 days. On day 2, pigs were divided into four groups, with pigs given a single injection of rhIGF-1/BP-3 (**Figure 1**): Pigs injected with 0.5 mg/kg intra-arterially without maternal plasma (IA-, $n = 3$), pigs injected with 0.5 mg/kg intra-arterially subsequent to 16 ml/kg maternal sow plasma (IA+, $n = 3$), pigs injected with 0.5 mg/kg subcutaneously with no sow's plasma (n=5) and pigs injected with 6 mg/kg orally, no maternal sow plasma and fed 10 ml/kg colostrum 0 and 1 h after IGF-1 ($n = 2$). Plasma for IGF-1 measurement was obtained *via* the umbilical arterial catheter at intervals from 30 min to 8 h after the single rhIGF-1/BP-3 injections. The preliminary investigation of IGF-1 levels after oral administration was to verify that the contribution from dietary IGF-1 to circulating IGF-1 levels would be minimal. Likewise, the studies with/without sow's plasma were to study the specific contribution of IGF-1 from sow's plasma, normally given in our studies on preterm pigs to provide them with passive immunity for survival and infection resistance (31). Based on the pharmacokinetic profile, with sustained levels of plasma IGF-1 within the desired physiological range (**Supplementary Figure 1**), a subcutaneous dose of 0.5 mg/kg rhIGF-1/BP-3 twice daily was chosen for the IGF-1 supplementation study (Experiment 3).

Experiment 3: IGF-1 Supplementation Study

Forty-nine piglets were delivered from two sows by cesarean section at 90% of gestation (day 106). Immediately after birth all pigs were injected intramuscularly with 0.1 ml doxapram and 0.1 ml flumazenil, transferred to our NICU facility and housed in temperature-regulated incubators with extra oxygen supply (1–2 l/min) for the first 12 h. The pigs were fitted with orogastric and umbilical arterial catheters for enteral feeding and vascular access. One pig was euthanized due to catheter-related problems and excluded from the study before randomization. Pigs were block-randomized according to birth weight and gender into two groups: pigs given 0.5 mg/kg rhIGF-1/BP-3 subcutaneously (SC) twice daily (rhIGF-1/BP-3, $n = 24$) at 7 am and 3 pm and pigs given equivalent volumes of vehicle SC twice daily (Controls, $n = 24$) at 7 am and 3 pm until they were euthanized at day 5 (**Figure 1**). *Via* the umbilical arterial catheter all pigs were immunized with maternal sow plasma (16 ml/kg) during the first 24 h and parenteral nutrition (PN) (Kabiven modified with Vamin, Soluvit, Vitalipid and Peditrace, all Fresenius Kabi, Uppsala, Sweden) was infused continuously throughout the study period (2–5 ml/kg/h) to

meet nutrient and fluid requirements of pigs (25). Every 3 h, the pigs were fed enteral formula composed of commercially available products used for feeding infants (formula composition shown in **Supplementary Table 1**). The enteral nutrition (EN) was provided *via* the orogastric catheter with increasing volumes (24–120 ml/kg/d) throughout the study period.

Clinical Observations and *in vivo* Tests

Pigs were weighed daily, monitored closely and euthanized immediately if severe respiratory distress or NEC symptoms were observed. Clinical and fecal status were evaluated twice daily using previously validated scoring systems (30) (except that fecal score 5 included diarrhea with visual blood). All involved personnel was trained and experienced in work with preterm pigs. The treatment groups were blinded by color codes on the stable records. Motor activity was captured by infrared video surveillance connected to a motion detection software (PigLWin, Ellegaard Systems, Faaborg, Denmark). Physical activity was analyzed from day 2, 8 am, since physical activity during the first 24 h of life mainly reflects wake-up movements after delivery and anesthesia. Intestinal permeability was assessed day 5 by peroral administration of a 5/5% lactulose/mannitol bolus (15 ml/kg) and urine recovery after 3 h. Concentration of lactulose and mannitol in urine were obtained and analyzed as previously described (32). Gastric residual was assessed by oral administration of a last feeding bolus (15 ml/kg) 60 min prior to euthanasia and postmortem measurement of the stomach content weight. Gastric pH was measured in the stomach content using a pH meter.

Blood Biochemistry, Hematology and Circulating IGF-1 Levels

For biochemistry and hematology, 1 ml blood was collected on day 4 in a heparin blood vacutainer (BD Diagnostics, Oxford, UK) *via* the umbilical catheter. Biochemistry of plasma and cell counting of full blood were analyzed using an Advia 1800 Chemistry System and an Advia 2120i Hematology system (Siemens Healthcare, Ballerup, Denmark), respectively. The plasma biochemistry profile included typical measures of metabolic, liver and kidney functions.

For circulating IGF-1 measurement blood samples were obtained two, six and 15 h post-dosing at day 4 *via* the umbilical catheter and at day 5 *via* intracardial puncture at euthanasia. One ml blood was collected in a serum tube with clot activator (BD diagnostics), rested until clotted (½-1 h), centrifuged at 1300 $\times$ *g* for 10 min and stored at −80°C. All serum samples were analyzed using a human IGF-1 ELISA kit (Mediagnost GmbH, Reutlingen, Germany) in a bioanalytical testing laboratory (PPD Laboratories, Richmond, Virginia). The quantitative limit of the analysis was 20 ng/mL, however, values between 10 and 20 ng/ml were also recorded for information. The detection limit of the analysis was 10 ng/ml and measurements lower than 10 ng/ml were assigned a value of 5 ng/ml for quantitative evaluations.

Tissue Collection and NEC Evaluation

On day 5, pigs were euthanized with an intracardial injection of sodium-pentobarbital (Euthanimal, Scanvet, Denmark). The entire gastrointestinal tract was removed from the abdomen and the stomach, proximal, middle and distal small intestine, caecum and colon were evaluated for pathological changes in a blinded fashion by two persons, using the following validated NEC scoring system for each of the gut regions (28): 1 = absence of lesions, 2 = local hyperaemia, 3 = hyperaemia, extensive edema and local hemorrhage, 4 = extensive hemorrhage, 5 = local necrosis or pneumatosis intestinalis, 6 = extensive necrosis and pneumatosis intestinalis. NEC was defined as a score of minimum 3 in at least one gut region, whereas a score of minimum 4 in at least one gut region was defined as "severe NEC." An average NEC severity score of the total gastrointestinal tract was calculated as the mean of the highest score of the small intestine parts (prox, mid or dist), the highest score of the colon parts (cecum or colon) and stomach. Organs were weighed and tissue from small intestine and colon was snap frozen and stored at −80°C to evaluate enzyme activities and levels of pro-inflammatory cytokines. Bone marrow was harvested from the distal femoral epiphysis with sterile instruments, cultured on blood agar at room temperature for 24 h, and stored at 4°C until colonies were enumerated.

Histological Examinations

Mid small intestine and colon tissue were fixed in 4% formaldehyde solution (CellPath, Newton, Powys, United Kingdom) routinely processed, embedded in paraffin blocks and sectioned at a thickness of 3 μm. The slides were stained with hematoxylin and eosin and Alcian-Blue-periodic acid Schiff for light-microscopic evaluation. Using a Leica DM2500 optical microscope images were taken by a lab technician unaware of treatment groups and villus length and crypt depth were quantified by an averaging value from 10 representative villi and crypts measured by ImageJ software (Laboratory for Optical and Computational Instrumentation, University of Wisconsin-Madison). Goblet cell density was calculated by the same lab technician using a stereological approach as the area of goblet cells relative to the total area of tunica mucosa (%).

To access the degree of proliferation, immunohistochemical staining was performed on tissue from small intestine mid sections. The slides were pre-treated with TEG buffer pH 8 for 2x5 min. Endogenous peroxidase was inhibited by incubation in 0.6% H_2O_2 for 15 min followed by Ultra V blocking (Thermo Fisher Scientific, Hvidovre, Denmark) for 5 min. Primary Ki-67 antibody (clone MIB-1, Dako, Glostrup, Denmark) was diluted 1:200 in 1% bovine serum albumin (BSA)/Tris-buffered saline (TBS) and slides were stained with the primary antibody overnight. Afterwards the sections were incubated for 20 min with Primary Antibody Enhancer followed by detection with HRP Polymer for 30 min (Thermo Fisher Scientific). Slides were then incubated with aminoethyl carbazole (AEC) solution for 10 min and counterstained with Meyer's hematoxylin. Finally, sections were dehydrated and mounted with glycerol-gelatine. Using a Leica DM2500 optical microscope, eight images of each small intestine section were taken in a standardized way and an automated digital image analysis of positive Ki67 staining areas in tunica mucosa was performed using

FIJI software (Fiji Is Just ImageJ, Laboratory for Optical and Computational Instrumentation). The analysis was run with vectors H DAB to detect cell nuclei and staining of specific Ki76 immunohistochemically positive areas (threshold = ∞-150, particle size, pixel^2 = 10-∞). The process was followed by a calculation step. Ki67 density was given as mean total Ki67 stained area of the total nuclei area in tunica mucosa (%).

Brush Border Enzyme Activity and Cytokine Expression

For activity of the brush border enzymes, lactase, maltase, sucrase, aminopeptidase N (ApN), aminopeptidase A (ApA), dipeptidylpeptidase IV (DPPIV) tissue samples from the mid small intestine were homogenized in 1% Triton X-100 buffer using a gentleMACS Dissociator (Miltenyi Biotec, Bergisch Gladbach, Germany). Assays were performed using specific substrates, as described previously (33). Interleukin (IL)-1β, IL-6, IL-8 and tumor necrosis factor (TNF)-α levels in mid small intestine and colon homogenates were analyzed using DuoSet ELISA kits (R&D systems, Minneapolis, MN) following the manufacturer's instruction. Each sample was tested in duplicate and measurements below detection limits were assigned a value of zero for the given analyte.

Statistical Analysis

The statistical software package R (version 3.6.1) was used for statistical analyses. Statistical significance of difference in continuous variables was analyzed by linear models if normally distributed. The model was tested for normality by Shapiro-Wilk's test and plots, data were transformed when required and non-parametric analysis was applied when data could not be transformed properly. Basal plasma IGF-1 levels measured in in Experiment 1 were analyzed by a non-parametric test with corrections for multiple testing. Binary data were analyzed by a logistic regression model. Ordered categorical outcomes, like NEC scores, were analyzed by a proportional odds logistic regression model. Repeated measurements were analyzed by the linear mixed effects modelif continuous and by cumulative link mixed models if ordered categorical. The above mentioned models were adjusted for possible cofounders like litter, sex and birth weight. For value comparisons, $p < 0.05$ was considered statistically significant. Values are expressed as mean ± standard error of mean (SEM) unless otherwise specified and levels of significance are assigned as $^{*}p < 0.05$, $^{**}p < 0.01$, $^{***}p < 0.001$.

RESULTS

Experiment 1: Basal IGF-1 Levels in Piglets

At day 1, 5, and 19, 23% (7/31), 0% (0/5) and 29% (31/107) of preterm pigs had plasma IGF-1 values above the pre-set lower quantitative limit of the assay, with an estimated mean level below 20 ng/ml. At day 19, more near-term pigs reared by their sow had IGF-1 values above the quantitative limit (83%, 10/12) and a higher estimated mean level than preterm pigs (both $p < 0.01$) and near-term pigs reared artificially (36%, 5/14 above the quantitative limit, both $p < 0.05$) (**Figure 2A**). Preterm pigs born with low birth weight [lowest 25% weight percentile (28/107)] showed a reduced estimated mean level at day 19 compared with remaining preterm pigs ($p < 0.001$, **Figure 2A**). Also, preterm pigs with extrauterine growth restriction (lowest 25% weight gain percentile, 26/106) had reduced estimated mean levels compared with the remaining pigs ($p < 0.05$, **Figure 2A**).

Experiment 2: Pharmacokinetics of IGF-1

Baseline plasma IGF-1 levels ($t = 0$) in preterm pigs were generally below the lower limit of quantitation, with an estimated mean level below 20 ng/ml. Following intra-arterial dosing of 0.5 mg rhIGF-1/BP-3, plasma IGF-1 levels peaked 30 min after injection and reached baseline levels by 8 h both in the IA+ and IA- group (**Supplementary Figure 1**, i.e., passive immunization with sow's plasma contributed minimally to IGF-1 levels). Following subcutaneous administration, IGF-1 levels peaked at 4 h and had sustained elevated levels within the desired physiological range (30–110 ng/ml) for up to 8 h. Finally, following oral administration of 6 mg/kg rhIGF-1/BP-3, plasma IGF-1 levels were comparable to baseline levels at all time points (**Supplementary Figure 1**, i.e., minimal enteral absorption of IGF-1).

Experiment 3: IGF-1 Supplementation Study

Circulating IGF-1 Levels

At birth, serum IGF-1 levels in cord blood of rhIGF-1/BP-3 and controls pigs were similar and generally near the quantitative limit of 20 ng/ml ($n = 24$–25). Two, six and 15 h after injection on day 4, the serum IGF-1 levels in pigs treated with rhIGF-1/BP-3 were 54.0 ± 3.6, 38.0 ± 2.6 and below 20 ng/ml, respectively (mean ± SEM). In corresponding control pigs, the estimated IGF-1 levels were below 20 ng/ml throughout (**Figure 2B**). When pigs were euthanized in a random sequence on day 5, serum IGF-1 levels in rhIGF-1/BP-3 pigs peaked 1.5-4.5 hrs after the last injection, with IGF-1 levels being 55–75 ng/ml. The IGF-1 levels then declined to 20–35 ng/ml 7–9 h after injection (**Figure 2C**). In all control pigs, values were below 20 ng/ml (**Figure 2C**, except for one control pig with a value of 24.8 ng/ml).

Clinical Observations, Organ Weights, Blood Chemistry, and NEC Lesions

Until day 4 all pigs were clinically stable with a clinical score = 1 (**Supplementary Table 2**). One control pig was euthanized on day 4 because of severe clinical NEC symptoms (abdominal distension, cyanosis and bloody diarrhea) while all others were killed on day 5 for planned tissue collection. No differences were found between rhIGF-1/BP-3 pigs and control pigs in birth weight, kill weight and average daily weight gain (**Table 1**). Likewise, rectal temperatures, clinical scores, fecal scores and physical activity were similar throughout the study period (**Supplementary Table 2**). At tissue collection on day 5, there were no differences among groups in relative organ weights, intestinal length or gastric pH (**Table 1**). At this time, hematological values and blood biochemistry values were similar between groups, except that rhIGF-1/BP-3 treatment increased the leukocyte and neutrophil counts ($p < 0.05$,

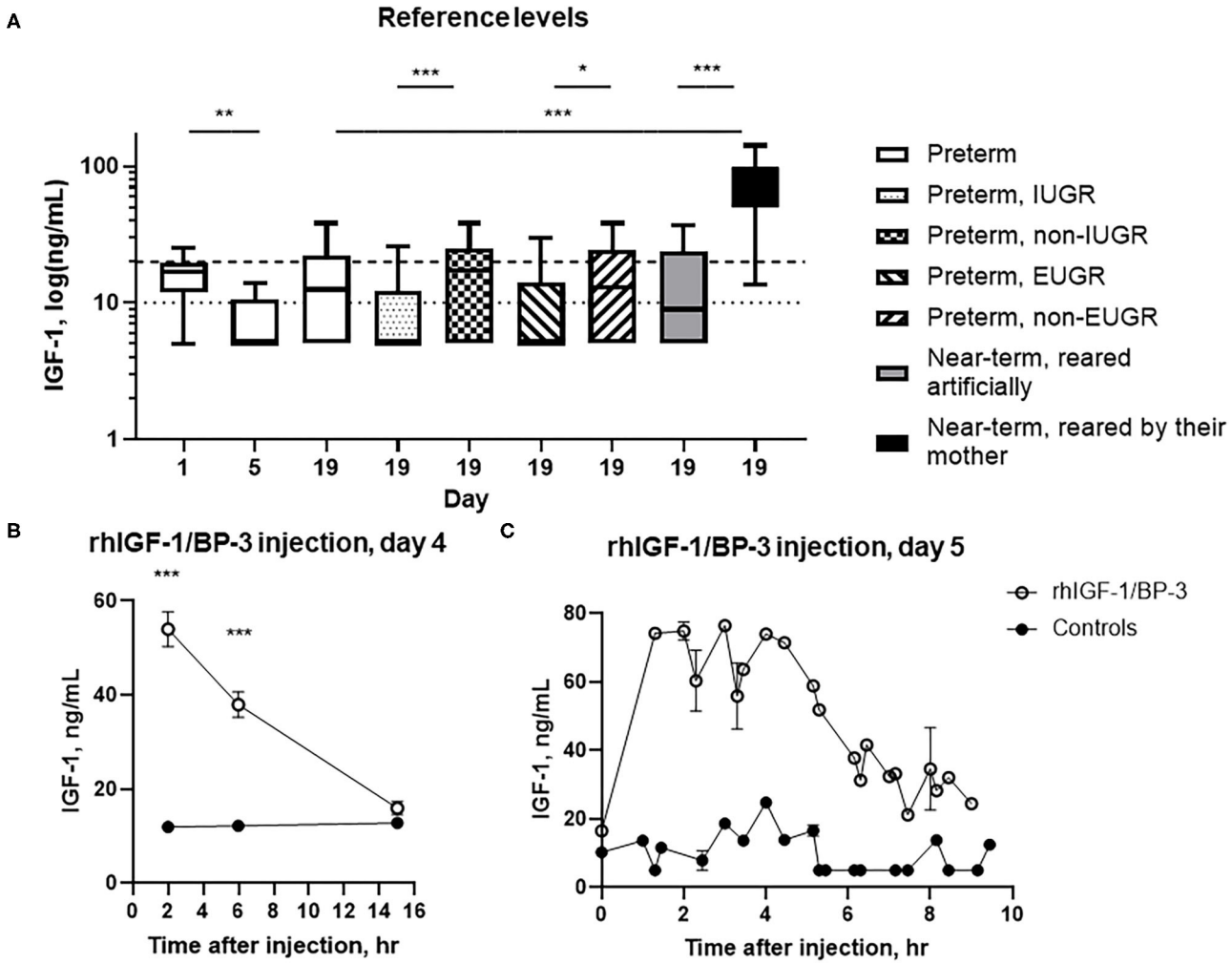

FIGURE 2 | Circulating IGF-1 levels and pharmacokinetics (mean ± SEM). **(A)** Basal IGF-1 plasma levels in 1–19 day-old preterm pigs reared in incubators (n = 7–107), near-term pigs reared in incubators (n = 14), and near-term pigs reared with their mother (n = 12). The 19 day-old preterm pigs were subdivided into pigs with intrauterine growth restriction (IUGR, n = 28) or non-IUGR (n = 79), and extrauterine growth restriction (EUGR, n = 26) or non-EUGR (n = 80), with growth restriction defined as the pigs with body weight within the lowest 25% of the growth percentiles. Data are presented as box plots (median and 25/75 percentiles) with whiskers = min to max. The interrupted horizontal line indicates the lower limit of quantitation (20 ng/ml) and the dotted horizontal line indicates the limit of detection (10 ng/ml) of the assay. **(B)** Serum IGF-1 levels in rhIGF-1/BP-3 and control preterm pigs after a single subcutaneous injection of rhIGF-1/BP-3 or vehicle on day 4 (n = 18–23) (mean ± SEM). **(C)** Serum IGF-1 levels at euthanasia 0–10 h after the last subcutaneous injections of rhIGF-1/BP-3 or vehicle on day 5 (n = 1–2 for samples taken 1-10 h after last dosing). t = 0 represents samples taken 15 h after last dosing (n = 16–19). $^{*}p < 0.05$, $^{**}p < 0.01$, $^{***}p < 0.001$.

Supplementary Tables 3, 4). Of note, basal plasma glucose levels were not significantly affected by rhIGF-1/BP-3 treatment.

When the incidence of NEC lesions included mild cases (score ≥3 in at least one gut region) there was no significant difference between groups (15/24 in rhIGF-1/BP-3 pigs vs. 20/24 in control pigs), but severe NEC lesions (score ≥4 in at least one gut region) was less frequent in rhIGF-1/BP-3 pigs than in control pigs (7/24 vs.16/24, $p = 0.01$, **Figure 3A**). Accordingly, average NEC severity across the entire gut and NEC scores in the colon region were lower in rhIGF-1/BP-3 vs. control pigs (**Figures 3B,C**, both $p < 0.05$). Stomach, small intestine and colon NEC lesions were present in 13 (37%), 8 (23%), and 32 (91%) out of the total 35 NEC cases, respectively (**Supplementary Table 5**). Thus, colon lesions occurred most frequently in 5 day-old preterm pigs, with three pigs (9%) having NEC in both colon and small intestine, nine pigs (26%) having NEC in both colon and stomach and 3 pigs (9%) having NEC in all three gut regions (**Supplementary Table 5**).

Intestinal Histology, Permeability, Digestive Enzymes and Cytokines

In the mid small intestine, rhIGF-1/BP-3 pigs had increased villus length compared with control pigs ($p < 0.05$, **Figure 3D**). When the four pigs with severe NEC lesions in this region (lesion score ≥ 4) were excluded from the analysis, the villus height difference between groups disappeared, indicating that

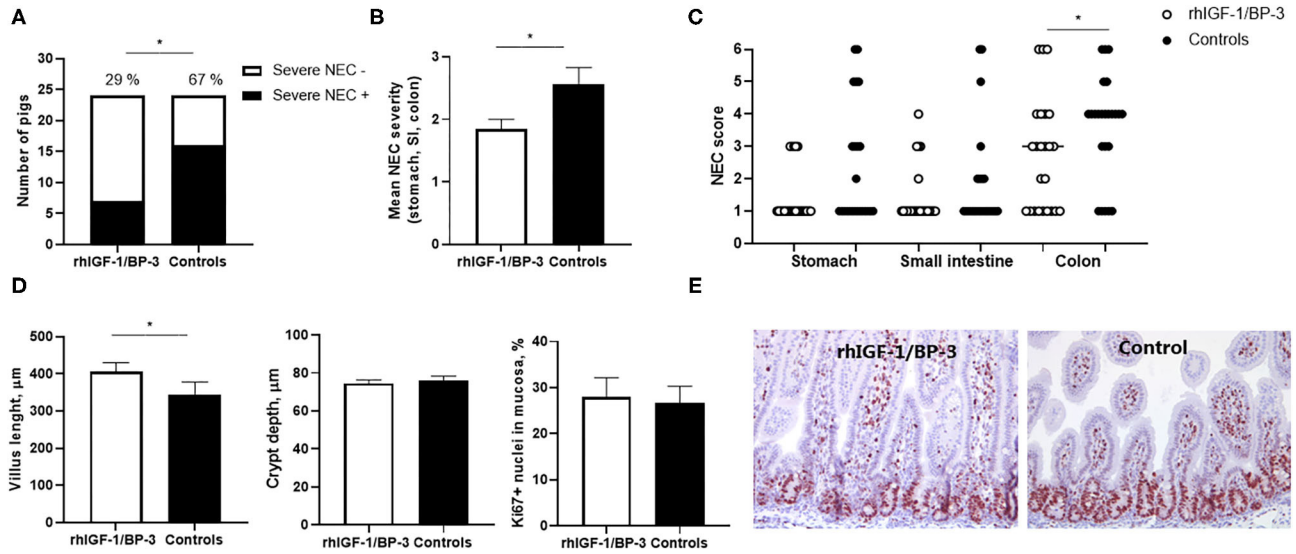

FIGURE 3 | Intestinal lesions and structure. **(A)** Incidence of severe NEC (defined as score ≥4 in at least one gut region) in rhIGF-1/BP-3 and control preterm pigs ($n = 24$). **(B)** NEC severity score across gut regions in rhIGF-1/BP-3 and control preterm pigs ($n = 24$). **(C)** Individual NEC scores in stomach, small intestine regions (highest score of the proximal, middle and distal section) and colon regions (highest score of the colon and cecum). **(D)** Villus length, crypt depth and Ki67 stained area relative to total nuclei area in tunica mucosa in mid small intestine ($n = 23$). Values are mean±SEM. **(E)** Immunohistochemically staining for Ki67 with hematoxylin counterstain in a representative middle small intestine section from a preterm pig treated with rhIGF-1/BP-3 and a control preterm pig. Pictures are 10x. $^{*}p < 0.05$, $^{**}p < 0.01$, $^{***}p < 0.001$.

TABLE 1 | Relative organ weights and parameters of preterm pigs treated with rhIGF-1/BP-3*.

Parameter	rhIGF-1/BP-3	Controls
Number of animals	23–24	22–24
Birth weight, g	1164 ± 63	1180 ± 60
Kill weight, g	1232 ± 66	1249 ± 61
Daily weight gain, g	14.9 ± 2.7	15.3 ± 2.5
SI length, cm/kg	285.7± 9.9	280.4 ± 8.0
SI weight:length, mg/cm	91.8 ± 2.6	89.9 ± 3.2
Stomach acidity, pH	3.8 ± 0.1	3.8 ± 0.1
Relative organ weights, g/kg:		
Liver	27.4 ± 0.7	28.0 ± 0.6
Spleen	2.7 ± 0.2	2.4 ± 0.1
Kidney	8.7 ± 0.3	8.2 ± 0.3
Stomach	6.2 ± 0.2	6.8 ± 0.4
Stomach content	25.8 ± 1.6	27.4 ± 2.5
Colon	16.0 ± 0.6	16.3 ± 0.7
SI total	25.8 ± 0.6	24.9 ± 0.7
SI Proximal	9.1 ± 0.3	8.6 ± 0.4
SI Middle	7.9 ± 0.6	7.3 ± 0.4
SI Distal	7.7 ± 0.2	7.6 ± 0.2

Values are mean ± SEM. There were no significant differences for any variable between groups (all $p > 0.05$). SI, Small intestine.

the rhIGF-1/BP-3 effect on villus morphology occurred *via* a NEC-protective effect. No differences in crypt depth or Ki67 density, reflecting the enterocyte proliferation rate, were observed (**Figures 3D,E**). In the colon, crypt depth (63.9 ± 1.6 vs. 64.1 ± 2.5 µm) and density of mucin-containing goblet cells (5.9 ± 0.7 vs. 5.3 ± 0.9 %) did not differ between rhIGF-1/BP-3 and control pigs.

No significant differences were observed between rhIGF-1/BP-3 and control pigs in intestinal permeability, as indicated by the urinary lactulose/mannitol ratio and accumulation of bacteria in the bone marrow (**Figures 4A,B**). Relative to control pigs, rhIGF-1/BP-3 pigs had a 44% ($p = 0.01$) and 31% ($p = 0.02$) increase in activity of the brush border peptidases ApN and DPPIV respectively, while ApA and disaccharidase activities (sucrase, maltase, lactase) did not differ between groups (**Figure 4C**). No significant differences in TNFα, IL-1β, IL-6 or IL-8 levels in the mid small intestine or colon were observed (**Figures 4D,E**).

DISCUSSION

Considering the ongoing clinical trials on IGF-1 supplementation in extremely preterm infants, it is important to understand how elevated IGF-1 levels in the postnatal period may affect organ development in preterm neonates short- and long-term. Using preterm NEC-sensitive pigs as models for such infants, we now examined the short-term effect of supplemental rhIGF-1/BP-3 on clinical variables, gut maturation and NEC incidence. Supporting our earlier studies (30), circulating IGF-1 levels remained low in preterm pigs for at least 3 weeks after birth (until the weaning transition period), at levels similar to those reported in hospitalized very and extremely preterm infants (2, 4). Conversely, IGF-1 values in 3 week-old near-term pigs reared by their sow were similar to values for normal *in*

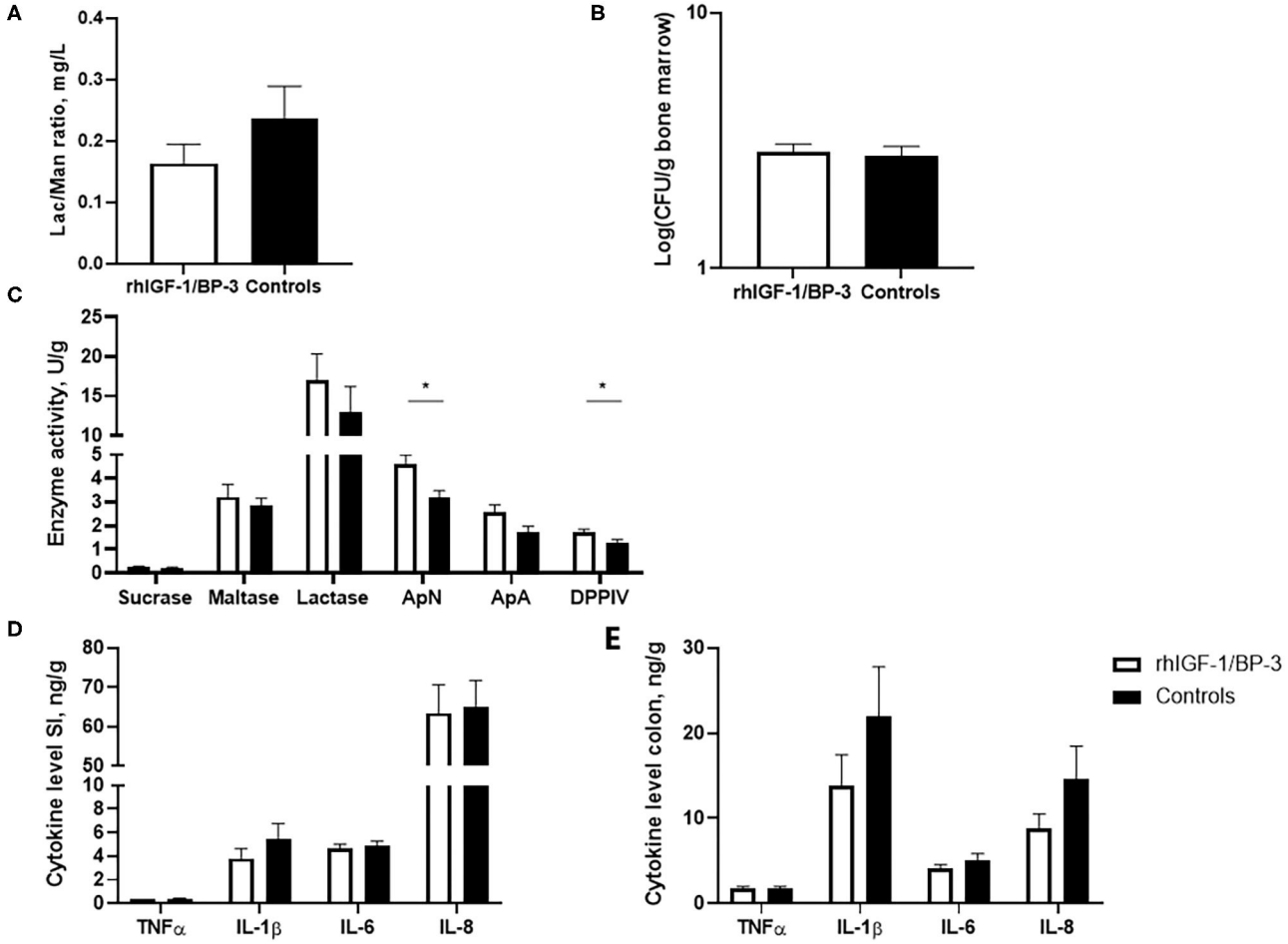

FIGURE 4 | Intestinal functions (means ± SEM). **(A)** Concentration of lactulose/mannitol (Lac/Man) ratio to asses intestinal permeability in the urine on day 5 ($n = 18$–22), and **(B)** bacterial load in bone marrow (colony forming units, CFU) to assess bacterial translocation on day 5 ($n = 23$–24). **(C)** Brush border enzyme activities in mid small intestine ($n = 24$, ApN, aminopeptidase N; ApA, aminopeptidase A; DPPIV, dipeptidylpeptidase). Pro-inflammatory cytokines in **(D)** middle small intestine and **(E)** colon ($n = 23$–24). $^{*}p < 0.05$, $^{**}p < 0.01$, $^{***}p < 0.001$.

utero human fetuses in the weeks before full-term birth (4). In control preterm pigs, we could only estimate the basal IGF-1 levels as most of the values were below the limit of optimal quantitation for our assay. Thus, a window of opportunity for supplemental IGF-1 may exist in the first week(s) after preterm birth. Our results suggest that IGF-1 supplementation in the first days after birth, restoring circulating IGF-1 levels for up to 6 h twice daily for 4 days, did not negatively affect clinical parameters, gut function or NEC. Rather, the treatment induced a moderate reduction in NEC incidence, accompanied by increased intestinal villus heights and peptidase activities that are good markers of villus integrity and function in preterm pigs (25–29). Further studies in both pigs and infants are required to confirm these findings.

It is well-documented that IGF-1 stimulates enterocyte proliferation and function (10, 12, 14, 15) but we were unable to demonstrate effects on epithelial proliferation, as tested by immunohistochemical staining. Enterocyte proliferation is relatively slow in fetuses and preterm neonates, especially in the more distal parts of the intestine, and IGF-1 may have worked to increase enterocyte lifespan and differentiation rather than stimulating proliferation, like in rodents after intestinal injury (9–11) or preterm pigs given milk diets rich in IGF-1 (34), supporting the effects of oral IGF-1 on gut growth, nutrient absorption, and enzyme activities in term pigs (13–15). Fresh milk contains important nutrients and multiple bioactive factors and the beneficial effects of mothers' milk and colostrum on gut maturation and NEC in infants are well-documented (20, 35). Colostrum and milk feeding also improve gut function and reduce NEC incidence and severity in preterm pigs relative to formula feeding (27, 29, 36). This may in part relate to high IGF-1 exposure (37, 38). Industrial processing of bovine milk for infant formula, for example, filtration and heat treatment steps, reduces the concentrations of bioactive proteins, including IGF-1 (34).

Impaired innate and adaptive immunity is a hallmark of prematurity and IGF-1 may play a role in this. In both preterm

pigs and infants, a low number of leucocytes, specifically neutrophils (neonatal neutropenia), may contribute to high susceptibility to infection, sepsis and NEC (23, 39, 40). However, in this study no correlation was observed between the number of leucocytes in the blood and the number of bacteria in the bone marrow of individual pigs (data not shown). In infants, IGF-1 has anti-inflammatory effects on newborn cord blood (41) and in rodents IGF-1 inhibits the TLR4/NF-κB signaling pathway and secretion of pro-inflammatory cytokines (42). The neutropenia and depressed immune function in preterm infants (40) and pigs (23, 39) may be partly prevented by IGF-1 treatment, like in other life stages (7, 43), but more studies are required to test this hypothesis.

Locally in intestinal epithelial cells, IGF-1 increases the expression of mucin and SIgA and protects against oxidative injury, thereby promoting mucosal barrier functions (8, 42). In this study, the macroscopic IGF-1 effects in the colon were not accompanied by changes in tissue cytokine levels or mucosal barrier function in the small intestine, as indicated by the urinary lactulose/mannitol ratio, bacterial load in the bone marrow or goblet cell density, despite that the overall NEC severity was similar to that reported in earlier similar studies in preterm pigs (39, 44, 45). However, some of these parameters may be mostly affected by NEC lesions in the small intestine vs. colon (where lesions occurred most frequently in this study), as shown in our previous study on region-dependent NEC effects on systemic inflammation in preterm pigs (46). In follow-up studies, we have quantified the expression levels of a series of immune-related genes specifically in the colon region (C3, CASP3, HIF1A, IL17, IL8, LBP, MPO, OFLM4, TLR2, TLR4, VEGF) but no significant differences were found between rhIGF-1/BP-3 pigs and control pigs on day 5 (unpublished observations). We conclude that the chosen treatment regimen, like dose, time and length of administration, had minimal effects on both intestinal and colonic immune responses in preterm pigs, despite the observed NEC-protective effects.

In the recent Swedish infant rhIGF-1/BP-3 intervention study, treatment reduced BPD and IVH severity, while the primary endpoint (retinopathy of prematurity, ROP) was unaffected (17). Conclusions regarding NEC effects were not possible due to low sample size and low NEC rate. The overall incidence of NEC was similar between groups (5–6 out of 60–61 infants), but the number of fatal NEC cases was highest in the rhIGF-1/BP-3 treated group (3 vs. 0), which raises some concerns despite the low number of cases. NEC remains a frequent and serious disease with potential fatal outcomes or long-term consequences for infants (18, 19, 21, 47). Current treatment strategies include bowel rest, nasogastric decompression, systemic antibiotics, respiratory and cardiovascular support and in the worst cases, surgical intervention (25–50% of NEC cases) (35, 48).

Preterm infants are a highly heterogeneous patient group and standardized rhIGF-1/BP-3 supplementation of all extremely preterm infants is unlikely to be appropriate. Because of the short circulating half-life of IGF-1 after subcutaneous and intravenous injections with rhIGF-1/BP-3, a current need for daily administration *via* indwelling catheters or repeated injections, is another challenge that needs to be overcome and adapted to clinical practice. The present pre-clinical safety and efficacy results in preterm pigs are promising but results should be interpreted with caution. Importantly, the short duration of twice daily subcutaneous dosing and the short half-life of rhIGF-1/BP-3 did not result in longer-lasting, continuous physiologic levels of circulating IGF-1 in preterm pigs. This may partly explain the limited effects and benefits across all the investigated clinical, blood and tissue parameters in preterm pigs during the first 5 days of life. We have recently tested the effects of a longer, higher and more frequent dose of rhIGF-1/BP-3 (0.75 mg/kg three times daily until day 9 after birth) and confirmed the reduction in NEC incidence, together with a clear increase in intestinal weight (unpublished observations). Provision of rhIGF-1/BP-3 at the right time and dose may be safe and support growth and organ development in subgroups of preterm infants, but more studies, across multiple organs, are required before rhIGF-1/BP-3 can used in clinical practice for groups of preterm infants.

Prematurity involves developmental deficits across multiple organs in the body, making exogenous IGF-1 an attractive early therapy for very preterm infants with its well-documented multi-functional physiological benefits in animal models and low levels after preterm birth in humans. Neonatal IGF-1 supplementation is clearly a therapy where the benefits vs. potential unforeseen treatment risks must be thoroughly investigated. Importantly, organ systems develop differently in various mammals relative to the normal time of birth, either preterm or term. This makes it a challenge to translate the effects of exogenous IGF-1 observed for one organ system at one time point in one species (e.g., pigs) to corresponding conditions in another species (e.g., infants). Preterm pigs are more sensitive to develop NEC lesions than very preterm infants and lesions often first appear in the colon region, unlike infants (39, 44, 48). However in both infants and pigs, the predisposing factors for NEC lesions are similar, for example, low gestational age, aggressive enteral (formula) feeding and adverse gut bacterial colonization (25–27, 29, 44). These interact with a number of other determinants, eventually leading to breakdown of the gut mucosal barrier and excessive mucosal inflammation (20, 35).

Future studies, potentially using pigs as models, should further study both short- and long-term NEC effects of IGF-1 and other critical morbidities known from very preterm infants, like BPD, IVH and ROP. In such studies, it will also be important to verify if IGF-1 supplementation in early life may alleviate the growth restriction and nutrient dysmetabolism often observed in very preterm infants.

DATA AVAILABILITY STATEMENT

The raw data supporting the conclusions of this article will be made available by the authors, without undue reservation.

ETHICS STATEMENT

The animal study was reviewed and approved by National Committee on Animal Experimentation, Denmark.

AUTHOR CONTRIBUTIONS

KH conceived and designed the experiments, acquired, analyzed and interpreted data, and wrote the paper. PS conceived and designed the experiments, analyzed and interpreted data, helped to draft the paper, and took final responsibility for its contents. XG and TT conceived and designed the experiments and acquired and interpreted data. XP, RN, and TM acquired data. TG analyzed and interpreted data. GC and NB conceived and designed the experiments. All authors revised the manuscript critically for important intellectual content and approved the final version. All authors agree to be accountable for all aspects of the work in ensuring that questions related to the accuracy or integrity of any part of the work are appropriately investigated and resolved.

FUNDING

The authors declare that this study received funding from Takeda, MA, USA (former Shire). This funder was not involved in the study design, collection, analysis, interpretation of data, the writing of this article or the decision to submit it for publication.

ACKNOWLEDGMENTS

The authors like to thank Elin Skytte and Kristina Møller for laboratory technical assistance and Jane Connie Povlsen, Britta Karlsson, Karoline Aasmul-Olsen, Nicole Lind Henriksen, Anders Brunse, Jing Sun, and Duc Ninh Nguyen for assistance with the many procures related to preterm pig care, for example, resuscitation, catheterization, clinical surveillance, drug administration, feeding, and sample collections.

SUPPLEMENTARY MATERIAL

The Supplementary Material for this article can be found online at: https://www.frontiersin.org/articles/10.3389/fped.2020.602047/full#supplementary-material

REFERENCES

1. Blencowe H, Cousens S, Oestergaard MZ, Chou D, Moller A-B, Narwal R, et al. National, regional, and worldwide estimates of preterm birth rates in the year 2010 with time trends since 1990 for selected countries: a systematic analysis and implications. *Lancet.* (2012) 379:2162–72. doi: 10.1016/S0140-6736(12)60820-4
2. Hansen-Pupp I, Hellstrom-Westas L, Cilio CM, Andersson S, Fellman V, Ley D. Inflammation at birth and the insulin-like growth factor system in very preterm infants. *Acta paediatrica.* (2007) 96:830–6. doi: 10.1111/j.1651-2227.2007.00276.x
3. Diaz-Gomez NM, Domenech E, Barroso F. Breast-feeding and growth factors in preterm newborn infants. *J pediatr gastroenterol nutr.* (1997) 24:322–7.
4. Hellstrom A, Ley D, Hansen-Pupp I, Hallberg B, Lofqvist C, van Marter L, et al. Insulin-like growth factor 1 has multisystem effects on foetal and preterm infant development. *Acta Pediatrica.* (2016) 105:576–86. doi: 10.1111/apa.13350
5. Rajaram S, Baylink DJ, Mohan S. Insulin-like growth factor-binding proteins in serum and other biological fluids: regulation and functions. *Endocr Rev.* (1997) 18:801–31. doi: 10.1210/edrv.18.6.0321
6. Sara VR, Hall K. Insulin-like growth factors and their binding proteins. *Physiol Rev.* (1990) 70:591–614. doi: 10.1152/physrev.1990.70.3.591
7. Smith TJ. Insulin-like growth factor-i regulation of immune function: a potential therapeutic target in autoimmune diseases? *Pharmacol Rev.* (2010) 62:199–236. doi: 10.1124/pr.109.002469
8. Baregamian N, Song J, Jeschke MG, Evers BM, Chung DH. IGF-1 protects intestinal epithelial cells from oxidative stress-induced apoptosis. *J Surg Res.* (2006) 136:31–7. doi: 10.1016/j.jss.2006.04.028
9. Hunninghake GW, Doerschug KC, Nymon AB, Schmidt GA, Meyerholz DK, Ashare A. Insulin-like growth factor-1 levels contribute to the development of bacterial translocation in sepsis. *Am J Respir Crit Care Med.* (2010) 182:517–25. doi: 10.1164/rccm.200911-1757OC
10. Jeschke MG, Bolder U, Chung DH, Przkora R, Mueller U, Thompson JC, et al. Gut mucosal homeostasis and cellular mediators after severe thermal trauma and the effect of insulin-like growth factor-i in combination with insulin-like growth factor binding protein-3. *Endocrinology.* (2007) 148:354–62. doi: 10.1210/en.2006-0883
11. Ozen S, Akisu M, Baka M, Yalaz M, Sozmen EY, Berdeli A, et al. Insulin-like growth factor attenuates apoptosis and mucosal damage in hypoxia/reoxygenation-induced intestinal injury. *Biol Neonate.* (2005) 87:91–6. doi: 10.1159/000081897
12. Fholenhag K, Arrhenius-Nyberg V, Sjogren I, Malmlof K. Effects of insulin-like growth factor i (IGF-I) on the small intestine: a comparison between oral and subcutaneous administration in the weaned rat. *Growth Factors.* (1997) 14:81–8.
13. Burrin DG, Wester TJ, Davis TA, Amick S, Heath JP. Orally administered IGF-I increases intestinal mucosal growth in formula-fed neonatal pigs. *Am J Physiol.* (1996) 270:R1085–91. doi: 10.1152/ajpregu.1996.270.5.R1085
14. Alexander AN, Carey HV. Oral IGF-I enhances nutrient and electrolyte absorption in neonatal piglet intestine. *Am J Physiol.* (1999) 277:G619–25. doi: 10.1152/ajpgi.1999.277.3.G619
15. Houle VM, Schroeder EA, Odle J, Donovan SM. Small intestinal disaccharidase activity and ileal villus height are increased in piglets consuming formula containing recombinant human insulin-like growth factor-I. *Pediatr Res.* (1997) 42:78–86. doi: 10.1203/00006450-199707000-00013
16. Hellstrom A, Engstrom E, Hard A-L, Albertsson-Wikland K, Carlsson B, Niklasson A, et al. Postnatal serum insulin-like growth factor i deficiency is associated with retinopathy of prematurity and other complications of premature birth. *Pediatrics.* (2003) 112:1016–20. doi: 10.1542/peds.112.5.1016
17. Ley D, Hallberg B, Hansen-Pupp I, Dani C, Ramenghi LA, Marlow N, et al. rhIGF-1/rhIGFBP-3 in preterm infants: a phase 2 randomized controlled trial. *J Pediatr.* (2019) 206:56–65.e8. doi: 10.1016/j.jpeds.2018.10.033
18. Hull MA, Fisher JG, Gutierrez IM, Jones BA, Kang KH, Kenny M, et al. Mortality and management of surgical necrotizing enterocolitis in very low birth weight neonates: a prospective cohort study. *J Am Coll Surg.* (2014) 218:1148–55. doi: 10.1016/j.jamcollsurg.2013.11.015
19. Juhl SM, Gregersen R, Lange T, Greisen G. Incidence and risk of necrotizing enterocolitis in denmark from 1994-2014. *PLoS ONE.* (2019) 14:e0219268. doi: 10.1371/journal.pone.0219268
20. Niño DF, Sodhi CP, Hackam DJ. Necrotizing enterocolitis: new insights into pathogenesis and mechanisms. *Nat Rev Gastroenterol Hepatol.* (2016) 13:590. doi: 10.1038/nrgastro.2016.119
21. Patel RM, Kandefer S, Walsh MC, Bell EF, Carlo WA, Laptook AR, et al. Causes and timing of death in extremely premature infants from 2000 through 2011. *N Engl J Med.* (2015) 372:331–40. doi: 10.1056/NEJMoa1403489

22. de Waard M, Li Y, Zhu Y, Ayede AI, Berrington J, Bloomfield FH, et al. Time to full enteral feeding for very low-birth-weight infants varies markedly among hospitals worldwide but may not be associated with incidence of necrotizing enterocolitis: the NEOMUNE-neonutrinet cohort study. *JPEN J Parenter Enteral Nutr.* (2019) 43:658–67. doi: 10.1002/jpen.1466
23. Nguyen DN, Jiang P, Frokiaer H, Heegaard PMH, Thymann T, Sangild PT. Delayed development of systemic immunity in preterm pigs as a model for preterm infants. *Sci Rep.* (2016) 6:36816. doi: 10.1038/srep36816
24. Ren S, Hui Y, Obelitz-Ryom K, Brandt AB, Kot W, Nielsen DS, et al. Neonatal gut and immune maturation is determined more by postnatal age than by postconceptional age in moderately preterm pigs. *Am J Physiol Gastrointest Liver Physiol.* (2018) 315:G855–67. doi: 10.1152/ajpgi.00169.2018
25. Sangild PT, Thymann T, Schmidt M, Stoll B, Burrin DG, Buddington RK. Invited review: the preterm pig as a model in pediatric gastroenterology. *J Anim Sci.* (2013) 91:4713–29. doi: 10.2527/jas.2013-6359
26. Bjornvad CR, Schmidt M, Petersen YM, Jensen SK, Offenberg H, Elnif J, et al. Preterm birth makes the immature intestine sensitive to feeding-induced intestinal atrophy. *Am J Physiol Regul Integr Comp Physiol.* (2005) 289:R1212–22. doi: 10.1152/ajpregu.00776.2004
27. Bjornvad CR, Thymann T, Deutz NE, Burrin DG, Jensen SK, Jensen BB, et al. Enteral feeding induces diet-dependent mucosal dysfunction, bacterial proliferation, and necrotizing enterocolitis in preterm pigs on parenteral nutrition. *Am J Physiol Gastrointest Liver Physiol.* (2008) 295:G1092–103. doi: 10.1152/ajpgi.00414.2007
28. Cilieborg MS, Boye M, Thymann T, Jensen BB, Sangild PT. Diet-dependent effects of minimal enteral nutrition on intestinal function and necrotizing enterocolitis in preterm pigs. *JPEN J Parenter Enteral Nutr.* (2011) 35:32–42. doi: 10.1177/0148607110377206
29. Sangild PT, Siggers RH, Schmidt M, Elnif J, Bjornvad CR, Thymann T, et al. Diet- and colonization-dependent intestinal dysfunction predisposes to necrotizing enterocolitis in preterm pigs. *Gastroenterology.* (2006) 130:1776–92. doi: 10.1053/j.gastro.2006.02.026
30. Andersen AD, Sangild PT, Munch SL, van der Beek EM, Renes IB, Ginneken C van, et al. Delayed growth, motor function and learning in preterm pigs during early postnatal life. *Am J Physiol Regul Integr Comp Physiol.* (2016) 310:R481–92. doi: 10.1152/ajpregu.00349.2015
31. Obelitz-Ryom K, Rendboe AK, Nguyen DN, Rudloff S, Brandt AB, Nielsen DS, et al. Bovine milk oligosaccharides with sialyllactose for preterm piglets. *Nutrients.* (2018) 10:1489. doi: 10.3390/nu10101489
32. Ostergaard MV, Shen RL, Stoy ACF, Skovgaard K, Krych L, Leth SS, et al. Provision of amniotic fluid during parenteral nutrition increases weight gain with limited effects on gut structure, function, immunity, and microbiology in newborn preterm pigs. *JPEN J Parenter Enteral Nutr.* (2016) 40:552–66. doi: 10.1177/0148607114566463
33. Jensen AR, Elnif J, Burrin DG, Sangild PT. Development of intestinal immunoglobulin absorption and enzyme activities in neonatal pigs is diet dependent. *J Nutr.* (2001) 131:3259–65. doi: 10.1093/jn/131.12.3259
34. Li Y, Ostergaard MV, Jiang P, Chatterton DEW, Thymann T, Kvistgaard AS, et al. Whey protein processing influences formula-induced gut maturation in preterm pigs. *J nutr.* (2013) 143:1934–42. doi: 10.3945/jn.113.182931
35. Knell J, Han SM, Jaksic T, Modi BP. Current status of necrotizing enterocolitis. *Curr Probl Surg.* (2019) 56:11–38. doi: 10.1067/j.cpsurg.2018.11.005
36. Stoy ACF, Heegaard PMH, Thymann T, Bjerre M, Skovgaard K, Boye M, et al. Bovine colostrum improves intestinal function following formula-induced gut inflammation in preterm pigs. *Clin Nutr.* (2014) 33:322–29. doi: 10.1016/j.clnu.2013.05.013
37. Donovan SM, McNeil LK, Jimenez-Flores R, Odle J. Insulin-like growth factors and insulin-like growth factor binding proteins in porcine serum and milk throughout lactation. *Pediatr Res.* (1994) 36:159–68. doi: 10.1203/00006450-199408000-00005
38. Baxter RC, Zaltsman Z, Turtle JR. Immunoreactive somatomedin-C/insulin-like growth factor i and its binding protein in human milk. *J Clin Endocrinol.* (1984) 58:955–9. doi: 10.1210/jcem-58-6-955
39. Nguyen DN, Fuglsang E, Jiang P, Birck MM, Pan X, Kamal SBS, et al. Oral antibiotics increase blood neutrophil maturation and reduce bacteremia and necrotizing enterocolitis in the immediate postnatal period of preterm pigs. *Innate Immun.* (2016) 22:51–62. doi: 10.1177/1753425915615195
40. Tissieres P, Ochoda A, Dunn-Siegrist I, Drifte G, Morales M, Pfister R, et al. Innate immune deficiency of extremely premature neonates can be reversed by interferon-gamma. *PLoS ONE.* (2012) 7:e32863. doi: 10.1371/journal.pone.0032863
41. Puzik A, Rupp J, Troger B, Gopel W, Herting E, Hartel C. Insulin-like growth factor-i regulates the neonatal immune response in infection and maturation by suppression of IFN-gamma. *Cytokine.* (2012) 60:369–76. doi: 10.1016/j.cyto.2012.07.025
42. Tian F, Liu G-R, Li N, Yuan G. Insulin-like growth factor i reduces the occurrence of necrotizing enterocolitis by reducing inflammatory response and protecting intestinal mucosal barrier in neonatal rats model. *Eur Rev Med Pharmacol Sci.* (2017) 21:4711–9.
43. Kooijman R, Coppens A, Hooghe-Peters E. IGF-I inhibits spontaneous apoptosis in human granulocytes. *Endocrinology.* (2002) 143:1206–12. doi: 10.1210/endo.143.4.8725
44. Birck MM, Nguyen DN, Cilieborg MS, Kamal SS, Nielsen DS, Damborg P, et al. Enteral but not parenteral antibiotics enhance gut function and prevent necrotizing enterocolitis in formula-fed newborn preterm pigs. *Am J Physiol Gastrointest Liver Physiol.* (2016) 310:G323–33. doi: 10.1152/ajpgi.00392.2015
45. Sun J, Li Y, Nguyen DN, Mortensen MS, van den Akker CHP, Skeath T, et al. Nutrient fortification of human donor milk affects intestinal function and protein metabolism in preterm pigs. *J Nutr.* (2018) 148:336–47. doi: 10.1093/jn/nxx033
46. Sun J, Pan X, Christiansen LI, Yuan X-L, Skovgaard K, Chatterton DEW, et al. Necrotizing enterocolitis is associated with acute brain responses in preterm pigs. *J Neuroinflammation.* (2018) 15:180. doi: 10.1186/s12974-018-1201-x
47. Fullerton BS, Hong CR, Velazco CS, Mercier CE, Morrow KA, Edwards EM, et al. Severe neurodevelopmental disability and healthcare needs among survivors of medical and surgical necrotizing enterocolitis: a prospective cohort study. *J Pediatr Surg.* (2017) S0022–3468:30651–6. doi: 10.1016/j.jpedsurg.2017.10.029
48. Feldens L, Souza JCK de, Fraga JC. There is an association between disease location and gestational age at birth in newborns submitted to surgery due to necrotizing enterocolitis. *J Pediatr (Rio J).* (2018) 94:320–4. doi: 10.1016/j.jped.2017.06.010

Conflict of Interest: TG, NB, RN, and GC were employed at Takeda, MA at the time of study. These co-authors did not participate in study execution, data acquisition or in drafting the manuscript with its text, results presentation, tables and figures.

The remaining authors declare that the research was conducted in the absence of any commercial or financial relationships that could be construed as a potential conflict of interest.

frontiers in Pediatrics

ORIGINAL RESEARCH
published: 11 February 2021
doi: 10.3389/fped.2021.626101

Sex-Specific Survival, Growth, Immunity and Organ Development in Preterm Pigs as Models for Immature Newborns

Ole Bæk[1†], Malene Skovsted Cilieborg[1†], Duc Ninh Nguyen[1], Stine Brandt Bering[1], Thomas Thymann[1] and Per Torp Sangild[1,2,3]*

[1] Comparative Pediatrics and Nutrition, Faculty of Health and Medical Sciences, University of Copenhagen, Frederiksberg, Denmark, [2] Department of Neonatology, Rigshospitalet, Copenhagen, Denmark, [3] Department of Pediatrics, Odense University Hospital, Odense, Denmark

OPEN ACCESS

Edited by:
Yuan Shi,
Children's Hospital of Chongqing Medical University, China

Reviewed by:
Ulrich Herbert Thome,
Leipzig University, Germany
Jonathan Michael Davis,
Tufts University, United States

****Correspondence:***
Per Torp Sangild
pts@sund.ku.dk

[†] *These authors share first authorship*

Specialty section:
This article was submitted to Neonatology, a section of the journal Frontiers in Pediatrics

Received: *04 November 2020*
Accepted: *21 January 2021*
Published: *11 February 2021*

Citation:
Bæk O, Cilieborg MS, Nguyen DN, Bering SB, Thymann T and Sangild PT (2021) Sex-Specific Survival, Growth, Immunity and Organ Development in Preterm Pigs as Models for Immature Newborns. Front. Pediatr. 9:626101. doi: 10.3389/fped.2021.626101

Background: After very preterm birth, male infants show higher mortality than females, with higher incidence of lung immaturity, neurological deficits, infections, and growth failure. In modern pig production, piglets dying in the perinatal period (up to 20%) often show signs of immature organs, but sex-specific effects are not clear. Using preterm pigs as model for immature infants and piglets, we hypothesized that neonatal survival and initial growth and immune development depend on sex.

Methods: Using data from a series of previous intervention trials with similar delivery and rearing procedures, we established three cohorts of preterm pigs (90% gestation), reared for 5, 9, or 19 days before sample collection (total $n = 1{,}938$ piglets from 109 litters). Partly overlapping endpoints among experiments allowed for multiple comparisons between males and females for data on mortality, body and organ growth, gut, immunity, and brain function.

Results: Within the first 2 days, males showed higher mortality than females (18 vs. 8%, $P < 0.001$), but less severe immune response to gram-positive infection. No effect of sex was observed for thermoregulation or plasma cortisol. Later, infection resistance did not differ between sexes, but growth rate was reduced for body (up to −40%) and kidneys (−6%) in males, with higher leucocyte counts (+15%) and lower CD4 T cell fraction (−5%) on day 9 and lower monocyte counts (−18%, day 19, all $P < 0.05$). Gut structure, function and necrotizing enterocolitis (NEC) incidence were similar between groups, but intestinal weight (−3%) and brush-border enzyme activities were reduced at day 5 (lactase, DPP IV, −8%) in males. Remaining values for blood biochemistry, hematology, bone density, regional brain weights, and visual memory (tested in a T maze) were similar.

Conclusion: Following preterm birth, male pigs show higher mortality and slower growth than females, despite limited differences in organ growth, gut, immune, and

brain functions. Neonatal intensive care procedures may be particularly important for compromised newborns of the male sex. Preterm pigs can serve as good models to study the interactions of sex- and maturation-specific survival and physiological adaptation in mammals.

Keywords: sex, gender, preterm, immune, animal model, cohort

INTRODUCTION

Across the lifespan, overall morbidity and mortality is higher in males than in females, caused by a multifaceted interaction among biological factors, societal conditions, and environmental determinants (1). The physiological mechanisms of the interacting sex- and age-related morbidities remain unknown and studies indicate that the male deficits are greatest at short gestational age at birth (2). Males are overrepresented among preterm infants and show an increased post-natal mortality compared with their female counterparts (3). Male sex is more prevalent with decreasing gestational age at birth, suggesting that male sex itself may be a risk factor for preterm birth (4). After preterm birth, deficient respiratory and immune functions may increase mortality (4, 5), potentially linked to later reduced body growth (6, 7) and more frequent neurological sequelae (4). While such complications may be specific for preterm birth, indications of increased mortality of term male infants, across the entire lifespan, imply that differences in survival capacity may exist between sexes, even after term birth (1, 8).

It is unknown if neonatal survival and adaptation is sex-specific across mammalian species. For pigs, perinatal mortality is high (15–25%) in both modern and traditional farming systems (9–15). A higher male piglet mortality is reported for outdoor, extensive systems with moderate litter size (16, 17) and impaired locomotion, hypothermia and lacking energy and passive immunity via sow's colostrum have been suggested as causative factors for increased male mortality (16). Intensive breeding programs for prolonged lean tissue growth (physiological immaturity) and large litter size in high-intensity facilities may increase the number of weak piglets (18–20). Considering the above knowledge of sex-specific effects for preterm infants, this may increase sex-specific neonatal morbidities for modern piglets. Pig growth rates and litter size are top in the world in Denmark (mean 18, range 15–30 piglets/sow) and perinatal mortality remains high, despite genetic selection for survival (9, 21). Previous studies in preterm pigs suggest that the combination of immaturity and growth restriction at birth negatively affects systemic and gut immunity (22–25).

Among the immune-related morbidities in preterm infants, necrotizing enterocolitis (NEC), a serious gut inflammatory disorder (26), does not appear to differ between males and females, although few studies report higher NEC incidence in males (27). Conversely, sex-specific differences in systemic immunity complications are reported, and full-term male infants show weaker innate and adaptive immunity, reduced vaccine response and poorer pathogen clearance (8, 28). These results indicate fundamental sex-specific differences in systemic immune functions, possibly driven by sex hormones, because differences accelerated after puberty in the above studies. Other hormones, such as glucocorticoids, critical for neonatal maturation and survival across many species, could also play a role for sex-specific survival after term birth (29, 30). Less is known for immature infants, but because sex-specific differences may manifest themselves already *in utero* (31), it is plausible that immaturity at birth pre-dispose to sex-specific effects on morbidity and mortality. Further, maternal inflammation and infection are known to affect infant immunity both in the neonatal period and beyond (32, 33). Male term and preterm infants also have higher risk of positive blood cultures and sepsis, indicating a higher post-natal sensitivity to infection (4, 34), and cord blood from male infants show greater pro-inflammatory response to lipopolysaccharide (LPS) (35). However, in other studies cord blood mononuclear cells from term and preterm infants did not show sex-specific differences in response to Toll-like receptor agonists (36). While these data confirm sex-specific responses and morbidities in some, but not all, human studies, they do not provide insight into mechanisms and whether sex effects exist across mammals with/without preterm birth. Observational studies in preterm infants provide limited insight into organ-specific mechanisms and results are often confounded by variable fetal conditions, gestational ages and post-natal treatments.

During 20 years, we have conducted numerous experiments with preterm pigs as models for preterm infants and immune-compromised newborn production pigs, using similar procedures for delivery (elective cesarean section at 90% gestation) and neonatal care (e.g., incubator rearing with supplemental oxygen, heating, and parenteral/enteral nutrition) (37, 38). This animal model has been used to assess effects of immaturity itself (reduced gestational age at birth) (39–45) and dietary, microbial and pharmacological interventions on nutritional (46), gastrointestinal (47, 48), immune (49, 50), and neurological endpoints (51–54). Across these separate experiments, no consistent sex-specific effects were reported. Larger cohorts of preterm pigs, across variable clinical complications and interventions, may be required to demonstrate sex-specific effects. We hypothesized that cohorts of preterm pigs, like preterm infants, show increased mortality of male offspring, potentially related to sex-specific development of organ growth and gut, immune and brain functions. This knowledge may help to define the need for sex-specific care procedures in pig production (e.g., intensive care procedures, artificial rearing, cross-fostering) as well as in human neonatatology.

TABLE 1 | Overview of cohorts of preterm pigs.

Duration (days)	Preterm pigs total *n*	Litters *n*	Separate studies *n*	Females *n*	Males *N*
5	1,398	79	27	698	700
9	319	18	5	163	156
19	221	12	5	104	117

METHODS

Animals and Their Treatment

All animal experiments were conducted under a license from the Danish National Committee on Animal Experimentation (2014-15-0201-00418). We compiled a database from previous experiments performed with preterm pigs 2009-2020, all using the same delivery procedures and rearing facilities (37). For all measured outcomes in total 1,938 preterm pigs from 109 litters across 37 experiments (**Table 1**), we collected sex-specific results when the same outcome parameter was measured across several experiments (aiming to have $n > 100$ for each sex). Across the different experiments, preterm pigs were reared for 4–5, 8–9, or 19 days and the three cohort groups were denoted 5, 9, and 19 day cohorts. An overview of the number of pigs, litters and experiments with specific interventions related to diet (e.g., feeding of formula, porcine, bovine or human milk, or colostrum), microbes (e.g., administration of pre-, pro- and antibiotics) or drugs (e.g., cortisol, IGF-1) is shown in **Supplementary Table 1**. While some biological endpoints were shared among experiments, other parameters were assessed only in some experiments, resulting in different n numbers for different parameters for each cohort. For immune endpoints, we first assessed the sex-specific responses to systemic infection for subgroups of pigs younger than 5 days, not included in the 5, 9, or 19 day cohorts (described in detail later).

All pigs (Duroc × Yorkshire × Danish Landrace) were delivered by elective cesarean section at 105–106 days gestation (term = 117 ± 1 days), and while anesthetized, piglets were fitted with oro-gastric feeding tubes and umbilical arterial lines. The pigs were reared in incubators with supplemental oxygen for the first 12 h (1–2 L/min), extra heating to prevent hypothermia and standardized parenteral and enteral feeding, as described previously (37). In the day 5 cohort, pigs had their rectal temperature taken at 2 h intervals for the first 12 h of life (data available for $n = 719$, 49% male). Furthermore, all pigs were infused with maternal plasma (16–20 mL/kg) within the first 24 h to ensure a standardized level of systemic passive immunity to support immunological protection (e.g., maternal IgG), independent of their sow's colostrum, thus excluding by this artificial rearing system any variability induced by differential piglet-sow interactions. **Figure 1** presents an overview of rearing conditions and possible clinical complications in 90% gestation preterm pigs when reared for 5, 9, or 19 days.

Several different enteral diets and interventions were used in the studies (see **Supplementary Table 1**) while the same formulation of parenteral nutrition (modified composition of Kabiven, Fresenius Kabi, Sweden) was used across experiments (41, 48, 51, 55). Across all experiments, pigs were randomly allocated to treatment groups stratified by sex and birth weight, thereby ensuring an even sex distribution in each intervention. During the studies, pigs were euthanized ahead of time if serious complications developed, defined as humane endpoints in accordance with criteria and the license from the Danish National Committee on Animal Experimentation. As described previously (37), the majority of mortalities for preterm pigs reared under such conditions occur within the first 48 h of life. Therefore, only pigs dying within this early neonatal period were included into mortality data for the present study. Pigs dying from iatrogenic causes (e.g., catheter-related complications with blood loss) were excluded from the analyses. At the end of the pre-defined study periods, all pigs were sacrificed by intracardial injection of phenobarbital after which organ weights were recorded and tissues sampled according to the different study protocols.

Neonatal Mortality and Blood Immunity, Hematology and Biochemistry

Across all experiments, we identified the litters where mortality within the first 48 h was accurately reported and noted as spontaneous death or euthanasia. Respiratory distress was commonly observed for such preterm pigs, but a detailed clinical and post-mortem organ investigation of the piglets was not performed. Hematology parameters were evaluated at birth (from the cord, during cesarean delivery), day 9 and day 19 (Advia 2120 Hematology System, Siemens Healthcare Diagnostics, Tarrytown, NY, USA) and plasma biochemistry was recorded at day 19 (Advia 1800 Chemistry System, Siemens, Erlangen, Germany).

Before analyzing organ data for the 5, 9, and 19 day cohorts, we explored the sex-specific differences in neonatal immune response by re-examining data from two previously conducted experiments modeling neonatal sepsis in infants (23, 56). These animals were not included among the 5, 9, or 19 day cohorts because the study length was shorter than 5 days. In short, preterm pigs were infused with live *Staphylococcus epidermidis* (1×10^8-5×10^9 CFU/kg body weight) bacteria through the umbilical caterer, either few hours after birth ($n = 38$, 53% male) or after 48 h ($n = 39$, 56% male), without prior provision of maternal plasma. The animals were followed for 24–48 h and hematological and arterial blood gas parameters evaluated. Animals inoculated with bacteria at birth were kept exclusively on parenteral nutrition whereas those inoculated after 48 h were supplemented with enteral milk diets. A detailed description of the experimental setup and bacterial inoculation procedure is available (23).

In the 9 day cohort, and in a subgroup of the 5 day cohort ($n = 75$, 40% male), spontaneous bacterial infection of the bone marrow was determined. After euthanasia, the femur head was dissected in a sterile manner and a sample of bone marrow collected. This sample was homogenized, serially diluted, plated out on agar and cultured for 24 h. Afterwards, bacterial density

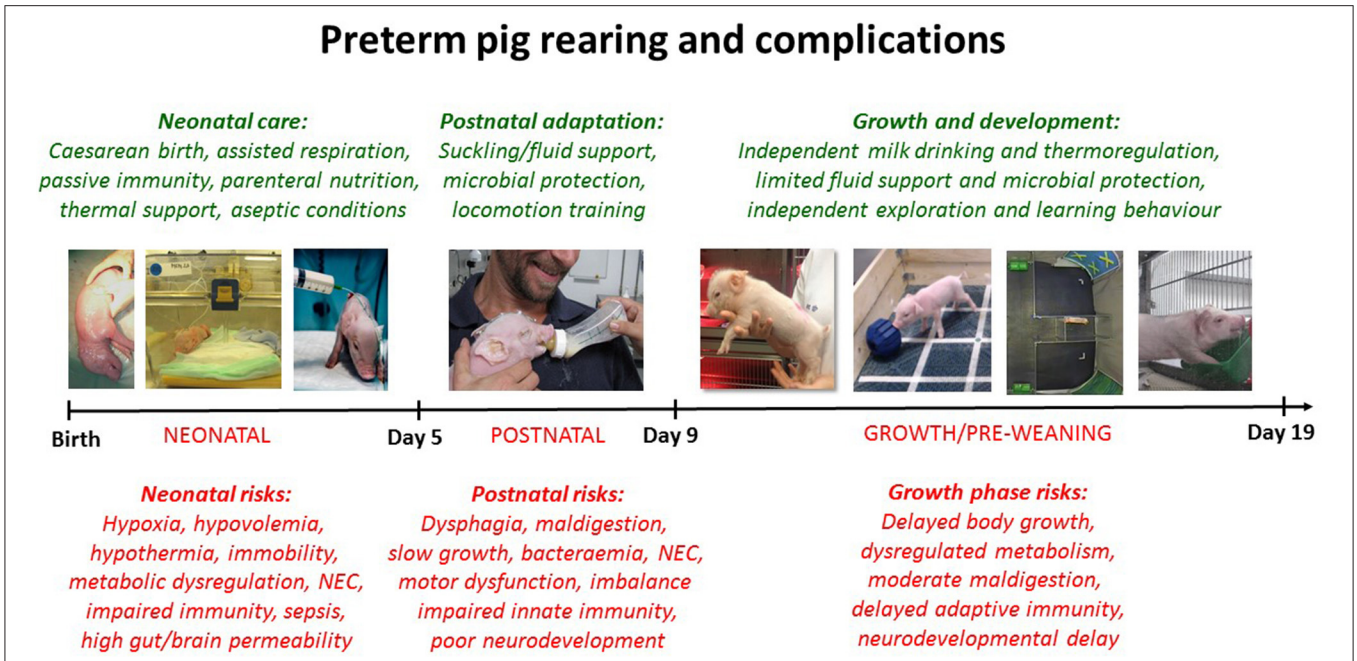

FIGURE 1 | Illustration of clinical care procedures (green text) and possible morbidities (red text) for cesarean-delivered 90% gestation preterm pigs, reared as models for preterm infants. Preterm pigs show clinical and physiological characteristics reflecting very preterm infants (<32 weeks gestation) but comparisons to infants are both age- and organ-specific (37). Based on the reports of gender-specific morbidities in preterm infants, we investigate if sex-specific effects are present in preterm pigs at different stages after preterm birth.

was calculated as culture-forming units (CFUs) per milliliter of bone marrow homogenate.

In 9 day pigs, and in a subgroup of day 19 pigs (n = 148, 51% male), flow cytometry (FACS) was used to determine T cell subsets, as described elsewhere (24). Using fluorescent-labeled antibodies against CD3, CD4, CD8, and FOXP3, the fraction of T cells, CD4+ T cells, CD8+ T cells and regulatory T cells (CD3+CD4+FOXP3+) were established. For the same pigs, the FACS equipment was used to determine neutrophil phagocytic function (57). In short, whole blood samples were incubated with fluorescent-labeled *Escherichia coli* (pH rhodo, Thermofischer, USA) and the phagocytic rate was defined as the fraction of neutrophils with internalized bacteria and the phagocytic capacity as the median fluorescent intensity of those neutrophils.

In the 9 day cohort, leucocyte gene expression at birth was evaluated using cord blood. Using primers against a panel of immune related genes, the relative expression of genes in whole blood, before and after stimulation with LPS, was calculated. Gene expression levels were presented as fold change, relative to a housekeeping gene. The same analysis was repeated at day 9 for a subgroup of animals (n = 38, 53% male). A full description of the genes investigated and methodologies are published elsewhere (22). Cortisol levels in plasma were measured by enzyme linked immune assay (R&D systems, USA) in cord blood (n = 112, 49% male) and at euthanasia in the day 5 (n = 164, 44% male) and day 19 cohorts (n = 60, 53% male).

Growth, Organ Weights and Gut Endpoints

Body weights at birth and euthanasia were used to calculate growth rate as relative daily weight gains across the study period (g/kg/day). At euthanasia, all major internal organs were evaluated and weight relative to body weight recorded. In a subgroup of the 19 day cohort (n = 86, 53% male) a full body dual-energy X-ray absorptiometry (DEXA, Lunar Prodigy scanner, GE Healthcare, Little Chalfont, UK) was performed at euthanasia to determine body composition, as described previously (41).

Sensitivity to NEC in preterm pigs is highest during the first 1–2 weeks after birth (58), and for the 5 and 9 day cohorts, the stomach, small intestine, and colon was visually inspected post-mortem for signs of inflammation and occurrence of NEC lesions, according to the same validated scoring system, with score 1–2 representing healthy tissue, 3–4 some evidence of NEC lesions, and 5–6 reflecting severe lesions (59). Brush border enzyme activities, including sucrase, maltase, lactase, aminopeptidase N (ApN), aminopeptidase A (ApA), and dipeptidyl peptidase IV (DPPIV), were evaluated across the small intestine for the 5 and 19-day cohorts (48). Using formalin-fixed small intestinal tissue, villus height and crypt depths were determined (48).

Neurodevelopment and Behavior

Brain weights were recorded and specifically for the 19 day cohort, the brains were further dissected to assess the relative size of each brain region [as percentage of the whole brain (60)].

Furthermore, in the 19 day studies, we performed a T maze-test, as a measure of spatial memory (**Figure 1**), explained in detail elsewhere (51, 52, 54). Briefly, from 10 days of age preterm pigs were placed in a T-shaped maze with a milk reward in one arm. Using visual clues on the walls, pigs could learn to find the reward following their daily tests in the maze. The number of days until pigs chose the right path in at least 80% of trials, was considered as the time taken to learn the task. The pigs were also subject to an open field test investigating explorative free movement behavior [**Figure 1**, (54)].

Statistical Analyses

All statistical analyses were performed using Stata 14.2 (StataCorp, Texas, USA). Categorical data was compared by Fischer's exact-test and an unadjusted odds ratio, with corresponding confidence interval (CI) calculated. Continuous data were compared using a linear mixed effect model with litter and diet type as fixed factors. Variables that could not conform to normal distribution were logarithmically transformed. If normal distribution could not be obtained, data was compared by Kruskal Wallis'-test. Data collected at several time points were mostly from independent samples and therefore compared separately for each time point. When analyzing immune related endpoints any animals treated with an antibiotic intervention were censored from analysis. Results were presented as means with corresponding standard error of the mean (SE).

RESULTS

Neonatal Mortality and Blood Immunity, Hematology and Biochemistry

Across the 109 litters of pigs, there were a mean of 17.8 live-born piglets per sow (**Table 1**). Mortality within the first 48 h was recorded for 833 live-born preterm pigs (48% male) from 18 experiments and 44 of these litters. From these litters, 107 (13%) died within 48 h of birth. The mortality was higher in male than female piglets (18 vs. 8%, $P < 0.001$). The unadjusted odds ratio for male piglets dying within 48 h compared to female was 2.4 (CI: 1.6–3.8, $P < 0.001$). Rectal temperatures decreased in the first 3–4 h after birth, despite being reared in incubators (to 34–35°C), but recovered thereafter to normal temperatures, as shown previously for preterm vs. term pigs (61). The temperature curve during the first 24 h after birth did not differ between male and female pigs (data not shown).

Hematological parameters at birth did not differ between female and male preterm pigs. By day 9, male piglets had higher total leucocyte counts (**Table 2**, $P < 0.05$) with a tendency to lower hemoglobin and haematocrit values (**Table 2**, both $P = 0.09$). At day 19, the male piglets showed lower hemoglobin concentration and haematocrit values (**Table 2**, both $P < 0.01$) with lower monocyte counts (**Table 2**, $P < 0.05$). Cortisol levels did not differ between the females and males, neither in cord blood (58.0 ± 2.1 vs. 63.4 ± 3.4 ng/mL, $P > 0.1$), at day 5 (87.5 ± 9.7 vs. 83.6 ± 7.5 ng/mL, $P > 0.1$) or by day 19 (60.0 ± 15.5 vs. 60.2 ± 18.2 ng/mL, $P > 0.1$). Furthermore, no differences in the serum biochemical parameters were found between female and male piglets on day 19, except higher aspartate aminotransferase levels in male piglets (**Table 3**, $P < 0.05$).

Animals inoculated with *S. epidermidis* right after birth showed marked sex-specific differences in their responses. Males showed higher neutrophil fractions and platelet counts with lower leucocyte fraction 6–12 h after inoculation (**Figures 2A–C**, $P < 0.05$–0.001). This result was coupled with a higher blood pH (**Figure 2D**, $P < 0.05$) and oxygen pressure (**Figure 2E**, $P < 0.01$–0.001), and with lower blood lactate (**Figure 2F**, $P < 0.001$). When the same experiment was conducted 48 h after birth, no differences in hematology or blood gas parameters between females and males were detected (data not shown).

There was no difference in the occurrence of spontaneous bacterial infection in bone marrow on day 5, but by day 9, male piglets tended to have a higher infection incidence (71 vs. 56%, **Figure 3A**, $P = 0.06$). However, the bacterial densities in the bone marrow did not differ between females or males, neither at day 5 nor at day 9 (**Figure 3B**, both $P > 0.1$). There were no differences in T cell subsets at birth or by day 19. However, by day 9, male preterm pigs showed lower fraction of T cells and CD4 positive T cells (**Figures 3C,D**, both $P < 0.05$). Neutrophil phagocytic function did not differ between female and male preterm piglets at birth, day 9 or day 19 (data not shown).

Leucocyte gene expression at birth was performed for 81 preterm pigs (51% male) and was repeated at day 9 for a smaller subgroup ($n = 38$, 53% male). At birth, male piglets showed higher expression of *IL2*, both before and after stimulation with LPS (**Figure 3E**, both $P < 0.05$), male pigs also had higher expression of *IFNG* after stimulation with LPS (**Figure 3F**, $P < 0.05$). Furthermore, male piglets had lower expression of *TLR2* and with higher expression of *MPO* than females (**Figures 3G,H**, both $P < 0.05$). By day 9, there was a tendency to higher expression of *IL2* in male pigs after LPS stimulation (**Figure 3E**, $P = 0.09$). No further differences between female and male preterm pigs were found at day 9.

Growth, Organ Weights and Gut Endpoints

Mean birth weight did not differ between female and male preterm piglets in any of the pig cohorts and ranged 912–998 g. However, relative daily weight gain was lower in male piglets, both at day 5, 9, and 19 (**Figure 4A**, all $P < 0.05$). For organ growth, 5 day male piglets showed lower relative kidney and small intestinal weight (**Table 4**, $P < 0.001$ and $P < 0.05$, respectively), with a tendency toward higher relative brain weight (**Table 4**, $P = 0.065$). In the cohort of pigs reared for 19 days, the relative kidney weight was still lower in male piglets ($P < 0.001$) whereas other organ weights did not differ, apart from a tendency to lower colon weight in male piglets both at day 9 and 19 (**Table 4**, $P < 0.10$). No sex-specific differences in body composition at day 19, as evaluated by DEXA scanning, were found (data not shown).

On day 5, 48% of pigs assessed for NEC ($n = 1{,}152$) showed mild-severe signs of NEC upon necropsy (score $\geq$3 in at least one region), while 36% showed more severe signs (score $\geq$4 in at least one region), but for both categories, no differences between males and females were observed (**Figure 4B**). Likewise, there was no difference in the average NEC severity score between males and females, even when stratifying across different regions of the gut

TABLE 2 | Hematological parameters of female and male preterm pigs on day 1, 9, and 19.

	Day 1		Day 9		Day 19	
	Female ($n = 109$)	**Male ($n = 116$)**	**Female ($n = 100$)**	**Male ($n = 102$)**	**Female ($n = 92$)**	**Male ($n = 95$)**
Total leucocytes (10^9 cells/L)	2.7 (0.0)	2.8 (0.0)	5.6 (0.3)	6.4 (0.3)*	9.9 (0.6)	9.5 (0.4)
Neutrophils (10^9 cells/L)	0.6 (0.0)	0.6 (0.0)	3.6 (0.3)	4.1 (0.3)	7.1 (0.8)	6.2 (0.4)
Lymphocytes (10^9 cells/L)	1.9 (0.0)	2.0 (0.1)	1.8 (0.1)	2.0 (0.1)	2.8 (0.1)	2.8 (0.1)
Monocytes (10^9 cells/L)	0.06 (0.01)	0.05 (0.00)	0.13 (0.01)	0.15 (0.01)	0.38 (0.03)	0.31 (0.03)*
Eosinophils (10^9 cells/L)	0.09 (0.01)	0.09 (0.01)	0.09 (0.05)	0.06 (0.01)	0.07 (0.01)	0.08 (0.01)
Basophils (10^9 cells/L)	0.01 (0.00)	0.01 (0.00)	0.02 (0.01)	0.01 (0.00)	0.02 (0.00)	0.02 (0.00)
Platelets (10^9 cells/L)	214 (8)	209 (9)	363 (20)	390 (22)	479 (20)	479 (22)
Red blood cells (10^{12} cells/L)	3.7 (0.0)	3.8 (0.0)	3.4 (0.1)	3.5 (0.1)	4.0 (0.1)	4.0 (0.1)
Hemoglobin (g/L)	5.2 (0.1)	5.2 (0.0)	4.4 (0.1)	4.2 (0.1)(*)	4.4 (0.1)	4.3 (0.1)**
Haematocrit (%)	28.1 (0.3)	28.1 (0.3)	23.8 (0.4)	23.2 (0.4)(*)	23.5 (0.5)	22.9 (0.5)**

*Data presented as means with corresponding SE. (*)Tendency to effect, $P < 0.1$, *$P < 0.05$, **$P < 0.01$.*

TABLE 3 | Serum biochemistry in female and male piglets at day 19.

	Female ($n = 95$)	**Male ($n = 105$)**
Albumin (g/L)	16.7 (0.3)	16.9 (0.3)
Total protein (g/L)	29.1 (0.5)	29.6 (0.6)
Alkaline phosphatase (U/L)	1,385 (81)	1,271 (69)
Alanine aminotransferase (U/L)	31.3 (0.8)	30.7 (0.8)
Total bilirubin (μmol/L)	2.0 (0.1)	2.3 (0.1)
Cholesterol (mmol/L)	2.7 (0.1)	2.7 (0.1)
Creatinine (μmol/L)	50.8 (1.1)	55.5 (2.1)
Creatine kinase (U/L)	241 (21.2)	245 (29.5)
Iron (μmol/L)	7.2 (0.6)	8.2 (0.5)
Phosphate (mmol/L)	2.1 (0.1)	2.1 (0.1)
Aspartate aminotransferase (U/L)	33.3 (1.4)	39.9 (2.7)*
Blood urea nitrogen (mmol/L)	3.7 (0.3)	4.5 (0.4)
Gamma-glutamyl transferase (U/L)	22.4 (0.9)	21.9 (0.9)
Calcium (mmol/L)	2.6 (0.0)	2.6 (0.0)
Magnesium (mmol/L)	0.9 (0.0)	0.9 (0.0)
Sodium (mmol/L)	142 (1.3)	143 (1.3)
Potassium (mmol/L)	4.4 (0.1)	4.4 (0.1)

*Data presented as means with corresponding SE. *$P < 0.05$.*

(data not shown). The corresponding values for day 9 piglets with NEC scores ($n = 319$) were 64 and 54%, again with no differences between males and females.

After 5 days, male piglets showed lower activity of lactase and DPPIV (**Figure 4C**, $P < 0.05$ and $P < 0.01$, respectively) with a tendency to higher activity of ApN ($P = 0.06$). In pigs reared for 19 days, there were no differences in brush border enzyme activities (data not shown). Likewise, there were no difference between villus height or crypt depth across gut regions in pigs reared for either 5 or 19 days (data not shown).

Neurodevelopment and Behavior

On day 19, male pigs had higher absolute weight of cerebellum (2.87 vs. 2.76 g, $P < 0.05$), and higher relative weights cerebellum (% of total brain weight, **Table 5**, $P < 0.001$), relative to female pigs. Other brain weight measures did not differ. Measured outcomes of motor function, explorative behavior, cognition, and visual memory (open field and T-maze-tests), did not show any significant differences between male and female piglets at any time points during the test (data not shown).

DISCUSSION

To optimize the care and treatment of immature neonates, it is important to know to which extent males and females have different risk factors and respond differently to treatments. Using our preterm pig model of immature birth, we studied preterm male and female pigs during the neonatal transition (5 days), post-natal adaptation (9 days) and initial growth phases of development (19 days, **Figure 1**). Following elective cesarean section in late gestation, this animal model mimics many of the complications of weak, compromised piglets at term, and of very preterm infants (e.g., immature lung, metabolic, thermoregulatory, gut, immune, and brain functions (37, 38, 62), yet it avoids the possible confounding effects of fetal factors leading to preterm birth in humans (e.g., maternal inflammation, hypertension, placental dysfunction). Further, our standardized rearing and feeding protocols ensure that we can isolate intrinsic biological differences between the sexes, independent of interactions with their mother for thermoregulation, nutrient uptake or passive immunity. Using this model we now show that neonatal mortality in immature preterm pigs is much higher in male vs. female pigs, despite a seemingly improved resistance to bacterial infection within the first days. There was a clear reduction in body growth in surviving male pigs, but apart from this the observed sex-specific gut, immunity and brain differences were marginal, at least compared with effects of most nutritional, microbial, or pharmacological interventions in preterm pigs (37). How sex-specific differences shortly after preterm birth may develop toward puberty and adulthood remains to be shown, and

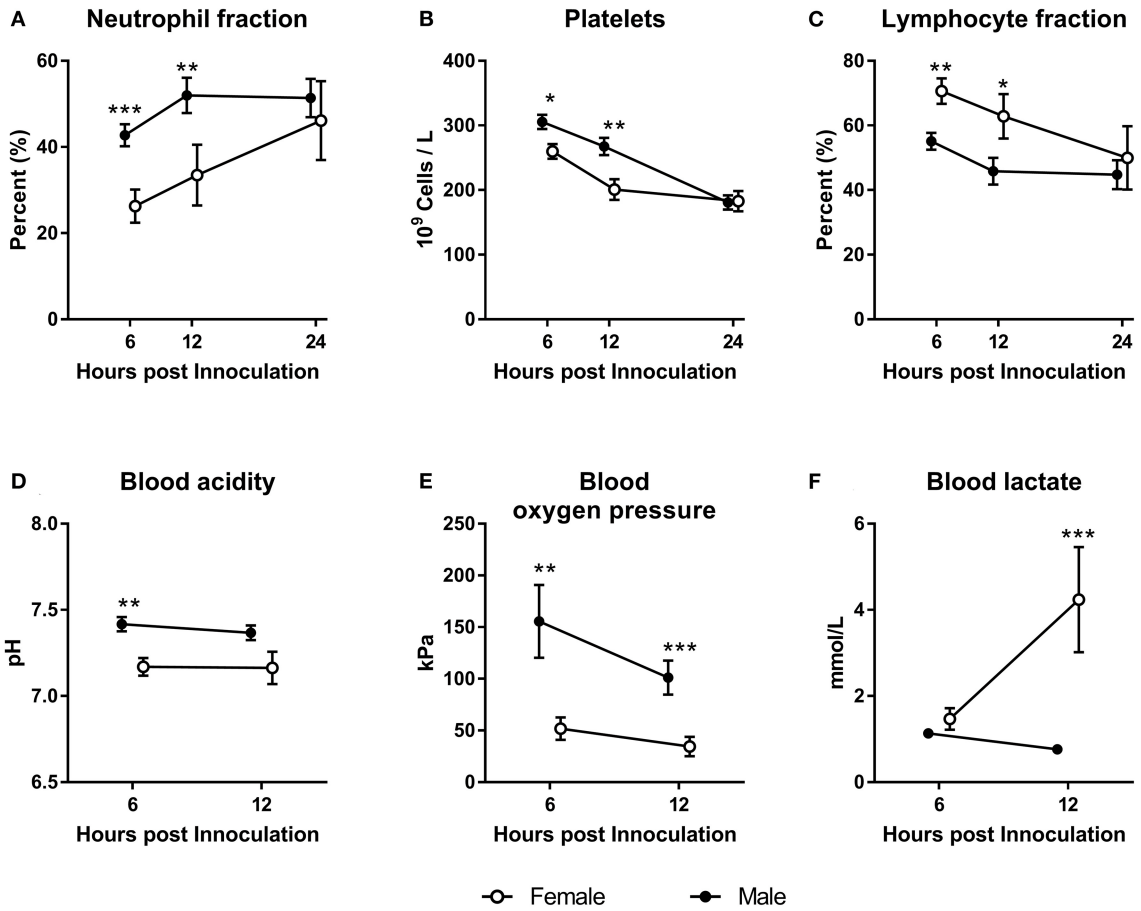

FIGURE 2 | Hematological and blood gas parameters in female and male preterm pigs (open and filled circles, respectively) inoculated with live *S. epidermidis* bacteria shortly after birth. Neutrophil fractions (**A**, $n = 38$). Platelet counts (**B**, $n = 38$). Lymphocyte fractions (**C**, $n = 38$). Blood acidity (**D**, $n = 38$). Blood oxygen pressure (**E**, $n = 38$). Blood lactate levels (**F**, $n = 38$). All shown as means with corresponding SE. $^{*}P < 0.05$, $^{**}P < 0.01$, $^{***}P < 0.001$.

in-depth studies on immunity, growth and organ functions are required in both pigs and infants.

Despite the clear difference in neonatal mortality, we are limited by the fact that our preterm pig studies did not include a detailed diagnosis of the cause of death. Yet, studies in infants suggest that poor respiratory function in preterm males is a key contributor to increased mortality (5) and cohort studies have shown that males, both late pre-terms and terms, have higher risk of respiratory distress syndrome (RDS) (63), possibly related to less surfactant production in late gestation (64, 65). Following cesarean section at 90% gestation, a large proportion of preterm pigs show RDS-like symptoms and lung immaturity, as assessed by reduced blood oxygen levels and macroscopic lung appearance at autopsy (atelectasis) (39, 41, 57, 61). However, we have not systematically registered the degree of post-natal respiratory distress in our studies. Interestingly, we did not detect any differences in cord blood levels of cortisol, a hormone well-known to stimulate lung development and respiratory function in preterm infants (66) although differences in cortisol production between the sexes may be masked by the cesarean section that may not stress the piglets as much as preterm labor. We have previously shown that blocking cortisol production in newborn pigs lead to increased neonatal mortality (29). Likewise, low cortisol levels at birth are associated with neonatal mortality in production pigs (30), highlighting the importance of this hormone after birth. Lower body temperature has also been observed in male production pigs and poor thermoregulation was suggested to contribute to increased mortality (16). However, we did not observe any differences in our study in the first 24 h of life but sex-specific differences in rectal temperature and thermoregulation could have been hidden by our tight control of temperatures in incubators.

Beyond the neonatal period, surviving male preterm pigs in our study showed reduced growth rate, kidney weight and activity of some digestive enzymes. Gut growth was not markedly affected although the slightly reduced intestinal weight on day 5, and tendency to reduced colon weight at day 9–19, may indeed reflect a slight delay in gut development in males. The magnitude of the transient male-specific reduction in

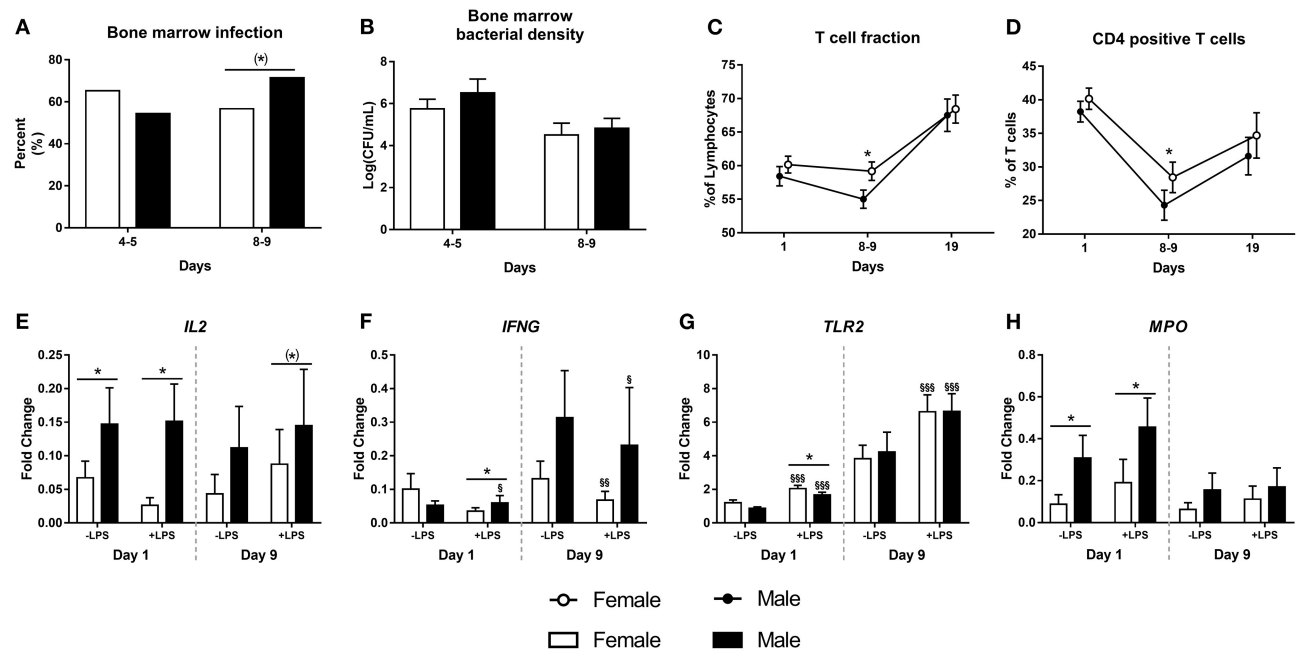

FIGURE 3 | Incidence of bone marrow bacterial infection (**A**, $n = 74$ and 130) with corresponding bacterial densities (**B**, $n = 74$ and 130), as well as fractions of T cells (**C**, $n = 52$–148), CD4 positive T cells (**D**, $n = 52$–148) and expressions of *IL2, IFNG, TLR2,* and *MPO* (**E–H**, $n = 38$–81) in male and female preterm pigs. Shown as fractions **(A)**, means with corresponding error **(B–D)** and fold- changes in relation to housekeeping gene, before and after stimulation with lipopolysaccharide (LPS, **E–H**). (*)Tendency to an effect, $P < 0.1$, $^{*}P < 0.05$. §Effect of LPS, $P < 0.1$, $^{§}P < 0.05$, $^{§§}P < 0.01$, $^{§§§}P < 0.001$.

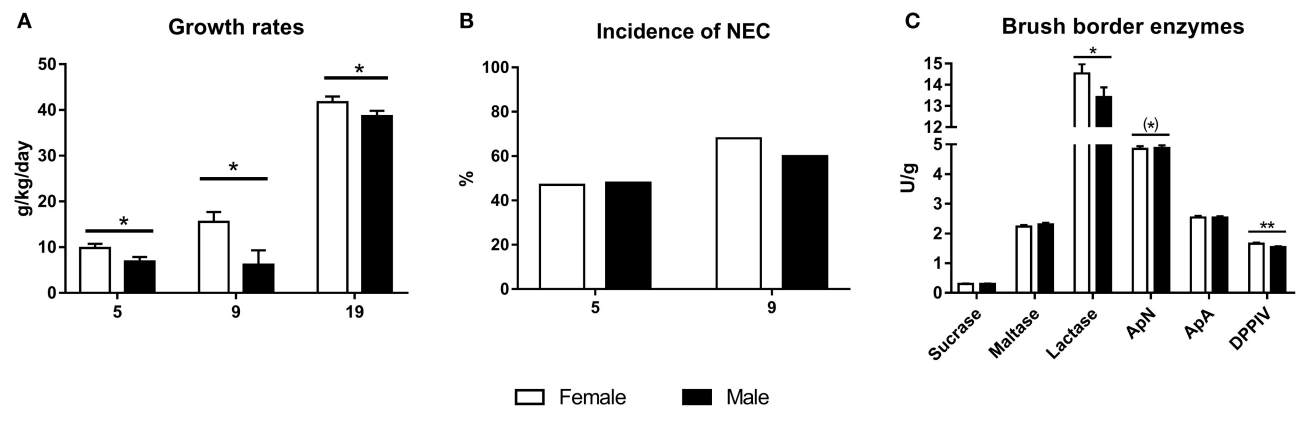

FIGURE 4 | Growth rates for 5, 9, and 19 day cohorts (**A**, g/kg/day, $n = 1{,}135$, 319, and 221), incidence of necrotizing enterocolitis (NEC score ≥3) at day 5 and 9 (**B**, $n = 1{,}152$ for day 5 and $n = 319$ for day 9), and brush border enzyme activities at day 5 (**C**, $n = 1{,}028$) for male and female preterm piglets. Shown as means with corresponding SE **(A,C)** or as proportion of animals (%) in the cohort **(B)**. (*)Tendency to effect, $P < 0.1$, $^{*}P < 0.05$, $^{**}P < 0.01$.

lactase and DPPIV activity on day 5 remained quantitatively of lower magnitude (e.g., 5–10% reduction) than those of feeding formula vs. intact milk diets or colostrum (47, 67) or changes to gut bacterial colonization (relative to germ-free rearing or antibiotics treatment) (47, 55, 68). The limited effect of sex on gut development and NEC in preterm pigs, despite their high NEC sensitivity in the first 1–2 weeks (37), is consistent with observations in preterm infants, where gender does not markedly affect NEC risk (27, 69, 70).

The slower body growth in male vs. female preterm pigs is consistent with the finding that male preterm infants are at a higher risk to develop extra-uterine growth restriction (6, 7). Among internal organs, only kidney growth was consistently reduced in male preterm pigs. In preterm infants, glomerular filtration rate is similar in males and females (71) but males show a higher risk of acute kidney injury (72, 73). At 19 days, male pigs had slightly lower hemoglobin and haematocrit values than females, potentially related to diminished erythropoiesis

TABLE 4 | Relative organ weights (g per kg body weight) of male and female preterm pigs.

	Day 5		Day 9		Day 19	
	Female (n = 501–568)	**Male (n = 457–514)**	**Female (n = 163)**	**Male (n = 156)**	**Female (n = 104)**	**Male (n = 116)**
Stomach	6.8 (0.1)	7.0 (0.1)	6.8 (0.2)	7.0 (0.3)	6.6 (0.1)	6.6 (0.1)
Small intestine	31.7 (0.3)	30.9 (0.3)*	32.5 (0.6)	33.8 (1.1)	40.2 (0.7)	39.5 (0.6)
Colon	12.2 (0.2)	11.9 (0.2)	16.4 (0.5)	15.5 (0.7)(*)	21.0 (1.3)	18.5 (1.3)(*)
Heart	8.1 (0.1)	7.9 (0.1)	7.5 (0.2)	8.0 (0.3)	7.2 (0.1)	7.3 (0.1)
Lungs	24.1 (0.3)	24.4 (0.3)	24.1 (0.6)	25.3 (0.9)	20.5 (0.6)	19.7 (0.6)
Liver	28.2 (0.2)	28.8 (0.2)	31.1 (0.7)	33.1 (0.8)*	25.7 (0.5)	25.5 (0.6)
Kidneys	10.6 (0.2)	10.0 (0.2)***	7.7 (0.2)	7.8 (0.3)	7.5 (0.1)	7.0 (0.1)***
Spleen	1.9 (0.0)	1.9 (0.0)	2.5 (0.1)	2.5 (0.1)	3.0 (0.1)	3.1 (0.1)
Brain†	28.3 (0.4)	29.9 (0.5)(*)	27.3 (0.8)	29.6 (1.1)	22.9 (0.6)	22.8 (0.7)

Data are means with corresponding SE. †*On day 5, brains were collected from a subgroup (n = 615, 47% male). (*)Tendency to effect, P < 0.1, *P < 0.05, ***P < 0.001.*

TABLE 5 | Brain parameters in male and female preterm pigs after 19 days.

	Female (n = 102)	**Male (n = 115)**
Water content (%)	82.7 (0.1)	82.8 (0.1)
Cerebellum (%)	10.4 (0.1)	10.8 (0.1)***
Cerebrum (%)	79.9 (0.1)	79.7 (0.1)
Brainstem (%)	9.2 (0.1)	9.3 (0.1)
Hippocampus (%)	1.8 (0.2)	1.6 (0.0)
Striatum (%)	1.0 (0.0)	1.0 (0.0)

*Data are means with corresponding SE. ***P < 0.001.*

by the smaller kidneys (74), but more studies are required to verify sex effects on renal structure and function. This organ could be particularly susceptible to perinatal stressors, as indicated by our recent studies on fetal inflammation on gut, lung, liver, immunity and kidney development in preterm pigs (33, 57, 75–77). In the literature on production pigs, males do not consistently show reduced neonatal survival and growth (18–20, 30), hence sex-specific survival, growth and adaptation may be most pronounced for immature newborns. Consequently, it may become increasingly relevant with sex-specific intensive care procedures for weak (immature) newborn pigs from hyperproliferative sows in modern pig production (e.g., resuscitation, cross-fostering, immunization, artificial rearing procedures, microbial protection).

Important sex-related differences were observed for some systemic immune endpoints just after birth, and these may interact with effects in internal organs. Despite that leucocyte or T cell subsets did not differ between preterm male and female piglets at birth, the leucocyte gene expression analysis showed that expression of genes encoding interleukin-2 (*IL2*) and interferon gamma (*IFNG*) were higher in males, also after stimulation with LPS. Both cytokines are important in development of a Th1-directed immune response (78). Together with a higher expression of myeloperoxidase (*MPO*) this may have made males more resilient to infection with *S. epidermidis*. Inoculation with the same bacteria later (48 h after birth) showed no differences between male and female piglets. However, the general response to infection was dampened from 2 to 3 days after preterm birth in pigs (23), potentially making sex-specific differences harder to detect from this age. A tendency to a higher rate of spontaneous infection from days 5 to 9 may indicate diminished immune function in males beyond the neonatal period. *Staphylococcus epidermidis* bacteria are considered pathogenic in preterm infants (79). Male preterm pigs also showed transiently lower T cell and CD4+ T cell fractions at day 9, but these disappeared by day 19, possibly reflecting age-related data from term 0 to 5 month old infants (80). We cannot exclude that species-specific differences in immune development between pigs and infants, including differential transfer of passive immunity (parentally via the placenta in infants vs. post-natally via colostrum uptake in the gut in pigs), affect our conclusions regarding sex effects. On the other hand, artificially-reared preterm pigs infused with maternal plasma to provide passive immunity (**Figure 1**) may very well reflect preterm infants normally born with low plasma levels of IgG and seldom receive mother's own milk or colostrum as their first enteral meals.

The only neurological parameter that differed between piglet sexes was the size of the cerebellum. While this may indicate better motor function, we saw no sex-related differences in the open field test, nor in the T-maze-test for visual memory capacity. In preterm infants, males have worse neurological outcomes following hypoxia, higher incidence of cerebral palsy and poorer long-term cognitive and language outcomes (81, 82), together with delayed myelination (83). The sex-differences in neurological outcomes are worse after more extreme prematurity (4). In this context, it is important to note that the brain, neurological outcomes and motor function are relatively mature in 90% gestation preterm pigs, relative to preterm infants, even if they show (temporary) post-natal deficits relative to term piglets (41, 43, 45, 60).

Across a large series of experiments with identical birth conditions (elective cesarean section) and clinically-relevant interventions in the same neonatal care facility, we aimed to mimic and standardize clinical responses to immaturity

at birth for both pigs and infants. Still, it remains unclear how to translate results from preterm pigs to preterm infants because species similarities and differences are both age- and organ-dependent. Similarly, it remains speculative how well 90% preterm piglets reflect the clinical complications for the large proportion of normal term pigs dying during delivery or shortly after birth in modern pig production. The inclusion of a large number of endpoints from different cohorts increases the risk of false discoveries in statistical testing, despite large sample size. Regardless, our model provides a well-controlled and sensitive tool to test the effects of interventions and biological co-variants when individuals show immaturity at birth, and without the variable maternal interactions known to influence sex-specific survival rates in both pigs (16) and infants (1–4). Our results document that preterm pigs mimic many of the sex-specific differences in mortality, growth, and immune functions in preterm infants, supporting the use of this model to investigate sex-specific diseases of immature newborns. The mechanisms related to differences in immune response in the neonatal period, as well as the small effects on body and organ growth and function later (e.g., lung, gut, immunity, brain) warrant further investigations. At the population level, such biological differences may affect clinical outcomes but it remains questionable, if they justify sex-specific clinical treatment of immature and/or mature newborn individuals, either pigs or infants.

DATA AVAILABILITY STATEMENT

The raw data supporting the conclusions of this article will be made available by the authors, without undue reservation.

ETHICS STATEMENT

The animal study was reviewed and approved by Danish National Committee on Animal Experimentation.

AUTHOR CONTRIBUTIONS

MC collected and organized the cohort data for analysis. OB analyzed data and produced the first draft of the manuscript. PS took responsibility for final editions in the text. All authors commented on the data, analyses and manuscript text, and approved the final version for submission.

FUNDING

The studies were supported by Grants from Innovation Fund Denmark (NEOMUNE, NEOCOL, InfantBrain), ARLA Foods Ingredients, Danone Baby Nutrition and Biofiber Damino.

ACKNOWLEDGMENTS

We acknowledge all the students, scientific and technical staff involved in the various animal experiments (see list of experiments in **Supplementary Table 1**). Christian Ritz is acknowledged for advice on statistical procedures.

SUPPLEMENTARY MATERIAL

The Supplementary Material for this article can be found online at: https://www.frontiersin.org/articles/10.3389/fped.2021.626101/full#supplementary-material

REFERENCES

1. Lozano R, Naghavi M, Foreman K, Lim S, Shibuya K, Aboyans V, et al. Global and regional mortality from 235 causes of death for 20 age groups in 1990 and 2010: A systematic analysis for the Global Burden of Disease Study 2010. *Lancet*. (2012) 380:2095–128. doi: 10.1016/S0140-6736(12)61728-0
2. Zisk JL, Genen LH, Kirkby S, Webb D, Greenspan J, Dysart K. Do premature female infants really do better than their male counterparts? *Am J Perinatol*. (2011) 28:241–6. doi: 10.1055/s-0030-1268239
3. Challis J, Newnham J, Petraglia F, Yeganegi M, Bocking A. Fetal sex and preterm birth. *Placenta*. (2013) 34:95–9. doi: 10.1016/j.placenta.2012.11.007
4. O'Driscoll DN, McGovern M, Greene CM, Molloy EJ. Gender disparities in preterm neonatal outcomes. *Acta Paediatr*. (2018) 107:1494–9. doi: 10.1111/apa.14390
5. Townsel CD, Emmer SF, Campbell WA, Hussain N. Gender differences in respiratory morbidity and mortality of preterm neonates. *Front Pediatr*. (2017) 5:6. doi: 10.3389/fped.2017.00006
6. Clark RH, Thomas P, Peabody J. Extrauterine growth restriction remains a serious problem in prematurely born neonates. *Pediatrics*. (2003) 111:986–90. doi: 10.1542/peds.111.5.986
7. Figueras-Aloy J, Palet-Trujols C, Matas-Barceló I, Botet-Mussons F, Carbonell-Estrany X. Extrauterine growth restriction in very preterm infant: etiology, diagnosis, and 2-year follow-up. *Eur J Pediatr*. (2020) 179:1469–79. doi: 10.1007/s00431-020-03628-1
8. Klein SL, Flanagan KL. Sex differences in immune responses. *Nat Rev Immunol*. (2016) 16:626–38. doi: 10.1038/nri.2016.90
9. Kobek-Kjeldager C, Moustsen VA, Theil PK, Pedersen LJ. Effect of litter size, milk replacer and housing on production results of hyper-prolific sows. *Anim Int J Anim Biosci*. (2020) 14:824–33. doi: 10.1017/S175173111900260X
10. Pedersen LJ, Larsen ML, Malmkvist J. The ability of different thermal aids to reduce hypothermia in neonatal piglets. *J Anim Sci*. (2016) 94:2151–9. doi: 10.2527/jas.2015-0219
11. Rangstrup-Christensen L, Krogh MA, Pedersen LJ, Sørensen JT. Sow-level risk factors for stillbirth of piglets in organic sow herds. *Anim Int J Anim Biosci*. (2017) 11:1078–83. doi: 10.1017/S1751731116002408
12. Pandolfi F, Edwards SA, Robert F, Kyriazakis I. Risk factors associated with the different categories of piglet perinatal mortality in French farms. *Prev Vet Med*. (2017) 137:1–12. doi: 10.1016/j.prevetmed.2016.12.005
13. Zeng ZK, Urriola PE, Dunkelberger JR, Eggert JM, Vogelzang R, Shurson GC, et al. Implications of early-life indicators for survival rate, subsequent growth performance, and carcass characteristics of commercial pigs. *J Anim Sci*. (2019) 97:3313–25. doi: 10.1093/jas/skz223
14. Calderón Díaz JA, Boyle LA, Diana A, Leonard FC, Moriarty JP, McElroy MC, et al. Early life indicators predict mortality, illness, reduced welfare and carcass characteristics in finisher pigs. *Prev Vet Med*. (2017) 146:94–102. doi: 10.1016/j.prevetmed.2017.07.018
15. Yuan TL, Zhu YH, Shi M, Li TT, Li N, Wu GY, et al. Within-litter variation in birth weight: impact of nutritional status in the sow. *J Zhejiang Univ Sci*. (2015) 16:417–35. doi: 10.1631/jzus.B1500010
16. Baxter EM, Jarvis S, Palarea-Albaladejo J, Edwards SA. The weaker sex? The propensity for male-biased piglet mortality. *PLoS ONE*. (2012) 7:e30318. doi: 10.1371/journal.pone.0030318

17. Bereskin B, Shelby CE, Cox DF. Some factors affecting pig survival. *J Anim Sci*. (1973) 36:821–7. doi: 10.2527/jas1973.365821x
18. Herpin P, Le Dividich J, Amaral N. Effect of selection for lean tissue growth on body composition and physiological state of the pig at birth. *J Anim Sci*. (1993) 71:2645–53. doi: 10.2527/1993.71102645x
19. Tuchscherer M, Puppe B, Tuchscherer A, Tiemann U. Early identification of neonates at risk: traits of newborn piglets with respect to survival. *Theriogenology*. (2000) 54:371–88. doi: 10.1016/S0093-691X(00)00355-1
20. Silalahi P, Tribout T, Billon Y, Gogué J, Bidanel JP. Estimation of the effects of selection on French large white sow and piglet performance during the suckling period. *J Anim Sci*. (2017) 95:4333–43. doi: 10.2527/jas2017.1485
21. Nielsen B, Su G, Lund MS, Madsen P. Selection for increased number of piglets at d 5 after farrowing has increased litter size and reduced piglet mortality. *J Anim Sci*. (2013) 91:2575–82. doi: 10.2527/jas.2012-5990
22. Bæk O, Ren S, Brunse A, Sangild PT, Nguyen DN. Impaired neonatal immunity and infection resistance following fetal growth restriction in preterm pigs. *Front Immunol*. (2020) 11:1808. doi: 10.3389/fimmu.2020.01808
23. Bæk O, Brunse A, Nguyen DN, Moodley A, Thymann T, Sangild PT. Diet modulates the high sensitivity to systemic infection in newborn preterm pigs. *Front Immunol*. (2020) 11:1019. doi: 10.3389/fimmu.2020.01019
24. Bæk O, Sangild PT, Thymann T, Nguyen DN. Growth restriction and systemic immune development in preterm piglets. *Front Immunol*. (2019) 10:2402. doi: 10.3389/fimmu.2019.02402
25. Che L, Thymann T, Bering SB, I LEH-L, D'Inca R, Zhang K, et al. IUGR does not predispose to necrotizing enterocolitis or compromise postnatal intestinal adaptation in preterm pigs. *Pediatr Res*. (2010) 67:54–9. doi: 10.1203/PDR.0b013e3181c1b15e
26. Niño DF, Sodhi CP, Hackam DJ. Necrotizing enterocolitis: new insights into pathogenesis and mechanisms. *Nat Rev Gastroenterol Hepatol*. (2016) 13:590–600. doi: 10.1038/nrgastro.2016.119
27. Carter BM, Holditch-Davis D. Risk factors for necrotizing enterocolitis in preterm infants: how race, gender, and health status contribute. *Adv Neonatal Care*. (2008) 8:285–90. doi: 10.1097/01.ANC.0000338019.56405.29
28. Muenchhoff M, Goulder PJR. Sex differences in pediatric infectious diseases. *J Infect Dis*. (2014) 209:120–6. doi: 10.1093/infdis/jiu232
29. Sangild PT, Diernaes L, Christiansen IJ, Skadhauge E. Intestinal transport of sodium, glucose and immunoglobulin in neonatal pigs. Effect of glucocorticoids. *Exp Physiol*. (1993) 78:485–97. doi: 10.1113/expphysiol.1993.sp003700
30. Leenhouwers JI, Knol EF, de Groot PN, Vos H, van der Lende T. Fetal development in the pig in relation to genetic merit for piglet survival. *J Anim Sci*. (2002) 80:1759–70. doi: 10.2527/2002.8071759x
31. Goldenberg RL, Andrews WW, Faye-Petersen OM, Goepfert AR, Cliver SP, Hauth JC. The Alabama preterm birth study: intrauterine infection and placental histologic findings in preterm births of males and females less than 32 weeks. *Am J Obstet Gynecol*. (2006) 195:1533–7. doi: 10.1016/j.ajog.2006.05.023
32. Wolfs TGAM, Jellema RK, Turrisi G, Becucci E, Buonocore G, Kramer BW. Inflammation-induced immune suppression of the fetus: a potential link between chorioamnionitis and postnatal early onset sepsis. *J Maternal Fetal Neonatal Med*. (2012) 25:8–11. doi: 10.3109/14767058.2012.664447
33. Ren S, Pan X, Gao F, Sangild PT, Nguyen DN. Prenatal inflammation suppresses blood Th1 polarization and gene clusters related to cellular energy metabolism in preterm newborns. *FASEB J*. (2020) 34:2896–911. doi: 10.1096/fj.201902629R
34. Albers MJIJ, De Gast-Bakker DAH, Van Dam NAM, Madern GC, Tibboel D. Male sex predisposes the newborn surgical patient to parenteral nutrition-associated cholestasis and to sepsis. *Arch Surg*. (2002) 137:789–93. doi: 10.1001/archsurg.137.7.789
35. Kim-Fine S, Regnault TR, Lee JS, Gimbel SA, Greenspoon JA, Fairbairn J, et al. Male gender promotes an increased inflammatory response to lipopolysaccharide in umbilical vein blood. *J Maternal fetal Neonatal Med*. (2012) 25:2470–4. doi: 10.3109/14767058.2012.684165
36. Sharma AA, Jen R, Brant R, Ladd M, Huang Q, Skoll A, et al. Hierarchical maturation of innate immune defences in very preterm neonates. *Neonatology*. (2014) 106:1–9. doi: 10.1159/000358550
37. Sangild PT, Thymann T, Schmidt M, Stoll B, Burrin DG, Buddington RK. Invited review: the preterm pig as a model in pediatric gastroenterology. *J Anim Sci*. (2013) 91:4713–29. doi: 10.2527/jas.2013-6359
38. Sangild PT. Gut responses to enteral nutrition in preterm infants and animals. *Exp Biol Med (Maywood, NJ)*. (2006) 231:1695–711. doi: 10.1177/153537020623101106
39. Ren S, Hui Y, Obelitz-Ryom K, Brandt AB, Kot W, Nielsen DS, et al. Neonatal gut and immune maturation is determined more by postnatal age than by postconceptional age in moderately preterm pigs. *Am J Physiol Gastrointest Liver Physiol*. (2018) 315:G855–67. doi: 10.1152/ajpgi.00169.2018
40. Kamal SS, Andersen AD, Krych L, Lauridsen C, Sangild PT, Thymann T, et al. Preterm birth has effects on gut colonization in piglets within the first 4 weeks of life. *J Pediatr Gastroenterol Nutr*. (2019) 68:727–33. doi: 10.1097/MPG.0000000000002259
41. Andersen AD, Sangild PT, Munch SL, van der Beek EM, Renes IB, Ginneken C, et al. Delayed growth, motor function and learning in preterm pigs during early postnatal life. *Am J Physiol Regul Integr Comp Physiol*. (2016) 310:R481–92. doi: 10.1152/ajpregu.00349.2015
42. Aunsholt L, Thymann T, Qvist N, Sigalet D, Husby S, Sangild PT. Prematurity reduces functional adaptation to intestinal resection in piglets. *JPEN*. (2015) 39:668–76. doi: 10.1177/0148607114528714
43. Bergström A, Kaalund SS, Skovgaard K, Andersen AD, Pakkenberg B, Rosenørn A, et al. Limited effects of preterm birth and the first enteral nutrition on cerebellum morphology and gene expression in piglets. *Physiol Rep*. (2016) 4:e12871. doi: 10.14814/phy2.12871
44. Hansen CF, Thymann T, Andersen AD, Holst JJ, Hartmann B, Hilsted L, et al. Rapid gut growth but persistent delay in digestive function in the postnatal period of preterm pigs. *Am J Physiol Gastrointest Liver Physiol*. (2016) 310:G550–60. doi: 10.1152/ajpgi.00221.2015
45. Plomgaard AM, Andersen AD, Petersen TH, van de Looij Y, Thymann T, Sangild PT, et al. Structural brain maturation differs between preterm and term piglets, whereas brain activity does not. *Acta Paediatr*. (2019) 108:637–44. doi: 10.1111/apa.14556
46. Vegge A, Thymann T, Lauritzen L, Bering SB, Wiinberg B, Sangild PT. Parenteral lipids and partial enteral nutrition affect hepatic lipid composition but have limited short term effects on formula-induced necrotizing enterocolitis in preterm piglets. *Clin Nutr (Edinburgh, Scotland)*. (2015) 34:219–28. doi: 10.1016/j.clnu.2014.03.004
47. Sangild PT, Siggers RH, Schmidt M, Elnif J, Bjornvad CR, Thymann T, et al. Diet- and colonization-dependent intestinal dysfunction predisposes to necrotizing enterocolitis in preterm pigs. *Gastroenterology*. (2006) 130:1776–92. doi: 10.1053/j.gastro.2006.02.026
48. Thymann T, Møller HK, Stoll B, Støy AC, Buddington RK, Bering SB, et al. Carbohydrate maldigestion induces necrotizing enterocolitis in preterm pigs. *Am J Physiol Gastrointest Liver Physiol*. (2009) 297:G1115–25. doi: 10.1152/ajpgi.00261.2009
49. Nguyen DN, Stensballe A, Lai JC, Jiang P, Brunse A, Li Y, et al. Elevated levels of circulating cell-free DNA and neutrophil proteins are associated with neonatal sepsis and necrotizing enterocolitis in immature mice, pigs and infants. *Innate Immun*. (2017) 23:524–36. doi: 10.1177/1753425917719995
50. Nguyen DN, Jiang P, Frøkiær H, Heegaard PM, Thymann T, Sangild PT. Delayed development of systemic immunity in preterm pigs as a model for preterm infants. *Sci Rep*. (2016) 6:36816. doi: 10.1038/srep36816
51. Ahnfeldt AM, Bæk O, Hui Y, Nielsen CH, Obelitz-Ryom K, Busk-Anderson T, et al. Nutrient restriction has limited short-term effects on gut, immunity, and brain development in preterm pigs. *J Nutr*. (2020) 150:1196–207. doi: 10.1093/jn/nxaa030
52. Andersen AD, Nguyen DN, Langhorn L, Renes IB, van Elburg RM, Hartog A, et al. Synbiotics combined with glutamine stimulate brain development and the immune system in preterm pigs. *J Nutr*. (2019) 149:36–45. doi: 10.1093/jn/nxy243
53. Cao M, Brunse A, Thymann T, Sangild PT. Physical activity and spatial memory are minimally affected by moderate growth restriction in preterm piglets. *Dev Neurosci*. (2019) 41:247–54. doi: 10.1159/000505726
54. Obelitz-Ryom K, Bering SB, Overgaard SH, Eskildsen SF, Ringgaard S, Olesen JL, et al. Bovine milk oligosaccharides with sialyllactose improves cognition in preterm pigs. *Nutrients*. (2019) 11:1335. doi: 10.3390/nu11061335

55. Birck MM, Nguyen DN, Cilieborg MS, Kamal SS, Nielsen DS, Damborg P, et al. Enteral but not parenteral antibiotics enhance gut function and prevent necrotizing enterocolitis in formula-fed newborn preterm pigs. *Am J Physiol Gastrointest Liver Physiol*. (2016) 310:G323–33. doi: 10.1152/ajpgi.00392.2015
56. Brunse A, Worsøe P, Pors SE, Skovgaard K, Sangild PT. Oral supplementation with bovine colostrum prevents septic shock and brain barrier disruption during bloodstream infection in preterm newborn pigs. *Shock*. (2019) 51:337–47. doi: 10.1097/SHK.0000000000001131
57. Nguyen DN, Thymann T, Goericke-Pesch SK, Ren S, Wei W, Skovgaard K, et al. Prenatal intra-amniotic endotoxin induces fetal gut and lung immune responses and postnatal systemic inflammation in preterm pigs. *Am J Pathol*. (2018) 188:2629–43. doi: 10.1016/j.ajpath.2018.07.020
58. Li Y, Pan X, Nguyen DN, Ren S, Moodley A, Sangild PT. Bovine colostrum before or after formula feeding improves systemic immune protection and gut function in newborn preterm pigs. *Front Immunol*. (2019) 10:3062. doi: 10.3389/fimmu.2019.03062
59. Siggers J, Sangild PT, Jensen TK, Siggers RH, Skovgaard K, Støy AC, et al. Transition from parenteral to enteral nutrition induces immediate diet-dependent gut histological and immunological responses in preterm neonates. *Am J Physiol Gastrointest Liver physiol*. (2011) 301:G435–45. doi: 10.1152/ajpgi.00400.2010
60. Holme Nielsen C, Bladt Brandt A, Thymann T, Obelitz-Ryom K, Jiang P, Vanden Hole C, et al. Rapid postnatal adaptation of neurodevelopment in pigs born late preterm. *Dev Neurosci*. (2018) 40:586–600. doi: 10.1159/000499127
61. Sangild PT, Petersen YM, Schmidt M, Elnif J, Petersen TK, Buddington RK, et al. Preterm birth affects the intestinal response to parenteral and enteral nutrition in newborn pigs. *J Nutr*. (2002) 132:3786–94. doi: 10.1093/jn/132.9.2673
62. Sangild PT, Ney DM, Sigalet DL, Vegge A, Burrin D. Animal models of gastrointestinal and liver diseases. Animal models of infant short bowel syndrome: translational relevance and challenges. *Am J Physiol Gastrointest Liver Physiol*. (2014) 307:G1147–68. doi: 10.1152/ajpgi.00088.2014
63. Anadkat JS, Kuzniewicz MW, Chaudhari BP, Cole FS, Hamvas A. Increased risk for respiratory distress among white, male, late preterm and term infants. *J Perinatol*. (2012) 32:780–5. doi: 10.1038/jp.2011.191
64. Fleisher B, Kulovich MV, Hallman M, Gluck L. Lung profile: sex differences in normal pregnancy. *Obstet Gynecol*. (1985) 66:327–30. Epub 1985/09/01.
65. Dammann CEL, Ramadurai SM, Mccants DD, Pham LD, Nielsen HC. Androgen regulation of signaling pathways in late fetal mouse lung development. *Endocrinology*. (2000) 141:2923–9. doi: 10.1210/endo.141.8.7615
66. Roberts D, Brown J, Medley N, Dalziel SR. Antenatal corticosteroids for accelerating fetal lung maturation for women at risk of preterm birth. *Cochrane Database Syst Rev*. (2017) 3:Cd004454. doi: 10.1002/14651858.CD004454.pub3
67. Shen RL, Thymann T, Østergaard MV, Støy AC, Krych Ł, Nielsen DS, et al. Early gradual feeding with bovine colostrum improves gut function and NEC resistance relative to infant formula in preterm pigs. *Am J Physiol Gastrointest Liver Physiol*. (2015) 309:G310–23. doi: 10.1152/ajpgi.00163.2015
68. Jensen ML, Thymann T, Cilieborg MS, Lykke M, Mølbak L, Jensen BB, et al. Antibiotics modulate intestinal immunity and prevent necrotizing enterocolitis in preterm neonatal piglets. *Am J Physiol Gastrointest Liver Physiol*. (2014) 306:G59–71. doi: 10.1152/ajpgi.00213.2013
69. Lu Q, Cheng S, Zhou M, Yu J. Risk factors for necrotizing enterocolitis in neonates: a retrospective case-control study. *Pediatr Neonatol*. (2017) 58:165–70. doi: 10.1016/j.pedneo.2016.04.002
70. Ahle M, Drott P, Elfvin A, Andersson RE. Maternal, fetal and perinatal factors associated with necrotizing enterocolitis in Sweden. A national case-control study. *PLoS ONE*. (2018) 13:e0194352. doi: 10.1371/journal.pone.0194352
71. Abitbol CL, Seeherunvong W, Galarza MG, Katsoufis C, Francoeur D, Defreitas M, et al. Neonatal kidney size and function in preterm infants: what is a true estimate of glomerular filtration rate? *J Pediatr*. (2014) 164:1026–31.e2. doi: 10.1016/j.jpeds.2014.01.044
72. Stojanović V, Barišić N, Milanović B, Doronjski A. Acute kidney injury in preterm infants admitted to a neonatal intensive care unit. *Pediatr Nephrol (Berlin, Germany)*. (2014) 29:2213–20. doi: 10.1007/s00467-014-2837-0
73. Nagaraj N, Berwal PK, Srinivas A, Berwal A. A study of acute kidney injury in hospitalized preterm neonates in NICU. *J Neonatal Perinat Med*. (2016) 9:417–21. doi: 10.3233/NPM-161614
74. Adamson JW, Eschbach J, Finch CA. The kidney and erythropoiesis. *Am J Med*. (1968) 44:725–33. doi: 10.1016/0002-9343(68)90254-4
75. Muk T, Jiang PP, Stensballe A, Skovgaard K, Sangild PT, Nguyen DN. Prenatal endotoxin exposure induces fetal and neonatal renal inflammation via innate and Th1 immune activation in preterm pigs. *Front Immunol*. (2020) 11:565484. doi: 10.3389/fimmu.2020.565484
76. Pan X, Zhang D, Nguyen DN, Wei W, Yu X, Gao F, et al. Postnatal gut immunity and microbiota development is minimally affected by prenatal inflammation in preterm pigs. *Front Immunol*. (2020) 11:420. doi: 10.3389/fimmu.2020.00420
77. Ren S, Hui Y, Goericke-Pesch S, Pankratova S, Kot W, Pan X, et al. Gut and immune effects of bioactive milk factors in preterm pigs exposed to prenatal inflammation. *Am J Physiol Gastrointest Liver Physiol*. (2019) 317:G67–77. doi: 10.1152/ajpgi.00042.2019
78. Levy O. Innate immunity of the newborn: basic mechanisms and clinical correlates. *Nat Rev Immunol*. (2007) 7:379–90. doi: 10.1038/nri2075
79. Dong Y, Speer CP. Late-onset neonatal sepsis: recent developments. *Arch Dis Child Fetal Neonatal Ed*. (2015) 100:F257–63. doi: 10.1136/archdischild-2014-306213
80. Lisse IM, Aaby P, Whittle H, Jensen H, Engelmann M, Christensen LB. T-lymphocyte subsets in West African children: impact of age, sex, and season. *J Pediatr*. (1997) 130:77–85. doi: 10.1016/S0022-3476(97)70313-5
81. Wood NS, Costeloe K, Gibson AT, Hennessy EM, Marlow N, Wilkinson AR. The EPICure study: associations and entecedents of neurological and developmental disability at the 30 months of age following extremely preterm birth. *Arch Dis Child Fetal Neonatal Ed*. (2005) 90:F134–40. doi: 10.1136/adc.2004.052407
82. Lauterbach MD, Raz S, Sander CJ. Neonatal hypoxic risk in preterm birth infants: the influence of sex and severity of respiratory distress on cognitive recovery. *Neuropsychology*. (2001) 15:411–20. doi: 10.1037/0894-4105.15.3.411
83. Skiöld B, Alexandrou G, Padilla N, Blennow M, Vollmer B, Ådén U. Sex differences in outcome and associations with neonatal brain morphology in extremely preterm children. *J Pediatr*. (2014) 164:1012–8. doi: 10.1016/j.jpeds.2013.12.051

Conflict of Interest: The authors declare that the research was conducted in the absence of any commercial or financial relationships that could be construed as a potential conflict of interest.

frontiers in Pediatrics

BRIEF RESEARCH REPORT
published: 03 March 2021
doi: 10.3389/fped.2021.606611

Safety of Red Blood Cell Transfusion Using Small Central Lines in Neonates: An *in vitro* Non-inferiority Study

Flavia Rosa-Mangeret[1]*, *Sophie Waldvogel-Abramowski*[2], *Riccardo E. Pfister*[1], *Olivier Baud*[1†] *and Sébastien Fau*[1†]

[1] Division of Neonatology, Geneva University Hospital (HUG), Geneva, Switzerland, [2] Division of Hematology, Geneva University Hospital (HUG), Geneva, Switzerland

OPEN ACCESS

Edited by:
Yuan Shi,
Children's Hospital of Chongqing Medical University, China

Reviewed by:
Andreas Repa,
Medical University of Vienna, Austria
Lu-Quan Li,
Chongqing Medical University, China
Shan He,
The First People's Hospital of Yunnan Province, China

***Correspondence:**
Flavia Rosa-Mangeret
flaviamangeret@gmail.com

[†] These authors have contributed equally to this work

Specialty section:
This article was submitted to Neonatology, a section of the journal Frontiers in Pediatrics

Received: 15 September 2020
Accepted: 25 January 2021
Published: 03 March 2021

Citation:
Rosa-Mangeret F, Waldvogel-Abramowski S, Pfister RE, Baud O and Fau S (2021) Safety of Red Blood Cell Transfusion Using Small Central Lines in Neonates: An in vitro Non-inferiority Study. Front. Pediatr. 9:606611. doi: 10.3389/fped.2021.606611

Aim: This study aimed to investigate the safety of transfusing red blood cell concentrates (RBCCs) through small [24 gauge (24G)] and extra-small [28 gauge [28G)] peripherally inserted central catheters (PICCs), according to guidelines of transfusion practice in Switzerland.

Methods: We performed a non-inferiority *in vitro* study to assess the safety of transfusing RBCC for 4 h at a 4 ml/h speed through 24G silicone and 28G polyurethane PICC lines, compared with a peripheral 24G short catheter. The primary endpoint was hemolysis percentage. Secondary endpoints were catheter occlusion, inline pressure, and potassium and lactate values.

Results: For the primary outcome, hemolysis values were not statistically different among catheter groups (0.06% variation, $p = 0.95$) or over time (2.75% variation, $p = 0.72$). The highest hemolysis values in both 24G and 28G PICCs were below the non-inferiority predefined margin. We did not observe catheter occlusion. Inline pressure varied between catheters but followed the same pattern of rapid increase followed by stabilization. Potassium and lactate measurements were not statistically different among tested catheters (0.139% variation, $p = 0.98$ for potassium and 0.062%, $p = 0.96$ for lactates).

Conclusions: This study shows that RBCC transfusion performed *in vitro* through 24G silicone and 28G polyurethane PICC lines is feasible without detectable hemolysis or pressure concerns. Also, it adds that, concerning hemolysis, transfusion of RBCC in small and extra-small PICC lines is non-inferior to peripheral short 24G catheters. Clinical prospective assessment in preterm infants is needed to confirm these data further.

Keywords: neonatal care, neonatal transfusion, premature (babies), quality of care/care delivery, blood transfusion, transfusion—alternative strategies

INTRODUCTION

Peripherally inserted central catheters (PICCs), usually ranging from 24 gauge (G) to 28G, are routinely used in very preterm infants for parenteral nutrition and drug infusion. They can be inserted at the bedside and maintained for several weeks. Their small diameter is also suitable for the most immature neonates, and the central positioning allows infusing high osmolality solutions (1).

Very preterm infants are at high risk of anemia due to impaired erythropoietin production, repeated blood draws, reduced red blood cell life span, iron depletion, and rapid growth. As a result, 80% of very low birth weight (VLBW) and 80–95% of extremely low birth weight (ELBW) neonates need at least one blood transfusion before discharge (2, 3). Potential risks of catheter occlusion and hemolysis exist when considering red blood cell concentrate (RBCC) transfusion through 24/28G PICC lines (1). However, securing a peripheral IV line for transfusions can be challenging and can lead to clinical instability in a critically ill neonate, moving some physicians toward performing them through an available PICC. To the best of our knowledge, there are no clear guidelines on transfusions using neonatal PICC lines, while there is also no evidence that using these devices with this purpose would be hazardous.

Few studies analyzed the feasibility and safety of transfusing RBCC through extra-small (27G) (4, 5) and small (24G) PICCs (6). However, no study compared the safety of transfusing RBCC using the polyurethane and silicone smallest PICC lines with the regularly used 24G short catheters, in conditions simulating a preterm neonate transfusion in the neonatal intensive care unit (NICU).

To understand this issue's relevance in Switzerland, we invited the nine Swiss level III NICU to answer a small self-administered questionnaire regarding PICC usage (available in the **Supplementary Material**). It revealed that 4/9 (44.4%) had already performed blood transfusion through 28G PICC lines. Among them, only one center declared that catheter blockage occurred. Furthermore, 7/9 (77.8%) units stated they would be willing to use catheters for transfusion if further safety evidence exists.

We then performed a non-inferiority *in vitro* study comparing the smallest PICCs available in Switzerland with the standard peripheral 24G short catheter. We hypothesize that transfusing RBCC through either small (24G) or extra-small (28G) PICC lines is as safe as transfusing RBCC through peripheral 24G short catheters in the NICU environment. The primary objective was to provide evidence for RBCC transfusion safety through extra-small PICC lines considering hemolysis, catheter blockage, and inline pressure levels.

MATERIALS AND METHODS

Setting

We performed a non-inferiority *in vitro* study to assess the safety of transfusing RBCC through small PICC lines compared with a peripheral 24G short catheter. We performed this study at Geneva University Hospital NICU. The Geneva Cantonal Ethics Commission waived the study (BASEC 2018−00823).

Red Blood Cell Concentrate Transfusion Setup

To do a mock neonatal RBCC transfusion, we performed the blood transfusion as per our unit protocol, into an incubator with the air temperature set at 37°C, considering the average body temperature of the neonate to be 37°C (**Figure 1**). In the setting, the incubator simulated the neonate, and the three different catheters underwent simultaneous standard RBCC transfusion in the incubator:

- peripheral 24G short catheter (24G BD Insyte-W™, Utah, USA), used as the control group (CTR);
- polyurethane catheter Premicath 1 Fr/28G 20 cm (Vygon Schweiz GmbH, Aachen, Germany), used as intervention Group #1 (PICC28);
- silicone catheter Epicutaneo 2 2 Fr/24G 30 cm (Vygon Schweiz GmbH, Aachen, Germany), used as intervention Group #2 (PICC24).

For each catheter, we added to the standard transfusion setup a three-way stopcock on the catheter entrance connected to a syringe pump with an embedded inline pressure sensor Alaris CC® (Becton Dickinson, Eysins, Switzerland). A data logger software registered inline pressure every 2 s. A minimal flow of 0.1 ml/h of NaCl 0.9% ran through this pressure measurement line.

The filtered RBCCs were gamma-irradiated immediately (25 Gray) before the procedure, and they were not older than 14 days. We calculated the volume and infusion rate based on a neonate of 1,000 g, who would need 15 ml/kg of RBCC transfusion infused within 4 h.

Procedure

Upon arrival, RBCC rested at room temperature (26°C) for at least 30 min, and then sampling for hemoglobin, hematocrit, potassium, and free hemoglobin took place before splitting it into three aliquots of 20 ml in 50 ml syringes.

Meanwhile, the three groups received a continuous infusion of parenteral nutrition (per 100 ml: amino-acid 3 g; glucose: 10.8 g; Na: 2 mmol; K: 1 mmol; Ca: 1.1 mmol; PO_4: 0.86 mmol; osmolarity: 1,000 mOsm/L) for 1 h, at a 4 ml/h speed, followed by a manual flush of 1 ml of NaCl 0.9%.

After parenteral nutrition infusion, RBCC infusion started simultaneously in all groups, at 4 ml/h for 4 h on the syringe pumps (Module DPS Fresenius Vial, Brézins, France). In order to avoid clotting, we placed catheter tips into an isotonic solution (NaCl 0.9%), avoiding direct contact between the red cells and air; and by the end of each hour (H1, H2, H3, and H4), we placed catheters tips into an Eppendorf Tube® 3810X 1.5 ml vial (Eppendorf AG, 22331 Hamburg, Germany) filled with 0.5 ml of NaCl 0.9% to complete 1.5 ml of total sample volume (**Figure 1**).

After that, we immediately analyzed samples for hemoglobin, hematocrit, and potassium (ABL835 Flex Radiometer Medical Inc., Brønshøj, Denmark) and centrifuged the remaining, in room temperature, at 2,000 rpm for 10 min; we collected 400 μl

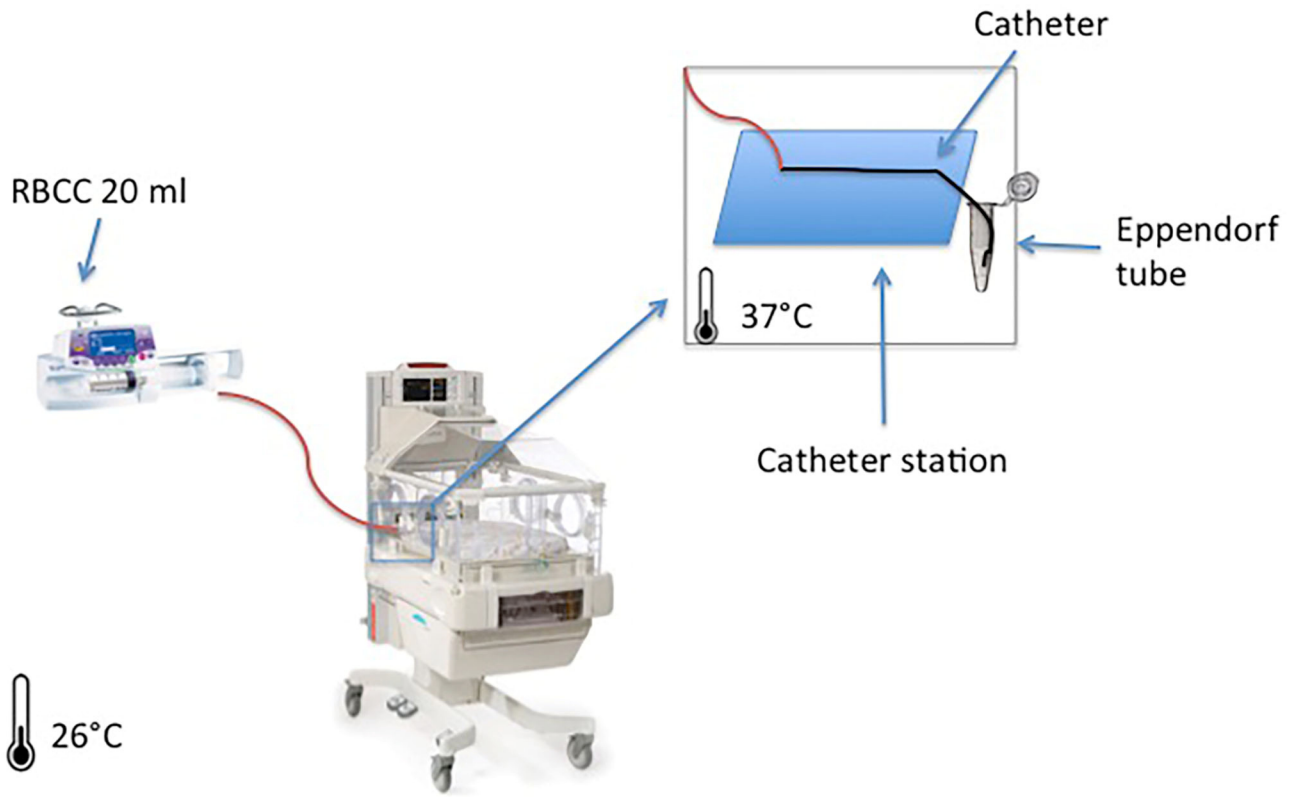

FIGURE 1 | System setup overview: the figure represents one red blood cell concentrate (RBCC) infusion through a peripherally inserted central catheter (PICC) line that lies on a support catheter station with the tip inserted on a collector tube filled in with NaCl 0.9% for sampling. The same setup was used for the three groups at the same time.

of the supernatant and froze it at −20°C until free hemoglobin testing (Spectrophotometer Biochrom Libra S70, Holliston, USA). Hemolysis in the RBCC bag was assessed (hemoglobin, hematocrit, and free hemoglobin) before and immediately after the procedure.

At the end of transfusion, all the lines were flushed with 1 ml of NaCl 0.9%, and the parenteral nutrition was restarted in the three systems for at least 1 h to determine pressure variation and possible catheter occlusion.

Outcomes

The primary outcome was hemolysis, measured as indicated in the European Guidelines (7): % hemolysis = [free hemoglobin (g/L) × (100 – hematocrit (%)]/total hemoglobin.

The secondary outcomes were as follows:

- potassium and lactate serum concentrations at baseline, H1, H2, H3, and H4;
- complete catheter occlusion during and after infusion, defined as inline pressure superior to 600 mmHg with a flush NaCl 0.9% in the 4 ml/h speed;
- inline pressure for each catheter during and after transfusion;

While lactate is not a hemolysis marker, it is considered a surrogate marker for blood storage (8). Hence, we assumed it was relevant to report its variation over time in our study.

Statistics

For sample size calculation, we considered a limit of the hemolysis parameter below 0.8% (9), and a non-inferiority margin of 0.2%. According to published data, the mean hemolysis for RBCC bags after 2 weeks of storage is 0.23 ± 0.12% (9). The reached sample size was eight separate RBCC transfusions, considering that the mean hemolysis at the end of the transfusion is at least equal to the control and intervention groups, reaching a significance level of 2.5% and 90% power. We compared the hemolysis values at the end of RBCC transfusion (H4) between the control and intervention groups using a one-way ANOVA and Friedman test for paired measures. We also compared hemolysis among catheters and over time, using repeated-measures two-way ANOVA with Geisser–Greenhouse correction. Hemolysis in RBCC bags was compared before and after the procedure using a Wilcoxon matched-pairs signed-rank test.

Secondary outcomes include catheter occlusion, inline pressure comparison before, during (at the steady state), and after RBCC infusion. Potassium and lactate hourly

measures were analyzed using repeated-measures two-way ANOVA with Geisser–Greenhouse correction. Statistical analyses used GraphPad PRISM version 6.0 (San Diego, CA).

RESULTS

Primary Outcome

Difference in means [standard deviations (SD)] of hemolysis values measured at the end of the transfusion procedures (H4) were not statistically significant between the control group [0.0675% (0.0205)], PICC28 [0.0700% (0.0239)], and PICC24 [0.0700% (0.02390)] ($p = 0.99$). For both intervention catheters (PICC28 and PICC24), the higher-margin values were significantly lower than the predefined non-inferiority margin of 0.2%. **Figure 2A** shows the mean hemolysis values in the three groups from the baseline to the end of transfusion. Comparing the hemolysis values between groups through the whole procedure on repeated-measures two-way ANOVA further confirms that hemolysis values were not statistically changed among catheter groups (0.06% variation, $p = 0.95$) or over time (2.75% variation, $p = 0.72$). The mean hemolysis in the RBCC that remained in the RBCC before and after transfusion was not found statistically different (0.0595% vs. 0.0706%, $p = 0.11$) (**Figure 2B**). The detailed data are available in the **Supplementary Materials**.

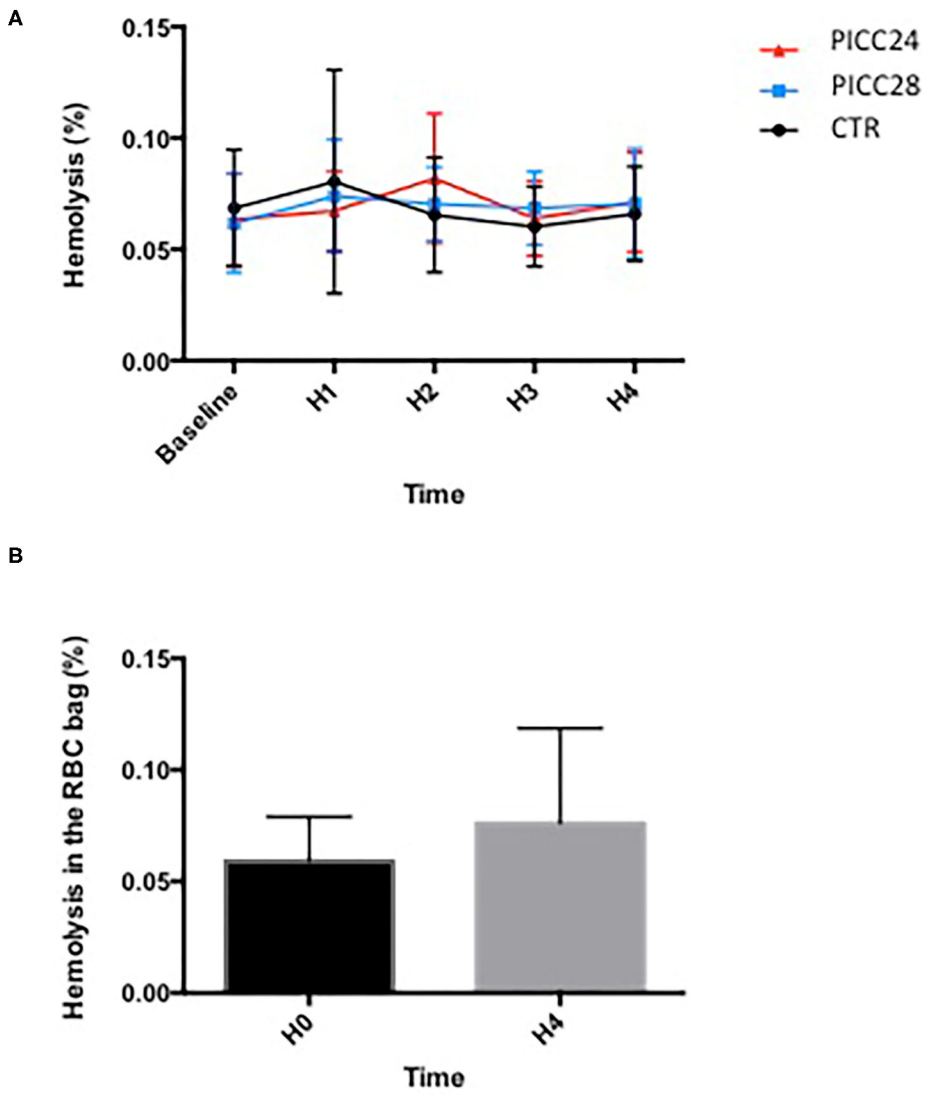

FIGURE 2 | Comparison of hemolysis over time during a 4 h transfusion according to IV line used. **(A)** Mean hemolysis for each catheter assessed each hour; data (mean ± SEM) were compared using a two-way ANOVA with time and catheter type as variables. **(B)** Comparison of hemolysis values (%) in red blood cell concentrate (RBCC) bag between baseline (H0) and the end of transfusion (H4). Data (mean ± SD) were compared using a Wilcoxon matched-pairs signed-rank test.

Secondary Outcomes

The potassium and lactate measurements analyzed on a two-way ANOVA revealed a non-significant variation among the three catheter groups (0.139% variation, $p = 0.98$ for potassium and 0.062%, $p = 0.96$ for lactates). Lactate increased significantly in all experimental groups overtime during the transfusion process (10.7% variation, $p < 0.001$). In contrast, potassium measurements remained remarkably stable (**Figure 3**).

Catheter occlusion did not happen during RBCC transfusions or parenteral nutrition infusion in the eight separate experiments. The recorded inline pressures were very reproducible among five experiments for the PICC28 group and four experiments for both the PICC24 and control groups (**Figure 4A**). During RBCC infusion, there was a rapid increase of pressures in the system, likely due to high blood viscosity, being the highest in the PICC28 group with a rise from 77 ± 5 mmHg during parenteral infusion to 183 ± 12 mmHg during transfusion. In the PICC24 group, pressure increased from 18 ± 8 to 55 ± 6 mmHg. In contrast, the pressure increase was limited from 3.3 ± 0.6 to 7.6 ± 5.3 mmHg in the control group (**Figure 4B**). Infusion of parenteral nutrition at the end of RBCC transfusion allowed, in all cases, a drop in pressure to similar values measured before the RBCC transfusion (84 ± 4, 24 ± 7, and 4.5 ± 1.0 mmHg for PICC28, PICC24, and control lines, respectively).

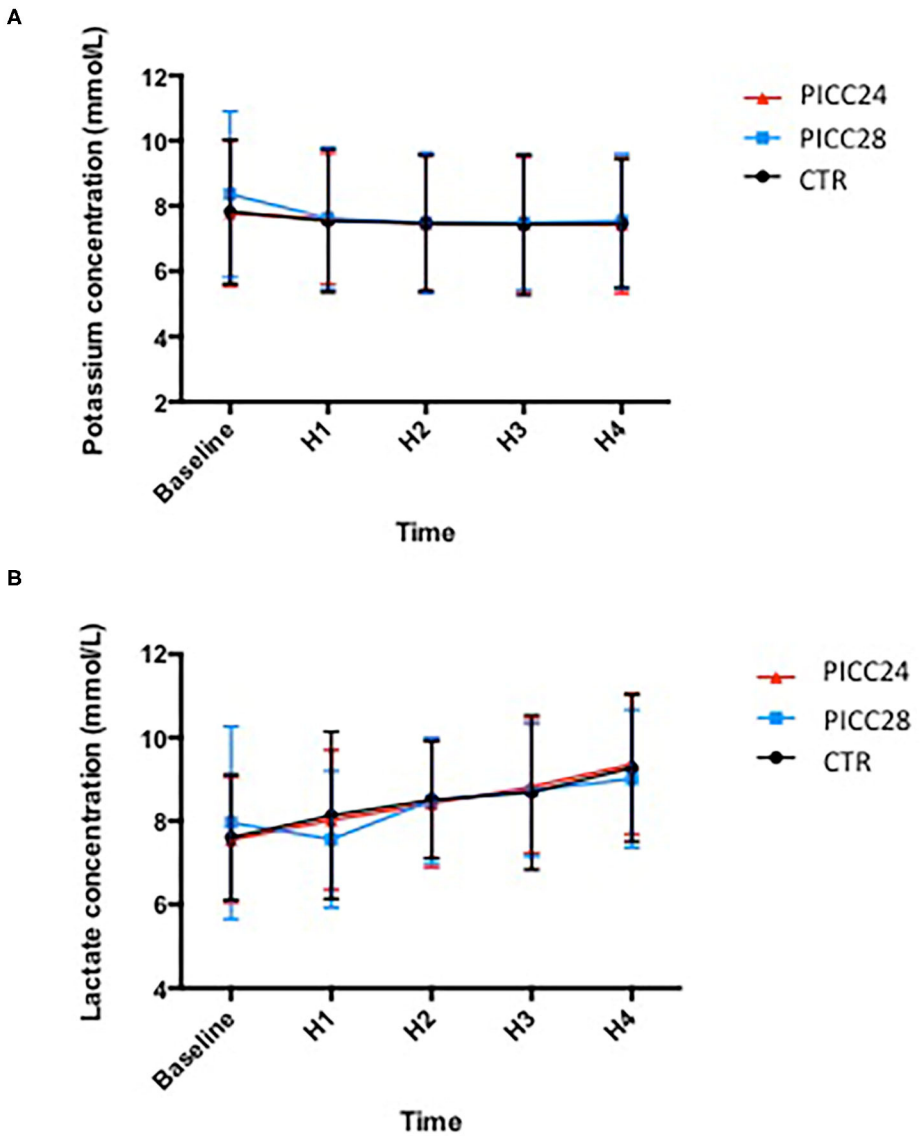

FIGURE 3 | Mean potassium **(A)** and lactate **(B)** concentrations in each IV line group during red blood cell concentrate (RBCC) transfusion.

DISCUSSION

RBCC transfusions are common interventions in very preterm infants admitted in NICUs and are dependent on available IV lines. In contrast to PICC lines usually already present when a transfusion is needed, peripheral IV lines are not; securing them to an already sick neonate is a challenge. In this *in vitro* non-inferiority study, for the primary outcome of hemolysis, transfusing RBCC in 24 and 28G PICCs was non-inferior to standard 24G short catheter. For the secondary outcomes, we have not detected catheter occlusion; inline pressures were measured within our pre-established limits; and

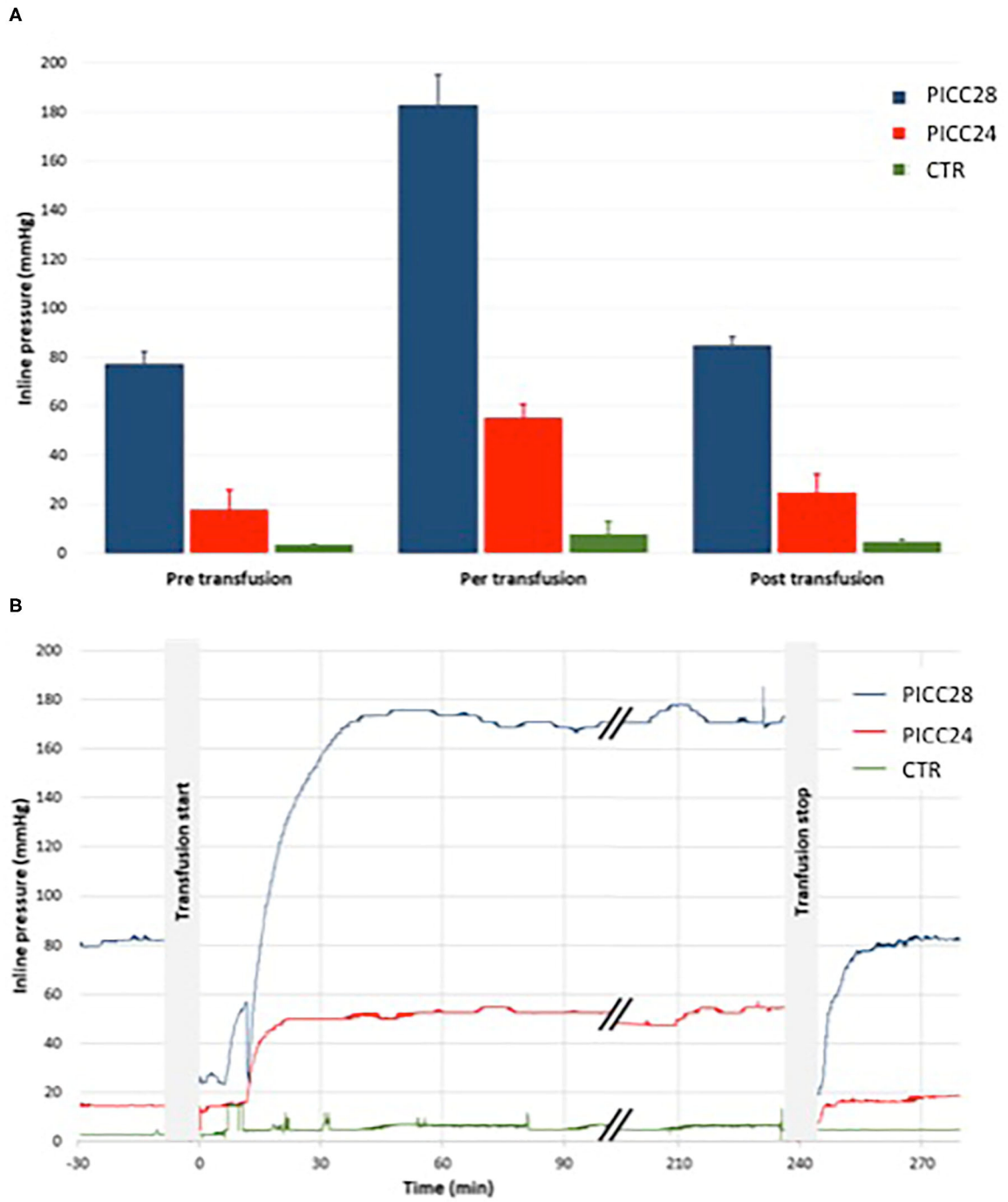

FIGURE 4 | Mean pressure within the lines before, during, and after the transfusion. Comparisons within IV line groups **(A)** and typical traces **(B)** in PICC28 line (blue), PICC24 line (red), and CTR peripheral control line (green).

there was no statistically significant difference in potassium and lactate concentrations among experimental groups during RBCC transfusion.

These observations are of interest in light of our Swiss national survey, which exhibits that most NICUs (7/9) would be ready to perform RBCC transfusions using small and extra-small PICC lines if further evidence of feasibility and safety available and some 44.4% (4/9) had already done it. This contrasts with a previous extensive survey performed in the United States, in which out of 186 NICUs, only five used (2.7%) PICC lines to transfuse blood products (10).

Our data show that free hemoglobin concentrations were found similar in PICC lines compared with peripheral IV lines. Also, no detectable adverse events were recorded. In a previous report, Repa et al. have tested *in vitro* the safety of RBCC transfusions in 27G 20 and 30 cm polyurethane PICC lines, without significant hemolysis (5). In another retrospective study, transfusion through a 27G PICC line was found feasible in 38 neonates, while free hemoglobin was not measured in this study, hemoglobin levels increased, and cardiovascular parameters remained stable without increase in potassium levels (4). Our data are consistent with those of previous studies and further support that transfusing RBCC through a 28G polyurethane 20 cm PICC line or a 24G silicone 30 cm PICC line is at least as safe as transfusing RBCC though a 24G short catheter.

Considering the inline pressure, the RBCC transfusion induced a substantial pressure increase. The blood viscosity infused at 4 ml/h through the PICC28 line generated pressures as high as 180 mmHg, far below 300 mmHg, which we and others consider as the safety threshold (11, 12). The rapid pressure drop after transfusion to the range of pre-RBCC transfusion values suggests that PICC resistance remained unchanged and is consistent with the absence of catheter occlusion, even partial, during the transfusion.

This *in vitro* study has several limitations. First, even if we set a system as close as possible to a neonatal RBCC transfusion with body temperature at 37°C and using same equipment and transfusion procedure as in our patients, it remains an *in vitro* study design and needs to be further completed by a clinical prospective study. Second, the speed of 4 ml/h during transfusion, fitting with standard care in a 1,000 g infant, appears to be the highest to avoid 300 mmHg of inline pressure usually considered a limit for safety reasons. We did not test lower speeds considering that they would not be clinically relevant. Third, we used a parenteral mixture with relatively low osmolarity, and catheters were unused for each experiment, all factors that may reduce the risk of catheter occlusion. Finally, we performed the RBCC transfusion alone and not in combination with simultaneous parenteral nutrition, which would not be recommended due to possible damage of RBC (13). However, most neonates needing transfusions are likely to be fed orally, and the sickest neonates will mostly have a two-lumen IV line.

In conclusion, this study showed that *in vitro* RBCC transfusion performed through 24 to 28G neonatal PICC lines was non-inferior to 24G short catheters, with no further evidence of catheter occlusion. These results might be useful in light of a practice that already exists in several NICUs, but safety of RBCC transfusion through PICC lines remains to be confirmed in a prospective clinical study.

DATA AVAILABILITY STATEMENT

The original contributions presented in the study are included in the article/**Supplementary Material**, further inquiries can be directed to the corresponding author/s.

AUTHOR'S NOTE

Red blood cell transfusions are a common intervention in very premature infants. Usually, they require a peripheral intravenous line, which can be very challenging to secure. Although very small neonates routinely have peripherally inserted central catheters (PICCs) to receive intravenous nutrition and medication infusion, only few studies are available regarding the safety of using PICCs for red blood cell transfusions. This study assessed the safety of performing blood transfusions through the smallest PICCs available (24 and 28 gauge) using an *in vitro* model that mimics preterm infants' environment, and its results might improve neonatal care to date.

AUTHOR CONTRIBUTIONS

FR-M designed the study, wrote the study protocol, performed all pilot tests and the main tests, and wrote the first draft and the last version. SW-A was the expert consultant, responsible to reach the ideal set up, provided the Red Blood Cell Concentrates, participated in the analysis of the samples and results, and edited the manuscript. RP was part of the study design, protocol, the conception and distribution of the survey, and read and edited manuscript. OB was part of the study design, writing of the protocol, ethics committee submission, survey conception, pilots conception, final setup, the statistics, analysis of results, and manuscript. SF was part of the setup conception, the monitoring up of pressures during transfusions, analysis of results, and manuscript editing. All authors revised the first draft of the manuscript and approved the final version.

SUPPLEMENTARY MATERIAL

The Supplementary Material for this article can be found online at: https://www.frontiersin.org/articles/10.3389/fped.2021.606611/full#supplementary-material

REFERENCES

1. Mccay AS, Elliott EC, Walden M. PICC placement in the neonate. *N Engl J Med*. (2014) 370:e17. doi: 10.1056/NEJMvcm1101914
2. Maier RF, Sonntag J, Walka MM, Liu G, Metze BC, Obladen M. Changing practices of red blood cell transfusions in infants with birth weights less than 1000g. *J Pediatr*. (2000) 136:220–4. doi: 10.1016/S0022-3476(00)70105-3
3. Widness JA, Seward VJ, Kromer IJ, Burmeister LF, Bell EF, Strauss RG. Changing patterns of red blood cell transfusion in very low birth weight infants. *J Pediatr*. (1996) 129:680–7. doi: 10.1016/S0022-3476(96)70150-6
4. Repa A, Mayerhofer M, Worel N, Cardona F, Deindl P, Pollak A, et al. Blood transfusions using 27 gauge PICC lines: a retrospective clinical study on safety and feasibility. *Klin Padiatr*. (2014) 226:3–7. doi: 10.1055/s-0033-1363244
5. Repa A, Mayerhofer M, Cardona F, Worel N, Deindl P, Pollak A, et al. Safety of blood transfusions using 27 gauge neonatal PICC lines : an *in vitro* study on hemolysis. *Klin Padiatr*. (2013) 225:379–82. doi: 10.1055/s-0033-1355329
6. Wong ECC, Schreiber S, Criss VR, LaFleur B, Rais-Bahrami K, Short B, et al. Feasibility of red blood cell transfusion through small bore central venous catheters used in neonates. *Pediatr Crit Care Med*. (2004) 5:69–74. doi: 10.1097/01.PCC.0000102225.49058.4B
7. Mayr WR. Guide to the preparation, use and quality assurance of blood components, 13th Edition. *Vox Sang*. (2017) 93:279. doi: 10.1111/j.1423-0410.2007.00965.x
8. Council of Europe. *Guide to the Preparation, Use and Quality Assurance*. (2011). Available online at: http://www.centronazionalesangue.it/sites/default/files/guida_edqm_16_edizione.pdf
9. Serrano K, Chen D, Hansen AL, Levin E, Turner TR, Kurach JDR, et al. The effect of timing of gamma-irradiation on hemolysis and potassium release in leukoreduced red cell concentrates stored in SAGM. *Vox Sang*. (2014) 106:379–81. doi: 10.1111/vox.12112
10. Sharpe E, Pettit J, Ellsbury DL. A national survey of neonatal Peripherally Inserted Central Catheter (PICC) Practices. *Adv. Neonatal Care*. (2013) 13:55–74. doi: 10.1097/ANC.0b013e318278b907
11. Keay S, Callander C. The safe use of infusion devices. *Contin Educ Anaesth Crit Care Pain*. (2004) 4:81–5. doi: 10.1093/bjaceaccp/mkh022
12. Pisciotto PT, Wong ECC. Chapter 11 – Technical considerations/mechanical devices. In: Hillyer CD, Strauss RG, Luban NLC, editors. *Handbook of Pediatric Transfusion Medicine*. Academic Press (2004). p. 121–30. doi: 10.1016/B978-012348776-6/50014-5
13. Sowemimo-Coke, SO. RBC hemolysis during processing.pdf. *Transfus Med Rev*. (2002) 16:46–60. doi: 10.1053/tmrv.2002.29404

Conflict of Interest: The authors declare that the research was conducted in the absence of any commercial or financial relationships that could be construed as a potential conflict of interest.

frontiers in Pediatrics

REVIEW
published: 09 March 2021
doi: 10.3389/fped.2021.615508

A Review of Placenta and Umbilical Cord-Derived Stem Cells and the Immunomodulatory Basis of Their Therapeutic Potential in Bronchopulmonary Dysplasia

Wai Kit Chia[1], Fook Choe Cheah[2], Nor Haslinda Abdul Aziz[3], Nirmala Chandralega Kampan[3], Salwati Shuib[1], Teck Yee Khong[4], Geok Chin Tan[1] and Yin Ping Wong[1]**

[1] Department of Pathology, Faculty of Medicine, Universiti Kebangsaan Malaysia, Kuala Lumpur, Malaysia, [2] Department of Pediatrics, Faculty of Medicine, Universiti Kebangsaan Malaysia, Kuala Lumpur, Malaysia, [3] Department of Obstetrics and Gynecology, Faculty of Medicine, Universiti Kebangsaan Malaysia, Kuala Lumpur, Malaysia, [4] Department of Pathology, SA Pathology, Women's and Children's Hospital, Adelaide, SA, Australia

OPEN ACCESS

Edited by:
Roland H. Hentschel, University of Freiburg Medical Center, Germany

Reviewed by:
Marius Alexander Möbius, Technische Universität Dresden, Germany
Tim Wolfs, Maastricht University, Netherlands

***Correspondence:**
Yin Ping Wong
ypwong@ppukm.ukm.edu.my
Geok Chin Tan
tangc@ppukm.ukm.edu.my

Specialty section:
This article was submitted to Neonatology, a section of the journal Frontiers in Pediatrics

Received: 09 October 2020
Accepted: 17 February 2021
Published: 09 March 2021

Citation:
Chia WK, Cheah FC, Abdul Aziz NH, Kampan NC, Shuib S, Khong TY, Tan GC and Wong YP (2021) A Review of Placenta and Umbilical Cord-Derived Stem Cells and the Immunomodulatory Basis of Their Therapeutic Potential in Bronchopulmonary Dysplasia. Front. Pediatr. 9:615508. doi: 10.3389/fped.2021.615508

Bronchopulmonary dysplasia (BPD) is a devastating lung disorder of preterm infants as a result of an aberrant reparative response following exposures to various antenatal and postnatal insults. Despite sophisticated medical treatment in this modern era, the incidence of BPD remains unabated. The current strategies to prevent and treat BPD have met with limited success. The emergence of stem cell therapy may be a potential breakthrough in mitigating this complex chronic lung disorder. Over the last two decades, the human placenta and umbilical cord have gained increasing attention as a highly potential source of stem cells. Placenta-derived stem cells (PDSCs) and umbilical cord-derived stem cells (UCDSCs) display several advantages such as immune tolerance and are generally devoid of ethical constraints, in addition to their stemness qualities. They possess the characteristics of both embryonic and mesenchymal stromal/stem cells. Recently, there are many preclinical studies investigating the use of these cells as therapeutic agents in neonatal disease models for clinical applications. In this review, we describe the preclinical and clinical studies using PDSCs and UCDSCs as treatment in animal models of BPD. The source of these stem cells, routes of administration, and effects on immunomodulation, inflammation and regeneration in the injured lung are also discussed. Lastly, a brief description summarized the completed and ongoing clinical trials using PDSCs and UCDSCs as therapeutic agents in preventing or treating BPD. Due to the complexity of BPD, the development of a safe and efficient therapeutic agent remains a major challenge to both clinicians and researchers.

Keywords: bronchopulmonary dysplasia, placenta, regenerative medicine, stem cell, umbilical cord

INTRODUCTION TO STEM CELL BIOLOGY

Stem cell therapy has evolved tremendously since its first success story of bone marrow cells in regenerating a rodent's infarcted myocardium (1). In recent years, it has been advocated as a novel yet promising treatment modality for a myriad of diseases, including cardiovascular, neurodegenerative, musculoskeletal, wound repair. Stem cells are unspecialized cells in the human body that have a remarkable capability to regenerate continually. The key abilities of stem cells to constantly self-renew, proliferate and differentiate into specialized cells under adapted physiological environment allow them to restore tissue to its pre-injurious state (2). Sources of stem cells include bone marrow, umbilical cord, cord blood and adipose tissue.

Stem cell potency is defined as its capability to self-renew and differentiate, thus classified as totipotent, pluripotent, multipotent, and unipotent. The term plasticity means the ability to be molded or change to adapt to the situation. Stem cell plasticity is defined as the ability to give rise to different cell types (3, 4). The potency of stem cells reduces with each journey of lineage differentiation from early embryogenesis to mature specialized cells (4). A zygote, which is formed following ovum fertilization by a sperm, is the classic example of a totipotent stem cell. It has the ability to generate the embryonic as well as extra-embryonic structures including placenta. The blastocyst, which is formed 5 days after fertilization, consists of the inner cell mass (also known as embryoblast) rimmed by trophoblasts (5). The latter will develop into the placenta. Human embryonic stem cells (hESCs) which originate from the inner cell mass, remain undifferentiated with pluripotent potential. Similar to totipotent stem cells, pluripotent stem cells are able to give rise to all cell types of any of the three primary germ layers (endoderm, mesoderm and ectoderm) in the body, but lacking the capability to produce extra-embryonic cells. Following differentiation of pluripotent stem cells into one of the germ layers, they become multipotent stem cells with differentiation potential restricted to only cells of that germ layer (5). Adult and fetal stem cells are the examples of multipotent stem cells. Adult stem cells, or somatic stem cells are found in adult somatic tissues (6), whereas fetal stem cells are obtained from cadaveric fetuses following medically terminated pregnancies. Unipotent stem cell has the narrowest differentiation ability to only one cell type (5). Progenitor cells are descendants of stem cells with limited ability to differentiate and replicate. Hematopoietic, neural and cardiac progenitor cells are among the examples (7).

Several categories of stem cells have been widely investigated over the last few decades, such as embryonic stem cells (ESCs), fetal stem cells and somatic/adult stem cells. Acquisition of pluripotent ESCs that involved destruction of a developing embryos and the use of fetal stem cells from aborted/living fetal tissue however, posed some ethical and legal implications (8). Moreover, these pluripotent ESCs and possibly fetal stem cells which possess similar oncogenic properties with cancer stem cells raise a major safety concern as these cells may undergo undesirable differentiation and pose a risk of malignant transformation post transplantation (9). For instance, *in vivo* teratoma when grafted in severe combined immunodeficient mice (10).

Human placenta, an ephemeral but crucial organ in pregnancy, is an alternative reservoir of stem cells. Apart from its fundamental role in determining optimal fetal growth trajectory *in utero*, it represents a rich source of stem cells that could offer additional advantages in terms of proliferation and plasticity compared to adult stem cells (11, 12). Placenta and umbilical cord are traditionally regarded as nothing but biological waste, is often discarded after parturition. This helps to resolve the ethical concern inherent in ESCs (8, 13). Unlike stem cells harvested from other sources such as the bone marrow, adipose tissue and endometrium, these placental and umbilical cord tissues are readily available in large quantities and its stem-cell derivatives are easily recovered without the donors incurring any invasive surgical procedures (14). These unique features of PDSCs and UCDSCs make them attractive alternatives in cell therapies and regenerative medicine.

In this review, we first provide an overview of bronchopulmonary dysplasia (BPD) and the disease pathogenesis, followed by the potential roles of human PDSCs and UCDSCs as effective therapeutic and possibly preventive modalities for BPD as the disease in focus. Unanswered fundamental challenges related to clinical translation of stem cells from bench to bedside in BPD are also discussed.

BRONCHOPULMONARY DYSPLASIA AND THE DISEASE PATHOGENESIS

Infants born extremely premature may have arrested lung development at the canalicular-saccular phase, before alveolarization could occur. These infants are inevitably exposed to postnatal interventions such as positive pressure mechanical ventilation, supplemental oxygen therapy and sustaining recurrent bouts of infections that may exert further harmful effects on the immature lung. Consequently, the prematurity-induced interruption of normal alveolar and distal vascular development, which is superimposed by pulmonary inflammation and aberrant reparative process may collectively contribute to the progression of BPD (15).

The lung of infants with BPD has three histopathological features: [1] widespread but occasionally patchy interstitial edema and fibrosis may give rise to areas of relative collapse and fibrosis accompanied by more distended emphysematous lung and thus less alveolar surface area; [2] arterial muscular hypertrophy and adventitial thickening of small pulmonary arteries leading to increased vascular resistance and pulmonary

Abbreviations: AECs, amniotic epithelial cells; AMSCs, amniotic mesenchymal stromal/stem cells; AM-MSCs, amniotic membrane-derived mesenchymal stromal/stem cells; BM-MSCs, bone marrow-derived mesenchymal stromal/stem cells; BPD, bronchopulmonary dysplasia; ECFCs, endothelial colony-forming cells; ESCs, embryonic stem cells; EVs, extracellular vesicles; hAECs, human amniotic epithelial cells; hUC-MSCs, human umbilical cord mesenchymal stromal/stem cells; L-MSCs, lung-resident mesenchymal stromal/stem cells; LPS, lipopolysaccharide; MSCs, mesenchymal stromal/stem cells; P-MSCs, placental mesenchymal stromal/stem cells; PDSCs, Placenta-derived stem cells; UCDSCs, umbilical cord-derived stem cells; UC-MSCs, umbilical cord mesenchymal stromal/stem cells.

hypertension; and [3] less usually nowadays, acute major airway pathology characterized by necrosis associated with an obliterative bronchiolitis, squamous metaplasia, and collapse of lung tissue distal to the obstructed airway (16).

Imbalance Between Pro- and Anti-inflammatory Activities

An imbalance between pro- and anti-inflammatory activities in the lung is proposed as the major mechanism resulting in BPD (17). It is characterized by influx of neutrophils and macrophages into the airways and lung parenchyma. Migration and accumulation of these inflammatory components in the lung may amplify and perpetuate further immune activation by release of potentially destructive pro-inflammatory cytokines, chemokines and tissue proteases such as tumor necrosis factor-alpha (TNF-α), interleukin-8 (IL-8), IL-1, IL-6, matrix metalloproteinase-8 (MMP-8) and MMP-9 (17).

Besides, adhesion molecules such as soluble E-selectin (sE-selectin) and intercellular adhesion molecule-1 (ICAM-1) were found elevated in the arterial plasma level of infants with BPD (18, 19). These adhesion molecules initiate effective immune response by triggering leukocyte rolling, adhesion and transendothelial migration to the site of injury (20). This results in an influx of neutrophils to the lung tissue, followed by recruitment of macrophages, which in turn produce macrophage inflammatory proteins (MIP-1a and MIP-1b), causing a disturbance in pro- and anti-inflammatory factors in the lung (21).

The release of pro-inflammatory cytokines such as TNF-α, IL-1β, IL-6 and IL-8 activates NLR Family Pyrin Domain Containing 3 (NLRP3) inflammasome protein complex (22), incites the upregulation of nuclear factor kappa B (NF-κB) signal transduction pathway. Bourbia et al. (23) revealed a high NF-κB transcription factor concentration in the tracheobronchial lavage of infants with BPD compared to those without (23). Iosef et al. (24) demonstrated that NF-κB inhibitor engendered alveolar simplification with marked reduction in pulmonary capillary density of neonatal mice, similar to that seen in BPD. Taken together, these suggest the physiological role of NK-κB in the developing lung by promoting angiogenesis and alveolarization (24). Intriguingly, whether NF-κB possesses pro- or anti-inflammatory property depends on the timing and degree of stimuli as well as the maturation status of the lung. By inhibiting NF-κB after the onset of inflammation aggravates the inflammatory response, while inhibiting NF-κB prior to injury showed otherwise (25). Similarly, NF-κB inhibition in the neonatal lung increased the inflammatory response, while the same treatment in adult mice gave a protective effect by repressing inflammation (26).

Aberrant Tissue Repair and Fibrosis

Inflammatory response is a double-edged sword, in which inflammation can be beneficial but at the same time detrimental to the host. Despite playing an active defense role against diverse insults and removing offending pathogens, exuberant inflammation can lead to paradoxical tissue destruction that trigger tissue repair, leading to fibrosis and scarring.

Developmental pathways particularly transforming growth factor-β (TGF-β) and Wnt signaling pathways that are involved in regulating various stages of lung development have been implicated in the pathogenesis of BPD. Wnt signal transduction cascade governs a myriad of developmental processes in the mammalian embryonic state, maintaining tissue homeostasis and controlling stem cells in postnatal life (27); while TGF-β is the key player in tissue healing by mediating fibroblastic activation, myofibroblastic transdifferentiation and extracellular matrix deposition.

Abnormal Pulmonary Vasculogenesis

In addition to defects in airway remodeling, dysmorphic vascular growth pattern within the distal airways were observed in various animal models of BPD, while some pulmonary arteries underwent structural remodeling with medial hypertrophy and distal arterial muscularization which contribute to pulmonary hypertension (28). Several angiogenic growth factors, such as vascular endothelial growth factor (VEGF) and nitric oxide (NO) were noticeably reduced in their expression in experimental models of BPD.

Dysfunction of Endogenous Lung-Resident Stem/Progenitor Cells

The discovery of resident undifferentiated stem/progenitor cell population residing in all organ systems including the lung, has opened up a new door to remarkable research in the field of regenerative medicine in recent years, with new knowledge on their physiological roles in lung development, pathogenesis and repair (29, 30) It is hypothesized that functional impairment or depletion of these lung-resident stem/progenitor cell populations has contributed to the disease pathogenesis in BPD (31).

Lung-resident stem/progenitor cells include cells of endothelial, mesenchymal and epithelial lineages. Endothelial progenitor cells are involved in vascular repair and regeneration by homing to the injury site to restore endothelial integrity and secure tissue perfusion. Endothelial colony-forming cells (ECFCs), a subset of endothelial progenitor cells with intrinsic self-renewal potential and capable of forming *de novo* vessels *in vivo* (32), were found to be in lower amount in the cord blood of infants with BPD (33). In contrast, those with high levels of ECFCs were protected from developing BPD, indicating its pivotal role in lung vascular maturation process. Baker et al. (34) revealed that ECFCs were highly susceptible to hyperoxia *in vitro* and lost their angiogenic potential. This observation linked the dysfunctional endogenous stem cell theory with occurrence of BPD in preterm neonates receiving postnatal oxygen therapy (34).

Lung-resident mesenchymal stromal/stem cells (L-MSCs) are stem cells found within the lung mesenchyme along with fibroblasts and extracellular matrix. They play a crucial role in the normal lung development and are recently discovered as the orchestrators in alveolarization through conduct of the tightly regulated processes of alveolar septation and angiogenesis in a developing lung (31, 35). In murine model, these L-MSCs were able to regenerate giving rise to differentiated daughter cells including airway smooth muscle cells or stalk mesenchyme

fibroblasts (36). In addition, L-MSCs directly coordinate the proliferation and maturation of lung epithelial stem/progenitor cells via epithelial-mesenchymal crosstalk.

Lung epithelial stem/progenitor cells, like other stem cells, are capable of giving rise to differentiated cell lineages. For instance, alveolar type 2 epithelial cells exhibited the ability to proliferate and differentiate into alveolar type 1 epithelial cells in hyperoxia-induced rodent models (37), nonetheless, under the instruction of L-MSCs. Antenatal and repetitive postnatal insults cause damage and injury to these progenitor cells through various mechanisms. Failure of these cells to repair themselves in the desired manner leads to simplification of alveolar structures and abnormal pulmonary angiogenesis resulting in pulmonary hypertension.

It is strongly believed that targeting inflammatory-related and angiogenic signaling pathways could reduce the severity of BPD (38). Hence, translation research aimed at modulating inflammation and angiogenesis might be a new hope for an effective remedy to treat or prevent this devastating disease of premature newborns. The potential therapeutic value of cell-based replacement therapy acting as anti-inflammatory and excellent reparative agent to ameliorate BPD is further explored in the following section.

HUMAN PLACENTA AND UMBILICAL CORD AND THEIR STEM CELL DERIVATIVES

The Normal Human Placenta and Umbilical Cord

The eutherian mammalian placentas show striking morphological and structural diversity across species (39), and are classified as epitheliochorial, endotheliochorial or hemochorial according to the number of tissue layers separating the maternal blood from that of the fetus (40). Similar to rodents, rabbits and primates, humans possess a hemochorial placental subtype, characterized by negligible cellular barrier between the maternal and fetal circulations, thus allowing effective transfer of nutrients to fetuses (41). A normal term human placenta has a flat, round to elliptical, disc-like shape that measures ∼22 and 2.5 cm in diameter and thickness, with an average weight of 500 g (42). It comprises both the fetus (chorionic plate) and maternal (basal plate) surfaces, held together by anchoring villi. These villi are organized into a series of 30 to 40 lobules or cotyledons, which are bathed directly by maternal blood filling the intervillous space, and epitomize the most important functional units for maternal-fetal exchange (43).

The outer surface of the chorionic villi constitutes the main cellular barrier between the fetal and maternal circulations and is formed by an outer layer of syncytiotrophoblasts and an inner layer of cytotrophoblasts, the latter of which diminishes as gestation progresses. The stroma of the villi is composed of sinusoidally dilated fetal capillaries embedded within loose connective tissues formed by mesenchymal cells, mesenchymal-derived macrophages (Hofbauer cells) and fibroblasts (44). The fetal membrane encompasses three distinct layers: [1] innermost amnion, [2] chorion laeve connective tissue, and [3] outermost decidua capsularis. Amnion comprises a single avascular layer of epithelial cells and connective tissue that contacts directly with the amniotic fluid and encloses the fetus. The chorion laeve is usually atrophic, composed of connective tissue containing fetal (chorio-allantoic) blood vessels, whereby decidua capsularis represents maternal modified endometrium (45). The developing embryo is connected to the chorionic plate (fetal surface) of placenta by an umbilical cord containing two arteries and one vein surrounded by gelatin-like mucoid substance, the Wharton's jelly. Wharton's jelly encompasses all loose connective tissue from the external surface of the tunica media of cord vessels to the inner margin of the amniotic epithelium (46). Wharton's jelly is important in keeping the integrity of umbilical cord. It prevents kinking of the cord and protects the umbilical blood vessels (47). The umbilical cord has an average length of 50 to 60 cm and diameter of 2 cm, with up to 40 helical turns (42).

Placenta and Umbilical Cord-Derived Stem Cells

The human placenta and umbilical cord represent a reliably high yield reservoir of stem cells compared to other sources. The observation that teratoma can arise from a term placenta suggests that it may harbor some multipotent germ cells (48). Studies have reported the placenta contains a population of multipotent stem cells that express stem cells markers such as c-KIT, octamer-binding transcription factor 4 (OCT4), sex determining region Y-box 2 (SOX2), stage-specific embryonic antigen-3 (SSEA3), SSEA4, T cell receptor alpha locus-1-60 (TRA-1-60) and TRA-1-81 (11). These cells possess mesodermal phenotype and demonstrate broad multilineage differentiation ability (12, 49, 50).

Different sources of placental stem/progenitor cells are derived from different layers of the placenta, namely amnion, chorion and decidua (51) as well as umbilical cord which constitutes the Wharton's jelly and cord blood vessels (52) (**Figure 1**). The two types of stem cells from the amniotic layer are amniotic epithelial cells (AECs), which originate from the epiblast and amniotic mesenchymal stromal/stem cells (AMSCs), derived from the hypoblast (53, 54). Deriving from the chorion sheets are chorionic MSCs from the inner chorionic mesoderm, which is similar to mesenchymal region of the amnion, and chorionic trophoblast cells from the outer layer of trophoblastic origin. The uterine component of the placenta, the decidua, also harbors decidual MSCs (55). Wharton's jelly of the umbilical cord serves as attractive source of MSCs while cord lining membrane (amniotic epithelium and subamniotic Wharton's jelly) is identified as a valuable source of epithelial stem cells and MSCs, respectively (52). The PDSCs and UCDSCs may be utilized in a wide range of clinical applications. In this review, we focused on stem cells harvested from placenta and umbilical cord that have demonstrated potential therapeutic value in BPD.

Human Amniotic Epithelial Cells (hAECs)

The human amniotic epithelial cells (hAECs) are valuable progenitor/stem cells for regenerative medicine as these cells offer great promise for therapeutic application due to their

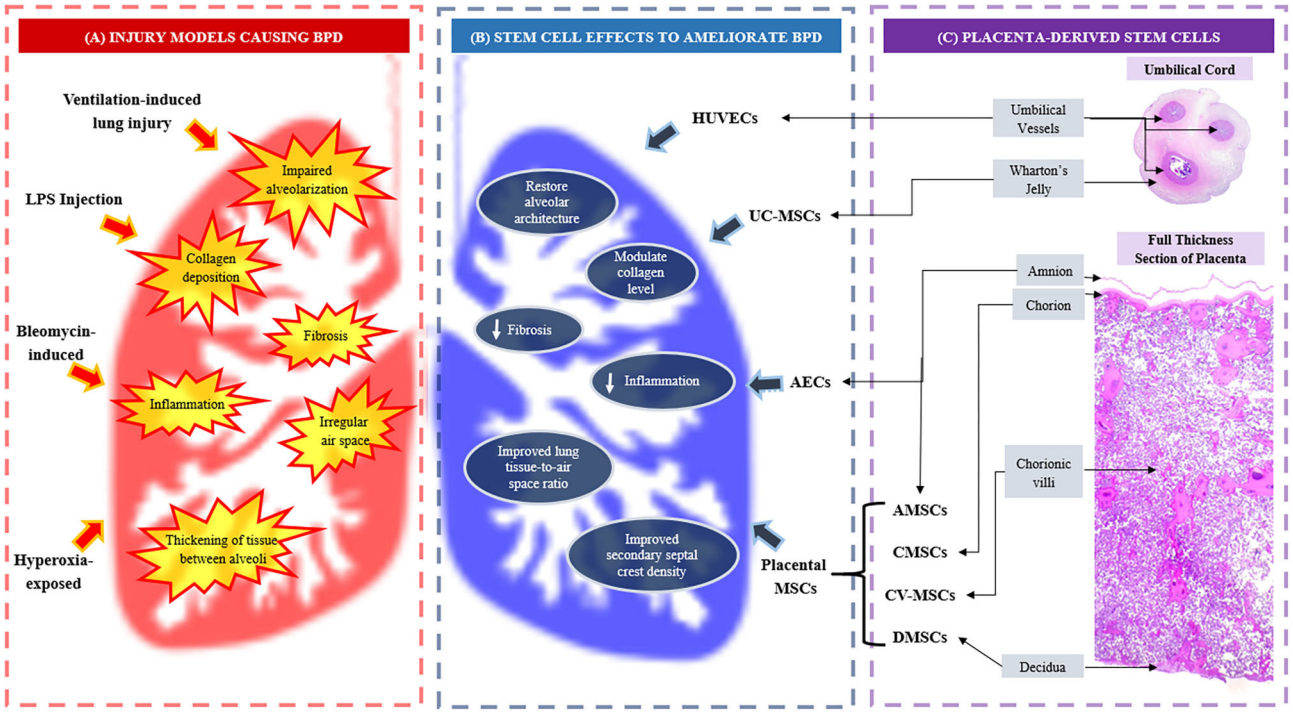

FIGURE 1 | (A) Injury models causing bronchopulmonary dysplasia (BPD) and BPD-like injuries; **(B)** Effects of placenta and umbilical cord-derived stem cells in ameliorating BPD, and **(C)** The origin of placenta and umbilical cord-derived stem cells. AECs, amniotic epithelial cells; AMSCs, amniotic mesenchymal stromal/stem cells; BPD, bronchopulmonary dysplasia; CMSCs, chorionic mesenchymal stromal/stem cells; CV-MSCs, chorionic villi mesenchymal stromal/stem cells; DMSCs, decidual mesenchymal stromal/stem cells; LPS, lipopolysaccharide; UC-MSCs, umbilical cord mesenchymal stromal/stem cells.

ease of isolation, multilineage potential, immune privilege, anti-inflammatory properties, do not have telomerase reverse transcriptase, show a stable karyotype, do not form tumors when injected and have a low risk of allogeneic rejection (2, 53, 56).

Cell surface antigens and other specific markers are often used to define the "stemness" of a cell type. Investigations demonstrated that hAECs displayed a similar set of stem cell marker profile to that of ESCs. hAECs expressed most of the ESCs transcription factors and cell surface markers in the early second trimester, namely OCT4, NANOG, SOX2, SOX3, SSEA3, SSEA4, TRA-1-60, TRA-1-81, and GCTM2 (53, 56, 57). Although most of these cells with stem cell markers are lost over time, some of them are still retained in the term placental amniotic epithelium (58). hAECs are pluripotent and have unlimited capacity for self-renewal as well as the ability to differentiate into the derivatives of the three primary germ layers; ectoderm, mesoderm and endoderm (53, 56, 58, 59).

Studies showed that hAECs have low expression of the major histocompatibility complex (MHC) class I molecules [human leukocyte antigen (HLA)-A, HLA-B, HLA-C and β2 microglobulin] and MHC class II molecules (HLA-DR) (58, 60, 61). Since the amnion does not express MHC class II antigens, hAECs can elude the immune system (51). The other suggested mechanism of induction of tolerance of hAECs is related to the expression of unique HLA class 1b molecules (62). These HLA class 1b molecules regulate immune response under autoimmune and transplantation conditions, while HLA class I and II molecules contribute to the allogeneic immune rejection (58).

hAECs express a number of distinct Toll-like receptors (TLRs) and induce the production of inflammatory cytokines as a part of their immunomodulatory responses. TLR4 expression induces apoptosis, and play a role in the pathogenesis of premature rupture of membrane. Study showed TLR4 expression in hAECs was accompanied by reduced BCL-2 expression and increased Bax protein (63). TLR5 and TLR6 recognize a variety of pathogens. Both TLR2 and TLR6 are expressed in respond to Mycoplasma-associated protein, while TLR5 ligand is expressed in reaction with flagellated Gram-positive and Gram-negative bacteria. Activation of TLR5 and TLR6 induced proinflammatory response. Together, these indicate hAECs possess self-regulatory mechanisms in immunomodulatory responses (58).

Placental Mesenchymal Stromal/Stem Cells (P-MSCs)

Human MSCs were first described by Friedenstein in the bone marrow in 1968 (64). Although bone marrow remains the most common source of MSCs, these cells can also be isolated from various human tissues, such as the lung (30), adipose tissue (65), umbilical cord (66), skeletal muscle (67), dental pulp (68), corneal stroma (69), synovium (70), cardiac tissue (71), spleen, liver, kidney (72), bone marrow (73), cord

blood (74), amniotic fluid (75), and placenta (76, 77). The placental mesenchymal stromal/stem cells (P-MSCs) express stromal markers, and are negative for the hematopoietic markers (78). Additionally, some studies reported P-MSCs expressed pluripotency markers (54, 79).

P-MSCs were first described in 2004 as plastic-adherent cells that share a similar immunophenotype with that of bone marrow MSCs and have multilineage differentiation potential (80). P-MSCs are of mesodermal origin. Depending on the layer they originate from, their stem cell derivatives include AMSCs, chorionic MSCs, chorionic villi MSCs and decidual MSCs (78, 81, 82). AMSCs (11, 83), chorionic MSCs (82, 84) and chorionic villi MSCs (78, 85) have been described as having a longer life span than the decidual MSCs population obtained from the maternal-derived decidua (82, 84).

P-MSCs have a much-limited differentiation repertoire compared to the pluripotent ESCs. These cells display the ability to differentiate *in vitro* into different mesodermal cell lineages, including adipocytes, chondrocytes, and osteoblasts (86). Another study suggested that P-MSCs may also be capable of neural differentiation (87). P-MSCs are widely studied in regenerative medicine. Other than their advantages in terms of the ease in isolation, high plasticity, low immunogenicity and tumorigenesis (51), P-MSCs display the ability to migrate to inflammatory microenvironments and tumors, involvement in angiogenesis and wound healing as well as tissue repair activity through paracrine actions, which are important therapeutic advantages of P-MSCs (88–90).

Umbilical Cord-Derived Stem Cells

Wharton's jelly is a popular source of umbilical cord mesenchymal stromal/stem cells (UC-MSCs) (91). Stem cells isolated from the Wharton's jelly show mesenchymal fibroblast-like morphology, with self-renewal ability and capable to differentiate into neuronal, osteo-chondral, adipocytic and muscular derivatives (92). Apart from having characteristics of MSCs as defined by the International Society for Cellular Therapy (93), UC-MSCs also exhibit properties attributed to ESCs, expressing markers such as TRA-1-60, TRA-1-81, SSEA1, SSEA-4 and alkaline phosphatase. In addition, ESC pluripotent markers that include OCT4, Sox-2, and NANOG are also detected at a lower level (94). Although UC-MSCs are not as pluripotent as ESCs, these cells are widely multipotent and do not develop into teratomas in immunocompromised mice (92).

Recently, Davies et al. (2017) proposed an anatomically/histologically-based nomenclature of the umbilical cord structures for the purpose of standardization and ease of comparison across cells harvested from different regions/zones of Wharton's jelly (46). Wharton's jelly is further divided into three distinct anatomical/histological zones: [1] subamnion, [2] intervascular and [3] perivascular Wharton's jelly. Interestingly, the stromal cells of Wharton's jelly are not uniformly distributed, but in a gradually increasing manner from the cord lining up to the proximity of umbilical vessels. Likewise, the tendency of myofibroblast differentiation of the stroma cells is the highest near the umbilical vessels with the least differentiated ones predominantly located in the subamniotic zone (95).

Accumulating evidence suggests that umbilical cord contains a unique cell family with different degree of stemness and phenotypic profiles residing in various parts of the umbilical cord (96). For instance, other than MSC markers (CD44, CD90 and CD105), stem cells harvested from perivascular Wharton's jelly demonstrated high expression of endothelial markers CD146 like that of CD146+ pericyte, a more differentiated MSC progenitor cells. They are however absent for CD73, a MSC marker. On the contrary, the intervascular Wharton's jelly yields stem cells positive for MSC markers but lacking that of endothelial markers (CD144, CD146 and CD34). The pericyte-like properties of the MSCs isolated from perivascular Wharton's jelly provide additional advantage in its rapid response to tissue damage upon engraftment and induce angiogenesis (97).

Comparison Between Placenta/Umbilical Cord-Derived Mesenchymal Stromal/Stem Cells and Bone Marrow-Derived Mesenchymal Stromal/Stem Cells

In vitro Comparison

Stem cells harvested from bone marrow are considered as the gold standard and the most characterized source of adult MSCs for various clinical applications. Acquisition of MSCs from bone marrow; however, requires invasive procedure with a risk of complications. Moreover, the cell yield from bone marrow declines with advancing donor age. When compared to young donor (<40 years old), older donors' MSCs revealed smaller-sized colonies and lower integrated density (98).

The P-MSCs and UC-MSCs are excellent alternatives to BM-MSCs. The former is shown to share similar morphology, cell surface markers and some pluripotency-related markers with BM-MSCs. Interestingly, BD-MSCs have additional advantages than BM-MSCs. For instance, a higher frequency of colony forming unit-fibroblasts was reported in UC nucleated cells (1:1609) compared to BM nucleated cells (1:35700) (99). Lower immunogenicity was seen in UC-MSCs over BM-MSCs with lower levels of lymphocyte proliferation following allogeneic lymphocyte stimulation assay. Likewise, UC-MSCs have a higher overall immunomodulatory effect with increased expression of potent immunosuppressive factors such as CD200, LIF, and TGF-β2 (99). *In vitro* study showed UC-MSCs underwent slower senescence, demonstrated a higher cell proliferation rate and greater anti-inflammatory effects than BM-MSCs (100). The challenges remain in understanding the heterogeneity of the isolated populations, and to standardize the diversity in isolation protocols and culture conditions (101).

P-MSCs were observed to consistently faster population doubling time and longer-term expandability (up to 15 passages) under identical culture condition compared with BM-MSCs (102). P-MSCs are more homogeneous as compared to BM-MSCs in culture (103). This might be due to the fact that P-MSCs are younger cells with less exposure to harmful substances such as reactive oxygen species, chemical and biological agents, and physical stressors (104), thus increasing

the efficacy and safety of the therapeutic applications of P-MSCs in regenerative medicine. Homing of P-MSCs to damaged tissue may be further enhanced with the demonstration of higher expression of VLA-4 (very late antigen-4) adhesion molecule on P-MSCs compared to BM-MSCs to allow adherence and migration through the endothelium (105). In addition, the advantage of P-MSCs over BM-MSCs and adipose tissue-derived stem cells includes the ability to be obtained using a non-invasive method and in larger quantity (106). Di Bernardo et al. (107) reported that P-MSCs played a pivotal role as potent stimulator of perinatal lung morphogenesis in *ex-vivo* fetal lung culture model compared with BM-MSCs (107).

In vivo Comparison

The therapeutic efficacy of BM-MSCs has been investigated in experimental models of lung injury in adult and newborn animals. Tian et al. (108) reported a significant improvement in radial alveolar count and reduction in lung inflammatory cytokines in hyperoxic mice model after intravenous BM-MSCs injection (108). Their findings were confirmed by other studies on hyperoxic rat models (109–111). Intra-tracheal delivery of BM-MSCs in hyperoxic neonatal rat lungs shown to confer protection with increased pulmonary vascular angiogenesis, reduced pulmonary hypertension and normalized alveolar structures (112). Conversely, intranasal administration of BM-MSCs in newborn mice lung injury model, failed to achieve epithelial reconstruction and transdifferentiation into respiratory epithelial cells (113). To date, the efficacy of BM-MSCs in larger animal BPD models such as preterm lambs, pigs and baboons have not been explored (114).

Although there have been extensive pre-clinical studies of BPD animal models using stem cells derived from bone marrow, placenta and umbilical cord, to the best of our knowledge, head-to-head comparative study on the efficacy of both the BM-MSCs and P-MSCs/UC-MSCs in BPD animal models is still lacking. This research gap needs to be further addressed.

MECHANISMS OF FUNCTION OF PLACENTA AND UMBILICAL CORD-DERIVED STEM CELLS

Cell-Contact-Mediated Effects

Upon transplantation, MSCs exert their immunomodulatory functions at damaged sites through a synergy of direct cell-cell contact. The direct cell-to-cell contact between PD-1 inhibitory molecule on T cells and its ligands PD-L1 on MSCs, inhibits CD3+ T cell proliferation, induces early apoptosis and suppressed effector T cell (e.g., IL-17 producing T cells, Th17) responses (115). Similarly, TNF receptor superfamily member 6 (Fas)-FasL interactions propagate the death signal and induce T cell apoptosis (116). In addition, expression of CD106 (VCAM-1) on P-MSCs (117) and CD54 (ICAM-1) on UC-MSCs (118) is crucial in mediating immunomodulatory functions on T cells.

Paracrine and Extracellular Vesicles-Mediated Effects

Despite the relatively poor *in vivo* engraftment rate (0–20%), pleiotropic lung protection following transplantation is believed to be attributed to paracrine factors such as lipid based mediators, growth factors and signaling peptides (119). Among the secreted bioactive substances include lipoxin A_4 (120), epithelial growth factors (e.g., keratinocyte growth factor, pro-angiogenic factors) (121) and TNF-α-stimulated gene/protein 6 (122), which have potent anti-inflammatory properties. With the presence of these molecules, administered stem cells are able to migrate to injured tissue and promote anti-inflammatory environment which support cell proliferation and inhibit apoptosis, thus enhance tissue regeneration, remodeling and survival.

MSCs influence both tissue resident stem cells and macrophages through paracrine effects like extracellular vesicles (EVs) other than cytokines and secreted soluble factors, which results in more efficient reparative process by tissue resident stem cells (123). EVs (such as exosomes and microvesicles) are nanometer-scale, cell membrane-enclosed packages of biomolecules that are released by cells into the surrounding environment to mediate signal transmission and cell-to-cell communication. These vesicular cargo biomolecules carry biological active compounds including amino acids, bioactive lipids and nuclei acids (124). These cell-free products may serve as safer alternatives to cell therapies. For large scale production, adipose tissue-derived MSCs and UC-MSCs exosomes will be easier to obtain compare to BM-MSCs (123). Compared to BM-MSCs, UC-MSCs have a higher production rate of EVs (125).

Kourembanas team was the first to discover pleiotropic protective effects of EVs-based therapy in experimental BPD models. In their study, they reported that intravenous administration of EVs derived from both BM-MSCs and UC-MSCs in hypoxic mice model were able to inhibit influx of alveolar macrophages and pro-inflammatory cytokines, besides ameliorate lung vascular remodeling and pulmonary hypertension. Moreover, the uptakes by macrophages cause a shift in balance to anti-inflammatory state (126). Following that, the same group of researchers reported that the lung functions of the EVs-treated mice were significantly improved with decreased fibrosis, arteriole muscularization and pulmonary hypertension. They concluded that restoration of lung function occurred partly related to macrophage immunomodulation induced by administration of EVs (127). Several subsequent studies have shown that early administration of human MSC-derived EVs improved histological and functional outcomes in experimental BPD (122, 128).

Similar therapeutic effects were observed in hyperoxia-induced neonatal lung injury in mice treated both with early and late EVs interventions (129). EVs might even potentially reverse the cardiorespiratory complications in children with developed BPD (129). In addition, Tan et al. (130) reported that the release of EVs from hAECs administered intranasally exerted similar beneficial effects to MSCs with significant reduction in lung inflammation,

improvement in tissue-to-airspace ratio and reduction in fibrosis in bleomycin-challenged aged mice (130). Willis et al. (129) and Bonadies et al. (131) suggested that MSCs and EVs are two most revolutionary treatments for BPD, not only effective in the prevention of BPD but also may potentially reverse the complications in children diagnosed with BPD (129, 131).

THERAPEUTIC POTENTIAL OF PLACENTA AND UMBILICAL CORD-DERIVED STEM CELLS IN BRONCHOPULMONARY DYSPLASIA

Experimental Therapeutics in Animal Models

Animal models play a crucial role in advancing our fundamental knowledge on the pathogenesis of this complex disease and to direct our future clinical trials into therapeutics. Mice and rats are among the widely used models since the newborn rodent pups are delivered at term in the saccular stage of lung development, equivalent to that of a preterm infant at risk of BPD. Other animal models for BPD that have been established are pigs (132), rabbits (133), lambs (134), and baboons (135). Arguably, larger animal models that require the need for mechanical ventilation and other life-support care after premature delivery are more clinically relevant and closely resemble human biology than rodents. Nonetheless, the use of these larger animal models increases the costs of experimentation and more labor intense, which might have precluded their use in preclinical studies (136). Methods of inducing BPD in animal models vary across studies and include the use of high concentration of oxygen (hyperoxia), mechanical ventilation, bleomycin, intrauterine inflammation via lipopolysaccharide (LPS) injection, postnatal continuous hypoxia or intrauterine prenatal hypoxia (137). Hyperoxia-induced lung injury is among the most used method.

Nonetheless, these animal models are not perfect representation of BPD in human. Induced animal models demonstrating alveolar simplification and vascular remodeling, may also reveal additional widespread fibrosis and inflammation (138). Recently, Zhang et al. (139) successfully created an innovative BPD model using premature hyperoxia-exposed rodents which showed characteristic histological features of BPD in humans (139), suggesting a new alternative model for future research. **Table 1** summarizes the effects of PDSCs and UCDSCs in BPD therapeutic experimental animal models while **Figure 1** illustrates how PDSCs/UCDSCs remedy the various BPD-like injuries inflicted in the models.

Human Amniotic Epithelial Cells (hAECs)

hAECs have been shown to reduce acute inflammation, accelerate repair and improve lung function in both immunodeficient and immunocompetent-mouse models with bleomycin-induced injury (140–142). Administration of hAECs to BPD models resulted in decreased gene expression of pro-inflammatory cytokines (TNF-α, TGF-β, IFN-γ, and IL-6), and decreased inflammatory cell infiltration (141). hAECs reduced scarring in lung injury by decreasing the collagen content (140). These cells were capable of mitigating lung inflammation and alveolar simplification in a murine model with BPD-like lung injury, by improving lung tissue-to-air space ratio and secondary septal crest density (143).

In larger animal like fetal sheep models, exposed to intraamniotic LPS injection, hAECs reduced the need of ventilation and reduced inflammatory changes (144, 145). In addition, it restored a normal lung tissue-to-air space ratio, reduced pro-inflammatory cytokines (145), normalized secondary septal crests, reduced collagen and elastin deposition and fibrosis (144). Deus et al. (152) described hAECs having beneficial effects by the production and secretion of various bioactive factors involved in anti-inflammation, immunomodulation, wound healing, angiogenesis, anti-fibrosis and anti-bacterial (152).

Studies showed host macrophages and T regulatory cells were the main contributors toward the reparative effects of hAECs (120, 153–155). Of note, the response to these cells was dependent on the timing of administration and the effects were best observed when they were administered at an early stage of injury (142, 143). Umezawa et al. (156) showed that placental amnion-derived cells can be reprogrammed to induced pluripotent stem cells. These cells maintained normal karyotype and chromosomal stability over a long period of passages. It can be easily isolated and expanded for industrial production of large quantities (156).

Placental Mesenchymal Stromal/Stem Cells (Placental MSCs)

Although not as widely utilized, P-MSCs attenuated perinatal inflammation- and hyperoxia-induced defective alveolarization and angiogenesis as well as reduced lung fibrosis. In LPS-injected rats, human MSCs derived from placentas improved vascular density, reduced TNF-α and IL-6 levels and collagen density, by exerting paracrine effects via increased VEGF and decreased connective tissue growth factor (CTGF) expression (146).

Cargnoni et al. (147) demonstrated that P-MSCs derived from fetal membrane showed stem cell phenotype, high plasticity, and displayed low immunogenicity both *in vitro* and *in vivo*. These MSCs also displayed the ability to engraft in the lung. A 1:1 mixture of hAECs and human AMSCs/human chorionic MSCs administered intratracheally into bleomycin-treated, immunocompetent C57/Bl6 mice exhibited a reduction in neutrophil infiltration and fibrosis, indicating the presence of the anti-fibrotic effect of PDSCs (147).

Umbilical Cord Mesenchymal Stromal/Stem Cells (UC-MSCs)

Umbilical cord mesenchymal stromal/stem cells (UC-MSCs) were injected into bleomycin-induced lung injury models and demonstrated reduced inflammation and fibrosis, with the injected cells found after 2 weeks and only in areas of inflammation and fibrosis (148). The treatment inhibited the expression of TGF-β, IFN-γ and proinflammatory cytokines macrophage migration inhibitory factor (MIF) and TNF-α. Collagen level was decreased, caused by up-regulation of MMP-2

TABLE 1 | Effects of placenta and umbilical cord-derived stem cells in BPD models.

Cell types	Effects	Evidence	References
hAECs	Anti-inflammatory	↓ Pro-inflammatory cytokines - TNF-α, TGF-β, IFN-γ, PDGF-α, PDGF-β, IL-1β, IL-10, IL-6 ↓ infiltration of inflammatory cells ↑ anti-inflammatory substances	(140–145)
	Anti-fibrosis	↓ collagen density	
	Lung function improvement	↓ peripheral pulmonary arterial remodeling ↑ density of pulmonary capillary bed Improved lung tissue-to-air space ratio Improved secondary septal crest density Restoration of alveolar architecture Preserved spatial pattern of elastin deposition Promoted pulmonary angiogenesis	
P-MSCs	Anti-inflammatory	↓ pro-inflammatory cytokines - IL-6, TNF-α	(146, 147)
	Anti-fibrosis	↑ VEGF ↓ CTGF ↓ collagen density ↓ infiltrating macrophages ↓ neutrophil infiltration	
	Lung function improvement	Restored vascular density	
hUC-MSCs	Anti-inflammatory	↓ Pro-inflammatory cytokines - TGF-β, IFN-γ, macrophage MIF and TNF-α	(148–151)
	Anti-fibrosis & ameliorate elastin remodeling	↓ Collagen density ↓ MMPs ↓ Elastin expression ↑ VEGF ↑ MMP-2 ↑ Vessel density ↑ Angiogenesis	
	Lung function improvement & accelerated repair	↓ BPD injury-related proteins - CX3CL1, TNF-α, TIM-1, hepassocin, neprilysin,osteoprotegerin, MMP-2, LIF ↑ alveolar septal widening ↑ septal crest density Restored lung alveolarization, vascularization and pulmonary vascular remodeling.	

BPD, bronchopulmonary dysplasia; CTGF, connective tissue growth factor; CX3CL1, C-X3-C motif chemokine ligand 1; hAECs, human amniotic epithelial cells; hUC-MSCs, human umbilical cord mesenchymal stromal/stem cells; IFN-γ, interferon-γ; IL, interleukin; LIF, leukocyte inhibitory factor; MIF, migratory inhibitory factor; MMPs, matrix metalloproteinases; P-MSCs, placental mesenchymal stromal/stem cells; PDGF, platelet derived growth factors; SMA, smooth muscle actin; TGF-β, transforming growth factor-β; TIM-1, T cell immunoglobulin and mucin domain; TNF-α, tumor necrosis factor-α; VEGF, vascular endothelial growth factor.

and reduced endogenous inhibitors, tissue inhibitors of MMPs. These results suggest that UC-MSCs harbor anti inflammation and antifibrotic properties and may augment lung repair (148).

In hyperoxia-exposed newborn mice, intraperitoneal administration of UC-MSCs at high dose (1 x 10^6 cells) restored lung structure and function (149). Characteristic arrest in alveolar growth with air space enlargement and loss of lung capillaries induced by hyperoxia were partially prevented and lung function and structure were somewhat preserved, without tumor formation following computed tomography scan assessment. While high dosage of intraperitoneal administration of UC-MSCs (1×10^6 cells) was associated with alveolar septal widening probably through the modification of the interstitial matrix, intranasal administration of UC-MSCs or lower dose at 0.1×10^6 cells intraperitoneal administration had no significant effects on lung function or alveolar remodeling. It is suggested that UC-MSCs may act via a paracrine effect. Purified exosomes from various sources of MSCs including Wharton's jelly-derived MSCs were also reported to restore lung architecture and improve lung development and function in hyperoxia-induced BPD animal models (129).

Moreira et al. (150) reported that the first intranasal administration of umbilical cord Wharton's jelly-derived MSC (UC-MSCs) to a hyperoxia-induced rat BPD model resulted in restoration of lung alveolarization, vascularization and pulmonary vascular remodeling. This was due to the combined effect on angiogenesis, immunomodulation, wound healing and cell survival of hUC-MSCs as indicated by the protein microarray results (150). The lungs of hUC-MSCs treated mice showed significantly lower levels of injury-related proteins associated

with immunomodulation (C-X3-C motif chemokine ligand 1 (CX3CL1), TNF-α, T cell immunoglobulin and mucin domain (TIM-1), hepassocin, neprilysin), cell survival (osteoprotegerin), and wound healing [MMP-2, leukocyte inhibitory factor (LIF)]. Moreira et al. (150) suggested the intranasal route of delivery as a feasible, non-invasive and effective method that may bear clinical applicability (150).

Elastin expressions stimulated by 90% O_2 in human lung fibroblasts (HLF) of a hyperoxia-induced rat model of BPD were reduced by intratracheal-delivered UC-MSCs. HLF trans-differentiation into myofibroblasts were also inhibited, indicating that UC-MSCs could inhibit lung elastase activity. These findings showed that UC-MSCs could ameliorate aberrant elastin expression and deposition in the lung of hyperoxia-induced BPD models, possibly through the suppression of TGF-β (151).

Clinical Translation: From Bench to Bedside

The results following extensive *in vitro* and *in vivo* experiments on animal BPD models using UC-MSCs and hAECs, are promising. This has created great enthusiasm in the scientific community with a surge in clinical trials, offering new hopes of cure for a myriad of diseases including BPD. Notably, hUC-MSCs are among the MSCs that had been extensively investigated over the past decades on various small and larger animal models.

There are currently 11 registered clinical trials of PDSCs and UCDSCs used for BPD listed in the United States National Institute of Health database at https://clinicaltrials.gov, while two are listed in the Australian New Zealand Clinical Trials Registry at https://anzctr.org.au (last accessed on 15 September 2020). At present, clinical trials are also being conducted at various countries including Korea, United States, Spain and China.

These clinical trials have collectively embraced umbilical cord as the main source of MSCs with only a few using hAECs. Most of them are phase 1 clinical trials, focusing on the safety and efficacy of PDSCs and UCDSCs in the treatment and prevention of BPD. Intratracheal and intravenous routes are the two preferred routes of administration, with a wide inter-study variation in the selection of dosage that ranges from 1 million cells/kg body weight up to 30 million cells/kg body weight. A summary of the ongoing and completed clinical trials (excluding 5 follow up studies—NCT03873506, NCT01632475, NCT04003857, NCT01897987, NCT02023788) is in **Table 2**.

hAECs were being explored for their safety and feasibility in treating BPD. Lim et al. (157) conducted the first in-human phase I clinical trial of allogeneic hAECs in 6 preterm babies with BPD via the intravenous route. They reported no immediate adverse events except one of the babies developed transient cardiorespiratory compromise due to pulmonary embolic event. In addition, serum C-reactive protein levels were slightly reduced or remained unchanged 48 h following hAECs administration. One of the six babies died a month after cell administration due to multiorgan failure. The rest of the babies were alive at the time of discharge (median, 174 days of life) (157) and after 2 years of follow up (158) (**Table 3**).

Translational Challenges in Cell-Based Therapy

Although cell-based intervention is hyped as the next therapeutic pillar in medicine, there are still many challenges to be overcome prior to its successful translation into clinical use. Comparing to small molecule and biologic drugs, cell-based therapies are considerably complex and are generally more challenging to control their biological behavior *in vivo*, which has posed a great obstacle to the scientific community toward establishing these cell sources as promising and rewarding therapeutic use in the clinics. In addition, other cell-based therapies such as ECFC and human umbilical vein endothelial cells (HUVEC) that had been comprehensively investigated in adult diseases (159, 160) may be explored for their potential benefits in treating BPD.

Safety remains a primary issue in cell transplantation. The complexity and lack of full understanding on the mode of action of PDSCs and UCDSCs *in vivo* remains a major issue (161). As compared with other small molecule or biologic drugs, these cells are living entities that are capable of metabolism, growth and reaction to environmental stimuli, affecting their therapeutic abilities.

Heterogeneity of PDSCs and UCDSCs may become a barrier that hinders treatment success. Notably, stem cells derived from different anatomic locations of the human placenta, although revealed to share common morphology and immunophenotypic pattern, differ significantly with regards to the numbers of cells in the host tissue, global gene expression patterns and their trilineage differentiation potential *ex vivo*. Careful biomolecular characterization of PDSCs and UCDSCs through genomic, epigenetic, secretomic and proteomic profiling can further refine their overlapping identities and hence reduce heterogeneity.

Standardization in isolation methods is hard to be achieved as different protocols exist for PDSCs/UCDSCs isolation from different anatomic locations. Isolation of cells from human amniotic membrane particularly could be problematic and at risk of cross-contamination due to both AECs and AM-MSCs located close to one another (54). Isolation of hAECs from amniotic fluid may inadvertently harvest trophoblast cells as well (162). Furthermore, the number of cells isolated is often not adequate for clinical use, requiring cell expansion by culture method to achieve a minimum of 1.5-6 $\times$ 10^7 cells per single dose (163). Large-scale production of MSCs is currently made possible with robust controlled bioreactor systems which enable rigorous process monitoring to ensure cell cultivation under optimum controlled conditions (164).

Lastly, it is imperative to note that the risk in transmitting of infections such as viruses, prions and mycoplasma from donors to the immunocompromised premature host although minimal, but extant (165). Stringent safety assurance system with appropriate donor selection and screening as well as employing sensitive screening tests for infectious diseases is mandatory.

CONCLUSION AND FUTURE PROSPECTS

Currently, there is no single effective therapy for BPD and as such, stem cells have emerged as a potential source of effective

TABLE 2 | Ongoing and completed clinical trials on bronchopulmonary dysplasia with placenta and umbilical cord-derived stem cell.

Identification code	Status	Cells	Phase	Study design			Age at treatment	Target	Country
				Interventional model	Dosage	Route of administration			
NCT04062136	Recruiting	hUC-MSCs	I	Single group	1×10^6/kg (×2)	Intravenous	1–6 months	10	Vietnam
NCT03558334	Recruiting	hUC-MSCs	I	Parallel assignment	1×10^6/kg, 5×10^6/kg	Intravenous	Child, adult, older adult	12	China
NCT03645525	Recruiting	hUC-MSCs	I-II	Parallel assignment	2×10^7/kg	Intratracheal	Up to 3 weeks	180	China
NCT03601416	Not yet Recruiting	hUC-MSCs	II	Parallel assignment	1×10^6/kg, 5×10^6/kg	Intravenous	Up to 1 year	57	China
NCT03631420	Recruiting	hUC-MSCs	I	Single group	3×10^6/kg, 1×10^7/kg, 3×10^7/kg	NA	36–48 weeks	9	Taiwan
NCT04255147	Not yet Recruiting	hUC-MSCs	I	Single group	1×10^6/kg, 3×10^6/kg, 1×10^7/kg	Intravenous	7–21 days	9	Canada
NCT03774537	Recruiting	hUC-MSCs	I-II	Parallel assignment	1×10^6/kg, 5 $\times 10^6$/kg	Intravenous	3–14 days	20	China
NCT01207869	Unknown	hUC-MSCs	I	Parallel assignment	3×10^6/kg	Intratracheal	Up to 6 months	10	Taiwan
NCT02443961	Recruiting	hUC-MSCs	I	Single group	5×10^6/kg (×3)	Intravenous	1 month to 28 weeks	10	Spain
ACTRN12618000920291	Recruiting	hAECs	I	Other	2×10^6/kg to 3×10^7/kg	Intravenous	14–16 days	24	Australia
**ACTRN12614000174684	Completed	hAECs	I	Single group	1×10^6/kg	Intravenous	More than 36 weeks	6	Australia

*HAECs, human amniotic epithelial cells; hUC-MSCs, human umbilical cord mesenchymal stromal/stem cells; hUCB-MSCs, human umbilical cord blood mesenchymal stromal/stem cells; NA, not available; **Published clinical trials.*

TABLE 3 | Published clinical trials on bronchopulmonary dysplasia with placenta derived stem cells.

Stem cells	Phase	Gestational age (weeks)	Mean age at treatment (days)	Mean birth weight (g)	Sample size, n	Study designs		Results	References
						Dosage	Route		
Allogeneic hAECs (ACTRN 12614000174684)	I	26	89 days	795	6	$1x10^6$/kg	Intravenous	5 alive, 1 died (due to multiorgan failure) 1 transient cardiorespiratory event No other adverse effect	(157)
								During the 2 years follow up: 2 resolved pulmonary hypertension No long-term transplant-related adverse effect	(158)

HAECs, human amnion epithelial cells.

therapy. Stem cell insufficiency in preterm infants may be one of the underlying pathological mechanisms for disordered development of alveolar and vascular structures. The placenta and umbilical cord are readily available source of stem cells, although the properties of these stem cells may differ depending on the regions they are isolated from.

To date, there are still very limited studies on the direct comparison between the value of MSCs from different sources, especially between BM-MSCs and P-MSCs/UC-MSCs. It would also be valuable to compare stem cells-derived EVs from various sources such as placenta, bone marrow, and adipose tissue. Accumulating evidence has demonstrated the beneficial effects of these placenta/umbilical cord-derived stem cells on both *in vitro* and *in vivo* experimental animal BPD models. Pre-clinical studies showed they are able to treat established BPD and can prevent BPD from developing in preterm neonates exposed to lung insults. The effects include reduced in the levels of inflammatory mediators such as IL-6 and TNF-α, improved

pulmonary angiogenesis, ameliorated lung fibrosis and restored alveolar structures in BPD experimental models. Although paracrine activities seemed to be the most likely mechanism involved, the exact functions of how these stem cells work *in vivo* remain unclear, leaving a knowledge gap in this area.

At the present moment, hAECs and hUC-MSCs are two stem-cell based therapies that are leading the way as potential treatment of BPD. In our opinion and backed by increasing evidence that the "game-changer" lies in the treatment with cell-free products via EVs which appear to yield similar benefits as stem cells. EVs are considered a novel discovery in stem cell biology. Although there are still many uncertainties and questions with regards to this product and that safety of this product has yet to be tested in any phase 1 clinical trial, EVs being cell-free do not have the inherent concerns of uncontrolled transformation. Future studies should investigate the properties of EVs isolated from different regions of placenta and umbilical cord. Lastly, standardized extraction methods and harvesting techniques are necessary to ensure quality and reproducibility of this stem cell product before it is released for use in human translational applications.

AUTHOR CONTRIBUTIONS

WKC, YPW, and GCT: writing—original draft preparation. SS, NHAA, and NCK: writing—review. GCT, TYK, and FCC: writing—critical review and editing. YPW, FCC, and GCT: funding acquisition. All authors have read and agreed to the published version of the manuscript.

FUNDING

This work was funded by the Ministry of Higher Education of Malaysia through the Fundamental Research Grant Scheme (FRGS/1/2016/SKK08/UKM/03/5).

REFERENCES

1. Orlic D, Kajstura J, Chimenti S, Jakoniuk I, Anderson SM, Li B, et al. Bone marrow cells regenerate infarcted myocardium. *Nature.* (2001) 410:701–5. doi: 10.1038/35070587
2. Antoniadou E, David AL. Placental stem cells. *Best Pract Res Clin Obstet Gynaecol.* (2016) 31:13–29. doi: 10.1016/j.bpobgyn.2015.08.014
3. Alison MR. Stem cell plasticity. In: Schwab M, editor. *Encyclopedia of Cancer*. Berlin: Springer Berlin Heidelberg (2011). p. 3511–3513. doi: 10.1007/978-3-642-16483-5_5492
4. Singh VK, Saini A, Kalsan M, Kumar N, Chandra R. Describing the stem cell potency: The various methods of functional assessment and *in silico* diagnostics. *Front Cell Dev Biol.* (2016) 4:134. doi: 10.3389/fcell.2016.00134
5. Zakrzewski W, Dobrzyński M, Szymonowicz M, Rybak Z. Stem cells: past, present, and future. *Stem Cell Res Ther.* (2019) 10:68. doi: 10.1186/s13287-019-1165-5
6. Biehl JK, Russell B. Introduction to stem cell therapy. *J Cardiovasc Nurs.* (2009) 24:98–105. doi: 10.1097/JCN.0b013e318197a6a5
7. Parolini O, Soncini M. Human placenta: a source of progenitor/stem cells? *J Reproduktionsmed Endokrinol.* (2006) 3:117–26.
8. Lo B, Parham L. Ethical issues in stem cell research. *Endocr Rev.* (2009) 30:204–13. doi: 10.1210/er.2008-0031
9. Volarevic V, Markovic BS, Gazdic M, Volarevic A, Jovicic N, Arsenijevic N, et al. Ethical and safety issues of stem cell-based therapy. *Int J Med Sci.* (2018) 15:36–45. doi: 10.7150/ijms.21666
10. Thomson JA, Itskovitz-Eldor J, Shapiro SS, Waknitz MA, Swiergiel JJ, Marshall VS, et al. Embryonic stem cell lines derived from human blastocysts. *Science.* (1998) 282:1145–7. doi: 10.1126/science.282.5391.1145
11. Parolini O, Alviano F, Bagnara GP, Bilic G, Bühring HJ, Evangelista M, et al. Concise review: isolation and characterization of cells from human term placenta: outcome of the first international Workshop on Placenta Derived Stem Cells. *Stem Cells.* (2008) 26:300–11. doi: 10.1634/stemcells.2007-0594
12. Pipino C, Shangaris P, Resca E, Zia S, Deprest J, Sebire NJ, et al. Placenta as a reservoir of stem cells: an underutilized resource? *Brit Med Bull.* (2013) 105:43–68. doi: 10.1093/bmb/lds033
13. Oliveira MS, Barreto-Filho JB. Placental-derived stem cells: Culture, differentiation and challenges. *World J Stem Cells.* (2015) 7:769–75. doi: 10.4252/wjsc.v7.i4.769
14. Pogozhykh O, Prokopyuk V, Figueiredo C, Pogozhykh D. Placenta and placental derivatives in regenerative therapies: Experimental studies, history, and prospects. *Stem Cells Int.* (2018) 2018:4837930. doi: 10.1155/2018/4837930
15. Thébaud B, Goss KN, Laughon M, Whitsett JA, Abman SH, Steinhorn RH, et al. Bronchopulmonary dysplasia. *Nat Rev Dis Primers.* (2019) 5:78. doi: 10.1038/s41572-019-0127-7
16. Khong TY. The respiratory system. In: Khong TY, Malcomson RDG, editors. *Keeling's Fetal and Neonatal Pathology*. New York, NY: Springer International Publishing (2015). p. 531–60. doi: 10.1007/978-3-319-19207-9_20
17. Speer CP. Pulmonary inflammation and bronchopulmonary dysplasia. *J Perinatol.* (2006) 26(Suppl. 1):S57–62; discussion S3–4. doi: 10.1038/sj.jp.7211476
18. Bose C, Laughon M, Allred EN, Van Marter LJ, O'Shea TM, Ehrenkranz RA, et al. Blood protein concentrations in the first two postnatal weeks that predict bronchopulmonary dysplasia among infants born before the 28th week of gestation. *Pediatr Res.* (2011) 69:347–53. doi: 10.1203/PDR.0b013e31820a58f3
19. Ballabh P, Kumari J, Krauss AN, Shin JJ, Jain A, Auld PAM, et al. Soluble E-selectin, soluble L-selectin and soluble ICAM-1 in bronchopulmonary dysplasia, and changes with dexamethasone. *Pediatrics.* (2003) 111:461–8. doi: 10.1542/peds.111.3.461
20. Ren G, Roberts AI, Shi Y. Adhesion molecules: key players in Mesenchymal stem cell-mediated immunosuppression. *Cell Adh Migr.* (2011) 5:20–2. doi: 10.4161/cam.5.1.13491
21. Niedermaier S, Hilgendorff A. Bronchopulmonary dysplasia - an overview about pathophysiologic concepts. *Mol Cell Pediatr.* (2015) 2:2. doi: 10.1186/s40348-015-0013-7
22. Liao J, Kapadia VS, Brown LS, Cheong N, Longoria C, Mija D, et al. The NLRP3 inflammasome is critically involved in the development of bronchopulmonary dysplasia. *Nat Commun.* (2015) 6:8977. doi: 10.1038/ncomms9977
23. Bourbia A, Cruz MA, Rozycki HJ. NF-kappaB in tracheal lavage fluid from intubated premature infants: association with inflammation, oxygen, and outcome. *Arch Dis Child Fetal Neonatal Ed.* (2006) 91:F36–F9. doi: 10.1136/adc.2003.045807
24. Iosef C, Alastalo T-P, Hou Y, Chen C, Adams ES, Lyu S-C, et al. Inhibiting NF-κB in the developing lung disrupts angiogenesis and alveolarization. *Am J Physiol Lung Cell Mol Physiol.* (2012) 302:L1023–36. doi: 10.1152/ajplung.00230.2011
25. Lawrence T, Gilroy DW, Colville-Nash PR, Willoughby DA. Possible new role for NF-kappaB in the resolution of inflammation. *Nat Med.* (2001) 7:1291–7. doi: 10.1038/nm1201-1291
26. Alvira CM, Abate A, Yang G, Dennery PA, Rabinovitch M. Nuclear factor-kappaB activation in neonatal mouse lung protects against lipopolysaccharide-induced inflammation. *Am J Respir Crit Care Med.* (2007) 175:805–15. doi: 10.1164/rccm.200608-1162OC

27. Nusse R, Clevers H. Wnt/β-Catenin signaling, disease, and emerging therapeutic modalities. *Cell.* (2017) 169:985–99. doi: 10.1016/j.cell.2017.05.016
28. Thébaud B, Abman SH. Bronchopulmonary dysplasia: Where have all the vessels gone? Roles of angiogenic growth factors in chronic lung disease. *Am J Respir Crit Care Med.* (2007) 175:978–85. doi: 10.1164/rccm.200611-1660PP
29. Kotton DN, Morrisey EE. Lung regeneration: mechanisms, applications and emerging stem cell populations. *Nat Med.* (2014) 20:822–32. doi: 10.1038/nm.3642
30. Möbius MA, Thébaud B. Bronchopulmonary dysplasia: Where have all the stem cells gone?: Origin and (potential) function of resident lung stem cells. *Chest.* (2017) 152:1043–52. doi: 10.1016/j.chest.2017.04.173
31. Collins JJ, Thébaud B. Lung mesenchymal stromal cells in development and disease: to serve and protect? *Antioxid Redox Signal.* (2014) 21:1849–62. doi: 10.1089/ars.2013.5781
32. Alphonse RS, Vadivel A, Fung M, Shelley WC, Critser PJ, Ionescu L, et al. Existence, functional impairment, and lung repair potential of endothelial colony-forming cells in oxygen-induced arrested alveolar growth. *Circulation.* (2014) 129:2144–57. doi: 10.1161/CIRCULATIONAHA.114.009124
33. Borghesi A, Massa M, Campanelli R, Bollani L, Tzialla C, Figar TA, et al. Circulating endothelial progenitor cells in preterm infants with bronchopulmonary dysplasia. *Am J Respir Crit Care Med.* (2009) 180:540–6. doi: 10.1164/rccm.200812-1949OC
34. Baker CD, Ryan SL, Ingram DA, Seedorf GJ, Abman SH, Balasubramaniam V. Endothelial colony-forming cells from preterm infants are increased and more susceptible to hyperoxia. *Am J Respir Crit Care Med.* (2009) 180:454–61. doi: 10.1164/rccm.200901-0115OC
35. Collins JJP, Thébaud B. Progenitor cells of the distal lung and their potential role in neonatal lung disease. *Birth Defects Res A Clin Mol Teratol.* (2014) 100:217–26. doi: 10.1002/bdra.23227
36. Kumar ME, Bogard PE, Espinoza FH, Menke DB, Kingsley DM, Krasnow MA. Defining a mesenchymal progenitor niche at single-cell resolution. *Science.* (2014) 346:1258810. doi: 10.1126/science.1258810
37. Hou A, Fu J, Yang H, Zhu Y, Pan Y, Xu S, et al. Hyperoxia stimulates the transdifferentiation of type II alveolar epithelial cells in newborn rats. *Am J Physiol Lung Cell Mol Physiol.* (2015) 308:L861–L72. doi: 10.1152/ajplung.00099.2014
38. Wright CJ, Kirpalani H. Targeting inflammation to prevent bronchopulmonary dysplasia: can new insights be translated into therapies? *Pediatrics.* (2011) 128:111–26. doi: 10.1542/peds.2010-3875
39. Longo LD, Reynolds LP. Some historical aspects of understanding placental development, structure and function. *Int J Dev Biol.* (2010) 54:237–55. doi: 10.1387/ijdb.082774ll
40. Furukawa S, Kuroda Y, Sugiyama A. A comparison of the histological structure of the placenta in experimental animals. *J Toxicol Pathol.* (2014) 27:11–8. doi: 10.1293/tox.2013-0060
41. Soares MJ, Varberg KM, Iqbal K. Hemochorial placentation: development, function, and adaptations. *Biol Reprod.* (2018) 99:196–211. doi: 10.1093/biolre/ioy049
42. Benirschke K, Burton GJ, Baerge RN. Macroscopic features of the delivered placenta. In: Benirschke K, Kaufmann P, Burton GJ, Baergen R, editors. *Pathology of the Human Placenta*. 6th edition. New York, NY: Springer (2012). p. 13–5. doi: 10.1007/978-3-642-23941-0_2
43. Burton GJ, Fowden AL. The placenta: a multifaceted, transient organ. *Philos Trans R Soc Lond B Biol Sci.* (2015) 370:20140066. doi: 10.1098/rstb.2014.0066
44. Kaufmann P, Stark J, Stegner HE. The villous stroma of the human placenta. I. The ultrastructure of fixed connective tissue cells. *Cell Tissue Res.* (1977) 177:105–21. doi: 10.1007/BF00221122
45. Benirschke K, Burton GJ, Baergen R. Anatomy and pathology of the placental membranes. In: Benirschke K, Kaufmann P, Burton GJ, Baergen R, editors. *Pathology of the Human Placenta*. 6th edition. New York, NY: Springer (2012). p. 249–95. doi: 10.1007/978-3-642-23941-0_11
46. Davies JE, Walker JT, Keating A. Concise Review: Wharton's jelly: the rich, but enigmatic, source of mesenchymal stromal cells. *Stem Cells Transl Med.* (2017) 6:1620–30. doi: 10.1002/sctm.16-0492
47. Chew MX, Teoh PY, Wong YP, Tan GC. Multiple umbilical cord strictures in a case of intrauterine foetal demise. *Malays J Pathol.* (2019) 41:365–8.
48. Tan GC SM, Nur Aireen I, Swaminathan M, Hayati AR, Zaleha AM. Large teratoma of the placenta. *Internet J Gynecol Obstet.* (2008) 11:11–4. doi: 10.5580/eeb
49. Delo DM, De Coppi P, Bartsch G, Jr., Atala A. Amniotic fluid and placental stem cells. *Methods Enzymol.* (2006) 419:426–38. doi: 10.1016/S0076-6879(06)19017-5
50. Miki T, Strom SC. Amnion-derived pluripotent/multipotent stem cells. *Stem Cell Rev.* (2006) 2:133–42. doi: 10.1385/SCR:2:2:133
51. de la Torre P, Pérez-Lorenzo M, Flores AI. Human placenta-derived mesenchymal stromal cells: a review from basic research to clinical applications. In: Valarmathi MT, editor. *Stromal Cells*. London: IntechOpen (2019). p. 230–2. doi: 10.5772/intechopen.76718
52. Alatyyat SM, Alasmari HM, Aleid OA, Abdel-maksoud MS, Elsherbiny N. Umbilical cord stem cells: Background, processing and applications. *Tissue Cell.* (2020) 65:101351. doi: 10.1016/j.tice.2020.101351
53. Miki T, Lehmann T, Cai H, Stolz DB, Strom SC. Stem cell characteristics of amniotic epithelial cells. *Stem Cells.* (2005) 23:1549–59. doi: 10.1634/stemcells.2004-0357
54. Ghamari S-H, Abbasi-Kangevari M, Tayebi T, Bahrami S, Niknejad H. The bottlenecks in translating placenta-derived amniotic epithelial and mesenchymal stromal cells into the clinic: Current discrepancies in marker reports. *Front Bioeng Biotechnol.* (2020) 8:180. doi: 10.3389/fbioe.2020.00180
55. Choi YS, Park YB, Ha CW, Kim JA, Heo JC, Han WJ, et al. Different characteristics of mesenchymal stem cells isolated from different layers of full term placenta. *PLoS ONE.* (2017) 12:e0172642. doi: 10.1371/journal.pone.0172642
56. Ilancheran S, Michalska A, Peh G, Wallace EM, Pera M, Manuelpillai U. Stem cells derived from human fetal membranes display multilineage differentiation potential. *Biol Reprod.* (2007) 77:577–88. doi: 10.1095/biolreprod.106.055244
57. Maymó JL, Riedel R, Pérez-Pérez A, Magatti M, Maskin B, Dueñas JL, et al. Proliferation and survival of human amniotic epithelial cells during their hepatic differentiation. *PLoS ONE.* (2018) 13:e0191489. doi: 10.1371/journal.pone.0191489
58. Miki T. Stem cell characteristics and the therapeutic potential of amniotic epithelial cells. *Am J Reprod Immunol.* (2018) 80:e13003. doi: 10.1111/aji.13003
59. Fatimah SS, Ng SL, Chua KH, Hayati AR, Tan AE, Tan GC. Value of human amniotic epithelial cells in tissue engineering for cornea. *Hum Cell.* (2010) 23:141–51. doi: 10.1111/j.1749-0774.2010.00096.x
60. Banas RA, Trumpower C, Bentlejewski C, Marshall V, Sing G, Zeevi A. Immunogenicity and immunomodulatory effects of amnion-derived multipotent progenitor cells. *Hum Immunol.* (2008) 69:321–8. doi: 10.1016/j.humimm.2008.04.007
61. Wolbank S, Peterbauer A, Fahrner M, Hennerbichler S, van Griensven M, Stadler G, et al. Dose-dependent immunomodulatory effect of human stem cells from amniotic membrane: A comparison with human mesenchymal stem cells from adipose tissue. *Tissue Eng.* (2007) 13:1173–83. doi: 10.1089/ten.2006.0313
62. Strom SC, Gramignoli R. Human amnion epithelial cells expressing HLA-G as novel cell-based treatment for liver disease. *Hum Immunol.* (2016) 77:734–9. doi: 10.1016/j.humimm.2016.07.002
63. Gillaux C, Méhats C, Vaiman D, Cabrol D, Breuiller-Fouché M. Functional screening of TLRs in human amniotic epithelial cells. *J Immunol.* (2011) 187:2766–74. Epub 2011/07/22. doi: 10.4049/jimmunol.1100217
64. Friedenstein AJ, Petrakova KV, Kurolesova AI, Frolova GP. Heterotopic of bone marrow. Analysis of precursor cells for osteogenic and hematopoietic tissues. *Transplantation.* (1968) 6:230–47. doi: 10.1097/00007890-196803000-00009
65. Zuk PA, Zhu M, Mizuno H, Huang J, Futrell JW, Katz AJ, et al. Multilineage cells from human adipose tissue: implications for cell-based therapies. *Tissue Eng.* (2001) 7:211–28. doi: 10.1089/107632701300062859
66. Iwatani S, Yoshida M, Yamana K, Kurokawa D, Kuroda J, Thwin KKM, et al. Isolation and characterization of human umbilical cord-derived mesenchymal stem cells from preterm and term infants. *J Vis Exp.* (2019) 143:e58806. doi: 10.3791/58806

67. Williams JT, Southerland SS, Souza J, Calcutt AF, Cartledge RG. Cells isolated from adult human skeletal muscle capable of differentiating into multiple mesodermal phenotypes. *Am Surg.* (1999) 65:22–6.
68. Gronthos S, Mankani M, Brahim J, Robey PG, Shi S. Postnatal human dental pulp stem cells (DPSCs) *in vitro* and *in vivo*. *Proc Natl Acad Sci USA.* (2000) 97:13625–30. doi: 10.1073/pnas.240309797
69. Pinnamaneni N, Funderburgh JL. Concise review: Stem cells in the corneal stroma. *Stem Cells.* (2012) 30:1059–63. doi: 10.1002/stem.1100
70. De Bari C, Dell'Accio F, Tylzanowski P, Luyten FP. Multipotent mesenchymal stem cells from adult human synovial membrane. *Arthritis Rheum.* (2001) 44:1928–42. doi: 10.1002/1529-0131(200108)44:8<1928::AID-ART331>3.0.CO;2-P
71. White IA, Sanina C, Balkan W, Hare JM. Mesenchymal stem cells in cardiology. *Methods Mol Biol.* (2016) 1416:55–87. doi: 10.1007/978-1-4939-3584-0_4
72. Klingemann H, Matzilevich D, Marchand J. Mesenchymal stem cells - sources and clinical applications. *Transfus Med Hemother.* (2008) 35:272–7. doi: 10.1159/000142333
73. Campagnoli C, Roberts IA, Kumar S, Bennett PR, Bellantuono I, Fisk NM. Identification of mesenchymal stem/progenitor cells in human first-trimester fetal blood, liver, and bone marrow. *Blood.* (2001) 98:2396–402. doi: 10.1182/blood.V98.8.2396
74. Amati E, Sella S, Perbellini O, Alghisi A, Bernardi M, Chieregato K, et al. Generation of mesenchymal stromal cells from cord blood: evaluation of *in vitro* quality parameters prior to clinical use. *Stem Cell Res Ther.* (2017) 8:14. doi: 10.1186/s13287-016-0465-2
75. Spitzhorn L-S, Rahman MS, Schwindt L, Ho H-T, Wruck W, Bohndorf M, et al. Isolation and molecular characterization of amniotic fluid-derived mesenchymal stem cells obtained from caesarean sections. *Stem Cells Int.* (2017) 2017:5932706. doi: 10.1155/2017/5932706
76. Siti Fatimah S, Chua k, Tan G, Azmi T, Tan A, Rahman H. Organotypic culture of human amnion cells in air-liquid interface as a potential substitute for skin regeneration. *Cytotherapy.* (2013) 15:1030–41. doi: 10.1016/j.jcyt.2013.05.003
77. Fariha MM, Chua KH, Tan GC, Tan AE, Hayati AR. Human chorion-derived stem cells: changes in stem cell properties during serial passage. *Cytotherapy.* (2011) 13:582–93. doi: 10.3109/14653249.2010.549121
78. Igura K, Zhang X, Takahashi K, Mitsuru A, Yamaguchi S, Takashi TA. Isolation and characterization of mesenchymal progenitor cells from chorionic villi of human placenta. *Cytotherapy.* (2004) 6:543–53. doi: 10.1080/14653240410005366-1
79. Battula VL, Bareiss PM, Treml S, Conrad S, Albert I, Hojak S, et al. Human placenta and bone marrow derived MSC cultured in serum-free, b-FGF-containing medium express cell surface frizzled-9 and SSEA-4 and give rise to multilineage differentiation. *Differentiation.* (2007) 75:279–91. doi: 10.1111/j.1432-0436.2006.00139.x
80. In 't Anker PS, Scherjon SA, Kleijburg-van der Keur C, de Groot-Swings GM, Claas FH, Fibbe WE, et al. Isolation of mesenchymal stem cells of fetal or maternal origin from human placenta. *Stem Cells.* (2004) 22:1338–45. doi: 10.1634/stemcells.2004-0058
81. Macias MI, Grande J, Moreno A, Domínguez I, Bornstein R, Flores AI. Isolation and characterization of true mesenchymal stem cells derived from human term decidua capable of multilineage differentiation into all 3 embryonic layers. *Am J Obstet Gynecol.* (2010) 203:495.e9-.e23. doi: 10.1016/j.ajog.2010.06.045
82. Soncini M, Vertua E, Gibelli L, Zorzi F, Denegri M, Albertini A, et al. Isolation and characterization of mesenchymal cells from human fetal membranes. *J Tissue Eng Regen Med.* (2007) 1:296–305. doi: 10.1002/term.40
83. Wolbank S, van Griensven M, Grillari-Voglauer R, Peterbauer-Scherb A. Alternative sources of adult stem cells: human amniotic membrane. *Adv Biochem Eng Biotechnol.* (2010) 123:1–27. doi: 10.1007/10_2010_71
84. Portmann-Lanz CB, Schoeberlein A, Huber A, Sager R, Malek A, Holzgreve W, et al. Placental mesenchymal stem cells as potential autologous graft for pre- and perinatal neuroregeneration. *Am J Obstet Gynecol.* (2006) 194:664–73. doi: 10.1016/j.ajog.2006.01.101
85. Chang CM, Kao CL, Chang YL, Yang MJ, Chen YC, Sung BL, et al. Placenta-derived multipotent stem cells induced to differentiate into insulin-positive cells. *Biochem Biophys Res Commun.* (2007) 357:414–20. doi: 10.1016/j.bbrc.2007.03.157
86. Fukuchi Y, Nakajima H, Sugiyama D, Hirose I, Kitamura T, Tsuji K. Human placenta-derived cells have mesenchymal stem/progenitor cell potential. *Stem Cells.* (2004) 22:649–58. doi: 10.1634/stemcells.22-5-649
87. Portmann-Lanz CB, Schoeberlein A, Portmann R, Mohr S, Rollini P, Sager R, et al. Turning placenta into brain: placental mesenchymal stem cells differentiate into neurons and oligodendrocytes. *Am J Obstet Gynecol.* (2010) 202:294.e1–.e11. doi: 10.1016/j.ajog.2009.10.893
88. Vegh I, Grau M, Gracia M, Grande J, de la Torre P, Flores AI. Decidua mesenchymal stem cells migrated toward mammary tumors *in vitro* and *in vivo* affecting tumor growth and tumor development. *Cancer Gene Ther.* (2013) 20:8–16. doi: 10.1038/cgt.2012.71
89. Moodley Y, Vaghjiani V, Chan J, Baltic S, Ryan M, Tchongue J, et al. Anti-inflammatory effects of adult stem cells in sustained lung injury: a comparative study. *PLoS ONE.* (2013) 8:e69299. doi: 10.1371/journal.pone.0069299
90. Bonomi A, Silini A, Vertua E, Signoroni PB, Coccè V, Cavicchini L, et al. Human amniotic mesenchymal stromal cells (hAMSCs) as potential vehicles for drug delivery in cancer therapy: an *in vitro* study. *Stem Cell Res Ther.* (2015) 6:155–. doi: 10.1186/s13287-015-0140-z
91. Wang HS, Hung SC, Peng ST, Huang CC, Wei HM, Guo YJ, et al. Mesenchymal stem cells in the Wharton's jelly of the human umbilical cord. *Stem Cells.* (2004) 22:1330–7. doi: 10.1634/stemcells.2004-0013
92. Fong CY, Richards M, Manasi N, Biswas A, Bongso A. Comparative growth behaviour and characterization of stem cells from human Wharton's jelly. *Reprod Biomed Online.* (2007) 15:708–18. doi: 10.1016/S1472-6483(10)60539-1
93. Dominici M, Le Blanc K, Mueller I, Slaper-Cortenbach I, Marini FC, Krause DS, et al. Minimal criteria for defining multipotent mesenchymal stromal cells. The International Society for Cellular Therapy position statement. *Cytotherapy.* (2006) 8:315–7. doi: 10.1080/14653240600855905
94. Taghizadeh RR, Cetrulo KJ, Cetrulo CL. Wharton's Jelly stem cells: future clinical applications. *Placenta.* (2011) 32(Suppl. 4):S311–5. doi: 10.1016/j.placenta.2011.06.010
95. Stefańska K, Ozegowska K, Hutchings G, Popis M, Moncrieff L, Dompe C, et al. Human Wharton's jelly-cellular specificity, stemness potency, animal models, and current application in human clinical trials. *J Clin Med.* (2020) 9:9–30. doi: 10.3390/jcm9041102
96. Conconi MT, Di Liddo R, Tommasini M, Calore C, Parnigotto P. Phenotype and differentiation potential of stromal populations obtained from various zones of human umbilical cord: An overview. *Open Tissue Eng Regen Med J.* (2011) 4:6–20. doi: 10.2174/1875043501104010006
97. Pittenger MF, Discher DE, Péault BM, Phinney DG, Hare JM, Caplan AI. Mesenchymal stem cell perspective: cell biology to clinical progress. *NPJ Regen Med.* (2019) 4:22. doi: 10.1038/s41536-019-0083-6
98. Ganguly P, El-Jawhari JJ, Burska AN, Ponchel F, Giannoudis PV, Jones EA. The analysis of *in vivo* aging in human bone marrow mesenchymal stromal cells using colony-forming unit-fibroblast assay and the $CD45^{low}$ $CD271^{+}$ phenotype. *Stem Cells Int.* (2019) 2019:5197983. doi: 10.1155/2019/5197983
99. Lu LL, Liu YJ, Yang SG, Zhao QJ, Wang X, Gong W, et al. Isolation and characterization of human umbilical cord mesenchymal stem cells with hematopoiesis-supportive function and other potentials. *Haematologica.* (2006) 91:1017–26.
100. Jin HJ, Bae YK, Kim M, Kwon S-J, Jeon HB, Choi SJ, et al. Comparative analysis of human mesenchymal stem cells from bone marrow, adipose tissue, and umbilical cord blood as sources of cell therapy. *Int J Mol Sci.* (2013) 14:17986–8001. doi: 10.3390/ijms140917986
101. Mathew SA, Naik C, Cahill PA, Bhonde RR. Placental mesenchymal stromal cells as an alternative tool for therapeutic angiogenesis. *Cell Mol Life Sci.* (2020) 77:253–65. doi: 10.1007/s00018-019-03268-1
102. Heo JS, Choi Y, Kim H-S, Kim HO. Comparison of molecular profiles of human mesenchymal stem cells derived from bone marrow, umbilical cord blood, placenta and adipose tissue. *Int J Mol Med.* (2016) 37:115–25. doi: 10.3892/ijmm.2015.2413
103. Barlow S, Brooke G, Chatterjee K, Price G, Pelekanos R, Rossetti T, et al. Comparison of human placenta- and bone marrow-derived

multipotent mesenchymal stem cells. *Stem Cells Dev.* (2008) 17:1095–107. doi: 10.1089/scd.2007.0154
104. Brandl A, Meyer M, Bechmann V, Nerlich M, Angele P. Oxidative stress induces senescence in human mesenchymal stem cells. *Exp Cell Res.* (2011) 317:1541–7. doi: 10.1016/j.yexcr.2011.02.015
105. Karlsson H, Erkers T, Nava S, Ruhm S, Westgren M, Ringdén O. Stromal cells from term fetal membrane are highly suppressive in allogeneic settings *in vitro*. *Clin Exp Immunol.* (2012) 167:543–55. doi: 10.1111/j.1365-2249.2011.04540.x
106. Vanover M, Wang A, Farmer D. Potential clinical applications of placental stem cells for use in fetal therapy of birth defects. *Placenta.* (2017) 59:107–12. doi: 10.1016/j.placenta.2017.05.010
107. Di Bernardo J, Maiden MM, Jiang G, Hershenson MB, Kunisaki SM. Paracrine regulation of fetal lung morphogenesis using human placenta-derived mesenchymal stromal cells. *J Surg Res.* (2014) 190:255–63. doi: 10.1016/j.jss.2014.04.013
108. Tian ZF, Du J, Wang B, Hong XY, Feng ZC. [Intravenous infusion of rat bone marrow-derived mesenchymal stem cells ameliorates hyperoxia-induced lung injury in neonatal rats]. *Nan Fang Yi Ke Da Xue Xue Bao.* (2007) 27:1692–5.
109. Aslam M, Baveja R, Liang OD, Fernandez-Gonzalez A, Lee C, Mitsialis SA, et al. Bone marrow stromal cells attenuate lung injury in a murine model of neonatal chronic lung disease. *Am J Respir Crit Care Med.* (2009) 180:1122–30. doi: 10.1164/rccm.200902-0242OC
110. Zhang H, Fang J, Wu Y, Mai Y, Lai W, Su H. Mesenchymal stem cells protect against neonatal rat hyperoxic lung injury. *Expert Opin Biol Ther.* (2013) 13:817–29. doi: 10.1517/14712598.2013.778969
111. Zhang H, Fang J, Su H, Yang M, Lai W, Mai Y, et al. Bone marrow mesenchymal stem cells attenuate lung inflammation of hyperoxic newborn rats. *Pediatr Transplant.* (2012) 16:589–98. doi: 10.1111/j.1399-3046.2012.01709.x
112. van Haaften T, Byrne R, Bonnet S, Rochefort GY, Akabutu J, Bouchentouf M, et al. Airway delivery of mesenchymal stem cells prevents arrested alveolar growth in neonatal lung injury in rats. *Am J Respir Crit Care Med.* (2009) 180:1131–42. doi: 10.1164/rccm.200902-0179OC
113. Fritzell JA, Mao Q, Gundavarapu S, Pasquariello T, Aliotta JM, Ayala A, et al. Fate and effects of adult bone marrow cells in lungs of normoxic and hyperoxic newborn mice. *Am J Respir Cell Mol Biol.* (2009) 40:575–87. doi: 10.1165/rcmb.2008-0176OC
114. Augustine S, Cheng W, Avey MT, Chan ML, Lingappa SMC, Hutton B, et al. Are all stem cells equal? Systematic review, evidence map, and meta-analyses of preclinical stem cell-based therapies for bronchopulmonary dysplasia. *Stem Cells Transl Med.* (2020) 9:158–68. doi: 10.1002/sctm.19-0193
115. D'Addio F, Riella LV, Mfarrej BG, Chabtini L, Adams LT, Yeung M, et al. The link between the PDL1 costimulatory pathway and Th17 in fetomaternal tolerance. *J Immunol.* (2011) 187:4530–41. doi: 10.4049/jimmunol.1002031
116. Yamada A, Arakaki R, Saito M, Kudo Y, Ishimaru N. Dual role of Fas/FasL-mediated signal in peripheral immune tolerance. *Front Immunol.* (2017) 8:403. doi: 10.3389/fimmu.2017.00403
117. Yang ZX, Han Z-B, Ji YR, Wang YW, Liang L, Chi Y, et al. CD106 Identifies a subpopulation of mesenchymal stem cells with unique immunomodulatory properties. *PLoS ONE.* (2013) 8:e59354. doi: 10.1371/journal.pone.0059354
118. Amable PR, Teixeira MVT, Carias RBV, Granjeiro JM, Borojevic R. Protein synthesis and secretion in human mesenchymal cells derived from bone marrow, adipose tissue and Wharton's jelly. *Stem Cell Res Ther.* (2014) 5:53. doi: 10.1186/scrt442
119. Yeung V, Willis GR, Taglauer E, Mitsialis SA, Kourembanas S. Paving the road for mesenchymal stem cell-derived exosome therapy in bronchopulmonary dysplasia and pulmonary hypertension. *Stem Cell-Based Therapy Lung Dis.* (2019) 133:131–52. doi: 10.1007/978-3-030-29403-8_8
120. Tan JL, Tan YZ, Muljadi R, Chan ST, Lau SN, Mockler JC, et al. Amnion epithelial cells promote lung repair via Lipoxin A(4). *Stem Cells Transl Med.* (2017) 6:1085–95. doi: 10.5966/sctm.2016-0077
121. Pierro M, Ionescu L, Montemurro T, Vadivel A, Weissmann G, Oudit G, et al. Short-term, long-term and paracrine effect of human umbilical cord-derived stem cells in lung injury prevention and repair in experimental bronchopulmonary dysplasia. *Thorax.* (2013) 68:475–84. doi: 10.1136/thoraxjnl-2012-202323
122. Chaubey S, Thueson S, Ponnalagu D, Alam MA, Gheorghe CP, Aghai Z, et al. Early gestational mesenchymal stem cell secretome attenuates experimental bronchopulmonary dysplasia in part via exosome-associated factor TSG-6. *Stem Cell Res Ther.* (2018) 9:173. doi: 10.1186/s13287-018-0903-4
123. Mitsialis SA, Kourembanas S. Stem cell-based therapies for the newborn lung and brain: Possibilities and challenges. *Semin Perinatol.* (2016) 40:138–51. doi: 10.1053/j.semperi.2015.12.002
124. Veziroglu EM, Mias GI. Characterizing Extracellular vesicles and their diverse RNA contents. *Front Genet.* (2020) 11:700–. doi: 10.3389/fgene.2020.00700
125. Ragni E, Banfi F, Barilani M, Cherubini A, Parazzi V, Larghi P, et al. Extracellular vesicle-shuttled mRNA in mesenchymal stem cell communication. *Stem Cells.* (2017) 35:1093–105. doi: 10.1002/stem.2557
126. Lee C, Mitsialis SA, Aslam M, Vitali SH, Vergadi E, Konstantinou G, et al. Exosomes mediate the cytoprotective action of mesenchymal stromal cells on hypoxia-induced pulmonary hypertension. *Circulation.* (2012) 126:2601–11. doi: 10.1161/CIRCULATIONAHA.112.114173
127. Willis GR, Fernandez-Gonzalez A, Anastas J, Vitali SH, Liu X, Ericsson M, et al. Mesenchymal stromal cell exosomes ameliorate experimental bronchopulmonary dysplasia and restore lung function through macrophage immunomodulation. *Am J Respir Crit Care Med.* (2018) 197:104–16. doi: 10.1164/rccm.201705-0925OC
128. Braun RK, Chetty C, Balasubramaniam V, Centanni R, Haraldsdottir K, Hematti P, et al. Intraperitoneal injection of MSC-derived exosomes prevent experimental bronchopulmonary dysplasia. *Biochem Biophys Res Commun.* (2018) 503:2653–8. doi: 10.1016/j.bbrc.2018.08.019
129. Willis GR, Fernandez-Gonzalez A, Reis M, Yeung V, Liu X, Ericsson M, et al. Mesenchymal stromal cell-derived small extracellular vesicles restore lung architecture and improve exercise capacity in a model of neonatal hyperoxia-induced lung injury. *J Extracell Vesicles.* (2020) 9:1790874. doi: 10.1080/20013078.2020.1790874
130. Tan JL, Lau SN, Leaw B, Nguyen HPT, Salamonsen LA, Saad MI, et al. Amnion epithelial cell-Derived exosomes restrict lung injury and enhance endogenous lung repair. *Stem Cells Transl Med.* (2018) 7:180–96. doi: 10.1002/sctm.17-0185
131. Bonadies L, Zaramella P, Porzionato A, Perilongo G, Muraca M, Baraldi E. Present and future of bronchopulmonary dysplasia. *J Clin Med.* (2020) 9:1539–64. doi: 10.3390/jcm9051539
132. Caminita F, van der Merwe M, Hance B, Krishnan R, Miller S, Buddington K, et al. A preterm pig model of lung immaturity and spontaneous infant respiratory distress syndrome. *Am J Physiol Lung Cell Mol Physiol.* (2015) 308:L118–29. doi: 10.1152/ajplung.00173.2014
133. D'Angio CT, Ryan RM. Animal models of bronchopulmonary dysplasia. *The preterm and term rabbit models. Am J Physiol Lung Cell Mol Physiol.* (2014) 307:L959–69. doi: 10.1152/ajplung.00228.2014
134. Albertine KH. Utility of large-animal models of BPD: chronically ventilated preterm lambs. *Am J Physiol Lung Cell Mol Physiol.* (2015) 308:L983–l1001. doi: 10.1152/ajplung.00178.2014
135. Escobedo MB, Leonard Hilliard J, Smith F, Meredith K, Walsh W, Johnson D, et al. A baboon model of bronchopulmonary dysplasia: I. Clinical features. *Exp Mol Pathol.* (1982) 37:323–34. doi: 10.1016/0014-4800(82)90045-4
136. Augustine S, Avey MT, Harrison B, Locke T, Ghannad M, Moher D, et al. Mesenchymal stromal cell therapy in bronchopulmonary dysplasia: Systematic review and meta-analysis of preclinical studies. *Stem Cells Transl Med.* (2017) 6:2079–93. doi: 10.1002/sctm.17-0126
137. Jobe AH. Animal Models, Learning lessons to prevent and treat neonatal chronic lung disease. *Front Med (Lausanne).* (2015) 2:49. doi: 10.3389/fmed.2015.00049
138. Ambalavanan N, Morty RE. Searching for better animal models of BPD: a perspective. *J Physiol Lung Cell Mol Physiol.* (2016) 311:L924–L7. doi: 10.1152/ajplung.00355.2016
139. Zhang X, Chu X, Weng B, Gong X, Cai C. An innovative model of bronchopulmonary dysplasia in premature infants. *Front Pediatr.* (2020) 8:271. doi: 10.3389/fped.2020.00271
140. Moodley Y, Ilancheran S, Samuel C, Vaghjiani V, Atienza D, Williams ED, et al. Human amnion epithelial cell transplantation abrogates lung fibrosis and augments repair. *Am J Respir Crit Care Med.* (2010) 182:643–51. doi: 10.1164/rccm.201001-0014OC

141. Murphy S, Lim R, Dickinson H, Acharya R, Rosli S, Jenkin G, et al. Human amnion epithelial cells prevent bleomycin-induced lung injury and preserve lung function. *Cell Transplant.* (2011) 20:909–23. doi: 10.3727/096368910X543385
142. Vosdoganes P, Wallace EM, Chan ST, Acharya R, Moss TJ, Lim R. Human amnion epithelial cells repair established lung injury. *Cell Transplant.* (2013) 22:1337–49. doi: 10.3727/096368912X657657
143. Zhu D, Tan J, Maleken AS, Muljadi R, Chan ST, Lau SN, et al. Human amnion cells reverse acute and chronic pulmonary damage in experimental neonatal lung injury. *Stem Cell Res Ther.* (2017) 8:257. doi: 10.1186/s13287-017-0689-9
144. Hodges RJ, Jenkin G, Hooper SB, Allison B, Lim R, Dickinson H, et al. Human amnion epithelial cells reduce ventilation-induced preterm lung injury in fetal sheep. *Am J Obstet Gynecol.* (2012) 206:448.e8–15. doi: 10.1016/j.ajog.2012.02.038
145. Vosdoganes P, Hodges RJ, Lim R, Westover AJ, Acharya RY, Wallace EM, et al. Human amnion epithelial cells as a treatment for inflammation-induced fetal lung injury in sheep. *Am J Obstet Gynecol.* (2011) 205:156.e26–33. doi: 10.1016/j.ajog.2011.03.054
146. Chou HC, Li YT, Chen CM. Human mesenchymal stem cells attenuate experimental bronchopulmonary dysplasia induced by perinatal inflammation and hyperoxia. *Am J Transl Res.* (2016) 8:342–53.
147. Cargnoni A, Gibelli L, Tosini A, Signoroni PB, Nassuato C, Arienti D, et al. Transplantation of allogeneic and xenogeneic placenta-derived cells reduces bleomycin-induced lung fibrosis. *Cell Transplant.* (2009) 18:405–22. doi: 10.3727/096368909788809857
148. Moodley Y, Atienza D, Manuelpillai U, Samuel CS, Tchongue J, Ilancheran S, et al. Human umbilical cord mesenchymal stem cells reduce fibrosis of bleomycin-induced lung injury. *Am J Pathol.* (2009) 175:303–13. doi: 10.2353/ajpath.2009.080629
149. Liu L, Mao Q, Chu S, Mounayar M, Abdi R, Fodor W, et al. Intranasal versus intraperitoneal delivery of human umbilical cord tissue-derived cultured mesenchymal stromal cells in a murine model of neonatal lung injury. *Am J Pathol.* (2014) 184:3344–58. doi: 10.1016/j.ajpath.2014.08.010
150. Moreira A, Winter C, Joy J, Winter L, Jones M, Noronha M, et al. Intranasal delivery of human umbilical cord Wharton's jelly mesenchymal stromal cells restores lung alveolarization and vascularization in experimental bronchopulmonary dysplasia. *Stem Cells Transl Med.* (2020) 9:221–34. doi: 10.1002/sctm.18-0273
151. Hou C, Peng D, Gao L, Tian D, Dai J, Luo Z, et al. Human umbilical cord-derived mesenchymal stem cells protect from hyperoxic lung injury by ameliorating aberrant elastin remodeling in the lung of O2-exposed newborn rat. *Biochem Biophys Res Commun.* (2018) 495:1972–9. doi: 10.1016/j.bbrc.2017.12.055
152. Deus IA, Mano JF, Custódio CA. Perinatal tissues and cells in tissue engineering and regenerative medicine. *Acta Biomater.* (2020) 110:1–14. doi: 10.1016/j.actbio.2020.04.035
153. Murphy SV, Shiyun SC, Tan JL, Chan S, Jenkin G, Wallace EM, et al. Human amnion epithelial cells do not abrogate pulmonary fibrosis in mice with impaired macrophage function. *Cell Transplant.* (2012) 21:1477–92. doi: 10.3727/096368911X601028
154. Tan JL, Chan ST, Wallace EM, Lim R. Human amnion epithelial cells mediate lung repair by directly modulating macrophage recruitment and polarization. *Cell Transplant.* (2014) 23:319–28. doi: 10.3727/096368912X661409
155. Tan JL, Chan ST, Lo CY, Deane JA, McDonald CA, Bernard CC, et al. Amnion cell-mediated immune modulation following bleomycin challenge: controlling the regulatory T cell response. *Stem Cell Res Ther.* (2015) 6:8. doi: 10.1186/scrt542
156. Umezawa A, Hasegawa A, Inoue M, Tanuma-Takahashi A, Kajiwara K, Makino H, et al. Amnion-derived cells as a reliable resource for next-generation regenerative medicine. *Placenta.* (2019) 84:50–6. doi: 10.1016/j.placenta.2019.06.381
157. Lim R, Malhotra A, Tan J, Chan ST, Lau S, Zhu D, et al. First-in-human administration of allogeneic amnion cells in premature infants with bronchopulmonary dysplasia: a safety study. *Stem Cells Transl Med.* (2018) 7:628–35. doi: 10.1002/sctm.18-0079
158. Malhotra A, Lim R, Mockler JC, Wallace EM. Two-year outcomes of infants enrolled in the first-in-human study of amnion cells for bronchopulmonary dysplasia. *Stem Cells Transl Med.* (2020) 9:289–94. doi: 10.1002/sctm.19-0251
159. Medina-Leyte D, Domínguez-Pérez M, Mercado del Río I, Villarreal-Molina M, Jacobo-Albavera L. Use of human umbilical vein endothelial cells (HUVEC) as a model to study cardiovascular disease: A review. *Appl Sci.* (2020) 10:938. doi: 10.3390/app10030938
160. Paschalaki KE, Randi AM. Recent advances in endothelial colony forming cells toward their use in clinical translation. *Front Med.* (2018) 5:295–. doi: 10.3389/fmed.2018.00295
161. Mastrolia I, Foppiani EM, Murgia A, Candini O, Samarelli AV, Grisendi G, et al. Challenges in clinical development of mesenchymal stromal/stem cells: Concise review. *Stem Cells Transl Med.* (2019) 8:1135–48. doi: 10.1002/sctm.19-0044
162. Khong TY. Trophoblastic regression of amnion: implications for amnion transplants. *Pathology.* (2017) 49:314–6. doi: 10.1016/j.pathol.2016.11.016
163. Jung S, Panchalingam KM, Wuerth RD, Rosenberg L, Behie LA. Large-scale production of human mesenchymal stem cells for clinical applications. *Biotechnol Appl Biochem.* (2012) 59:106–20. doi: 10.1002/bab.1006
164. Elseberg CL, Salzig D, Czermak P. Bioreactor expansion of human mesenchymal stem cells according to GMP requirements. *Methods Mol Biol.* (2015) 1283:199–218. doi: 10.1007/7651_2014_117
165. Noroozi-Aghideh A, Kheirandish M. Human cord blood-derived viral pathogens as the potential threats to the hematopoietic stem cell transplantation safety: A mini review. *World J Stem Cells.* (2019) 11:73–83. doi: 10.4252/wjsc.v11.i2.73

Conflict of Interest: The authors declare that the research was conducted in the absence of any commercial or financial relationships that could be construed as a potential conflict of interest.

frontiers in Pediatrics

REVIEW
published: 11 March 2021
doi: 10.3389/fped.2021.592571

CRISPR Gene-Editing Models Geared Toward Therapy for Hereditary and Developmental Neurological Disorders

*Poh Kuan Wong[1], Fook Choe Cheah[2], Saiful Effendi Syafruddin[3], M. Aiman Mohtar[3], Norazrina Azmi[1], Pei Yuen Ng[1] and Eng Wee Chua[1]**

[1] Drug and Herbal Research Centre, Faculty of Pharmacy, Universiti Kebangsaan Malaysia, Kuala Lumpur, Malaysia, [2] Department of Paediatrics, Universiti Kebangsaan Malaysia Medical Centre, Kuala Lumpur, Malaysia, [3] UKM Medical Molecular Biology Institute, Universiti Kebangsaan Malaysia, Kuala Lumpur, Malaysia

Hereditary or developmental neurological disorders (HNDs or DNDs) affect the quality of life and contribute to the high mortality rates among neonates. Most HNDs are incurable, and the search for new and effective treatments is hampered by challenges peculiar to the human brain, which is guarded by the near-impervious blood-brain barrier. Clustered Regularly Interspaced Short Palindromic Repeat (CRISPR), a gene-editing tool repurposed from bacterial defense systems against viruses, has been touted by some as a panacea for genetic diseases. CRISPR has expedited the research into HNDs, enabling the generation of *in vitro* and *in vivo* models to simulate the changes in human physiology caused by genetic variation. In this review, we describe the basic principles and workings of CRISPR and the modifications that have been made to broaden its applications. Then, we review important CRISPR-based studies that have opened new doors to the treatment of HNDs such as fragile X syndrome and Down syndrome. We also discuss how CRISPR can be used to generate research models to examine the effects of genetic variation and caffeine therapy on the developing brain. Several drawbacks of CRISPR may preclude its use at the clinics, particularly the vulnerability of neuronal cells to the adverse effect of gene editing, and the inefficiency of CRISPR delivery into the brain. In concluding the review, we offer some suggestions for enhancing the gene-editing efficacy of CRISPR and how it may be morphed into safe and effective therapy for HNDs and other brain disorders.

Keywords: Clustered Regularly Interspaced Short Palindromic Repeat (CRISPR), gene-editing, gene therapy, hereditary neurological disorders, neonates, pharmacogenomics, caffeine, drug responsiveness

OPEN ACCESS

Edited by:
Evan Yale Snyder, Sanford Burnham Institute for Medical Research, United States

Reviewed by:
Surendra Sharma, Women & Infants Hospital of Rhode Island, United States
Tomo Tarui, Tufts Medical Center, United States

****Correspondence:***
Eng Wee Chua
cew85911@ukm.edu.my

Specialty section:
This article was submitted to Neonatology, a section of the journal Frontiers in Pediatrics

Received: *07 August 2020*
Accepted: *19 February 2021*
Published: *11 March 2021*

Citation:
Wong PK, Cheah FC, Syafruddin SE, Mohtar MA, Azmi N, Ng PY and Chua EW (2021) CRISPR Gene-Editing Models Geared Toward Therapy for Hereditary and Developmental Neurological Disorders. Front. Pediatr. 9:592571. doi: 10.3389/fped.2021.592571

INTRODUCTION

The human brain is the most complex organ in our body, consisting of a multitude of neurons communicating with each other. It is the command center that governs our bodily functions, including senses, movements, emotions, language, communication, thoughts, and memory. The intricate neural circuits of the brain are built *in utero* and continue to grow till adulthood. The process is orchestrated by a collection of genes that encode signals for triggering neural cell differentiation and migration; but many of the genes are still unknown (1, 2). Defects in these

genes impair prenatal brain development and cause hereditary neurological disorders (HNDs) (3). Currently, there is no cure for most of the HNDs, as the underlying pathogenesis is often obscure and poorly understood; and effective treatments of HNDs are impeded by the blood-brain barrier (BBB) that prevents drugs from being delivered to their target sites. For many of the known HNDs, symptomatic treatments are the only feasible avenues to clinical care (4, 5). However, a major caveat is that some HNDs may not become manifest until after the neonatal period, and critical treatment opportunities may be missed (6).

Gene-editing systems, such as Zinc Finger Nucleases (ZFN) and Transcription Activator-Like Effector Nuclease (TALEN), are potentially powerful approaches for the disease-modifying treatment of HNDs (7). However, they are complex, time-consuming, and have low gene-editing efficiency. To date, Clustered Regularly Interspaced Short Palindromic Repeat (CRISPR) is the most efficient and simplest genome editing system and has been widely used in different cell types and organisms to edit single or multiple target genes (8). CRISPR can be directed to different genetic loci simply by redesigning the sgRNAs (**Table 1**), unlike ZFN and TALEN which would require time-consuming synthesis of new guiding proteins (9). The ease of reconstructing sgRNAs enables CRISPR to target multiple loci simultaneously, needing only an assortment of gene-specific sgRNAs. Moreover, wild-type Cas9 can be reprogrammed into catalytically inactive Cas9 (dead Cas9 or dCas9) that can modulate target gene expression when it is fused to transcriptional modifiers (10).

The number of clinical trials looking into CRISPR-based therapy, especially that of cancer, is growing, (11). Recently, a patient with Leber congenital amaurosis, a hereditary disorder that causes blindness, became the first patient to undergo *in vivo* gene editing using CRISPR (ClinicalTrials.gov identifier: NCT03872479). Although CRISPR has not yet reached the clinical stages of testing in humans with HNDs, pre-clinical results have demonstrated the efficacy of CRISPR in correcting faulty genes associated with HNDs (12). Therefore, CRISPR-based treatments could help to reduce the mortality and morbidity in neonates who suffer HNDs. A viable treatment strategy would be pre-emptive CRISPR gene editing that could prevent the causal genetic defects from developing into full-blown HNDs (6).

Besides, CRISPR can be utilized to generate models to study the effects of genetic variation on drug response (13, 14). Caffeine has a beneficial effect on the developing brain, improving cognitive outcomes in infants treated with it (15). However, caffeine sensitivity varies between neonates, possibly owing to genetic variation. The outcome of caffeine therapy was shown to be adversely affected by rs16851030, a DNA variant located in the 3'-untranslated region of the *ADORA1* gene—the target of caffeine. Individuals who are homozygous for the rs16851030 C-allele may respond better to caffeine than those who harbor the T-allele (16).

In this review, we discuss how CRISPR may progress from laboratory benches into clinics to improve neonatal care. We cover a particularly interesting but challenging subject—the management of HNDs, which affect the vulnerable, growing brains of newborns. We include only relevant HNDs that are manifest during the neonatal period and those that occur later. We also discuss how CRISPR may help us to understand the genetic basis of the variable caffeine sensitivity among neonates with apnea of prematurity, given the large amount of evidence pointing to a beneficial effect of caffeine on brain development.

CRISPR GENE-EDITING VS. TRADITIONAL GENE THERAPY

Gene therapy has the potential to treat a wide range of inherited diseases, such as cystic fibrosis and muscular dystrophy (17, 18). Traditional gene therapy replaces faulty genes with the correct versions or, with the help of a vector, introduces new genes into cells to produce functional proteins (19) (**Figure 1**). However, not all gene constructs can fit into a vector. The gene expression system has a size limit, and large genes are difficult to package and deliver into cells (20). Traditional gene therapy works well for autosomal recessive disorders as the mechanism is straightforward. Most autosomal recessive disorders are caused by loss-of-function exonic variants, and inserting normal copies of the target gene into cells is sufficient to restore protein function (21). In contrast, autosomal dominant disorders are caused by gain-of-function exonic variants and require more elaborate gene editing. This includes an exogenous supply of functional gene constructs to restore protein function, and the use of antisense oligonucleotides and small interfering RNAs to silence the transcription of disease-causing genes (22, 23). The additional requirement for gene silencing means that repeat doses would be needed to maintain therapeutic efficacy (24). This would not be necessary with gene edits created by CRISPR, as the outcome is long-lasting.

Deaths reported following gene therapy have cast serious concerns on its safety. For example, two patients suffered liver dysfunction and died after they received high doses of adeno-associated viruses (AAV) that delivered a gene therapy for X-linked myotubular myopathy (25). An 18-year-old patient passed away 4 days after he was given an intra-artery dose of a gene therapy that was designed to remedy ornithine transcarbamylase deficiency. The cause of death was determined to be a severe immune reaction to the AAV vector that carried the corrective gene (26).

THE MECHANICS OF CRISPR

CRISPR is an adaptive immune defense used by archaea and bacteria against viruses (27). Upon infection by a virus, the host will integrate fragments of the viral genetic material into its genome, which will serve as memory for recognizing and destroying the virus in subsequent infections. The virus will be targeted and destroyed by the CRISPR-associated protein (Cas), an endonuclease that cleaves DNA strands. Between 2011 and 2013, substantial efforts by many researchers led to the successful repurposing of this CRISPR-Cas system to enable gene editing in

TABLE 1 | Gene-editing glossary (62, 63).

Term	Definition
Autosomal dominant	A pattern of inheritance in which an affected individual has a copy of a mutant gene and a normal gene on a pair of autosomal chromosomes
Autosomal recessive	A pattern of inheritance in which an affected individual has a mutant gene on each autosomal chromosome
Cas9 nickase	Cas9 mutant with a single functional endonuclease domain and is only able to introduce single-stranded DNA nicks
CRISPR-associated protein 9 (Cas9)	An enzyme that cuts DNA at specific sites, guided by gRNA
Double-strand break (DSB)	A break in the DNA double helix that is formed when both strands are cut by Cas9. This is different from a single-strand break or "nick."
Guide RNA (gRNA)	A short segment of RNA, usually 20 nucleotides, used to direct a DNA-cutting enzyme, such as Cas9, to the target location in the genome. It contains sequences which are complementary to the target sequence. It is also frequently referred to as single guide RNA (sgRNA).
Homology-directed repair (HDR)	A DNA repair mechanism that uses a template that is homologous to the site of DNA double-strand break to repair the break
Insertion/deletion (Indels)	Mutations that could disrupt an entire protein-coding frame of amino acids and abrogate gene function
Non-homologous end-joining (NHEJ)	A natural repair process used to join the two ends of a broken DNA strand. This is prone to errors where short indels are introduced.
Off-target effect	An undesired effect that occurs when Cas9 cuts at an unintended site, which typically resembles the target site
Protospacer adjacent motif (PAM)	A short segment of a few nucleotides adjacent to the sequence that is cleaved by Cas9
Ribonuclear protein complex (RNP)	A complex of gRNA and Cas9 that cuts DNA at specific sites

eukaryotes. The mechanics of CRISPR-Cas are simple and readily reproducible outside the microbes (28, 29).

CRISPR has been widely used to edit single or multiple target genes in a variety of cells and organisms (8). For a detailed discussion of the mechanisms of CRISPR and the requirements for successful gene edits, the readers are referred to another review (30). A functional CRISPR toolkit needs only: (I) the Cas nuclease, commonly the Cas9, and (II) a guide RNA complementary to the target sequence. The basic scheme can be altered to suit a variety of gene-editing needs (28). The guide RNA directs the Cas9 nuclease to the targeted DNA region, which must contain a protospacer adjacent motif (PAM) at the 3′ end. The binding of Cas9 nuclease to the target region induces DNA double-strand breaks (DSBs), which subsequently trigger endogenous mechanisms to repair the DSBs. DSBs can be repaired either by non-homologous end joining (NHEJ) or homology-directed repair (HDR). In actively dividing human cells, NHEJ is the prevailing DNA repair mechanism, remedying 75% of naturally occurring DSBs, while HDR is responsible for the remaining 25% (31). NHEJ is an error-prone process and causes random DNA insertions or deletions (indels), which could generate frameshift mutations (32). Thus, NHEJ is useful when the resultant edits are intended to abolish gene expression. For precise gene edits such as single-base substitutions, a donor repair template is needed to shift the DNA repair pathways from NHEJ to HDR (33) (**Figure 2A**). HDR enhances the precision of CRISPR, but the issue remains that unlike NHEJ which is active throughout the cell cycle, HDR is only active at the G_2 and S phases. This decreases the efficiency of HDR; and the problem is exacerbated in post-mitotic cells, which are not actively dividing (34).

The discovery of DNA base editors in 2016 offered an HDR-independent solution to the problem (35). These base editors utilize Cas9-nickase or dCas9 conjugated with deaminase to induce single-base transitions from C to T or A to G (36, 37) (**Figure 2B**). Prime editing expands the types of base substitutions that can be created by the base editors, using its dual-functioning guide RNA to prime the *synthesis* of DNA edits by a reverse transcriptase (**Figure 2C**). Instructed by a template embedded in the guide RNA, the reverse transcriptase can create precise indels or any of the 12 possible point mutations (C → T, G → A, A → G, T → C, C → A, C → G, G → C, G → T, A → C, A → T, T → A, and T → G) without the need for DSBs or an HDR template (37).

Precise single-base editing would be an important, clinically relevant modality of gene editing, as ∼50% of disease-causing mutations are single-nucleotide substitutions rather than small indels. The Cas9-deaminase base editors may find use in correcting those mutations and treating the associated disorders (37, 38). For instance, a base editor has been shown to correct a mutation that caused Niemann-Pick disease type C and accumulation of lipids in mouse brain tissue (39). Prime editing is expected to surpass the base editors in therapeutic utility, as it could edit up to 89% of known genetic variants associated with human diseases (37).

GENERATION OF CELL AND ANIMAL MODELS OF HNDS USING CRISPR

Genes hold the blueprint for how the brain matures and functions. However, the roles of many genes in the developing human brain are still poorly understood, making the search for new HND treatments a difficult undertaking (40). *In vitro* and *in vivo* disease models are useful for understanding the molecular mechanisms and the pathogeneses of HNDs and exploring novel therapies. However, the generation of disease models using the conventional transgenesis technique, which introduces an altered version of a gene (harbored in a vector) into a host organism, is time-consuming and inefficient. Cells naturally reject foreign

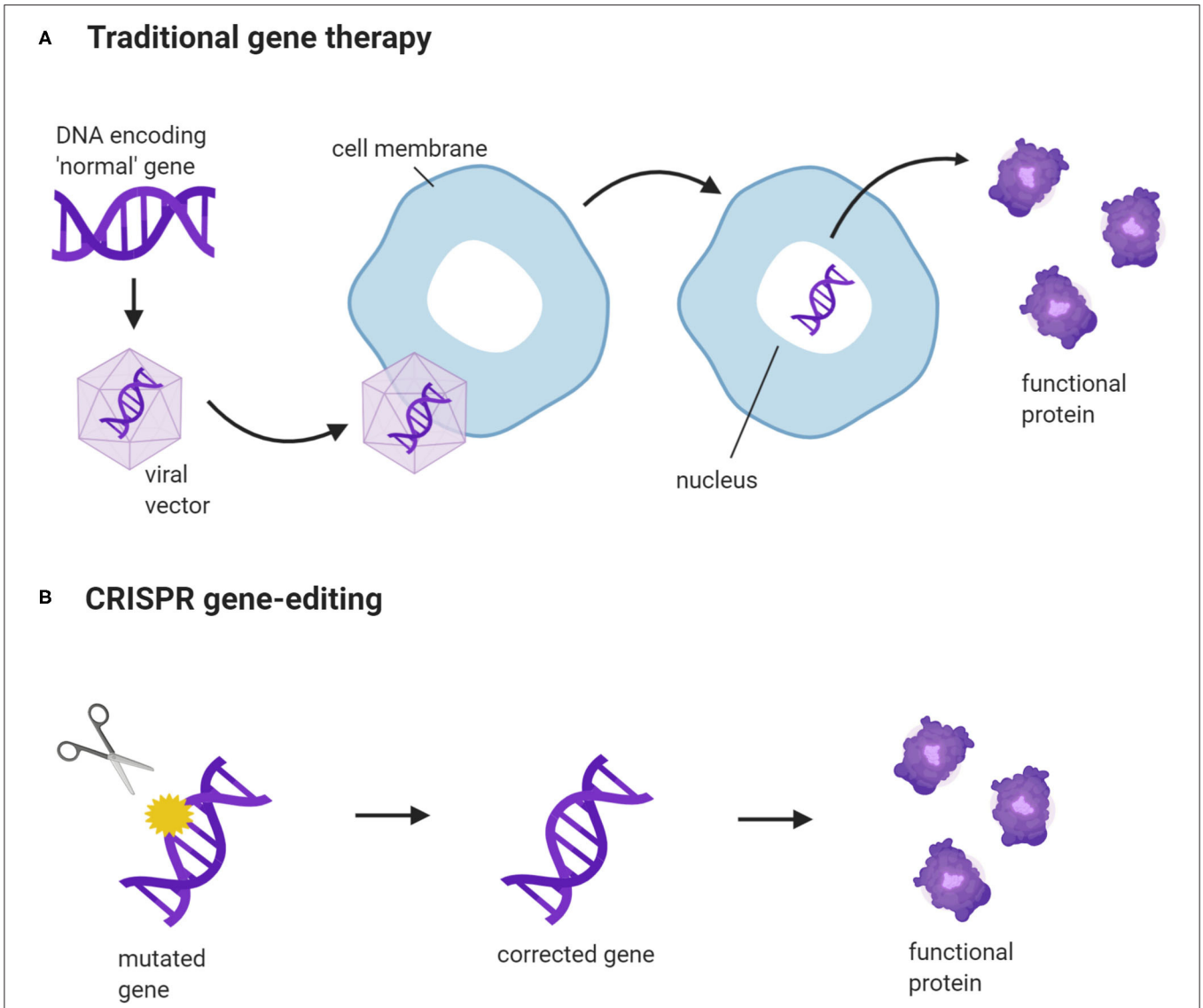

FIGURE 1 | CRISPR gene-editing vs. traditional gene therapy. **(A)** A new gene construct is packaged into a viral vector. The vector binds to the cell membrane and releases the gene construct into the cell nucleus. This enables the cells to produce normal, functional proteins, encoded by the construct. **(B)** CRISPR targets a specific gene and corrects a disease-causing DNA variant. The corrected gene can now be transcribed and translated into a functional protein. (Created with BioRender.com).

substances, so the expression of the mutant gene is usually lost after several rounds of cell division (41). CRISPR obviates this limitation, creating inheritable and permanent changes in nuclear (native) DNA (42).

CRISPR has been used to rapidly create *in vivo* and *in vitro* models to elucidate the pathogenetic mechanisms of genetic diseases and to identify potential treatments (**Table 2**). For instance, to facilitate the study on how the loss of *UBE3A*, which regulates synaptic development, in neurons leads to Angelman syndrome, *in vitro* and *in vivo* (rat) models were generated by knocking out *UBE3A* using CRISPR. *UBE3A*-deficient rats showed signs similar to what have been observed in patients with Angelman syndrome, namely cognitive and motor impairment. Neurons lacking functional *UBE3A* lose the ability to fire mature action potentials—the electrical signals that connect neurons and underpin the workings of the brain (43, 44). By silencing *UBE3A*, CRISPR has helped to pinpoint the genetic switch of neural circuits and the causal gene for Angelman syndrome.

Mice and rats are popular choices of model organisms for studies of human diseases. However, they are not always compatible with human HNDs. Though the brains of humans, mice, and rats share the same general layout, they differ in some key aspects, making it impossible to create valid mouse or rat models for certain HNDs. The cortex of the human brain is heavily folded to house dense networks of neurons that perform

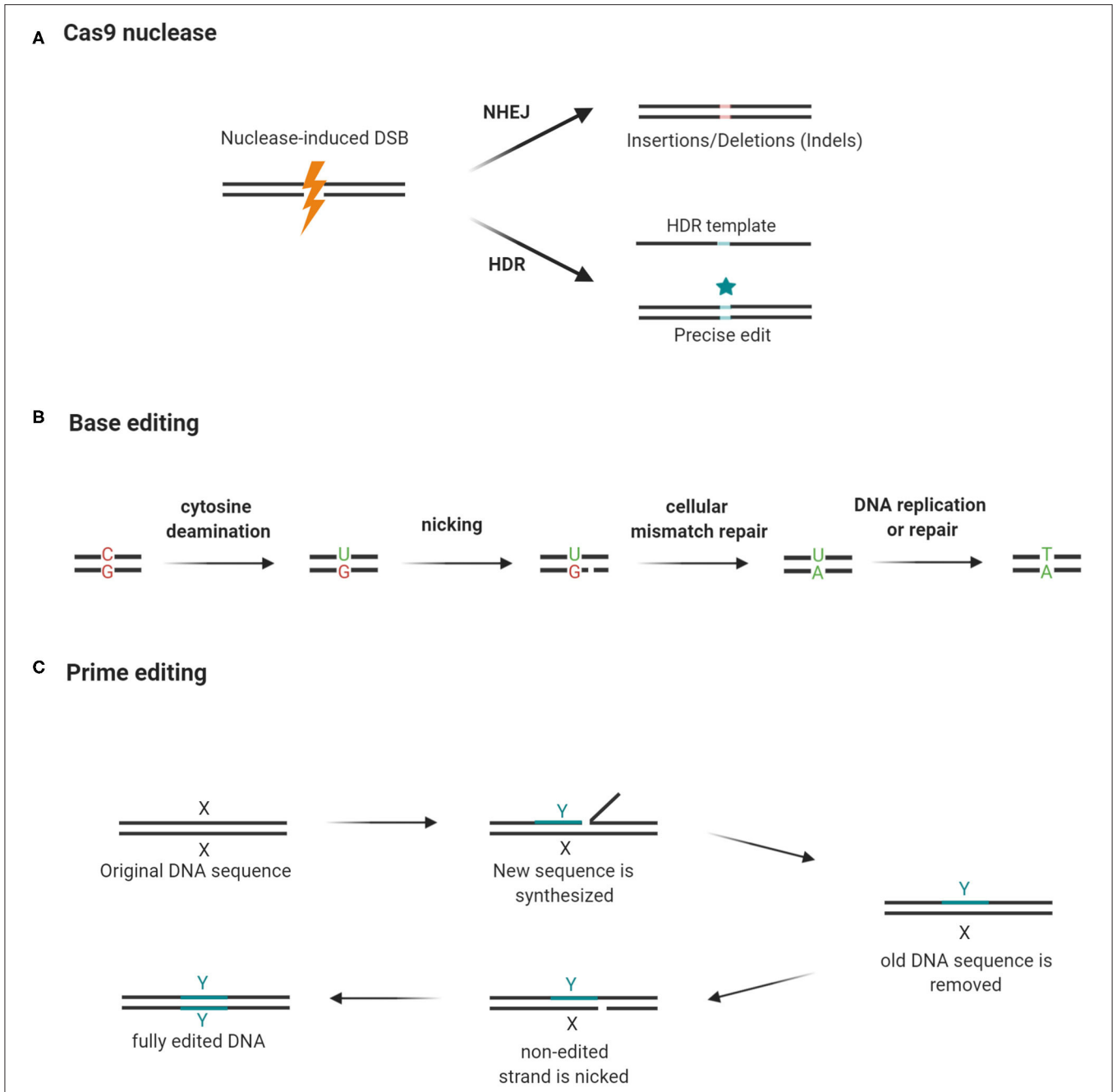

FIGURE 2 | Cas9 nuclease, base editing, and prime editing. **(A)** Guide RNA guides Cas9 nuclease to cut a DNA segment that is 3 bases upstream of the PAM. The resultant double-strand break (DSB) triggers NHEJ, which may cause frame-shifting indels and abolish gene expression. By using a repair template, the repair machinery can be shifted to HDR and introduce precise edits while rejoining the broken DNA strands. **(B)** Cytidine deaminase converts cytosine to uracil while deoxyadenosine deaminase (not shown in the figure) converts adenosine to guanine. Cas9 nickase cuts the opposite strand and triggers a mismatch repair mechanism. As a result, in repairing the nick previously created by the Cas9 nickase, the cell uses the edited DNA strand as a template and copies the "mutation" into the complementary strand. **(C)** Prime editing requires a prime editor and a prime editing guide RNA (pegRNA) to modify gene sequences. The prime editor is a chimera of a Cas9 nickase and a reverse transcriptase (RT). The pegRNA guides the prime editor to the target site where editing should occur. It also carries a primer-binding site (PBS) and a short stretch of a template sequence containing the desired edit. The reverse transcriptase converts the template sequence into complementary DNA, which is then incorporated into the target site after the original DNA sequence is excised by an endogenous endonuclease. Then, the edited strand serves as a template for the repair of the unedited strand after it is nicked by Cas9 nickase. Hence, both DNA strands have the desired edit. X: original DNA sequence; Y: edited DNA sequence (Created with BioRender.com).

TABLE 2 | HNDs models generated by CRISPR.

HNDs	Targeted gene	Species	*In vitro*/ *in vivo*	Genetic alteration	Delivery method	Editing method	References
Angelman syndrome	*UBE3A*	Human	*In vitro*	NHEJ-mediated gene knockout	Transfection	Cas9 and sgRNA	(43)
		Rat	*In vivo*	NHEJ-mediated gene knockout	Embryo microinjection	Cas9 and sgRNA	(44)
Lissencephaly	*Dcx*	Ferret	*In vivo*	NHEJ-mediated gene knockout	Embryo microinjection	Cas9 mRNA and sgRNA	(45)
	Cdk5	Ferret	*In vivo*	NHEJ-mediated gene knockout	*In utero* electroporation	Plasmid expressing Cas9 and sgRNA	(46)
Infantile neuronal ceroid lipofuscinoses	*PPT1*	Ovine	*In vivo*	HDR-mediated mutation	Zygote microinjection	Cas9 mRNA, sgRNA and HDR template (90 mer single-stranded oligodeoxynucleotide)	(47)

high-level cognitive functions—an anatomical feature that is absent from the brains of mice and rats (48, 49). Beneath the cortical sheath, neurons are grouped by the genes they actively express into a variety of functional classes. Many of the neuron classes are conserved between humans and mice, but some putative counterparts were found to have notably varied patterns of gene expression (50). This means the molecular workings of some human brain diseases are species-specific and may only be accurately replicated in animals that are closely related to humans.

Medium-sized animals, such as sheep, monkeys, pigs, and ferrets resemble humans more closely than mice or rats and are therefore better model organisms for use in CRISPR-based studies of HNDs (51). For instance, CRISPR-mediated genome editing was applied to develop a ferret model to study lissencephaly, which causes loss of cortical folding in the human brain (45). In this study, a CRISPR system targeting *Dcx* was injected into single-cell ferret embryos, which were then implanted into surrogate females. This abolished the function of *Dcx* and resulted in the birth of ferrets who had smooth brains, confirming the importance of *Dcx* in enabling neuronal migration during cortical folding (45). Infants born with lissencephaly have small brains and severe intellectual disability (40). In another study, by delivering a CRISPR system using *in utero* electroporation, researchers proved that *Cdk5* can be another gene required for cortical folding, as knocking out this gene resulted in smooth-surfaced brains (46). Both studies used ferrets, as cortical folds are present in ferrets but not in rodents (45, 46).

It is evident that the choice of an animal model depends on the characteristics of the disease in question. For instance, a CRISPR-ovine model is the logical choice for infantile neuronal ceroid lipofuscinoses, where deleterious mutations in the palmitoyl-protein thioesterase 1 (*PPT1*) gene cause progressive death of nerve cells. The incurable disease affects children and severely reduces their life expectancy to ∼10% of the average lifespan of humans, as death typically occurs at ∼9 years of age. Sheep are more effective disease models than ferrets in this case, though both have brain structures similar to humans. The longer lifespans of sheep would allow us to thoroughly map out the development of the disease (47, 52, 53).

Overall, the studies curated in **Table 1** have clearly shown the utility of CRISPR, when coupled with medium-sized animal models, in helping us to understand the pathogeneses of HNDs. However, the high costs, long breeding periods, ethical concerns, and strict regulations may still limit the use of those animal models in the future (51, 54).

CRISPR-MEDIATED TREATMENT OF HEREDITARY OR DEVELOPMENTAL NEUROLOGICAL DISORDERS

Besides its potential in the generation of effective models of human diseases, CRISPR can also be used to treat HNDs (**Table 3**). Here we discuss in detail the pre-clinical findings reported by studies of a variety of HNDs, namely fragile X syndrome, Down syndrome, and sphingolipidoses. CRISPR-based therapy could be achieved using different approaches in the clinical settings, namely *in vitro* germline editing, *in utero* gene editing, and *in vivo* and *ex vivo* gene editing (**Figure 3**). We detail the rationales and challenges of different strategies for CRISPR editing of HND-causing DNA variants in **Table 4**.

Fragile X Syndrome

CRISPR-Gold, a non-viral delivery system, was found to effectively edit *mGluR5*, an autism-associated gene, in a mouse model of fragile X syndrome. *mGluR5* editing reduces the signaling between brain cells and thus decreases the repetitive behaviors caused by this disorder (**Figure 4**). In the study that examined the therapeutic potential of CRISPR-Gold, the CRISPR system was injected directly into mouse brains to limit gene editing to the striatum, which mediates repetitive behaviors. As a result, *mGluR5* mRNA and protein levels were reduced by 40–50%, and this was sufficient to rescue the treated mice from repetitive behaviors (12). However,

TABLE 3 | CRISPR-mediated treatment of HNDs.

HNDs	Targeted gene	Species	*In vitro/ in vivo*	Genetic alteration	Delivery method	Editing method	References
Fragile X syndrome	*mGluR5*	Mouse	*In vivo*	NHEJ-mediated gene knockout	Intracranial injection	CRISPR–Gold Cas9 sgRNA RNPs	(12)
Down syndrome	Chromosome 21	Mouse, human	*In vitro*	CRISPR-mediated chromosome deletion	Transfection	Plasmid expressing Cas9 and sgRNA	(55)
Tay-Sachs	*HEXA*	Mouse	*In vivo*	cDNA-mediated Hex enzyme expression	Hydrodynamic injection	AAV-SaCas9 and AAV-*HEXM*-gRNA plasmids	(56)
	HEXA 1278 + TATC	Human	*In vitro*	TATC deletion	Transfection	Prime editing (PE3/PE3b plasmid, pegRNA plasmid, sgRNA plasmid)	(37)
Sandhoff disease	*HEXB*	Mouse	*In vivo*	cDNA-mediated Hex enzyme expression	Hydrodynamic injection	AAV-SaCas9 and AAV-*HEXM*-gRNA plasmids	(56)
Niemann-Pick disease type C	*NPC1* c.3182T>C	Mouse	*In vivo*	C → T	Retro-orbital injection	AAV-mediated cytosine base editor	(39)

it could be a challenge for researchers to determine the extent of *mGluR5* reduction that would cause a similar effect in humans. Fragile X syndrome is associated with an imbalance of glutamatergic and GABAergic signaling (64). *mGluR5* serves a role in excitatory glutamatergic neurotransmission and completely knocking out this gene can further disrupt GABAergic signaling and impair human brain function (65, 66). Hence, the nuanced balance between the glutamatergic and GABAergic signals in the brain dictates the level of *mGluR5* inhibition that would be therapeutic in humans (67).

Down Syndrome

Down syndrome, also known as trisomy 21, is caused by an error in cell division that leads to an extra chromosome 21 (68). It is a well-known genetic disorder that impairs neurodevelopment in newborns. The extra chromosome 21 causes overexpression of >100 genes that drive brain development or function (69). Several gene editing strategies, including CRISPR, have been applied to eliminate the surplus chromosome (70). For instance, two gRNAs were designed to target repetitive sequences at the long arm of chromosome 21, induce cleavage at multiple sites, and eliminate the whole chromosome. The deletion of an entire chromosome is challenging as it is difficult to efficiently induce multiple DNA cleavages. Although the initial trial of the chromosome-removing strategy was successful in stem cells derived from patients with Down syndrome, the same outcome was not replicable in embryos, probably because chromosomal deletion was lethal to embryonic cells (55). Recently, two alternative strategies were proposed. The suggestions were aimed at inactivating instead of deleting the extra chromosome 21 (71). Guided by sgRNAs, the Cas9 nuclease could home in on and cut off the Down syndrome critical regions in chromosome 21, which harbor the culprit genes that cause Down syndrome and inhibit neuronal development. Alternatively, the enzyme could edit out a non-functional segment within chromosome 21 in exchange for a regulatory DNA construct which contains *XIST* that inactivates the chromosome (71, 72). With this proposed approach, chromosomal inactivation by *XIST* which normally occurs at the pluripotent stage could be induced in non-pluripotent neural stem cells and differentiated neurons (73). Both the proposed methods could rescue neurogenesis and improve cognitive performance in Down syndrome patients.

Sphingolipidoses

CRISPR has also demonstrated its genome editing efficacy in mouse models of Tay-Sachs and Sandhoff diseases. Mutations in *HEXA*, which encodes the Hex α subunit, lead to Tay-Sachs disease while mutations in *HEXB*, which encodes the Hex β subunit, cause Sandhoff disease. Mutations in the *HEXA* and *HEXB* genes reduce the activity of beta-hexosaminidase, which breaks down G_{M2} ganglioside, a normal component of the neuronal membrane. As a result, G_{M2} ganglioside accumulates to a level which is toxic to neurons in the brain and the spinal cord, causing intellectual disability and seizures (74). Instead of targeting the brain, a CRISPR system delivered by AAV was used to turn hepatocytes into machinery that produces a modified human Hex μ subunit, by integrating cDNA encoding the protein into the albumin gene. The enzymes expressed and secreted from the edited hepatocytes were then carried by the bloodstream to the brain to break down G_{M2} ganglioside (56).

With new techniques being rapidly developed, several alternative strategies—one of which being prime editing—have become available for editing *HEXA* mutations in Tay-Sachs disease (37). The most common mutation found in patients with Tay-Sachs disease is a 4-bp insertion, i.e., TATC in exon 11 of the *HEXA* gene (75). In an *in vitro* model, prime editing was shown to correct the mutation by removing the 4-bp insertion without DSB (37). To determine which CRISPR system is optimal, criteria such as safety, costs, delivery vectors, and how well the system works in cells should be considered. Most importantly, more supporting evidence should be garnered from pre-clinical studies before moving into clinical trials.

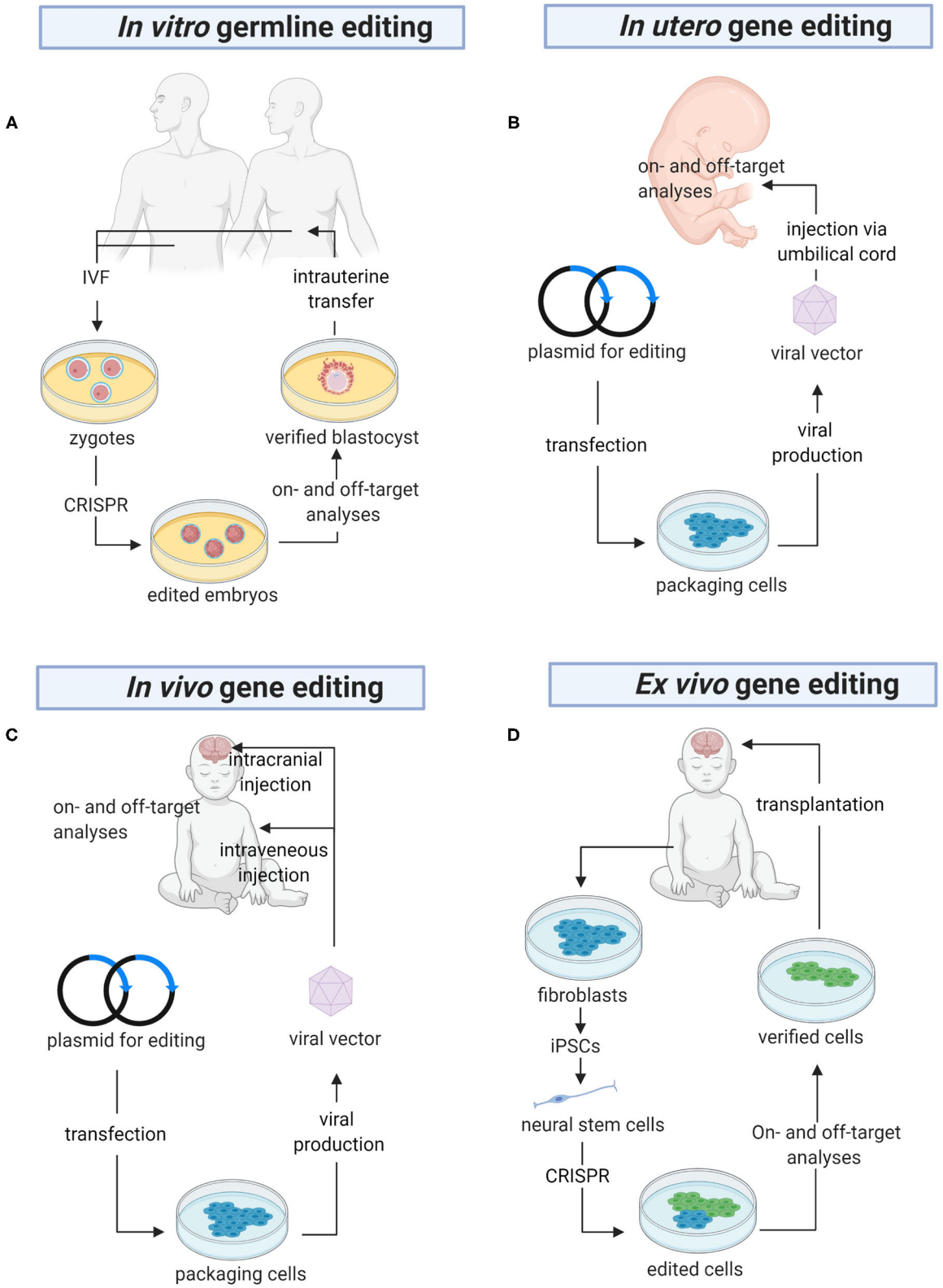

FIGURE 3 | The future of gene editing in HNDs. **(A)** *In vitro* germline editing is initiated with the creation of zygotes. CRISPR constructs are microinjected into the zygotes, which are allowed to grow into embryos harboring the desired DNA edits. PGD is carried out to ensure there are no off-target mutations before the embryos

(Continued)

FIGURE 3 | are transferred into the uterus. **(B)** A viral vector harboring a genome editor is injected into the umbilical cord for direct delivery into the fetus. Alternatively, the editor can be delivered using a non-viral vector (not shown in the figure). Before the baby is born, a variety of tests will be performed to confirm on-target gene edits and detect off-target mutations. **(C)** CRISPR is packaged in a viral or non-viral vector for systemic delivery or direct injection into the brain. **(D)** *Ex vivo* gene editing begins with isolation of fibroblasts from the patients. The cells are reprogrammed into iPSCs, differentiated into neural stem cells, and CRISPR-edited. Then, the edited cells are analyzed for on- and off-target gene edits before they are transplanted into the brain. PGD, pre-implantation genetic diagnosis; IVF, *in vitro* fertilization; iPSCs, induced pluripotent stem cells (Created with BioRender.com).

TABLE 4 | Advantages and disadvantages of different strategies of CRISPR-based gene editing in HNDs.

	Advantages/rationales	Disadvantages/challenges
(A) *In vitro* germline editing (57)	• The risk of affecting the mother is low. • Gene edits are not inheritable. • May allow parents who are homozygous carriers of recessively transmitted diseases to have a healthy child.	• Ethical, legal and social issues. • Its use is not justified as inherited genetic disorder can be prevented by embryo screening in most of the cases.
(B) *In utero* gene editing (58)	• Avoids the manifestation of life-threatening genetic diseases. • BBB is more permissive; vectors can be easily delivered to brain cells via systemic delivery. • Actively proliferating cells increase the efficiency of HDR. • Immune system can tolerate the gene editing system. • Decreases therapeutic dosing as the fetus is small in size.	• The safety of both the mother and the fetus should be ensured. • Off-target effects need careful evaluation in pre-clinical settings. • Difficult to determine the timing of intervention. • Risk of unintended germline editing (59).
(C) *In vivo* gene editing (post-natal)	• Ameliorates disease symptoms for conditions diagnosed after birth. • Poor engraftment of edited cells can be avoided. • Mother is not affected by the gene editing system.	• Presence of pre-existing immune response to the viral vector or CRISPR constructs, limiting the efficacy of repeat doses that may be necessary (58). • Important to select an appropriate vector to cross the BBB and target neuronal cells.
(D) *Ex vivo* gene editing (post-natal)	• Ameliorates disease symptoms for after birth diagnosis. • Precise selection of genetically modified cells without off-target mutations (60). • Minimal immune response. • Mother is not affected by the gene editing system.	• Time-consuming as the procedure is complicated. • Poor engraftment of edited cells (61).

GENE-EDITING TO STUDY DRUG RESPONSIVENESS

Caffeine, an antagonist of adenosine A1 (ADORA1) and A2A receptors (ADORA2A), is a key modality of the management of apnoea of prematurity. Administration of caffeine in pre-mature, apneic infants was found to improve symptoms and significantly reduce death rates and the severity of neurocognitive impairment (76). Caffeine has also been shown to have a variety of neuroprotective effects *in vitro* and *in vivo*. It protects against cell death and preserves background electrical activity in the hypoxic-ischemic brains (77–80) and enhances the connection between neurons by activating genes that control neuron projection. This is especially important to the developing brains of infants. Together, the protective mechanisms of caffeine act to improve neurodevelopment in preterm infants (81).

Individual genetic differences can affect the pharmacology of some drugs and cause inter-individual variability in drug response. This would affect drug therapy outcomes. Because of genetic variation, not all infants given caffeine will respond optimally to the drug. Rs16851030, a DNA variant located in the 3′-untranslated region of the *ADORA1* gene, was shown to adversely affect the outcome of caffeine therapy. A prospective case-control study was conducted to assess the variability of caffeine sensitivity in relation to single-nucleotide variants in the *ADORA1* gene. All infants who were >28 weeks old and homozygous for the rs16851030 reference C-allele were found to have responded favorably to caffeine therapy, in comparison with a 57% response rate among those harboring the alternate T-allele. The discrepancies in the treatment outcomes may be due to the influence of rs16851030 on the expression of the adenosine A1 receptor (16); but this remains an unconfirmed theory. Furthermore, we do not know whether the genetic variation in caffeine response could be overcome by dosage adjustment (82). In caffeine-sensitive individuals, the augmented effects of caffeine could be offset by lowering caffeine doses to avoid toxicity, such as tachycardia and seizure (83). Conversely, individuals who are less caffeine-responsive may benefit from higher caffeine doses to reduce the risk of apnea and to prevent complications such as hypoxia-induced brain damage. CRISPR has been used to create a mutant breast cancer cell line with a single base edit to elucidate the mechanism of drug resistance (14). Therefore, by creating a cell-based model using CRISPR and treating the cells carrying the C- or T-allele with different concentrations of caffeine, we could then gauge whether the underlying genetic influence could be overcome by adjustments to the dosage of caffeine. The resultant findings would be valuable for optimizing the management of apnea of prematurity and improving neurodevelopmental outcomes in preterm infants.

Using a base editor to investigate how rs16851030 affects the outcome of caffeine therapy could be challenging as there are multiple Cs around the target C (in brackets) within the editing

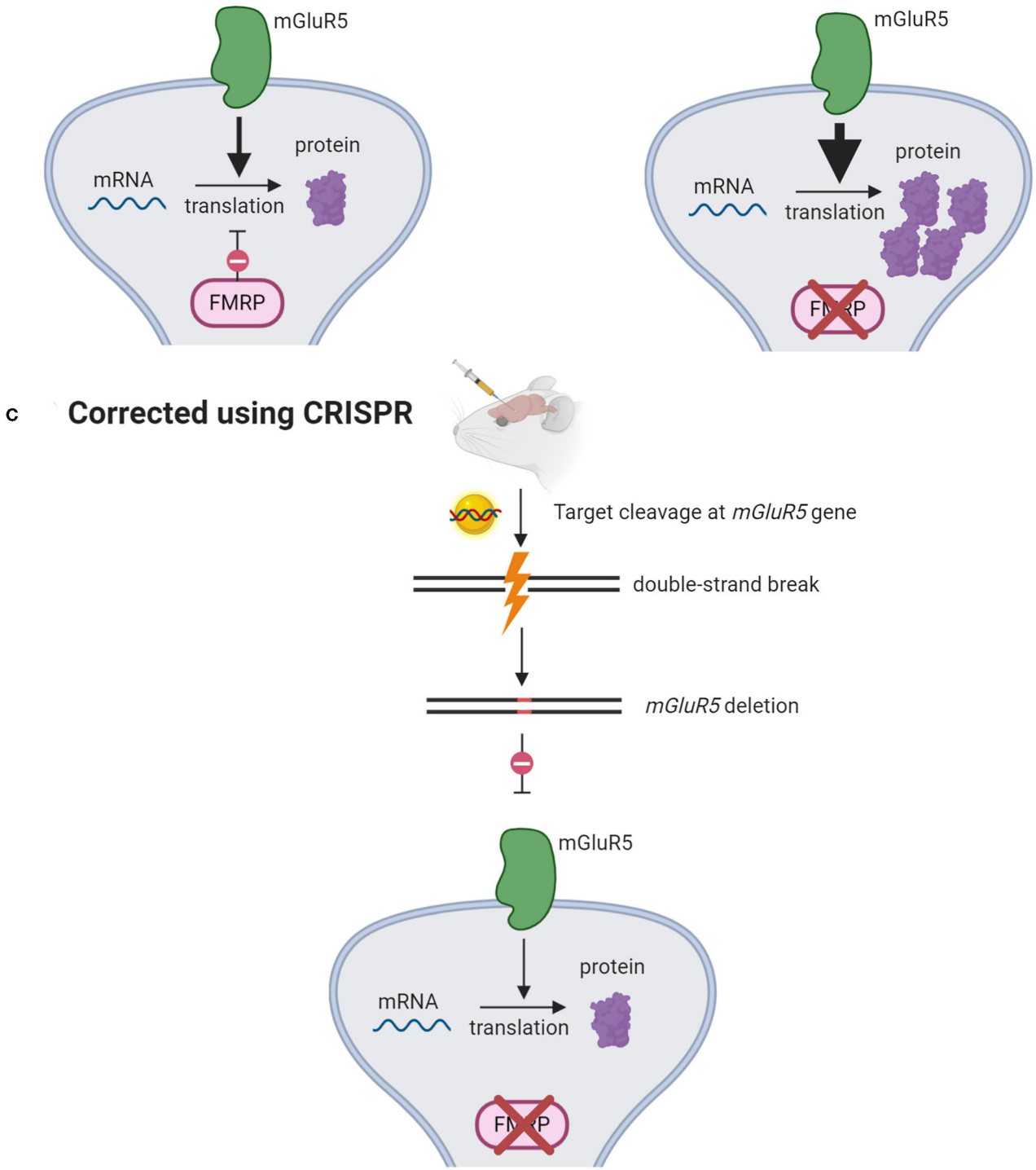

FIGURE 4 | mGluR5 signaling reduction rescues fragile X syndrome in mice. **(A)** mGluR5 signaling activates protein synthesis. FMRP opposes mGluR5 and suppresses the translation of mRNAs into proteins. **(B)** In FMRP-knockout mice, mGluR5 signaling is exaggerated, causing excessive synthesis of proteins. **(C)** CRISPR-Gold is injected intracranially to knock out *mGlur5* gene. This has been shown to decrease mGlurR5 mRNAs by 40–50% and restore protein synthesis to its normal levels (12). (Created with BioRender.com).

window, as shown in the flanking sequences of rs16851030, TCTTAGATGTTGGTGGTGCAGC[C/T]CCAGGACCAAGCT TA**AGG**AGAG. The editing of additional Cs can cause harmful effects. CRISPR base editors with narrow editing windows were reported recently but they still would not be able to precisely edit the target C, owing to bystander effects (84, 85); and the editing may result in a non-T (86, 87). Prime editing would be a fitting alternative to the base editors (**Figure 2C**), as it creates precise point mutations by directly copying the desired gene edits into the target DNA segments (37). Another advantage of prime editing is that unlike the other base editors, it can perform gene editing in post-mitotic cells, including neurons in the brain (37).

LIMITATIONS OF CRISPR AND THE WAY FORWARD

In this section, we detail the roadblocks to CRISPR attaining its maximal utility in neuroscience research: off-target effects, potential difficulties in crossing the blood-brain barrier, and immunogenicity of Cas9 and vulnerability of neuronal cells to the adverse effect of CRISPR editing (or the system that delivers it).

Off-Target Effects

The specificity of CRISPR is ensured by its companion gRNA, which consists of sequences complementary to the target DNA region. However, the specificity is not absolute, and unintended binding between gRNA and non-target DNA sequences is possible. Off-target activity must be avoided because it can lead to adverse side effects. Current tactics for curbing off-target editing have focused on two key aspects of how CRISPR operates, i.e., the need for specific gRNAs, and the fundamental gene editing mechanics.

DISCOVER-Seq (discovery of *in situ* Cas off-targets and verification by sequencing) is a tool for detecting possible *in vitro* or *in vivo* off-targets of CRISPR, helping researchers to validate the guide RNAs they have designed *in silico*. By checking the interaction between a DSB repair protein, MRE11, with Cas9 cut sites, DISCOVER-Seq can identify the exact locations in the genome where a cut has been made by CRISPR. The MRE11-bound DNA segments are captured by chromatin immunoprecipitation and sequenced on a high-throughput platform. DISCOVER-Seq is superior to other tools as it can be used to detect off-target events *in vivo* (88). This may in then inform corresponding strategies to eradicate the off-target editing.

Prime editing overhauls the mechanism of base editing and could be an option that is relatively free of off-target editing. It was reported to have increased target specificity (37). However, the safety and efficacy of prime editors in neuronal cells are still unclear. Further studies are needed to explore the utility of this newly developed gene editor in the neuroscience space.

Crossing the Blood-Brain Barrier

For gene expression studies and treatment of HNDs, the main challenge is to deliver a CRISPR system across the BBB. The BBB prevents the entry of foreign substances into the brain, including toxins and pathogens (89). The protective mechanism is a two-edged sword, as it also cuts off the access of CRISPR systems to the brain. There are several strategies to tackle the BBB, such as viral delivery and nanoparticles. AAV is a popular method for shipping CRISPR expression constructs to the target brain cells. To make room for CRISPR, the virus is emptied of its protein-coding genes, leaving only the capsids and the sequences that regulate DNA replication. The passage of AAV-CRISPR across the BBB is made possible by the inherent ability of viruses to bind to and invade host cells (90).

However, wild-type AAVs are inefficient in crossing the BBB and need direct injection into the brain (91). Besides, they have low transduction efficiency *in vitro* and *in vivo* (92, 93). To counter the drawbacks, a 7-mer peptide, PHP.B, was inserted into the capsids of wild-type AAVs to facilitate the penetration of BBB and to increase transduction efficiency in neuronal cells (93, 94). However, a high viral load of AAV-PHP.B would be required ($\geq 1 \times 10^{12}$ vg per adult mouse) for genetic modification in the brain, and this translates into a high risk of immune reactions. With the development of AAV-PHP.eB, which varies from AAV-PHP.B at only two amino acids adjacent to the initial 7-mer peptide insertion, neuronal cells can be edited using a lower viral load (95). Some studies showed that PHP.B and PHP.eB require the LY6A receptor (lymphocyte antigen 6 complex) to reach the mouse brain. *Ly6a* disruption decreases, while *Ly6a* overexpression enhances, transduction efficiency (96, 97). Nonetheless, this mechanism utilized by AAVs to cross the BBB is mouse-specific and there is no direct homolog to *Ly6a* in humans. Further experiments should focus on pinpointing a gene which can be targeted to increase AAV transduction in the human brain (98).

Another way to deliver the CRISPR system across the BBB has been developed recently using *in vitro* BBB models and holds promises in the eradication of neuroHIV. It was achieved by packaging the CRISPR system bound with magneto-electric nanoparticles (MENPs) in a nanoformulation. A magnetic field was then applied on the nanoformulation to release CRISPR from the surfaces of MENPs and to facilitate cell uptake. This would then result in intracellular release of CRISPR and inhibition of HIV (99). Neonates acquire neuroHIV when the virus enters their brains, and this could delay their brain development (100, 101). Although HIV is not an inherited disease, the same approach to delivery across the BBB could be applied in the treatment of HNDs. However, it is unclear whether the BBB has fully formed during the neonatal period (89). This would affect the concentration of a CRISPR system to be safely delivered into the brain. Future efforts should focus on determining the optimum concentration of CRISPR before this technique can be adopted clinically.

Immunogenicity of Cas9 and Vulnerability of Neuronal Cells to the Adverse Effect of CRISPR Delivery Systems

The most common Cas9 orthologs are derived from *Staphylococcus aureus* (SaCas9) and *Streptococcus pyogenes* (SpCas9) (102). Because of their bacterial origins, Cas9 proteins face pre-existing adaptive immune responses in humans. Antibodies against SaCas9 and SpCas9 have been detected in 86 and 73%, respectively, of the serum samples obtained from

cord blood donors (103). The potential immunogenicity of Cas9 proteins warrants caution in future clinical trials examining the use of CRISPR in neonates.

Besides, the delivery methods of CRISPR systems may also induce immune responses and impact neuronal cells. Viral vectors are commonly used to deliver CRISPR constructs across the BBB (12, 104). However, viral delivery causes protracted CRISPR expression, which is toxic to neuronal cells and alters neuronal phenotypes (12). Moreover, it has been demonstrated that persistent Cas9 expression elicits cytotoxic immune response, which removes genetically edited cells. The removal of modified cells in the brain could lead to adverse consequences, as brain cells have limited capacity to regenerate (105). The finding also means that CRISPR edits are not necessarily permanent, so repeat administration of CRISPR therapy would be required (106). Hence, non-viral delivery methods have received great interest recently; for instance, gold nanoparticles have been used to deliver Cas9 ribonucleoproteins targeting *mGluR5* in a mouse model of fragile X syndrome (12). Gold nanoparticles are safe, as they were not found to cause cytotoxicity or changes to neuronal functions at low doses. Also, they did not induce immune responses—a common problem arising from the delivery of CRISPR systems via viral methods (12).

Overall, nanoparticles seem an ideal carrier for delivering CRISPR systems into brain cells. Nanoparticles are versatile as their surfaces can be engineered to target specific cells. For instance, gold nanoparticles coated with exosomes have been shown to be able to cross the BBB via endocytosis (107, 108). To selectively target brain cells, the exosomes can be modified with a neuron-specific peptide derived from the rabies virus glycoprotein. This peptide specifically binds to the acetylcholine receptors expressed by neuronal cells (109, 110). Therefore, by modifying the surfaces of nanoparticles, we can ensure a CRISPR system is able to pass through the BBB and reach its target brain cells.

ETHICAL AND FUTURE PERSPECTIVES

In the last few years, CRISPR-driven research is rapidly increasing, and new cell and animal models have been created to elucidate the pathogenesis of HNDs. This is important groundwork for future research into new therapies. The family of CRISPR-Cas9 gene editors has been growing steadily. A variety of base editors and prime editors are continually being discovered that may improve the precision and efficacy of gene editing. Studies trialing the gene editors have resulted in various success rates. The simple mechanics of CRISPR make it a robust gene-editing tool; however, off-target editing is still a major concern and could have severe consequences (111). The safety of CRISPR editing should be guaranteed in two aspects. First, enhancing the precision of gene editing should remain at the core of future CRISPR-centric research. It may be helpful to pinpoint "hotspots" in the genome where off-target edits are most likely to arise. This may then lead to strategies that can effectively curb off-target editing in those DNA segments. Second, the chosen mode of CRISPR delivery should be non-toxic to neuronal cells and non-immunogenic. The body's immune response may suppress CRISPR gene therapy, and pose a health risk to the person receiving the treatment. Screening for potential immunological or allergic reactions to CRISPR should be performed before commencing therapy.

An appealing use of the CRISPR technique would be pre-emptive *in utero* editing of pathogenic gene mutations coupled with prenatal genetic testing (112–114). This would be better than delaying gene therapy until after birth, when the disease would have become manifest and the damage established. Some of the HNDs develop before birth; for instance, lissencephaly impairs cortical folding and is irreversible once the prenatal brain development is completed (115).

However, a long road lies ahead for the adoption of CRISPR-based gene editing in the clinics. What is therapeutic and what is not; or defining which genetic diseases should take priority for CRISPR therapy, are some difficult choices to make even in settings with relatively abundant health care resources. CRISPR therapy is likely to be costly—some estimates have priced it at USD $0.5 to $2 million, so funding it would be a challenge for most countries or insurance companies. Owing to the exorbitant costs of emerging gene therapies, health insurers may become increasingly selective in choosing their clients, excluding those diagnosed with "pre-existing conditions" (116, 117).

Ethical concerns are also important considerations before CRISPR can be used in humans. Genome editing in clinical settings is currently limited to somatic cells, as this is less likely than germline editing to be misused for non-ethical purposes. Potential problems may arise if "designer babies" are created using CRISPR. For instance, undetected off-target effects can be passed down to future generations and the undesirable negative consequences may be grave. Other ethical considerations include using CRISPR to achieve better phenotypic characteristics, such as height, intelligence, and athletic performance. This highlights the need for strict regulations and judicial frameworks on human germline editing. The National Institute of Health supports the call for an international moratorium on human germline editing in the clinical settings until certain conditions are met (118). Global discussions involving scientists and ethicists are needed to address how germline editing should be performed and ethically acceptable before the moratorium can be lifted.

In summary, CRISPR is an effective research tool for studying HNDs. If important safety and ethical concerns can be addressed, it has immense potential as a new treatment modality for HNDs. We expect more established CRISPR-based treatment strategies that bring new hopes for HNDs in the future.

AUTHOR CONTRIBUTIONS

All authors listed have made a substantial, direct and intellectual contribution to the work, and approved it for publication.

FUNDING

This work was supported by a grant from the Ministry of Higher Education, Malaysia, Fundamental Research Grant Scheme (FRGS/1/2019/SKK08/UKM/03/4).

REFERENCES

1. Cardoso AR, Lopes-Marques M, Silva RM, Serrano C, Amorim A, Prata MJ, et al. Essential genetic findings in neurodevelopmental disorders. *Hum Genom*. (2019) 13:31. doi: 10.1186/s40246-019-0216-4
2. Stiles J, Brown TT, Haist F, Jernigan TL. Brain and cognitive development. *Handb Child Psychol Dev Sci*. (2015) 2:1–54. doi: 10.1002/9781118963418.childpsy202
3. Qu H, Lei H, Fang X. Big data and the brain: peeking at the future. *Genom Proteomics Bioinform*. (2019) 17:333–6. doi: 10.1016/j.gpb.2019.11.003
4. Ingusci S, Verlengia G, Soukupova M, Zucchini S, Simonato M. Gene therapy tools for brain diseases. *Front Pharmacol*. (2019) 10:724. doi: 10.3389/fphar.2019.00724
5. Simonato M, Bennett J, Boulis NM, Castro MG, Fink DJ, Goins WF, et al. Progress in gene therapy for neurological disorders. *Nat Rev Neurol*. (2013) 9:277–91. doi: 10.1038/nrneurol.2013.56
6. Sondhi D, Peterson DA, Edelstein AM, del Fierro K, Hackett NR, Crystal RG. Survival advantage of neonatal CNS gene transfer for late infantile neuronal ceroid lipofuscinosis. *Exp Neurol*. (2008) 213:18–27. doi: 10.1016/j.expneurol.2008.04.022
7. Laoharawee K, DeKelver RC, Podetz-Pedersen KM, Rohde M, Sproul S, Nguyen H-O, et al. Dose-dependent prevention of metabolic and neurologic disease in murine MPS II by ZFN-mediated *in vivo* genome editing. *Mol Ther*. (2018) 26:1127–36. doi: 10.1016/j.ymthe.2018.03.002
8. Gupta RM, Musunuru K. Expanding the genetic editing tool kit: ZFNs, TALENs, and CRISPR-Cas9. *J Clin Invest*. (2014) 124:4154–61. doi: 10.1172/JCI72992
9. Li H, Yang Y, Hong W, Huang M, Wu M, Zhao X. Applications of genome editing technology in the targeted therapy of human diseases: mechanisms, advances and prospects. *Signal Transduct Targeted Ther*. (2020) 5:1. doi: 10.1038/s41392-019-0089-y
10. McCarty NS, Graham AE, Studená L, Ledesma-Amaro R. Multiplexed CRISPR technologies for gene editing and transcriptional regulation. *Nat Commun*. (2020) 11:1281. doi: 10.1038/s41467-020-15053-x
11. Stadtmauer EA, Fraietta JA. CRISPR-engineered T cells in patients with refractory cancer. *Science*. (2020) 367:eab7365. doi: 10.1126/science.aba7365
12. Lee B, Lee K, Panda S, Gonzales-Rojas R, Chong A, Bugay V, et al. Nanoparticle delivery of CRISPR into the brain rescues a mouse model of fragile X syndrome from exaggerated repetitive behaviours. *Nat Biomed Eng*. (2018) 2:497–507. doi: 10.1038/s41551-018-0252-8
13. Abe S, Kobayashi K, Oji A, Sakuma T, Kazuki K, Takehara S, et al. Modification of single-nucleotide polymorphism in a fully humanized CYP3A mouse by genome editing technology. *Sci Rep*. (2017) 7:15189. doi: 10.1038/s41598-017-15033-0
14. Harrod A, Fulton J, Nguyen VTM, Periyasamy M, Ramos-Garcia L, Lai CF, et al. Genomic modelling of the ESR1 Y537S mutation for evaluating function and new therapeutic approaches for metastatic breast cancer. *Oncogene*. (2017) 36:2286–96. doi: 10.1038/onc.2016.382
15. Moschino L, Zivanovic S, Hartley C, Trevisanuto D, Baraldi E, Roehr CC. Caffeine in preterm infants: where are we in 2020? *ERJ Open Res*. (2020) 6:00330-2019. doi: 10.1183/23120541.00330-2019
16. Kumral A, Tuzun F, Yesilirmak DC, Duman N, Ozkan H. Genetic basis of apnoea of prematurity and caffeine treatment response: role of adenosine receptor polymorphisms: genetic basis of apnoea of prematurity. *Acta paediatrica (Oslo, Norway: 1992)*. (2012) 101:e299–303. doi: 10.1111/j.1651-2227.2012.02664.x
17. Burney TJ, Davies JC. Gene therapy for the treatment of cystic fibrosis. *Appl Clin Genet*. (2012) 5:29–36. doi: 10.2147/TACG.S8873
18. Asher DR, Thapa K, Dharia SD, Khan N, Potter RA, Rodino-Klapac LR, et al. Clinical development on the frontier: gene therapy for duchenne muscular dystrophy. *Expert Opin Biol Ther*. (2020) 20:263–74. doi: 10.1080/14712598.2020.1725469
19. Goswami R, Subramanian G, Silayeva L, Newkirk I, Doctor D, Chawla K, et al. Gene therapy leaves a vicious cycle. *Front Oncol*. (2019) 9:297. doi: 10.3389/fonc.2019.00297
20. Niibori Y, Lee SJ, Minassian BA, Hampson DR. Sexually divergent mortality and partial phenotypic rescue after gene therapy in a mouse model of dravet syndrome. *Hum Gene Ther*. (2019) 31:339–51. doi: 10.1089/hum.2019.225
21. Turner TN, Douville C, Kim D, Stenson PD, Cooper DN, Chakravarti A, et al. Proteins linked to autosomal dominant and autosomal recessive disorders harbor characteristic rare missense mutation distribution patterns. *Hum Mol Genet*. (2015) 24:5995–6002. doi: 10.1093/hmg/ddv309
22. Yu-Wai-Man P. Genetic manipulation for inherited neurodegenerative diseases: myth or reality? *Br J Ophthalmol*. (2016) 100:1322. doi: 10.1136/bjophthalmol-2015-308329
23. Watts JK, Corey DR. Silencing disease genes in the laboratory and the clinic. *J Pathol*. (2012) 226:365–79. doi: 10.1002/path.2993
24. Aguiar S, van der Gaag B, Cortese FAB. RNAi mechanisms in Huntington's disease therapy: siRNA versus shRNA. *Transl Neurodegen*. (2017) 6:30. doi: 10.1186/s40035-017-0101-9
25. High-dose AAV gene therapy deaths. *Nat Biotechnol*. (2020) 38:910. doi: 10.1038/s41587-020-0642-9
26. Sibbald B. Death but one unintended consequence of gene-therapy trial. *CMAJ*. (2001) 164:1612.
27. Datsenko KA, Pougach K, Tikhonov A, Wanner BL, Severinov K, Semenova E. Molecular memory of prior infections activates the CRISPR/Cas adaptive bacterial immunity system. *Nat Commun*. (2012) 3:945. doi: 10.1038/ncomms1937
28. Jinek M, Chylinski K, Fonfara I, Hauer M, Doudna JA, Charpentier E. A programmable dual-RNA-guided DNA endonuclease in adaptive bacterial immunity. *Science (New York, NY)*. (2012) 337:816–21. doi: 10.1126/science.1225829
29. Cong L, Ran FA, Cox D, Lin S, Barretto R, Habib N, et al. Multiplex genome engineering using CRISPR/Cas systems. *Science (New York, NY)*. (2013) 339:819–23. doi: 10.1126/science.1231143
30. Anzalone AV, Koblan LW, Liu DR. Genome editing with CRISPR-Cas nucleases, base editors, transposases and prime editors. *Nat Biotechnol*. (2020) 38:824–44. doi: 10.1038/s41587-020-0561-9
31. Mao Z, Bozzella M, Seluanov A, Gorbunova V. Comparison of nonhomologous end joining and homologous recombination in human cells. *DNA Repair*. (2008) 7:1765–71. doi: 10.1016/j.dnarep.2008.06.018
32. Ryu SM, Hur JW, Kim K. Evolution of CRISPR towards accurate and efficient mammal genome engineering. *BMB Rep*. (2019) 52:475–81. doi: 10.5483/BMBRep.2019.52.8.149
33. Okamoto S, Amaishi Y, Maki I, Enoki T, Mineno J. Highly efficient genome editing for single-base substitutions using optimized ssODNs with Cas9-RNPs. *Sci Rep*. (2019) 9:4811. doi: 10.1038/s41598-019-41121-4
34. Devkota S. The road less traveled: strategies to enhance the frequency of homology-directed repair (HDR) for increased efficiency of CRISPR/Cas-mediated transgenesis. *BMB Rep*. (2018) 51:437–43. doi: 10.5483/BMBRep.2018.51.9.187
35. Zeng Y, Li J, Li G, Huang S, Yu W, Zhang Y, et al. Correction of the marfan syndrome pathogenic FBN1 mutation by base editing in human cells and heterozygous embryos. *Mol Ther*. (2018) 26:2631–7. doi: 10.1016/j.ymthe.2018.08.007
36. Komor AC, Kim YB, Packer MS, Zuris JA, Liu DR. Programmable editing of a target base in genomic DNA without double-stranded DNA cleavage. *Nature*. (2016) 533:420–4. doi: 10.1038/nature17946
37. Anzalone AV, Randolph PB, Davis JR, Sousa AA, Koblan LW, Levy JM, et al. Search-and-replace genome editing without double-strand breaks or donor DNA. *Nature*. (2019) 576:149–57. doi: 10.1038/s41586-019-1711-4
38. Zhou C, Zhang M, Wei Y, Sun Y, Sun Y, Pan H, et al. Highly efficient base editing in human tripronuclear zygotes. *Protein Cell*. (2017) 8:772–5. doi: 10.1007/s13238-017-0459-6
39. Levy JM, Yeh WH. Cytosine and adenine base editing of the brain, liver, retina, heart and skeletal muscle of mice *via* adeno-associated viruses. *Nat Biomed Eng*. (2020) 4:97–110. doi: 10.1038/s41551-019-0501-5
40. Dixon-Salazar TJ, Gleeson JG. Genetic regulation of human brain development: lessons from Mendelian diseases. *Ann NY Acad Sci*. (2010) 1214:156–67. doi: 10.1111/j.1749-6632.2010.05819.x
41. Burgio G. Redefining mouse transgenesis with CRISPR/Cas9 genome editing technology. *Genome Biol*. (2018) 19:27. doi: 10.1186/s13059-018-1424-2
42. Foulkes AL, Soda T, Farrell M, Giusti-Rodríguez P, Lázaro-Muñoz G. Legal and ethical implications of crispr applications in psychiatry. *N C Law Rev*. (2019) 97:1359–98.

43. Fink JJ, Robinson TM, Germain ND, Sirois CL, Bolduc KA, Ward AJ, et al. Disrupted neuronal maturation in Angelman syndrome-derived induced pluripotent stem cells. *Nat Commun*. (2017) 8:15038. doi: 10.1038/ncomms15038
44. Dodge A, Peters MM, Greene HE, Dietrick C, Botelho R, Chung D, et al. Generation of a novel rat model of angelman syndrome with a complete Ube3a gene deletion. *Autism Res*. (2020) 13:397–409. doi: 10.1002/aur.2267
45. Kou Z, Wu Q, Kou X, Yin C, Wang H, Zuo Z, et al. CRISPR/Cas9-mediated genome engineering of the ferret. *Cell Res*. (2015) 25:1372–5. doi: 10.1038/cr.2015.130
46. Shinmyo Y, Terashita Y, Dinh Duong TA, Horiike T, Kawasumi M, Hosomichi K, et al. Folding of the cerebral cortex requires Cdk5 in upper-layer neurons in gyrencephalic mammals. *Cell Rep*. (2017) 20:2131–43. doi: 10.1016/j.celrep.2017.08.024
47. Eaton SL, Proudfoot C, Lillico SG, Skehel P, Kline RA, Hamer K, et al. CRISPR/Cas9 mediated generation of an ovine model for infantile neuronal ceroid lipofuscinosis (CLN1 disease). *Sci Rep*. (2019) 9:9891. doi: 10.1038/s41598-019-45859-9
48. Sun T, Hevner RF. Growth and folding of the mammalian cerebral cortex: from molecules to malformations. *Nat Rev Neurosci*. (2014) 15:217–32. doi: 10.1038/nrn3707
49. Ellenbroek B, Youn J. Rodent models in neuroscience research: is it a rat race? *Dis Model Mech*. (2016) 9:1079. doi: 10.1242/dmm.026120
50. Hodge RD, Bakken TE, Miller JA, Smith KA, Barkan ER, Graybuck LT, et al. Conserved cell types with divergent features in human versus mouse cortex. *Nature*. (2019) 573:61–8.
51. Yang W, Li S, Li X-J. A CRISPR monkey model unravels a unique function of PINK1 in primate brains. *Mol Neurodegen*. (2019) 14:17. doi: 10.1186/s13024-019-0321-9
52. Marini RP, Otto G, Erdman S, Palley L, Fox JG. Biology and diseases of ferrets. *Lab Anim Med*. (2002):483–517. doi: 10.1016/B978-012263951-7/50016-8
53. Nibe K, Miwa Y, Matsunaga S, Chambers JK, Uetsuka K, Nakayama H, et al. Clinical and pathologic features of neuronal ceroid-lipofuscinosis in a ferret (*Mustela putorius furo*). *Vet Pathol*. (2011) 48:1185–9. doi: 10.1177/0300985811400441
54. Yang W, Liu Y, Tu Z, Xiao C, Yan S, Ma X, et al. CRISPR/Cas9-mediated PINK1 deletion leads to neurodegeneration in rhesus monkeys. *Cell Res*. (2019) 29:334–6. doi: 10.1038/s41422-019-0142-y
55. Zuo E, Huo X, Yao X, Hu X, Sun Y, Yin J, et al. CRISPR/Cas9-mediated targeted chromosome elimination. *Genome Biol*. (2017) 18:224. doi: 10.1186/s13059-017-1354-4
56. Ou L, Przybilla MJ, Tăbăran A-F, Overn P, O'Sullivan MG, Jiang X, et al. A novel gene editing system to treat both Tay-Sachs and Sandhoff diseases. *Gene Ther*. (2020) 27:226–36. doi: 10.1038/s41434-019-0120-5
57. von Hammerstein AL, Eggel M, Biller-Andorno N. Is selecting better than modifying? An investigation of arguments against germline gene editing as compared to preimplantation genetic diagnosis. *BMC Med Ethics*. (2019) 20:83. doi: 10.1186/s12910-019-0411-9
58. Peranteau WH, Flake AW. The future of *in utero* gene therapy. *Mol Diagn Ther*. (2020) 24:135–42. doi: 10.1007/s40291-020-00445-y
59. Coller BS. Ethics of human genome editing. *Ann Rev Med*. (2019) 70:289–305. doi: 10.1146/annurev-med-112717-094629
60. Jacinto FV, Link W, Ferreira BI. CRISPR/Cas9-mediated genome editing: from basic research to translational medicine. *J Cell Mol Med*. (2020) 24:3766–78. doi: 10.1111/jcmm.14916
61. Ho BX, Loh SJH, Chan WK, Soh BS. *In vivo* genome editing as a therapeutic approach. *Int J Mol Sci*. (2018) 19:2721. doi: 10.3390/ijms19092721
62. Rui Y, Wilson DR, Green JJ. Non-viral delivery to enable genome editing. *Trends Biotechnol*. (2019) 37:281–93. doi: 10.1016/j.tibtech.2018.08.010
63. Jackson M, Marks L, May GHW. The genetic basis of disease. *Essays Biochem*. (2018) 62:643–723. doi: 10.1042/EBC20170053
64. Paluszkiewicz SM, Martin BS, Huntsman MM. Fragile X syndrome: the GABAergic system and circuit dysfunction. *Dev Neurosci*. (2011) 33:349–64. doi: 10.1159/000329420
65. Dölen G, Osterweil E, Rao BS, Smith GB, Auerbach BD, Chattarji S, et al. Correction of fragile X syndrome in mice. *Neuron*. (2007) 56:955–62. doi: 10.1016/j.neuron.2007.12.001
66. Barnes SA, Pinto-Duarte A, Kappe A, Zembrzycki A, Metzler A, Mukamel EA, et al. Disruption of mGluR5 in parvalbumin-positive interneurons induces core features of neurodevelopmental disorders. *Mol Psychiatry*. (2015) 20:1161–72. doi: 10.1038/mp.2015.113
67. Erickson CA, Davenport MH, Schaefer TL, Wink LK, Pedapati EV, Sweeney JA, et al. Fragile X targeted pharmacotherapy: lessons learned and future directions. *J Neurodev Disord*. (2017) 9:7. doi: 10.1186/s11689-017-9186-9
68. Kazemi M, Salehi M, Kheirollahi M. Down syndrome: current status, challenges and future perspectives. *Int J Mol Cell Med*. (2016) 5:125–33. doi: 10.1038/s41586-019-1506-7
69. Haydar TF, Reeves RH. Trisomy 21 and early brain development. *Trends Neurosci*. (2012) 35:81–91. doi: 10.1016/j.tins.2011.11.001
70. Akutsu SN, Fujita K, Tomioka K, Miyamoto T. Applications of genome editing technology in research on chromosome aneuploidy disorders. *Cells*. (2020) 9:239. doi: 10.3390/cells9010239
71. Tafazoli A, Behjati F, Farhud DD, Abbaszadegan MR. Combination of genetics and nanotechnology for down syndrome modification: a potential hypothesis and review of the literature. *Iran J Public Health*. (2019) 48:371–8. doi: 10.18502/ijph.v48i3.878
72. Czermiński JT, Lawrence JB. Silencing trisomy 21 with XIST in neural stem cells promotes neuronal differentiation. *Dev Cell*. (2020) 52:294–308.e3. doi: 10.1016/j.devcel.2019.12.015
73. Panning B. X-chromosome inactivation: the molecular basis of silencing. *J Biol*. (2008) 7:30. doi: 10.1186/jbiol95
74. Karimzadeh P, Jafari N, Nejad Biglari H, Jabbeh Dari S, Ahmad Abadi F, Alaee MR, et al. GM2-gangliosidosis (Sandhoff and Tay Sachs disease): diagnosis and neuroimaging findings (An Iranian pediatric case series). *Iran J Child Neurol*. (2014) 8:55–60.
75. Boles DJ, Proia RL. The molecular basis of HEXA mRNA deficiency caused by the most common Tay-Sachs disease mutation. *Am J Hum Genet*. (1995) 56:716–24.
76. Schmidt B, Roberts RS, Davis P, Doyle LW, Barrington KJ, Ohlsson A, et al. Long-term effects of caffeine therapy for apnea of prematurity. *N Engl J Med*. (2007) 357:1893–902. doi: 10.1056/NEJMoa073679
77. Winerdal M, Urmaliya V, Winerdal ME, Fredholm BB, Winqvist O, Ådén U. Single Dose Caffeine Protects the Neonatal Mouse Brain against Hypoxia Ischemia. *PLoS ONE*. (2017) 12:e0170545. doi: 10.1371/journal.pone.0170545
78. Tanaka K, Ishitsuka Y, Kurauchi Y, Yamaguchi K, Kadowaki D, Irikura M, et al. Comparative effects of respiratory stimulants on hypoxic neuronal cell injury in SH-SY5Y cells and in hippocampal slice cultures from rat pups. *Pediatr Int*. (2013) 55:320–7. doi: 10.1111/ped.12079
79. Di Martino E, Bocchetta E, Tsuji S, Mukai T, Harris RA, Blomgren K, et al. Defining a time window for neuroprotection and glia modulation by caffeine after neonatal hypoxia-ischaemia. *Mol Neurobiol*. (2020) 57:2194–205. doi: 10.1007/s12035-020-01867-9
80. Sun H, Gonzalez F, McQuillen PS. Caffeine restores background EEG activity independent of infarct reduction after neonatal hypoxic ischemic brain injury. *Dev Neurosci*. (2020) 42:72–82. doi: 10.1159/000509365
81. Yu NY, Bieder A, Raman A, Mileti E, Katayama S, Einarsdottir E, et al. Acute doses of caffeine shift nervous system cell expression profiles toward promotion of neuronal projection growth. *Sci Rep*. (2017) 7:11458. doi: 10.1038/s41598-017-11574-6
82. Mokhtar WA, Fawzy A, Allam RM, Zidan N, Hamed MS. Association between adenosine receptor gene polymorphism and response to caffeine citrate treatment in apnea of prematurity; An Egyptian single-center study. *Egypt Pediatr Assoc Gazette*. (2018) 66:115–20. doi: 10.1016/j.epag.2018.09.001
83. Kumar VHS, Lipshultz SE. Caffeine and clinical outcomes in premature neonates. *Children (Basel, Switzerland)*. (2019) 6:118. doi: 10.3390/children6110118
84. Kim YB, Komor AC, Levy JM. Increasing the genome-targeting scope and precision of base editing with engineered Cas9-cytidine deaminase fusions. *Nat Biotechnol*. (2017) 35:371–6. doi: 10.1038/nbt.3803
85. Tan J, Zhang F, Karcher D, Bock R. Expanding the genome-targeting scope and the site selectivity of high-precision base editors. *Nat Commun*. (2020) 11:629. doi: 10.1038/s41467-020-14465-z

86. Lee HK, Smith HE, Liu C, Willi M, Hennighausen L. Cytosine base editor 4 but not adenine base editor generates off-target mutations in mouse embryos. *Commun Biol*. (2020) 3:19. doi: 10.1038/s42003-019-0745-3
87. Jin S, Zong Y, Gao Q, Zhu Z, Wang Y, Qin P, et al. Cytosine, but not adenine, base editors induce genome-wide off-target mutations in rice. *Science (New York, NY)*. (2019) 364:292–5. doi: 10.1126/science.aaw7166
88. Wienert B, Wyman SK. Unbiased detection of CRISPR off-targets *in vivo* using DISCOVER-Seq. *Science*. (2019) 364:286–9. doi: 10.1126/science.aav9023
89. Ek CJ, Dziegielewska KM, Habgood MD, Saunders NR. Barriers in the developing brain and Neurotoxicology. *Neurotoxicology*. (2012) 33:586–604. doi: 10.1016/j.neuro.2011.12.009
90. Wang D, Tai PWL, Gao G. Adeno-associated virus vector as a platform for gene therapy delivery. *Nat Rev Drug Discov*. (2019) 18:358–78. doi: 10.1038/s41573-019-0012-9
91. Dong X. Current strategies for brain drug delivery. *Theranostics*. (2018) 8:1481–93. doi: 10.7150/thno.21254
92. Hanlon KS, Meltzer JC, Buzhdygan T, Cheng MJ, Sena-Esteves M, Bennett RE, et al. Selection of an efficient AAV vector for robust CNS transgene expression. *Mol Ther Methods Clin Dev*. (2019) 15:320–32. doi: 10.1016/j.omtm.2019.10.007
93. Lau CH, Ho JW, Lo PK, Tin C. Targeted transgene activation in the brain tissue by systemic delivery of engineered AAV1 expressing CRISPRa. *Mol Ther Nucleic Acids*. (2019) 16:637–49. doi: 10.1016/j.omtn.2019.04.015
94. Deverman BE, Pravdo PL, Simpson BP, Kumar SR, Chan KY, Banerjee A, et al. Cre-dependent selection yields AAV variants for widespread gene transfer to the adult brain. *Nat Biotechnol*. (2016) 34:204–9. doi: 10.1038/nbt.3440
95. Chan KY, Jang MJ, Yoo BB, Greenbaum A, Ravi N, Wu WL, et al. Engineered AAVs for efficient noninvasive gene delivery to the central and peripheral nervous systems. *Nat Neurosci*. (2017) 20:1172–9. doi: 10.1038/nn.4593
96. Hordeaux J, Yuan Y, Clark PM, Wang Q, Martino RA, Sims JJ, et al. The GPI-linked protein LY6A drives AAV-PHP.B transport across the blood-brain barrier. *Mol Ther*. (2019) 27:912–21. doi: 10.1016/j.ymthe.2019.02.013
97. Huang Q, Chan KY, Tobey IG, Chan YA, Poterba T, Boutros CL, et al. Delivering genes across the blood-brain barrier: LY6A, a novel cellular receptor for AAV-PHP.B capsids. *PLoS ONE*. (2019) 14:e0225206. doi: 10.1371/journal.pone.0225206
98. Batista AR, King OD, Reardon CP, Davis C, Shankaracharya, Philip V, et al. Ly6a differential expression in blood-brain barrier is responsible for strain specific central nervous system transduction profile of AAV-PHP.B. *Hum Gene Ther*. (2019) 31:90–102. doi: 10.1089/hum.2019.186
99. Kaushik A, Yndart A, Atluri V, Tiwari S, Tomitaka A, Gupta P, et al. Magnetically guided non-invasive CRISPR-Cas9/gRNA delivery across blood-brain barrier to eradicate latent HIV-1 infection. *Sci Rep*. (2019) 9:3928. doi: 10.1038/s41598-019-40222-4
100. Van Rie A, Harrington PR, Dow A, Robertson K. Neurologic and neurodevelopmental manifestations of pediatric HIV/AIDS: a global perspective. *EJPN*. (2007) 11:1–9. doi: 10.1016/j.ejpn.2006.10.006
101. Wilmshurst JM, Hammond CK, Donald K, Hoare J, Cohen K, Eley B. NeuroAIDS in children. *Handb Clin Neurol*. (2018) 152:99–116. doi: 10.1016/B978-0-444-63849-6.00008-6
102. Yourik P, Fuchs RT, Mabuchi M, Curcuru JL, Robb GB. *Staphylococcus aureus* Cas9 is a multiple-turnover enzyme. *RNA (New York, NY)*. (2019) 25:35–44. doi: 10.1261/rna.067355.118
103. Charlesworth CT, Deshpande PS, Dever DP, Camarena J, Lemgart VT, Cromer MK, et al. Identification of preexisting adaptive immunity to Cas9 proteins in humans. *Nat Med*. (2019) 25:249–54. doi: 10.1038/s41591-018-0326-x
104. Swiech L, Heidenreich M, Banerjee A, Habib N, Li Y, Trombetta J, et al. *In vivo* interrogation of gene function in the mammalian brain using CRISPR-Cas9. *Nat Biotechnol*. (2015) 33:102–6. doi: 10.1038/nbt.3055
105. Li A, Tanner MR, Lee CM, Hurley AE, De Giorgi M, Jarrett KE, et al. AAV-CRISPR gene editing is negated by pre-existing immunity to Cas9. *Mol Ther*. (2020) 28:1432–41. doi: 10.1016/j.ymthe.2020.04.017
106. Yang S, Chang R, Yang H, Zhao T, Hong Y, Kong HE, et al. CRISPR/Cas9-mediated gene editing ameliorates neurotoxicity in mouse model of Huntington's disease. *J Clin Invest*. (2017) 127:2719–24. doi: 10.1172/JCI92087
107. Betzer O, Perets N, Angel A, Motiei M, Sadan T, Yadid G, et al. *In vivo* neuroimaging of exosomes using gold nanoparticles. *ACS Nano*. (2017) 11:10883–93. doi: 10.1021/acsnano.7b04495
108. Chen CC, Liu L, Ma F, Wong CW, Guo XE, Chacko JV, et al. Elucidation of exosome migration across the blood-brain barrier model *in vitro*. *Cell Mol Bioeng*. (2016) 9:509–29. doi: 10.1007/s12195-016-0458-3
109. Khongkow M, Yata T, Boonrungsiman S, Ruktanonchai UR, Graham D, Namdee K. Surface modification of gold nanoparticles with neuron-targeted exosome for enhanced blood-brain barrier penetration. *Sci Rep*. (2019) 9:8278. doi: 10.1038/s41598-019-44569-6
110. Alvarez-Erviti L, Seow Y, Yin H, Betts C, Lakhal S, Wood MJA. Delivery of siRNA to the mouse brain by systemic injection of targeted exosomes. *Nat Biotechnol*. (2011) 29:341–5. doi: 10.1038/nbt.1807
111. Zhang X-H, Tee LY, Wang X-G, Huang Q-S, Yang S-H. Off-target effects in CRISPR/Cas9-mediated genome engineering. *Mol Ther Nucleic Acids*. (2015) 4:e264. doi: 10.1038/mtna.2015.37
112. Ma H, Marti-Gutierrez N, Park SW, Wu J, Lee Y, Suzuki K, et al. Correction of a pathogenic gene mutation in human embryos. *Nature*. (2017) 548:413–9. doi: 10.1038/nature23305
113. Rose BI, Brown S. Genetically modified babies and a first application of clustered regularly interspaced short palindromic repeats (CRISPR-Cas9). *Obstet Gynecol*. (2019) 134:157–62. doi: 10.1097/AOG.0000000000003327
114. Rossidis AC, Stratigis JD, Chadwick AC, Hartman HA, Ahn NJ, Li H, et al. *In utero* CRISPR-mediated therapeutic editing of metabolic genes. *Nat Med*. (2018) 24:1513–8. doi: 10.1038/s41591-018-0184-6
115. Alhasan M, Mathkour M, Milburn JM. Clinical images: postterm newborn with lissencephaly presented with seizure: case report and review of literature. *Ochsner J*. (2015) 15:127–9.
116. Sherkow JS. CRISPR, Patents, and the public health. *Yale J Biol Med*. (2017) 90:667–72.
117. Wilson RC, Carroll D. The daunting economics of therapeutic genome editing. *CRISPR J*. (2019) 2:280–4. doi: 10.1089/crispr.2019.0052
118. Wolinetz CD, Collins FS. NIH supports call for moratorium on clinical uses of germline gene editing. *Nature*. (2019) 567:175. doi: 10.1038/d41586-019-00814-6

Conflict of Interest: The authors declare that the research was conducted in the absence of any commercial or financial relationships that could be construed as a potential conflict of interest.

frontiers in Pediatrics

BRIEF RESEARCH REPORT
published: 11 March 2021
doi: 10.3389/fped.2021.614209

Studying the Effects of Granulocyte-Macrophage Colony-Stimulating Factor on Fetal Lung Macrophages During the Perinatal Period Using the Mouse Model

Fook-Choe Cheah[1], Pietro Presicce[2,3], Tian-Lee Tan[1], Brenna C. Carey[2] and Suhas G. Kallapur[2,3]*

[1] Neonatal Intensive Care Unit, Department of Paediatrics, Faculty of Medicine, Universiti Kebangsaan Malaysia Medical Centre, Hospital Canselor Tuanku Muhriz, Kuala Lumpur, Malaysia, [2] Division of Pulmonary Biology, Cincinnati Children's Hospital Medical Center, Cincinnati, OH, United States, [3] David Geffen School of Medicine, University of California, Los Angeles, Los Angeles, CA, United States

OPEN ACCESS

Edited by:
Henry J. Rozycki,
Virginia Commonwealth University,
United States

Reviewed by:
Trent E. Tipple,
University of Oklahoma Health Sciences Center, United States
Vineet Bhandari,
Cooper University Hospital,
United States

***Correspondence:**
Fook-Choe Cheah
cheahfc@ppukm.ukm.edu.my

Specialty section:
This article was submitted to Neonatology, a section of the journal Frontiers in Pediatrics

Received: 05 October 2020
Accepted: 17 February 2021
Published: 11 March 2021

Citation:
Cheah F-C, Presicce P, Tan T-L, Carey BC and Kallapur SG (2021) Studying the Effects of Granulocyte-Macrophage Colony-Stimulating Factor on Fetal Lung Macrophages During the Perinatal Period Using the Mouse Model. Front. Pediatr. 9:614209. doi: 10.3389/fped.2021.614209

Background: Granulocyte-macrophage colony-stimulating factor (GM-CSF) is a pro-inflammatory cytokine that is increased in the amniotic fluid in chorioamnionitis and elevated in the fetal lung with endotoxin exposure. Although GM-CSF has a pivotal role in fetal lung development, it stimulates pulmonary macrophages and is associated with the development of bronchopulmonary dysplasia (BPD). How antenatal GM-CSF results in recruitment of lung macrophage leading to BPD needs further elucidation. Hence, we used a transgenic and knock-out mouse model to study the effects of GM-CSF focusing on the fetal lung macrophage.

Methods: Using bitransgenic (BTg) mice that conditionally over-expressed pulmonary GM-CSF after doxycycline treatment, and GM-CSF knock-out (KO) mice with no GM-CSF expression, we compared the ontogeny and immunophenotype of lung macrophages in BTg, KO and control mice at various prenatal and postnatal time points using flow cytometry and immunohistology.

Results: During fetal life, compared to controls, BTg mice over-expressing pulmonary GM-CSF had increased numbers of lung macrophages that were $CD68^{+}$ and these were primarily located in the interstitium rather than alveolar spaces. The lung macrophages that accumulated were predominantly $CD11b^{+}F4/80^{+}$ indicating immature macrophages. Conversely, lung macrophages although markedly reduced, were still present in GM-CSF KO mice.

Conclusion: Increased exposure to GM-CSF antenatally, resulted in accumulation of immature macrophages in the fetal lung interstitium. Absence of GM-CSF did not abrogate but delayed the transitioning of interstitial macrophages. Together, these results suggest that other perinatal factors may be involved in modulating the maturation of alveolar macrophages in the developing fetal lung.

Keywords: bronchopulmonary dysplasia, chorioamnionitis, GM-CSF overexpression, intrauterine inflammation or infection, GM-CSF knockout, interstitial macrophages, alveolar macrophages, transgenic mice

INTRODUCTION

Granulocyte-macrophage colony-stimulating factor (GM-CSF) is a glycoprotein which was discovered as a hemopoietic growth factor based on its ability to stimulate bone marrow cell proliferation in a mouse lung-conditioned medium (1). It is now evident that GM-CSF also exhibits immunomodulatory effects and serves as one of the major cytokines during inflammation (2–4). In the lung, the locally expressed GM-CSF have both autocrine and paracrine functions on type II alveolar epithelial cells and alveolar macrophages, respectively (5, 6). During pregnancy, the level of GM-CSF is developmentally regulated and is elevated in the presence of chorioamnionitis and other inflammatory conditions (7, 8). Endotoxin-induced chorioamnionitis resulted in increased GM-CSF in the amniotic fluid and fetal sheep lung, but not in the fetal circulation, suggesting that chorioamnionitis induced local expression of GM-CSF and could have profound effects on the developing fetal lung (9).

Intriguingly, augmentation of GM-CSF resulted in the proliferation of type II alveolar epithelial cells, restoration of alveolar epithelial barrier function, increased vascular endothelial growth factor expression, enhancement of lung growth and surfactant phospholipid production in several animal models, suggesting the role of this cytokine in the lung reparative and remodeling process (5, 10–12). These may underlie clinical observations of a lesser burden of respiratory distress syndrome in preterm infants with intrauterine exposure to chorioamnionitis (13–15). In fact, GM-CSF is essential for alveolar macrophage (AM) phenotypic and functional maturation via its downstream transcriptional factor PU.1 and peroxisome proliferator-activated receptor-γ (PPAR-γ) (16–19). As the AM is also crucial in alveolar surfactant catabolism (16, 17), ablation of the mice genetic loci for GM-CSF, although does not perturb lung morphogenesis (10), leads to the abnormal deposition of surfactant in the alveolar space, a typical characteristic of pulmonary alveolar proteinosis (16, 20).

The development of fetal AM is thought to begin antenatally in the lung interstitium and translocate into the alveolar sacs in the first week of postnatal life (18, 21–24). The fetal monocytes first colonize the developing lung and differentiate into the primitive AM from embryonic day 18.5 in the lung interstitium, which corresponds to the saccular phase of alveolar development (18). Subsequently, the primitive AM differentiates into mature AM under the influence of GM-CSF surge that occurs in the perinatal period, and they reside in the alveoli with minimal turnover (18). However, more recently, the study on the ontogeny of lung macrophages elegantly showed that during postnatal and adult life, the lung interstitium could be re-populated in a third "wave" with non-embryonic bone marrow-derived macrophages (25). This phase may be less dependent on GM-CSF as Dranoff et al. in their seminal paper surmised that the ablation of this cytokine did not appear to critically affect basal hematopoesis (26).

During an inflammatory process, macrophage recruitment in the alveolar sacs are associated with delayed alveolar and pulmonary vasculature development, similar to lung changes seen in infants with bronchopulmonary dysplasia (BPD) (27–29). In preterm infants, the early alteration in pulmonary expression of GM-CSF during postnatal life has been found to precede the development of BPD (30).

Together, these observations suggest a balance in GM-CSF levels may exist during the perinatal period affecting AM trafficking and maturation, which is still largely unclear. Disruption of this balance may predispose to the development of BPD in preterm infants. Therefore, we used animal models with GM-CSF over-expression and knock-out to study the effects on the AM during the saccular phase of alveolar development in late gestation and early postnatal life. The results may serve as a platform for the further evaluation of the direct effects of GM-CSF on BPD development.

MATERIALS AND METHODS

Mice

Animal experiments were performed following protocols approved by the Cincinnati Children's Hospital Medical Center Animal Care Committee (IACUC S3D01004). Wild type mice (Charles River, Wilmington MA), and transgenic mice in this study were on the C57Bl/6 background. All mice were housed in a barrier facility with a continuous supply of purified water, air and food, which was supplemented with doxycycline (Dox) if indicated. The female mice were checked for vaginal plug the morning after the night of breeding, and plug presence was recorded as embryonic day 0.5 (E0.5). For the study of fetal lungs, the pregnant dams were euthanized by carbon dioxide narcosis, the fetuses surgically delivered and mouse pups were sacrificed with intraperitoneal pentobarbital injection.

GM-CSF Overexpressing and GM-CSF Knockout Mice

Inducible lung-specific GM-CSF expressing bi-transgenic mice (BTg) were generated previously by crossing the reverse

tetracycline-activator (rtTA)-Clara cell secretory protein (CCSP) line with the (tet-O)$_7$-CMV-GM-CSF line. In this system, inducible expression of GM-CSF is mediated by rtTA binding to the tet-operator, switched on by Dox administered in the food. Lung epithelial-specific GM-CSF expression is mediated by the CCSP promoter, which directs transgene expression at high levels in non-ciliated respiratory epithelial cells of the tracheal-bronchial and bronchiolar regions of the lung starting at embryonic day 14.5 (31). To generate single transgenic (STg) mice [rtTA-CCSP or (tet-O)$_7$-CMV-GM-CSF] and WT mice as littermate controls for BTg mice, male BTg mice were bred with WT females. Pregnant mice received daily Dox starting at gestational day E14.5. The GM-CSF KO mice, generated by Dr. Glenn Dranoff (26), were backcrossed for at least eight generations into the C57Bl/6 strain.

Genotyping

Mouse tails were digested using proteinase K (1 mg/mL) in lysis buffer containing Tris HCL pH 8, 0.5 M EDTA, 5 M NaCl, and 20% SDS. The samples were precipitated with KOAc and washed with pure ETOH followed by 70% ETOH, dried, and the pellets were reconstituted in Tris-EDTA buffer. Genotyping was done using the following primers with GoTaq Green Master Mix (Promega Corporation, Madison, WI) with minor modifications of the manufacturer's protocol.

CCSP-rtTA 5′ ACT GCC CAT TGC CCA AAC AC
CCSP-rtTA 3′ AAA ATC TTG CCA GCT TTC CCC
(tet-O)$_7$-GM-CSF 5′ GCC ATC CAC GCT GTT TTG AC
(tet-O)$_7$-GM-CSF 3′ CCT GGG CTT CCT CAT TTT TGG.

Animal Procedures

To obtain bronchoalveolar lavage fluid (BALF), the fetal (E18.5) and neonatal (postnatal, PN day 1–14) mice were dissected under a microscope, trachea exposed and cannulated and flushed with 0.5–1.0 mL cold sterile PBS (pH 7.4) through a 25 Fr gauge needle. BALF was used for cell counts and differential counts using Diff-Quik staining, flow cytometry cell studies and for GM-CSF protein measurement in the supernatant collected from select animals using ELISA assay (Endogen, Inc., Boston, MA). Lung cell suspensions were made in tissue culture media (RPMI + 10% FCS) by mincing the left lung under gentle pressure and filtered using a 50 μm nylon mesh.

Flow Cytometric Analyses

Lung cells were suspended at a density of 1×10^6 cells/100 μL media. Cell viability was determined using trypan blue exclusion and was found to be >90% viable for all the experiments. The antibodies used in the study were based on validated markers for immunophenotyping lung monocyte/macrophage (32). The following antibodies were used: Rat anti-mouse F4/80 - FITC (BM8) (Abcam, Cambridge, MA), CD11b - APC (M1/70) (BD Pharmingen, San Diego, CA) and CD68 - RPE (AbD Serotec, Raleigh, NC). Appropriate isotype-control antibodies were used. The cells were reacted with the antibodies for 30 min on ice followed by washing × 3. At least 10,000 events were recorded for each sample using the BD FACSCalibur™ flow cytometer (Becton, Dickinson and Co., Franklin Lakes, NJ), and analyses were done using the FlowJo software (Ver 9.5.2, Treestar, Ashland, OR). Cells above the isotype background intensity were considered as positively stained cells. The values were expressed as proportions of positively labeled cells.

Lung Tissue Immunohistochemistry

For lung tissue immunohistochemistry, thoraces from embryonic and PN day 1 pups were immersed in ice-cold 4% paraformaldehyde in PBS overnight. For PN day 4, 7, and 14 mouse pups, after cannulation of the trachea, the lungs were inflation fixed with 4% paraformaldehyde at 25 cm H_2O pressure. The fixed lung tissues were washed three times in PBS and dehydrated in ethanol before paraffin embedding or immersed in 30% sucrose followed by mounting in the cryoprotectant OCT and frozen at −80°C before immunostaining. Lung tissues for CD68 were immunostained using 5 μm sections from OCT embedded lung specimen (Rat anti-mouse CD68 AbD Serotec, Raleigh, NC). Myeloperoxidase (MPO) staining of lung samples was done on formalin fixed lung tissue cut in 5 μm sections (rabbit polyclonal anti-MPO Cell Marque Corp., Rocklin, CA). For the paraffin embedded sections, antigen retrieval was performed by boiling the tissues in citrate buffer followed by quenching of endogenous peroxidase activity with hydrogen peroxide. Non-specific binding was blocked with 5% goat serum before overnight incubation at 4°C with anti-CD68 (1:100) or anti-MPO antibody (1:200). The sections were washed followed by incubation at room temperature for 1 h with a secondary biotinylated goat anti-rabbit antibody (Vector Laboratories, Burlingame, CA) diluted at 1:200. Immunoreactivity was determined by the diaminobenzidine method. The tissues were counterstained with nuclear fast red. Quantitative cell counts were performed in a blinded fashion by counting $CD68^+$ cells in 5 random microscopic fields per animal in at least 3 animals per group.

Statistics

Statistical analyses were performed with SigmaStat v.1.0 (Jandel, San Rafael, CA) and GraphPad, Prism v.6.03 (GraphPad Software, Inc., La Jolla, CA). Comparisons of two groups were made with unpaired *t*-tests and the results are presented as means and SD. For comparisons of more than two groups, ANOVA followed by Student-Newman-Keuls tests for *post-hoc* analyses were used. Significance was accepted at $P < 0.05$.

RESULTS

We used both WT and STg littermates as controls for the BTg experimental fetal mice. We confirmed the non-inducible GM-CSF expression in the WT and STg littermates showing no differences in the percentages of positive F4/80 and CD11b cells on flow cytometry or CD68 positive macrophages on lung immunohistology after Dox treatment at E16.5 and E18.5 (**Supplementary Figure 1**). Thus, the controls used in this study were a composite of WT and/or STg genotypes. Similarly, in the CCSP-rtTA model with constitutive and inducible *Fgf*-7, WT and STg did not overexpress when given Dox as compared with the BTg (31).

Antenatal GM-CSF Overexpression Increased Macrophages in the Fetal Lung

Switching on with Dox resulted in markedly increased GM-CSF in BALF of BTg, E18.5 fetal mice (236 ± 171 pg/mL for BTg mice vs. 2.5 ± 2.8 pg/mL, for controls, respectively, $p < 0.05$. There was no difference in mean GM-CSF levels between the WT and STg; 3.2 and 2.3 pg/mL, respectively). This was consistent with a previously reported study that constitutive levels of GM-CSF in the BALF of these mice were at the limit of detection of the assay, 5 pg/mL (10). Concordantly, compared to littermate controls, BTg fetuses exposed to Dox at E14.5 showed accumulation of $CD68^+$ macrophages by immunohistology on days E16.5 and E18.5 (**Figures 1A–E**). These cells had a typical mononuclear morphology (**Figure 1E**, inset), and lacked MPO expression. Almost all the lung macrophages in the E18.5 BTg mice were interstitial with <5% alveolar macrophages (**Figure 1F**). Immuno-phenotyping results of these interstitial cells by flow cytometry of fetal lung suspensions in response to GM-CSF is shown in **Figure 1G**. Compared to control littermates, BTg fetuses had a 3-fold increase in lung $CD68^+$ cells (**Figure 1H**).

It has been reported that interstitial lung macrophages are $CD11b^+$ and $F4/80^{low}$ while alveolar macrophages are $CD11b^-$ and $F4/80^{high}$ in adult mice (32). Moreover, immature macrophages have lower side and forward scatter properties (18). We therefore sought to further determine the characteristics of antenatal GM-CSF driven accumulation of macrophages. In control fetuses at E18.5, the alveolar phenotype $CD11b^-$ $F4/80^+$ macrophages were 5-fold more abundant compared to $CD11b^+$ $F4/80^+$ macrophages (**Figures 2A,B**). In contrast, the predominant population of macrophages in BTg fetuses at the similar timepoint showed predominantly the interstitial type $CD11b^+$ $F4/80^+$ macrophages. The alveolar:interstitial ($CD11b^-$:$CD11b^+$) macrophage ratio showed a reversal in phenotype with fewer alveolar but more interstitial at 1:2 ratio in BTg fetuses compared to 5:1 in controls. Finally, GM-CSF KO at E18.5 had cells with lower side and forward scatter properties compared to BTg fetuses (**Figure 2C**). These KO fetuses had the lowest alveolar type $CD11b^-$ $F4/80^+$ macrophages compared to both controls and BTg fetuses (**Figure 2B**).

Fetal Lung Interstitial Macrophages Are Reduced but Not Absent in GM-CSF KO Mice

We next investigated whether GM-CSF was essential for the development of lung macrophages. At E14.5 there were very few $CD68^+$ cells in the lung interstitium of both control and GM-CSF KO mice but the $CD68^+$ cell counts were similar between these groups (**Figures 3A,B,E**). In the controls, there was a progressive increase in $CD68^+$ interstitial macrophages from E14.5 to E16.5 and E18.5 (**Figure 3E**, see also, **Figures 1A,B,D**). In contrast, the $CD68^+$ cell counts did not increase from E14.5 to E18.5 in the GM-CSF KO mice (**Figures 3B–E**), and the proportions of these $CD68^+$ cells were lower in the GM-CSF KO mice compared to the controls (**Figure 3E**). Consistently, there were no alveolar macrophages in the fetal lungs of controls and KO.

Lung Interstitial Macrophages Maturing as Alveolar Type Postnatally May Be Dependent on GM-CSF

Absence of GM-CSF signaling causes disruption of alveolar macrophage function resulting in pulmonary alveolar proteinosis in an adult mouse model (16, 20). There is limited data to indicate if this phenomenon occurs even at the early neonatal period. To understand the postnatal ontogeny of lung macrophage and its dependence on GM-CSF, we compared immunohistology for CD68 in the lung tissue from GM-CSF KO vs. controls. As in the preceding antenatal period, despite the absence of GM-CSF in KO, $CD68^+$ cells were still present in the lungs at postnatal days 1, 4, 7, and 14, although they appeared fewer than controls (**Figure 4**). Notably, on PN14, $CD68^+$ cells were abundantly seen in the alveolar space of controls but not in the GM-CSF KO mice (compare **Figures 4G,H**). In the lung tissue, $CD68^+$ cell numbers in the GM-CSF KO mice were decreased at PN1 and PN4 compared to controls, but were similar for PN7 and PN14 (**Figure 4I**). Similarly, $CD11b^-$ $F4/80^+$ macrophages were fewer in KO mice on PN1 than controls (**Figure 4J**). In BALF, a distinct population of cells from the alveolar space appeared with high forward and side scatter properties in the controls but this was completely absent in the KO mice (**Supplementary Figures 2A,B**). Consistent with immunohistology, KO mice also had fewer $CD68^+$ cells (**Supplementary Figure 2C**) and $CD11b^-$ $F4/80^+$ macrophages in the BALF (**Supplementary Figure 2D**) than controls.

DISCUSSION

Our results demonstrate that antenatal surge of GM-CSF increased the population of CD68 and CD11b/F4/80 double-positive cells. These lung macrophages in the fetus just before birth were almost exclusively located in the interstitium rather than the alveoli. Although some loss of alveolar macrophages may occur during tissue processing, the overwhelming interstitial macrophage presence compared to controls was remarkably significant (**Figure 1**). Furthermore, compared with macrophages of postnatal day 14 mice, the lung macrophage from E18.5 fetuses had a significantly lower F4/80 expression and lower scatter properties, suggesting that antenatal GM-CSF increases the population of immature macrophages in the interstitium. A recent ontogeny study reported the three "waves" in lung macrophage development. The first two "waves" are "primitive" macrophages originating from the yolk sac and fetal liver, and they are located primarily in the lung interstitium with F4/80 and Mac2 (low F4/80) expression. These are gradually replaced by the postnatal form of "definitive" interstitial macrophages, also having F4/80 expression but presumably regulated by progenitors from bone-marrow dependent hematopoeisis (25). It is recognized that interstitial macrophages are involved in tissue repair and lung remodeling while alveolar macrophages are considered as the "police" of the alveolar space involved in phagocytosis of foreign particles and surfactant catabolism. The functional potential of interstitial macrophages is less clear, but macrophages from fetal mice can

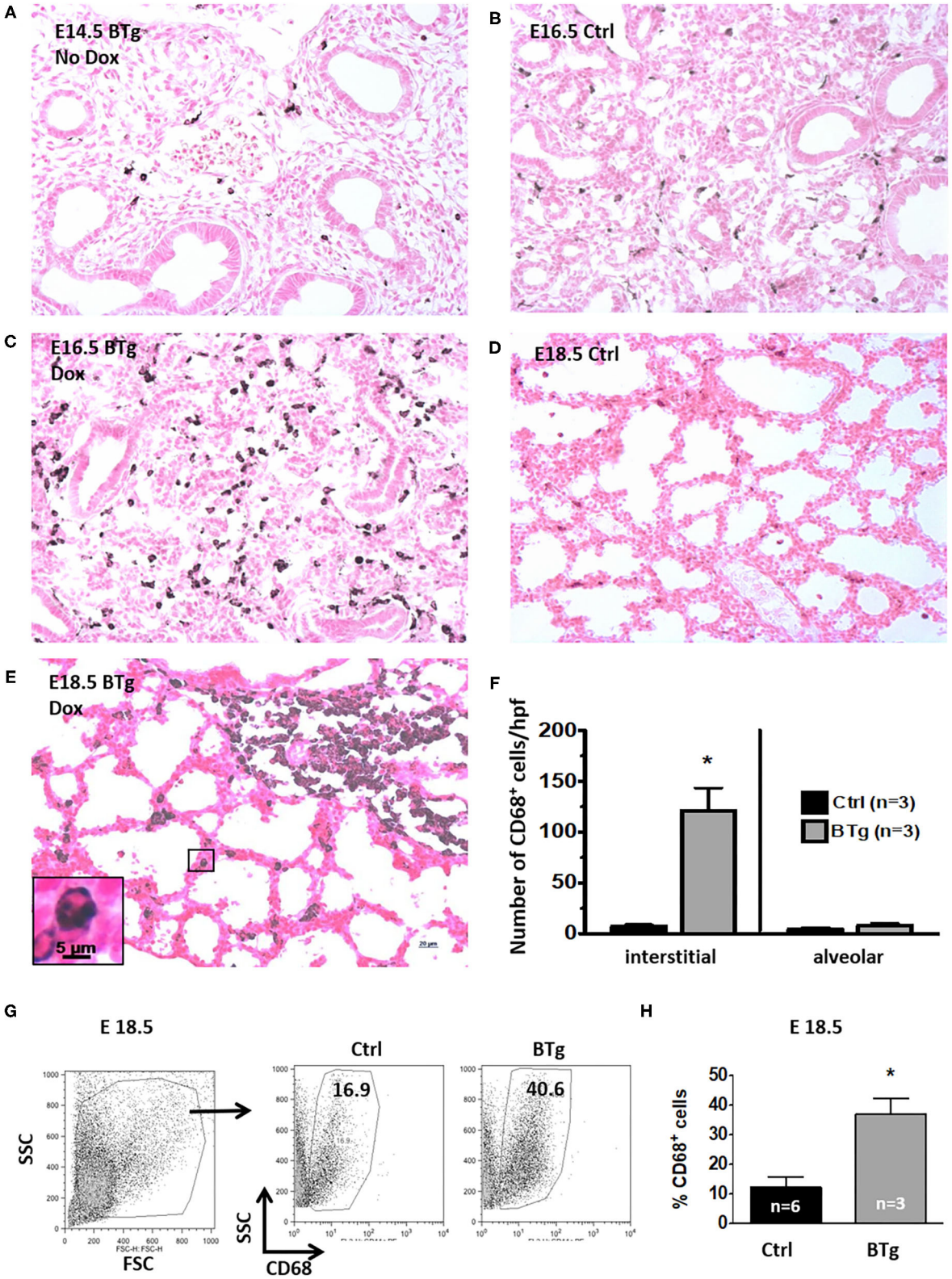

FIGURE 1 | Antenatal GM-CSF increased interstitial CD68$^+$ cells in the fetal lung. Representative immunohistology for CD68 using lung sections (20X objective) from **(A)** Bitransgenic (BTg) mice at E14.5 without exposure to doxycycline (Dox), **(B)** control E16.5 and **(D)** control E18.5 fetuses. Sections from BTg fetuses after

(Continued)

FIGURE 1 | exposure to Dox at **(C)** E16.5 and **(E)** E18.5. Inset in **(E)** shows a magnification of a $CD68^+$ cell in the interstitium with the characteristic mononuclear morphology. Increased staining for CD68 (dark brown/black staining) expressing cells were noted in the interstitium of BTg mice at E16.5 and E18.5. **(F)** Quantification of interstitial vs. alveolar location of $CD68^+$ cells (by immunohistology) in E18.5 BTg fetuses. **(G,H)** Flow cytometry quantification using E18.5 fetuses shows more than two-fold increase in $CD68^+$ cells in BTg fetal lungs compared to control lungs (*$p < 0.05$ vs. controls).

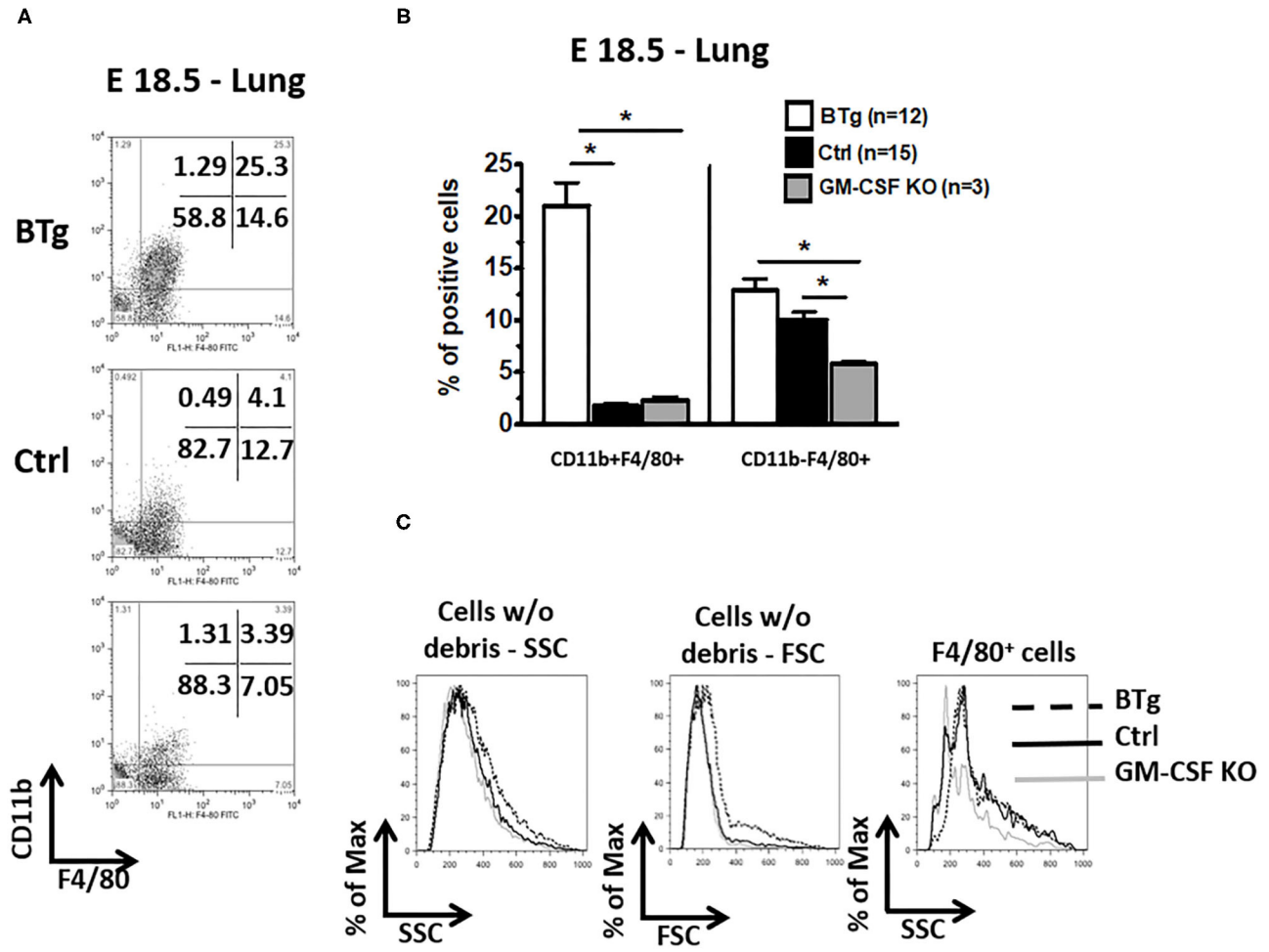

FIGURE 2 | Increased double positive CD11b/F4/80 ($CD11b^+$ $F4/80^+$) fetal lung macrophages after antenatal GM-CSF exposure. Lung cell suspensions were made from fetuses at E18.5 with the genotypes BTg on Dox starting at E14.5, GM-CSF KO, and controls. Cell suspensions were labeled with anti-CD11b and anti-F4/80 for flow cytometry. **(A)** Representative dot plots, **(C)** the corresponding quantitation for the gated cells in **(A)** are shown, **(B)** histogram showing scatter properties of the lung cells from the three groups. The major lung macrophage population in the BTg fetuses was $CD11b^+$ $F4/80^+$ (*$p < 0.05$ vs. controls).

respond to LPS *in vitro* with the production of IL-1β and TNF-α (33). Our previous work in a preterm sheep model indicated that lung monocytes/macrophages from controls did not respond with oxidative burst to an inflammatory stimulus, but with prior intrauterine exposure to LPS it significantly increases the oxidative ability of these lung monocytes/macrophages (9). The functional competency of the interstitial lung macrophage induced by antenatal inflammation with cytokines such as GM-CSF surge *in vivo* awaits further studies. As GM-CSF levels have been reported to be increased in chorioamnionitis (7, 9, 34, 35), we speculate that these macrophages may be primed to a more robust response to extrauterine stresses such as hyperoxia and volutrauma from mechanical ventilation. As observed by Tan and Krasnow, physiologically, a population of interstitial macrophages (Mac2) began to populate the alveolar spaces at the end of the first postnatal week (25). Furthermore, a recent study showed that exposure to hyperoxia in the first 10 days postnatal life induced accumulation of macrophages in the alveolar space, possibly including a population of interstitial macrophages (36). We speculate the first "hit" from intrauterine infection upregulates GM-CSF and increases interstitial macrophages in the fetal lung. The second "hit"

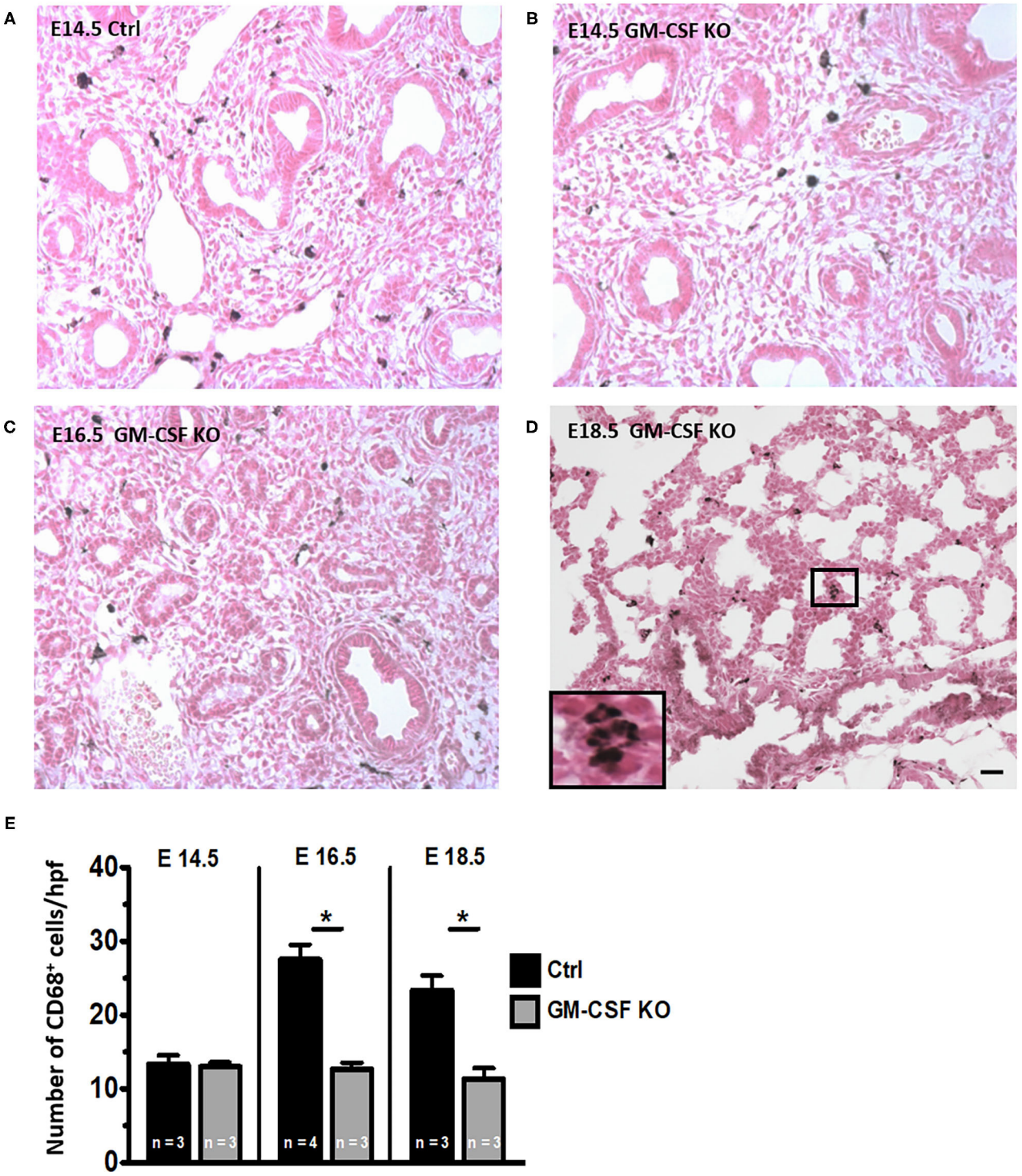

FIGURE 3 | Decreased $CD68^+$ macrophages in fetal lungs of GM-CSF KO fetuses. Representative immunohistology for CD68 using lung sections (20X objective) from **(A)** Control fetal lung at E14.5. **(B–D)** Fetal lungs from GM-CSF KO mice at the indicated gestational ages. Inset in **(D)** shows magnification of a group of interstitial CD68 staining macrophages with their characteristic morphology. **(E)** Quantitation of $CD68^+$ cells based on the average number of cells present in at least five random high power fields (hpf) is shown. The number of macrophages was lower in GM-CSF KO compared to control lungs at E16.5 and E18.5. (*$p < 0.05$ vs. controls).

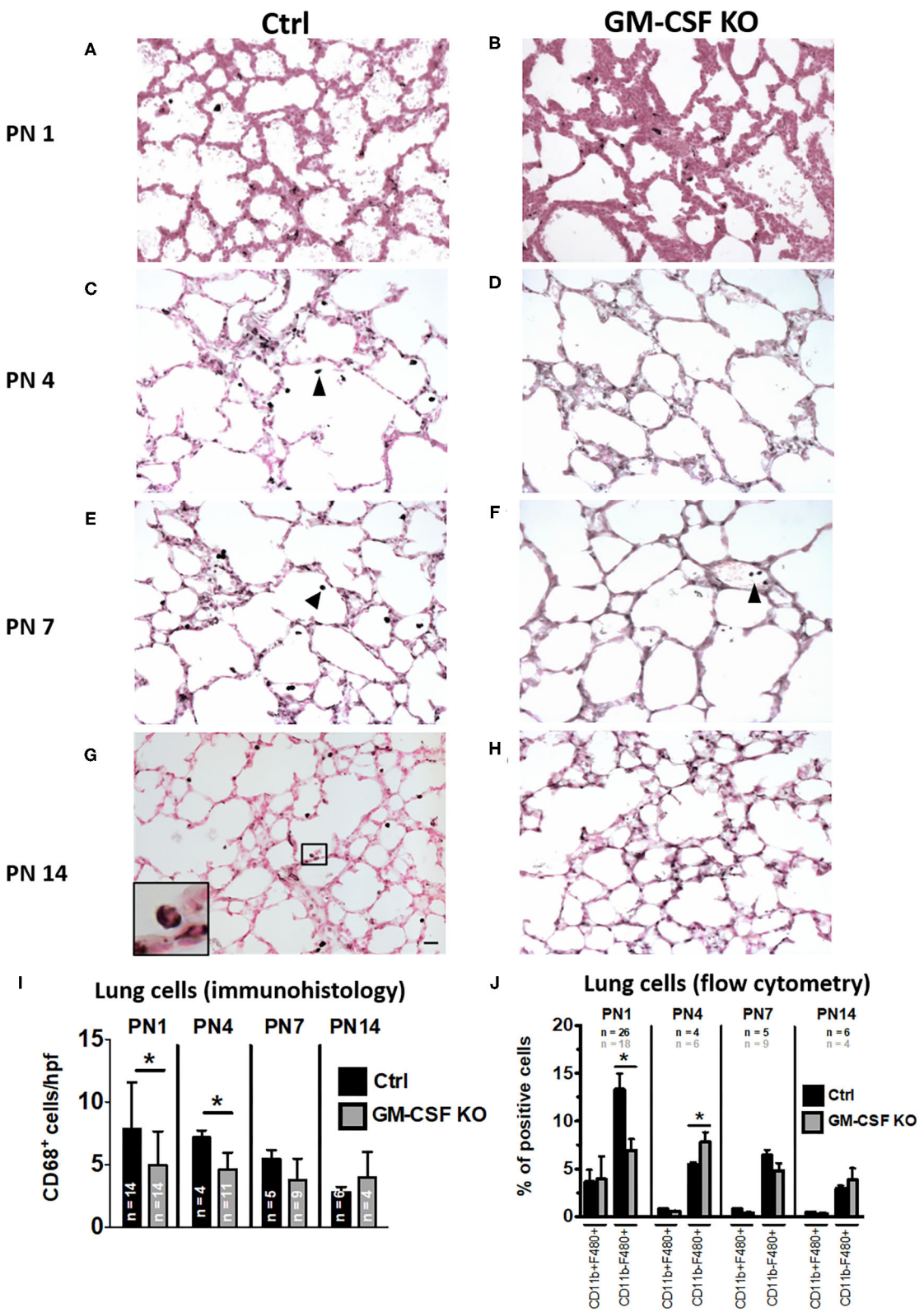

FIGURE 4 | Decreased CD68$^+$ macrophages in lungs of GM-CSF KO neonatal mice. Representative immunohistology of neonatal mouse lungs at postnatal (PN) days 1, 4, 7, and 14 (20X objective). **(A,C,E,G)** show immunostaining in control mice and **(B,D,F,H)** show immunostaining in GM-CSF KO mice. There were more alveolar macrophages (arrowhead showing dark brown/black staining cells) in the controls compared to the GM-CSF KO group. Inset in **(G)** shows a magnified

(Continued)

FIGURE 4 | $CD68^+$ alveolar macrophage in control mice, but $CD68^+$ cells were not seen in the alveolar space of GM-CSF KO mice ($N = 4$–13 animals/group). Immunohistology quantitation of the lung $CD68^+$ cells comparing control and GM-CSF KO mice **(I)**. Flow cytometry quantitation of lung homogenates for proportions of cells positive for CD11b and/or F4/80 **(J)**. Differences in $CD68^+$, $CD11b^+$, and $F4/80^+$ expression between controls and GM-CSF KO mice noted on PN1 and PN4 were no longer seen at PN7 and PN14 ($^*p < 0.05$ vs. controls).

during postnatal life such as hyperoxia, triggers the release of these accumulated interstitial macrophages into the alveolar space. This "double-hit" hypothesis has been proposed by some authors in the pathogenesis of BPD (37, 38).

Even though the administration of GM-CSF may increase surfactant production in preterm rabbits (39), activated interstitial macrophages as the result of local GM-CSF surge impaired airway branching morphogenesis, which, together are some features of the new BPD (33). In a clinical study, GM-CSF levels were elevated in the tracheal aspirates of preterm infants who developed BPD (34). Together, tight regulation of GM-CSF levels appears to be necessary for normal fetal lung development and the maturation of alveolar macrophages.

Our study concludes that a surge of antenatal GM-CSF, as might happen in intrauterine inflammation, stimulates an increase in the interstitial macrophage population in the developing fetal lung. These GM-CSF-induced interstitial macrophages have the characteristics that are lacking of the mature alveolar type. Our results were consistent with what have been previously reported (18, 25). We further demonstrated that postnatally, GM-CSF is required for the early transition to this population of mature macrophages in the alveolar space. Also, the absence of GM-CSF showed a slower accumulation of $CD68^+$ cells in the lung during the early postnatal period. Similarly, in the experiment by Kalymbetova et al. in depleting *Csf1r*-expressing monocytes or macrophages by Fas-induced apoptosis, few macrophages were still detected in the alveolar spaces (36). Collectively, our results suggest a novel finding that GM-CSF is necessary, but not the sole determinant for interstitial macrophage recruitment and alveolar macrophage maturation during the perinatal period. Other stimuli, perhaps the mechanical stretch from respiration postnatally, oxygen sensing or other cytokine signals, are likely needed for the accumulation of mature alveolar macrophages. Intuitively, interstitial macrophages and intrauterine factors may be the major modulators of the "new" BPD whereas alveolar macrophages may play a greater role in the more severe or "old" BPD (40).

CONCLUSION

The Dox-inducible CCSP-promoter based transgenic mice model has been successfully developed for tight control of various gene expression to study lung development and disease pathogenesis. Concerns regarding toxicity of the rtTA system associated with emphysematous change in the lung structure of adult mice (41) was not evident at the perinatal or neonatal stages in our mouse model when comparing between the wild type and single transgene littermates. Of note, this transgenic model has rarely been used in studying antenatal inducible events followed by postnatal exposures to agents of interest.We hope our preliminary results and the models utilized here may serve as a platform to further study the mechanisms of disruption in the control and balance of GM-CSF during the perinatal period. How this could interfere with normal lung development and functional outcomes when complicated by postnatal factors such as hyperoxia and sepsis in the pathogenesis of BPD also warrant further studies.

DATA AVAILABILITY STATEMENT

The raw data supporting the conclusions of this article will be made available by the authors, without undue reservation.

ETHICS STATEMENT

The animal study was reviewed and approved by Cincinnati Children's Hospital Medical Center Animal Care Committee (IACUC S3D01004).

AUTHOR CONTRIBUTIONS

F-CC and SGK were involved in designing of the study, analyses of the data, interpreting the results, and writing of this report. BCC was primarily involved with breeding of the animals, conducting the animal experiments, and data collection. PP was involved in the flow cytometry analyses, data interpretation, and reporting. T-LT was involved in analysis and writing of the manuscript. All authors contributed to the article and approved the submitted version.

FUNDING

This study was funded by NIH HD57869 (to SGK). The funder had no role in the study design, data collection and analysis, decision to publish, or preparation of the manuscript.

ACKNOWLEDGMENTS

We wish to thank Dr. Ross Ridsdale for his expert guidance on fetal mice tracheal cannulation; Drs. Anna Perl, Cindy Bachurski, and Susan Wert for their valuable advice on the genetics, breeding of the mice and immunohistology; Tiffany Crane, Amy Whitescarver, and Manuel Alvarez for their technical assistance. Our appreciation to Dr. Jerrold Teo for his help in some of the manuscript revision work. We also thank Professors Bruce Trapnell, Alan Jobe, and Jeffrey Whitsett for their advice and input in this study. Some of the results were presented at the May 2011 Pediatric Academic Societies and the Asian Society for Pediatric Research Joint Meeting.

SUPPLEMENTARY MATERIAL

The Supplementary Material for this article can be found online at: https://www.frontiersin.org/articles/10.3389/fped.2021.614209/full#supplementary-material

Supplementary Figure 1 | Immunohistology and flow cytometry quantification of lung macrophages using CD68, F4/80 and CD11b markers in mice with constitutive and inducible GM-CSF backgrounds. **(A–E)** Represent results from E14.5 mice on regular chow and from mice who were on Dox at E16.5 and E18.5. There were no differences in CD68, F4/80 and CD11b positive macrophages between WT and STg at E14.5, E16.5 or E18.5. However, significantly more of these macrophages were present in BTg on Dox at E16.5 and E18.5. WT, wild type; STg, single transgenic; BTg, bitransgenic; $^*p < 0.05$ vs. controls.

Supplementary Figure 2 | Immunophenotyping of BALF cells for monocyte/macrophage surface markers in control and GM-CSF KO neonatal mice. Flow cytometry was performed on BALF cells from control and GM-CSF KO neonatal mice at PN14. **(A)** Representative dot plots and **(B)** histogram of the forward-scatter (FSC) and side-scatter (SSC) properties of BALF cells. **(C)** Quantitation of $CD68^+$ cells and **(D)** $CD11b^+$ and $F4/80^+$ cells. In contrast to the subtle differences between cell populations in lung homogenates (**Figure 4J**), BALF from GM-CSF KO mice had strikingly lower $CD68^+$ cells, and lower $CD11b^-$ $F4/80^+$ cells compared to controls ($^*p < 0.05$ vs. controls).

REFERENCES

1. Burgess A, Camakaris J, Metcalf D. Purification and properties of colony-stimulating factor from mouse lung-conditioned medium. *J Biol Chem.* (1977) 252:1998–2003. doi: 10.1016/S0021-9258(18)71855-3
2. Hamilton JA, Stanley ER, Burgess AW, Shadduck RK. Stimulation of macrophage plasminogen activator activity by colony-stimulating factors. *J Cell Physiol.* (1980) 103:435–45. doi: 10.1002/jcp.1041030309
3. Whetton AD, Dexter TM. Myeloid haemopoietic growth factors. *BBA Rev Cancer.* (1989) 989:111–32. doi: 10.1016/0304-419X(89)90038-3
4. Thomas D, Lopez A. Granulocyte-macrophage colony-stimulating factor (GM-CSF). In: Henry H, Norman A, editors. *Encyclopedia of Hormones*. New York, NY: Academic Press. (2003). p. 202–8.
5. Joshi PC, Applewhite L, Mitchell PO, Fernainy K, Roman J, Eaton DC, et al. GM-CSF receptor expression and signaling is decreased in lungs of ethanol-fed rats. *Am J Physiol Lung Cell Mol Physiol.* (2006) 291:1150–8. doi: 10.1152/ajplung.00150.2006
6. Baleeiro CEO, Christensen PJ, Morris SB, Mendez MP, Wilcoxen SE, Paine R. GM-CSF and the impaired pulmonary innate immune response following hyperoxic stress. *Am J Physiol Lung Cell Mol Physiol.* (2006) 291:L1246–55. doi: 10.1152/ajplung.00016.2006
7. Bry K, Hallman M, Teramo K, Waffarn F. Granulocyte-macrophage colony-stimulating factor in amniotic fluid and in airway specimens of newborn infants. *Pediatr Res.* (1997) 41:105–9. doi: 10.1203/00006450-199701000-00016
8. Keelan J, Blumenstein M, Helliwell R, Sato T. Cytokines, prostaglandins and parturition–a review. *Placenta.* (2003) 24 (Suppl. A):S33–46. doi: 10.1053/plac.2002.0948
9. Kramer BW, Joshi SN, Moss TJM, Newnham JP, Sindelar R, Jobe AH, et al. Endotoxin-induced maturation of monocytes in preterm fetal sheep lung. *Am J Physiol Lung Cell Mol Physiol.* (2007) 293:L345–53. doi: 10.1152/ajplung.00003.2007
10. Huffman Reed JA, Rice WR, Zsengellér ZK, Wert SE, Dranoff G, Whitsett JA. GM-CSF enhances lung growth and causes alveolar type II epithelial cell hyperplasia in transgenic mice. *Am J Physiol Lung Cell Mol Physiol.* (1997) 273:L715–25. doi: 10.1152/ajplung.1997.273.4.L715
11. Baytur YB, Ozbilgin K, Yuksel H, Kose C. Antenatal administration of granulocyte-macrophage colony-stimulating factor increases fetal lung maturation and endothelial nitric oxide synthase expression in the fetal rat lung. *Eur J Obstet Gynecol Reprod Biol.* (2008) 136:171–7. doi: 10.1016/j.ejogrb.2007.03.010
12. Yuksel H, Yilmaz O, Baytur YB, Ozbilgin K. Prenatal administration of granulocyte-macrophage colony-stimulating factor increases mesenchymal vascular endothelial growth factor expression and maturation in fetal rat lung. *Exp Lung Res.* (2008) 34:550–8. doi: 10.1080/01902140802341736
13. Richardson CJ, Pomerance JJ, Cunningham MD, Gluck L. Acceleration of fetal lung maturation following prolonged rupture of the membranes. *Am J Obstet Gynecol.* (1974) 118:1115–8. doi: 10.1016/0002-9378(74)90691-7
14. Andrews WW, Goldenberg RL, Faye-Petersen O, Cliver S, Goepfert AR, Hauth JC. The Alabama Preterm Birth study: polymorphonuclear and mononuclear cell placental infiltrations, other markers of inflammation, and outcomes in 23- to 32-week preterm newborn infants. *Am J Obstet Gynecol.* (2006) 195:803–8. doi: 10.1016/j.ajog.2006.06.083
15. Lahra MM, Beeby PJ, Jeffery HE. Maternal versus fetal inflammation and respiratory distress syndrome: a 10-year hospital cohort study. *Arch Dis Child Fetal Neonatal Ed.* (2009) 94:F13–6. doi: 10.1136/adc.2007.135889
16. Shibata Y, Berclaz PY, Chroneos ZC, Yoshida M, Whitsett JA, Trapnell BC. GM-CSF regulates alveolar macrophage differentiation and innate immunity in the lung through PU.1. *Immunity.* (2001) 15:557–67. doi: 10.1016/S1074-7613(01)00218-7
17. Berclaz PY, Shibata Y, Whitsett JA, Trapnell BC. GM-CSF, via PU.1, regulates alveolar macrophage FcγR-mediated phagocytosis and the IL-18/IFN-γ-mediated molecular connection between innate and adaptive immunity in the lung. *Blood.* (2002) 100:4193–200. doi: 10.1182/blood-2002-04-1102
18. Guilliams M, De Kleer I, Henri S, Post S, Vanhoutte L, De Prijck S, et al. Alveolar macrophages develop from fetal monocytes that differentiate into long-lived cells in the first week of life via GM-CSF. *J Exp Med.* (2013) 210:1977–92. doi: 10.1084/jem.20131199
19. Schneider C, Nobs SP, Kurrer M, Rehrauer H, Thiele C, Kopf M. Induction of the nuclear receptor PPAR-γ 3 by the cytokine GM-CSF is critical for the differentiation of fetal monocytes into alveolar macrophages. *Nat Immunol.* (2014) 15:1026–37. doi: 10.1038/ni.3005
20. Bonfield TL, Raychaudhuri B, Malur A, Abraham S, Trapnell BC, Kavuru MS, et al. PU.1 regulation of human alveolar macrophage differentiation requires granulocyte-macrophage colony-stimulating factor. *Am J Physiol Lung Cell Mol Physiol.* (2003) 285:1132–6. doi: 10.1152/ajplung.00216.2003
21. Alenghart E, Esterly J. Alveolar macrophages in perinatal infants. *Pediatrics.* (1984) 74:221–3.
22. Jacobs RF, Wilson CB, Palmer S, Springmeyer SC, Henderson WR, Glover DM, et al. Factors related to the appearance of alveolar macrophages in the developing lung. *Am Rev Respir Dis.* (1985) 131:548–53. doi: 10.1164/arrd.1985.131.4.548
23. van de Laar L, Saelens W, De Prijck S, Martens L, Scott CL, Van Isterdael G, et al. Yolk sac macrophages, fetal liver, and adult monocytes can colonize an empty niche and develop into functional tissue-resident macrophages. *Immunity.* (2016) 44:755–68. doi: 10.1016/j.immuni.2016.02.017
24. Scott C, Guilliams M. Tissue unit-ed: lung cells team up to drive alveolar macrophage development. *Cell.* (2018) 175:898–900. doi: 10.1016/j.cell.2018.10.031
25. Tan SYS, Krasnow MA. Developmental origin of lung macrophage diversity. *Dev.* (2016) 143:1318–27. doi: 10.1242/dev.129122
26. Dranoff G, Crawford AD, Sadelain M, Ream B, Rashid A, Bronson RT, et al. Involvement of granulocyte-macrophage colony-stimulating factor in pulmonary homeostasis. *Science.* (1994) 264:713–6. doi: 10.1126/science.8171324
27. Willet KE, Jobe AH, Ikegami M, Newnham J, Brennan S, Sly PD. Antenatal endotoxin and glucocorticoid effects on lung morphometry in preterm lambs. *Pediatr Res.* (2000) 48:782–8. doi: 10.1203/00006450-200012000-00014
28. Coalson JJ. Pathology of new bronchopulmonary dysplasia. *Semin Neonatol.* (2003) 8:73–81. doi: 10.1016/S1084-2756(02)00193-8
29. Kallapur SG, Bachurski CJ, Le Cras TD, Joshi SN, Ikegami M, Jobe AH. Vascular changes after intra-amniotic endotoxin in

preterm lamb lungs. *Am J Physiol Lung Cell Mol Physiol.* (2004) 287:L1178–85. doi: 10.1152/ajplung.00049.2004
30. Been J V., Debeer A, Van Iwaarden JF, Kloosterboer N, Passos VL, Naulaers G, et al. Early alterations of growth factor patterns in bronchoalveolar lavage fluid from preterm infants developing bronchopulmonary dysplasia. *Pediatr Res.* (2010) 67:83–9. doi: 10.1203/PDR.0b013e3181c13276
31. Tichelaar JW, Lu W, Whitsett JA. Conditional expression of fibroblast growth factor-7 in the developing and mature lung. *J Biol Chem.* (2000) 275:11858–64. doi: 10.1074/jbc.275.16.11858
32. Zaynagetdinov R, Sherrill TP, Kendall PL, Segal BH, Weller KP, Tighe RM, et al. Identification of myeloid cell subsets in murine lungs using flow cytometry. *Am J Respir Cell Mol Biol.* (2013) 49:180–9. doi: 10.1165/rcmb.2012-0366MA
33. Blackwell TS, Hipps AN, Yamamoto Y, Han W, Barham WJ, Ostrowski MC, et al. NF-κB signaling in fetal lung macrophages disrupts airway morphogenesis. *J Immunol.* (2011) 187:2740–7. doi: 10.4049/jimmunol.1101495
34. Papoff P, Christensen RD, Calhoun DA, Juul SE. Granulocyte colony-stimulating factor, granulocyte macrophage colony-stimulating factor and neutrophils in the bronchoalveolar lavage fluid of premature infants with respiratory distress syndrome. *Biol Neonate.* (2001) 80:133–41. doi: 10.1159/000047132
35. Stallmach T, Hebisch G, Joller H, Kolditz P, Engelmann M. Expression pattern of cytokines in the different compartments of the feto-maternal unit under various conditions. *Reprod Fertil Dev.* (1995) 7:1573–80. doi: 10.1071/RD9951573
36. Kalymbetova TV, Selvakumar B, Rodríguez-Castillo JA, Gunjak M, Malainou C, Heindl MR, et al. Resident alveolar macrophages are master regulators of arrested alveolarization in experimental bronchopulmonary dysplasia. *J Pathol.* (2018) 245:153–9. doi: 10.1002/path.5076
37. Collins JJP, Tibboel D, de Kleer IM, Reiss IKM, Rottier RJ. The future of bronchopulmonary dysplasia: emerging pathophysiological concepts and potential new avenues of treatment. *Front Med.* (2017) 4:61. doi: 10.3389/fmed.2017.00061
38. Davidson L, Berkelhamer S. Bronchopulmonary dysplasia: chronic lung disease of infancy and long-term pulmonary outcomes. *J Clin Med.* (2017) 6:4. doi: 10.3390/jcm6010004
39. Uy C, Bry K, Lappalainen U, Hallman M. Granulocyte-macrophage colony-stimulating factor increases surfactant phospholipid in premature rabbits. *Pediatr Res.* (1999) 46:613–20. doi: 10.1203/00006450-199911000-00020
40. Abman SH, Bancalari E, Jobe A. The evolution of bronchopulmonary dysplasia after 50 years. *Am J Respir Crit Care Med.* (2017) 195:421–4. doi: 10.1164/rccm.201611-2386ED
41. Sisson TH, Hansen JM, Shah M, Hanson KE, Du M, Ling T, et al. Expression of the reverse tetracycline-transactivator gene causes emphysema-like changes in mice. *Am J Respir Cell Mol Biol.* (2006) 34:552–60. doi: 10.1165/rcmb.2005-0378OC

Conflict of Interest: The authors declare that the research was conducted in the absence of any commercial or financial relationships that could be construed as a potential conflict of interest.

frontiers in Pediatrics

ORIGINAL RESEARCH
published: 01 April 2021
doi: 10.3389/fped.2021.636638

Co-bedding of Preterm Newborn Pigs Reduces Necrotizing Enterocolitis Incidence Independent of Vital Functions and Cortisol Levels

Anders Brunse[1], *Yueming Peng*[1,2], *Yanqi Li*[1,3], *Jens Lykkesfeldt*[4] *and Per Torp Sangild*[1,5,6]*

[1] Comparative Pediatrics and Nutrition, Department of Veterinary and Animal Sciences, Faculty of Health and Medical Sciences, University of Copenhagen, Copenhagen, Denmark, [2] Department of Neonatology, Shenzhen People's Hospital (The Second Clinical Medical College, Jinan University; The First Affiliated Hospital, Southern University of Science and Technology), Shenzhen, China, [3] Nordic Bioscience Clinical Development A/S, Herlev, Denmark, [4] Experimental Animal Models, Department of Veterinary and Animal Sciences, Faculty of Health and Medical Sciences, University of Copenhagen, Copenhagen, Denmark, [5] Department of Neonatology, Rigshospitalet, Copenhagen, Denmark, [6] Hans Christian Andersen Children's Hospital, Odense, Denmark

Background: Preterm infants are born with immature organs, leading to morbidities such as necrotizing enterocolitis (NEC), a gut inflammatory disease associated with adverse feeding responses but also hemodynamic and respiratory instability. Skin-to-skin contact including "kangaroo care" may improve infant survival and health *via* improved vital functions (e.g., pulmonary, cardiovascular) and endocrine influences by adrenal glucocorticoids. Clinical effects of skin-to-skin contact for newborn siblings ("co-bedding") are not known. Using NEC-susceptible Preterm pigs as models, we hypothesized that co-bedding and exogenous glucocorticoids improve vital functions and NEC resistance.

Methods: In experiment 1, cesarean-delivered, formula-fed Preterm pigs were reared in incubators with (co-bedding, COB, $n = 30$) or without (single-bedding, SIN, $n = 29$) a sibling until euthanasia and tissue collection on day four. In experiment 2, single-bedded Preterm pigs were treated postnatally with a tapering dose of hydrocortisone (HC, $n = 19$, 1–3 mg/kg/d) or saline (CON, $n = 19$).

Results: Co-bedding reduced NEC incidence (38 vs. 65%, $p < 0.05$) and increased the density of colonic goblet cells (+20%, $p < 0.05$) but had no effect on pulmonary and cardiovascular functions (respiration, blood pressure, heart rate, blood gases) or cortisol levels. There were limited differences in intestinal villous architecture and digestive enzyme activities. In experiment 2, HC treatment increased NEC lesions in the small intestine without any effects on pulmonary or cardiovascular functions.

Conclusion: Co-bedding may improve gut function and NEC resistance independently of cardiorespiratory function and cortisol levels, but pharmacological cortisol treatment predispose to NEC. Preterm pigs may be a useful tool to better understand the physiological effects of co-bedding, neonatal stressors and their possible interactions with morbidities in Preterm neonates.

Keywords: necrotizing enterocolitis, skin-to-skin care, co-bedding, hydrocortisone, preterm (birth)

OPEN ACCESS

Edited by:
Yuan Shi,
Children's Hospital of Chongqing Medical University, China

Reviewed by:
Lu-Quan Li,
Chongqing Medical University, China
David Hackam,
Johns Hopkins Medicine, United States

***Correspondence:**
Per Torp Sangild
pts@sund.ku.dk

Specialty section:
This article was submitted to Neonatology, a section of the journal Frontiers in Pediatrics

Received: *01 December 2020*
Accepted: *02 March 2021*
Published: *01 April 2021*

Citation:
Brunse A, Peng Y, Li Y, Lykkesfeldt J and Sangild PT (2021) Co-bedding of Preterm Newborn Pigs Reduces Necrotizing Enterocolitis Incidence Independent of Vital Functions and Cortisol Levels. Front. Pediatr. 9:636638. doi: 10.3389/fped.2021.636638

INTRODUCTION

Preterm birth (birth before 37 weeks' gestation) interrupts intrauterine development and results in premature exposure of the developing fetus to the extra-uterine environment, leading to a range of morbidities, including necrotizing enterocolitis (NEC). NEC is a life-threatening gut inflammatory disease that develops in part due to dysfunctional barrier and motility of the gut following enteral feeding, especially with formula, and the presence of opportunistic pathogenic bacteria (1). However, physiological stressors and the mesenteric blood supply may also play a role in NEC etiology, exemplified by the reduction in NEC incidence after surgical ligation of patent ductus arteriosus in extremely low birth weight infants (2).

Parent-infant skin-to-skin contact (termed "kangaroo care") may serve to reduce negative stress effects, thereby increasing cardiovascular and respiratory stability in Preterm infants (3–5). A meta-analysis, including more than 3,000 low birth weight infants, showed that kangaroo care decreased overall mortality and infection rates and increased body weight gain (6). Skin-to-skin contact between infant siblings (termed "co-bedding") may provide the same benefits as kangaroo care, but few clinical studies are available and effects on survival, vital functions, NEC and infection rates are unknown (7). The mechanisms whereby kangaroo care or co-bedding may improve survival and health remain unknown but could relate to changes in circulating cortisol levels, a key regulator of perinatal organ maturation and cardiovascular and respiratory stability (8). However, the relations among care procedures, circulating cortisol and neonatal morbidities in Preterm infants are not clear (9, 10).

Cortisol is a critical birth adaptation hormone and an essential drug for Preterm infants. This was elegantly demonstrated in the pioneering studies by Liggins et al., incidentally discovering a partial lung expansion in fetal lambs exposed to synthetic cortisol (11), and later showing improved survival and prevention of lung disease in Preterm infants after antenatal betamethasone treatment (12). Besides the beneficial effects on lung maturation, antenatal corticosteroid treatment reduces the risk of NEC (13), but it is unclear whether this is an independent effect or due to improved pulmonary function. Conversely, postnatal corticosteroid therapy does not appear to have organ maturational effects and may even have negative effects on immunity and brain development (e.g., cerebral palsy) (14). Regardless, early postnatal hydrocortisone (HC) treatment is commonly used to support neonatal cardiovascular function and blood pressure (15) and may improve pulmonary function in extremely Preterm infants (16). Effects on gut functions and NEC sensitivity are unknown.

The Preterm pig is a highly translational animal model in experimental neonatology with similarities to moderately Preterm infants in size, physiology, anatomy and presence of a range of relevant physiological immaturities (17). At 80% gestation, Preterm pigs have lower mean arterial blood pressure and require antenatal corticosteroid treatment to survive (17) while at 90% gestation, neither exogenous corticosteroids or mechanical ventilation are strictly required for survival. However, Preterm newborn pigs have lower serum cortisol levels than term counterparts (18), and treatment with adrenocorticotropic hormone (ACTH) or cortisol to pig fetuses or cesarean-delivered near-term pigs improves maturation of the gut, pancreas and liver (19–22). In 90% gestation Preterm pigs, formula feeding alone, without further physiological stressors, is sufficient to induce high sensitivity to develop gut lesions with a high degree of clinical, radiographic and pathological similarity to human NEC (23).

On this background, we hypothesized that neonatal co-bedding and HC treatment are two clinically relevant interventions that together or independently improve cardiovascular and respiratory functions and protect against NEC in Preterm neonates. Using Preterm pigs as models for Preterm infants, we first compared co-housed animals with single-housed siblings and subsequently performed a saline-controlled HC intervention study in single-housed animals. Pulmonary and cardiovascular functions were longitudinally recorded before gut pathological assessment a few days later when Preterm formula-fed pigs are known to be highly NEC sensitive.

MATERIALS AND METHODS

Experiment 1: Co-bedding

Fifty-nine Preterm piglets from three pregnant sows (Danish Landrace × Large White × Duroc) were delivered by cesarean section at 90% gestation (gestational day 106) and resuscitated as previously described (24) (see study design in **Figure 1**). The newborn pigs were stratified by sex and birth weight and randomly allocated for single-housing (SIN, $n = 29$) or co-bedding (COB, $n = 30$) immediately after birth. Co-bedded animals were paired with a littermate pig and shared a single heated incubator (32–36°C), as shown in **Figure 1**. In contrast to our standard rearing of Preterm pigs (24), no supplemental oxygen was provided to the incubators within the first 12 h, to allow the piglets to demonstrate their independent ability to reach respiratory stability after some hours. On the first day, co-bedded piglets were wrapped together in a dry cotton cloth, while on subsequent days, they were placed in skin-to-skin contact (**Figure 1**, bottom panel) whenever they were not walking around in incubators (typically after 24–48 h).

Within 2–3 h after birth, animals were fitted with orogastric and umbilical arterial catheters for gavage feeding and vascular access (6 and 4 Fr size, respectively, Portex, Kent, UK), as previously described (24). To compensate for the lack of transplacental immunoglobulin transfer, animals were passively immunized with 16 ml/kg body weight of intra-arterially administered maternal plasma within the first 24 h after birth. The animals were gavage-fed at 3-h intervals with increasing volumes of infant formula (40 ml/kg/d on day 1, increasing to 80 ml/kg/d on day 4–5 (see nutrient compositions in **Supplementary Table 1**). Throughout the experiment, until euthanasia for tissue collection at ∼72 h after birth, the animals were continuously infused with parenteral nutrition *via* the arterial catheter (4 ml/kg/h, Kabiven, Fresenius-Kabi, Bad Homburg, Germany).

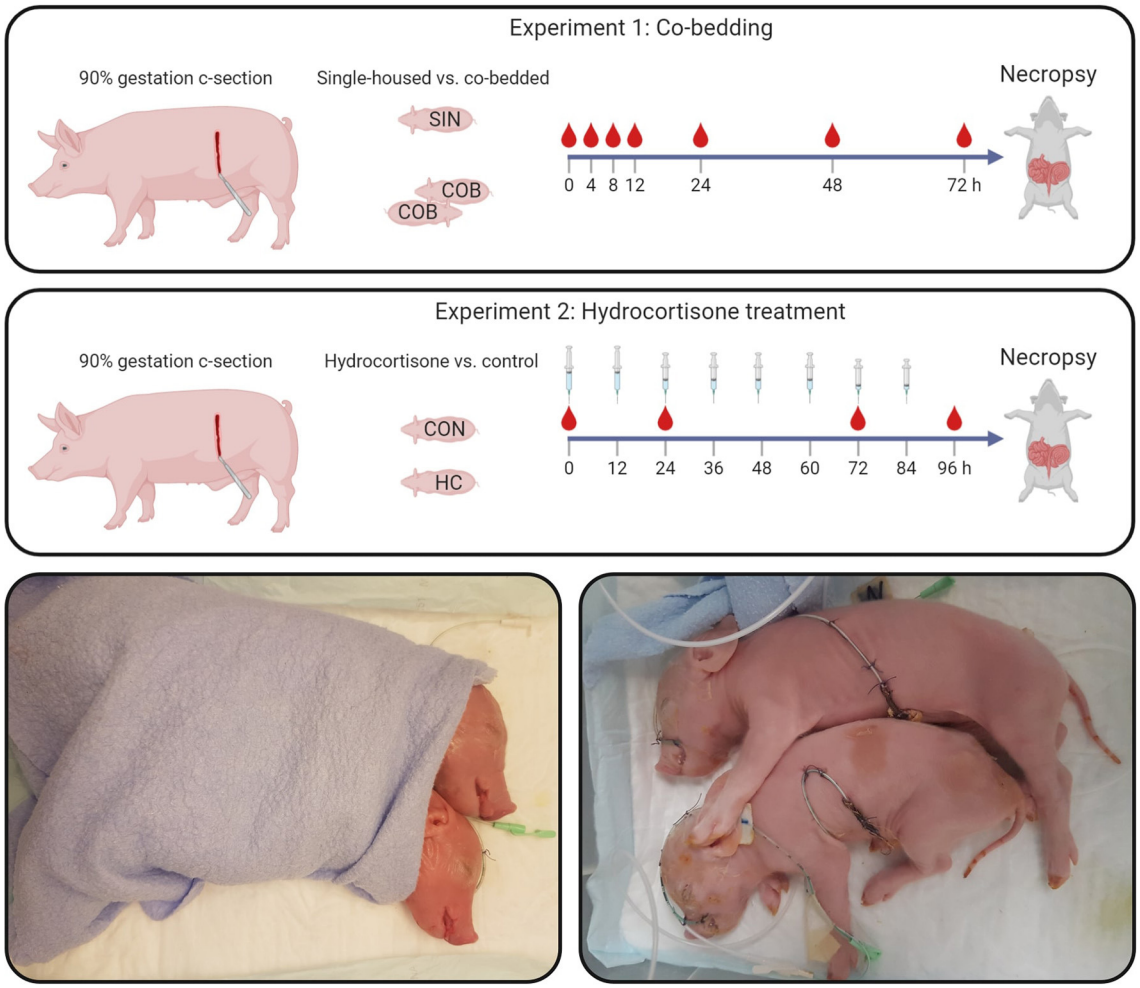

FIGURE 1 | Study design (upper panels). In Experiment 1, single-housed (SIN) and co-bedded (COB) Preterm cesarean-delivered piglets were studied for 72 h, including a period of longitudinal monitoring of vital functions and blood gases. In Experiment 2, Preterm pigs receiving a tapering dose of hydrocortisone (HC) were compared with controls (CON) for 96 h. Main outcomes in both experiments were vital signs, cardiovascular and respiratory functions, as well as gut structure and function, including NEC-like lesions. Lower panels show how co-bedded piglet siblings were wrapped together just after birth and fitted with umbilical catheters and feeding tubes.

Experiment 2: Hydrocortisone Treatment

Thirty-eight Preterm piglets from two sows were stratified by sex and birth weight and randomly allocated for intra-arterial hydrocortisone injection (HC, $n = 19$; Solu-Cortef, Pfizer, Ballerup, Denmark) or saline (CON, $n = 19$). The tapering dose of HC was 3 mg/kg twice daily on day 1, decreasing to 2 mg/kg on days 2–3, and 1 mg/kg on day 4. The dose regimen was based on clinical HC use for hypotension treatment (25) and prevention of bronchopulmonary dysplasia (26). Animals were euthanized ∼96 h after birth. All other procedures were as described above for Experiment 1.

Vital Signs, Blood Gases, and Cortisol

In the co-bedding experiment, assessment of vital signs and arterial blood sampling for blood gas measurements was done at 0, 4, 8, 12, 24, 48, and 72 h after birth. Serum cortisol levels were measured at 48 and 72 h. In the hydrocortisone experiment, vital signs were recorded at 0, 6, 24, 48, and 72 h after birth, except for arterial blood pressure (only at 24 and 72 h). Arterial blood gases were measured at 24 h, while serum cortisol levels were measured at birth, and at 72 and 96 h (12 h after the final HC administration). Core body temperature was measured using a rectal thermometer. Respiratory frequency was manually counted in 2-min intervals. Heart rate and oxygen saturation were measured using pulse oximetry with the sensor attached to the upper left forelimb. Arterial blood pressure was measured by connecting the umbilical catheter to a saline-filled tubing system pressurized to 200 mmHg and equipped with transducer and monitor (Datex Ohmeda Compact S5, GE Healthcare, Brondby, Denmark). Data was stored and analyzed using Datex-Ohmeda S/5 Collect software. Arterial blood gases were measured using the GEM Premier 3000 system (Intrumentation

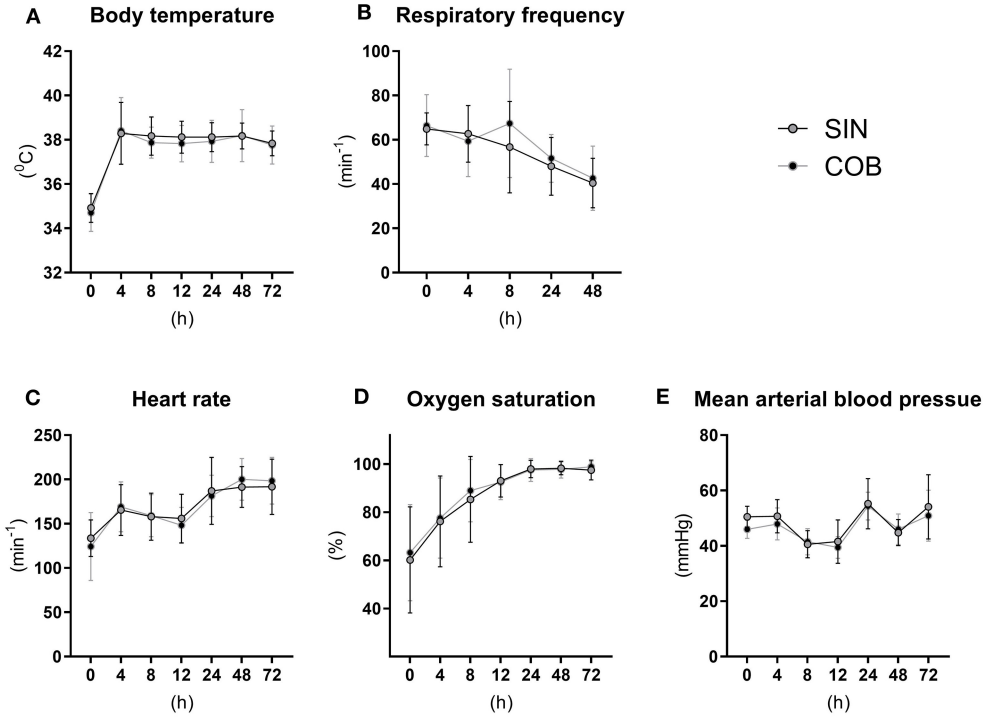

FIGURE 2 | Core body temperature **(A)** and pulmonary and cardiovascular functions **(B–E)** in single-housed (SIN) and co-bedded (COB) Preterm piglets. Data is presented as means with standard deviations.

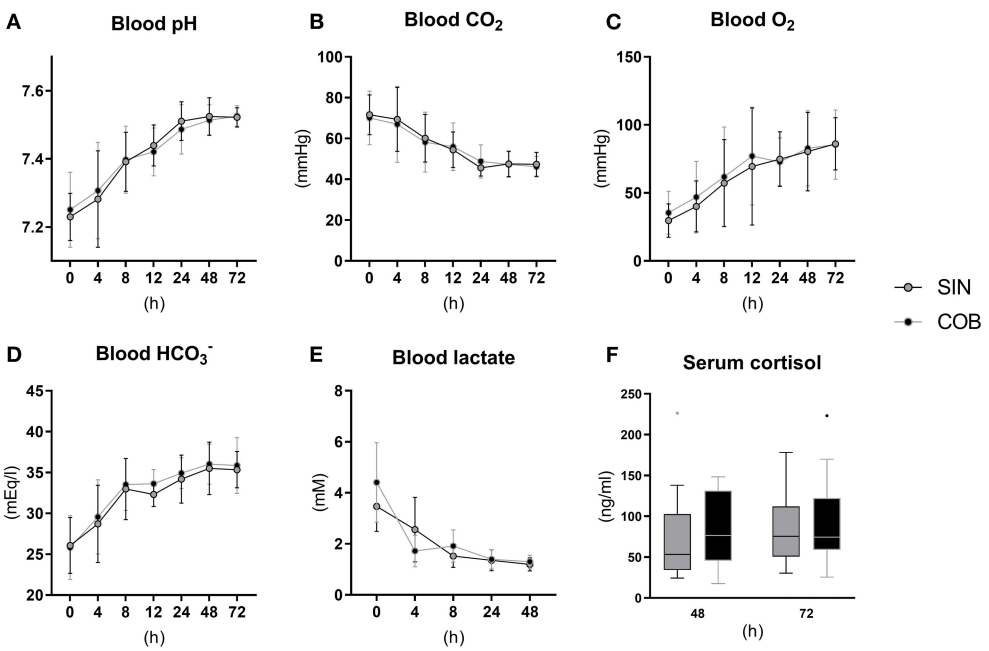

FIGURE 3 | Arterial blood gas values **(A–E)** and serum cortisol levels **(F)** in single-housed (SIN) and co-bedded (COB) Preterm piglets. Longitudinal data is presented as means with standard deviations, and cortisol data is presented in box plots (box edges denote interquartile ranges and horizontal line denotes the median value) with Tukey whiskers (outliers shown as dots).

Laboratory, Bedford, MA, USA). Cortisol levels were measured in serum samples using an enzyme-linked immunosorbent assay (KGE008B, R&D Systems, Abingdon, UK).

Euthanasia, Tissue Collection, and NEC Evaluation

Three hours prior to euthanasia, all animals received an oro-gastric 15 ml/kg bolus of 5/5% lactulose/mannitol solution for the assessment of intestinal permeability by urinary recovery of the sugar marker molecules. Furthermore, animals in the co-bedding experiment received a standardized oro-gastric formula bolus of 15 mL/kg to assess gastric emptying. Animals were then anesthetized and blood collected by cardiac puncture for hematological cell counting and blood biochemistry (only for the HC experiment) measurements, followed by euthanasia with a lethal cardiac injection of barbiturate. Urine was collected by cystocentesis for measurement of lactulose and mannitol, as previously described (27). Abdominal and thoracic organs were excised and brains collected for recording of their wet weights. Macroscopic lesions of small intestine and colon were graded according to a previously validated six-grade NEC scoring system (see **Supplementary Figure 1**), where NEC was defined as the presence of a lesion score of three (focal hemorrhage) or above in any of the gut segments (28). Biopsies of proximal, mid and distal small intestine were dissected and either immersion fixed to assess mucosal morphometry or snap-frozen for later measurement of brush-border enzyme activity and oxidative stress markers (only for the HC experiment), while a biopsy from the transverse colon was collected and immersion fixed for estimation of goblet cell mucin density (only for the co-bedding experiment).

Gut Structure and Function

Duplicate biopsies from three small intestinal regions were paraffin-embedded, and tissue sections stained with hematoxylin-eosin. Villus lengths and crypt depths were measured with ImageJ software in four 10× magnification photomicrographs per region capturing mainly well-oriented villus structures. Further, duplicate biopsies from transverse colon were embedded in paraffin, and tissue sections stained with Alcian blue-periodic acid Schiff to visualize mucin-laden goblet cells. Relative goblet cell area was quantified using ImageJ software. Small intestinal brush-border enzyme activities were measured as previously described (29). Finally, markers of oxidative status in small intestinal homogenate were measured. Superoxide dismutase (SOD) acticity was analyzed using the Ransod colorimetric assay (Randox, Crumlin, UK). Oxidized (GSSG) and reduced (GSH) glutathione were analyzed by a fluorometric assay (30), Vitamin E (α- and γ-tocopherol), ascorbic acid and malondialdehyde (MDA), a lipid peroxidation end product, were analyzed by high-performance liquid chromatography (31–33).

Statistics

All statistical analyses were performed using R statistical software (version 1.3.1093). Analysis of dichotomous outcomes (NEC and diarrhea incidences) was done using a generalized linear model (glm), while continuous outcomes were analyzed using a general linear model (lm). Longitudinal data (vital functions, blood gases, mucosa morphometry) were analyzed using a linear mixed-effects (lme) model with animal ID as a random effect parameter. All models included adjustments for litter, sex and birth weight as fixed-effects parameters. Residuals were checked using Q-Q and residual vs. fit plots and data log-transformed, if these did not adhere to model assumptions of normality and homoscedasticity. Probability values <0.05 were considered significant.

TABLE 1 | Blood hematology of three-day old single-housed or co-bedded piglets.

	SIN	COB
Total erythrocytes (10^{12}/l)	3.79 (0.57)	3.66 (0.49)
Hemoglobin (mmol/l)	4.92 (0.62)	4.75 (0.46)
Hematocrit (g/kg)	0.26 (0.03)	0.25 (0.03)
Platelets (10^9/l)	276 (46.5)	233 (33.2)
Total leucocytes (10^9/l)	1.78 (1.04)	1.44 (0.76)
Neutrophils (10^9/l)	0.79 (0.83)	0.68 (0.68)
Lymphocytes (10^9/l)	0.77 (0.26)	0.66 (0.15)
Monocytes (10^9/l)	0.07 (0.10)	0.05 (0.02)

All data is presented as means with standard deviations in parentheses. SIN, single-housing; COB, co-bedding. No differences between the groups were found in the statistical analysis.

RESULTS

Experiment 1: Co-bedding

The vital functions of co-bedded and single-housed Preterm piglets were closely monitored for 72 h (**Figure 2**). Following transient hypothermia in the hours following Preterm birth, the core body temperature increased to normal levels in both groups (38–39°C) within 4 h (**Figure 2A**). The respiratory frequency decreased gradually, and similarly in the groups, together with increasing heart rate and oxygen saturation (**Figures 2B–D**). Large intra- and inter-individual variation (e.g., 40–50 mmHg) were observed in mean arterial blood pressures with no obvious effect of time or treatment (**Figure 2E**).

Pronounced changes over time were also observed for arterial blood gas parameters (**Figures 3A–E**), measured at similar time points as the vital signs. Piglets were mildly acidotic just after birth (mean arterial blood pH around 7.2, **Figure 3A**) but blood acidity was normalized within the first 24 h, and similarly in the two groups. Accordingly, CO_2 partial pressure (**Figure 3B**) and lactate levels decreased over time (**Figure 3E**), whereas O_2 partial pressure and bicarbonate levels increased (**Figures 3C,D**), with no effect of co-bedding vs. single-bedding. Likewise, serum cortisol levels measured at 48 and 72 h (**Figure 3F**), and blood hematology at 72 h (**Table 1**), showed no differences between the groups.

Until euthanasia at 72 h, daily growth rate was similar between the groups (**Figure 4A**) and no differences were observed for organ weights (**Supplementary Table 2**). At this time, the NEC incidence was significantly lower in co-bedded animals

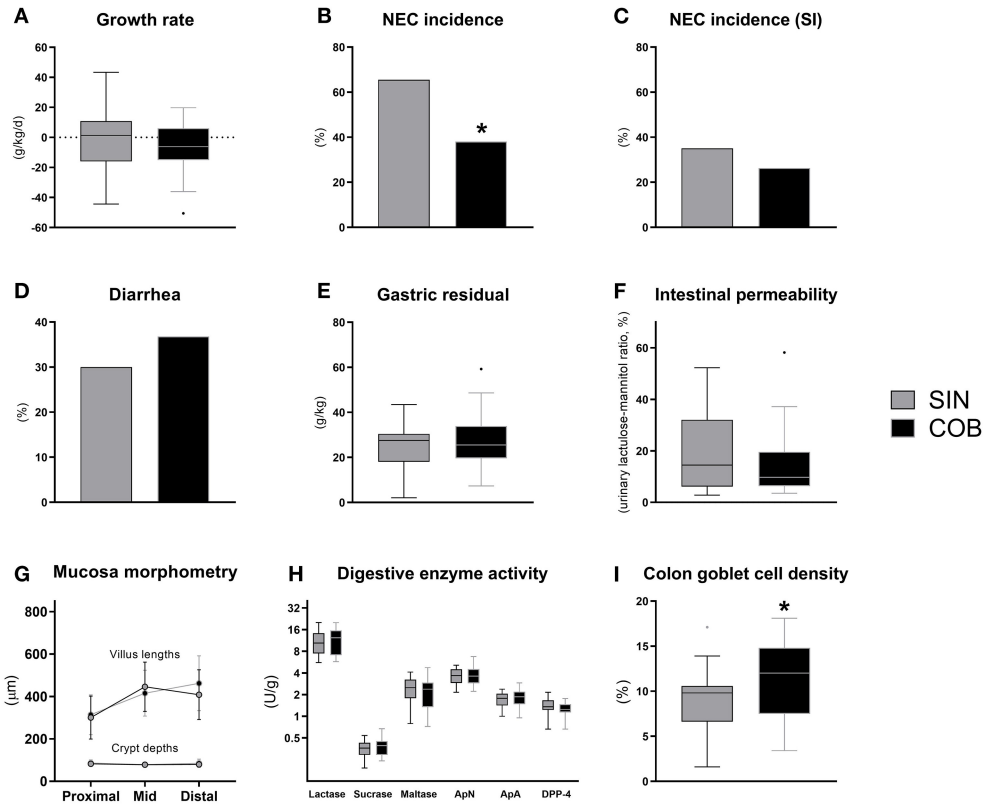

FIGURE 4 | Body growth rate **(A)**, overall and small intestinal (SI) NEC incidence **(B,C)**, proportion of pigs with diarrhea **(D)**, gastric residual volume **(E)**, urinary lactulose-mannitol ratio as a measure of intestinal permeability **(F)**, small intestinal villus and crypt morphology **(G)**, activity of brush-border disaccharidases (lactase, sucrase, maltase) and aminopeptidases (aminopeptidase N, ApN; aminopeptidase A, ApA; dipeptidyl peptidase-4, DPP-4) **(H)**, and relative area of colonic goblet cells **(I)**. Dichotomous data is reported as frequencies. Longitudinal data is presented as means with standard deviations, while remaining continuous data is presented as box plots (box edges denote interquartile ranges and horizontal line denotes the median value) with Tukey whiskers (outliers shown as dots). *Denotes a probability value below 0.05. SIN, single-housing; COB, co-bedding.

relative to single-housed littermates ($p < 0.05$, **Figure 4B**). This was due to a reduction in colonic NEC-like lesions, as the small intestinal NEC incidences were similar (**Figure 4C**). Conversely, diarrhea incidence, gastric emptying rate and intestinal permeability (**Figures 4D–F**) were not affected by co-bedding. Likewise, small intestinal villi and crypts were of similar lengths (**Figure 4G**), and disaccharidase and aminopeptidase activities did not differ (**Figure 4H**). However, supporting the reduced colonic NEC incidence, significantly higher colonic goblet cell density was observed in co-bedded animals ($p < 0.05$, **Figure 4I**).

Experiment 2: Hydrocortisone Treatment

Following the tapering HC dose over 4 days, serum cortisol levels were measured at birth and 72 h (shortly after HC administration) and at euthanasia (∼12 h after the last HC injection (**Figure 5A**). Cortisol levels at birth were ∼50 ng/ml on average and increased to a concentration just above 100 ng/ml at 72 and 96 h in CON animals. Cortisol levels were more than six-fold higher in HC animals relative to CON at 72 h ($p < 0.001$) but appeared to decrease to control levels 12 h after treatment discontinuation (**Figure 5A**). Vital functions followed a similar longitudinal trend as observed in Experiment 1, with increasing core body temperature, pulse and oxygen saturation (**Figures 5B,D,E**) and decreasing respiratory frequency (**Figure 5C**). Like in Experiment 1, all blood gas values were largely normalized by 24 h after birth, and there were no clear effect of HC treatment on these (**Figure 5G**) or on blood pressure (**Figure 5F**). In addition, blood hematology (**Supplementary Table 3**) and biochemical profiles (**Supplementary Table 4**) measured at euthanasia showed no effects of HC treatment.

Until euthanasia at 96 h after birth, daily growth rate was not affected by HC treatment (**Figure 6A**) and organ weights did not differ (**Supplementary Table 5**). The incidence of small intestinal NEC lesions was significantly increased in the HC group, relative to CON ($p < 0.05$), without effects on the overall NEC incidence across gut regions (**Figures 6B,C**). The incidence of diarrhea was similarly high in both groups (**Figure 6D**), while the HC group showed a tendency to reduced intestinal permeability (**Figure 6E**, $P = 0.07$). Further, no treatment effects were observed for small intestinal villous architecture, brush-border enzyme activities and markers of oxidative status (**Figures 6F–H**). However, across groups animals with NEC showed increased MDA levels relative to littermates without NEC ($p < 0.05$, data not shown).

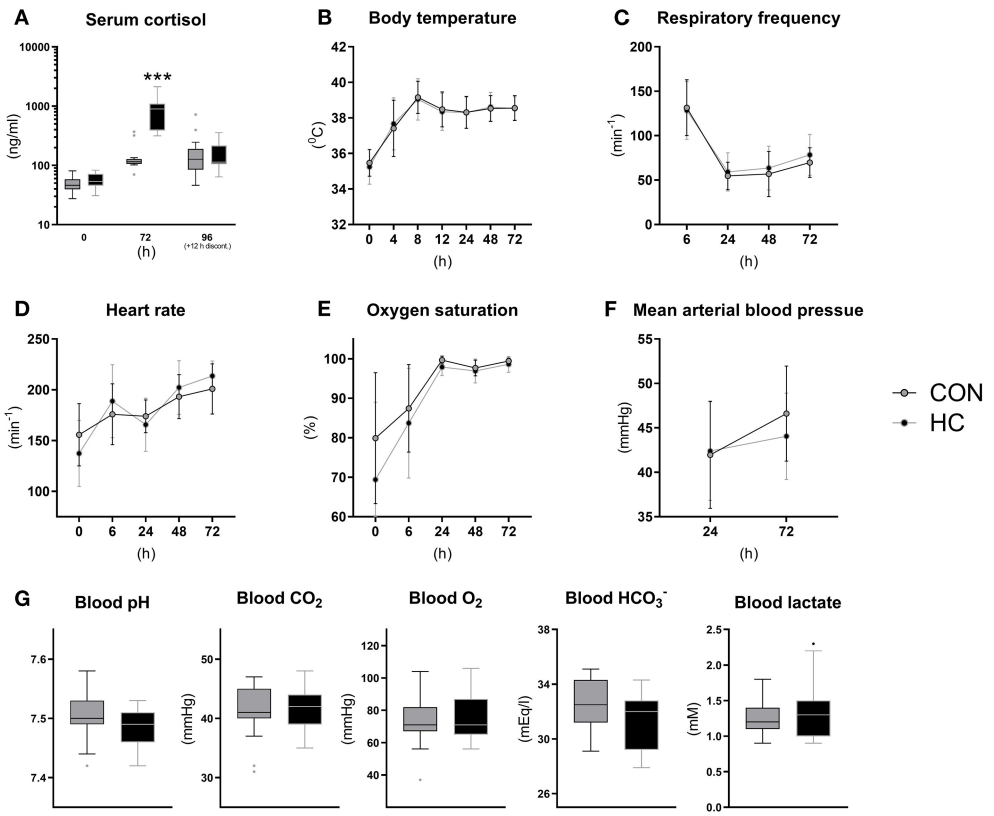

FIGURE 5 | Serum cortisol levels **(A)**, core body temperature **(B)**, pulmonary and cardiovascular functions **(C–F)** and arterial blood gas parameters at 24 h **(G)** for hydrocortisone (HC) and control (CON) Preterm piglets. Longitudinal data is presented as means with standard deviations, and remaining data is presented as box plots (box edges denote interquartile ranges and horizontal line denotes the median value) with Tukey whiskers (outliers shown as dots). ***Denotes a probability value below 0.001.

DISCUSSION

With increasing survival of extremely Preterm infants, improving the care for these patients remains a priority to facilitate optimal growth and development and reduce the risk of serious morbidities. Skin-to-skin contact appears to provide organism-wide benefits to Preterm infants, but detailed knowledge about physiological effects requires the use of animal models. With the use of Preterm pigs, we examined the potential of Preterm sibling skin-to-skin contact (co-bedding) as well as pharmacological cortisol treatment to improve vital functions and prevent the life-threatening disease NEC. Cardiovascular and respiratory function were not notably affected by either treatment but co-bedding decreased overall NEC incidence while HC treatment increased NEC specifically in the small intestine. The two experiments provide preliminary insights into some clinically relevant interventions for Preterm infants but more studies are required to better understand mechanisms and possible interactions across organs and functions.

Co-bedding and kangaroo care share the concept of skin-to-skin contact and possible effects on neuro-endocrine regulatory pathways, but they also differ in many aspects. The majority of clinical data on skin-to-skin clinical care in Preterm infants is based on kangaroo care, documented to increase survival, growth and infection resistance (6), in addition to possible effects on the oral and stool microbiome (34, 35). The latter effect may arise from exposure to maternal skin microbiota, a factor that we have excluded in our co-bedding mediated skin-to-skin experiments. Growth and feeding results from studies of kangaroo care should also be interpreted with caution, as it is often difficult to differentiate between the effects of breastmilk intake and skin-to-skin contact *per se*. In this perspective, it is attractive from a scientific standpoint to use cesarean-delivered (sterile) Preterm pigs, not affected by prenatal complications, and fed without contact to their mother in highly standardized conditions, in studies on skin-to-skin contact *via* siblings, affecting relevant physiological, clinical and pathological endpoints.

Across all mammals, organ structure and function develop differently in relation to the normal time of birth (24, 36). In pigs, gut and immune functions are relatively immature until close to term, making them highly susceptible to gut dysfunctions (e.g., NEC) and infections when delivered at 90% gestation (37, 38). For these pigs, the development in vital organ functions just after birth was characterized by a transient hypothermia, tachypnea, low oxygen saturation and blood pH as well as elevated lactate but all these parameters resolved to normal

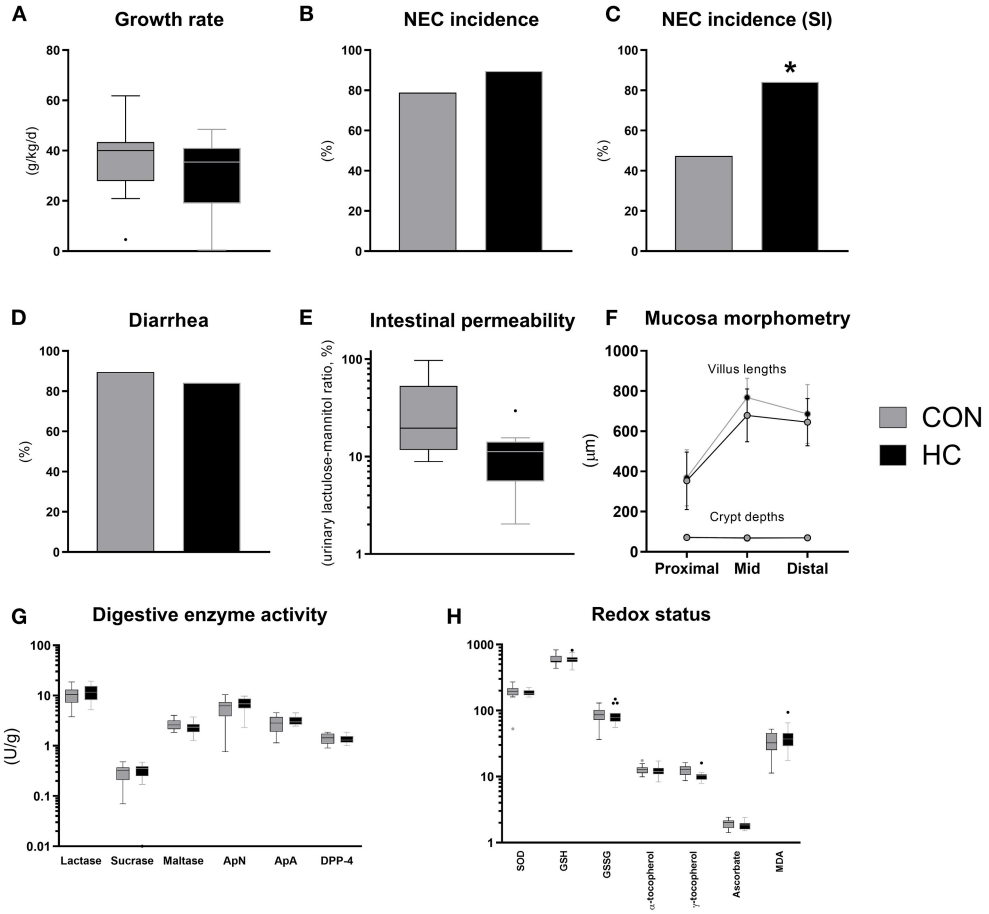

FIGURE 6 | Body growth rate **(A)**, overall and small intestinal (SI) NEC incidence **(B,C)**, proportion of pigs with diarrhea **(D)**, urinary lactulose-mannitol ratio as a measure of intestinal permeability **(E)**, small intestinal villus and crypt morphology **(F)**, activity of brush-border disaccharidases (lactase, sucrase, maltase) and aminopeptidases (aminopeptidase N, ApN; aminopeptidase A, ApA; dipeptidyl peptidase-4, DPP-4) **(G)**, markers of oxidative stress in small intestinal tissue (superoxide dismutase activity, SOD, U/g; reduced (GSH) and oxidized glutathione, GSSG, both nmol/g; α- and γ-tocopherol, both nmol/g; ascorbate, µmol/g; malondialdehyde, MDA, nmol/g) **(H)**. Dichotomous data is reported as frequencies. Longitudinal data is presented as means with standard deviations, while remaining continuous data is presented as box plots (box edges denote interquartile ranges and horizontal line denotes the median value) with Tukey whiskers (outliers shown as dots). *Denotes a probability value below 0.05. HC, hydrocortisone; CON, control.

levels within 24–48 h after birth when pigs were kept in heated incubators with fluid and nutrition supply (parenteral nutrition), and even without oxygen supplementation. In this regard, neonatal viability of 90% gestation Preterm pigs may reflect that in moderately Preterm infants (32–37 weeks gestation), rather than very or extreme Preterm infants (<32 weeks gestation). This is supported by the limited need for surfactant, oxygen and mechanical ventilation for survival of 90% gestation Preterm pigs. A large proportion of these pigs have an open ductus arteriosus (PDA) at 24 h after birth, relative to term pigs (20–40 vs. 0%, our unpublished observations). In addition to a moderate cardiovascular and respiratory immaturity in 90% gestation Preterm pigs, anesthesia of the pregnant sow during the cesarean section, could also have contributed to the compromised physiological state in the first day of life. The fact that normalization of vital functions during the first 1–2 days was not accelerated by co-bedding or HC treatment may indicate that such interventions are most pronounced in more extreme states of prematurity.

Antenatal glucocorticoid treatment is among the most well-documented medical treatments for Preterm infants with beneficial effects on survival and pulmonary function (13). After Preterm birth on the other hand, it has proven difficult to identify the proper drug and dose regimen to patients with insufficient endogenous glucocorticoid production to ensure optimal clinical benefit (e.g., treatment of hypotension) without adverse treatment effects (14). A frequent side effect to postnatal glucocorticoid treatment is gastrointestinal bleeding (14). In this study, we found an increased incidence of small intestinal hemorrhage (NEC-like lesions) in HC treated Preterm pigs, which may be due to excessive circulating cortisol levels. Oxidative tissue damage was confirmed by increased levels of MDA, a lipid peroxidation product shown in animals with hemorrhagic small intestine. Establishing

reference values for serum cortisol levels in Preterm infants is difficult due to fluctuations and numerous influencing factors (e.g., antenatal glucocorticoids, delivery mode, glucose levels, infection). However, 20–200 ng/ml has been proposed as a relatively wide range reflecting cortisol levels in non-symptomatic Preterm infants (39) and is in accordance with that of Preterm pigs in the neonatal period (40). In this regard, co-bedded and single-housed Preterm pigs had cortisol levels in the normal range, whereas HC treated animals largely exceeded these reference values. The initial HC dose used in this study (3 mg/kg/d) is three-fold higher than the dose that has been shown to be safe and efficacious for prevention of bronchopulmonary dysplasia in Preterm infants (16). In summary, 90% gestation pigs may not benefit from exogenous cortisol postnatally with regards to their cardiaovascular and respiratory functions, potentially because these functions are relatively mature. This contrasts the marked effects of ACTH or HC treatment on gut functions in both near-term or term pigs (20, 21).

We found that skin-to-skin contact between Preterm newborn pigs increased the resistance to NEC-like colonic inflammation in ways that are unlikely to depend on cardiopulmonary functions or cortisol levels. The benefits of co-bedding on NEC was confined to the colon region, which showed less NEC-like pathology and higher relative area of goblet cells in co-bedded animals. The suggestion that Preterm skin-to-skin contact improves stress coping *via* neuroendocrine mechanisms (41) may help to explain how co-bedding could reduce NEC incidence without affecting vital functions. Heart rate variability, an accepted marker for cardiac vagal tone and parasympathetic nervous activity, is altered in Preterm relative to term infants (42), and reduced by kangaroo care in response to pain (43). Further, massage of Preterm infants, another type of skin-to-skin contact, improves gastric motility in addition to increasing vagal tone. Whereas increases in vagal tone is usually accompanied by decreased cortisol levels, evidence from inflammatory bowel disease patients indicates that this inverse association may be uncoupled during disease states (44). The gut microbiota is closely associated with gut inflammatory status and NEC, but to which degree it is affected by co-bedding and whether this is causally related with NEC development remains to be explored. To address this issue, we propose a future experiment, where gut microbiota from co-bedded Preterm neonates is transplanted into single-housed recipients to investigate causality of the gut microbiota in this regard. Collectively, we speculate that skin-to-skin contact during co-bedding increases vagal tone, thereby promoting gastrointestinal motility and improves NEC resistance, possibly through modulation of the gut microbiota.

Kangaroo care has become standard practice in most neonatal clinics, but in situations where a parent is not able to be in contact with the infant (e.g., culture, tradition, socioeconomic reasons), co-bedding may provide an alternative, even among non-siblings if deemed safe. Regardless, the causal relationships among skin-to-skin contact, vagal tone, gastrointestinal motility and inflammation clearly warrants further investigations and the Preterm pig may be of value to in this context to study detailed effects of clinical care procedures.

DATA AVAILABILITY STATEMENT

The raw data supporting the conclusions of this article will be made available by the authors, without undue reservation.

ETHICS STATEMENT

All *in vivo* procedures were approved by the Danish Animal Experiments Inspectorate (license no. 2020-15-0201-00520), which complies with the EU Directive 2010/63 (legislation for the use of animals in research).

AUTHOR CONTRIBUTIONS

AB and PTS: conception and design, data interpretation, writing original draft, and critical review and editing. AB and YP: data acquisition. AB, YP, YL, and JL: data analysis. All authors: editing and approval of the final manuscript.

FUNDING

The NEOCOL project granted by Innovation Fund Denmark (NEOCOL Project No. 6150-00004B).

ACKNOWLEDGMENTS

We would like to thank Yan Xudong, Malene Birck, Elin Skytte, Jane C. Povlsen, Thomas Thymann, Line Møller Willumsen, Paivi Worsøe, and Kristina Møller from Comparative Pediatrics and Nutrition for support in animal procedures and technical support with biochemical analyses.

SUPPLEMENTARY MATERIAL

The Supplementary Material for this article can be found online at: https://www.frontiersin.org/articles/10.3389/fped.2021.636638/full#supplementary-material

REFERENCES

1. Niño DF, Sodhi CP, Hackam DJ. Necrotizing enterocolitis: new insights into pathogenesis and mechanisms. *Nat Rev Gastroenterol Hepatol*. (2016) 13:590–600. doi: 10.1038/nrgastro.2016.119
2. Cassady G, Crouse DT, Kirklin JW, Strange MJ, Joiner CH, Godoy G, et al. A randomized, controlled trial of very early prophylactic ligation of the ductus arteriosus in babies who weighed 1000 g or less at birth. *N Engl J Med*. (1989) 320:1511–6. doi: 10.1056/NEJM198906083202302
3. Ludington-Hoe SM, Anderson GC, Swinth JY, Thompson C, Hadeed AJ. Randomized controlled trial of kangaroo care: cardiorespiratory and thermal effects on healthy preterm infants. *Neonatal Netw*. (2004) 23:39–48. doi: 10.1891/0730-0832.23.3.39

4. Kommers DR, Joshi R, van Pul C, Atallah L, Feijs L, Oei G, et al. Features of heart rate variability capture regulatory changes during kangaroo care in preterm infants. *J Pediatr*. (2017) 182:92–8.e1. doi: 10.1016/j.jpeds.2016.11.059
5. Sehgal A, Nitzan I, Jayawickreme N, Menahem S. Impact of skin-to-skin parent-infant care on preterm circulatory physiology. *J Pediatr*. (2020) 222:91–7.e2. doi: 10.1016/j.jpeds.2020.03.041
6. Conde-Agudelo A, Díaz-Rossello JL. Kangaroo mother care to reduce morbidity and mortality in low birthweight infants. *Cochrane Database Syst Rev*. (2016) 2016 doi: 10.1002/14651858.CD002771.pub4
7. Lai NM, Foong SC, Foong WC, Tan K. Co-bedding in neonatal nursery for promoting growth and neurodevelopment in stable preterm twins. *Cochrane Database Syst Rev*. (2016) 2016:CD008313. doi: 10.1002/14651858.CD008313.pub3
8. Grier DG, Halliday HL. Effects of glucocorticoids on fetal and neonatal lung development. *Treat Respir Med*. (2004) 3:295–306. doi: 10.2165/00151829-200403050-00004
9. Mörelius E, Theodorsson E, Nelson N. Salivary cortisol and mood and pain profiles during skin-to-skin care for an unselected group of mothers and infants in neonatal intensive care. *Pediatrics*. (2005) 116:1105–13. doi: 10.1542/peds.2004-2440
10. Mitchell AJ, Yates CC, Williams DK, Chang JY, Hall RW. Does daily kangaroo care provide sustained pain and stress relief in preterm infants? *J Neonatal Perinatal Med*. (2013) 6:45–52. doi: 10.3233/NPM-13 64212
11. Liggins GC. Premature delivery of foetal lambs infused with glucocorticoids. *J Endocrinol*. (1969) 45:515–23. doi: 10.1677/joe.0.0450515
12. Liggins GC, Howie RN. A controlled trial of antepartum glucocorticoid treatment for prevention of the respiratory distress syndrome in premature infants. *Pediatrics*. (1972) 50:515–25.
13. Roberts D, Brown J, Medley N, Dalziel SR. Antenatal corticosteroids for accelerating fetal lung maturation for women at risk of preterm birth. *Cochrane Database Syst Rev*. (2017) 3:CD004454. doi: 10.1002/14651858.CD004454.pub3
14. Doyle LW, Cheong JL, Ehrenkranz RA, Halliday HL. Early (< 8 days) systemic postnatal corticosteroids for prevention of bronchopulmonary dysplasia in preterm infants. *Cochrane Database Syst Rev*. (2017) 2017:CD001146. doi: 10.1002/14651858.CD001146.pub5
15. Johnson PJ. Hydrocortisone for treatment of hypotension in the newborn. *Neonatal Netw*. (2015) 34:46–51. doi: 10.1891/0730-0832.34.1.46
16. Baud O, Maury L, Lebail F, Ramful D, El Moussawi F, Nicaise C, et al. Effect of early low-dose hydrocortisone on survival without bronchopulmonary dysplasia in extremely preterm infants (PREMILOC): a double-blind, placebo-controlled, multicentre, randomised trial. *Lancet*. (2016) 387:1827–36. doi: 10.1016/S0140-6736(16)00202-6
17. Eiby YA, Wright LL, Kalanjati VP, Miller SM, Bjorkman ST, Keates HL, et al. A pig model of the preterm neonate: anthropometric and physiological characteristics. *PLoS ONE*. (2013) 8:e68763. doi: 10.1371/journal.pone.0068763
18. Andersen AD, Sangild PT, Munch SL, van der Beek EM, Renes IB, Ginneken C van, et al. Delayed growth, motor function and learning in preterm pigs during early postnatal life. *Am J Physiol Regul Integr Comp Physiol*. (2016) 310:R481–92. doi: 10.1152/ajpregu.00349.2015
19. Sangild PT, Weström BR, Fowden AL, Silver M. Developmental regulation of the porcine exocrine pancreas by glucocorticoids. *J Pediatr Gastroenterol Nutr*. (1994) 19:204–12. doi: 10.1097/00005176-199408000-00011
20. Sangild P, Diernaes L, Christiansen I, Skadhauge E. Intestinal transport of sodium, glucose and immunoglobulin in neonatal pigs. Effect of glucocorticoids. *Exp Physiol*. (1993) 78:485–97. doi: 10.1113/expphysiol.1993.sp003700
21. Sangild PT. Stimulation of gastric proteases in the neonatal pig by a rise in adrenocortical secretion at parturition. *Reprod Fertil Dev*. (1995) 7:1293–8. doi: 10.1071/RD9951293
22. Sangild PT, Sjöström H, Noren O, Fowden AL, Silver M. The prenatal development and glucocorticoid control of brush-border hydrolases in the pig small intestine. *Pediatr Res*. (1995) 37:207–12. doi: 10.1203/00006450-199502000-00014
23. Sangild PT, Siggers RH, Schmidt M, Elnif J, Bjornvad CR, Thymann T, et al. Diet- and colonization-dependent intestinal dysfunction predisposes to necrotizing enterocolitis in preterm pigs. *Gastroenterology*. (2006) 130:1776–92. doi: 10.1053/j.gastro.2006.02.026
24. Sangild PT, Thymann T, Schmidt M, Stoll B, Burrin DG, Buddington RK. Invited review: the preterm pig as a model in pediatric gastroenterology. *J Anim Sci*. (2013) 91:4713–29. doi: 10.2527/jas.2013-6359
25. Peeples ES. An evaluation of hydrocortisone dosing for neonatal refractory hypotension. *J Perinatol*. (2017) 37:943–6. doi: 10.1038/jp.2017.68
26. Onland W, Offringa M, Cools F, De Jaegere AP, Rademaker K, Blom H, et al. Systemic hydrocortisone to prevent bronchopulmonary dysplasia in preterm infants (the SToP-BPD study); a multicenter randomized placebo controlled trial. *BMC Pediatr*. (2011) 11:102. doi: 10.1186/1471-2431-11-102
27. Birck MM, Nguyen DN, Cilieborg MS, Kamal SS, Nielsen DS, Damborg P, et al. Enteral but not parenteral antibiotics enhance gut function and prevent necrotizing enterocolitis in formula-fed newborn preterm pigs. *Am J Physiol Gastrointest Liver Physiol*. (2016) 310:G323–33. doi: 10.1152/ajpgi.00392.2015
28. Bjornvad CR, Thymann T, Deutz NE, Burrin DG, Jensen SK, Jensen BB, et al. Enteral feeding induces diet-dependent mucosal dysfunction, bacterial proliferation, and necrotizing enterocolitis in preterm pigs on parenteral nutrition. *Am J Physiol Gastrointest Liver Physiol*. (2008) 295:G1092–103. doi: 10.1152/ajpgi.00414.2007
29. Østergaard MV, Shen RL, Støy ACF, Skovgaard K, Krych Ł, Leth SS, et al. Provision of amniotic fluid during parenteral nutrition increases weight gain with limited effects on gut structure, function, immunity, and microbiology in newborn preterm pigs. *J Parenter Enter Nutr*. (2016) 40:552–66. doi: 10.1177/0148607114566463
30. Hissin PJ, Hilf R. A fluorometric method for determination of oxidized and reduced glutathione in tissues. *Anal Biochem*. (1976) 74:214–26. doi: 10.1016/0003-2697(76)90326-2
31. Sattler W, Mohr D, Stocker R. Rapid isolation of lipoproteins and assessment of their peroxidation by high-performance liquid chromatography postcolumn chemiluminescence. *Methods Enzymol*. (1994) 233:469–89. doi: 10.1016/S0076-6879(94)33053-0
32. Lykkesfeldt J. Determination of malondialdehyde as dithiobarbituric acid adduct in biological samples by HPLC with fluorescence detection: comparison with ultraviolet-visible spectrophotometry. *Clin Chem*. (2001) 47:1725–7. doi: 10.1093/clinchem/47.9.1725
33. Lykkesfeldt J. Ascorbate and dehydroascorbic acid as reliable biomarkers of oxidative stress: analytical reproducibility and long-term stability of plasma samples subjected to acidic deproteinization. *Cancer Epidemiol Biomarkers Prev*. (2007) 16:2513–6. doi: 10.1158/1055-9965.EPI-07-0639
34. Hendricks-Muñoz KD, Xu J, Parikh HI, Xu P, Fettweis JM, Kim Y, et al. Skin-to-skin care and the development of the preterm infant oral microbiome. *Am J Perinatol*. (2015) 32:1205–16. doi: 10.1055/s-0035-1552941
35. Rozé JC, Ancel PY, Marchand-Martin L, Rousseau C, Montassier E, Monot C, et al. Assessment of neonatal intensive care unit practices and preterm newborn gut microbiota and 2-year neurodevelopmental outcomes. *JAMA Netw Open*. (2020) 3:e2018119. doi: 10.1001/jamanetworkopen.2020.18119
36. Sangild PT. Gut responses to enteral nutrition in preterm infants and animals. *Exp Biol Med*. (2006) 231:1695–711. doi: 10.1177/153537020623101106
37. Ren S, Hui Y, Obelitz-Ryom K, Brandt AB, Kot W, Nielsen DS, et al. Neonatal gut and immune maturation is determined more by postnatal age than by postconceptional age in moderately preterm pigs. *Am J Physiol Liver Physiol*. (2018) 315:G855–67. doi: 10.1152/ajpgi.00169.2018
38. Bæk O, Brunse A, Nguyen DN, Moodley A, Thymann T, Sangild PT. Diet modulates the high sensitivity to systemic infection in newborn preterm pigs. *Front Immunol*. (2020) 11:e01019. doi: 10.3389/fimmu.20 20.01019
39. Heckmann M, Wudy SA, Haack D, Pohlandt F, Heckmann M, Wudy SA, et al. Reference range for serum cortisol in well preterm infants. *Arch Dis Child Fetal Neonatal Ed*. (1999) 81:171–4. doi: 10.1136/fn.81.3.F171
40. Cao M, Brunse A, Thymann T, Sangild PT. Physical activity and spatial memory are minimally affected by moderate growth restriction in preterm piglets. *Dev Neurosci*. (2020) 41:247–54. doi: 10.1159/000505726
41. Bergman NJ. Birth practices: maternal-neonate separation as a source of toxic stress. *Birth Defects Res*. (2019) 111:1087–109. doi: 10.1002/bdr2.1530

42. Patural H, Pichot V, Jaziri F, Teyssier G, Gaspoz JM, Roche F, et al. Autonomic cardiac control of very preterm newborns: a prolonged dysfunction. *Early Hum Dev*. (2008) 84:681–7. doi: 10.1016/j.earlhumdev.2008.04.010
43. Cong X, Ludington-Hoe SM, McCain G, Fu P. Kangaroo care modifies preterm infant heart rate variability in response to heel stick pain: pilot study. *Early Hum Dev*. (2009) 85:561–7. doi: 10.1016/j.earlhumdev.2009.05.012
44. Diego MA, Field T, Hernandez-Reif M. Vagal activity, gastric motility, and weight gain in massaged preterm neonates. *J Pediatr*. (2005) 147:50–5. doi: 10.1016/j.jpeds.2005.02.023

Conflict of Interest: The authors declare that the research was conducted in the absence of any commercial or financial relationships that could be construed as a potential conflict of interest.

Advantages of publishing in Frontiers

OPEN ACCESS
Articles are free to read for greatest visibility and readership

FAST PUBLICATION
Around 90 days from submission to decision

HIGH QUALITY PEER-REVIEW
Rigorous, collaborative, and constructive peer-review

TRANSPARENT PEER-REVIEW
Editors and reviewers acknowledged by name on published articles

Frontiers
Avenue du Tribunal-Fédéral 34
1005 Lausanne | Switzerland

Visit us: www.frontiersin.org
Contact us: frontiersin.org/about/contact

REPRODUCIBILITY OF RESEARCH
Support open data and methods to enhance research reproducibility

DIGITAL PUBLISHING
Articles designed for optimal readership across devices

FOLLOW US
@frontiersin

IMPACT METRICS
Advanced article metrics track visibility across digital media

EXTENSIVE PROMOTION
Marketing and promotion of impactful research

LOOP RESEARCH NETWORK
Our network increases your article's readership